

The Effects of Inflammatory Bowel Disease Drugs on the Autophagy Pathway

Kirsty Marie Hooper

A thesis submitted in partial fulfillment of the
requirements of Edinburgh Napier University, for the
award of Doctor of Philosophy

May 2019

For Mum, Dad, Mark and Jamie

Abstract

Crohn's disease (CD), one of the main forms of Inflammatory Bowel Disease (IBD), is a complex disorder characterised by chronic inflammation of the gastrointestinal (GI) tract. The aetiology of CD involves genetics and environmental factors that trigger an abnormal immune response to intestinal bacteria. Genome-wide association studies have strongly linked genes involved in autophagy, such as *ATG16L1*, to CD. Autophagy is a cellular degradation process that clears intracellular bacteria and regulates inflammatory responses. Recent studies suggest that enhancing autophagy in CD patients may be therapeutically beneficial. The aim of this study was to characterise the mechanism of action of a panel of commonly used IBD drugs in the context of autophagy and autophagy-related pathways, such as the unfolded protein response (UPR) and apoptosis.

Modulation of autophagy was assessed *in vitro*, and in peripheral blood mononuclear cells (PBMCs) and GI biopsies from paediatric IBD patients. Several complimentary techniques to monitor the autophagy marker LC3 and master regulator of autophagy, mechanistic target of rapamycin (mTORC1), were used. Varying stages of apoptosis were assessed using a range of techniques and activity of UPR mediators was measured using RT-qPCR and western immunoblotting. The clearance of CD-associated adherent-invasive *E. coli* (AIEC) was assessed using gentamicin protection assays, and pro-inflammatory cytokines were monitored by RT-qPCR.

Our results reveal that the immunosuppressant drug azathioprine is a strong inducer of autophagy and this response was independent of apoptosis. Azathioprine induced autophagy via inhibition of mTORC1 and up-regulation of the UPR. Azathioprine also enhanced the clearance of intracellular AIEC and dampened pro-inflammatory cytokine responses. Furthermore, azathioprine induced autophagy in paediatric patient samples, and this response was more pronounced in patients harbouring the CD-associated *ATG16L1* variant. A better understanding of IBD drug mechanism of action can contribute to patient stratification for the development of a more personalised therapeutic approach.

Contents

ABSTRACT	II
CONTENTS	III
LIST OF FIGURES	IX
DECLARATION	1
ACKNOWLEDGMENTS	2
LIST OF ABBREVIATIONS	3
1. INTRODUCTION	12
1.1 Inflammatory Bowel Disease	12
1.1.1. Paediatric IBD	13
1.1.2. Aetiology of Crohn's Disease	14
1.1.2.1. CD-associated NOD2 variants	14
1.1.2.2. Genome Wide Association Studies	15
1.1.2. Intestinal Microbiota, Microbial Dysbiosis and CD-associated pathogens	16
1.1.3. Intestinal Epithelial Barrier in CD	18
1.1.4. Intestinal and Systemic Immune cells in CD	21
1.1.4.1. Haematopoiesis and Immune cell subsets	21
1.1.4.2. Myeloid cells in CD	23
1.1.4.3. T cells in CD	24
1.1.4.4. B cells in CD	24
1.1.4.5. NK cells in CD	25
1.2. Autophagy	25
1.2.1. Autophagosome biogenesis	26
1.2.2. Autophagy regulatory pathways	29
1.2.3. Transcriptional Regulation of Autophagy	31
1.2.4. Autophagy and Cell Death are intrinsically linked	32
1.2.4.1. Apoptosis	33
1.2.4.2. Interactions of Autophagy and Apoptosis	34

1.2.4.3.	Autophagic-Cell Death (ACD)	36
1.2.5.	Xenophagy: Autophagic Degradation of Microorganisms	37
1.2.6.	Mitophagy: Autophagic degradation of mitochondria	38
1.3.	Autophagy and Crohn's Disease	39
1.3.1.	<i>ATG16L1</i> variant linked to CD	39
1.3.2.	Implications of impaired NOD2-ATG16L1 interactions in CD pathogenesis	41
1.3.3.	<i>IRGM</i> variants and CD pathogenesis	42
1.3.4.	<i>LRRK2</i> variants and CD pathogenesis	42
1.3.5.	AIEC, CD and autophagy	43
1.3.6.	Autophagy control of cytokines in CD	44
1.3.7.	Autophagy involved in adaptive immune responses in CD	44
1.3.8.	Mitophagy and CD	46
1.4.	ER-stress and the Unfolded Protein Response	47
1.4.1.	ER stress and UPR linked to Intestinal Inflammation and IBD	50
1.4.2.	Autophagy and the UPR intersect: Implications in Crohn's disease	52
1.5.	Current IBD treatments and Autophagy	55
1.5.1.	Corticosteroids	59
1.5.2.	Aminosalicylates	63
1.5.3.	Thiopurines	64
1.5.4.	Immunomodulators: Methotrexate, Cyclosporin and Tacrolimus	69
1.5.5.	Biological agents: Anti-TNF- α	71
1.6.	Hypothesis and Aims	74
2.	MATERIALS AND METHODS	75
2.1	Cell culture	75
2.2	Cell treatments and Reagents	75
2.3	Transfection and plasmids	76
2.3.1	Plasmid propagation	76
2.4	Antibodies	77
2.5	Western immunoblotting	79
2.6	Immunofluorescence microscopy	80
2.6.1	Confocal Microscopy with fixed cells	80

2.6.2	Live-cell imaging	80
2.6.3	GFP-LC3 autophagy assay	81
2.6.4	TUNEL assay	81
2.7	Flow cytometry	81
2.7.1	CD14 flow cytometry	81
2.7.2	GFP-LC3 and endogenous LC3 flow cytometry	82
2.7.3	Annexin-V/PI assay	82
2.7.4	Cytospins	83
2.8	RT-qPCR	83
2.9	Bacterial infection assays	85
2.9.1	Bacterial strains, plasmids and transformation	85
2.9.2	Growth Curve	86
2.9.3	Infection model and analysis	87
2.10	AlamarBlue assay	88
2.11	IDEA study	90
2.11.1	Patients and sample collection	90
2.11.2	PBMC isolation and Flow cytometry	94
2.11.3	Genotyping	95
2.11.4	Immunohistochemistry	95
2.12	Statistical analysis	97

Results

3.	INVESTIGATING IBD DRUG MODULATION OF AUTOPHAGY	98
3.1	Introduction	98
3.2	Results	99
3.2.1	AlamarBlue® Cytotoxicity Assay to Identify Non-Toxic Concentration Range of IBD Drugs in HEK293 cells	99
3.2.2	Live-cell Imaging Time-Course to Identify IBD Drugs that Modulate Autophagy in HEK293 GFP-LC3 Cells	101
3.2.3	Fixed-Cell Confocal Microscopy to Monitor Autophagy Modulation by Azathioprine and Infliximab in HEK293 GFP-LC3 Cells	105
3.2.4	LC3 Western Immunoblot to Confirm Azathioprine-Induced Autophagy in HEK293 cells	107

3.2.5	LC3 Western Immunoblot to Monitor Autophagy in HEK293 Cells Treated with Infliximab	110
3.2.6	Flow Cytometry to Monitor Autophagy in HEK293 GFP-LC3 cells Treated with Azathioprine and Infliximab	110
3.2.7	HEK293 Cells Transiently Transfected with RFP-GFP-LC3 to Confirm Azathioprine-Induced Autophagy Flux	114
3.2.8	AlamarBlue® Cytotoxicity to Identify Non-Toxic Concentration Range of Azathioprine in THP-1-Derived Macrophages	117
3.2.9	LC3 Immunostain to Monitor Azathioprine-Induced Autophagy in THP-1-Derived Macrophages	118
3.2.10	THP-1-derived macrophages LC3 flow cytometry	121
3.3	Summary	123
4.	INVESTIGATING THE EFFECTS OF IBD DRUGS ON CELL DEATH	125
4.1	Introduction	125
4.2	Results	126
4.2.1	Cleaved-PARP Western Immunoblot to Monitor Apoptosis in HEK293 and SW480 Cells Treated with Azathioprine	126
4.2.2	TUNEL Assay to Monitor Apoptosis in HEK293 cells treated with Azathioprine	127
4.2.3	Annexin-V/PI Flow Cytometry to Monitor Apoptosis and Necrosis in HEK293 cells and THP-1-derived macrophages treated with Azathioprine	129
4.3	Summary	134
5	IBD DRUG MODULATION OF AUTOPHAGY AND UPR SIGNALLING PATHWAYS	136
5.1	Introduction	136
5.2	Results	136
5.2.1	Human Autophagy RT-PCR Array in THP-1-Derived Macrophages Treated with Azathioprine	136
5.2.2	CXCR4 Expression Altered by Azathioprine Treatment in THP-1-Derived Macrophages	141
5.2.3	Expression of Unfolded Protein Response Markers Altered by Azathioprine Treatment	141
5.2.4	Western Immunoblot for UPR markers in THP-1-Derived Macrophages Treated with Azathioprine	144
5.2.5	Western Immunoblot for rpS6 and Phosphorylated rpS6 to Monitor mTORC1 Activity in THP-1-Derived Macrophages	146
5.2.6	Azathioprine inhibits mTORC1 activity independent of PERK	149
5.2.7	Azathioprine-induced autophagy is dependent on PERK	151

5.3	Summary	153
6.	EFFECTS OF AZATHIOPRINE-INDUCED AUTOPHAGY ON CLEARANCE OF CD-ASSOCIATED ADHERENT INVASIVE <i>E. COLI</i>	154
6.1	Introduction	154
6.2	Results	154
6.2.1	AIEC infection of THP-1-derived macrophages	154
6.2.2	Azathioprine decreased intracellular AIEC survival as monitored by live-cell imaging	155
6.2.3	Azathioprine decreased intracellular AIEC survival as monitored by gentamicin protection assay with enumeration of CFU	157
6.2.4	Azathioprine increased autophagy induction in correlation with enhanced bacterial clearance	158
6.2.5	Azathioprine dampens pro-inflammatory cytokine responses to both AIEC infection and LPS	160
6.3	Summary	161
7.	THE IDEA STUDY - AZATHIOPRINE MODULATION OF AUTOPHAGY IN PAEDIATRIC IBD PATIENT SAMPLES	163
7.1	Introduction	163
7.2	Results	163
7.2.1	Paediatric patient genotype: <i>ATG16L1</i> and <i>NOD2</i> CD-associated variants	163
7.2.2	Comparison of autophagy levels in gastrointestinal biopsies from non-IBD and IBD paediatric patients	165
7.2.3	Effect of azathioprine on PBMC sub-populations	168
7.2.4	Effect of azathioprine on autophagy in PBMC sub-populations	171
7.2.5	<i>Ex vivo</i> azathioprine treatment preferentially increases autophagy in paediatric patient PBMC populations with <i>ATG16L1 T300A</i> SNP	171
7.3	Summary	173
8	DISCUSSION	175
8.1	Summary of results	175
8.2	The effect of anti-TNF-α agents on autophagy	175

8.3	The effect of corticosteroids, aminosalisylates and immunomodulators on autophagy	176
8.4	The effect of thiopurines on autophagy and apoptosis	177
8.5	Azathioprine mechanism of action in the context of autophagy	182
8.6	The effect of azathioprine-induced autophagy on clearance of AIEC	186
8.7	The IDEA study and clinical implications of azathioprine-induced autophagy	188
8.7.1	Autophagy levels in GI biopsies from paediatric patients	188
8.7.2	Effects of azathioprine on PBMC populations and autophagy in paediatric PBMCs	189
8.8	Clinical Implications of azathioprine-induced autophagy	194
8.9	On-going and Future research	196
8.10	Final Conclusions	199
9.	SUPPLEMENTARY RESULTS: OPTIMISATION OF TECHNIQUES TO MONITOR AUTOPHAGY	200
9.1	Introduction	200
9.2	Results	201
9.2.1	Optimisation of the autophagy response: Confocal imaging of HEK293 GFP-LC3 cells	201
9.2.2	Optimisation of the autophagy response: Western Immunoblot of LC3 in PC3 cells	209
9.2.3	Optimisation of the autophagy response: Western Immunoblot of LC3 in HEK293 cells	212
9.2.4	Differentiation of THP-1 monocytes into macrophage-like cells	216
9.2.5	Endogenous LC3 Immunostaining in THP-1-derived Macrophages	217
9.2.6	Endogenous LC3 Flow cytometry in THP-1-derived Macrophages	219
9.3	Summary	220
10.	SUPPLEMENTARY FIGURES	221
11.	REVIEW PAPER	228
12.	REFERENCES	238

List of Figures and Tables

Figures

1. Introduction

Figure 1.1: Intestinal Epithelial Barrier	20
Figure 1.2: Peripheral Blood Mononuclear Cell Haematopoiesis	22
Figure 1.3: Autophagy Pathway and Autophagosome Biogenesis	27
Figure 1.4: Autophagy Regulatory Pathways	30
Figure 1.5: Extrinsic and Intrinsic Apoptosis pathways.....	34
Figure 1.6: The Unfolded Protein Response	49
Figure 1.7: IBD Drug Modulation of Autophagy.....	59
Figure 1.8: Thiopurine Metabolism, Mechanism of Action and Modulation of Autophagy	68

2. Methods

Figure 2.1: Annexin-V/PI experimental staining controls and gating strategy	83
Figure 2.2: IPTG-inducible x-light mCherry plasmid	86
Figure 2.3: AIEC infection and treatment regime in THP-1-derived macrophages to assess intracellular survival	88
Figure 2.4: IDEA Study sample collection and analysis	91

3. Investigating IBD drug modulation of autophagy

Figure 3.1: AlamarBlue® Toxicity Time-course and Concentration Range Analysis with IBD Drugs in HEK293 Cells	100
Figure 3.2: Live-cell Imaging to monitor IBD drug modulation of Autophagy in HEK293 GFP-LC3 cells	104
Figure 3.3: Fixed-cell Confocal Microscopy to Monitor Autophagy in HEK293 GFP-LC3 Treated with Azathioprine and Infliximab	106

Figure 3.4: LC3 Western Immunoblot to Monitor Autophagy in HEK293 cells Azathioprine and Infliximab	109
Figure 3.5: Flow Cytometry to Monitor Autophagy in HEK293 GFP-LC3 Cells Treated with Azathioprine and Infliximab	113
Figure 3.6: HEK293 Cells Transiently Transfected with GFP-RFP-LC3 to Monitor Azathioprine-Induced Autophagy Flux using Confocal Microscopy	116
Figure 3.7: AlamarBlue Toxicity Time-course and Concentration Range Analysis in THP- 1-derived Macrophages Treated with Azathioprine	118
Figure 3.8: Azathioprine-Induced Autophagy in THP-1-derived Macrophages Monitored by LC3 Immunostaining.....	120
Figure 3.9: Endogenous LC3 Flow Cytometry to monitor Autophagy Induction in THP-1- derived Macrophages	122

4. Investigating the effects of IBD drug on cell death

Figure 4.1: Cleaved-PARP Western Immunoblot to Monitor Apoptosis in Cells Treated with Azathioprine	127
Figure 4.2: TUNEL Assay to Monitor Apoptosis in Cells Treated with Azathioprine	129
Figure 4.3: Annexin-V/PI Flow Cytometry to Monitor Apoptosis and Necrosis in HEK293 Cells Treated with Azathioprine	132
Figure 4.4: Annexin-V/PI Flow Cytometry to Monitor Apoptosis and Necrosis in THP-1- derived macrophages Treated with Azathioprine	134

5. IBD drug modulation of autophagy and UPR signalling pathways

Figure 5.1: RT ² Profiler™ PCR Array for Human Autophagy Genes for Analysis of Azathioprine-Induced Autophagy	138
Figure 5.2: RT-qPCR for Unfolded Protein Response Markers	143
Figure 5.3: Unfolded Protein Response Markers Protein Expression Modulated by Azathioprine	145
Figure 5.4: Western Immunoblot for rpS6 and Phospho-rpS6 to Monitor mTORC1 Activity Modulation by Azathioprine	148

Figure 5.5: Azathioprine-induced inhibition of mTORC1 is not PERK dependent	150
Figure 5.6: Azathioprine-induced autophagy is PERK dependent	152

6. Effects of azathioprine-induced autophagy on clearance of AIEC

Figure 6.1: AIEC growth curve when treated with Azathioprine	155
Figure 6.2: Azathioprine-induced clearance of mCherry AIEC monitored by live-cell imaging	157
Figure 6.3: Azathioprine-induced clearance of AIEC monitored by gentamicin protection assay with CFU enumeration	158
Figure 6.4: Azathioprine-induced clearance of mCherry AIEC and autophagy stimulation monitored by LC3 immunostaining.....	159
Figure 6.5: Azathioprine dampens AIEC- and LPS-induced pro-inflammatory cytokine expression	161

7. IDEA study - Azathioprine modulation of autophagy in paediatric samples

Figure 7.1: LC3 immunohistochemistry in paediatric patient GI biopsies.....	168
Figure 7.2: Paediatric patient PBMC populations	170
Figure 7.3: Paediatric patient LC3 flow cytometry	173

8. Discussion

Figure 8.1: Proposed mechanism of action of azathioprine in the context of autophagy	185
Figure 8.2 Summary of effect of azathioprine on autophagy activity in PBMC populations	194

Tables

1. Introduction

Table 1.1: PBMC population and their role in IBD	23
Table 1.2: IBD Drug Mechanism of Action	57
Table 1.3: IBD Drug Modulation of Autophagy	58

2. Methods

Table 2.1: Details of reagents used for cell treatments.....	76
Table 2.2: Details of antibodies.....	78
Table 2.3: Details of primers used for RT-qPCR.....	85
Table 2.4: IDEA study paediatric patient demographics.....	93

5. IBD drug modulation of autophagy and UPR signalling pathways

Table 5.1: Differentially Expressed Genes from RT ² Profiler™ PCR Array for Human Autophagy Genes	140
---	-----

7. IDEA study - Azathioprine modulation of autophagy in paediatric samples

Table 7.1: IDEA Study Paediatric Patient Genotypes.....	165
---	-----

Supplementary Results Chapter Figures

Supplementary Figure 9.1: Confocal Microscopy Imaging of HEK293 GFP-LC3 cells to Analyse Response to Autophagy Modulating Agents.....	206
Supplementary Figure 9.2: HEK293 GFP-LC3 Cells Treated with EBSS for Autophagy Induction via Nutrient Deprivation	208
Supplementary Figure 9.3: Optimisation of LC3 Western Immunoblot of LC3-I and LC3- II Positive Protein Lysates	211
Supplementary Figure 9.4: Comparison of LC3 Antibodies for Western immunoblot of HEK293 and HEK293 GFP-LC3 Cells Treated with Bafilomycin	214

Supplementary Figure 9.5: Comparison of Transfer Buffers for LC3 western Immunoblot of HEK293 cells.....	215
Supplementary Figure 9.6: THP-1 Cell Line Differentiated to Macrophage-Like Cells .	217
Supplementary Figure 9.7: Comparison of LC3 antibodies for immunostaining in THP-1- derived macrophages.....	218
Supplementary Figure 9.8: Optimisation of antibody concentration for endogenous LC3 Flow cytometry in THP-1-derived macrophages.....	219

Supplementary Figures

Supplementary Figure 10.1: Azathioprine-Induced Autophagy in THP-1-derived Macrophages Monitored by LC3 Immunostaining	221
Supplementary Figure 10.2: Cleaved-PARP Western Immunoblot to Monitor Apoptosis	222
Supplementary Figure 10.3: LC3 Immunostaining to Monitor Autophagy Activity for Human Autophagy Gene Array	223
Supplementary Figure 10.4: <i>CXCR4</i> Gene Expression Up-Regulated by Azathioprine in THP-1-Derived Macrophages	224
Supplementary Figure 10.5: Optimisation of Brefeldin A treatment as a positive control for BiP and PERK qPCR	225
Supplementary Figure 10.6: Optimisation of THP-1-derived macrophages infection with AIEC	226
Supplementary Figure 10.7: Live-cell confocal imaging of THP-1-derived macrophages infected with mCherry-AIEC.....	227

Declaration

The IDEA study was a collaborative project with supervisor Dr Paul Henderson, at the Royal Hospital for Sick children, who undertook all patient recruitment and collection of patient samples and demographics. Ms Suzie McGinley and Ms Sadie Kemp performed some experimental work included in the thesis, under the supervision of Ms Kirsty Hooper, as indicated in figure legends. The Centre for Comparative Pathology, University of Edinburgh, and the Genetics Core, Edinburgh Clinical Research Facility, provided vital technical services, as indicated in figure legends. All other work included in the thesis was performed by Ms Kirsty Hooper.

This PhD studentship was funded by Crohn's in Childhood Research Association (CICRA). The Research team also acknowledges the financial support of NHS Research Scotland (NRS), through Edinburgh Clinical Research Facility.

A journal article was published in the *Journal of Crohn's and Colitis* during this PhD studentship:

Hooper KM, Barlow PG, Stevens C, and Henderson P (2017). Inflammatory Bowel Disease Drugs: A Focus on Autophagy. *J Crohns Colitis*. **11(1)**:118-127.

A research article arising from data from this thesis has been submitted for publication:

Hooper KM, Casanova V, Kemp S, Staines KA, Satsangi J, Barlow PG, Henderson P and Stevens C (2018). Azathioprine modulates autophagy via mTORC1 and the unfolded protein response sensor PERK: implications for inflammatory bowel disease.



Kirsty Hooper

July 2018

Acknowledgments

Firstly, I would like to thank my Director of Studies, Dr Craig Stevens and the other members of the supervisory team, Dr Peter Barlow and Dr Paul Henderson, for sharing their expertise and providing guidance and support throughout the PhD. Also, the members of our lab group Dr Victor Casanova, Filipa Sousa, Olga Biskou, Beatriz Cotharz and Sophie Shepherd for their advice and encouragement, and most importantly making the PhD an enjoyable journey. Dr Katherine Staines and Dr Jack Satsangi also provided integral guidance and advice that aided the direction of the research. I would also like to thank Dr Clare Taylor for her support as Independent Panel Chair throughout my PhD.

I am extremely grateful for the support from all of the technical staff within the lab and the assistance in experimental procedures provided by Ms. Sadie Kemp and Ms. Suzie McGinley. The Centre for Comparative Pathology, University of Edinburgh, and Genetics Core, Edinburgh Clinical Research Facility, also provided vital technical services.

For the IDEA study I would like to thank all the patients and families that agreed to take part in the study. Also, Dr Paul Henderson for his support throughout the study and all other clinicians and staff at the Royal Hospital for Sick Children that were involved in the study. Importantly, I would like to acknowledge the financial support from CICRA for this PhD.

Finally, this would not have been possible without the love and support from my wonderful family and friends. Thank you for keeping my motivation and spirits high.

List of Abbreviations

3BDO	3-benzyl-5-((2-nitrophenoxy) methyl)-dihydrofuran-2(3H)-one
3-MA	3-methyladenine
4EBP1	EIF4E binding protein 1
5-ASA	5-Aminosalicylate
6-MMP	6-methylmercaptapurine
6-MP	6-mercaptapurine
6-thioGMP	6-thioguanosine monophosphate
6-thioGTP	6-thioguanosine triphosphate
6-TIMP	6-thioinosine monophosphate
6-TU	Thiouric acid
AARE	Amino Acid Response Element
ACD	Autophagic-Cell Death
AIEC	Adherent Invasive <i>Escherichia coli</i>
AIF	Apoptosis Inducing Factor
Akt	Protein kinase B
ALFY	Autophagy-linked FYVE protein
AMBRA1	Autophagy And Beclin 1 Regulator 1
AMP	Adenosine monophosphate
AMPK	AMP activated protein kinase
APAF1	Apoptotic Protease Activating Factor 1
APC	Antigen Presenting Cell
Ask1	Apoptosis signal-regulating kinase 1
ATF4	Activated Transcription Factor 4
ATF6	Activated Transcription Factor 6
ATG	Autophagy-related protein
ATG16L1	Autophagy-related protein 16L1
ATP	Adenosine triphosphate
BAD	Bcl-2-associated death promoter
BAK	Bcl-2 Antagonist or Killer
BAX	Bcl-2-Associated X protein

Bcl-2	B cell lymphoma 2
Bcl-xL	B-cell lymphoma-extra large
BCP	B cell progenitor
BH3	Bcl-2-Homology 3
BID	BH3-Interacting Domain Death Agonist
BIM	Bcl-2-Interacting Mediator of cell death
BiP	Binding Immunoglobulin Protein
Snip3	BCL2/adenovirus E1B 19 kDa protein-interacting protein 3
Breg	Regulatory B cell
Calcoco3	Calcium-binding and coiled-coil domain-containing protein 3
CAPS	3-Cyclohexylamino-1-propanesulfonic acid
CARE	C/EBP-ATF Response Element
CCL20	Chemokine (C-C motif) ligand 20
CCR9	C-C chemokine receptor type 9
CD	Crohn's disease
cDNA	Complementary DNA
c-di-AMP	Cyclic-di-AMP
CEACAM6	Carcinoembryonic antigen-related cell adhesion molecule 6
C/EBP	CCAAT/enhancer-binding protein
CFU	Colony forming units
CHOP	C/EBP Homologous Protein
CHOP-RE	CHOP-Response Element
CLEAR	Coordinated lysosomal expression and regulation
CLN3	Battenin
CLP	Common lymphoid progenitor
CMA	Chaperone-mediated autophagy
CMP	Common myeloid progenitor
CTSD	Cathespin D
CXCL	Chemokine (C-X-C motif) ligand
CXCR	C-X-C chemokine receptor type
DAMP	Damage Associated Molecular Pattern
DAPI	4',6-diamidino-2-phenylindole

DAPK	Death-Associated Protein Kinase
DC	Dendritic cell
DDIT4	DNA damage-induced transcript 4
DMEM	Dulbecco's modified Eagle medium
DMP	Differentially methylated position
DMSO	Dimethyl sulfoxide
dPBS	Distilled PBS
DRAM1	DNA damage-Regulated Autophagy Modulator 1
DSS	Dextran Sodium Sulphate
<i>E.</i>	<i>Escherichia</i>
E2F1	E2F Transcription Factor 1
EBSS	Earle's Balanced Salt Solution
ECM	Extracellular Matrix
EDTA	Ethylenediaminetetra acetic acid
ER	Endoplasmic Reticulum
ERAD	ER-associated protein degradation
ERK	Extracellular signal-regulated kinases
EIF2 α	Elongation Initiation Factor 2 α
EIF2AK3	Eukaryotic Translation Initiation Factor 2 Alpha Kinase 3
EIF4E	Eukaryotic initiation factor 4E
EIF4G1	Eukaryotic Translation Initiation Factor 4 Gamma 1
<i>F.</i>	<i>Faecalibacterium</i>
FADD	FAS-Associated Death Domain
fALS	familial Amyotrophic Lateral Sclerosis
FBS	Foetal Bovine Serum
FKBP12	FK506 binding protein 12
FKBP51	FK506-binding protein 51
FIP200	FAK family kinase interacting protein of 200 kDa
FITC	Fluorescein isothiocyanate
FMO	Fluorescence Minus One Control
FOXO	Forkhead box protein O
FSC	Forward scatter

G908R	p.Gly908Arg
GAA	Glucosidase α
GABARAP	Gamma-aminobutyric acid receptor-associated protein
GATA1	GATA-binding factor 1
GCN2	General Control Nonderepressible 2
GFP	Green Fluorescent Protein
GI	Gastrointestinal
GM	Granulocyte-macrophage progenitor
GMPS	Guanosine monophosphate synthetase
GP	Granulocyte progenitor
GRP78	Glucose Regulated Protein 78
GSH	Glutathione
GST	Glutathione S-transferase
GTP	Guanosine triphosphate
GWAS	Genome-wide association study
HCEC	Human colon epithelial cells
HDAC6	Histone Deacetylase 6
HEK293	Human Embryonic Kidney cells 293
HGS	Hepatocyte growth factor
HLA-DR	Human Leukocyte Antigen – antigen D Related
HMGB1	High mobility group box chromosomal protein 1
HPRT	Hypoxanthine-guanine phosphoribosyl transferase
HtrA	High-temperature requirement A
HTS	High Throughput System
HTT	Huntingtin
IBD	Inflammatory Bowel Disease
IBDU	Inflammatory Bowel Disease Unclassified
IGF1	Insulin-like growth factor 1
IHC	Immunohistochemistry
IHH	Immortalized human hepatic
IMPDH	Inosine monophosphate dehydrogenase
IRE1	Inositol-Requiring transmembrane kinase Endonuclease 1

IDEA	IBD Drug Effect on Autophagy
IEC	Intestinal Epithelial Cell
IFN- γ	Interferon gamma
Ig	Immunoglobulin
IL	Interleukin
IPTG	Isopropyl β -D-1-thiogalactopyranosid
IRGM	Immunity-related GTPase family M protein
ISC	Intestinal Stem Cell
JNK	c-Jun N-terminal kinase
L1007fs	p.Leu1007fsX1008
LB	Luria-Bertani
LC3B	Microtubule-associated proteins 1A/1B light chain 3B
LKB1	Liver Kinase B1
LMP	Lysosomal Membrane Permeabilisation
LPS	Lipopolysaccharide
LRRK2	Leucine rich repeat kinase 2
M Φ 1	IFN- γ induced macrophages
M Φ 2	IL-4-induced macrophages
M Φ ind	Anti-TNF-induced macrophages
MAMP	Microbial associated molecular pattern
MAP	<i>Mycobacterium avium</i> subspecies <i>paratuberculosis</i>
MAPK	Mitogen-activated protein kinases
Mbtps1	Membrane-bound transcription factor peptidase S1P-encoding gene
MCL1	Myeloid cell leukaemia sequence 1
MDP	Muramyldipeptide
MEC	Mammary Epithelial Cells
MHC	Major histocompatibility complex
MIF	Macrophage migration inhibitory factor
MIR	miRNA
miRNA	microRNA
MMR	Mismatch repair
MOI	Multiplicity of Infection

MOMP	Mitochondrial Outer Membrane Permeabilisation
MP	Monocyte-DC progenitor
mRNA	Messenger RNA
mtDNA	Mitochondrial DNA
mTORC1	Mechanistic Target of Rapamycin Complex 1
MUC2	Mucin 2
Nbr1	Neighbour of Brca1 Gene 1
NDP52	Nuclear Domain 10 Protein 52
NFAT1	Nuclear factor of activated T cells
NF- κ B	Nuclear factor kappa-light-chain-enhancer of activated B cells
NHS	National Health Service
NIX	NIP3-like protein X
NK	Natural killer
NKP	NK cell Progenitor
NIpl	New lipoprotein I
NLR	Nod-like receptor
NOD2	Nucleotide-binding oligomerisation domain-containing protein 2
NR1D1	Nuclear Receptor Subfamily 1 Group D Member 1
OA-FLS	Osteoarthritis fibroblast-like synovial
OMV	Outer membrane vesicle
OSCC	Oral squamous cell carcinoma
PAMP	Pathogen Associated Molecular Pattern
PARK2	Parkinson Juvenile Disease Protein 2
PBMC	Peripheral blood mononuclear cell
PBS	Phosphate Buffered Saline
PBST	PBS + 0.1% Tween 20
PDI	Protein disulphide isomerase
PE	Phosphatidylethanolamine
PERK	Protein Kinase RNA-like Endoplasmic Reticulum Kinase
PFA	Paraformaldehyde
PHB	Prohibitin 1
PI	Propidium Iodide

PI3K	Phosphatidylinositide 3-kinases
PI3P	Phosphatidyl inositol triphosphate
PINK1	PTEN-induced putative kinase protein 1
PKA	Protein Kinase A
PKD	Protein Kinase D
PMA	Phorbol myristate acetate
PML	Promyelocytic leukaemia
PRAS40	Proline-rich Akt substrate of 40 kDa
PRR	Pattern recognition receptor
PT	Permeability transition
PUMA	p53 Upregulated Modulator of Apoptosis
PVDF	Polyvinylidene difluoride
PTP	Permeability Transitions Pores
R702W	p.Arg702Trp
RAC1	Ras-related C3 botulinum toxin substrate 1
RAPTOR	Regulatory-associated protein of mTOR
RAW	Ralph and William's cell line
Rb	Rabbit
RBC	Red Blood Cell
REC	Research Ethics Committee
RFP	Red Fluorescent Protein
RGS19	Regulator Of G Protein Signaling 19
Rheb	RAS homologue enriched in brain
RIDD	Regulates IRE1-dependent decay
RIPK-2	Receptor-interacting serine-threonine kinase 2
ROS	Reactive oxygen species
RPM	Revolutions per minute
RPMI	Roswell Park Memorial Institute
(p-)rpS6	(Phosphorylated) S6 ribosomal protein
RT	Room temperature
RT-qPCR	Quantitative reverse transcription PCR
S1P	Site 1 Protease

S2P	Site 2 Protease
S6K	S6 ribosomal protein kinase
SASP	Salicylazosulfapyridine
SCC	Squamous cell carcinoma
SDS-PAGE	Sodium dodecyl sulfate-polyacrylamide gel electrophoresis
SE	Standard Error
siRNA	Small interfering RNA
SLR	Sequestosome 1/p62-like receptors
SMURF1	SMAD specific E3 ubiquitin protein ligase 1
SNP	Single nucleotide polymorphism
SOD1	Superoxide dismutase-1
SSC	Side scatter
ssDNA	Single stranded DNA
STING	Stimulator of interferon genes
Syk	Spleen tyrosine kinase
T300A	Threonine to alanine at position 300
T3SS	Type 3 secretion system
TCA	Tricarboxylic acid
TCP	T cell Progenitor
TdT	Terminal deoxynucleotidyl transferase
TE	Tris-EDTA
TFEB	Transcription factor EB
TGF	Transforming growth factor
TGM2	Transglutaminase 2
TLR	Toll-like receptor
TMEM	Transmembrane protein
TNF	Tumour Necrosis Factor
TNFR1	TNF-Receptor 1
TNP	T cell and NK cell progenitor
TPMT	Thiopurine methyltransferase
TRADD	TNFR1-Associated Death Domain
TRAF2	TNF receptor-associated factor 2

TRAILR	TNF-Related Apoptosis-Inducing Ligand Receptor
Treg	Regulatory T cell
TSC	Tuberous Sclerosis Complex
TUNEL	TdT dUTP Nick-End Labeling
UA	Ursolic acid
UC	Ulcerative colitis
ULK	UNC51 like Ser/Thr kinases
UPR	Unfolded Protein Response
UVEC	Umbilical vein endothelial cells
UVRAG	UV-irradiation resistance-associated gene
VMP1	Vacuole membrane protein 1
Vps	Vacuolar protein sorting
XBP1	X-box binding protein 1
XOD	Xanthine Oxidase
ZFPM1	Zinc Finger Protein, FOG Family Member 1
ZKSCAN3	Zinc Finger With KRAB And SCAN Domains 3

1. Introduction

1.1 Inflammatory Bowel Disease

Inflammatory Bowel Disease (IBD) is characterised by chronic inflammation of the gastrointestinal (GI) tract and encompasses Crohn's disease (CD), ulcerative colitis (UC) and colonic IBD, type unclassified (IBDU). The incidence rate for IBD is approximately 50-200 per 100,000 persons per year in Western countries (Gasparetto and Guariso, 2013) and prevalence exceeds 0.3% in North America, Oceania and many counties in Europe (Ng et al., 2017). In the UK, a recent National Health Service (NHS) review revealed a prevalence of up to 400 in 100,000 persons (NHS, 2013). Furthermore, in newly industrialised countries in Africa, Asia and South America, the incidence of IBD has been steadily rising since 1990 (Ng et al., 2017). The survival rate for CD is 93.7% at 15 years, but morbidity is a major issue and CD patients have 4-20 times more risk of developing colon cancer compared to the general public (Diefenbach and Breuer, 2006). Several reports have shown that mortality is not affected by UC; however, a recent study of a large Danish cohort over a 30 year time-period revealed that UC patients have 10% increased risk of mortality, while CD patients have a 50% increased risk (Kassam et al., 2014). UC patients have a more pronounced risk of colon cancer compared to CD patients with an annual incidence of 1% in patients diagnosed for more than 10 years (Diefenbach and Breuer, 2006).

CD is distinguished from the other main IBD subtype, UC, due to the presence of submucosal or transmural inflammation and ulcers that occur in patches at any location along the digestive tract (Gasparetto and Guariso, 2013). UC is localised to the colon and inflammation is limited to the mucosa and epithelial lining of the GI tract (Fakhoury et al., 2014). Patients can also be diagnosed with IBDU, when a conclusive distinction between CD and UC cannot be made.

The clinical presentation of IBD occurs as periods of relapse and remission and commonly includes abdominal pain, chronic diarrhoea, weight loss, lethargy, fever, nausea, vomiting and extraintestinal manifestations such as arthritis (Fakhoury et al., 2014). Diagnosis is usually established from endoscopic, histological and radiological findings (Fernandes et al., 2016). At present there is no cure for IBD, and medications such as corticosteroids, aminosalicylates, thiopurines, immunomodulators and

biological agents are aimed at inducing and maintaining remission of disease by modifying inflammatory processes (Neurath, 2017). A recent review estimated IBD treatment costs of £720 million per year (NHS, 2013), with roughly a quarter of these costs directly attributed to drug treatments (Bassi et al., 2004).

1.1.1. Paediatric IBD

Paediatric IBD is the diagnosis of the disease before the age of 17, with early-onset IBD being diagnosed before the age of 10 and very early onset IBD in children younger than 6 years old (Ashton et al., 2017). The occurrence of complications leading to surgery is more common in paediatric patients and other issues such as growth impairment and psychological stress are also factors involved with childhood CD (Diefenbach and Breuer, 2006). The Paris classification was adapted from Montreal classification for the phenotypic assessment of paediatric IBD, with the main distinction between these systems being the consideration of age and growth failure (Levine et al., 2011). It has been estimated that 25-30% of CD patients are <20 years of age (Diefenbach and Breuer, 2006) and the incidence of paediatric IBD is rising worldwide. One study investigating Scotland-wide trends showed a 76% increase in paediatric IBD diagnosis from 4.75/100,000/year between 1990-1995 to 7.82/100,000/year between 2003-2008 (Henderson et al., 2012). This study also found that the mean age of diagnosis decreased from 12.7 years to 11.9 years. Furthermore, in Canada, early-onset IBD incidence has risen by 7.4% per year between 1994-2009 (Benchimol et al., 2014).

Paediatric IBD more often involves genetic susceptibility and is often associated with rapid progression and a more severe outcome (Marcuzzi et al., 2013). More than 200 genes have been associated with early-onset IBD (Ashton et al., 2017) and rare monogenic disorders are more common, especially in very-early onset IBD (Uhlir et al., 2014). Furthermore, exclusive enteral nutrition, which is a treatment involving a controlled diet of basic nutrients, is very effective in paediatric IBD, suggesting an important role for diet and gut microbiota in early-onset IBD (Heuschkel, 2009; Kaakoush et al., 2015). Due to the distinct characteristics of childhood IBD, the continuation of studies solely focusing on paediatric cases is imperative for improvements in understanding and treatment of the disease.

1.1.2. Aetiology of Crohn's Disease

The aetiopathogenesis of IBD is multifactorial in nature, with genetic predisposition, environmental triggers and a dysregulated immune response to intestinal microflora all contributing (Boyapati et al., 2015). The environmental risk factors include smoking, appendectomy, diet, pollution, antibiotics and stress (Gasparetto and Guariso, 2013).

1.1.2.1. CD-associated NOD2 variants

Nucleotide-binding oligomerisation domain-containing protein 2 (NOD2) was the first gene to be linked to CD susceptibility in 2001 (Hampe et al., 2001; Hugot et al., 2001; Ogura et al., 2001a). NOD2 is a member of the Nod-like receptor (NLRs) family of pattern recognition receptor (PRR). NOD2 is located in the cytosol and plasma membrane of white blood cells and intestinal epithelial cells and recognises the bacterial wall component muramyl dipeptide (MDP) to induce innate immune responses (Marcuzzi et al., 2013). Membrane recruitment of NOD2 is essential for responses to MDP (Barnich et al., 2005). Upon activation, NOD2 recruits receptor-interacting serine-threonine kinase 2 (RIPK-2), which leads to the activation of NF- κ B (nuclear factor kappa-light-chain-enhancer of activated B cells) and MAPK (mitogen-activated protein kinases)/ERK (extracellular signal-regulated kinases) pathways (Homer et al., 2010; Ogura et al., 2001b). This induces the release of cytokines and chemokines for immune cell recruitment and the release of host defence peptides (Marcuzzi *et al.*, 2013). Therefore, NOD2 and the subsequent signalling pathways play a key role in the innate immune system and regulating inflammatory responses.

The CD-associated *NOD2* variants, which are found in roughly one third of Crohn's patients (Niess et al., 2012), disrupt binding to MDP and normal immune responses initiated by this receptor (Hugot et al., 2001). The NOD2 variant can also have "gain-of-function" actions by actively suppressing the transcription of anti-inflammatory cytokine, interleukin (IL)-10 (Muzes *et al.*, 2013). Three CD-associated *NOD2* variants exist, two of which contain a single-nucleotide polymorphism (SNP) (*p.Arg702Trp (R702W)* and *p.Gly908Arg (G908R)*) and the last is a frame-shift mutation (*p.Leu1007fsX1008 (L1007fs)*) (Hampe et al., 2001; Hugot et al., 2001; Ogura et al., 2001a). Heterozygosity for the *NOD2* variant can increase the risk of CD from 1.5 to 4.5-

fold, whereas the presence of homozygous variant alleles increases the risk to between 20- to 40-fold (Ahmad et al., 2002; Brant et al., 2003; Lesage et al., 2002). The *NOD2 L1007fs* variant has also been associated with increased risk of early-onset CD (Pranculiené et al., 2016).

1.1.2.2. Genome Wide Association Studies

A genome-wide association study (GWAS) compares allele frequency of thousands of SNPs between cases and controls, to identify SNPs that are associated with disease susceptibility. Several GWAS's and meta-analyses have been undertaken for IBD, and have identified SNPs in three distinct categories, including autophagy, the IL-23/IL-17 axis and failure to suppress aberrant immune responses (Verstockt et al., 2018). A meta-analysis of 15 international GWAS's identified 163 IBD susceptibility loci; of which 110 were shared between CD and UC, 30 were specific to CD and 23 were specific to UC (Jostins et al., 2012). A more recent GWAS has increased the number of IBD susceptibility loci to 241, with most of the loci inferring susceptibility for both CD and UC (Lange et al., 2017) and another study has found four genome-wide significant loci associated with IBD prognosis (Lee et al., 2017).

In 2007, GWAS confirmed the previously recognised association with *NOD2*, but also identified *autophagy-related protein 16L1 (ATG16L1)*, associated specifically with CD (Hampe et al., 2007; Rioux et al., 2007). The CD-associated *ATG16L1* SNP (rs2241880) causes a single amino acid change from threonine to alanine at position 300 (*T300A*) (Hampe et al., 2007), and is present in up to 30% of CD patients (Hampe et al., 2007; Rioux et al., 2007). Heterozygous presentation of the *ATG16L1 T300A* allele increases risk of CD by 1.4-fold, whereas homozygous *T300A* genotype increases risk of CD by 1.9-fold (Zhang et al., 2009). In paediatric CD patients, homozygous *ATG16L1 T300A* alleles increased risk of disease by 3-fold (Amre et al., 2009). *ATG16L1 T300A* has also been associated with increased risk of complicated fistulating disease (Salem et al., 2015). Additionally, the autophagy genes *Immunity-related GTPase family M protein (IRGM)* and *leucine rich repeat kinase 2 (LRRK2)* have been associated with CD susceptibility (Barrett et al., 2008; Franke et al., 2010; Parkes et al., 2007), with *IRGM* risk variant also being identified in a cohort of early-onset CD (Pranculiené et al., 2016). These genetic studies have led to an increase in research linking autophagy dysregulation to CD pathogenesis.

Genetic studies have also identified association with endoplasmic reticulum (ER) stress/Unfolded Protein Response (UPR) genes in IBD. Genetic association with the transcription factor *x-box-binding protein 1 (XBP1)*, a key component of the UPR, was identified with both CD and UC (Kaser et al., 2008). Furthermore, *Anterior gradient 2 (AGR2)*, which is a member of the ER protein disulphide isomerase (PDI) family, has been associated with IBD (Zheng et al., 2006).

Interestingly, recent advances have been made in investigating the epigenome in IBD. An integrative epigenome-wide analysis identified 439 differentially methylated positions (DMPs) and 5 differentially methylated regions (DMRs) in IBD, which related to underlying genotype and revealed differing gene expression profiles in specific cell types (Ventham et al., 2016).

1.1.2. Intestinal Microbiota, Microbial Dysbiosis and CD-associated pathogens

The intestinal microbiota is integral to GI homeostasis. Commensal and symbiotic bacteria provide protection against pathogens, possess anti-inflammatory properties and are also involved in immune system maturation, within the intestine and systemically (Elson and Cong, 2012). Commensal bacteria competitively colonise the GI tract to prevent pathogen expansion in a process known as colonisation resistance (Buffie and Pamer, 2013), and can also produce metabolites that are toxic to certain pathogens (Kamada et al., 2012).

In IBD, dysregulated immune responses can be in response to commensal microflora or specific microorganisms that are associated with IBD. However, it is unclear whether alterations in intestinal microbiota contribute to the cause, or the effect, of IBD. Nevertheless, there is an increased abundance of mucosa-associated bacteria (Png et al., 2010; Schultsz et al., 1999), with the largest population of bacteria found in terminal ileum and colon (Carrière et al., 2014), which is the most common location for lesions in CD (Dorn et al., 2004). Microbial dysbiosis (altered microbiota composition) is also associated with IBD (Fujimoto et al., 2013; Nishino et al., 2018; Takahashi et al., 2016). Microbial dysbiosis in IBD is characterised by reduced microbial diversity (Walker et al., 2011) or a decrease in commensal bacteria, such as *Faecalibacterium (F.) prausnitzii*,

Blautia faecis, *Roseburia inulinivorans*, *Ruminococcus torques*, and *Clostridium lavalense* (Fujimoto et al., 2013; Takahashi et al., 2016). This causes increased susceptibility to pathogens, such as *Bacteroidetes* and *Proteobacteria* (Frank et al., 2007). Furthermore, the commensal bacteria decreased in IBD patients can have anti-inflammatory properties (Frank et al., 2007). For instance, *F. prausnitzii* can enhance production of anti-inflammatory cytokine IL-10 and reduce pro-inflammatory cytokines IL-12 and interferon gamma (IFN- γ) (Sokol et al., 2008). Decreases in *F. prausnitzii* are associated with CD recurrence after surgery (Walker et al., 2011).

IBD pathogenesis cannot be attributed to one specific bacterial species, as one strain that may be detrimental to one host genotype could be beneficial to another (Elson and Cong, 2012). A recent study has identified a microbial signature for CD, with eight microbial groups specifically altered in CD (Pascal et al., 2017). This microbial signature was used with high sensitivity and specificity for the detection of CD patients versus healthy controls and UC patients, meaning it can potentially be used as a microbiomarker. However, some specific bacterial strains have been associated with the disease including *Mycobacterium avium* subspecies *paratuberculosis* (MAP), *Yersinia*, *Listeria* and *Helicobacter* (Carrière et al., 2014).

The role of *Escherichia (E.) coli* in CD aetiopathogenesis has been extensively explored. A specific pathovar has been described in CD known as Adherent Invasive *E. coli* (AIEC). AIEC are highly prevalent in the ileal mucosa of CD patients (Boudeau et al., 1999; Darfeuille-Michaud et al., 2004, 1999; Frank et al., 2011; Martin et al., 2004; Thomazini et al., 2011) and have an increased ability to adhere and invade intestinal epithelial cells (IECs) (Boudeau et al., 2001, 1999; Martin et al., 2004). AIEC isolated from CD patients have been shown to induce IL-8 and Chemokine (C-C motif) ligand 20 (CCL20) secretion in IEC cell lines and promote Dendritic cell (DC) migration (Eaves-Pyles et al., 2008). Furthermore, AIEC strains are able to survive and replicate in human macrophages (Bringer et al., 2006, 2005; Cieza et al., 2015; Lapaquette et al., 2012; P. Lapaquette et al., 2010; Negroni et al., 2016; Sadabad et al., 2015; Vazeille et al., 2015), causing prolonged inflammatory responses involving the release of Tumour Necrosis Factor (TNF)- α (Bringer et al., 2012; Glasser et al., 2001). The bacteria reside in low pH phagolysosomal compartments within macrophages (Bringer et al., 2006) and the increased levels of TNF- α in turn enhances intracellular replication of AIEC (Bringer et

al., 2012). AIEC persistence within intestinal macrophages and prolonged pro-inflammatory signalling causes continued recruitment of immune cells, ultimately resulting in granuloma formation, which is a distinctive feature of CD (Meconi et al., 2007). Accordingly, *E. coli* DNA has been detected in 80% of CD granulomas (Ryan et al., 2004).

Identifying key virulence factors of AIEC has allowed for further understanding of its aetiopathogenesis in CD. Some of these adaptations allow AIEC to subvert host immune defences such as autophagy. The type 1 pili system facilitates AIEC adhesion by binding carcinoembryonic antigen-related cell adhesion molecule 6 (CEACAM6) on eukaryotic cells, which is also vital for perturbation of host defences to allow AIEC invasion (Boudeau et al., 2001; Dreux et al., 2013). Interestingly, ileal expression of CEACAM6 is increased in CD and *CEACAM6* variants have been identified in IBD patients (Glas et al., 2011). Additionally, the *ibeA* virulence gene was identified as a key component for AIEC invasion into IECs, survival in macrophages and inflammatory responses in murine intestine (Cieza et al., 2015). The *high-temperature requirement A (HtrA)* gene encoding stress protein HtrA is also essential for replication in macrophages as it enables AIEC survival in low-pH vacuoles of phagocytic cells (Bringer et al., 2005). Furthermore, lipoprotein, Nlpl (new lipoprotein I), Flagella protein, YfgL, and outer membrane vesicles (OMVs), including OmpC and OmpA, are vital for AIEC adhesion and invasion capacities (Barnich et al., 2004, 2003; Rolhion et al., 2007, 2005). Analysis of *E. coli* isolates from paediatric CD patients compared to non-IBD patients revealed a higher abundance of AIEC and an increased incidence of genes encoding virulence factors K1, *fyuA* and *ibeA* in AIEC isolated from CD patients (Conte et al., 2014).

1.1.3. Intestinal Epithelial Barrier in CD

The epithelial barrier of the GI tract is composed of a number of different IECs organised into crypts and villi (Figure 1.1). The primary purpose of the intestinal epithelial barrier is to segregate the microbiota in the lumen from the host immune cells in the lamina propria, thus preventing unnecessary inflammatory responses. To reinforce barrier integrity, multi-protein complexes, including tight junctions, adheren junctions and desmosomes, form between IECs to prevent paracellular permeability (Dupaul-Chicoine et al., 2013). Pro-inflammatory cytokines that are often overexpressed in IBD, such as

TNF- α and IFN- γ , can disrupt tight junctions and induce IEC apoptosis, causing epithelial barrier permeability (Marini et al., 2003). Increased intestinal permeability is a prominent feature of active CD that is reduced during remission phases (Benjamin et al., 2008).

At the bottom of crypts, pluripotent progenitor cells proliferate and differentiate into distinct intestinal epithelial cell types including goblet cells, Paneth cells, absorptive cells, enteroendocrine cells, M cells, cup cells and Tuft cells (Figure 1.1) (Coskun, 2014). These cell types play very distinct roles in intestinal homeostasis and constant renewal of these cells, through stem cell differentiation, is key to maintain this. In IBD, genes to enable effective differentiation of these cells are aberrantly expressed (Ahn et al., 2008; Coskun et al., 2012; Zheng et al., 2011).

Goblet cells generate mucous and highly glycosylated mucin proteins that form a tight layer to prevent bacterial cell adhesion to the intestinal epithelium. The *Muc2* gene encodes the main mucin protein produced by goblet cells. In *Muc2*-deficient mice, there is diminished mucosal layer formation and elevated pro-inflammatory cytokine production, which culminate in spontaneous colitis (Sluis et al., 2006). Furthermore, in IBD, genetic risk loci in *Muc1* and *Muc19* have been identified (Franke et al., 2010; Jostins et al., 2012). Moreover, in CD patients, goblet cell depletion can occur, which depletes mucus layer protection against bacterial adhesion (Elson and Cong, 2012).

Paneth cells are found in the base of crypts of the small intestine and function to release host defence peptides, including defensins, into the mucous layer (Figure 1.1) (Henderson et al., 2011). This controls microbiota growth and prevents interaction of microbes with IECs (Coskun, 2014). *NOD2* is highly expressed in Paneth cells (Ogura et al., 2003), and *NOD2* variants cause abnormal Paneth cell functions (Wehkamp et al., 2004). This includes decreased NF- κ B signalling (Bonen et al., 2003) and diminished granule exocytosis of α -defensins, which is a key factor in CD pathogenesis (Wehkamp et al., 2004). Furthermore, *NOD2* knock-out (k/o) mice were more susceptible to infection and death caused by *Listeria monocytogenes*, due to decreased α -defensin production (Kobayashi, 2005). Therefore, the formation of a protective mucous layer containing host defence peptides is vital for intestinal homeostasis, and dysregulation of this protective feature is a key factor of CD pathogenesis.

If pathogens are able to interact with the epithelial barrier, IECs are capable of eliciting innate immune responses, due to their expression of PRRs, NLRs and toll-like receptors (TLRs) (Dupaul-Chicoine et al., 2013). NLRs and TLRs, can mount a strong innate immune response when in contact with Pathogen Associated Molecular Patterns (PAMPs). This response involves inflammatory signalling to promote host defence peptide production and maturation of antigen-presentation cells, ultimately to resolve infection (Henderson et al., 2011). To prevent excessive immune activation, TLRs are primarily expressed at basolateral sides of IECs at the base of crypts and are specifically upregulated during inflammation (Cario and Podolsky, 2000; Gewirtz et al., 2001).

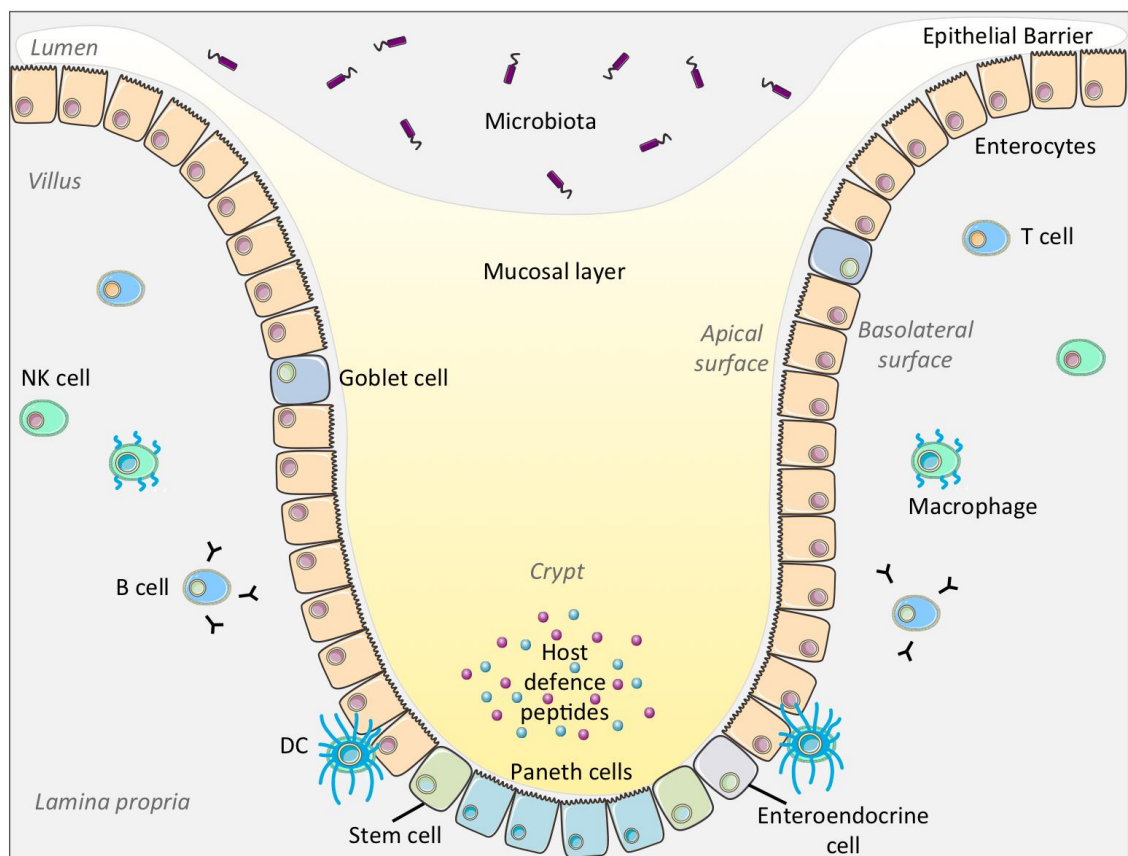


Figure 1.1: Intestinal Epithelial Barrier

The epithelial barrier is structured into crypts and villi and separates microbiota in the lumen from the lamina propria. The epithelial barrier is composed of intestinal epithelial cells: enterocytes, Paneth cells, goblet cells, enteroendocrine cells and intestinal stem cells. Goblet cells secrete mucous to form the mucosal layer and Paneth cells release host defence peptides into the mucosal layer. Immune cells including T cells, B cells, natural killer (NK) cells, macrophages and dendritic cells (DCs) reside within the lamina propria.

1.1.4. Intestinal and Systemic Immune cells in CD

Intestinal immune cells in the lamina propria provide vital protection from pathogens that have crossed the epithelial barrier. The adaptive immune cells, T and B cells, in the lamina propria represent the majority of lymphoid cells in the body (Figure 1.1) (Elson and Alexander, 2015). Furthermore, there is an abundance of innate immune cells including macrophages and dendritic cells (Figure 1.1).

1.1.4.1. *Haematopoiesis and Immune cell subsets*

Haematopoiesis and differentiation of peripheral blood mononuclear cells (PBMCs), as described by Rieger and Schroeder (2012), is shown in Figure 1.2. Common myeloid progenitor (CMP) cells and common lymphoid progenitor (CLP) cells are derived from multi-potent stem cells. From CLP cells arise T cells, NK cells and B cells that differentiate from their respective progenitors, and plasmacytoid DCs. From CMP cells, granulocyte progenitors (GP) produce basophils, neutrophils and eosinophils, and monocyte-DC progenitors (MP) differentiate to monocytes or myeloid DCs. Monocytes differentiate into macrophages within tissue (Furth and Cohn, 1968) and can differentiate into myeloid DCs while in circulation (Romani et al., 1994).

Monocyte sub-sets are categorised by their expression of the surface markers CD14 and CD16, and nomenclature used is described in Ziegler-Heitbrock et al., (2010), as shown in Table 1.1. Classical monocytes express high levels of CD14 and do not express CD16, so are referred to as CD14⁺⁺CD16⁻ or CD14^{high}CD16⁻. Monocytes that express high levels of CD14 but also express CD16, CD14⁺⁺CD16⁺ or CD14^{high}CD16⁺, are known as intermediate monocytes. Finally, low expression of CD14 and the presence of CD16 denotes non-classical monocytes, which is referred to as either CD14⁺CD16⁺⁺ or CD14^{low}CD16⁺⁺. Classical monocytes are professional phagocytes with an anti-inflammatory phenotype, whereas intermediate monocytes are extremely inflammatory and expand in a wide range of inflammatory diseases. Non-classical monocytes patrol vessel walls and are generally considered anti-inflammatory; however, they can mount highly pro-inflammatory responses (Cros et al., 2010).

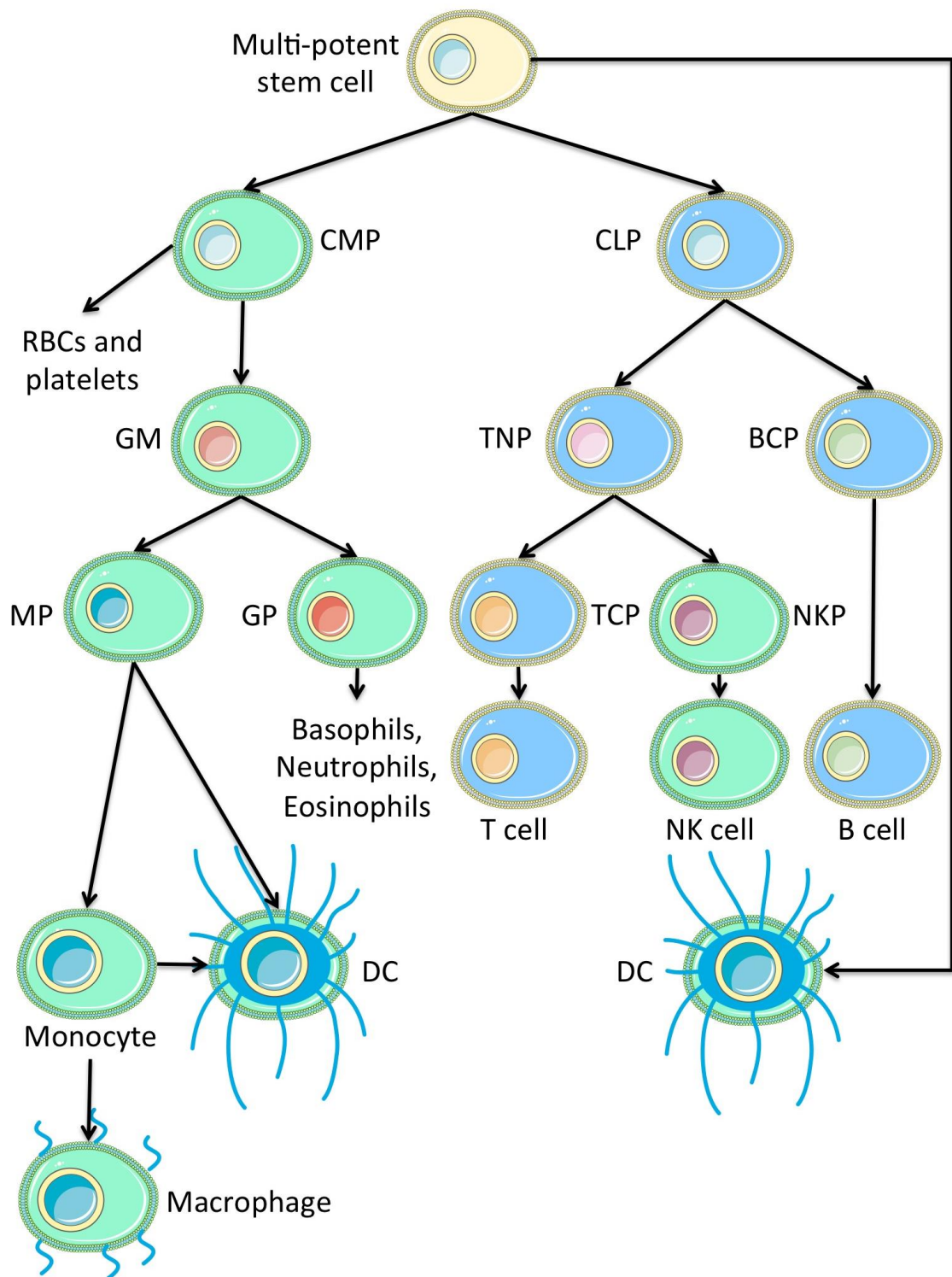


Figure 1.2: Peripheral Blood Mononuclear Cell Haematopoiesis

CMP Common Myeloid Progenitor, *CLP* Common Lymphoid Progenitor, *RBC* Red Blood Cell, *GM* Granulocyte-macrophage Progenitor, *TNP* T cell NK cell Progenitor, *BCP* B cell Progenitor, *MP* Monocyte-DC Progenitor, *GP* Granulocyte Progenitor, *TCP* T cell Progenitor, *NKP* NK cell Progenitor, *DC* Dendritic cell.

Table 1.1: PBMC population and their role in IBD

PBMC populations and monocyte subsets are shown, with basic immune function. Aberrant functions of PBMC populations has been linked to IBD pathogenesis (Erokhina et al., 2018¹; Grip et al., 2007²; Janssen et al., 2012³; Koch S. et al., 2010⁴; Nedjic et al., 2008⁵; Ng et al., 2009⁶; Oka et al., 2014⁷; Olson et al., 2004⁸; Shale et al., 2013⁹; Steel et al., 2010¹⁰; Timmermans et al., 2016¹¹)

Subsets	Surface markers	Normal Function	Link to IBD
T cells	CD3+	Adaptive	<ul style="list-style-type: none"> Imbalance between effector and regulatory T cells⁹ Lack of immune tolerance⁵
NK cells	CD56+	Innate	Expanded HLA-DR+ and CD16+ NK cells ^{6,10} ; produce high levels of IFN- γ to increase T cell activation ¹
B cells	CD19+	Adaptive (humoral)	<p>Pathogenic:</p> <ul style="list-style-type: none"> High levels of auto-reactive and anti-microbial antibodies¹¹ Granuloma formation³ Suppress Tregs⁸ <p>Regulatory:</p> <ul style="list-style-type: none"> Decreased IL-10 producing Bregs that control monocytes and T cells⁷
Monocytes	CD14+	Innate	Expanded in CD ^{2,4}
• Classical	CD14++ CD16-	Phagocytosis	
• Inter-mediate	CD14++ CD16+	Pro-inflammatory	
• Non-classical	CD14+ CD16++	Patrolling	

1.1.4.2. Myeloid cells in CD

In the intestinal environment myeloid cells are prominently tolerogenic. In a healthy gut environment, macrophages are usually refractory to inflammatory stimulation, but do retain phagocytic and bactericidal capabilities (Smythies et al., 2005). The primary function of the antigen presenting cells (APCs), DCs, in the gut is to prime naïve T cells to induce differentiation to either effector or regulatory T cells phenotype.

IBD-associated loci are enriched for genes that regulate monocyte differentiation and activation (Baillie et al., 2017), and CD has been linked to the systemic expansion of the pro-inflammatory, intermediate monocyte subset (Grip *et al.*, 2007; Koch *et al.*, 2010) (Table 1.1). In the intestine, pro-inflammatory macrophages become the most

prominent immune population during CD (Zigmond et al., 2012). These macrophages upregulate TLRs and NOD2, to become more permissive to bacterial-induced responses (Zigmond et al., 2012), produce excessive amounts of pro-inflammatory cytokines and contribute to IL-17-associated effector T cell responses (Kamada et al., 2008). CD-patient derived macrophages are more susceptible to AIEC infection, and exhibit more pronounced inflammatory responses (Vazelle et al., 2015).

DCs are known to accumulate in the intestinal mucosa of IBD patients, as well as in experimental murine models of colitis. A pro-inflammatory subtype of DCs that express E-cadherin, can promote intestinal inflammation and are preferentially expanded in inflamed colon (Siddiqui et al., 2010). Furthermore, during T-cell-induced colitis, pro-inflammatory DCs expand to prime effector T cells (Rivollier et al., 2012) and inhibition of DC-T cell interaction can prevent the experimental colitis (Uhlir et al., 2006).

1.1.4.3. T cells in CD

Intestinal homeostasis is largely dependent on balances between effector T cells and regulatory T cells. In the normal gut this balance is shifted towards Treg function (Elson and Alexander, 2015) that can restrain effector T cell function, dampen innate immune cell activities (Li and Flavell, 2008) and promote effective immunoglobulin (Ig)A production, which is vital for mucosal surface homeostasis (Cong et al., 2009). In CD effector T cells, mainly CD4+, and in particular, Th1 (IFN- γ) and Th17, are expanded with enhanced activity (Cader and Kaser, 2013). Th17 cells are activated by IL-23 derived from DCs and intestinal macrophages in CD (Becker et al., 2003; Kamada et al., 2008), and produce high levels of pro-inflammatory cytokines (Littman and Rudensky, 2010). These effector cells expand at the expense of Treg populations, therefore, results in expansion of other effector T cells that are repressed by Tregs (Cader and Kaser, 2013). Although Th1 cells are strongly associated with CD pathogenesis, exacerbated Th2 cell responses in mice also resulted in spontaneous colitis (Kabat et al., 2016).

1.1.4.4. B cells in CD

When DCs detect pathogens, presentation of antigens to B cells in the lamina propria promotes production of IgA. IgA helps to maintain commensal microbiota, as it prevents exposure of microbial antigens to the systemic immune system, which reduces systemic inflammatory responses to commensal bacteria (Konrad et al., 2006). In IBD B cells have

a conflicting role as they can have regulatory or pathogenic functions. Malfunctioning B cells within the intestine during IBD can produce high levels of anti-self (Mizoguchi and Bhan, 2012) and anti-microbial antibodies (Lodes et al., 2004), and there is a serological shift from IgA- to IgG-dominant responses (Brandtzaeg et al., 2006). In one study, CD clinical activity correlated with elevated activation of B cell with higher expression of TLR2 and IL-8 (Noronha et al., 2009). Furthermore, B cells can block Treg function (Olson et al., 2004) and are key to the formation of granulomas, particularly in paediatric CD patients harbouring *NOD2* SNPs (Janssen et al., 2012; Timmermans et al., 2016). In contrast, decreases in specific B cell populations have been associated with IBD, such as IgM+ memory “natural effector” B cells (Sabatino et al., 2005; Timmermans et al., 2016) and IL-10 producing regulatory B cells (Bregs) that control pro-inflammatory cytokine production from monocytes and T cells (Oka et al., 2014; Zheng et al., 2017). Therefore, IBD pathogenesis is linked to imbalances in B cell populations and a lack of regulation of B cell functions.

1.1.4.5. NK cells in CD

Intestinal NK cells are phenotypically similar to “helper” NK cells and are important for anti-pathogen responses and maintaining intestinal homeostasis (Yadav et al., 2011). NK cell activities are generally reduced in IBD, although pro-inflammatory cytokine stimulation of NK cells can promote TNF- α and IFN- γ production and cytolytic activities in IBD (Yadav et al., 2011). Increases in NK cells expressing high levels of CD16+ (Steel et al., 2010) or activation marker Human Leukocyte Antigen – antigen D Related (HLA-DR) (Ng et al., 2009) has been associated with IBD. These populations have a less mature phenotype, have high cytolytic activity and produce high levels of IFN- γ , which subsequently enhances activation of T cells (Burt et al., 2008; Erokhina et al., 2018). The expansion of this inflammatory subset of NK cells has a vital role in IBD pathogenesis.

1.2. Autophagy

Autophagy is an intracellular process that degrades excessive, damaged or aged proteins and organelles to maintain cellular homeostasis (Yang and Klionsky, 2010). This pathway differs from the ubiquitin proteasome system, which degrades only single targeted proteins (Van Limbergen et al., 2009). Autophagy affects many essential cellular

processes including development, differentiation, survival, senescence and innate and adaptive immunity; with dysregulated autophagy linked to a multitude of diseases (Levine and Kroemer, 2008).

Autophagy can be categorised into macro-, micro- and chaperone-mediated autophagy (CMA) depending on the route of delivery of cargo to the lysosome and the main physiological functions. CMA is the process by which the cytoplasm is directly engulfed and degraded by the lysosome (Orenstein and Cuervo, 2010); while microautophagy engulfs specific cytosolic proteins by inward vesicle budding (Mijaljica et al., 2011).

Macroautophagy (hereafter referred to as autophagy) is the most prominent type of autophagy implicated in disease pathogenesis, and involves the formation of autophagosomes to mediate its functions. It is usually active at a basal level to maintain homeostasis, and varying stimuli enhance this activity. Non-selective (canonical) autophagy is stimulated by cellular stresses, such as nutrient or growth factor deprivation; whereas selective autophagy is directed towards specific target cargo (Lamb et al., 2013). Selective autophagy uses cargo receptors and adaptor proteins to associate cargo with the autophagosome machinery (Birgisdottir et al., 2013), and can be further classified based on the target proteins, lipids and/or organelles. For example, aggrephagy is the degradation of aggregated proteins (Lamark and Johansen, 2012), mitophagy targets damaged mitochondria (Narendra et al., 2008) and xenophagy degrades bacteria (Baxt et al., 2013) and viruses (Kim et al., 2010).

1.2.1. Autophagosome biogenesis

When autophagy is initiated, the isolation membrane, an expanding lipid bilayer, forms a double membrane vesicle (the autophagosome) around the cargo to be degraded (Figure 1.3). This isolation membrane, originally known as the phagophore, is often derived from ER membranes (Lamb et al., 2013). The mature autophagosome then fuses with a lysosome to form an autophagolysosome, in which lysosomal enzymes degrade the inner membrane and cargo (Figure 1.3). The process of autophagy is controlled by the coordinated activity of 37 ATG proteins in yeast, but the core ATG proteins, which are conserved in mammalian cells, are much fewer (Lamb et al., 2013).

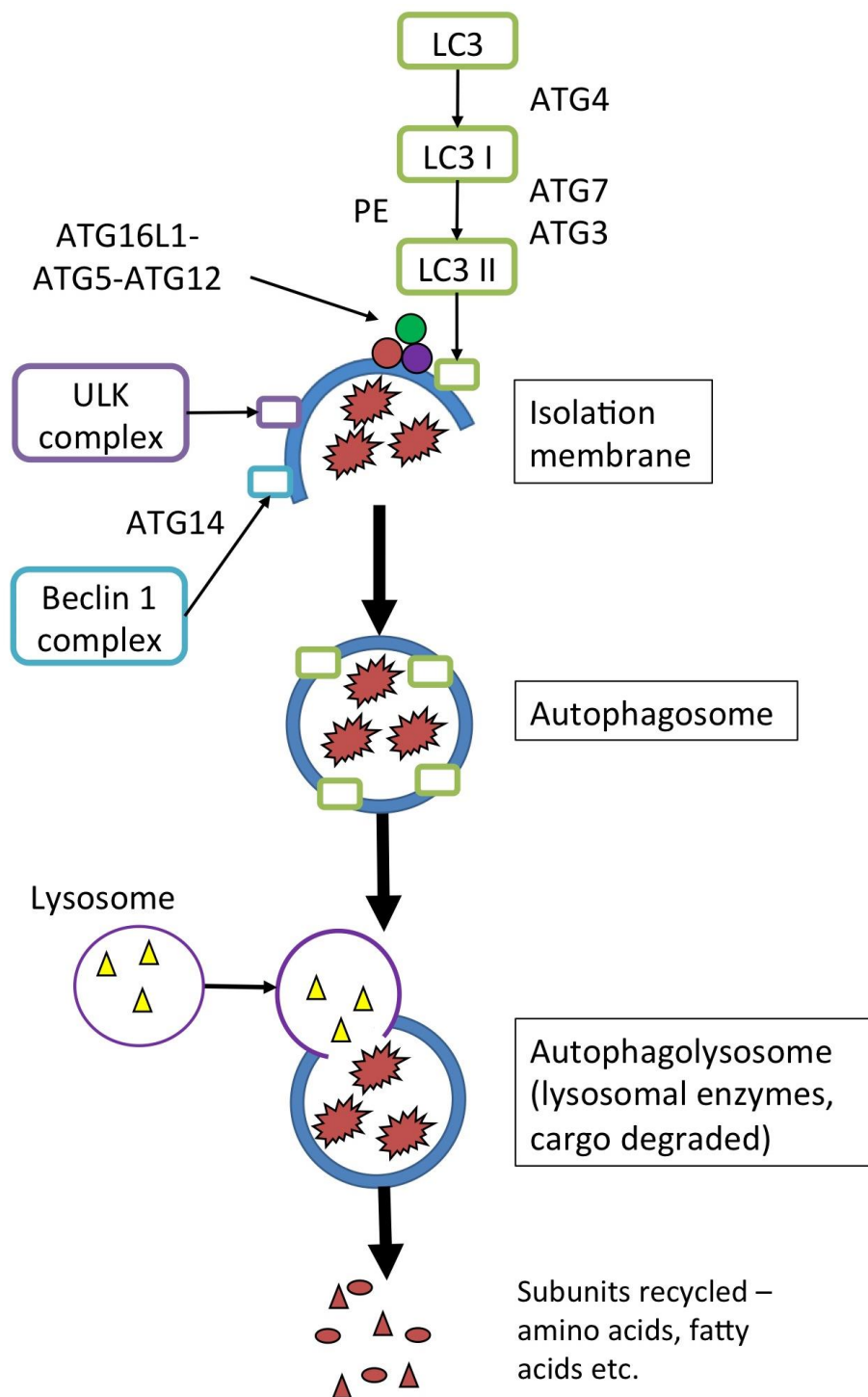


Figure 1.3: Autophagy Pathway and Autophagosome Biogenesis

During the initial stages of autophagy, the isolation membrane forms a double membrane vesicle (the autophagosome) around the cargo to be degraded. ULK complex (ULK1-ULK2-ATG13-FIP200-ATG101) and Beclin 1 (Vps34-Vps150-Beclin1) complex, through interaction with ATG14, recruit autophagy proteins and complexes to the autophagosome membrane. ATG12 is conjugated to ATG5 and forms a complex with ATG16L1 (ATG16L1 complex). The ATG16L1 complex is proposed to specify the site of LC3 lipidation for autophagosome formation. LC3 is conjugated to PE to form lipidated LC3-II and is associated with the autophagosome outer membrane. Upon autophagosome closure, LC3 localises to the inner membrane and other autophagy

proteins and complexes dissociate for recycling. The mature autophagosome then fuses with a lysosome to form an autophagolysosome, in which cargo are degraded by lysosomal enzymes and subunits are recycled.

Autophagy initiation requires the ULK complex, which consists of UNC51 like Ser/Thr kinases (ULK)1 and ULK2, ATG13, FAK family kinase interacting protein of 200 kDa (FIP200) and ATG101 (Akers et al., 2012). Under normal conditions in mammalian cells, ULK complex is bound and inhibited by mTORC1 (Mechanistic Target of Rapamycin Complex 1) complex (Wirth et al., 2013) and mTORC1 also phosphorylates ULK1 and ATG13 to inhibit the ULK complex (Fujita et al., 2008). Inactivation of mTORC1, during nutrient deprivation, allows kinase activity of ULK1 and ULK2 for phosphorylation of substrates FIP200 and ATG13, and thus activation of the ULK complex (Wirth et al., 2013). The ULK complex then localises to the site of autophagosome formation and is vital for recruitment and activation of other autophagy machinery proteins and complexes (Figure 1.3) (Chan et al., 2009; Ragusa et al., 2012).

Formation of the class III phosphatidylinositide 3-kinases (PI3K) complex (Beclin 1 complex), which is composed of vacuolar protein sorting (Vps)34, Vps150 and Beclin1 is also key to initiation of autophagosome formation (Figure 1.4). Interaction of the Beclin complex with ATG14 is important for recruitment of autophagy proteins to the autophagosome membrane during early stages of the pathway (Figure 1.3) (Suzuki et al., 2007). Furthermore, when in this complex Vps34, generates phosphatidyl inositol triphosphate (PI3P), which is required for ATG protein recruitment and phagophore elongation, in the initial steps of autophagy (Devereaux et al., 2013).

During expansion of the isolation membrane, the microtubule-associated proteins 1A/1B light chain 3B (LC3B) precursor is converted by ATG4 into LC3-I and is then conjugated with phosphatidylethanolamine (PE) to form lipidated LC3-II by Atg7 and Atg3 (Figure 1.3) (Lamb et al., 2013). Simultaneously, ATG5 and ATG12 conjugate and form a complex with ATG16L1, known as the ATG16L1 complex, on the isolation membrane (Figure 1.3) (Fujita et al., 2008). The ATG16L1 complex is proposed to specify the site of LC3 lipidation for autophagosome formation (Fujita et al., 2008).

Prior to autophagosome closure ATG proteins associated with the membrane dissociate and are recycled, except for LC3-II that becomes localized to the inner membrane of the

autophagosome (Figure 1.3) (Lamb et al., 2013). Autophagosome fusion with the lysosome forms the autophagolysosome for cargo degradation and the degraded cargo then re-enters the cytosol through membrane permeases for macromolecule synthesis and metabolism (Figure 1.3) (Glick et al., 2010; Muzes et al., 2013; Van Limbergen et al., 2009).

1.2.2. Autophagy regulatory pathways

Autophagy is largely regulated, but not exclusively, by the mTORC1 and Beclin1/B cell lymphoma 2 (Bcl-2) signalling pathways (Figure 1.4). The mTORC1 pathway plays a central role in the inhibition of autophagy, for example blocking mTORC1 activity with the small macrolide antibiotic rapamycin stimulates autophagy. The small GTP (guanosine triphosphate)-ase, Rheb (RAS homologue enriched in brain), constitutively enhances mTORC1 activity (Huang and Manning, 2009). Upon nutrient deprivation, AMP (adenosine monophosphate) activated protein kinase (AMPK) detects an imbalance in AMP to ATP (adenosine triphosphate) ratio and phosphorylates the tuberous sclerosis complex (TSC) to inactivate Rheb and relieve mTORC1 repression of autophagy (Dibble et al., 2012). AMPK can also directly phosphorylate mTORC1 subunit RAPTOR (regulatory-associated protein of mTOR) to induce mTORC1 inhibition (Gwinn et al., 2008).

Class I PI3K, Akt (protein kinase B) and MAPK/ERK signalling pathways are involved in the activation of mTORC1 and subsequent inhibition of autophagy (Lamb et al., 2013). When growth factors, such as insulin, are detected by Class I PI3K/Akt, phosphorylation of TSC2 occurs resulting in Rheb activation of mTORC1 (Inoki et al., 2002; Miyazaki et al., 2010). Furthermore, Akt, in response to growth factor signalling can phosphorylate mTORC1 complex component, PRAS40 (proline-rich Akt substrate of 40 kDa), to relieve mTORC1 inhibition (Sancak et al., 2007). TSC2 phosphorylation can also be induced by the MAPK/ERK pathway in response to growth factors to achieve the same mTORC1 activating result (Lamb et al., 2013).

In contrast, when energy levels are reduced, class III PI3K Vps34 can act to induce autophagosome formation by forming the Beclin 1 complex (Devereaux et al., 2013). AMPK in response to starvation, can activate ULK1 through its phosphorylation at

distinct sites from mTORC1 phosphorylation (Egan et al., 2011; Kim et al., 2011). Activated ULK1 (Kim et al., 2013; Russell et al., 2013) and AMPK (Kim et al., 2013) then phosphorylate Beclin1 to promote formation of the Beclin 1 complex. Beclin 1 is bound to Bcl-2 during normal nutrient conditions but Bcl-2 dissociates to allow binding to Vps34 during periods of nutrient starvation. This is stimulated by Beclin 1-interacting proteins, UVRAG (UV-irradiation resistance-associated gene) and AMBRA1 (Autophagy And Beclin 1 Regulator 1) (Glick et al., 2010).

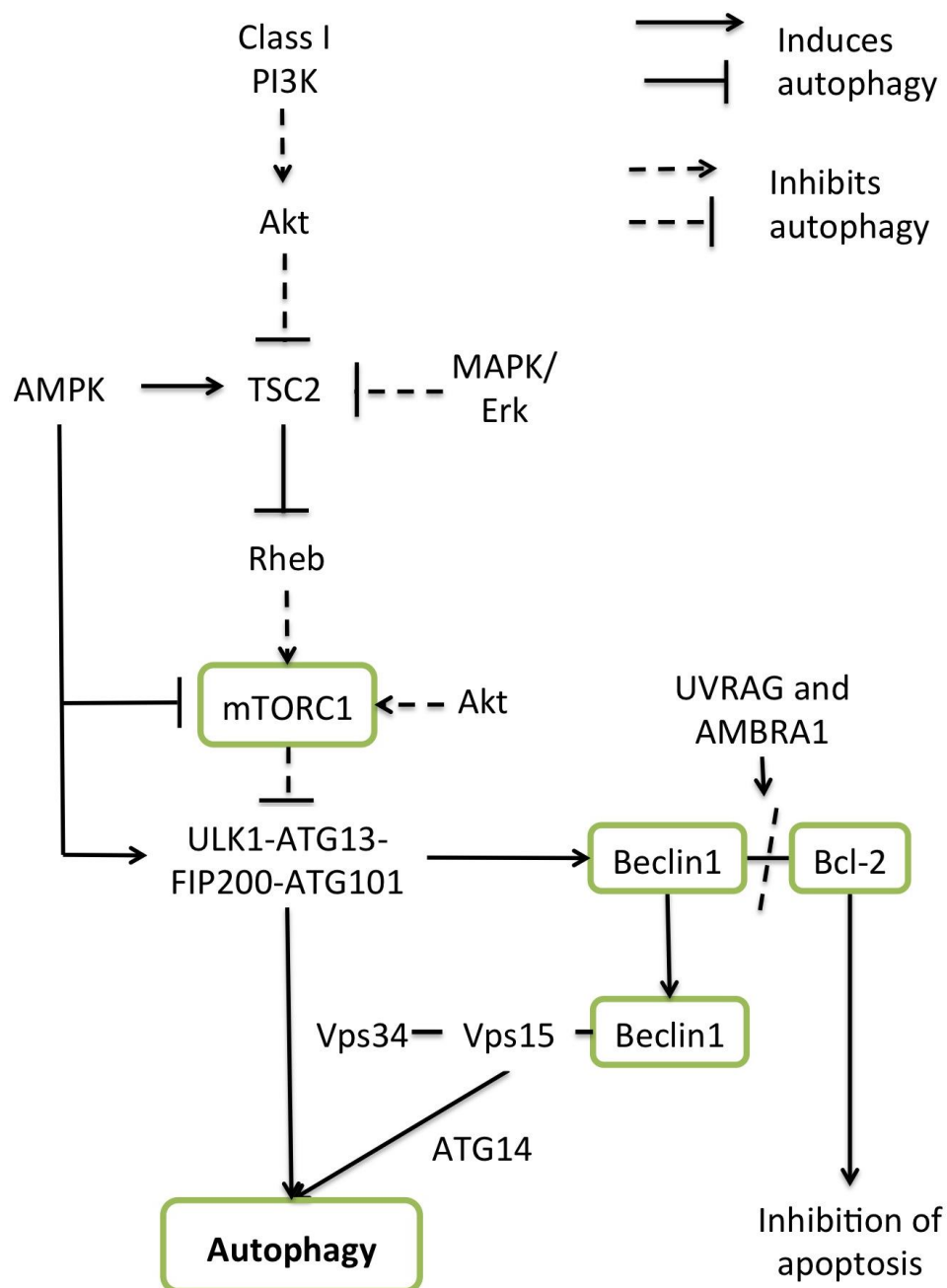


Figure 1.4: Autophagy Regulatory Pathways

The central pathways in autophagy regulation are mTORC1 and Beclin1/Bcl-2. Class I PI3K via Akt, and MAPK/Erk signalling pathways phosphorylate TSC2 to promote Rheb-dependent activation of mTORC1. When active, mTORC1 inhibits formation of the ULK complex, which is necessary for initiation of autophagy. Conversely, AMPK is involved in the inhibition of mTORC1 and stimulates autophagy via phosphorylation of ULK1 at sites distinct from mTORC1. UVRAG and AMBRA1 stimulate dissociation of Bcl-2 from Beclin 1 via JNK-1-dependent phosphorylation of Bcl-2 (not shown). Bcl-2 is then free to inhibit apoptosis and Beclin 1 is free to bind Vps34-Vps150 to induce autophagy. The Beclin 1 complex binds to ATG14 to induce further ATG protein recruitment and elongation of the isolation membrane in the initial stages of autophagy. Activated ULK1 and AMPK can also directly phosphorylate Beclin 1 for the induction of autophagy.

1.2.3. Transcriptional Regulation of Autophagy

Increased autophagy activity is accompanied by transcriptional changes in a wide range of autophagy-related proteins including *ATG5* (Haim et al., 2015; Kovsan et al., 2011; Rodríguez-Muela et al., 2012), *ATG12* (Kouroku et al., 2007), *ATG7* (Bernard et al., 2015; Bernard and Klionsky, 2015; Vázquez et al., 2012), *ATG16L1*, *LC3* (Kirisako et al., 1999; Mitroulis et al., 2010; Nara et al., 2002; Vázquez et al., 2012), *ATG9* (Jin et al., 2014), *ATG14* (Xiong et al., 2012), *GABARAP* (*Gamma-aminobutyric acid receptor-associated protein*) (Sandri, 2010), *Bnip3* (*BCL2/adenovirus E1B 19 kDa protein-interacting protein 3*), *Becn1* (Vázquez et al., 2012), *PARK2* (*Parkinson Juvenile Disease Protein 2*), *VMP1* (*Vacuole membrane protein 1*) (Ropolo et al., 2007) and *ULK1* (Klionsky et al., 2016). Transcriptional increases in many of these genes enables autophagy initiation, however, autophagy proteins that are primarily involved in autophagosome formation and maturation, such as LC3 and ATG5, are more likely to be up-regulated for replenishment of protein when autophagy flux is extensive or prolonged (Kouroku et al., 2007; Rouschop et al., 2010; Sandri, 2010).

Several transcription factors have been implicated in the regulation of autophagy gene expression. FOXO (Forkhead box protein O) transcription factors (FOXO1 and FOXO3) have been shown to regulate autophagy gene expression (Mammucari et al., 2007; Xiong et al., 2012; Zhao et al., 2007) and GATA1 (GATA-binding factor 1) along with co-regulator ZFP1 (Zinc Finger Protein, FOG Family Member 1) increases transcription of autophagy components (Kang et al., 2012). Using promoter analysis assays, it has been shown that when transcription factor E2F1 (E2F Transcription Factor 1) binds to the *LC3B* promoter, expression of several autophagy genes was increased, resulting in increased autophagy flux (Haim et al., 2015; Kovsan et al., 2011).

Nuclear Receptor Subfamily 1 Group D Member 1 (NR1D1) (also known as Rev-erb- α) acts to repress transcription of *ULK1*, *Bnip3*, *ATG5*, *PARK2/parkin* and *Becn1* (Woldt et al., 2013). ZKSCAN3 (Zinc Finger With KRAB And SCAN Domains 3) also transcriptionally represses autophagosome and lysosome biogenesis and is translocated to the nucleus upon stimulation of autophagy (Chauhan et al., 2013). This is thought to prevent excessive autophagy in response to stimuli.

A major hub of transcriptional regulation of both autophagosome and lysosome biogenesis is the CLEAR (coordinated lysosomal expression and regulation) network (Palmieri et al., 2011; Sardiello et al., 2009; Settembre et al., 2011). Transcription factor EB (TFEB) is central to the control of CLEAR, and is regulated via phosphorylation by MAPK1/ERK2 and mTORC1 pathways (Martina et al., 2012; Settembre et al., 2012, 2011). mTORC1 phosphorylates TFEB on lysosome surfaces to prevent nuclear translocation and subsequent activation of autophagy genes (Settembre et al., 2012). This network highlights the concomitant transcriptional regulation of both lysosomes and autophagosomes to promote an effective degradative process. Although post-translational modifications of autophagy proteins and formation of complexes is central to autophagy initiation and regulation, these studies show that there are key points of transcriptional regulation within the autophagy pathway.

1.2.4. Autophagy and Cell Death are intrinsically linked

Cell death can be mediated by several different pathways and cell death modalities can be distinguished by morphological classification as well as biochemical pathways. Necrosis is a detrimental form of cell death that is not regulated by the cell and culminates in cell membrane rupturing and uncontrolled release of Damage Associated Molecular Patterns (DAMPs). In contrast, programmed cell death, including apoptosis and autophagic-cell death (ACD), is a highly regulated process. Apoptosis is essential for the removal of unwanted, damaged or infected cells through their controlled dismantling, which is integral to cellular suicide. Autophagy can interact with apoptosis in several context-dependent processes. Distinct from these interactions is ACD, which is strictly defined as cell death mediated by increased autophagic flux, with inhibition of autophagy preventing cell death (Pattingre et al., 2005).

1.2.4.1. Apoptosis

Apoptosis is identified, morphologically, by nuclear condensation and fragmentation, followed by plasma membrane blebbing. Extrinsic apoptosis eliminates abnormal cells based on aberrant development or tumorigenic qualities (Figure 1.5) (Mariño et al., 2014). The extrinsic pathway is triggered upon ligation of death receptors, such as TNF receptor 1 (TNFR1) or TNF-related apoptosis-inducing ligand receptor (TRAILR) (Mariño et al., 2014). Once activated, these receptors recruit pro-apoptotic proteins to stimulate lysosomal membrane permeabilisation (LMP) that releases cathepsin proteases into the cytosol, resulting in general proteolysis and caspase-independent apoptosis (Boya and Kroemer, 2008). Recruitment of caspase 8 during extrinsic apoptosis proteolytically activates downstream caspase cascades, causing caspase-dependent cell death and also truncates the BH3 (Bcl-2-Homology 3)-only protein, BID (BH3-Interacting Domain Death Agonist) to activate intrinsic apoptosis (Mariño et al., 2014).

Intrinsic apoptosis occurs in response to cytotoxic stress, exposure to xenobiotics, mitochondrial damage and general developmental cues (Figure 1.5). The defining process of intrinsic apoptosis is Mitochondrial Outer Membrane Permeabilisation (MOMP). Upon activation of BH3-only proteins by caspase 8 or p53 in response to DNA damage (Vousden and Lane, 2007), pro-apoptotic proteins Bcl-2-associated X protein (BAX) and Bcl-2 antagonist or killer (BAK) are recruited to the mitochondria to induce MOMP (Adams and Cory, 2007; Galonek and Hardwick, 2006; Kroemer et al., 2007). Due to the permeabilisation of the mitochondria, cytochrome c is released to induce caspase-dependent apoptosis, and Apoptosis Inducing Factor (AIF) and Endonuclease G are released to cause caspase-independent apoptosis (Kroemer and Martin, 2005). Caspase-independent apoptosis is characterised by reactive oxygen species (ROS) production, DNA damage, proteolysis and chromatin condensation.

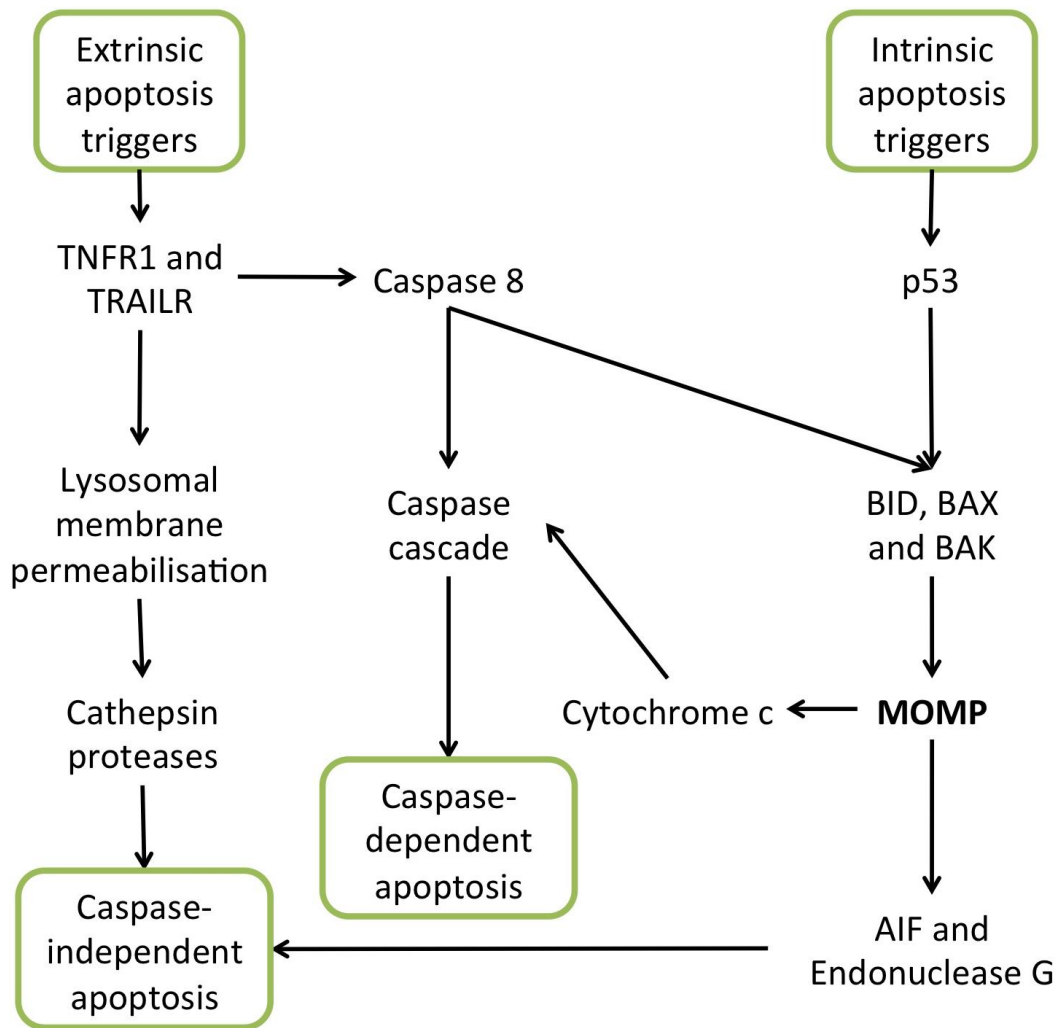


Figure 1.5: Extrinsic and Intrinsic Apoptosis pathways

Extrinsic apoptosis is triggered by binding of receptors TNFR1 and TRAILR to induce lysosomal membrane permeabilisation (LMP), which releases cathepsin proteases, causing general proteolysis and caspase-independent apoptosis. Extrinsic apoptosis receptors also activate caspase 8 to induce caspase-dependent apoptosis and intrinsic apoptosis. Intrinsic apoptosis is characterised by mitochondrial outer membrane permeabilisation (MOMP), facilitated by BH3-only proteins that localise to the mitochondria when caspase 8 and p53 are activated. MOMP releases cytochrome c for caspase cleavage and AIF and endonuclease G for caspase-independent apoptosis.

1.2.4.2. Interactions of Autophagy and Apoptosis

In response to cellular stress, autophagy often precedes apoptosis in an attempt to promote survival, which can involve autophagy actively suppressing apoptosis. However, when cellular stress is prolonged and/or more intense the cell will undergo apoptosis to protect neighbouring cells. In this instance autophagy can act to initiate

apoptosis and active apoptosis can then suppress cytoprotective autophagy to accelerate cell death.

Beclin 1 was originally identified as an interacting protein with Bcl-2 (Liang et al., 1998), the anti-apoptotic protein that inhibits autophagy when it is in complex with Beclin 1 (Maiuri et al., 2007; Pattingre et al., 2005). In response to nutrient deprivation, c-Jun N-terminal kinase (JNK)-1-mediated phosphorylation of Bcl-2 occurs, causing the dissociation of the Beclin 1-Bcl-2 complex and induction of autophagy (Wei et al., 2008). Under these conditions Bcl-2 will bind to and inhibit pro-apoptotic proteins, including BAX and BAK, to promote survival. However, during periods of prolonged nutrient deprivation, extensive levels of Bcl-2 phosphorylation prevents Bcl-2 from binding to pro-apoptotic proteins (Bassik et al., 2004; Wei et al., 2008). Cells and mice expressing Bcl-2 with mutant phosphorylation sites are resistant to autophagy and apoptosis induction in response to stress (He et al., 2012). Therefore, Bcl-2 phosphorylation can act as a switch between autophagy and apoptosis (Wei et al., 2008).

Due to the Beclin 1-Bcl-2 interaction, induction of pro-apoptotic signalling can also induce autophagy. One of the mechanisms by which BH3-only proteins, induce apoptosis is by neutralizing anti-apoptotic Bcl-2 family proteins, Bcl-2 and MCL1 (Myeloid cell leukaemia sequence 1), which indirectly enhances autophagy by disrupting inhibitory interactions of Bcl-2 and MCL1 with Beclin1 (Mariño et al., 2014). Furthermore, Death-Associated Protein Kinase (DAPK), which has varying pro-apoptotic effects, can also promote autophagy through phosphorylation of Beclin 1, which inhibits interaction with Bcl-2 (Choi et al., 2013; Zalckvar et al., 2009). DAPK also triggers protein kinase D (PKD) phosphorylation of Vps34 to promote formation of the Vps34-Vps15-Beclin1 complex for autophagy induction (Eisenberg-Lerner and Kimchi, 2012).

p53 can also act to initiate both autophagy and apoptosis in response to DNA damage. Cytosolic p53 constitutively represses autophagy by interacting with FIP200, thus inhibiting the ULK complex that is essential for autophagosome formation (Tasdemir et al., 2008). Upon DNA damage, p53 translocates to the nucleus and mitochondria, which prevents inhibitory interaction with FIP200 (Tasdemir et al., 2008). In the mitochondria p53 interacts with cyclophilin D to cause formation of permeability transition pores (PTP) (Vaseva et al., 2012). PTP activates autophagic clearance of mitochondria (mitophagy), but if PTP reaches a critical threshold MOMP occurs, triggering intrinsic apoptosis

(Galluzzi et al., 2012; Youle and Narendra, 2011a). Furthermore, when translocated to the nucleus p53 up-regulates expression of genes for pro-apoptotic as well as pro-autophagic proteins (Riley et al., 2008). The co-regulatory capacity of these pathways can be explained by the concept of pre-mortem autophagy, as the signalling pathways induce autophagy when cellular stress is more modest and then induce apoptosis if the cellular stress is prolonged.

Autophagy can also inhibit apoptosis in its attempts to promote cell survival. Mitophagy plays an important role in preventing apoptosis, as removal of damaged mitochondria prevents release of mitochondrial activators of intrinsic apoptosis. Furthermore, autophagy can also selectively degrade pro-apoptotic proteins, such as caspase 8 and BAX, to attenuate cell death (Amir et al., 2013; Hou et al., 2010). Autophagic inhibition of apoptosis is an attempt to restore homeostasis and promote survival in cells exposed to low levels of stress.

When autophagy is not capable of restoring homeostasis in response to cellular stress, apoptosis is essential to protect neighbouring cells. To accelerate apoptosis it is pertinent that autophagy is inhibited. This can be achieved by caspase digestion of essential autophagy proteins, such as ATG3 (Oral et al., 2012), Beclin1 (Luo and Rubinsztein, 2010; Wirawan et al., 2010) and AMBRA1 (Pagliarini et al., 2012). Furthermore, the fragments of caspase-digested autophagy proteins, such as Beclin 1 (Wirawan et al., 2010), ATG5 (Yousefi et al., 2006) and ATG4D (Betin and Lane, 2009) can acquire pro-apoptotic functions. A carboxy-terminal fragment of Beclin 1 can localise at the mitochondria to induce cytochrome c release through mitochondrial permeabilisation (Wirawan et al., 2010). The complex relationship between autophagy and apoptotic cell death highlights the need to monitor cytotoxicity when investigating autophagy.

1.2.4.3. Autophagic-Cell Death (ACD)

A rheostat model proposed by Pattingre *et al.* (2005) suggests that when autophagy exceeds physiological levels then autophagic-cell death can occur due to over-digestion of essential cellular components. ACD is defined as cell death mediated by autophagy in which suppression of autophagy prevents cell death, as opposed to cell death accompanied by autophagy flux. This phenomenon has mostly been described in model

organisms such as nematodes (Erdélyi et al., 2011) and *Drosophila melanogaster* (Denton et al., 2009), but there is some evidence in mammals. For example, cell death induced by overexpression of the RAS oncogene (Byun et al., 2009; Elgendy et al., 2011), hypoxia (Koike et al., 2008) or influenza virus infection increased ATG5, ATG7 or Beclin 1 levels (Sun et al., 2012).

1.2.5. Xenophagy: Autophagic Degradation of Microorganisms

Xenophagy (a specific type of autophagy that degrades microorganisms) is central to innate immune response. It can target and degrade intracellular pathogens, stimulate the production of host defence peptides, regulate pro-inflammatory signalling and present antigens to initiate the adaptive immune response (Deretic et al., 2013). This process is particularly important for the bacterial handling of certain pathogens that can elude phagocytic vacuoles, such as *Listeria monocytogenes*, as well as bacteria that remain in intracellular vacuoles such as *Salmonella enterica* (Travassos et al., 2010). Interestingly, antibiotic-induced microbial dysbiosis in the gut has been shown to enhance expression of autophagy genes (Singh et al., 2017).

During infection, microorganisms are detected via PAMPs by PRRs located on the surface or within the cytosol of host cells. PRRs involved in xenophagy include the NLRs, TLRs and sequestosome 1/p62-like receptors (SLRs) (Delgado et al., 2009). NLRs are primarily cytosolic but have been described at the plasma membrane (Barnich et al., 2005). NLRs including NLRP3, NLRP4, NLRP10, and NLRC4 can be found in complexes with Beclin1, but their mechanism in autophagy regulation has yet to be fully elucidated (Jounai et al., 2011). NOD1 and NOD2 can initiate autophagy in response to muramyl peptides in bacterial walls, which will be discussed further in Section 1.3.2.

TLRs are plasma membrane bound PRRs, central to innate immunity, and have been implicated in the stimulation of autophagy. Different TLRs are stimulated by different PAMPs and it has been found that ligands for TLR4 and TLR7, which are lipopolysaccharide and single-stranded DNA respectively, provoke the greatest autophagy response (Van Limbergen et al., 2009). TLR-mediated autophagy can be mediated via disruption of the Beclin1-Bcl-2 complex (Shi and Kehrl, 2008).

SLRs or autophagy receptors can target cytosolic pathogens to initiate autophagy (Nys et al., 2013). There are five main SLRs including sequestosome 1/p62, NBR1 (Neighbor of BRCA1 gene 1) (Kirkin et al., 2009), NDP52 (Nuclear Domain 10 Protein 52) (Thurston et al., 2009), the NDP52-like receptor calcoco3 (Calcium-binding and coiled-coil domain-containing protein 3) (Newman et al., 2012), and optineurin (Wild et al., 2011). SLRs can bind ubiquitin tags on invading pathogens (Dupont et al., 2009; Thurston et al., 2009; Wild et al., 2011) or galectin, which binds galactose residues exposed on damaged phagosomes (Li et al., 2013; Thurston et al., 2012). SLRs have another binding motif, the LC3-interacting region (LIR), which allows direct interaction with the autophagy machinery (Johansen and Lamark, 2011). The activity of SLRs can be enhanced by cargo adaptors. For instance, the adaptor, autophagy-linked FYVE protein (ALFY) can bind ubiquitinated pathogens via p62 and promote association with the autophagy machinery through binding to ATG5 (Filimonenko et al., 2010).

1.2.6. Mitophagy: Autophagic degradation of mitochondria

Mitophagy is the autophagic degradation of damaged or excessive mitochondria. This process is required for turnover of mitochondria, adjustment of mitochondria quantity in response to alterations in metabolic requirements and during developmental stages, for example red blood cell differentiation (Youle and Narendra, 2011b). Loss of autophagy proteins ATG5 or ATG7 leads to accumulation of damaged mitochondria and enhanced ROS production (Mortensen et al., 2010; Saitoh et al., 2008; Stephenson et al., 2009).

The main mediators of mitophagy are E3 ligase parkin and PTEN-induced putative kinase protein 1 (PINK1). PINK1 is degraded by proteolysis in healthy mitochondria; however, when mitochondrial inner membrane potential decreases in damaged mitochondria, PINK1 proteolysis is inhibited (Narendra et al., 2010). This causes PINK1 accumulation in damaged mitochondria, which subsequently recruits parkin to the mitochondrial membrane from the cytosol (Narendra et al., 2008). PINK1 binding and phosphorylation of parkin activates its E3 ubiquitin ligase activity (Sha et al., 2010). Parkin then ubiquitinates substrates embedded in the outer mitochondrial membrane, which are then bound by ubiquitin-binding adaptor proteins p62 and histone deacetylase 6

(HDAC6) (Geisler et al., 2010; Lee et al., 2010; Okatsu et al., 2010). These adaptor proteins then transport the ubiquitinated mitochondria to autophagosomes for mitophagy initiation. Pink1 and parkin variants dramatically reduce parkin recruitment to mitochondria and inhibit mitochondrial degradation (Geisler et al., 2010; Lee et al., 2010; Narendra et al., 2010). NIP3-like protein X (NIX) can also promote parkin translocation to the mitochondria to induce mitophagy in human red blood cells and mouse embryonic fibroblasts (Ding et al., 2010).

1.3. Autophagy and Crohn's Disease

Breakdown of autophagic homeostasis has been linked to several diseases, including neurodegenerative diseases, cancer and infectious diseases (Levine and Kroemer, 2008). Part of autophagy's homeostatic function is its ability to limit inflammation by degrading pathogens, controlling NF- κ B signalling and pro-inflammatory responses, and activating effective adaptive immune responses (Van Limbergen *et al.*, 2009). Loss of this inflammatory regulation has been linked to the chronic GI inflammation observed in CD.

Several studies have shown impaired autophagy responses in a range of cell types derived from CD patients including dendritic cells, lymphoblastoid cells and PBMCs (Plantinga *et al.*, 2011; Cooney *et al.*, 2010; Homer *et al.* 2010). Moreover, functional studies have linked dysregulated autophagy in CD to major CD-associated genetic variants including *NOD2*, *ATG16L1*, *IRGM* and *LRRK2*.

1.3.1. *ATG16L1* variant linked to CD

In 2007, the first autophagy gene, *ATG16L1*, was linked to CD susceptibility, followed by the identification of variants in autophagy genes *IRGM* and *LRRK2* (Franke et al., 2010; Hampe et al., 2007). *ATG16L1* is widely expressed in intestinal epithelial cells and is also expressed in macrophages and lymphocytes (Muzes et al., 2013; Rioux et al., 2007). Interestingly, it has recently been suggested that CD-associated *ATG16L1 T300A* acts as a dominant negative variant by interacting with the function of WT *ATG16L1* allele in macrophages from heterozygous mice (Gao et al., 2017).

Mice with the CD-associated *ATG16L1 T300A* SNP do not spontaneously develop intestinal inflammation, but do show evidence of Paneth cell and Goblet cell dysfunction (Cadwell et al., 2010, 2008; Lassen et al., 2014). This is also observed in Paneth cells from patients homozygous for the *T300A* allele (Cadwell et al., 2008). Paneth cells and Goblet cells are vital for intestinal homeostasis; therefore, their aberrant function is an integral component of CD pathogenesis. Furthermore, in *ATG16L1* deficient mice, macrophage function is disrupted leading to increased ROS production, impaired mitophagy, decreased microbial clearance and reduced antigen processing (Zhang et al., 2017).

In mice with *ATG16L1 T300A* knock-in there are slight decreases in basal levels of autophagy but xenophagy levels are significantly inhibited (Lassen et al., 2014). Furthermore, in IEC cell lines transfected with the *T300A* SNP, impaired capture of *Salmonella* within autophagosomes is observed (Kuballa et al., 2008). Therefore, the *ATG16L1 T300A* variant decreases the capacity for antibacterial autophagy, despite minimal effect on non-selective autophagy.

The *ATG16L1* protein has two functional regions. The N-terminal region is vital for autophagy activity, as it is responsible for LC3 conjugation. The C-terminal contains the WD40 domain that is crucial for unconventional autophagy, such as xenophagy. A recent study has shown that the *T300A* SNP inhibited xenophagy in cells, but not basal or rapamycin-induced autophagy, which was due to impaired binding of adaptor protein, transmembrane protein (TMEM) 59, to the WD40 domain (Boada-Romero et al., 2016). Recent functional studies, using a *T300A* knock-in mouse model, have demonstrated that this SNP creates a caspase cleavage site, making *ATG16L1* more susceptible to caspase-3-mediated degradation (Lassen et al., 2014; Murthy et al., 2014). The enhanced caspase cleavage did not affect the N-terminal region, but disrupted the functions of the WD40 domain. This meant that canonical (non-selective) autophagy activity was maintained, but WD40-mediated xenophagy was impaired (Boada-Romero et al., 2016). Therefore, the preferential disruption of xenophagy by the *T300A* SNP is due to loss of function in the WD40 domain in the C-terminal of *ATG16L1*.

ATG16L1 is post-transcriptionally inhibited by miRNA, *MIR142-3p*, which leads to attenuated starvation- and MDP-induced autophagy (Zhai et al., 2014). Dysregulated miRNAs have been implicated in CD pathogenesis (Cao et al., 2017; F. Wu et al., 2010; Wu et al., 2011). Due to its link to *ATG16L1* and autophagy, *MIR142-3p* may have a role

in CD pathogenesis. Therefore, in CD, decreased translation of *ATG16L1* due to dysregulated miRNA could generally impair autophagy activity, and not specifically xenophagy.

1.3.2. Implications of impaired NOD2-ATG16L1 interactions in CD pathogenesis

The immunoregulatory properties of NOD2 have been linked to autophagy. CD susceptibility is heightened when *ATG16L1* and *NOD2* variants present in combination causing synergistic genetic epistasis (Rioux et al., 2007; Weersma et al., 2009). This implies a significant interaction between these proteins in the autophagy pathway.

Cells harbouring CD-associated *NOD2* variants and/or the *ATG16L1 T300A* SNP exhibit a number of disrupted functions linked to autophagy and have similar phenotypes, suggesting that NOD2-ATG16L1 functionally intersect. Paneth cell abnormalities causing reduced antibacterial processes were found in CD patients with *NOD2* or *ATG16L1* variants (Homer et al., 2010). In IECs and DCs that harbour the *NOD2 L1007f/s* or *ATG16L1 T300A* variants, MDP-induced autophagy is diminished, leading to ineffective killing of pathogens such as *Salmonella typhimurium*, *Shigella flexneri* and AIEC (Cooney et al., 2010; Homer et al., 2010). Furthermore, in monocytes from CD patients with CD-associated *ATG16L1* and *NOD2* variants, deficient autophagy led to increased accumulation of bacterial products and enhanced pro-inflammatory responses (Wolkamp et al., 2014).

A functional interaction between these proteins has been observed, as NOD2 recruits ATG16L1 to the site of bacterial entry at the plasma membrane to initiate autophagy (Travassos *et al.*, 2010). The CD-associated NOD2 variant failed to recruit ATG16L1, which led to impaired formation of a phagophore around the invading bacteria (Travassos *et al.*, 2010). Therefore, there is a strong link between impaired NOD2-ATG16L1 interactions, caused by CD-associated mutations, and defective autophagy. This can ultimately lead to decreased bacterial clearance, causing persistent infection and excessive pro-inflammatory responses that are characteristic of CD.

1.3.3. *IRGM* variants and CD pathogenesis

A deletion polymorphism immediately upstream of *IRGM* causes *IRGM* to segregate into CD risk variant (deletion) and protective variant (no deletion) (McCarroll et al., 2008; Parkes et al., 2007). Subsequently it has been shown that miR-196, which is overexpressed in the inflammatory intestinal epithelia of individuals with CD, downregulates the *IRGM* protective variant but not the risk-associated variant (Brest et al., 2011). *Irgm1*-deficient mice also exhibit abnormalities in Paneth cells, accompanied by increased susceptibility to inflammation in the colon and ileum (Liu et al., 2013).

Functionally, the loss of *IRGM* protective variant expression compromises autophagy responses to intracellular bacteria (Brest et al., 2011). Interestingly, a recent study has placed *IRGM* in a central role for the orchestration of core autophagy machinery as it regulates the formation of a complex containing NOD2 and ATG16L1 that is necessary for the induction of xenophagy (Chauhan et al., 2015). The interaction of *IRGM* with NOD2 also stimulates phosphorylation cascades involving AMPK, ULK1 and Beclin1 that regulate autophagy initiation complexes (Chauhan et al., 2015).

1.3.4. *LRRK2* variants and CD pathogenesis

LRRK2 regulates the autophagy pathway via Beclin1 and independently of mTORC1 (Manzoni et al., 2016). *LRRK2* involvement in autophagy regulation has mainly been investigated in the context of Parkinson's disease (Roosen and Cookson, 2016); however, the *LRRK2* locus has been associated with CD in GWA studies (Barrett et al., 2008; Franke et al., 2010). *LRRK2* variants have been shown to affect autophagy activity, as well as age of onset and disease location in CD patients (Hui et al., 2018). *LRRK2* deficiency confers enhanced susceptibility to experimental colitis in mice, which was associated with enhanced nuclear localisation of the transcription factor nuclear factor of activated T cells (NFAT1), important for regulating innate immune responses (Liu et al., 2011). *LRRK2* can also enhance NF κ B-dependent transcription, while small interfering RNA (siRNA) knockdown of *LRRK2* in murine Ralph and William's cell line (RAW) 264.7 macrophage-like cells interferes with ROS production and bacterial killing (Gardet et al., 2010).

1.3.5. AIEC, CD and autophagy

Defects in autophagy have been linked to AIEC persistence in macrophages (Lapaquette et al., 2010, 2012; Sadabad et al., 2015) and enhanced expression of TNF- α , IL-1 β and IL-8 in response to AIEC (Negroni et al., 2016). Furthermore, in IECs and DCs with CD-associated *NOD2*, *ATG16L1* and *IRGM* variants, there were diminished autophagy responses to AIEC infection, causing unsuccessful clearance of the intracellular bacteria (Brest et al., 2011; Cooney et al., 2010).

Various bacterial strains can perturb autophagy responses, such as *Listeria monocytogenes* and *Shigella flexneri* that can block recruitment of Beclin1 and ATG7 to the autophagosome (Birmingham et al., 2007; Ogawa et al., 2005), and *Salmonella* that can deubiquitinate autophagy proteins to inhibit autophagosome formation and maturation (Mesquita et al., 2012). The AIEC strain LF82 can escape autophagy in IECs (Lapaquette et al., 2010), and AIEC were able to survive in neutrophils by disrupting autophagy flux, which exacerbated IL-8 production (Chargui et al., 2012). In human intestinal epithelial T84 cells and in mouse enterocytes, AIEC infection upregulated miRNA (MIR) 30C and MIR130A via NF κ B activation, which decreased levels of ATG5 and ATG16L1 (Nguyen et al., 2014). This resulted in inhibition of autophagy, which augmented AIEC replication and pro-inflammatory responses. In ileal biopsies from CD patients, increased MIR30C and MIR130A levels correlated with decreased ATG5 and ATG16L1. The enterohaemorrhagic strain of *E. coli* (O157:H7) can also inhibit autophagy. The type 3 secretion system (T3SS) in *E. coli* O157:H7 translocates Tir protein into host cells to act as a receptor for bacterial adhesion (Xue et al., 2017). Tir then activates protein kinase A (PKA) to facilitate adhesion and inhibit autophagy via suppression of ERK1/2 and enhanced PI3K/Akt signalling. PKA can also phosphorylate ATG13 protein to cause dissociation from the autophagosome (Stephan et al., 2009).

Defective autophagy can be caused by host genetic variants in key autophagy proteins, as well as AIEC modulation of host defences. Regardless of the cause, deficient autophagy results in enhanced survival of intracellular AIEC and augmented pro-inflammatory responses in CD.

1.3.6. Autophagy control of cytokines in CD

The increased levels of pro-inflammatory cytokines observed in CD patients has also been linked to autophagy dysregulation. Autophagy removes endogenous damage signals, such as ROS, and damaged organelles, such as the mitochondria, which decreases basal levels of inflammasome activation (Nys *et al.*, 2013). This indirectly inhibits inflammasome activation of caspase 1, which converts pro-IL-1 β to IL-1 β and matures IL-18 (Shi *et al.*, 2012). Caspase-1 in inflammasomes can also induce a process called pyroptosis in macrophages (Suzuki *et al.*, 2007). Pyroptosis is a process in which immune cells affronted with infection will swell and burst to release cytokines. Autophagy has the capacity to directly eliminate active inflammasomes (Shi *et al.*, 2012) and can protect the cells from pyroptosis (Suzuki *et al.*, 2007). This suggests that pyroptosis could occur more readily in response to infection in cells from CD patients with defective autophagy.

NOD2 and ATG16L1 proteins also regulate pro-inflammatory cytokine production. The *T300A* SNP was associated with augmented IL-1 β , IL-6 and IL-18 production in response to bacterial infection and NOD2 ligands in PBMCs from CD patients (Glubb *et al.*, 2011; Salem *et al.*, 2015) and healthy donors (Plantinga *et al.*, 2011), and in *ATG16L1*-deficient or *T300A* knock-in mice (Lassen *et al.*, 2014; Saitoh *et al.*, 2008). One study revealed that ATG16L1 regulates NOD2-mediated cytokine release by interfering with poly-ubiquitination and recruitment of RIPK-2 (Sorbara *et al.*, 2013). Therefore, when bound to NOD2, ATG16L1 acts as a modulator of NOD2 activity, shifting the balance between autophagy and cytokine production. Loss of functional ATG16L1 shifts NOD2 activity towards RIPK-2-mediated pro-inflammatory signalling (Plantinga *et al.*, 2011).

1.3.7. Autophagy involved in adaptive immune responses in CD

Autophagy is required for presentation of antigens derived from degraded bacterial components to the adaptive immune system (Deretic *et al.*, 2013). Autophagosomes containing degraded peptides can fuse with the multivesicular major histocompatibility complex (MHC)-loading compartments for processing of the antigen (Cooney *et al.*, 2010), which is then presented on the surface of the cell to activate adaptive immune cells.

As DCs are APCs they have an important role in appropriate activation of adaptive immune responses. Autophagy-deficient monocyte-derived DCs from paediatric CD patients expressing the *NOD2 L1007f/s* or *ATG16L1 T300A* variants have disrupted antigen sampling and processing (Strisciuglio et al., 2013), and antigen presentation via MHC II (Cooney et al., 2010). Furthermore, autophagy-deficient DCs present cytoskeletal defects, which reduce mobility (Wildenberg et al., 2017). Impaired migration can be linked to decreased antigen sampling, resulting in inadequate development of immune self-tolerance (Wildenberg et al., 2017). These studies might suggest that autophagy defects in DCs would lead to decreased T cell activation. In contrary, knockdown of *ATG16L1* in DCs enhanced T-cell proliferation in a co-culture environment (Strisciuglio et al., 2013). This could be due to autophagy's role in destabilizing the synapse between DCs and T cells. This is highlighted in cells from CD patients with the *ATG16L1* risk allele, as there is increased T cell activation due to hyper-stable immunological synapses with DCs (Wildenberg et al., 2012). It appears there is a culmination of factors regarding antigen-presentation that link autophagy deficiency in DCs to the development of IBD. Firstly, insufficient antigen sampling and processing could impair appropriate activation of adaptive immune responses to resolve infections, and also impede development of self-tolerance. However, when antigen presentation is able to occur, lack of autophagy means there is over-activation of T cells due to hyper-stability of immunological synapses, and reduced mobility could cause DC inability to egress from inflamed peripheral tissue and lymph nodes.

Autophagy within T cell populations is also directly related to IBD pathogenesis. In mice with a *ATG16L1* deletion specifically in T cells, decreased autophagy caused impaired Treg survival and exacerbated inflammatory Th2 responses, resulting in spontaneous colitis (Kabat et al., 2016). On the other hand, Treg populations can be expanded by treatment with autophagy inducer rapamycin (Kabat et al., 2016) or enhancing autophagy by increasing *ATG16L1* transcription through knock-down of inhibitory miRNA, miR-142-3p (Lu et al., 2018). Autophagy can also help maintain T cell homeostasis and tolerance in the thymus. One study found that in *ATG5* knockout mice, T cell selection in the thymus was altered and this disrupted the generation of a self-tolerant T-cell repertoire, which resulted in severe colitis (Nedjic et al., 2008). Therefore, the role of T cells in CD is associated with imbalances between regulatory and effector

T cells (Shale et al., 2013) and a lack of immune self-tolerance, both of which are related to autophagy defects.

Although a direct link between autophagy in B cells and IBD has not been made, autophagy is essential for normal B cell differentiation, survival and functioning (Miller et al., 2008). In an *ATG5* knockout mouse model, autophagy was essential for survival of peripheral B cells, plasma cell development and survival, and humoral responses (Arnold et al., 2016). Humoral production of IgA is a key feature of intestinal mucosa, which suggests that autophagy may play a role in maintenance of IgA in mucosal layers. As aberrant B cell responses have been linked to CD pathogenesis, lack of autophagy may be pivotal to this.

1.3.8. Mitophagy and CD

Mitochondrial damage has been implicated in IBD pathogenesis (Novak and Mollen, 2015), with a recent study determining that mitochondrial DNA (mtDNA), which can act as a pro-inflammatory DAMP, was elevated in plasma samples from patients with active IBD (Boyapati et al., 2018). Furthermore, analysis of GWAS's revealed that ~5% of IBD susceptibility genes identified had a direct role in regulation of mitochondrial homeostasis (Ho et al., 2018).

Failure in mitochondrial regulation in IBD can be, in part, attributed to deficient autophagy responses, as defective autophagy can cause accumulation of ROS and damaged mitochondria (Saitoh et al., 2008). IRGM, which can be dysfunctional in CD, plays an integral role in mitophagy and localizes to mitochondrial membrane (Singh et al., 2010). Furthermore, the mitochondrial protein prohibitin 1 (PHB) can modulate autophagy via ROS signalling (Kathiria et al., 2012), and is decreased in active IBD and animals with experimental colitis (Hsieh et al., 2006; Theiss et al., 2007). Finally, the *SMAD specific E3 ubiquitin protein ligase 1 (SMURF1)* gene has also been associated with IBD (Franke et al., 2010) and is key for promotion of mitophagy by facilitating transport of damaged mitochondria to autophagosomes (Novak and Mollen, 2015).

Mitochondria are the most abundant source of ROS in the cell, and ROS levels are enhanced when damaged mitochondria accumulate due to lack of mitophagy (Novak and Mollen, 2015). Increased ROS has been found in intestinal epithelium of IBD patients

(Novak and Mollen, 2015) and there are reductions in antioxidant levels in IBD patients (Geerling et al., 2000). ROS can exert DNA damage and lipid oxidation, and mitochondria are also a major target of deleterious effects of oxidative stress. Therefore, it is unclear whether increased ROS in IBD is part of the cause or effect of the disease.

1.4. ER-stress and the Unfolded Protein Response

ER stress is caused by an accumulation of unfolded and misfolded protein in the ER and the UPR is activated to resolve ER stress. To reduce the accumulation of unfolded/misfolded proteins the UPR promotes protein re-folding, inhibits protein synthesis and induces degradation of unfolded and misfolded proteins through ER-associated protein degradation (ERAD) and autophagy (Figure 1.6). If these survival mechanisms are unsuccessful the UPR will induce apoptosis, as reviewed by Sano and Reed (2013). The three major regulators of the UPR are the ER-membrane resident proteins PERK (protein kinase RNA-like endoplasmic reticulum kinase), inositol-requiring transmembrane kinase endonuclease 1 (IRE1) and activated transcription factor (ATF) 6. In an inactive state these proteins are bound to the binding immunoglobulin protein (BiP), also known as glucose regulated protein 78 (GRP78) (Cao, 2015). When misfolded proteins accumulate during ER stress, BiP binds the misfolded proteins and dissociates from the ER-membrane resident proteins to allow their transition to active state (Cao, 2015).

PERK inactivates elongation initiation factor 2 α (EIF2 α) via phosphorylation, which causes inhibition of general protein synthesis (Guan et al., 2014) and specific up-regulation of activated ATF4 (Vattem and Wek, 2004). ATF4 transcriptionally up-regulates several UPR genes including CCAAT/enhancer-binding protein (C/EBP) homologous protein (CHOP) (Figure 1.6) (Harding et al., 2000; Nishitoh, 2012). CHOP is also a transcription factor that regulates several UPR genes and under conditions of prolonged ER stress can promote pro-apoptotic gene expression (Harding et al., 2000; Nishitoh, 2012).

IRE1 exists in two forms: IRE1 α that is ubiquitously expressed and IRE1 β that is only expressed in the GI tract and lung epithelial cells (Wang et al., 1998). During ER stress, IRE1 is activated through dimerization and auto-phosphorylation (Shamu and Walter,

1996; Tirasophon et al., 2000). The IRE1 α RNase domain is essential for creating transcriptionally activate X-box binding protein 1 (*XBP1*) messenger RNA (mRNA) via splicing, which acts as a transactivator of UPR genes (Figure 1.6) (Calfon et al., 2002; Lee et al., 2003, 2002; Yoshida et al., 2001). IRE1 endoribonuclease activity also facilitates degradation of specific mRNA in a process known as RIDD (regulated IRE1-dependent decay) (Hollien, 2006).

ATF6 translocates to the Golgi apparatus once released from its complex with BiP (Shen et al., 2002). This allows cleavage by site 1 and site 2 proteases (S1P and S2P), which releases the transcriptionally active cytoplasmic domain of ATF6 (ATF6-N) that induces UPR-associated genes (Figure 1.6) (Haze et al., 1999; M. Li et al., 2000; Ye et al., 2000). Among the ATF6 upregulated genes are *CHOP* and *XBP1* (Hirsch et al., 2014).

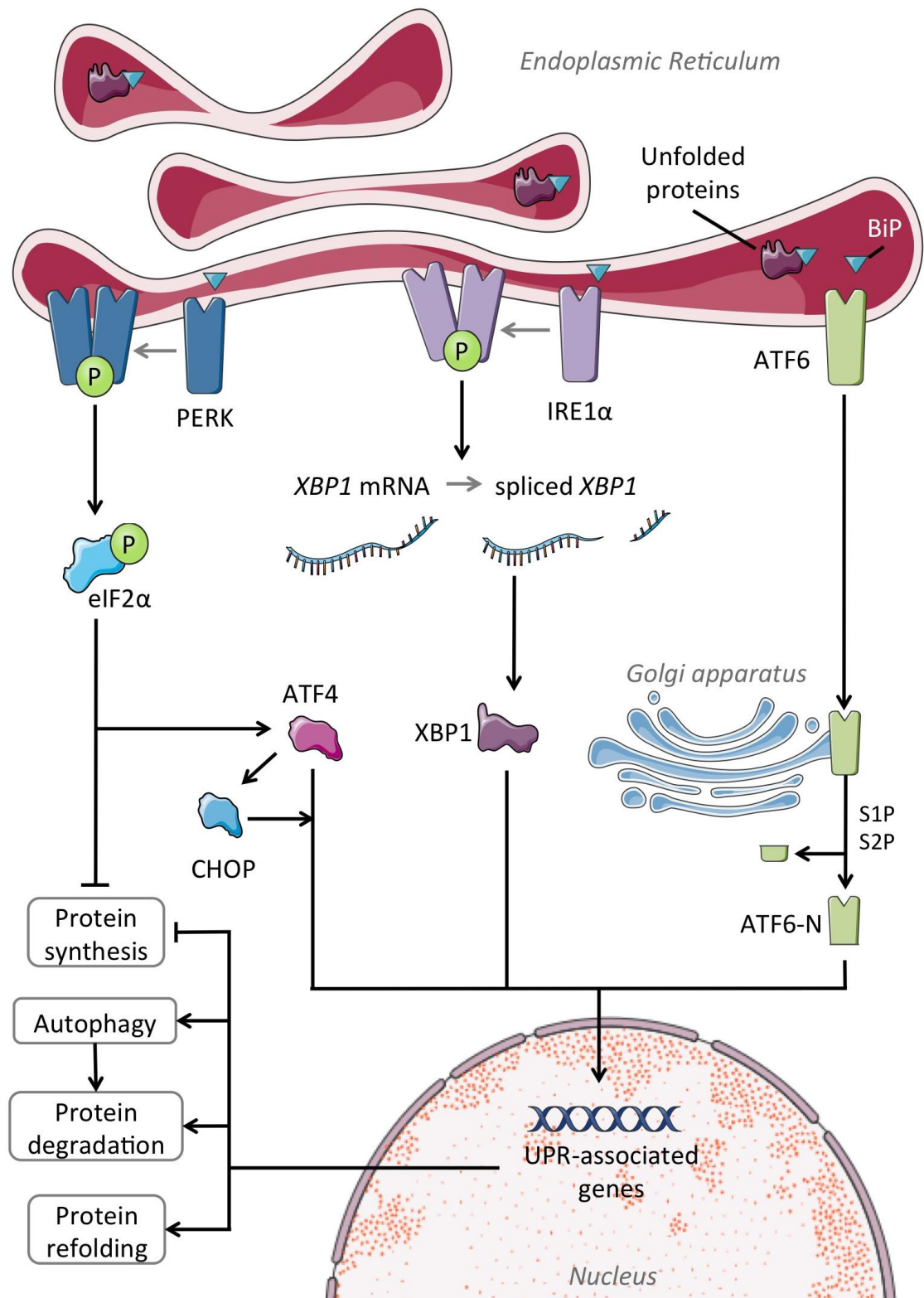


Figure 1.6: The Unfolded Protein Response

BiP chaperone protein binds unfolded/misfolded proteins in the ER and dissociates from transmembrane receptors upon accumulation of the toxic proteins. The transmembrane receptors PERK, IRE1 α and ATF6 become activated. PERK phosphorylates EIF2 α , which downregulates global translation but specifically upregulates ATF4 and CHOP that upregulate UPR-associated genes. IRE1 α splices XBP1 to its active form and ATF6 is cleaved by S1P and S2P to active ATF6-N, which both translocate to the nucleus to

upregulate UPR-associated genes. The main function of these UPR-associated genes is to increase protein refolding, inhibit synthesis of new protein and degrade unfolded/misfolded proteins through autophagy and ERAD.

1.4.1. ER stress and UPR linked to Intestinal Inflammation and IBD

Genetic studies have identified several ER-stress/UPR genes in association with IBD pathogenesis (McGuckin et al., 2010). *XBP1* and *Anterior gradient 2 (AGR2)*, which is a member of the ER PDI family, have both been identified as risk loci associated with IBD (Kaser et al., 2008; Zheng et al., 2006). There is evidence that ER-stress levels are enhanced in ileal and colonic biopsies from Crohn's disease patients, as levels of BiP, chaperone protein Gp96, and spliced *XBP1* are enhanced (Deuring et al., 2012; Kaser et al., 2008; Rolhion et al., 2010; Shkoda et al., 2007). In Ulcerative colitis increased *BiP* expression, enhanced levels of active ATF6 and ultrastructural evidence of ER stress were exhibited in colonic tissue (Heazlewood et al., 2008; Tréton et al., 2011). This link between aberrant ER stress responses and IBD can be elucidated further when considering the distinct cell types present in the intestinal epithelium. Cells that naturally secrete large amounts of protein, such as Paneth cells are more susceptible to ER-stress, therefore rely heavily on the UPR (Todd et al., 2008).

Winnie mice are characterised by a missense mutation in *Muc2*, which causes abnormalities in intestinal goblet cells, leading to aberrant mucous production and spontaneous colitis. *Winnie* mice also exhibit severe ER stress in Goblet cells (Heazlewood et al., 2008), which causes up to four-fold increases in activated DCs in the colonic lamina propria, and aberrant adaptive immune responses with strong IL-23/Th17 responses (Eri et al., 2011). Goblet cell abnormalities are also apparent in mice deficient in UPR transcription factor OASIS, which causes increased ER stress and susceptibility to DSS-colitis (Asada et al., 2012; Hino et al., 2014).

As *XBP1* is the most prominent IBD-associated loci, several studies have focused on IRE1-XBP1 signalling in murine models. In mice with *XBP1* deletion specifically in IECs (*XBP1^{ΔIEC}* mice), spontaneous inflammation of the small intestine and increased susceptibility to DSS-induced colitis was observed (Kaser et al., 2008). In *XBP1^{ΔIEC}* mice, increased ER stress, evidenced by elevated levels of BiP, and increased apoptosis of Goblet cells and

Paneth cells led to decreased host defence peptides and higher susceptibility to *Listeria monocytogenes* infection. Furthermore, *XBP1* has been shown to suppress experimental colitis-associated cancer (Niederreiter et al., 2013), and was essential for efficient TLR-mediated pro-inflammatory responses to infection in macrophages (Martinon et al., 2010). These studies confirm that the *XBP1* is necessary for protective functions of IECs and macrophages.

Although the UPR primarily acts to maintain homeostasis, hyper-activation of certain UPR components can create a pro-inflammatory state. It was observed that in *XBP1^{ΔIEC}* mice there was increased activation of IRE1 α , causing hyperactivation of NF κ B, which was essential for spontaneous inflammation (Adolph et al., 2013). In contrary, IRE1 β knock-out mice have enhanced sensitivity to DSS-induced colitis (Bertolotti et al., 2001). Furthermore, IRE1 β knock-out mice exhibit Goblet cell abnormalities with exaggerated MUC2 accumulation, whereas IRE1 α knock-out mice displayed normal Goblet cells (Tsuru et al., 2013). In murine Paneth cells IRE1 α and IRE1 β have distinct roles with overactivation of IRE1 α driving CD-like ileitis, and IRE1 β having a protective role (Tschurtschenthaler et al., 2017).

Association between aberrant PERK-EIF2 α and ATF6 pathways, and intestinal inflammation has also been observed. A mouse model expressing non-phosphorylatable EIF2 α in IECs resulted in functional abnormalities in Paneth cells and increased susceptibility to *Salmonella* infection and DSS-induced colitis (Cao et al., 2014). ATF6 α deficient mice exhibit increased ER stress as detected by elevated levels of BiP, ATF4, CHOP and spliced *XBP1*, which ultimately resulted in enhanced sensitivity to DSS-induced colitis (Cao et al., 2013). Additionally, hypomorphic mutation in *membrane-bound transcription factor peptidase S1P-encoding gene (Mbtps1)* that encodes S1P for cleavage of ATF6 causes enhanced susceptibility to DSS-induced colitis (Brandl et al., 2009). Although there is less extensive evidence for the role of aberrant PERK-EIF2 α and ATF6 pathways in IBD pathogenesis, their importance for appropriate ER stress responses in intestinal epithelium is apparent.

1.4.2. Autophagy and the UPR intersect: Implications in Crohn's disease

It is well known that the UPR can elicit an autophagy response in its attempts to relieve ER stress (Hart et al., 2012; Li et al., 2008; Ogata et al., 2006; Shimodaira et al., 2014; Wang et al., 2016). ER-stress-induced autophagy degrades misfolded proteins, aggregates and damaged organelles. There is also a distinct form of ER-stress-induced autophagy known as ER-phagy, that specifically degrades ER membranes and the autophagosomes are, at least in part, derived from the ER membrane (Song et al., 2017).

A recent study has shown that ER stress can be mediated by the innate immune sensor, stimulator of interferon genes (STING), in response to cyclic-di-AMP (c-di-AMP), a vital PAMP in live gram-positive bacteria (Moretti et al., 2017). This process induces autophagy via mTORC1 inhibition and interferon responses that localize STING to autophagosomes, and ultimately inhibits macrophage cell death.

Autophagy activity is high in Paneth cells (Adolph et al., 2013) to counterbalance high levels of ER-stress (Ogata et al., 2006), therefore ER-stress is a significant risk when the UPR or autophagy is not functional. Consistent with this, in Paneth cells of CD patients harbouring *ATG16L1 T300A* risk alleles, BiP and pEIF2 α were highly expressed (Deuring et al., 2014). *ATG16L1;XBP1 Δ IEC* mice develop similar phenotypic ileitis but earlier in life than *ATG16L1 Δ IEC* mice, due to increased ER stress (Adolph et al., 2013; Tschurtschenthaler et al., 2017). ERAD can regulate the degradation of IRE1 α to prevent accumulation of toxic IRE1 α aggregates, however persistent ER stress will inhibit ERAD degradation of IRE1 α . When this occurs autophagy has an important role in the clearance of supramolecular clusters of IRE1 α . In *ATG16L1 Δ IEC* mice, development of spontaneous CD-like ileitis is associated with defective autophagy resulting in toxic accumulation of IRE1 α in Paneth cells (Tschurtschenthaler et al., 2017). In humans homozygous for *ATG16L1 T300A*, a similar accumulation of IRE1 α was observed in intestinal epithelial crypts (Tschurtschenthaler et al., 2017). This has led to suggestion that the *ATG16L1 T300A* SNP may define a specific subtype of patients with CD, characterised by Paneth cell ER stress which correlates with bacterial persistence, and reduced antimicrobial functionality (Deuring et al., 2014). Furthermore, the synergistic

and compensatory relationship between the UPR and autophagy, which is contextualised by the CD-associated SNPs in *ATG16L1* and *XBP1*, is also highlighted.

Interestingly, a recent study has demonstrated a direct link between NOD1/2 and the IRE1 α pathway in the context of ER-stress-induced inflammation (Keestra-Gounder et al., 2016). When activated the IRE1 α kinase domain activates the JNK pathway and recruits TRAF2 (TNF receptor-associated factor 2) to the ER membrane to trigger NF κ B signalling (Kaneko et al., 2003; Urano et al., 2000) and autophagy induction (Castillo et al., 2011; Ding et al., 2007; Ogata et al., 2006). In mouse and human cells, ER stress induced by chemical ER stress inducers or infection with *Brucella abortus* and *Chlamydia muridarum* increased inflammation and IL-6 production (Keestra-Gounder et al., 2016). This response was dependent on NOD1/2 and RIP2, but also on IRE1 α kinase activity and TRAF2-induced NF κ B signalling (Keestra-Gounder et al., 2016). This suggests there is a functional intersection between the IRE1 α pathway and NOD1/2 signalling, which is facilitated by TRAF2.

In a range of colonic cell lines, chemical ER stress inducers activated autophagy, regulated by enhanced CHOP expression, which also promoted the IRE1 α pathway (Shimodaira et al., 2014). In endothelial cells IRE1 α -dependent splicing of *XBP1* mRNA activated autophagy via up-regulation of *Beclin-1* (Margariti et al., 2013). Contrary to expectations, *XBP1* deletion in a familial amyotrophic lateral sclerosis (fALS) mouse model increased autophagy, which enhanced clearance of accumulated toxic superoxide dismutase-1 (SOD1) aggregates (Hetz et al., 2009). It was suggested that in this scenario autophagy is induced in a compensatory manner due to attenuated UPR.

The UPR and autophagy also intersect at the PERK-EIF2 α -ATF4 pathway (Avivar-Valderas et al., 2013; Ji et al., 2015; Jia et al., 2015; Kouroku et al., 2007; Moon et al., 2016; Zhao et al., 2013). In an *in vitro* model of osteosarcoma, PERK induced autophagy via mTORC1 inhibition, to promote survival in response to ER stress-conferred chemoresistance to apoptosis (Ji et al., 2015). Additionally, PERK mediated autophagy via AMPK-dependent inhibition of mTORC1, in response to extracellular matrix (ECM) detachment in mammary epithelial cells (MECs) (Avivar-Valderas et al., 2013). The main purpose of PERK signalling is to reduce protein synthesis and the inhibition of mTORC1 promotes this effect as mTORC1 pathway controls synthesis of ~15-20% of protein within the cell

(Laplante and Sabatini, 2012). This, therefore, has a dual purpose of inhibiting protein synthesis and inducing autophagy to degrade misfolded proteins.

The PERK-EIF2 α -ATF4 pathway can also be involved in the transcriptional up-regulation of autophagy genes. Polyglutamine-induced ER stress was associated with increased LC3-I to LC3-II conversion, facilitated by pEIF2 α up-regulation of *ATG12* to promote ATG5-ATG12-ATG16L1 complex formation in mouse embryonic carcinoma cells (Kouroku et al., 2007). During amino acid deprivation ATF4 and CHOP can bind specific C/EBP-ATF Response Elements (CAREs), known as Amino Acid Response Elements (AAREs) and CHOP-Response Elements (CHOP-REs), either independently or bound together in heterodimers, to induce transcription of autophagy genes including *ATG16L1*, *MAP1LC3B*, *ATG12*, *ATG3*, *Becn1*, *Sqmt1*, *Nbr1*, *ATG7*, *ATG10*, *ATG5* and *Gabarap* (B'chir et al., 2013). In other studies, hypoxia or ECM detachment can induce PERK-dependent autophagy, associated with up-regulation of *MAP1LC3B*, *Becn1* and *ATG5* via ATF4 and CHOP (Avivar-Valderas et al., 2011; Rouschop et al., 2010; Rzymiski et al., 2010). This up-regulation of autophagy gene transcription by ATF4 and CHOP was shown to replenish autophagy proteins to promote survival during cellular stress (Rouschop et al., 2010). However, if the cellular stress is prolonged or intense the transcription factor CHOP can also act to up-regulate genes for apoptosis. This identifies yet another mechanism for regulating the relationship between autophagy and apoptosis in response to cellular stress.

ATF6 has also been implicated mechanistically in autophagy induction. In response to cellular stress IFN- γ activates the Ask1 (Apoptosis signal-regulating kinase 1)/MAPK pathway, which phosphorylates ATF6 to allow its proteolytic activation (Gade et al., 2014). ATF6 interaction with C/EBP- β is then essential for IFN- γ -induced *DAPK1* up-regulation and subsequent stimulation of autophagy (Gade et al., 2012). Mice lacking either ATF6 or Ask1 were highly susceptible to bacterial infection due to defective autophagy (Gade et al., 2014, 2012). Furthermore, activated ATF6 was shown to stimulate Akt, which resulted in the negative regulation of mTORC1, and ULK1 activation (Appenzeller-Herzog and Hall, 2012; Yamazaki et al., 2009).

In a recent study in MCF-7 human breast cancer cells, the chemopreventative agent ursolic acid (UA)-induced ER-stress was an effect rather than cause of autophagy activation (Zhao et al., 2013). UA induced autophagy via MAPK1/3 signalling, and

subsequent promotion of PERK signalling activated MCL1, the Bcl-2 related protein, to inhibit apoptosis. Furthermore, another study in human ovarian cancer cells showed interdependent activation of autophagy and the PERK-EIF2 α UPR pathway when treated with metformin, which causes energy starvation (Moon et al., 2016). In these scenarios an unconventional relationship between autophagy and ER stress was uncovered, which remains to be mechanistically solved. Nonetheless, in these circumstances the intertwining of the UPR and autophagy pathways has pro-survival outcomes.

The convergence between autophagy and UPR pathways is important for efficient resolution of ER stress to maintain intestinal homeostasis, which ultimately confers protection against intestinal infections and inflammation. This, therefore, provides new opportunity for the treatment of IBD. For example, modulation of the UPR in combination with autophagy inducers is a promising therapeutic strategy.

1.5. Current IBD treatments and Autophagy

The efficacy of current drugs for the treatment of IBD continues to come under scrutiny as response to treatment often diminishes over time, resulting in disease complications including abscesses, fistulas and strictures. Furthermore, a review of worldwide cohorts estimated that between 10–35% of CD patients required surgery within a year of diagnosis and up to 61% by 10 years (Bernstein et al., 2012). Development of new drugs is a long and expensive process associated with high failure rates; therefore making better use of drugs that have already been approved for clinical use is essential. The Crohn's and Colitis Foundation of America has highlighted this need for research into optimising medical therapies (Denson et al., 2013), with patient stratification and personalised medicine of key importance in this context (Fiocchi, 2015). In order to improve the efficacy of existing drugs a more comprehensive characterisation of their mechanism of action is required.

There is evidence that inducing autophagy can have therapeutic benefits for the treatment of IBD, as several studies have investigated the role of autophagy inducers as adjuvant therapies for IBD. Rapamycin analogues, sirolimus and everolimus, inhibit mTORC1 to induce autophagy and are already approved for clinical use for post-transplantation management. In IL-10-deficient mice, everolimus treatment alleviated

spontaneous colitis and reduced CD4+ T cells and IFN- γ (Matsuda et al., 2007). In a case study sirolimus improved symptoms and intestinal healing in a patient with severe refractory CD (Massey *et al.*, 2008). In another case study, symptoms were controlled with everolimus treatment for 1 ½ years in a refractory UC patient (Dumortier et al., 2008). Moreover, in a study of refractory paediatric IBD, sirolimus induced clinical remission in 45% of UC patients and 100% of CD patients; however, sample size was small (Mutalib et al., 2014). Everolimus had comparable safety and tolerability as azathioprine when used to maintain steroid-induced remission in a cohort of adult CD patients (Reinisch et al., 2008).

Progress has been made in recent years towards characterising IBD drug effects (Table 1.2), with the modulation of immunoregulatory signalling pathways often linked directly or indirectly to the autophagy response (Table 1.3). These heterogeneous studies have been conducted in a wide variety of disease settings and cell types; highlighting the need to explore the effect of these drugs on autophagy pathway activity in the context of IBD.

Table 1.2: IBD Drug Mechanism of Action

Five main IBD drug classes shown, with examples of drugs in each class and known mechanism of action (Campregher and Gasche, 2011¹; Ciechomska et al., 2013²; Kuenzig et al., 2014³; Stocco et al., 2015⁴; Tiede et al., 2003⁵; Van den Brande et al., 2003⁶).

Drug Class	Examples	Mechanism of action
Corticosteroids	Prednisolone, Budesonide	<ul style="list-style-type: none"> • Downregulation of pro-inflammatory cytokines³ • Interference with NFκB inflammatory signalling³
Aminosalicylates	Sulfasalazine, Mesalazine	<ul style="list-style-type: none"> • ROS scavenging, anti-oxidant upregulation and inhibition of nitric oxide formation¹ • Inhibition of leukocyte motility and activation¹ • Interference with NFκB and pro-inflammatory cytokines¹ • Prevention of mitochondrial damage¹ • Colonic epithelial cell arrest in S-phase¹
Thiopurines	Azathioprine, 6-mercaptopurine	<ul style="list-style-type: none"> • Inhibition of DNA, RNA and protein synthesis, results in immune-suppression and cytotoxicity⁴ • Induce T cell apoptosis through co-stimulation of CD28 due to the blockage of RAC1 activation of NFκB⁵
Immuno-modulators	Methotrexate, cyclosporine and tacrolimus	<ul style="list-style-type: none"> • Methotrexate inhibits DNA and RNA synthesis in rapidly dividing cell² • Cyclosporine and tacrolimus alter IL-2 transcription causing reduced T-cell activity²
Biological Agents (Anti-TNF agents)	Infliximab, Adalimumab	<ul style="list-style-type: none"> • Neutralize TNF-α to prevent pro-inflammatory functions • Induce apoptosis in activated T cells and monocytes⁶

Table 1.3: IBD Drug Modulation of Autophagy

Five main IBD drug classes and evidence of modulation of autophagy pathway (Chacon-Cabrera et al., 2014¹; Ciechomska et al., 2013²; Fatkhullina et al., 2014³; J. Gao et al., 2016⁴; W. Gao et al., 2016⁵; Han et al., 2014⁶; Harr et al., 2010⁷; Harris and Keane, 2010⁸; He et al., 2016⁹; Kim et al., 2014¹⁰; Kimura et al., 2013¹¹; Kyrmizi et al., 2013¹²; Laane et al., 2009¹³; Levin et al., 2016¹⁴; Nakagaki et al., 2013¹⁵; Oancea et al., 2017¹⁶; Pallet et al., 2008¹⁷; Shi et al., 2015¹⁸; Swerdlow et al., 2008¹⁹; Tang et al., 2018²⁰; Tsai et al., 2013²¹; Varshney and Saini, 2018²²; Wang et al., 2006²³; Wildenberg et al., 2017²⁴; Xia et al., 2010²⁵; Xie et al., 2017²⁶; Xu et al., 2015²⁷; Xue et al., 2016²⁸; Zeng et al., 2007²⁹; Zeng and Kinsella, 2010³⁰, 2008³¹).

Drug Class	Evidence of autophagy modulation
Corticosteroids	<ul style="list-style-type: none"> Inhibition of mTORC1 to induce autophagy in a range of cell types^{3, 4, 7, 9, 23, 28} Induction of autophagy to promote viability in osteocytes^{18,25} Dexamethasone induced autophagy and apoptosis in T lymphocytes^{13,19} Prednisolone inhibited autophagy <i>in vivo</i> and in cell lines^{5,20} Inhibition of autophagy in human monocytes infected with <i>Aspergillus fumigatus</i>¹²
Aminosalicylates	<ul style="list-style-type: none"> Sulfasalazine decreased autophagy via NFκB inhibition in a murine model of cachectic cancer¹ Sulfasalazine induced autophagic cell death via inhibition of Akt and activation of ERK pathway in an OSCC cell line⁶
Thiopurines	<ul style="list-style-type: none"> Increased autophagy and apoptosis mediated by MMR-processing²⁹⁻³¹ Inhibition of RAC1 restores DC migration defect caused by autophagy deficiency²⁴ Increased autophagy due to rapid local bacterial conversion of thioguanine pro-drug in murine colitis model¹⁶
Immunomodulators	<ul style="list-style-type: none"> Methotrexate inhibited autophagy via mTORC1 activation in SCC cells²¹ Methotrexate induced autophagy in OA-FLS cells and keratinocytes via HMGB1 and Beclin 1^{22, 27} Cyclosporine cytotoxicity induced autophagy as a survival process in a range of cell types^{2, 11, 17} Cyclosporine induced autophagic-cell death in a rat pituitary cell line¹⁰ Tacrolimus induced autophagy in neuronal cells¹⁵
Biological Agents (Anti-TNF agents)	<ul style="list-style-type: none"> Anti-TNF agents can induce reactivation of TB, partially due to decreased autophagy⁸ Infliximab increased and prolonged autophagy in murine model of retinal detachment²⁶ Anti-TNF agents induce differentiation of monocytes to regulatory macrophages via augmented autophagy¹⁴

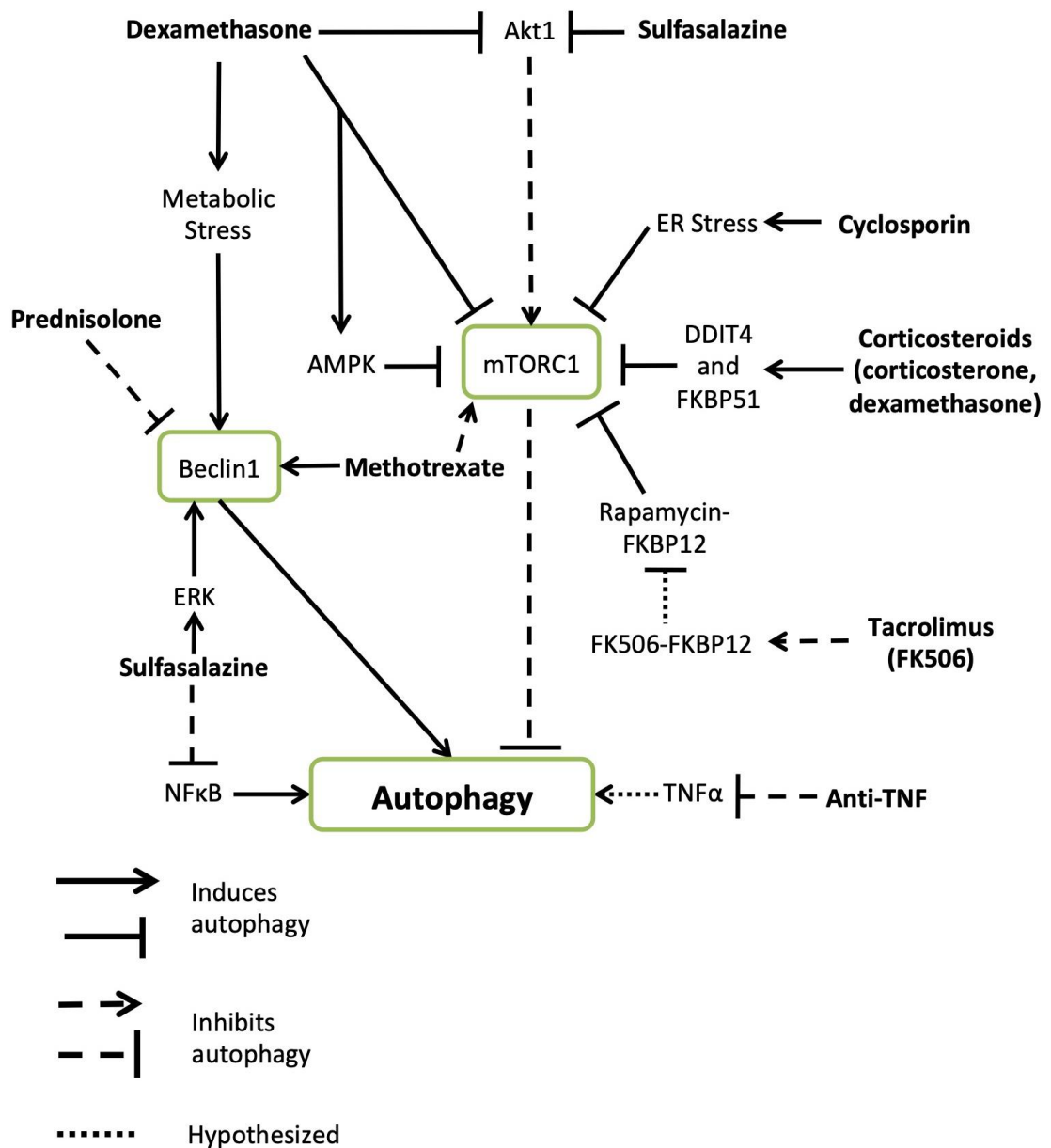


Figure 1.7: IBD Drug Modulation of Autophagy

Evidence of corticosteroid, aminosalicylate, immunomodulator and biological agent modulation of autophagy and autophagy signalling. Further details in Section 1.5

1.5.1. Corticosteroids

First-line treatment for CD and UC is often corticosteroids. These drugs are used to treat many autoimmune diseases, such as rheumatoid arthritis and lupus, due to their anti-inflammatory properties. Most studies with paediatric IBD have been undertaken using prednisolone or methylprednisolone, but other corticosteroids can be used, including Budesonide (Wilson et al., 2010). Corticosteroids downregulate pro-inflammatory cytokines including IL-1, IL-6 and TNF- α by inhibiting the transcription of genes involved

in their production and affecting the stability of mRNA to inhibit protein expression (Table 1.2) (Kuenzig et al., 2014). Furthermore, inflammatory signalling induced by NF κ B is decreased due to interaction with corticosteroid receptors (Table 1.2) (Kuenzig et al., 2014).

Corticosteroid therapy can be very effective for IBD treatment, as it has been shown to induce remission in up to 84% of children with CD (Markowitz, 2008). However, the adverse side effects of corticosteroids can be very severe due to their non-specific downregulation of immune processes and other metabolic pathways. The side effects include increased risk of infection, osteoporosis, growth retardation, pancreatitis, glucose intolerance, adrenal insufficiency, cataracts, glaucoma, Cushing syndrome, hypertension, weight gain, acne and mood disturbances (Diefenbach and Breuer, 2006; Markowitz, 2008). Therefore, prolonged use of corticosteroids in paediatric cases is undesirable. Nevertheless, steroid dependence is common with 30-40% of patients remaining on steroids at one year, when a common course is recommended for only 8-10 weeks (Wilson et al., 2010).

There has been progress in understanding the effect of corticosteroids on autophagy activity in a range of disease settings. Clinical response to corticosteroids in UC patients has been linked to mTORC1. In a transcriptomics study, it was observed that miRNA and mRNA profiles in the rectal mucosa of UC patients differed between responders and non-responders to corticosteroid treatment (Naves et al., 2015). The mRNA with the most significant differential expression between groups was DNA damage-induced transcript 4 (DDIT4), an inhibitor of mTORC1 activity, which was upregulated in responders after three days of corticosteroid treatment (Figure 1.7).

In the hippocampus of rats, it has also been shown that corticosterone treatment affects mTORC1 signalling pathways (Polman et al., 2012). In this study, corticosterone up-regulated the expression of DDIT4, as well as FK506-binding protein 51 (FKBP51), but down-regulated DDIT3. DDIT4 and FKBP51 inhibit mTORC1 activity, whereas the pro-apoptotic transcription factor DDIT3 is itself regulated by mTORC1 (Figure 1.7) (Polman et al., 2012). In agreement, Wang *et al.* (2006) found that dexamethasone treatment of *in vivo* skeletal muscle and cultured L6 myoblasts increased DDIT4 expression and confirmed that DDIT4 down-regulates mTORC1 activity (Figure 1.7 and Table 1.3). In a

rat model of placental angiogenesis, a rat cell line representing muscle atrophy and in human umbilical vein endothelial cells (UVEC) corticosteroids inhibited the Akt pathway, a known mTORC1 activator, (Girón et al., 2015; Ozmen et al., 2016, 2015) and activated the AMPK pathway, an inhibitor of mTORC1 (Figure 1.7) (Troncoso et al., 2014). Another study, investigating the effects of dexamethasone treatment on T-lymphocytes from healthy donors, found that there was a reduction in mTORC1 expression (Figure 1.7 and Table 1.3) (Fatkhullina et al., 2014). Furthermore, dexamethasone inhibition of mTORC1 resulted in increased autophagy activity in rat chondrocytes (Xue et al., 2016), a human placental choriocarcinoma cell line (BeWo) (He et al., 2016) a osteocyte-like cell line (MLO-Y4) and in primary murine calvarial osteocytes (Figure 1.7 and Table 1.3) (J. Gao et al., 2016). These studies strongly suggest that the mechanism of action of corticosteroids is, in part, through the inhibition of the mTORC1 pathway and increased autophagy.

Several studies have investigated the effects of corticosteroids on osteocyte cell fate. Glucocorticoids have been shown to enhance osteoclastogenesis, *in vitro* and *in vivo*, in an ROS-induced autophagy dependent manner (Table 1.3) (Shi et al., 2015). Furthermore, low doses of prednisolone and dexamethasone, *in vitro* and *in vivo*, induce autophagy in osteocytes and this is associated with increased osteocyte viability (Table 1.3) (Xia et al., 2010). However, higher doses of corticosteroids induced apoptosis, suggesting that autophagy may act as a protective mechanism against the cytotoxic effects of corticosteroids (Weinstein et al., 1998).

Corticosteroids are also used to treat lymphoid malignancies and it has been shown that glucocorticoids induce autophagy in immature T cell populations (Harr et al., 2010), lymphoid cell lines (Swerdlow et al., 2008) and primary leukaemia cells (Table 1.3) (Laane et al., 2009). The dexamethasone-induced autophagy was also associated with inhibition of mTORC1, possibly through regulation of the Src kinase Fyn pathway (Figure 1.7) (Harr et al., 2010). Swerdlow *et al.* (2008) suggested that a contributing factor to dexamethasone-induced autophagy could be metabolic stress caused by reduced glycolysis and glucose uptake in corticosteroid-treated lymphocytes (Figure 1.7).

Autophagy stimulation by glucocorticoids is relevant for treatment of lymphoid malignancies as it is intimately linked to the induction of apoptosis in T lymphocytes (Laane et al., 2009; Swerdlow et al., 2008). Corticosteroids are able to induce apoptosis

in immature T lymphocytes as these cells lack the inhibitor of apoptosis protein Bcl-2 (Swerdlow et al., 2008). Although Bcl-2 usually acts to inhibit autophagy by binding to Beclin1 (Figure 1.4), it has been shown that overexpression of Bcl-2 in immature T lymphocytes can increase autophagy levels, presumably due to inhibition of apoptosis (Swerdlow et al., 2008). Furthermore, autophagy induction prolonged the survival of dexamethasone-treated cells (Swerdlow et al., 2008). In contrast Laane *et al.* (2009) found that autophagy played a positive role in dexamethasone-induced apoptosis in lymphoid leukaemia cells. In this study dexamethasone induced cell death through promyelocytic leukaemia (PML) protein-dependent dephosphorylation of the autophagy inhibitor Akt, stimulating the induction of autophagy.

In certain scenarios corticosteroids have demonstrated autophagy-inhibiting activity. In a rat model of osteoporosis, prednisolone inhibited autophagy, as observed by downregulation of Beclin1, Atg5 and LC3-II, and induced apoptosis (Table 1.3) (Tang et al., 2018). Methylprednisolone also suppressed autophagy activity in a neuroblastoma cell line (Neuro-2a) (Table 1.3) (W. Gao et al., 2016). Additionally, autophagy was activated in spinal cord injuries (SCL) along with apoptosis and necrosis, but rats treated with methylprednisolone exhibited decreased autophagy post-SCL (Chen et al., 2012). The effects of methylprednisolone on autophagy in this study may therefore be attributed to direct inhibition of autophagy or due to a decrease in inflammation associated with injury, which indirectly reduces autophagy.

Corticosteroids also block autophagy protein recruitment to pathogen-containing phagosomes in human monocytes infected with *Aspergillus fumigatus* (Kymizi et al., 2013). Detection of the fungal ligand β -glucan by Dectin-1 receptors, triggered Syk (Spleen tyrosine kinase) kinase-dependent production of ROS, which stimulated autophagy (Kymizi et al., 2013). When autophagy was directly inhibited, or cells were treated with corticosteroids (*in vivo* and *ex vivo*), phagosome maturation (including fusion with the lysosome) and *A. fumigatus* killing were impaired (Table 1.3) (Kymizi et al., 2013). This highlights the importance of autophagy as a defence mechanism against fungal infections, but contradicts studies suggesting that autophagy is induced by corticosteroid treatment.

The contrasting results in these studies could be due to differences in the disease pathogenesis investigated, the types of corticosteroids used, or the different types of

autophagy that were investigated. For instance, studies showing decreased autophagy used prednisolone/methylprednisolone instead of other corticosteroids often used in cancer therapy, or focused on the effects of corticosteroids on xenophagy with *A. fumigatus*. Whereas, opposing studies focused on non-selective autophagy induced by cellular stress. This serves to highlight the cell-type specific and context-dependent nature of autophagy and the need to investigate the effect of corticosteroids on cell types that are relevant to IBD.

1.5.2. Aminosalicylates

Aminosalicylates are effective as first line drugs to induce and maintain remission in mild to moderate cases of UC (Turner et al., 2012), and there is some evidence of their efficacy in prevention of post-operative CD recurrence (Z. Yang et al., 2014). Despite the minimal evidence for their efficacy in CD treatment, they are often prescribed as adjuvant therapy due to minimal side effects, low cost and chemo-preventative properties (Diefenbach and Breuer, 2006; Schoepfer et al., 2014). Sulfasalazine or salicylazosulfapyridine (SASP) was originally developed for rheumatoid arthritis and contains 5-Aminosalicylate (5-ASA) bound to sulfapyridine (CCFA, 2013). Sulfapyridine exhibits direct antimicrobial activity, and treatments with sulfapyridine have been linked to alterations in faecal bacterial profiles (Campregher and Gasche, 2011). Sulfapyridine has been associated with additional adverse effects (Diefenbach and Breuer, 2006), leading to the development of other forms of aminosalicylates without sulfapyridine, including Mesalazine and its pro-drugs Balsalazide and Olsalazine (CCFA, 2013).

The anti-inflammatory activities of 5-ASA include scavenging of damaging ROS, upregulation of endogenous antioxidant systems, inhibition of leukocyte motility, leukotriene and platelet activation, interference with NF κ B1, TNF- α , IL-1 and TGF- β , inhibition of nitric oxide formation, prevention of mitochondrial damage and colonic epithelial cell-cycle arrest in S-phase (Table 1.2) (Campregher and Gasche, 2011). In theory, many of these activities could directly or indirectly affect autophagy due to a reduction of cellular stress. One study, investigating sulfasalazine as an NF κ B inhibitor in an *in vivo* murine model of cancer cachexia, reported a decrease in autophagy (Figure 1.7 and Table 1.3) (Chacon-Cabrera et al., 2014). This could be due to a direct effect of

NFκB inhibition, as NFκB signalling regulates autophagy in a context-dependent manner (Salminen et al., 2012), or through one or more of the other pathways regulated by sulfasalazine. In addition, this response may be specific to the disease or to the muscle tissues being examined in murine models.

In contrast, Han *et al.* (2014) reported that sulfasalazine treatment in an oral squamous cell carcinoma (OSCC) cell line, HSC-4, induced autophagic cell death through inhibition of the Akt pathway and activation of the ERK pathway (Figure 1.7 and Table 1.3). The seemingly opposing effects of sulfasalazine observed in these studies may be due to differences in dosage. Dosage is extremely difficult to compare between *in vitro* and *in vivo* studies, however it is possible the induction of autophagic cell death observed by Han *et al.* (2014) may be representative of a cytotoxic concentration range.

1.5.3. Thiopurines

Thiopurines, including azathioprine, 6-mercaptopurine and 6-thioguanine, are immunosuppressant drugs used to treat IBD (Guijarro et al., 2012). They have a relatively slow onset, but can maintain remission in moderate to severe cases of CD and have also shown some effectiveness for the induction of remission (Diefenbach and Breuer, 2006; Gisbert et al., 2011). However, only 30% of CD patients achieve complete steroid-free remission after 6 months of azathioprine therapy (Colombel et al., 2010). Furthermore, adverse effects are observed in 25-30% of children treated with thiopurines (Kirschner, 1998), and 15-20% of adult patients treated with thiopurines have to discontinue treatment due to these side effects (Stocco et al., 2015). The most severe side effects of thiopurines are myelosuppression and hepatotoxicity, which are observed in 10-15% paediatric patients (Dubinsky, 2004) and 3.5-4.5% of adult patients (Giverhaug et al., 1996; Shaye et al., 2007). Erythrocyte concentrations of thiopurine metabolites can be monitored to maintain therapeutic levels and avoid toxicity (Gardiner et al., 2008). Due to higher levels of drug metabolites with 6-TG treatment compared to 6-MP and azathioprine, there is more hepatic toxicity with this treatment; therefore, 6-TG is used mainly for cancer therapy instead of IBD (Dubinsky, 2004).

The commonly used pro-drug azathioprine is converted to 6-mercaptopurine (6-MP) with release of the imidazole ring through a conjugation reaction with anti-oxidant

glutathione (GSH) in the intestinal wall, which can lead to GSH depletion (Figure 1.8) (Eklund et al., 2006). This can occur spontaneously or can be facilitated by glutathione S-transferases (GST), which generates ROS (Aarbakke et al., 1997). 6-MP is then metabolised to the inactive metabolites thiouric acid (6-TU) by xanthine oxidase (XOD), generating more ROS (Alice U. Lee and Farrell, 2001), or 6-methylmercaptopurine (6-MMP) by thiopurine methyltransferase (TPMT) (Figure 1.8). 6-MP is also converted to active 6-thioinosine monophosphate (6-TIMP) by hypoxanthine-guanine phosphoribosyl transferase (HPRT). 6-TIMP can be methylated by TPMT to methyl-6-TIMP, which prevents *de novo* synthesis of purines (Figure 1.8). 6-TIMP is also metabolized in a multi-step reaction to 6-thioguanosine monophosphate (6-thioGMP) by inosine monophosphate dehydrogenase (IMPDH) and guanosine monophosphate synthetase (GMPS) (Figure 1.8). 6-thioGMP is phosphorylated several times to 6-thioguanosine triphosphate (6-thioGTP) (Figure 1.8) (Elion, 1989). 6-TG, on the other hand, is directly metabolised to 6-thioGMP by HPRT, then phosphorylated to 6-thioGTP (Figure 1.8) (Elion, 1989).

6-thioGTP has been shown to induce T cell apoptosis through co-stimulation of the CD28 receptor due to blockage of Ras-related C3 botulinum toxin substrate 1 (Rac1) activation of NFκB (Figure 1.8 and Table 1.2) (Tiede et al., 2003). 6-thioGTP is also incorporated into genomic DNA (Figure 1.8 and Table 1.2) (Elion, 1989). Once incorporated into the DNA 6-thioGTP is methylated by S-adenosylmethionine to S⁶-methylthioguanine, which pairs with thymine and cytosine during DNA replication, causing mismatched base pairs (Swann et al., 1996). In response, DNA mismatch repair (MMR) is activated to excise damaged DNA (Figure 1.8) (Yan et al., 2003). This, however, can cause DNA single-stranded breaks, activating apoptosis (Figure 1.8) (Yan et al., 2003). Furthermore, protein complexes that are recruited to the single stranded DNA (ssDNA) and MMR proteins that bind to O⁶-methylguanine adducts cause p53-induced apoptosis (O'Brien and Brown, 2006).

It has been shown, in MMR-proficient colonic cell lines (HCT116 and HT29), that activated p53 is also essential for 6-TG-induced autophagy, potentially by enhancing expression of autophagy genes (Figure 1.8 and Table 1.3) (Zeng et al., 2007). It was subsequently shown that the BH3-only protein BNIP3 is also required for 6-TG-induced autophagy and that its enhanced transcription is mediated by p53 (Zeng and Kinsella,

2010). BNIP3 causes PTP in mitochondria, decreasing mitochondrial potential and resulting in release of ROS. Enhanced ROS production triggered autophagy to promote degradation of damaged mitochondria in cells treated with all three thiopurine drugs (Figure 1.8) (Chaabane et al., 2016; Zeng and Kinsella, 2010). This ROS-dependent increase in autophagy activity has a pro-survival role as it inhibits apoptosis (Chaabane et al., 2016; Zeng et al., 2007).

Investigating this further, it was found that 6-TG-induced autophagy in HCT116 MMR-proficient cells and HT29 cells was regulated by mTORC1. Contradictory to the established function of mTORC1; in this scenario mTORC1 positively regulated both autophagy and apoptosis through S6K1 (Ribosomal protein S6 kinase beta-1) activation (Zeng and Kinsella, 2008). This was mediated via inhibition of Akt, which can act to inhibit both autophagy and cell death (Zeng and Kinsella, 2008). Inhibition of mTORC1 also abrogated 6-TG-induced increases in BNIP3 (Zeng and Kinsella, 2010). As mTORC1-S6K1 has an important role in protein translation, it was speculated that S6K1 enhances translation of BNIP3 in response to 6-TG, which overrode the negative regulation of autophagy by mTORC1.

A recent study has correlated *ATG16L1* genotype and response to thiopurines in two IBD cohorts, specifically showing the association in patients with CD but not with UC (Wildenberg et al., 2017). Furthermore, autophagy-deficient DCs, and DCs from CD patients with the *T300A* variant had cytoskeletal defects that reduced mobility of the myeloid cells, due to hyperactivation of RAC1 (Wildenberg et al., 2017). RAC1, a member of the Rho family of GTPases, is a known target for inhibition by thiopurines (Poppe et al., 2006; Tiede et al., 2003); therefore, thiopurine treatment reversed the cytoskeletal aberrations and restored DC migration via RAC1 inhibition and potentially induction of autophagy (Figure 1.8 and Table 1.3) (Wildenberg et al., 2017). RAC1 inhibition also destabilizes APC-T cell synapses (Poppe et al., 2006), meaning thiopurines have a role in regulation of APC activation of the adaptive immune system (Figure 1.8). It has been suggested that *ATG16L1* genotyping could be used to identify patients that would benefit from thiopurine treatment (Wildenberg et al., 2017).

In another recent study the rapid local bacterial conversion of thioguanine pro-drug to active metabolite was shown to augment autophagy in epithelial cells (Table 1.3). This

resulted in immune activation in animal colitis models, resulting in increased intracellular bacterial killing and decreased intestinal inflammation (Oancea, 2016).

Thiopurines seem to have two distinct mechanisms that affect autophagy activity. The ability of thiopurine metabolites to incorporate into genomic DNA primarily causes cytotoxicity, but autophagy is stimulated in this scenario to attenuate cell death. On the other hand, thiopurine inhibition of RAC1 can be linked to stimulation of autophagy activity and regulation of APC functions.

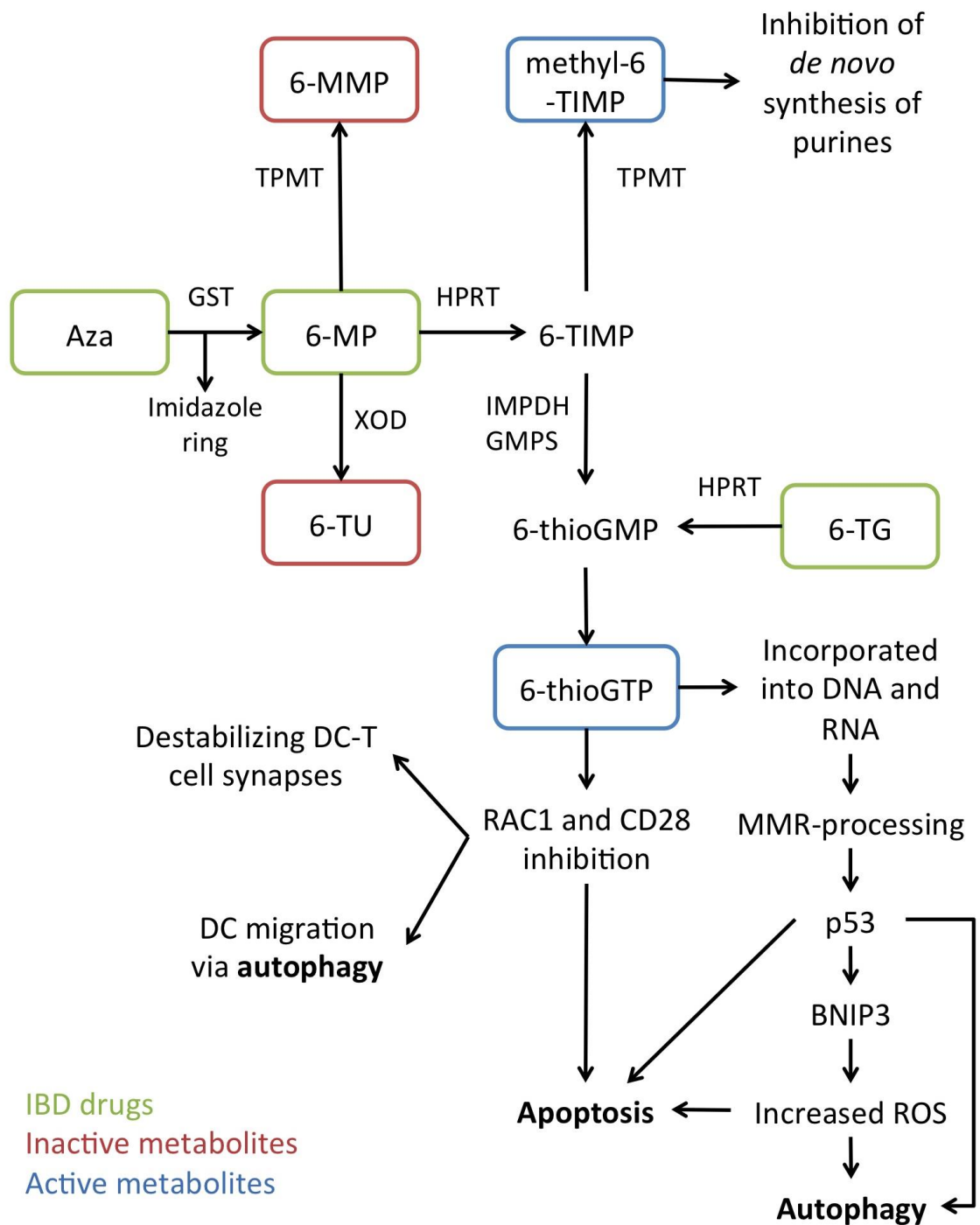


Figure 1.8: Thiopurine Metabolism, Mechanism of Action and Modulation of Autophagy

Metabolism of azathioprine, 6-mercaptopurine and 6-thioguanine, and known mechanism of action linked to autophagy and apoptosis. Further details in Section 1.5.3.

1.5.4. Immunomodulators: Methotrexate, Cyclosporin and Tacrolimus

Methotrexate, cyclosporin and tacrolimus are immunomodulatory drugs used mainly as second-line treatments to maintain remission in severe, steroid-refractory CD (Markowitz et al., 2002) with more recent evidence suggesting a role for tacrolimus in UC (Nuki et al., 2016). The use of these drugs is limited in CD patients due to severe side effects including myelosuppression, hepatitis, and renal and neurological effects (Diefenbach and Breuer, 2006).

Methotrexate, often used as a cancer therapy, inhibits DNA and RNA synthesis in rapidly dividing cells (Table 1.2) (Ciechomska et al., 2013). In squamous cell carcinoma (SCC) cells, methotrexate suppressed the autophagy pathway by phosphorylating and enhancing mTORC1 activity (Figure 1.7 and Table 1.3) (Tsai et al., 2013). However, in osteoarthritis fibroblast-like synovial (OA-FLS) cells (Xu et al., 2015) and keratinocytes (Varshney and Saini, 2018) methotrexate has been shown to induce autophagy. The mechanism of methotrexate-induced autophagy was not associated with modulation of the Akt/mTORC1 pathway, but was rather mediated through enhanced expression of high mobility group box chromosomal protein 1 (HMGB1) and Beclin 1 (Figure 1.7 and Table 1.3) (Xu et al., 2015).

Cyclosporin, originally used to prevent organ transplant rejection, acts by blocking lymphocyte and other immune cell activation due to altered IL-2 transcription (Table 1.2) (Ciechomska et al., 2013). As this drug has very cytotoxic effects, several studies have shown that treatment with cyclosporin can induce autophagy in response to the toxicity either as a survival process or as part of a cell death mechanism (Table 1.3) (Ciechomska et al., 2013; Kimura et al., 2013; Pallet et al., 2008). Toxic levels of cyclosporin induced autophagy *in vivo* and *in vitro* in malignant glioma cells (Ciechomska et al., 2013). This was accompanied by mTORC1 inhibition and an ER stress response, with blockage of ER signalling decreasing accumulation of the autophagy marker LC3-II (Figure 1.7 and Table 1.3) (Ciechomska et al., 2013). Furthermore, when autophagy is inhibited, by blocking of ULK1, Atg5 or Atg7, cyclosporin-induced cell death was shown to increase (Ciechomska et al., 2013). These results suggest that autophagy is induced as a protective response to the cytotoxic effects of cyclosporin.

In a study of cyclosporin-induced nephrotoxicity, ER stress-dependent autophagy induction (Figure 1.7 and Table 1.3) has been demonstrated in primary cultured human renal tubular cells and *in vivo* within rat kidneys (Pallet et al., 2008). In addition, cyclosporin can cause chronic metabolic stress, which leads to autophagy induction in kidney proximal tubule epithelial cells (Kimura et al., 2013). In this study, autophagy-competent cells allow for metabolic adaptation to cyclosporin treatment, whereas autophagy deficiency resulted in cyclosporin-induced deterioration of the tricarboxylic acid (TCA) cycle and the overall energy status of the cell. In a rat pituitary cell line model, cyclosporin induced apoptosis and autophagic-cell death in a dose-dependent manner (Kimura et al., 2013). From these studies, it appears that autophagy is stimulated by cyclosporin only as a secondary response to the drug's cytotoxic effects.

The mechanism of action of tacrolimus, also known as FK506, is similar to cyclosporin as both drugs inhibit the protein phosphatase calcineurin to block T cell function and IL-2 transcription (Ciechomska et al., 2013). FK506 inhibits calcineurin by forming a complex with the immunophilin FKBP12 (FK506 binding protein 12), which is involved in immunoregulation (Liu et al., 1992). FKBP12 is also the direct target of rapamycin, the mTORC1 inhibitor.

A recent study by Ge *et al.* (2014) investigating a novel activator of mTORC1, 3-benzyl-5-((2-nitrophenoxy) methyl)-dihydrofuran-2(3H)-one (3BDO), demonstrated that 3BDO could activate mTORC1 by occupying the rapamycin-binding site in FKBP12 (Amiot and Peyrin-Biroulet, 2015). This study suggested that FK506, through a mechanism involving the formation of an FK506-FKBP12 complex, has the potential to act as an mTORC1 activator and autophagy inhibitor (Figure 1.7). However, in another study, investigating the use of FK506 as a novel therapeutic for prion infections, FK506 was shown to induce autophagy in mouse neuroblastoma (N2a58) and mouse microglial (MG20) cell lines and in the brains of mice (Table 1.3) (Nakagaki et al., 2013). FK506 treatment significantly increased LC3-II, Atg5, Atg7 and autolysosome formation, concomitant with decreased prion protein levels in cell cultures and increased survival of mice due to delayed accumulation of prion proteins (Nakagaki et al., 2013). Therefore, the effect of tacrolimus on autophagy needs to be investigated more extensively in varying scenarios to conclusively determine its effect on mTORC1 and autophagy.

1.5.5. Biological agents: Anti-TNF- α

Overproduction of pro-inflammatory cytokines and chemokines are a common feature associated with inflammatory diseases. Monoclonal antibodies that target and neutralise cytokines such as TNF- α , IL-12, IL-23, IL-21, IL-22, IL-32 and IFN- γ are used for the treatment of IBD (Nys et al., 2013). The most commonly used biological agent for IBD is the anti-TNF- α antibody, Infliximab. Other anti-TNF- α treatments approved for treatment of IBD patients include Adalimumab, Golimumab for UC only, and Certolizumab pegol, which is approved in the USA, Switzerland and Russia. Anti-TNF- α biosimilars, which are less expensive versions of licensed biological agents whose patents have now expired, have also recently been developed (de Ridder et al., 2015). These biological agents are usually reserved for the treatment of refractory CD or steroid-dependent patients to induce and maintain remission. Studies have shown that Infliximab can only induce remission in roughly 50% of CD patients (Akobeng and Zachos, 2004) but in a recent study of paediatric cases, the treatment induced remission in 85% of patients (Ruemmele et al., 2009). This reiterates the differences between adult and paediatric cases of CD and therefore the need for separate investigations of the disease. One of the main causes of diminished response to biological agents is the development of anti-drug antibodies in patients. However, combination with low dose immunosuppressant thiopurines can reduce risk of antibodies to anti-TNF- α and enhances the probability of clinical remission (Boyapati et al., 2017). The side effects associated with biological agents remain severe and can include infusion reaction, nausea, fever/chills, hives, fatigue and even a long-term risk of T cell lymphoma (Diefenbach and Breuer, 2006).

Anti-TNF- α antibodies in IBD, neutralize TNF- α mainly produced by inflammatory macrophages and T cells, but can also induce apoptosis of activated T cells and monocytes (Table 1.2) (Van den Brande et al., 2003). TNF- α plays a major role in modulating inflammatory responses, and while the effects of TNF- α have been extensively studied in a variety of cell types, its mechanism of action in the gut remains unclear. One confirmed effect of TNF- α is the modulation of autophagy, which has been observed in synovial fibroblasts from rheumatoid arthritis patients (Connor et al., 2012), in skeletal muscle (Keller et al., 2011), in atherosclerotic vascular smooth cells (Jia et al., 2006) and in trophoblastic cells (Cha et al., 2014). Furthermore, mouse macrophages

activated by TNF- α have increased mitophagy resulting in increased mitochondrial protein degradation and enhanced MHC I presentation to T cells (Bell et al., 2013).

Taken together, these studies imply that anti-TNF agents would inhibit autophagy (Figure 1.7). Although there are no studies that have directly confirmed this, there is support for this hypothesis as anti-TNF agents can induce reactivation of *Mycobacterium tuberculosis*, at least partially due to decreased autophagy (Table 1.3) (Harris and Keane, 2010). This effect is likely due to the protective antibacterial and anti-inflammatory roles of autophagy in epithelial cells infected with this non-motile bacillus (Castillo et al., 2012). Additionally, *Andrographis paniculata* plant extract (HMPL-400), which is currently being studied in IBD trials for reduction of TNF- α , IL-1 β , IFN- γ and IL-22 expression, has been shown to inhibit autophagy in cancer (Zhou et al., 2012). This may be due to the reduction of cytokines or another mechanism affected by HMPL-400.

It is worth noting, however, that TNF- α can also have inhibitory effects on autophagy in some contexts. A study investigating the effects of elevated TNF- α on congestive heart failure in H9C2 rat cardiomyoblasts found that although TNF- α induces autophagy, autophagic protein degradation is disrupted, as evidenced by accumulation of p62 and increased ubiquitin-proteasome pathway activity (Opperman and Sishi, 2015). Furthermore, there is growing evidence that anti-TNF agents also have the ability to increase autophagy activity. In a murine model, infliximab augmented and prolonged autophagy responses to retinal detachment, which promoted cell survival (Table 1.3) (Xi et al. 2017).

It has also been shown that anti-TNF-induced macrophages (M Φ ind) have enhanced levels of autophagy compared to IFN- γ induced macrophages (M Φ 1) and IL-4-induced macrophages (M Φ 2), which was dependent on autophagy-related protein cathepsin S (Table 1.3) (Levin et al., 2016). Macrophages induced by anti-TNF agents harboured a regulatory macrophage phenotype similar to M2 macrophages (CD206 positive). Macrophage polarisation to M2 phenotype is autophagy dependent (Chang et al., 2013; Roca et al., 2009; M. Yang et al., 2014) and this macrophage subset can reduce intestinal inflammation in murine colitis models (Hunter et al., 2010; Leung et al., 2013). IBD patients who responded to anti-TNF therapy had increased levels of intestinal M2 macrophages (Vos et al., 2012), which were able to inhibit prolonged inflammation and promote wound healing (Vos et al., 2012, 2011). Furthermore, stimulation of the

autophagy pathway has been proven key for the effectiveness of anti-TNF therapy (Wildenberg et al., 2017). Additionally, anti-TNF-induced differentiation to M2 macrophage phenotype, expression of CD206 and immunosuppression of T cell proliferation were correlated with number of *ATG16L1* wild type alleles (Levin et al., 2016). These studies have identified that anti-TNF agents promote development of regulatory macrophage populations via enhanced autophagy and this response in patients is determined by *ATG16L1* genotype.

There are contradictory results regarding the effect of anti-TNF agents on autophagy activity. Most studies describe autophagy-stimulating properties of TNF- α , however, there is little evidence that anti-TNF agents inhibit the pathway. In contrary, some studies have found that anti-TNF-induction of autophagy was key to differentiation of regulatory macrophages. There could be modes of action of anti-TNF agents that are distinct from TNF- α neutralization, but are capable of inducing autophagy. Furthermore, the effect of anti-TNF agents could be cell type dependent and depend on differentiation stage of cells like monocytes and macrophages. As macrophages play a crucial role in innate immunity and inflammation within the gastrointestinal tract, the effects of anti-TNF- α on autophagy in this cell type is particularly relevant to IBD.

1.6. Hypothesis and Aims

Evidence suggests that enhancing autophagy may be therapeutically beneficial for the treatment of CD. We hypothesise that current IBD drugs exert their effects, in part, through stimulation of the autophagy pathway.

The principal aim of this study was to determine activity and mechanism of action of current IBD drugs in the context of autophagy. The specific aims were to:

1. Determine whether IBD drugs modulate autophagy activity
2. Characterise the molecular mechanisms by which IBD drugs modulate autophagy
3. Assess the effect of IBD drugs on the invasion and survival properties of CD-associated AIEC.
4. Confirm *in vitro* results in PBMCs and GI biopsies isolated from paediatric IBD patients: The IDEA (IBD Drug Effect on Autophagy) study

2. Materials and Methods

2.1 Cell culture

Human embryonic kidney cells 293 (HEK293) were grown in Dulbecco's modified Eagle medium (DMEM) with 4.5g/l glucose, L-glutamine, NaHCO_3 and pyridoxine HCl (Gibco™, ThermoFisher Scientific, Paisley, UK) supplemented with 10% heat inactivated foetal bovine serum (FBS) (Invitrogen™, ThermoFisher Scientific) and 1% antibiotics; 500µg/ml Streptomycin and 500µg/ml Penicillin (Gibco™). HEK293 cells, stably expressing LC3 protein tagged with green fluorescent protein (GFP), were provided as a gift from Dr Craig Stevens (Edinburgh Napier University, Edinburgh, UK) and were cultured in DMEM growth media. THP-1 cells were grown in RPMI (Roswell Park Memorial Institute) 1640 (Sigma-Aldrich, Irvine, UK), supplemented with 10% FBS, 1% penicillin streptomycin and 200mM L-glutamine (Gibco™). Cells were incubated at 37°C and 5% CO_2 and were passaged every 3-4 days by washing in NaCl solution (Baxter Healthcare, Newbury, UK) and detaching cells with 0.05% Trypsin-Ethylenediaminetetra acetic acid (EDTA) for adherent cells (Gibco™). Cell counts were performed using a haemocytometer to determine seeding density. For experiments HEK293 cells were seeded in growth media overnight at 37°C and 5% CO_2 until an 80-90% confluent cell monolayer had formed. For differentiation to macrophages, THP-1 cells were incubated in RPMI supplemented with 10ng/ml phorbol myristate acetate (PMA) (Sigma-Aldrich) for 48 hours, then rested for 24 hours in fresh RPMI prior to experiments.

2.2 Cell treatments and Reagents

Cells were washed in NaCl then treated with the pharmacological agents diluted in growth media for the appropriate incubation time. All reagents used are detailed in Table 2.1, and equivalent amounts of dimethyl sulfoxide (DMSO) (Sigma) were used as vehicle control. For nutrient deprivation, cells were incubated with Earle's Balanced Salt Solution (EBSS) (Gibco™).

Table 2.1: Details of reagents used for cell treatments

Reagents	Stock conc.	Working conc.	Manufacturer
Azathioprine, 6-mercaptopurine, methotrexate, methylprednisolone, sulfasalazine	400mM in DMSO	1-150µM	Tocris, Abingdon, UK
Bafilomycin A1	1mg/ml in DMSO	160nM	Santa Cruz Biotechnology, Dallas, Texas, USA
Brefeldin A from <i>Penicillium brefeldianum</i>	10mg/ml in DMSO	0.5µg/ml	Sigma-Aldirch
(S)-(+)-Camptothecin >90% (HPLC)	1mg/ml in DMSO	30µM	Sigma, Life Sciences
PERK inhibitor I (GSK2606414)	5µM in DMSO	50nM	Calbiochem®, Millipore
Rapamycin	2mg/ml	100nM	Sigma, Life Sciences, UK
Remicade® (infliximab)	10mg/ml in dH ₂ O	5-100µg/ml	Janssen Immunology, High Wycombe, UK

2.3 Transfection and plasmids

For transfection of HEK293 cells, Nucleofector Kit V (Lonza Ltd, Manchester, UK) was used according to the manufacturer's instructions with the Nucleofector™ 2b Device (Lonza Ltd). The GFP-LC3 (Kabeya et al., 2000), red fluorescent protein (RFP)-GFP-LC3 (Kimura et al., 2007) and TNFR plasmids have been described previously, and were provided as gifts from Dr Craig Stevens (Edinburgh Napier University, Edinburgh, UK).

2.3.1 Plasmid propagation

On ice, 25µl of Efficiency® DH5α™ Competent *E. coli* (Invitrogen™) were transformed with 17.5ng of plasmid and incubated for 30 minutes. *E. coli* were heat shocked at 42°C for 1 minute and returned to ice for 2 minutes before being incubated at 37°C in Luria-Bertani (LB) broth (10% tryptone, 5% yeast extract and 5% NaCl in dH₂O) for 2 hours. The *E. coli* were then grown on LB nutrient agar plates supplemented with selection antibiotic overnight at 37°C. Single resistant colonies were picked and grown in LB broth

shaking at 37°C for 2 hours. The *E. coli* plasmid cultures were then diluted in LB broth containing selection antibiotic for reselection overnight at 37°C. The plasmid was then isolated from *E. coli* using the Plasmid Midi Kit (Qiagen, Crawley, UK) according to manufacturer's protocol.

2.4 Antibodies

Details in Table 2.2

Table 2.2: Details of antibodies

Type	Antibody	Clone	Use (Conc.)	Manufacturer
Primary Antibodies	Ms actin	ACTN05 [C4]	WB (1 in 5000)	Abcam, Cambridge, UK
	Rb phospho-eIF2 α (S51)	119A11	WB (1 in 500)	Cell Signalling, Hitchin, UK
	Rb GRP78 BiP	Ab21685	WB (1 in 1000)	Abcam
	Ms LC3	2G6	WB (1 in 1000)	NanoTools Teningen, Germany
	Rb LC3	2775S	WB (1 in 1000)	Cell Signalling
	Rb LC3	PM036	IF (1 in 1000), IHC (1 in 1000), F (1 in 500)	MBL Intl., MA, USA
	Rb cleaved-PARP	D214	WB (1 in 1000)	Cell Signalling
	Ms PDI	RL90	WB (1 in 1000)	Abcam
	Ms rpS6	54D2	WB (1 in 1000)	Cell Signalling
	Rb phospho-rpS6 (S235/236)	2F9	WB (1 in 1000)	Cell Signalling
	Rb Tubulin	GR187587-1	WB (1 in 5000)	Abcam
PBMC surface markers	PE-Cy [™] 7 Ms Anti-Human CD3	UCHT1 (MOPC-21)	F (1 in 40)	BD Pharmingen [™] , Oxford, UK
	PE-Ms Anti-Human CD14	M5E2	F (1 in 10)	BD Pharmingen [™]
	PerCP-Cy [™] 5.5 Ms Anti-Human CD16	3G8	F (1 in 40)	BD Pharmingen [™]
	BV786 Ms Anti-Human CD19	HIB19 (X40)	F (1 in 40)	BD Horizon [™] , Oxford, UK
	BV650 Ms Anti-Human CD56	NCAM16.2 (27-35)	F (1 in 40)	BD Horizon [™]
	BV421 Ms Anti-Human HLA-DR	G46-6 (Polyclonal)	F (1 in 40)	BD Horizon [™]
Secondary Antibodies	Goat anti-Rb and anti-Ms IgG/HRP	F:1.0 and F:1.5	WB (1 in 5000)	Dako, Glostrup, Denmark
	Goat anti-Rb IgG-FITC		IF (1 in 1000), F (1 in 500)	Sigma
	Biotinylated Secondary Ab (R.T.U. Universal Elite [®] ABC Vectastain [®] Kit)		IHC (no dilution)	Vector Laboratories

F Flow cytometry, *IF* immunofluorescent staining, *IHC* immunohistochemistry, *Ms* Mouse, *Rb* rabbit, *WB* western blot.

2.5 Western immunoblotting

Treated cells were washed with phosphate buffered saline (PBS) (Thermo Fisher Scientific Oxoid Ltd, Basingstoke, UK), then cell pellets were prepared by gently scraping cells from 6-well plates into PBS, followed by centrifugation at 300G for 5 minutes and removal of supernatant. Cells were lysed in ice-cold extraction buffer (50mM Tris [pH 7.6], 150mM NaCl, 5mM EDTA, 0.5% NP-40, 5mM NaF, 1mM sodium vanadate, 1 × Pierce Protease Inhibitor Cocktail [Thermo Scientific™]) for 30 min followed by centrifugation at 17000G for 15 minutes at 4°C to remove cell debris. Protein concentration of the supernatant was determined by adding 5µl of sample or BSA standard to 195µl of Bradford reagent (Sigma-Aldrich) and measuring absorbance at 595nm using the MRX II absorbance reader (Dynex Technologies, Worthing, UK) with the Revelation 4.25 software. Between 10µg and 50µg of protein lysates and 2.5µl of PageRuler™ Plus prestained protein ladder (Thermo Scientific™) were resolved by sodium dodecyl sulfate-polyacrylamide gel electrophoresis (SDS-PAGE). SDS-PAGE was performed in the Mini-PROTEAN® Tetra Vertical Electrophoresis Cell (Bio-Rad, Perth, UK) using a discontinuous buffer system with a stacker gel (pH 6.8) and an 8-15% bis-acrylamide (Sigma-Aldrich) resolving gel (pH 8.8). Proteins were then electrotransferred to Immobilon®-FL polyvinylidene difluoride (PVDF) membrane (Millipore, Cork, Ireland) using either Tris-Glycine Buffer or CAPS (3-(Cyclohexylamino)-1-propanesulfonic acid) buffer (Sigma) in the Mini-PROTEAN® Cell (Bio-Rad). Ponceau stain (Sigma-Aldrich) was used to assess transfer quality before membranes were blocked for an hour in 10% w/v non-fat skimmed milk in PBS + 0.1% Tween 20 (PBST) (Sigma-Aldrich). Membranes were incubated at 4°C overnight with constant agitation in the primary antibody diluted between 1 in 1000 to 1 in 5000 in 5% w/v non-fat skimmed milk in PBST. Membranes were washed in PBST for 10 minutes (x3) prior to incubation with secondary antibodies, which were diluted 1 in 5000 in 0.5% w/v non-fat skimmed milk in PBST, for 1 hour at room temperature (RT) with constant agitation. Membranes were washed in PBST for 10 minutes (x3) and incubated with the ECL™ select western blotting detection reagent (GE Healthcare Bio-Sciences AB, Uppsala, Sweden), before proteins were visualised using Bio-Rad ECL system (Bio-Rad) or G: BOX system (Syngene, Cambridge, UK). Relative intensity of bands was measured using Image J software (Schindelin et al., 2012) (National Institutes of Health, Bethesda, MD, USA).

2.6 Immunofluorescence microscopy

Cells were seeded on 21-mm borosilicate glass cover slips (VWR International, Lutterworth, UK), 8 chamber polystyrene vessel CultureSlides (Falcon®, Fisher Scientific, Loughborough, UK) or 35mm imaging dishes (Ibidi, Thistle Scientific, Uddingston, UK).

2.6.1 Confocal Microscopy with fixed cells

Upon treatment completion, cells were washed with PBS (x3). Cells were fixed by addition of 4% paraformaldehyde (PFA) (Sigma-Aldrich) directly onto the cell monolayer and incubated at RT for 10-15 minutes before washing with PBS (x3). For transfected cells, with no immunostaining required, cells were then counterstained with 4',6-diamidino-2-phenylindole (DAPI) or mounted with Vectashield® mounting medium for fluorescence with DAPI (Vector Laboratories, Burlingame, CA).

For immunostaining with antibodies, after fixation, cells were permeabilized with 0.2% Triton-X and incubated at RT for 3-5 minutes. After another wash in PBS (x3), cells were blocked with PBS containing 10% FBS or 10% goat's serum (Gibco™) with 2.5% Human TruStain FcX™ (BioLegend®, San Diego, USA) and incubated at RT for 20-30 minutes. Primary antibodies were incubated overnight at 4°C, then washed with PBS (x3) prior to secondary antibody incubation for 30 minutes to 1hr at RT. Both primary and secondary antibodies were diluted in 1% FBS or goat's serum. Isotype controls and secondary only controls were used where appropriate. Cells were counterstained with DAPI or mounted with Vectashield® mounting medium for fluorescence with DAPI (Vector Laboratories). Images were captured using Carl Zeiss LSM880 confocal microscope (Carl Zeiss Ltd., Cambridge, UK) and analysed using Image J software (National Institutes of Health).

2.6.2 Live-cell imaging

Immediately after treatment, cells were transferred to the live-cell imaging chamber attached to Carl Zeiss LSM880 confocal microscope and maintained at 37°C and 5% CO₂ for the duration of the experiment. Images were taken every 2 minutes over an appropriate time period and images were analysed using Image J software (Schindelin et al., 2012) (National Institutes of Health).

2.6.3 GFP-LC3 autophagy assay

The basal threshold number of GFP-LC3 foci per cell was established as 5, as untreated cells that represented basal autophagy usually had between 1-4 GFP-LC3 foci. Therefore, cells exhibiting >5 GFP-LC3 foci were regarded as having modulated autophagy activity. The basal threshold number of RFP-GFP-LC3 plus RFP-LC3 foci per cell was established as 10. Percentage of cells displaying greater than the threshold number of foci was calculated.

2.6.4 TUNEL assay

The Terminal deoxynucleotidyl transferase (TdT) dUTP Nick-End Labeling (TUNEL) Assay was performed using the ApopTag Plus Fluorescein In Situ Apoptosis Detection Kit (Millipore). All buffers and reagents were prepared according to manufacturer's instructions. The assay was performed on cells grown on glass coverslips and the protocol was adapted to fit this application. Coverslips were then mounted on glass slides with Vectashield® mounting medium for fluorescence with DAPI (Vector Laboratories).

2.7 Flow cytometry

After treatments in 12-well plates, cells were gently detached using 0.05% trypsin or Cell Dissociation Solution Non-enzymatic (Sigma) at 37°C for 10 min. Centrifugation steps were at 350G or 400G for 5 minutes. Cells were acquired using the BD Biosciences (Oxford, UK) Celesta flow cytometer or the FACSCalibur (BD) with a stopping gate of 20,000 (cell lines) or 50,000 (PBMCs) events. Data analysis performed using BD FACSDiva Software or FlowJo software. Cell debris was excluded by forward scatter (FSC) and side scatter (SSC), and then single cell events were selected by FSC-H and FSC-A.

2.7.1 CD14 flow cytometry

After collection of THP-1s, cells were blocked with 2.5% Human TruStain FcX™, then incubated with CD14 surface marker or IgG fluorescent isotype diluted in Brilliant Stain

Buffer (BD Horizon™) for 25 minutes, both at RT. Cells were then washed with distilled PBS (dPBS) and acquired.

2.7.2 GFP-LC3 and endogenous LC3 flow cytometry

HEK293 GFP-LC3 cells were collected then washed in 0.05% w/v saponin (Sigma) diluted in PBS to remove the unbound cytosolic LC3 (Eng et al., 2010). Prior to acquisition cells were washed in dPBS. For endogenous LC3 staining, following saponin wash, cells were fixed with 1% PFA for 20 minutes at 4°C. Cells were then washed with 0.05% saponin, blocked with 2.5% Human TruStain FcX™ in 0.05% saponin for 20 minutes, then incubated overnight with primary LC3 antibody or rabbit (Rb) IgG Isotype control (Invitrogen™) diluted in 1% goat serum in 0.05% saponin at 4°C. After washing cells with 0.05% saponin (x3), cells were incubated with Anti-rabbit Fluorescein isothiocyanate (FITC) secondary antibody in 1% goat serum in 0.05% saponin and incubated at 4°C for 30 minutes. Prior to acquisition cells were washed twice in 0.05% saponin and then once in dPBS.

2.7.3 Annexin-V/PI assay

Cells were stained using the FITC Annexin V Apoptosis Detection Kit I (BD Pharmingen™) according to manufacturer's instructions. To calculate voltage compensation and apply gating strategy, experimental staining controls were used. Unstained cells were untreated, Annexin-V only stained cells that were transfected with TNFR and propidium iodide (PI) only stained cells that were scraped (Figure 2.1). For THP-1-derived macrophages annexin-V and PI only cells were both treated with camptothecin.

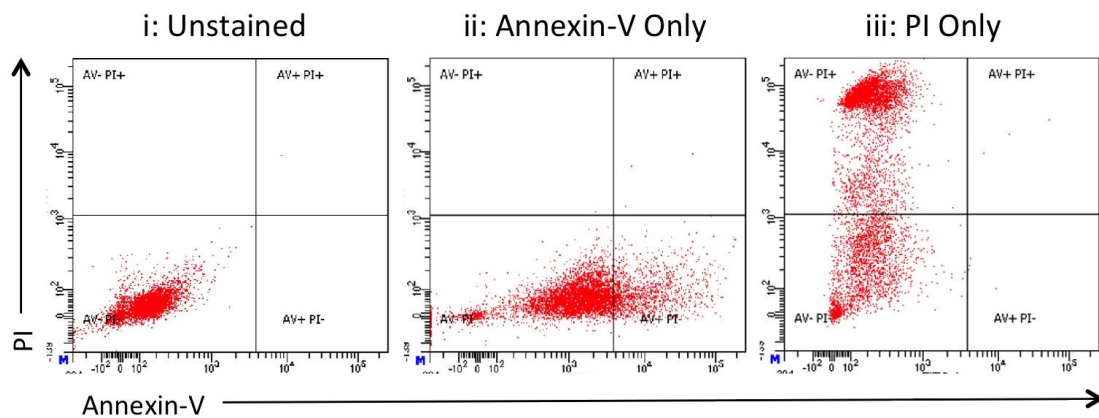


Figure 2.1: Annexin-V/PI experimental staining controls and gating strategy

HEK293 cells were untreated for unstained control (i), transfected with TNFR for annexin-V staining only (ii) or detached by scraping for PI staining only (iii).

2.7.4 Cytospins

After flow cytometry acquisition, remaining cells were cytospun onto glass slides for confocal analysis where required. Cell suspensions were transferred to the Shandon Cytospin 3 (Thermo Fisher Scientific) chambers and cytocentrifuged at 800G for 3 minutes. Cells were mounted with Vectashield® mounting medium for fluorescence with DAPI (Vector Laboratories). Images were captured using Carl Zeiss LSM880 confocal microscope (Carl Zeiss Ltd.) and analysed using Image J software (National Institutes of Health).

2.8 RT-qPCR

After appropriate treatments in 12-well plates, cells were scraped into RNeasy® RT (Sigma-Aldrich) and immediately frozen at -80°C. After thawing total RNA was extracted according to manufacturer's instructions and was quantified using a NanoDrop 2000 Spectrophotometer (Thermo Scientific). The integrity of Total RNA was assessed using an Agilent 2100 Bioanalyzer (Agilent Technologies, Stockport, UK) with RNA Nano Chips and Agilent RNA 6000 Nano Reagents (Agilent Technologies). mRNA was converted to complementary DNA (cDNA) using nanoScript 2, Reverse Transcription Premix (PrimerDesign Ltd, Chandler's Ford, UK) according to manufacturer's instructions and a control of RNA with addition of no reverse transcriptase was included. For quantitative reverse transcription PCR (RT-qPCR) analysis of gene expression, PrecisionPLUS

Mastermix with SYBR green and ROX with inert blue dye (PrimerDesign) was used according to manufacturer's instructions with RT-qPCR Grade Water (Invitrogen™) and the StepOnePlus Real-time PCR System (Applied Biosystems, ThermoFisher). Primers are detailed in (Table 2.3). A geNorm kit (PrimerDesign) was used for the selection of appropriate reference genes with the qbase+ software (Vandesompele et al., 2002). $2^{-\text{ddCT}}$ was used for relative quantification of gene expression (Livak and Schmittgen, 2001).

For the RT² Profiler™ PCR Array of Human Autophagy genes (Qiagen) RNA was extracted from cells using the RNeasy® mini kits following manufacturers protocols (Qiagen). RNA was converted to cDNA using RT² First Strand Kit (Qiagen) and the PCR array was performed according to manufacturer instructions with RT² SYBR Green Mastermix (Qiagen). Analysis was performed according to manufacturer's instructions.

Table 2.3: Details of primers used for RT-qPCR

Target Gene	FW Primer	RV Primer	Manufacturer
<i>Actin</i>	GGACTTCGAGCAAGAGATGG	AGGAAGGAAGGCTGGAAGAG	Eurofins Genomics, Ebersberg, Germany
<i>ATF4</i>	CTCCGGGACAGATTGGATGTT	GGCTGCTTATTAGTCTCTGGAC	Eurofins Genomics
<i>BiP (GRP78)</i>	TATGGTGCTGCTGTCCAGG	CTGAGACTTCTTGGTAGGCAC	Eurofins Genomics
<i>CHOP</i>	AGCTGGAAGCCTGGTATGAGG	GTGCTTGTGACCTCTGCTGG	Eurofins Genomics
<i>CXCR4</i>	ACTACACCGAGGAAATGGGCT	CCCACAATGCCAGTTAAGAAGA	Eurofins Genomics
<i>IL-18</i>	TTCGAGGCACAAGGCACAAC	CTGGAAGGAGCACTTCATCTGT	Eurofins Genomics
<i>IL-6</i>	GGTACATCCTCGACGGCATCT	GTGCCTCTTTGCTGCTTTCAC	Eurofins Genomics
<i>PERK</i>	GGAAACGAGAGCAGGATTTATT	ACTATGTCCATTATGGCAGCTTC	Eurofins Genomics
<i>PDI</i>	TGCCCAAGAGTGTGTCTGAC	CTGGTTGTCGGTGTGGTC	Eurofins Genomics
<i>RPL13A</i>	Primer Mix	Primer Mix	PrimerDesign Ltd, Chandler's Ford, UK
<i>TNFα</i>	GCTGCACTTTGGAGTGATCG	GCTTGAGGGTTTGCTACAACA	Eurofins Genomics

FW forward and RV reverse primer sequences.

2.9 Bacterial infection assays

2.9.1 Bacterial strains, plasmids and transformation

The AIEC strain CUICD541-10 (Baumgart et al., 2007) was selected and transformed with the isopropyl β -D-1-thiogalactopyranosid (IPTG)-inducible x-light mCherry plasmid, (Mills et al., 2013). Repression of the x-light mCherry plasmid is relieved upon metabolism of IPTG in viable bacteria to allow synthesis of fluorescent protein (Figure 2.2).

Electrocompetent CUICD541-10 were prepared using an established method of washing the bacterial culture in decreasing volumes of ice-cold 10% glycerol (Miller and Nickoloff, 1995). Aliquots of glycerol stocks were frozen at -80°C , at a concentration of roughly $1-3 \times 10^{10}$ cells/ml (Miller and Nickoloff, 1995). At 4°C , $2\mu\text{l}$ of plasmid in Tris-EDTA (TE)

buffer from the Plasmid Midi Kit (Qiagen) was mixed with 40µl of electrocompetent CUICD541-10 glycerol stock and incubated for 1 minute on ice before electroporation at 2483 volts and 12.4-field strength for 5.3 milliseconds using the GenePulser Xcell™ electroporator (BioRad). CUICD541-10 was immediately resuspended in 1ml of SOC medium (Sigma) and incubated at 37°C for 1 hour, shaking at 225 revolutions per minute (RPM). Selection of transformed CUICD541-10 was achieved by spreading on LB agar plates with 100µg/ml ampicillin sodium salt (Sigma-Aldrich).

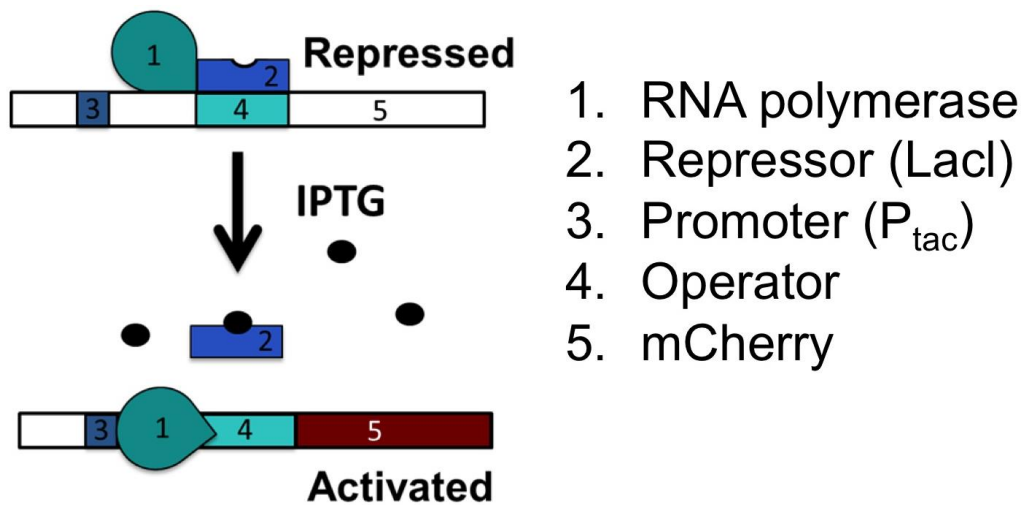


Figure 2.2: IPTG-inducible x-light mCherry plasmid

Plasmid is repressed by LacI repressor. When IPTG is present LacI repressor dissociates from Operator and RNA polymerase is able to transcribe plasmid for mCherry expression in bacteria.

2.9.2 Growth Curve

10ml of LB broth was inoculated from an overnight culture of CUICD541-10 to an optical density of 0.05 at 600nm using the Jenway 6300 spectrophotometer. Cultures were treated appropriately and incubated at 37°C with 200RPM shaking. Optical density was measured at 600nm every 30 minutes.

2.9.3 Infection model and analysis

To assess intracellular survival of AIEC an infection protocol was designed (Figure 2.3). Cells were infected with CUICD541-10 at a multiplicity of infection (MOI) (MOI= colony forming unit (CFU)/Host Cell Number) of 10 for 3 hours, incubated for 1 hour in 100µg/ml gentamicin (Gibco™) to kill extracellular bacteria, then maintained for a further 24h in 20µg/ml gentamicin. Appropriate treatments were added for the final 6 hours.

The survival of intracellular bacteria was assessed by gentamicin protection assay with enumeration of CFU, or with confocal microscopy to visualise and enumerate fluorescent intracellular bacteria. For immunofluorescence, cells were infected with CUICD541-10 transformed with an x-light mCherry plasmid and 30 minutes prior to immunostaining cells were incubated with 0.1mM IPTG (Sigma) to promote bacterial fluorescence. IPTG and 5µM Cell Tracker™ Green BODIPY® (Invitrogen™) were added for the duration of the live-cell imaging of infected cells.

For CFU enumeration, cells were washed in PBS and then lysed for 10 minutes using 1% Triton X100 in PBS. PBS wash and lysates were serially diluted and spread on LB agar plates for overnight incubation at 37°C. CFU of PBS wash was subtracted from CFU of lysates, then CFU/ml of intracellular bacteria was calculated.

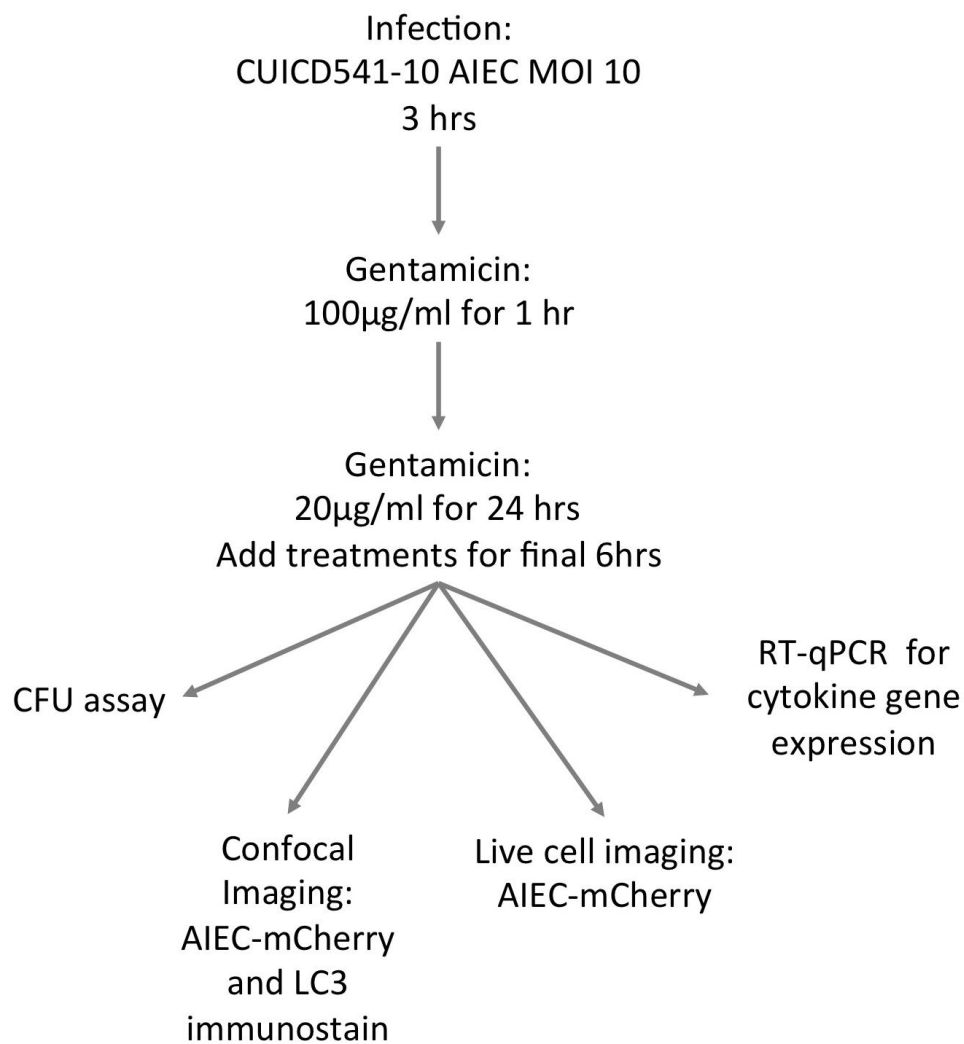


Figure 2.3: AIEC infection and treatment regime in THP-1-derived macrophages to assess intracellular survival

THP-1-derived macrophages infected with CUICD541-10 at MOI 10 for 3 hours. Cells treated with 100µg/ml gentamicin for 1 hour to kill extracellular bacteria. Cells were maintained in 20µg/ml gentamicin for a total of 24 hours. For the final 6 hours appropriate treatments were added. To analyse survival of intracellular AIEC, colony forming unit (CFU) enumeration and live-cell and fixed-cell confocal imaging of AIEC-mCherry was undertaken. To monitor autophagy, fixed-cell confocal imaging was combined with LC3 immunostain. Pro-inflammatory cytokine expression was quantified by RT-qPCR.

2.10 AlamarBlue assay

AlamarBlue® assay (Invitrogen) was adapted from manufacturer's protocol for use in 24-hour time-course experiments. Pharmacological treatments, prepared in growth media,

were supplemented with 10% alamarBlue® reagent prior to cell treatment. This was repeated for no-cells controls.

Cells were seeded in a Microtest™ 96-well assay plate, Optilux, with black sides and clear bottom (BD Falcon, Oxford, UK) for fluorescence assays. Fluorescence was read via bottom optics with an excitation wavelength of 544nm and an emission wavelength of 590nm after gain adjustment was applied to the entire plate, using the FLUOstar Omega with software version 1.2 fluorescent plate reader (BMG Labtech, Aylesbury, UK). The metabolic activity of cells was calculated according to the manufacturer's instructions and calculations were performed as follows:

FI590: Fluorescent intensity at 590nm emission (544nm excitation)

Percentage difference between treated and control cells = $\frac{(\text{FI590 of test agent treated cells} - \text{FI590 of test agent only}) \times 100}{(\text{FI590 of untreated cells} - \text{FI590 of media only})}$

Absorbance was measured using the MRX II Microplate Reader (Dynex Technologies), with absorbance wavelength at 550nm and reference wavelength at 595nm. Flat bottom 96-well assay plates were used. In accordance with the manufacturer's protocol, the metabolic activity of cells was calculated as follows:

O1: molar extinction coefficient (E) of oxidized alamarBlue® (Blue) at 550 nm (0.431)

O2: E of oxidized alamarBlue® at 595 nm (0.795)

A1: absorbance of test wells at 550 nm

A2: absorbance of test wells at 595 nm

P1: absorbance of positive growth control well (cells plus alamarBlue® but no test agent) at 550 nm

P2: absorbance of positive growth control well (cells plus alamarBlue® but no test agent) at 595 nm

Percentage
$$\frac{((O2 \times A1) - (O1 \times A2)) \times 100}{((O2 \times P1) - (O1 \times P2))}$$

difference =

between treated

and control cells

2.11 IDEA study

Patient recruitment and sample collection was performed at the Royal Hospital for Sick Children in Edinburgh, and processing and analysis was performed at Edinburgh Napier University. All samples were collected with local institutional and NHS ethical approvals (reference 16/WW/0210).

2.11.1 Patients and sample collection

Inclusion criteria were: (1) aged 6-18 years on date of colonoscopy; (2) Already confirmed Crohn's disease, ulcerative colitis or IBDU (Levine et al., 2014) or undergoing first upper and lower GI endoscopy due to gastrointestinal symptoms suggestive of possible bowel inflammation (e.g. abdominal pain, PR bleeding, weight loss). Non-IBD patients were defined as those with both microscopically and macroscopically normal colonoscopy. Patients were excluded if they had previously undergone colonoscopy for anything other than known IBD, were found to have anything other than IBD following a full investigative cycle, or who could not provide written consent. Eligible patients were approached at least 48hrs prior to colonoscopy and following consent whole blood samples (maximum 15ml), GI biopsies (two standard biopsies were collected from the rectum in all patients and also two biopsies from either terminal ileum or caecum if

ileum was not intubated) and saliva samples were collected from patients for analysis (Figure 2.4).

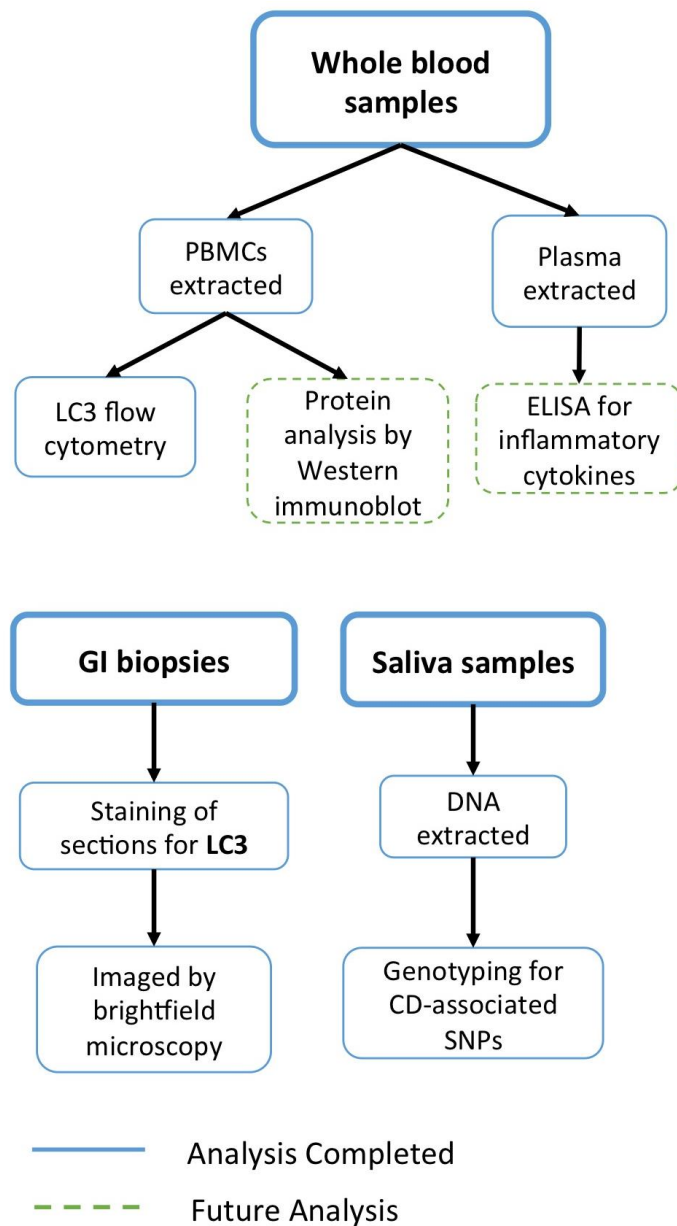


Figure 2.4: IDEA Study sample collection and analysis

Samples collected from paediatric patients, PBMCs frozen at -80°C for 3-9 months and analysis completed within study. Plasma and PBMC protein lysates have also been stored at -80°C for any future analysis.

Patients ranged between 8.4 and 16.9 years of age, of which 20 were IBD cases and 9 were non-IBD controls (Table 2.4). Within the IBD patient group, there were 12 patients diagnosed with CD, 7 with UC and one with IBDU. Due to new diagnosis, most of the IBD

cases were not receiving therapy. However, one CD patient was receiving an immunosuppressant drug, four CD patients were receiving biological agents, one of which in combination with thiopurines, and three UC patients were receiving 5-aminosalicylates, one of which in combination with biological agents and two in combination with thiopurines.

Table 2.4: IDEA study paediatric patient demographics

	Non-IBD	CD	UC	IBDU
Cohort (n=29)	9	12	7	1
Age years (mean +/- SD)	10.7 +/- 3.3	12.8 +/- 2.7	13.4 +/- 2.5	9.7 +/- 0
Disease duration: years (mean +/- SD)	N/A	1.4 +/- 2.3	1.9 +/- 3.4	0
Disease Location ^a				
L1	N/A	1	N/A	N/A
L2	N/A	1	N/A	N/A
L3	N/A	2	N/A	N/A
L1/L4a	N/A	1	N/A	N/A
L2/L4a	N/A	1	N/A	N/A
L3/L4a	N/A	5	N/A	N/A
Disease Location ^b				
E1	N/A	N/A	0	0
E2	N/A	N/A	3	1
E3	N/A	N/A	1	0
E4	N/A	N/A	3	0
Disease Behaviour ^a				
B1	N/A	8	N/A	N/A
B2	N/A	1	N/A	N/A
B3	N/A	0	N/A	N/A
B1p	N/A	2	N/A	N/A
Disease Behaviour ^b				
S0	N/A	N/A	5	1
S1	N/A	N/A	2	0
Therapy (n)				
None	N/A	7	4	1
Immunosuppressants	N/A	1	0	0
Biologics	N/A	3	0	0
Biologics, thiopurines	N/A	1	0	0
Biologics, 5-ASA	N/A	0	1	0
5-ASA, thiopurines	N/A	0	2	0

CD Crohn's disease, UC Ulcerative colitis, IBDU IBD unclassified. SD Standard deviation.

^aPorto Criteria for CD: L1 ileal, L2 colonic, L3 ileocolonic, L4a upper disease proximal to ligament of Treitz*; B1 non-stricturing and non-penetrating, B2 stricturing, B3 penetrating, p perianal disease modifier (Levine et al., 2011). ^bPorto Criteria for UC: E1 ulcerative proctitis, E2 left-sided UC (distal to splenic flexure), E3 extensive (hepatic flexure distally), E4 pancolitis (proximal to hepatic flexure); S0 never severe, S1 ever severe as defined by Paediatric Ulcerative Colitis Activity Index (PUCAI) (Levine et al., 2014). 5-ASA 5-aminosalicylates.

2.11.2 PBMC isolation and Flow cytometry

Whole blood samples, up to a volume of 15ml, were collected in EDTA coated tubes and stored at RT for 1 to 2 hours before isolating PBMCs. Firstly, whole blood was mixed with dPBS at 1:1 volume ratio, then layered on top of Ficoll-Paque™ PLUS solution (GE Healthcare Bio-Sciences AB), at a 4:3 ratio of blood and dPBS to Ficoll volume. This was then centrifuged at 700G for 30 minutes, with the brake disabled. Plasma was collected and stored at -80°C for future analysis. The PBMC layer was collected and washed twice with dPBS by centrifugation at 300G for 10 minutes. PBMCs were re-suspended in 1ml of heat inactivated FBS supplemented with 10% DMSO and gradually cooled to -80°C for storage for 3-9 months.

Once recruitment was completed, batch analysis of PBMCs by flow cytometry was undertaken. PBMCs were thawed rapidly at 37°C and immediately washed, twice, in RPMI growth media. PBMCs were seeded at 2×10^5 cells per well in a 96-well round-bottom plate, then rested overnight. Cells were kept in the 96-well rounded-bottom plate for the entire protocol and flow cytometry acquisition was achieved using the BD High Throughput System (HTS) attachment on the BD Biosciences Celesta flow cytometer. The protocol described in section 2.7.2 was also altered to accommodate for PBMC surface marker staining.

After treatments in duplicate, cells were gently detached using Cell Dissociation Solution Non-enzymatic (Sigma) on ice for 10 minutes, then washed in RPMI growth media then dPBS. Cells were blocked with 2.5% Human TruStain FcX™, then incubated with PBMC surface markers or IgG isotypes diluted in Brilliant Stain Buffer (BD Horizon™) for 25 minutes, both at RT. Cells were washed in 0.05% saponin (Sigma), which does not alter expression of membrane antigens (Jacob et al., 1991) and fixed with 1% PFA. Cells were washed with 10% goat serum in 0.05% saponin prior to overnight incubation with primary antibody or Isotype control. Prior to acquisition cells were re-suspended in 200µl of dPBS.

To calculate voltage compensation and apply gating strategy, experimental staining controls were used, which consisted of single fluorochrome staining and Fluorescence Minus One Control (FMO) staining (LC3 intracellular stain excluded). The gating strategy

was undertaken as follows. LC3 stained PBMCs were selected by FITC histogram by reference to isotype control staining. CD3+ T cells, CD56+ NK cells and CD19+ B cells were selected by scatterplots against LC3. Monocytes were selected firstly by exclusion of CD56+ and CD3+ cells; as CD3+ T cells are the largest population and CD56+ NK cells also express the monocyte marker CD16. Then CD14 and CD16 were used to select monocytes. HLA-DR+ PBMCs were selected by HLA-DR versus LC3 scatterplot and HLA-DR+ T cells, NK cells, B cells and monocytes were selected by scatterplot of HLA-DR versus respective PBMC surface marker. Percentage of cell populations and LC3 geometric mean within each population was analysed.

2.11.3 Genotyping

Saliva samples were collected using Oragene DNA kits (DNA Genotek, Ontario, Canada) and stored at RT prior to genotyping analysis. Due to unforeseen circumstances saliva samples were not able to be collected for one IBDU patient (AUT026) and one non-IBD patient (AUT004). Saliva samples were sent to Wellcome Trust Clinical Research Facility in Edinburgh, for analysis within the Genetics Core with all materials provided at this site. DNA was extracted from saliva samples using Isohelix Kit and placed on rotating wheel to ensure complete re-suspension in 1ml TE buffer. DNA yield was measured using Picogreen, and DNA was subsequently stored at -20°C. Taqman Genotyping for each sample was undertaken for the following SNPs: *ATG16L1 T300A* (rs2241880), *NOD2 L1007f/s* (p.Leu1007fsX1008) (rs2066847), *NOD2 R702W* (rs2066844) and *NOD2 G908R* (rs2066845).

2.11.4 Immunohistochemistry

For each patient two biopsies were collected from the rectum and two from either terminal ileum or caecum. Due to unavoidable circumstances biopsies were not able to be collected from one UC patient (AUT014) and only rectal biopsies were able to be collected from one CD patient (AUT023). Biopsies were immediately fixed in 10% neutral buffered formalin for 24 hours then stored in 70% ethanol.

Once study recruitment was completed, biopsies were processed using Leica 1020 tissue processor (Leica Biosystems, Newcastle):

- 1) 70% ethanol for 1 hour 30 mins at RT
- 2) 80% ethanol for 1 hour 30 mins at RT
- 3) 90% ethanol for 1 hour 30 mins at RT
- 4) 95% ethanol for 1 hour 30 mins at RT
- 5) 95% ethanol for 1 hour 30 mins at RT
- 6) Absolute ethanol for 2 hours at RT
- 7) Absolute ethanol for 2 hours at RT
- 8) Xylene for 1 hour at RT
- 9) Xylene for 1 hour at RT
- 10) Paraffin wax supplemented with Bouin's dye (Sigma-Aldrich) for 1 hour at 60°C
- 11) Paraffin wax supplemented with Bouins dye for 1 hour at 60°C

Paraffin wax infused biopsies were then orientated and embedded in Paraplast® paraffin wax (Sigma). Paraffin blocks were section to 5µM at the Centre for Comparative Pathology (University of Edinburgh, Edinburgh, UK).

For IHC staining of sections, wax was removed with AnalaR NORMAPUR Xylene (VWR PROLABO® Chemicals, Lutterworth, UK) and tissue was then rehydrated with decreasing concentrations of EtOH at RT:

- 1) Xylene for 5 mins
- 2) Xylene for 5 mins
- 3) Absolute ethanol for 2 mins
- 4) Absolute ethanol for 2 mins
- 5) 90% ethanol for 1 min
- 6) 70% ethanol for 1 min
- 7) Distilled water for 5 mins

Antigen retrieval was performed using 10mM citrate buffer, pH 6.0, and microwaving on full power for 5 minutes followed by a 1 minute rest, then microwaving for a further 5 minutes followed by a 20 minute rest. Endogenous peroxidase was blocked with 3% Hydrogen Peroxide solution (Fischer Scientific) for 10 minutes. After washing sections twice with PBS for 5 minutes, sections were blocked for 30 minutes in Normal Horse Serum from the R.T.U. Universal Elite® ABC Vectastain® Kit (Vector Laboratories). Then sections were incubated overnight at 4°C with 1 in 1000 primary LC3 antibody or Rb IgG

isotype control diluted in Normal Horse Serum, and then were washed in PBS + 0.1% tween-20 (PBS-T), twice, for 5 minutes. Using the same ABC kit, sections were incubated in biotinylated secondary antibody, then Avidin-Biotin Conjugate complex, each for 30 minutes at RT and followed by two PBS-T washes for 5 minutes. Sections were exposed to 3'-Diaminobenzidine (DAB) substrate from the Peroxidase Substrate Kit (Vector Laboratories), followed by haematoxylin Gill's formula (Vector Laboratories) counterstain, both for 2 minutes. The DAB reaction was stopped by placing slides in distilled water and excess haematoxylin was removed by 1 minute in 2% acetic acid, followed by 1 minute in Scots tap water substitute (Cell Path, Newtown, UK). Tissue was dehydrated with increasing concentrations of EtOH and xylene, as described above, in reverse, prior to mounting with Pertex® (HistoLab®, Västra Frölunda, Sweden).

Sections were imaged by brightfield microscopy using Leica DM2500 microscope and Leica DFC425 camera. LC3 staining intensity was scored blinded, by two independent investigators. Overall LC3 staining intensity was scored as follows:

0 – No staining

1 – Low intensity staining

2 – Medium intensity staining

3 – High intensity staining

2.12 Statistical analysis

Results are reported as the mean \pm Standard Error Mean (SEM) assuming normally distributed variables with statistical analysis conducted by using GraphPad Prism version 7.0 (GraphPad Software, CA, USA). One-way or two-way ANOVAs were performed with Tukey's or Dunnett's multiple comparisons tests, as appropriate. For certain analysis within the IDEA study, paired, two-tailed t-tests were performed.

3. Investigating IBD drug modulation of autophagy

3.1 Introduction

There are five main classes of drugs commonly used for the treatment of IBD. In this chapter, azathioprine and 6-mercaptopurine (thiopurines), Infliximab (biological agent), Methotrexate (immunomodulatory), Methylprednisolone (corticosteroid) and Sulfasalazine (aminosalicylate) were screened for their ability to modulate autophagy. As described in section 1.5 and shown in Table 1.3, the mechanism of action of these drugs has previously been linked either directly, or indirectly, to the modulation of autophagy in a variety of cell types and disease settings (Hooper et al., 2017). Corticosteroids (Fatkhullina et al., 2014; Harr et al., 2010; Kyrnizi et al., 2013; Laane et al., 2009; Swerdlow et al., 2008; Wang et al., 2006) and sulfasalazine (Chacon-Cabrera et al., 2014; Han et al., 2014) have been shown to both induce and inhibit autophagy. Thiopurines (Chaabane et al., 2016; Oancea et al., 2017; Wildenberg et al., 2017; Zeng et al., 2007; Zeng and Kinsella, 2010, 2008), cyclosporine (Ciechomska and Kaminska, 2012; Kim et al., 2014; Kimura et al., 2013; Pallet et al., 2008) and tacrolimus (Nakagaki et al., 2013) have been shown to induce autophagy. Anti-TNF- α biological agents have been shown to inhibit autophagy (Harris and Keane, 2010), but also induce differentiation of macrophages that have enhanced autophagy activity (Levin et al., 2016). Due to a lack of consensus, it was necessary to determine the effect of each IBD drug on autophagy in our chosen experimental cell line.

The HEK293 cell line is well-characterised and has been extensively used for investigating autophagy (Musiwaro et al., 2013). Moreover, HEK293 cells engineered to stably express the autophagy marker LC3 fused to green fluorescent protein (HEK293 GFP-LC3) were available as a powerful tool to use in experimental work. Several studies that had previously used IBD drugs to investigate modulation of autophagy *in vitro* were referred to, and this informed on the concentration ranges (Agnholt and Kaltoft, 2001; Han et al., 2014; Harr et al., 2010; Henderson, 2013; Kyrnizi et al., 2013; Laane et al., 2009; Petit et al., 2008; Swerdlow et al., 2008; Wittstock et al., 2015). Initially, well-characterised stimulators and inhibitors of autophagy, including serum starvation,

rapamycin and bafilomycin were used to optimise techniques for measuring autophagy (Supplementary Results: chapter 9).

3.2 Results

3.2.1 AlamarBlue[®] Cytotoxicity Assay to Identify Non-Toxic Concentration Range of IBD Drugs in HEK293 cells

The AlamarBlue[®] assay was used to assess whether IBD drugs disrupted the metabolic activity of HEK293 cells over a 24-hour time-course. AlamarBlue[®] measures cytotoxicity via detection of a colorimetric change from the blue reagent resazurin that is metabolically reduced to the pink and highly fluorescent resorufin. Fluorescent intensity or absorbance can be measured to quantify levels of oxidation in the cell, which are an indirect indicator of cell viability or cytotoxicity. As resazurin and resorufin are non-toxic, this assay can be used for time-course analysis at prolonged time points.

The effect of drug treatment and concentration on metabolic activity, expressed as mean percentage of untreated metabolic activity (indicated by the red line at 100% metabolic activity), was assessed within each time-point (Figure 3.1). There was no effect of the vehicle control, DMSO, on the metabolic activity of cells, and when treated with 0.5% Triton-X, as a positive control for cell death, metabolic activity significantly decreased to 1% throughout the time-course (data not shown).

Metabolic activity of cells was unaffected by treatment with azathioprine, infliximab, methotrexate, methylprednisolone or sulfasalazine throughout the time-course and corresponding concentration ranges (Figure 3.1: i-ii, iv-vi). A concentration of 60 μ M of 6-MP at the 2-hour time-point showed a significant decrease in metabolic activity to 80% (Figure 3.1: iii). However, higher concentrations and longer incubation times with 6-MP had no significant effect on metabolic activity (Figure 3.1: iii).

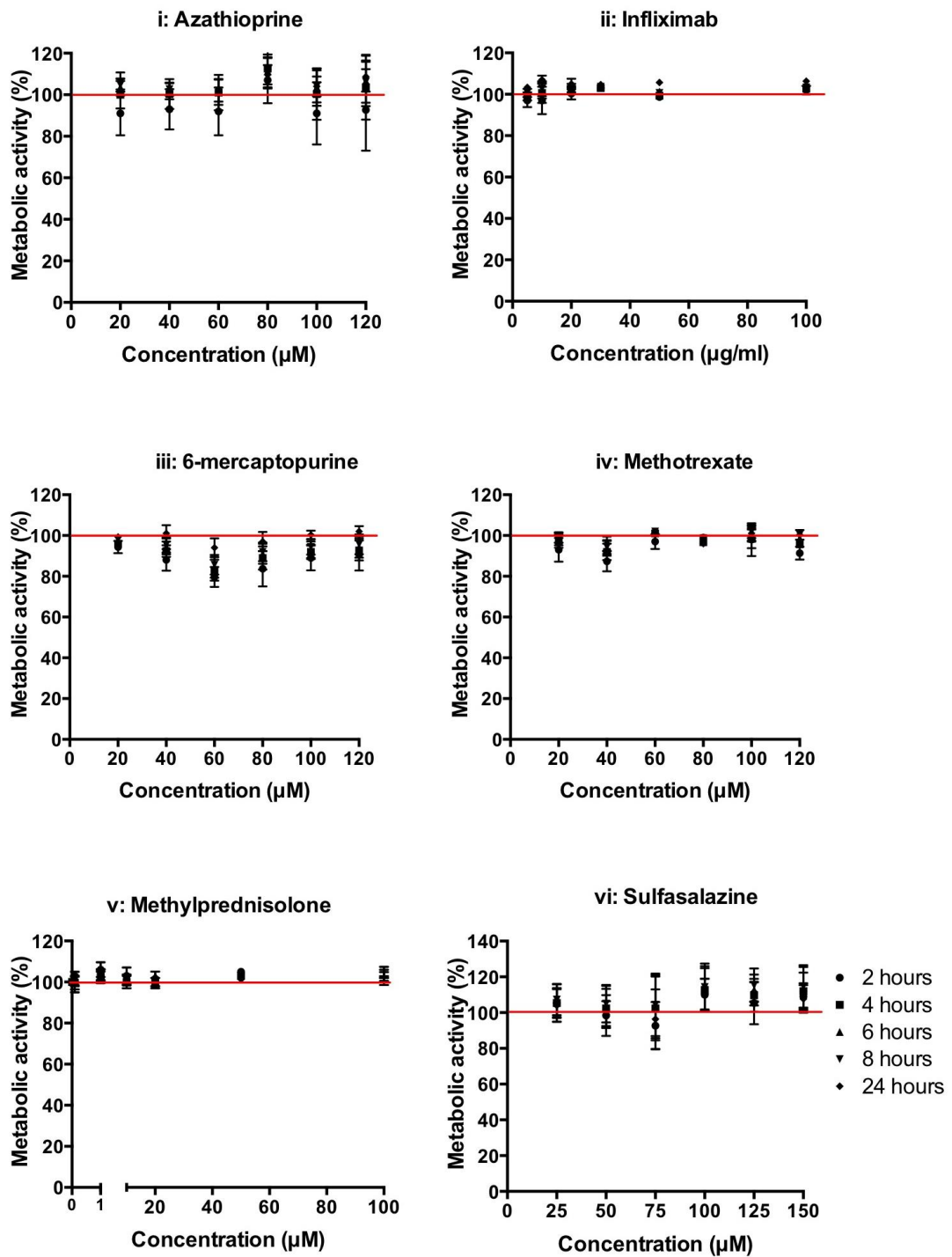


Figure 3.1: AlamarBlue® Toxicity Time-course and Concentration Range Analysis with IBD Drugs in HEK293 Cells

HEK293 cells were treated with IBD drugs for 24-hours in the presence of 10% alamarBlue® reagent (n=3). Cells were treated with 0-120 μM of Azathioprine (i), 0-100 $\mu\text{g/ml}$ Infliximab (ii), 0-120 μM 6-mercaptopurine (iii), 0-120 μM Methotrexate (iv), 0-100 μM methylprednisolone (v) or 0-150 μM sulfasalazine (vi). Fluorescence was read at 2, 4, 6, 8 and 24 hours. Percentage difference between fluorescent intensity of treated and untreated cells (0 μM or 0 $\mu\text{g/ml}$: red line) was calculated after fluorescent intensity of corresponding “no cells” controls were subtracted. Mean percentage metabolic activity (+/- SEM) is displayed. Two-way ANOVA with Tukey’s multiple comparison test

was performed for each drug to compare the effect of treatment and concentration within each time-point.

3.2.2 Live-cell Imaging Time-Course to Identify IBD Drugs that Modulate Autophagy in HEK293 GFP-LC3 Cells

As the concentrations of IBD drugs tested in section 3.2.1 were not cytotoxic, the highest concentration of each drug was used to treat HEK293 GFP-LC3 cells for up to 12 hours. GFP-LC3 foci formation was monitored with live-cell imaging on the confocal microscope.

At 0 hours of confocal imaging, the percentage of cells exhibiting >5 GFP-LC3 foci was between 5% and 17% (Figure 3.2B). The percentage of cells with >5 GFP-LC3 foci remained low in the negative control (untreated) and vehicle control (DMSO), fluctuating between 1% and 13% throughout the time-course (Figure 3.2B). EBSS treatment was used as a positive control to induce autophagy via nutrient deprivation. With EBSS treatment the percentage of cells exhibiting >5 GFP-LC3 increased to 22% at 0.5 hours, then increased significantly to 35% at 1 hour and fluctuated between 64% and 79% up to 12 hours, with optimum autophagy induction at 6 hours (Figure 3.2A and B).

Azathioprine treatment increased autophagy slightly from 0.5 to 2 hours with between 17% and 20% of cells exhibiting >5 LC3 foci (Figure 3.2B). There was a significant increase in percentage of cells exhibiting >5 GFP-LC3 foci compared to DMSO between 3 and 12 hours fluctuating between 33% and 49%, with optimum autophagy induction at 6 hours (Figure 3.2A and B).

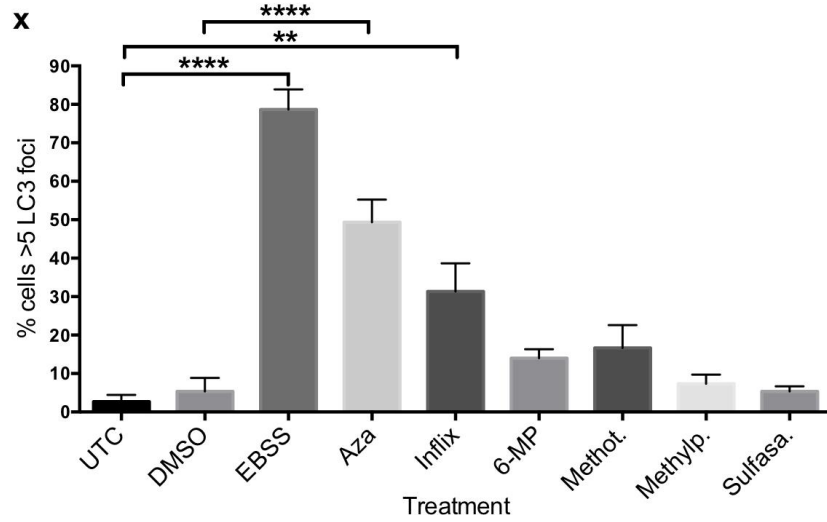
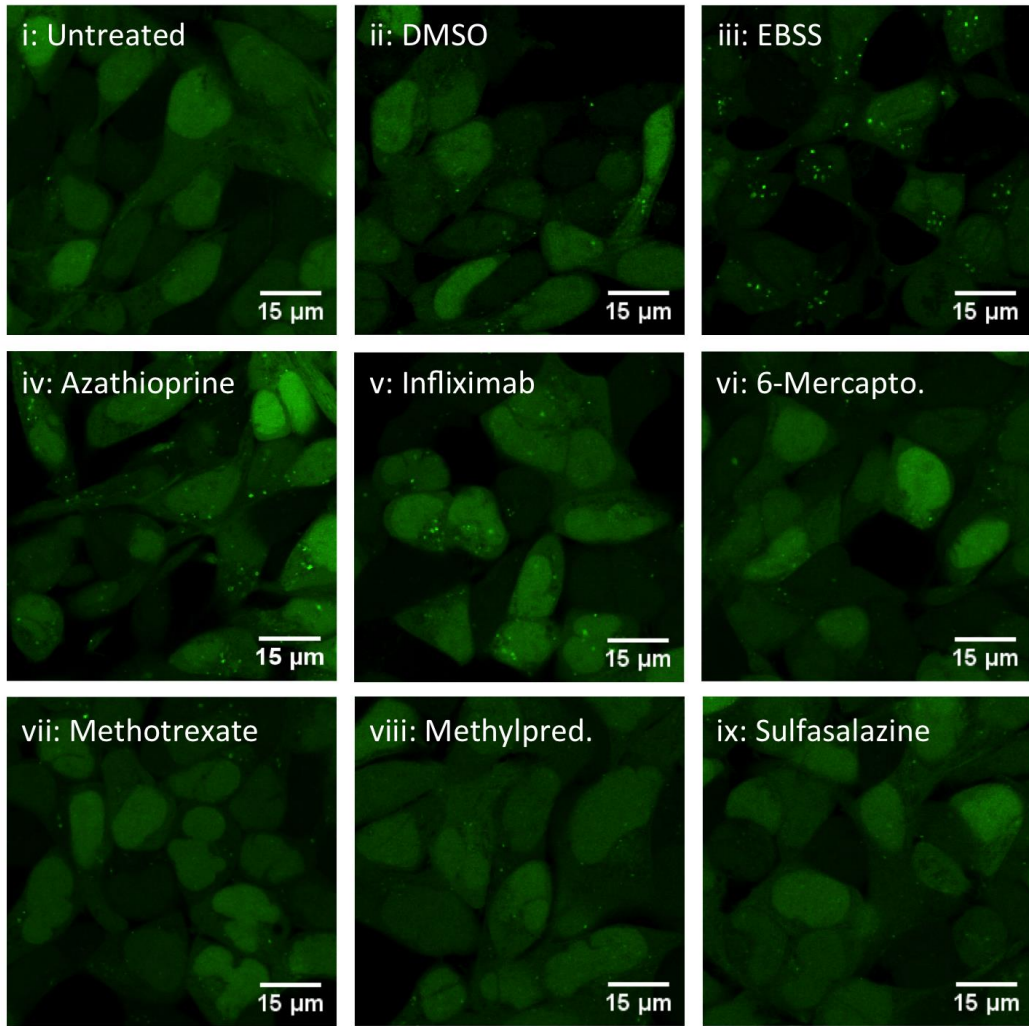
When HEK293 GFP-LC3 cells were treated with infliximab, the percentage of cells exhibiting >5 GFP-LC3 foci increased from 17% at 0 hours to 27% at 0.5 hours and fluctuated between 16% and 23% from 1 to 5 hours (Figure 3.2B). As infliximab neutralizes TNF- α , it is important to note that HEK293 cells express low levels of the TNF receptor (TNFR) (McFarlane et al., 2002). The percentage of cells with >5 GFP-LC3 foci increased significantly to an optimal level of 31% at 6 hours (Figure 3.2A and B). At 7 and 8 hours treatment with infliximab the significant increase in autophagy was sustained

with 27% and 25% of cells with >5 GFP-LC3 foci, respectively (Figure 3.2B). At 9 hours 25% of cells exhibited >5 GFP-LC3 foci and this decreased to 21-23% from 10 to 12 hours (Figure 3.2B).

Neither 6-mercaptopurine, methotrexate, methylprednisolone nor sulfasalazine induced significant increases in percentage of cells exhibiting >5 GFP-LC3 foci at any time-point. At 0.5 hours a slight increase in percentage of cells with >5 GFP-LC3 foci to 21%, 18% and 20% was induced by methotrexate, methylprednisolone and sulfasalazine, respectively (Figure 3.2). However, this decreased to between 6% and 17% for these treatments between 1 and 12 hours (Figure 3.2). There was no increase at 0.5 hours induced by 6-mercaptopurine as percentage of cells exhibiting >5 GFP-LC3 remained between 7% and 16% throughout the time-course (Figure 3.2).

As the optimum time-point for increases in percentage of cells with >5 GFP-LC3 foci was 6 hours for treatments azathioprine, infliximab and EBSS, the 6-hour time-point has been shown separately for comparison of all treatments (Figure 3.2A).

A



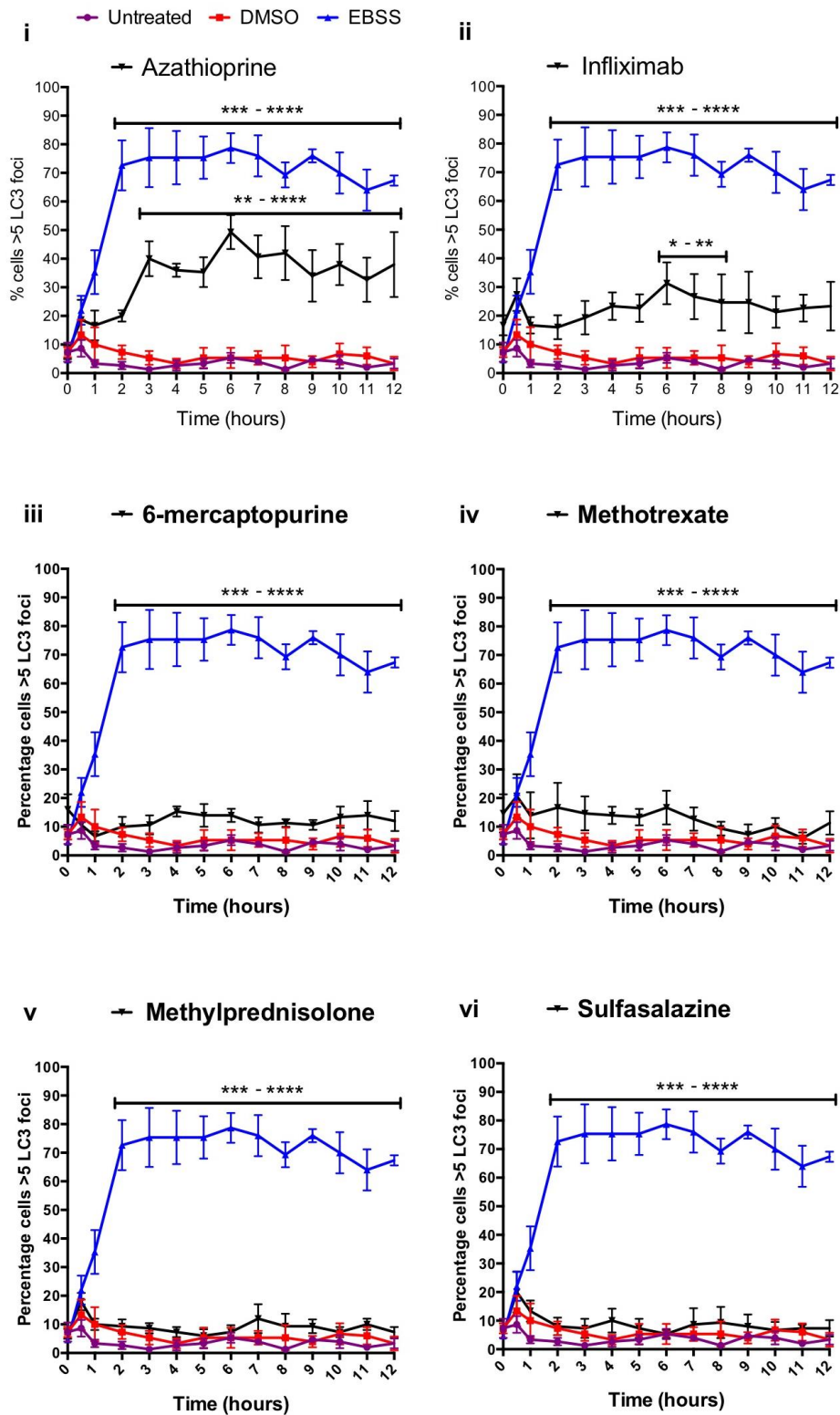
B

Figure 3.2: Live-cell Imaging to monitor IBD drug modulation of Autophagy in HEK293 GFP-LC3 cells

HEK293 GFP-LC3 cells were untreated (i); treated with DMSO (vehicle control) (ii), EBSS (nutrient deprivation) (iii), 120 μ M Azathioprine (iv), 100 μ g/ml Infliximab (v), 120 μ M 6-mercaptopurine (vi), 120 μ M Methotrexate (vii), 100 μ M methylprednisolone (viii) or 150 μ M sulfasalazine (ix) and imaged by live-cell confocal microscopy for 12 hours. Mean

percentage of cells with >5 GFP-LC3 foci per cell (+/- SEM) were calculated from n=3 and fifty cells were counted in 1 field of view for each condition.

A: Confocal microscopy images (i-ix) and quantification (x) for 6 hour time-point shown. One-way ANOVA with Tukey's multiple comparison test was performed on data for the 6-hour time-point **p < 0.01; ****p < 0.0001.

B: Quantification of all time-points shown. Two-way ANOVA with Tukey's multiple comparison test was performed on data to compare the effect of different treatments within each time-point *p <0.05; ** p <0.01; ****p < 0.0001 (azathioprine vs. DMSO; EBSS and infliximab vs. untreated).

3.2.3 Fixed-Cell Confocal Microscopy to Monitor Autophagy Modulation by Azathioprine and Infliximab in HEK293 GFP-LC3 Cells

Fixed-cell confocal fluorescence microscopy was used to confirm the effect of azathioprine and infliximab on autophagy. HEK293 GFP-LC3 cells were treated with azathioprine and infliximab for 6 hours. Untreated cells and cells treated with DMSO showed a basal levels of autophagy with 15% of cells exhibiting >5 GFP-LC3 foci (Figure 3.3). When cells were treated with EBSS the percentage of cells with >5 GFP-LC3 foci increased significantly to 91% (Figure 3.3). The percentage of cells exhibiting >5 GFP-LC3 foci were significantly increased to 61% with azathioprine treatment (Figure 3.3). However, infliximab treatment did not appear to modulate autophagy as only 6% of cells exhibited >5 GFP-LC3 foci (Figure 3.3).

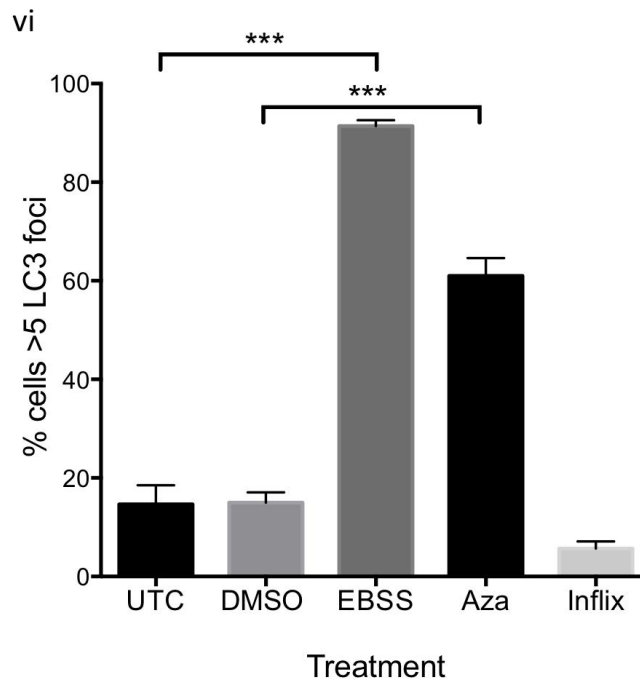
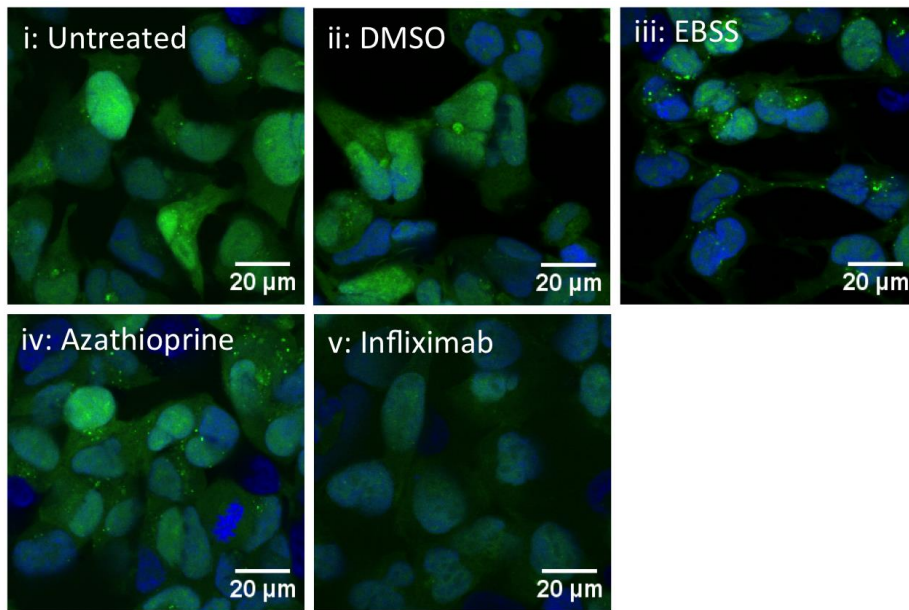


Figure 3.3: Fixed-cell Confocal Microscopy to Monitor Autophagy in HEK293 GFP-LC3 Treated with Azathioprine and Infliximab

HEK293 GFP-LC3 cells were untreated (i) or treated with DMSO (ii), EBSS (iii), 120 μ M Azathioprine (iv) or 100 μ g/ml Infliximab (v) and mounted with DAPI Vectashield (blue) (n=3). 30 cells were counted in 3 fields of view per treatment and mean percentage cells with >5 GFP-LC3 (green) foci was quantified (+/- SEM) (vi). One-way ANOVA with Tukey's multiple comparison test was performed ***p < 0.0001.

3.2.4 LC3 Western Immunoblot to Confirm

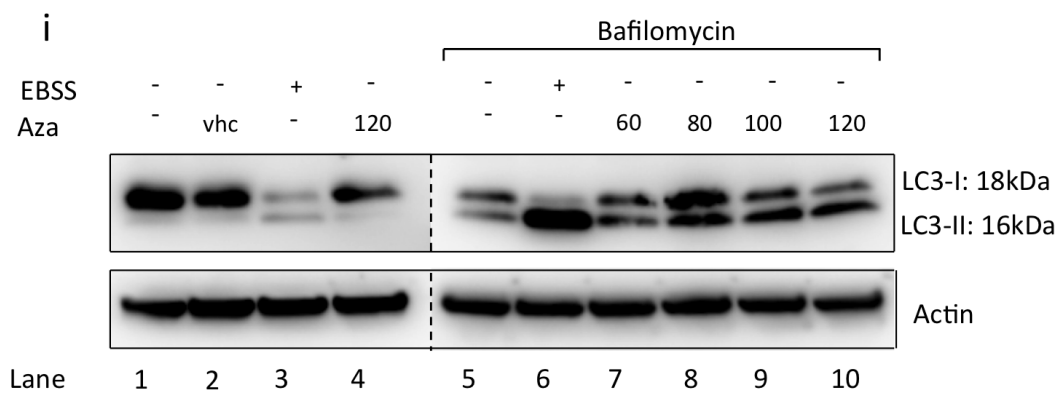
Azathioprine-Induced Autophagy in HEK293 cells

LC3 western immunoblot was used to confirm azathioprine-induced autophagy and determined the optimum concentration. HEK293 cells were treated with 60-120 μ M of azathioprine for 6 hours and bafilomycin was used to block degradation of LC3-II positive autophagosomes in combination with azathioprine and EBSS.

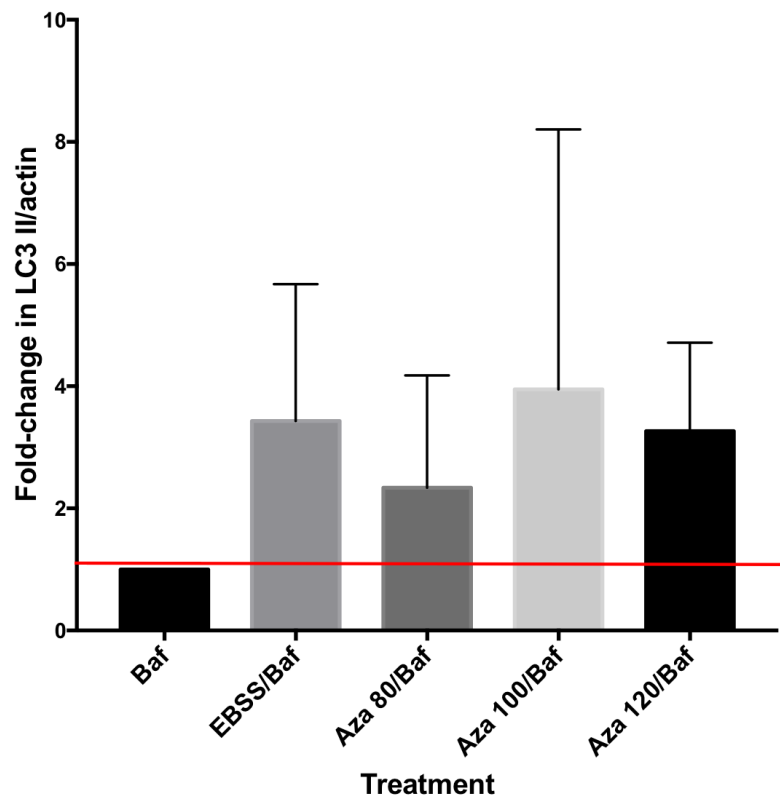
Mean LC3-II density was 0.7% of β -actin in untreated cells and 0.3% in cells treated with DMSO (Figure 3.4A). When treated with EBSS or 120 μ M azathioprine, mean LC3-II density increased to 10.7% and 3.0%, respectively (Figure 3.4A). As bafilomycin treatments were on a separate blot the quantification was analysed separately with LC3-II density at 39.7% of β -actin in bafilomycin only treated cells (Figure 3.4A). LC3-II density increased to 76.0% when bafilomycin was combined with EBSS, which was a fold-change of 3.4 (Figure 3.4A i-ii). When cells were treated with azathioprine LC3-II density increased to 48.7%, 67.0% and 99.0% of β -actin for concentrations of 80, 100 and 120 μ M, respectively (Figure 3.4A). Mean fold-change from bafilomycin was 2.3-, 4.0- and 3.3- fold increase when combined with increasing concentrations of azathioprine, respectively (Figure 3.4A: ii). There was a consistent, yet non-significant, trend showing that azathioprine increased autophagosome-bound LC3-II, which accumulated upon combination with bafilomycin.

The optimal concentration of azathioprine for fold-increase from bafilomycin was 100 μ M (Figure 3.4A: ii). However, there was high variability at 100 μ M azathioprine and the mean LC3-II density was optimal with 120 μ M azathioprine combined with bafilomycin. Therefore, it was determined that the optimal concentration for azathioprine-induced autophagy at 6 hours was 120 μ M.

A

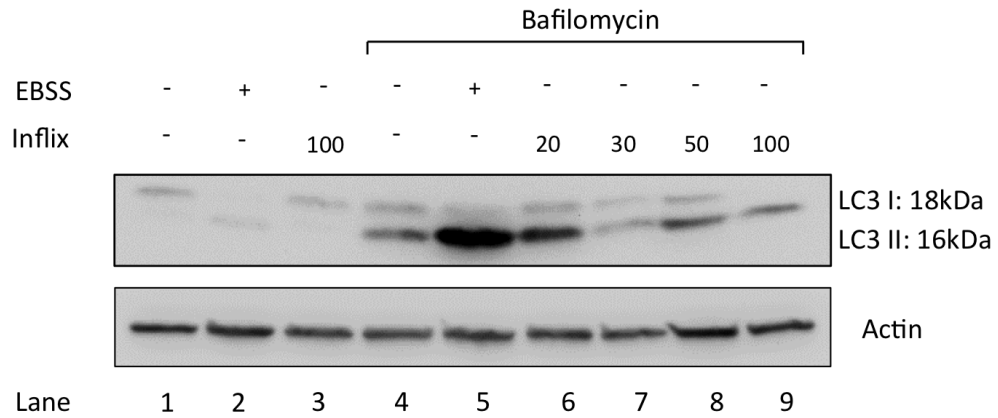


ii



B

i



ii

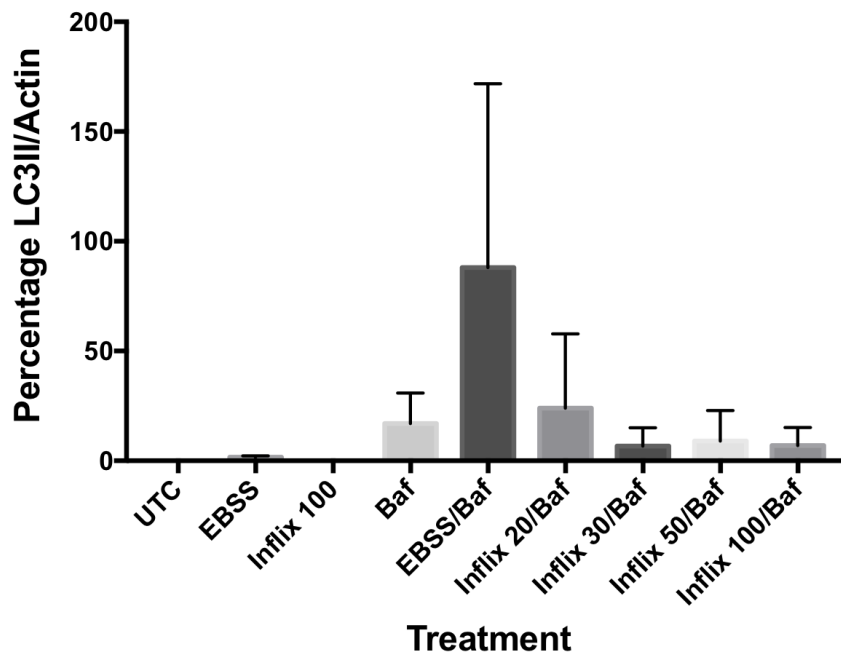


Figure 3.4: LC3 Western Immunoblot to Monitor Autophagy in HEK293 cells Azathioprine and Infliximab

HEK293 cells were untreated; treated with DMOS (vhc), EBSS for nutrient deprivation, 120 μ M azathioprine (A) or 100 μ g/ml infliximab (B) for 6 hours. Cells were also treated with either 160nM bafilomycin only or bafilomycin in combination with EBSS, 60-120 μ M azathioprine (A) or 20-100 μ g/ml infliximab (B) for 6 hours. Protein lysates were separated on a 15% SDS-page gel and immunoblotted for LC3, with a representative western immunoblot from n=3 shown. ImageJ software was used for western densitometry. A: Fold-change from bafilomycin only treatment in LC3-II (16kDa) bands normalized to β -actin was quantified from n=3 (+/- SEM), and not including 60 μ M azathioprine treatment. B: Mean percentage LC3-II bands normalized to β -actin was quantified from n=3 (+/- SEM).

3.2.5 LC3 Western Immunoblot to Monitor

Autophagy in HEK293 Cells Treated with Infliximab

The LC3 western immunoblot was used as an alternative method to assess autophagy modulation induced by infliximab. Bafilomycin was used to block degradation of LC3-II positive autophagosomes in HEK293 cells and was combined with EBSS and 20-100 μ g/ml infliximab for 6 hours.

Mean LC3-II density was between 0% and 2% of β -actin in cells without bafilomycin treatment (Figure 3.4B). Bafilomycin treatment increased LC3-II density to 17% of β -actin (Figure 3.4B). LC3-II density increased to 88% when bafilomycin was combined with EBSS, but increased more modestly to 24% when combined with 20 μ g/ml infliximab (Figure 3.4B). However, when bafilomycin was combined with higher concentrations of infliximab, 30-100 μ g/ml, LC3-II density decreased to between 7% and 9% (Figure 3.4B).

3.2.6 Flow Cytometry to Monitor Autophagy in

HEK293 GFP-LC3 cells Treated with Azathioprine and Infliximab

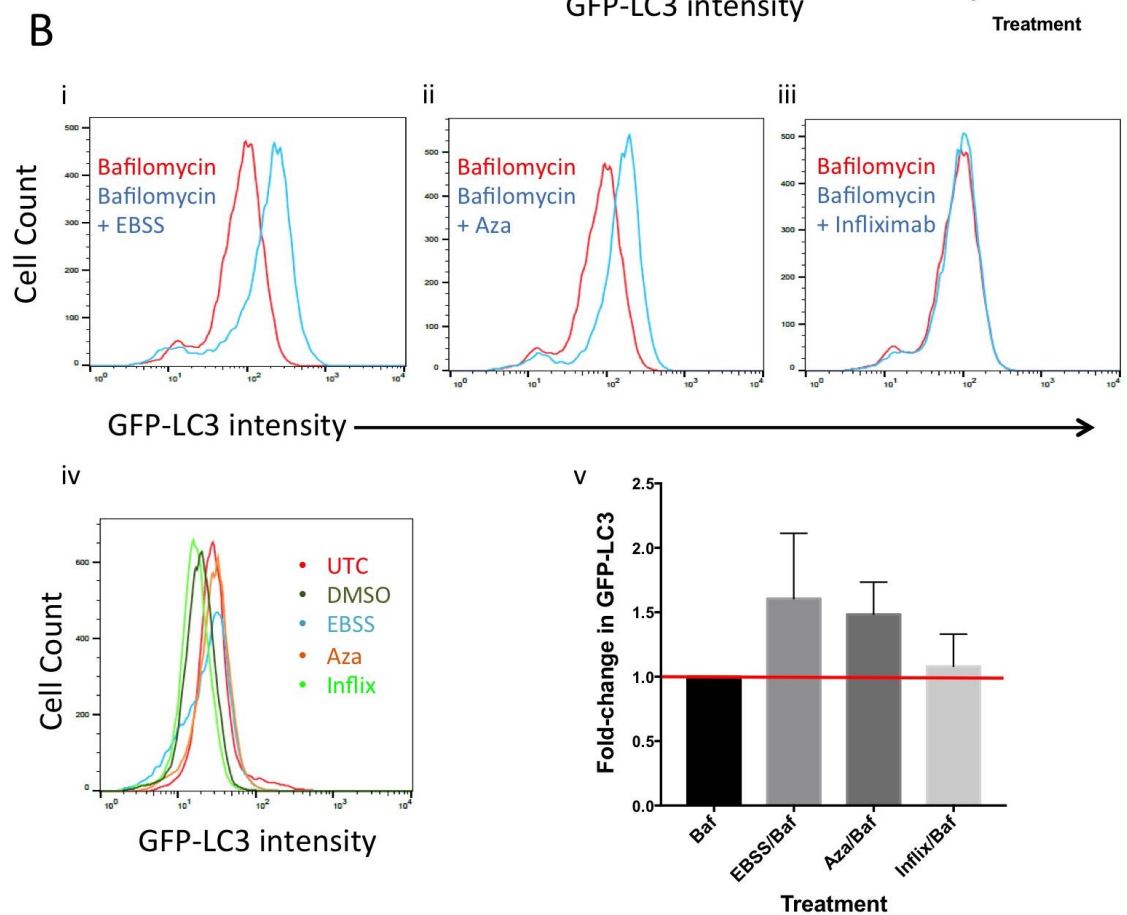
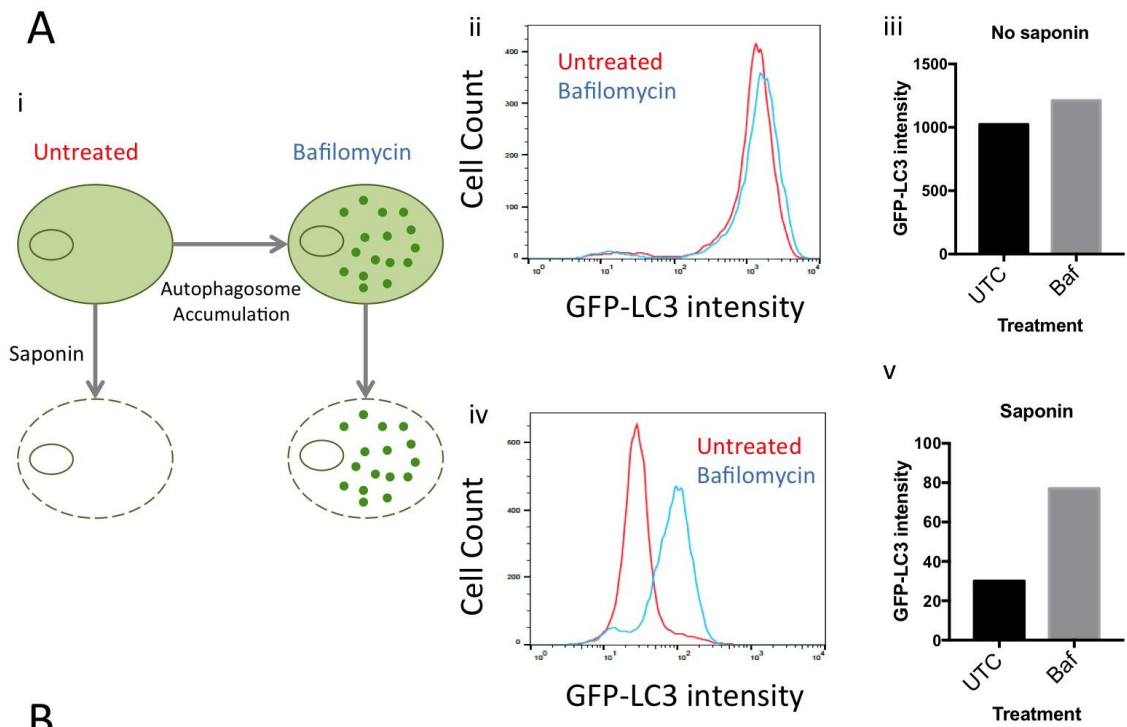
Flow cytometry for GFP-LC3 analysis was used as a complementary technique to support the finding that azathioprine induces autophagy. As LC3 does not increase in abundance but rather re-localises to the autophagosome membrane upon autophagy induction, to quantify autophagy levels by flow cytometry, cytosolic LC3 must be removed (Figure 3.5A: i). This allowed for quantification of GFP-LC3 to indicate levels of autophagy activity in the cell (Figure 3.5A). HEK293 GFP-LC3 cells were left untreated or treated with bafilomycin to block degradation of GFP-LC3 positive autophagosomes for 6 hours (Figure 3.5A). Initially, geometric mean of GFP-LC3 fluorescent intensity was used to compare cells permeabilised with saponin to cells not permeabilised, to assess efficacy of cytosolic GFP-LC3 removal (Figure 3.5A). The GFP-LC3 geometric mean of non-permeabilised cells was 1023 for untreated cells, which increased slightly to 1212 when treated with bafilomycin (Figure 3.5A: ii-iii). When cytosolic GFP-LC3 was removed the geometric mean was markedly lower (30 for untreated) but when cells were treated with bafilomycin, the geometric mean more than doubles to 77 (Figure 3.5A: iv-v). Therefore, although the fluorescent intensity was lower overall when cytosolic GFP-LC3

was removed, the increase in autophagosome-bound GFP-LC3 when treated with bafilomycin can be clearly observed.

HEK293 GFP-LC3 cells were then untreated or treated with DMSO, EBSS for nutrient deprivation, azathioprine or infliximab for 6 hours (Figure 3.5 B: iv). Bafilomycin was used to block degradation of autophagosomes, and EBSS (i), azathioprine (ii) and infliximab (iii) treatments were also combined with bafilomycin (Figure 3.5B). Cells were permeabilised with saponin to remove cytosolic GFP-LC3 for flow cytometry analysis and were then cytopinned on to microscope slides for confocal microscopy analysis to allow visualisation of the location and intensity of GFP-LC3.

The GFP-LC3 geometric mean in untreated cells was 22, which remained relatively constant (~19-22), when cells were treated with DMSO, EBSS and infliximab (Figure 3.5B). There was a small increase in GFP-LC3 intensity to 25 with azathioprine treatment (Figure 3.5B). When cells were treated with bafilomycin there was a significant increase in GFP-LC3 intensity to a geometric mean of 84 (Figure 3.5B). The fold-change from GFP-LC3 geometric mean of cells treated with bafilomycin to cells treated with bafilomycin combined with EBSS, azathioprine or infliximab was shown in Figure 3.5B (v) to allow assessment of the augmentation of GFP-LC3 accumulation. When bafilomycin was combined with infliximab, GFP-LC3 intensity remained constant at 85 (Figure 3.5B). However, when EBSS was combined with bafilomycin the geometric mean increased to 125, which was a fold-change of 1.67 compared to bafilomycin (Figure 3.5B). Furthermore, when azathioprine was combined with bafilomycin, GFP-LC3 intensity increased to a geometric mean of 122, which was a fold-increase of 1.52 compared to bafilomycin (Figure 3.5B). Despite the notable increase in GFP-LC3 intensity from bafilomycin induced by combination with EBSS or azathioprine, the changes were not statistically significant. However, the trend observed does support the statistically significant observations found with previous complimentary methods such as live-cell and fixed-cell imaging.

Saponin treatment and cytopinning of the cells caused GFP-LC3 to appear diffuse within the cell, however the untreated control cells had no visible GFP-LC3, and therefore it was assumed that all cytosolic GFP-LC3 had been removed (Figure 3.5C). Furthermore, there was a visible increase in GFP-LC3, when comparing bafilomycin only (xv) to bafilomycin combined with EBSS (xvi) or azathioprine (xvii) (Figure 3.5C).



C

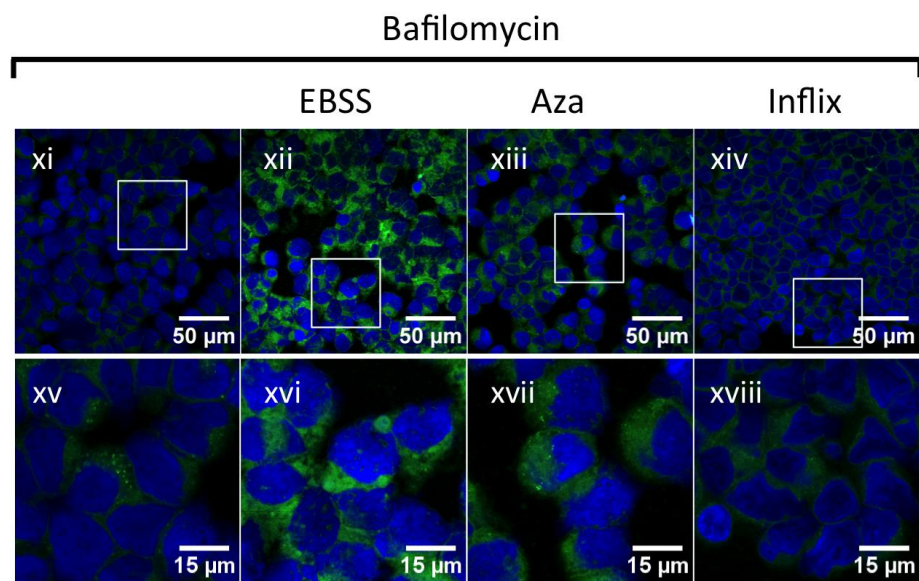
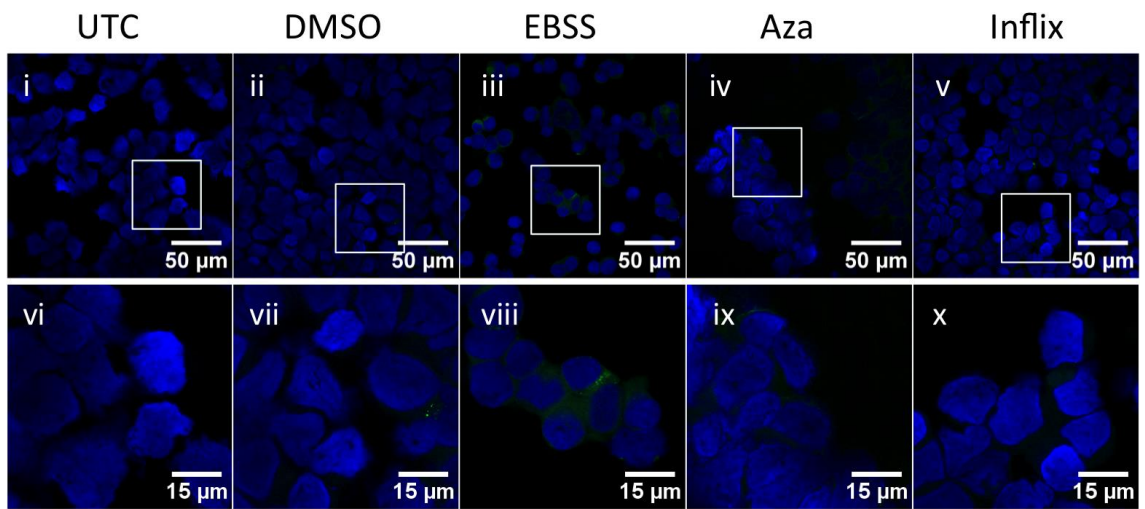


Figure 3.5: Flow Cytometry to Monitor Autophagy in HEK293 GFP-LC3 Cells Treated with Azathioprine and Infliximab

A: Schematic diagram showing cell permeabilisation with 0.05% saponin to remove cytosolic GFP-LC3 to allow flow cytometry analysis (Eng et al., 2010) (i). HEK293 GFP-LC3 cells were either untreated or treated with 160nM bafilomycin for 6 hours (ii-v). Cells were washed without (ii-iii) or with (iv-v) cell permeabilisation with 0.05% saponin to remove cytosolic GFP-LC3 before fixation. Geometric mean of GFP-LC3 fluorescent intensity of cells was quantified by flow cytometry and analysed using FlowJo software.

B: HEK293 GFP-LC3 cells were treated with either 160nM bafilomycin only or bafilomycin with EBSS for nutrient deprivation (i), 120μM azathioprine (ii) or 100μg/ml Infliximab (iii). Cells were also treated without bafilomycin (iv). After 6-hour incubation,

cells were washed with 0.05% saponin. Geometric mean of GFP-LC3 intensity of cells was quantified by flow cytometry and analysed using FlowJo software. Histograms were selected to represent n=3 and fold-change in GFP-LC3 geometric mean from bafilomycin only was quantified from n=3 (+/- SEM) (v).

C: Cells used for flow cytometry were cytospinned and mounted with DAPI Vectashield (blue) for confocal microscopy imaging and analysis of GFP-LC3 (green): untreated (i, vi), DMSO (ii, vii), EBSS (iii, viii), 120µM azathioprine (iv, ix), 100µg/ml Infliximab (v, x), bafilomycin only (xi, xv) and bafilomycin in combination with EBSS (xii, xvi), 120µM azathioprine (xiii, xvii) or 100µg/ml Infliximab (xiv, xvii).

3.2.7 HEK293 Cells Transiently Transfected with RFP-GFP-LC3 to Confirm Azathioprine-Induced Autophagy Flux

LC3-II and autophagosomes can accumulate due to activation or inhibition of the autophagy pathway. To clarify the effect of azathioprine on autophagy, HEK293 cells were transfected with the tandem fluorescent-tagged RFP-GFP-LC3 plasmid and treated with azathioprine, bafilomycin or EBSS for 6 hours. When RFP-GFP-LC3 proteins are localised to autophagosomes (early stage of the pathway), both GFP and RFP proteins are stable and can be observed as yellow foci in merged images (Figure 3.6A). When autophagosomes fuse with lysosomes (late stage of the pathway) GFP is quenched leaving only the more stable RFP-LC3 bound to autophagolysosomes (Mizushima et al., 2010) (Figure 3.6A).

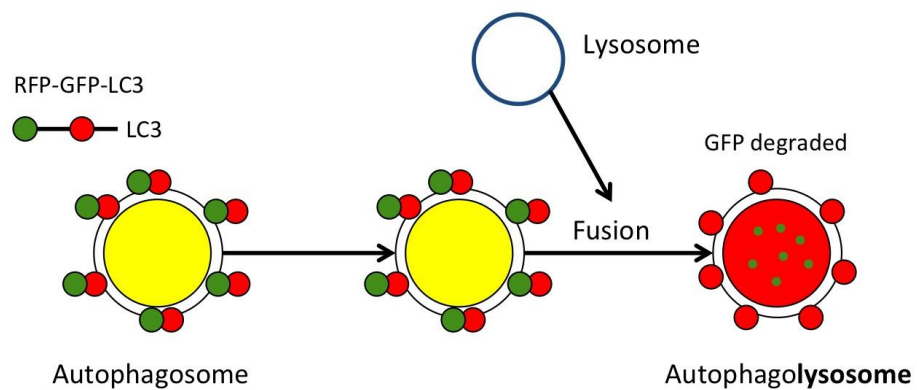
When autophagy activity was induced by EBSS there was an increase in autophagosome formation, therefore an increase in percentage of cells with >10 yellow RFP-GFP-LC3 foci (Figure 3.6B: xi, xiv). As EBSS induces autophagy flux, there was also an increase in autophagosome fusion with lysosomes, which degrades GFP causing an accumulation of red late stage autophagolysosomes (Figure 3.6B: xi, xiv). When autophagosome fusion with lysosomes was inhibited, with bafilomycin treatment, only an accumulation of yellow RFP-GFP-LC3 foci was visible (Figure 3.6B: x, xiii). Azathioprine treatment induced autophagy activity, as both yellow RFP-GFP-LC3 (xii, xv) and red RFP-LC3 foci (xii, xv: indicated with arrow) were visible (Figure 3.6B: iv).

For quantification of autophagy modulation, the percentage of transfected cells with >10 LC3 foci was quantified (Figure 3.6B: xvi) and compared to untreated. As expected,

all three treatments caused significant increases in autophagosome accumulation compared to untreated (Figure 3.6B, panel xvi).

To determine the proportion of late stage autophagosomes and therefore the mode of autophagy modulation, the percentage of RFP-LC3 foci (autophagolysosomes), normalised to total LC3 foci (red autophagolysosomes plus yellow autophagosomes), was quantified (Figure 3.6B: xvii). In untreated cells basal autophagy flux was observed with 85% of autophagosomes appearing red, therefore having fused with lysosomes. Upon treatment with EBSS and azathioprine, autophagy flux was not disrupted as the percentage of red autophagosomes remained between 78% and 86%, respectively (Figure 3.6B, panel xvii). However, as fusion with the lysosome and subsequent degradation of GFP was blocked with bafilomycin treatment, there was a significant decrease in percentage of red autophagosome compared to untreated cells, to only 5% (Figure 3.6B, panel xvii).

A



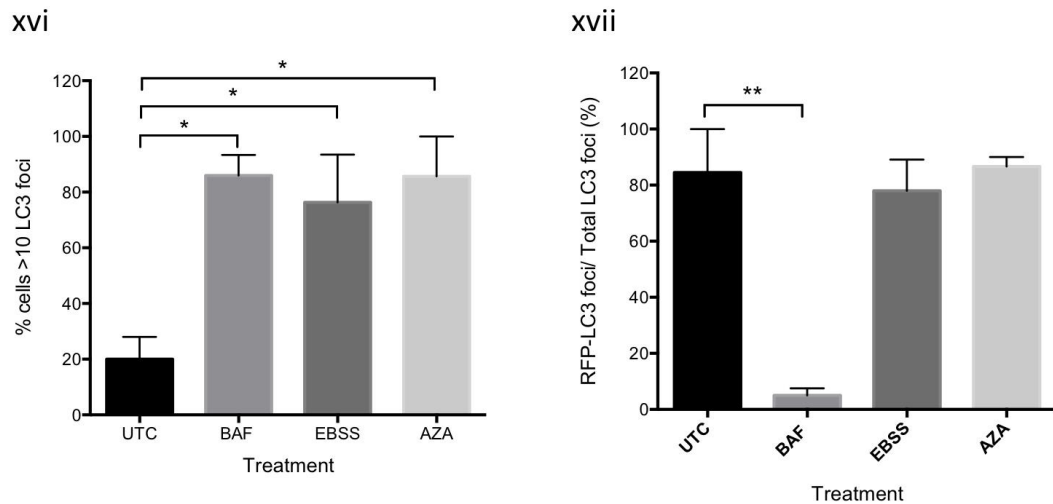
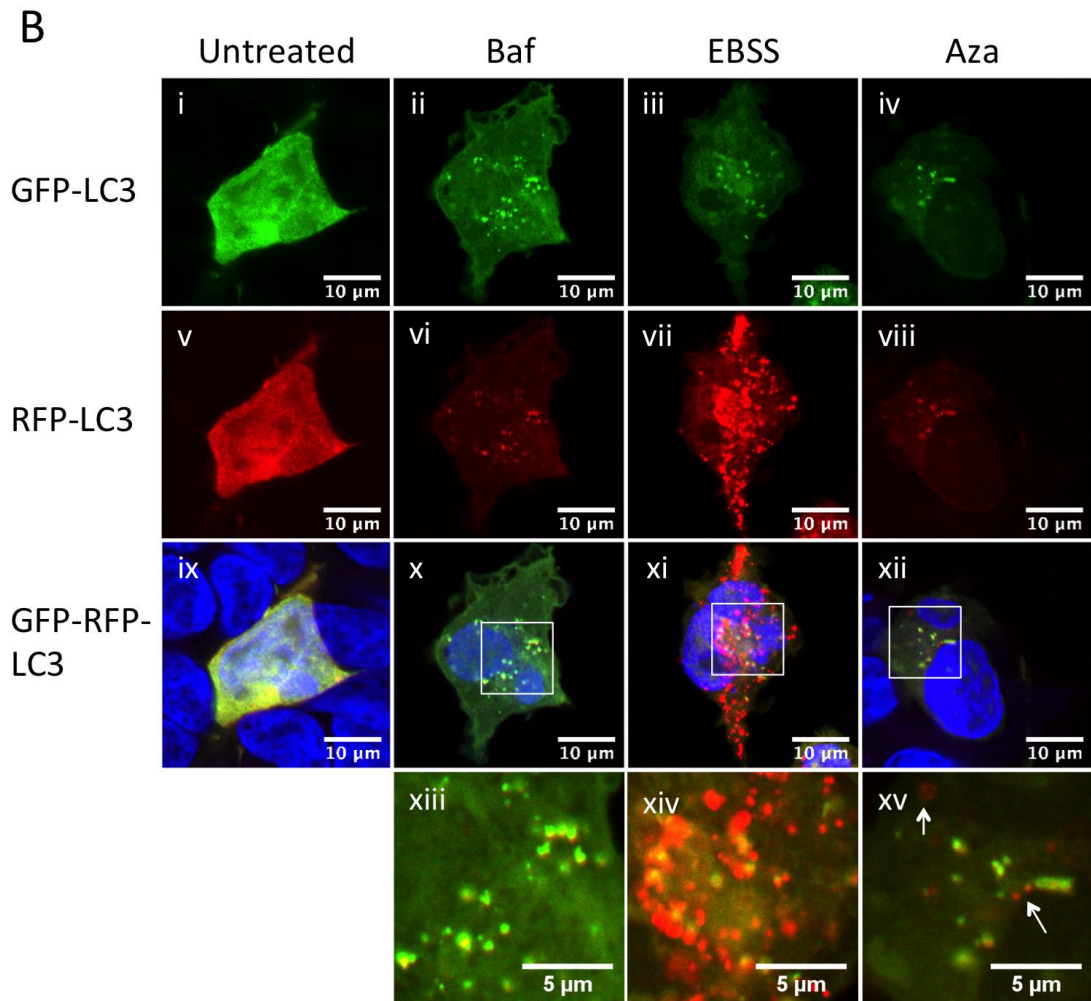


Figure 3.6: HEK293 Cells Transiently Transfected with GFP-RFP-LC3 to Monitor Azathioprine-Induced Autophagy Flux using Confocal Microscopy

A: Schematic diagram of RFP-GFP-LC3 plasmid used to track autophagosome progression through pathway. When GFP-RFP-LC3 proteins are bound to autophagosomes, yellow foci are visible. Fusion with the lysosome quenches GFP and autophagolysosomes appear as red foci.

B: HEK293 cells were transfected by nucleofection with RFP-GFP-LC3 plasmid and left untreated (i, v, ix) or treated with 160nM Bafilomycin (ii, vi, x, xiii), EBSS (iii, vii, xi, xiv), or 120µM azathioprine (iv, viii, xii, xv) for 6 hours and mounted with DAPI Vectashield (blue). Percentage of transfected cells with >10 LC3 foci was quantified (+/-SEM) (n=5) (xvi) *p value <0.05. Percentage of RFP-LC3 foci (autophagolysosomes) normalised to total LC3 foci (red autophagolysosomes plus yellow autophagosomes) was quantified (+/-SEM) (n=5) (xvii) **p <0.01, ***p <0.001.

3.2.8 AlamarBlue® Cytotoxicity Assay to Identify Non-Toxic Concentration Range of Azathioprine in THP-1-Derived Macrophages

Resident macrophages have an important role in maintaining GI tract homeostasis, and macrophages from CD patients are more susceptible to pathogen infection and persistence, with more pronounced pro-inflammatory responses (Vazeille et al., 2015), in part due to defects in autophagy (Lapaquette et al., 2010, 2012; Negroni et al., 2012; Sadabad et al., 2015). Therefore, the human monocyte cell line, THP-1's, differentiated into macrophages using PMA (Supplementary Results: Chapter 9), were used as a more physiologically relevant cell line for investigating autophagy in the context of CD.

As described in section 3.2.1, the alamarBlue® cytotoxicity assay indirectly measures cell viability by assessing metabolic activity, and can be used for time-course studies. The THP-1-derived macrophages were left untreated (indicated by red line) or treated with 60-160µM azathioprine for 24 hours in the presence of 10% alamarBlue® reagent. Absorbance was measured at 2, 4, 6 and 24 hours and metabolic activity was calculated as a percentage of the metabolic activity of untreated cells for each time-point (Figure 3.7).

When cells were treated with DMSO there was no significant change in metabolic activity compared to untreated cells. However, when cells were treated with 0.5% Triton-X, as a positive control for cell death, metabolic activity significantly decreased throughout the time-course (data not shown).

It was found that azathioprine did not induce a decrease in metabolic activity with the lowest metabolic activity being 94% of untreated (Figure 3.7). There were some increases in metabolic activity observed, with the highest value being 154% at 2 hours

with 100 μ M (Figure 3.7), although none of these increases were statistically significant and did not correlate with concentration or incubation time.

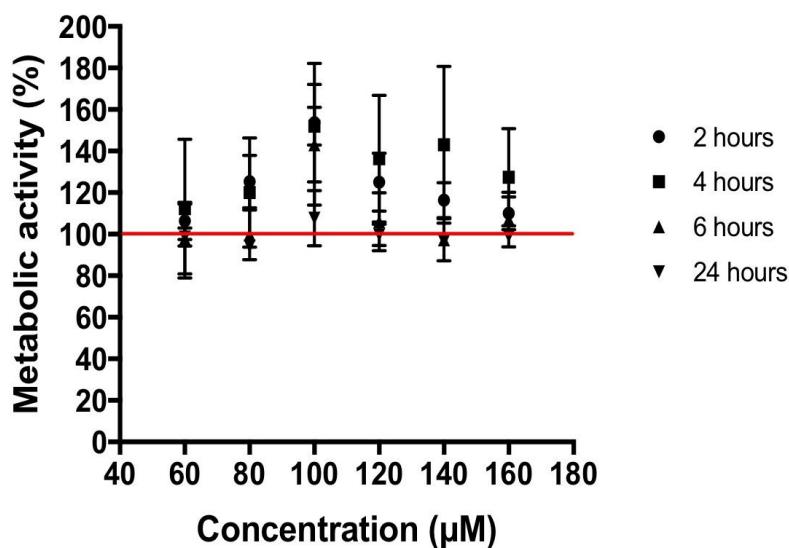


Figure 3.7: AlamarBlue[®] Toxicity Assay Time-course and Concentration Range Analysis in THP-1-derived Macrophages Treated with Azathioprine

THP-1-derived macrophages were untreated or treated with 60-160 μ M azathioprine for 24-hours in the presence of 10% alamarBlue[®] reagent (n=3). Fluorescence was read at 2, 4, 6 and 24 hours. Percentage difference between fluorescent intensity of treated and untreated cells (red line) was calculated after fluorescent intensity of corresponding “no cells” controls were subtracted. Mean percentage metabolic activity (+/- SEM) is displayed. A two-way ANOVA with Tukey’s multiple comparison test was used to compare the effect of treatments and concentration within each time-point. Experimental procedure was performed by Ms Suzie McGinley under the supervision of Ms Kirsty Hooper.

3.2.9 LC3 Immunostain to Monitor Azathioprine-Induced Autophagy in THP-1-Derived Macrophages

LC3 immunostaining was used to determine if azathioprine modulates autophagy in THP-1-derived macrophages. Although alamarBlue[®] analysis detected no cytotoxic effects of azathioprine up to 160 μ M and 24-hour incubation, the concentration used in THP-1-derived macrophages was 120 μ M to replicate findings in HEK293 cells. To determine the optimal time-point for azathioprine-induced autophagy in THP-1-derived macrophage, cells were untreated or treated with azathioprine for 2, 4, 6, 8, 16 and 24 hours.

Although notable increases in percentage of cells with >5 LC3 foci were visible between 6 and 24 hours, an optimal increase was observed at 6-hour incubation time (Supplementary Figure 10.1). At this time-point, the percentage of THP-1-derived macrophages with >5 LC3 foci increased from 17% in untreated cells to 62% in azathioprine-treated cells (Supplementary Figure 10.1: xiii).

At the optimal 6-hour time-point cells were left untreated (i), or treated with DMSO (ii), azathioprine (iii), or EBSS (iv) (Figure 3.8). Untreated cells and DMSO-treated cells exhibited >5 LC3 foci in 9% and 15% of cells, respectively (Figure 3.8B). A significant increase in the percentage of cells with >5 LC3 foci was observed when cells were treated with azathioprine to 43% (Figure 3.8). There was a slightly more pronounced increase in percentage of cells exhibiting >5 LC3 foci when treated with EBSS to 59% (Figure 3.8).

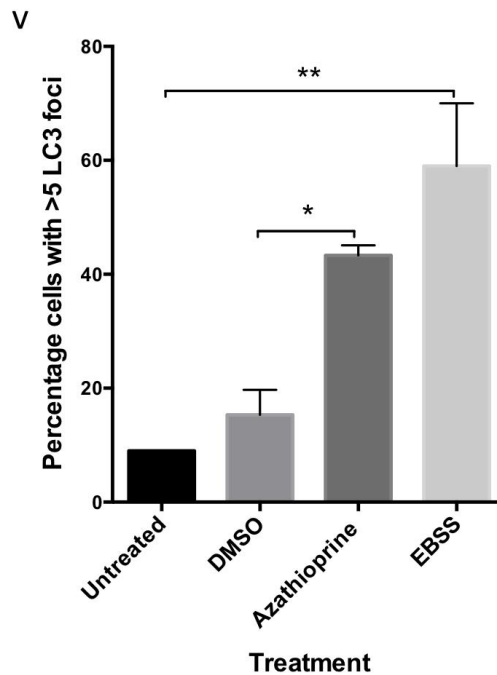
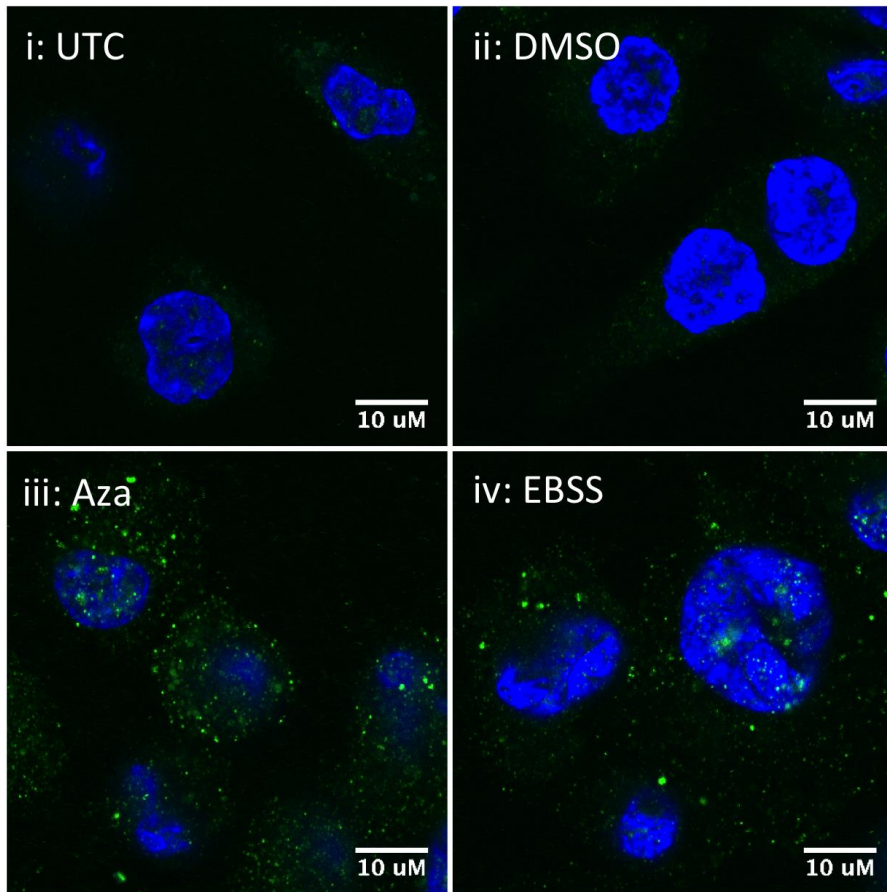


Figure 3.8: Azathioprine-Induced Autophagy in THP-1-derived Macrophages Monitored by LC3 Immunostaining

Cells were untreated (i), or treated with DMSO vehicle control (ii), 120 μ M azathioprine (iii), or EBSS (nutrient deprivation) (iv) for 6 hours (n=3). Cells were then immunostained for LC3 (green) and mounted with DAPI Vectashield (blue). 30 cells were counted in 3 fields of view per treatment and percentage cells with >5 GFP-LC3 foci quantified from

n=3 (+/- SEM). One-way ANOVA with Tukey's multiple comparisons was performed *p <0.05; **p < 0.01.

3.2.10 THP-1-derived macrophages LC3 flow cytometry

Flow cytometry for endogenous LC3 was investigated as a supplementary method for monitoring autophagy in THP-1-derived macrophages. Cells were treated with DMSO, azathioprine, EBSS, bafilomycin, EBSS with bafilomycin and azathioprine with bafilomycin for 6 hours and immunostained for endogenous LC3 for flow cytometry analysis, as optimised in Supplementary Results (Chapter 9). The representative histograms demonstrate an increase in LC3-II from untreated compared to bafilomycin treated cells (Figure 3.9: i), which was augmented by addition of azathioprine (Figure 3.9: ii), and to a lesser extent, EBSS treatment (Figure 3.9: iii). However, quantification of mean geometric mean showed that results obtained with this method were not reproducible, as responses to autophagy-modulating controls appeared to be inconsistent due to highly variable LC3-II/FITC immunostaining intensities. Therefore, in this cell type, flow cytometry for endogenous LC3 could not be used to confirm autophagy induction by azathioprine.

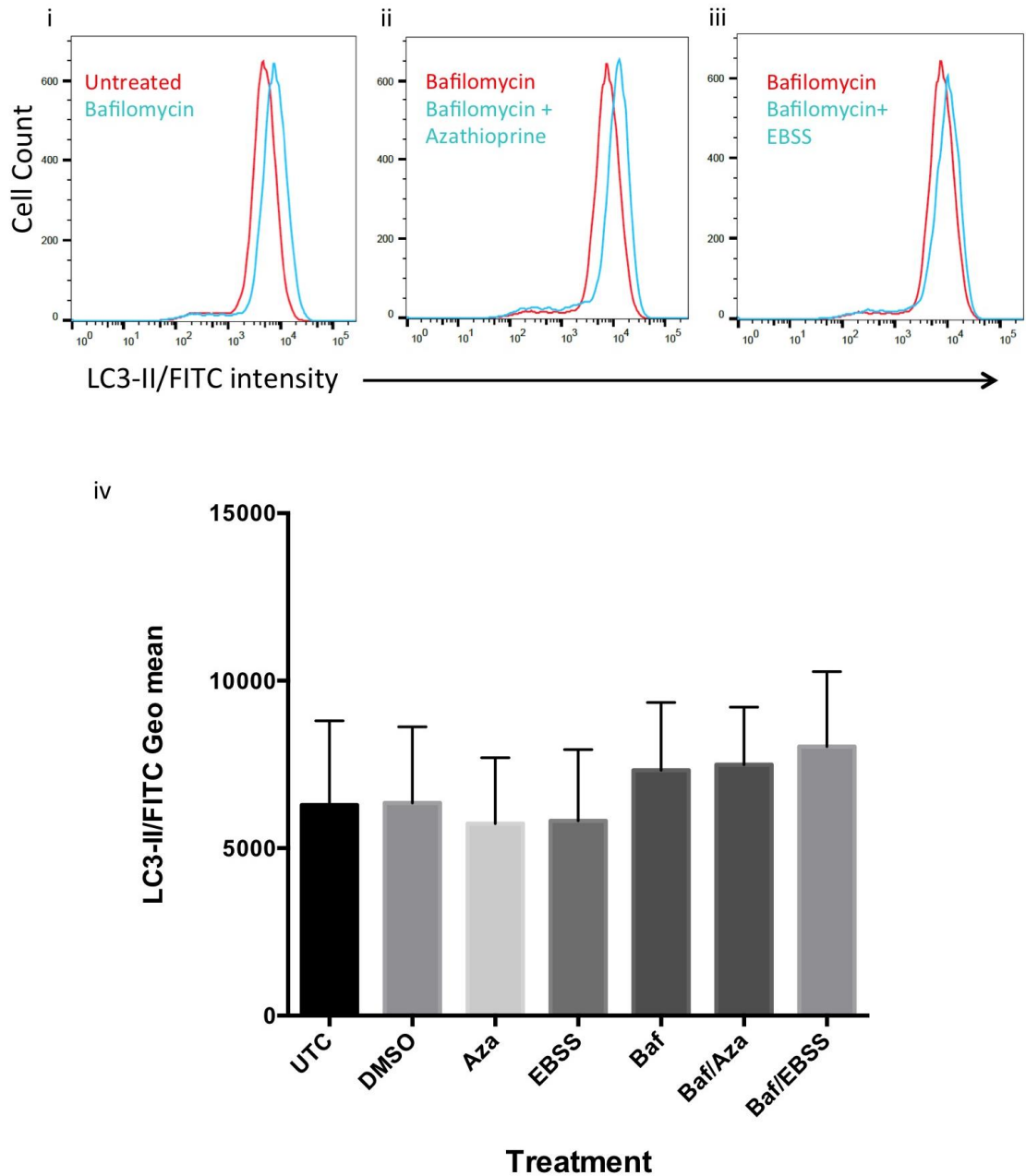


Figure 3.9: Endogenous LC3 Flow Cytometry to monitor Autophagy Induction in THP-1-derived Macrophages

THP-1-derived macrophages were treated with either 160nM bafilomycin only or bafilomycin with EBSS for nutrient deprivation (i), 120 μ M azathioprine (ii) or 100 μ g/ml Infliximab (iii). Cells were also treated without bafilomycin (iv). After 6-hour incubation, cells were washed with 0.05% saponin and immunostained for LC3. Geometric mean of LC3 intensity of cells was quantified by flow cytometry and analysed using FlowJo software. Histograms were selected to represent n=3 and mean LC3 geometric mean was quantified from n=3 (+/- SEM) (iv).

3.3 Summary

Six commonly used IBD drugs were selected from the five main drug classes used for CD treatment. Using the alamarBlue® cytotoxicity assay, it was confirmed that none of the drugs selected had cytotoxic effects in the HEK293 cells at the concentrations and time-points investigated. Using live-cell imaging to monitor GFP-LC3 foci formation in HEK293 GFP-LC3 cells, it was identified that azathioprine, and to a lesser extent, infliximab, modulated autophagy activity, while the other IBD drugs screened induced minimal or no effect.

At the optimum time-point of 6 hours, complementary techniques were used in an attempt to confirm these results. However, infliximab treatment of HEK293 GFP-LC3 cells for 6 hours failed to increase autophagy activity as assessed by fixed-cell confocal microscopy and flow cytometry analysis of GFP-LC3. Western immunoblot revealed slight decreases in accumulated LC3-II with some concentrations, which may suggest that infliximab causes inhibition of autophagy activity. However, the varying effect of concentration and the opposing findings from live-cell imaging contradict this conclusion. The discrepancies in results for infliximab between live-cell imaging and the additional techniques is likely due to the higher sensitivity of the live-cell imaging technique.

In contrast, azathioprine induced strong autophagy responses in HEK293 and HEK293 GFP-LC3 cells, and THP1-1-derived macrophages. Fixed-cell and flow cytometry analysis of GFP-LC3 formation and western immunoblot for LC3-II in HEK293 cells confirmed azathioprine-induced autophagy modulation and identified optimum time-point as 6 hours and optimal concentration as 120µM. Although there was a lack of statistical significance observed with some techniques, the result remains valuable to supplement previous significant results, especially when it is considered that the positive control, EBSS, shows a similar trend to azathioprine that was also not statistically significant. Azathioprine treatment modulated autophagy in THP-1-derived macrophages at the same time-point and concentration that was optimal for autophagy induction in HEK293 cells, as monitored by LC3 immunostaining.

When treating cells with bafilomycin, the GFP-LC3 foci and LC3-II that accumulate represent the autophagosomes that are formed and usually degraded during basal

autophagy activity. When bafilomycin is combined with treatments that increase autophagy activity and autophagosome formation, GFP-LC3 and LC3-II accumulation would be augmented. If bafilomycin were combined with treatments that modulate autophagy in a similar manner to bafilomycin, accumulated GFP-LC3 foci and LC3-II would likely remain constant. When azathioprine was combined with bafilomycin it increased GFP-LC3 foci and LC3-II compared with bafilomycin treatment alone. To corroborate that azathioprine induces autophagy flux as opposed to blocking autophagosome turnover, HEK293 cells were transfected with RFP-GFP-LC3 to differentiate between early and late stage autophagosomes. Azathioprine treatment resulted in the accumulation of both autophagosomes and autophagolysosomes, confirming that azathioprine induces flux through the entire autophagy pathway.

In conclusion, azathioprine has been identified as a strong inducer of autophagy in the HEK293 cells and THP-1-derived macrophages, and optimal concentrations and incubation times have been identified for autophagy induction. These findings set the foundations for subsequent investigation of the mechanism of action of azathioprine and its effect on pathogen clearance in the context of autophagy. Furthermore, this enables examination of the effect of this IBD drug in primary immune cells derived from paediatric IBD patients.

4. Investigating the effects of IBD Drugs on Cell Death

4.1 Introduction

Autophagy is intimately linked with cell death as described in section 1.2.4. When exposed to mild stress, the autophagy pathway promotes cell survival and inhibits apoptosis (Mariño et al., 2014). When stress is prolonged or intense, however, the cell will initiate apoptosis, and actively suppress autophagy to accelerate cell death (Mariño et al., 2014). Therefore, autophagy often precedes apoptosis when cells undergo stress. In a different model of cell death and autophagy; autophagic cell death (ACD) can be caused by excessive autophagy causing degradation of essential cellular components (Pattingre et al., 2005). This is distinct from apoptosis that is accompanied by autophagy, as ACD is cell death directly mediated by autophagy and if autophagy is prevented, cell death will not occur (Pattingre et al., 2005).

When thiopurine nucleotides incorporate into DNA, DNA mismatch-repair (MMR) is activated, which can lead to DNA single-stranded breaks that activate apoptosis via p53 (O'Brien and Brown, 2006; Yan et al., 2003). In MMR-proficient HCT116, HT29 and human endometrial cancer cells (HEC59), thiopurines induce both apoptosis and autophagy (Chaabane et al., 2016; Zeng et al., 2007; Zeng and Kinsella, 2010, 2008), regulated by p53-mediated responses to MMR processing (Zeng et al., 2007). The increased autophagy activity had a pro-survival role as it inhibited apoptosis, and it was suggested that the most likely mechanism was through the degradation of damaged mitochondria (Chaabane et al., 2016; Zeng et al., 2007). The aim of this chapter is to determine whether azathioprine-induced autophagy is linked to cell death by using complementary techniques to analyse different types of cell death.

4.2 Results

4.2.1 Cleaved-PARP Western Immunoblot to Monitor Apoptosis in HEK293 Cells Treated with Azathioprine

To determine if azathioprine treatment induces cell death, cleaved- Poly (ADP-ribose) polymerase (PARP) western immunoblotting was used. Both intrinsic and extrinsic pathways can induce caspase-3 dependent apoptosis, which results in the cleavage of PARP. Therefore, the accumulation of cleaved PARP on a western immunoblot is indicative of caspase-dependent apoptosis. To identify an effective positive control for PARP cleavage (TNFR) HEK293 and HEK293 GFP-LC3 cells were transfected with the p55 TNF receptor, as ligation of this receptor triggers extrinsic apoptosis. Cell lysates were prepared and western immunoblotted for full length PARP (116kDa) and cleaved PARP (89kDa) (Supplementary Figure 10.2). In transfected cells there is a clear increase in cleaved-PARP compared to non-transfected for both cell lines (Supplementary Figure 10.2).

Following on from this HEK293 cells were left untreated, treated with DMSO or with azathioprine for 6 and 24 hours (Figure 4.1). There was no increase in cleaved-PARP observed with azathioprine or DMSO for either time-point, however TNFR transfection induced a considerable increase in cleaved-PARP (Figure 4.1).

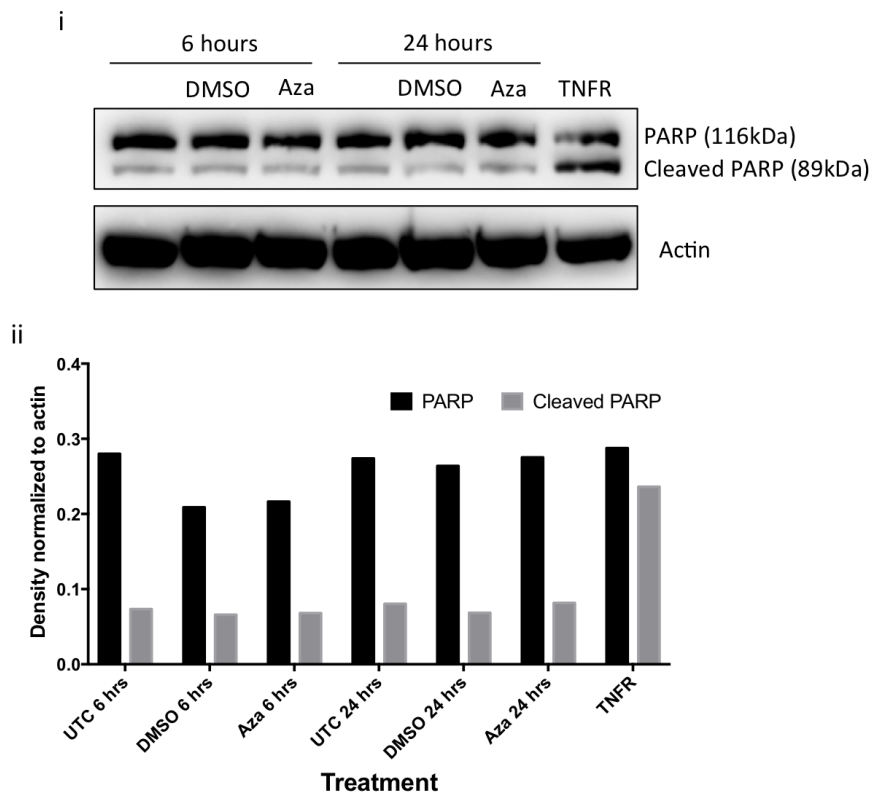


Figure 4.1: Cleaved-PARP Western Immunoblot to Monitor Apoptosis in Cells Treated with Azathioprine

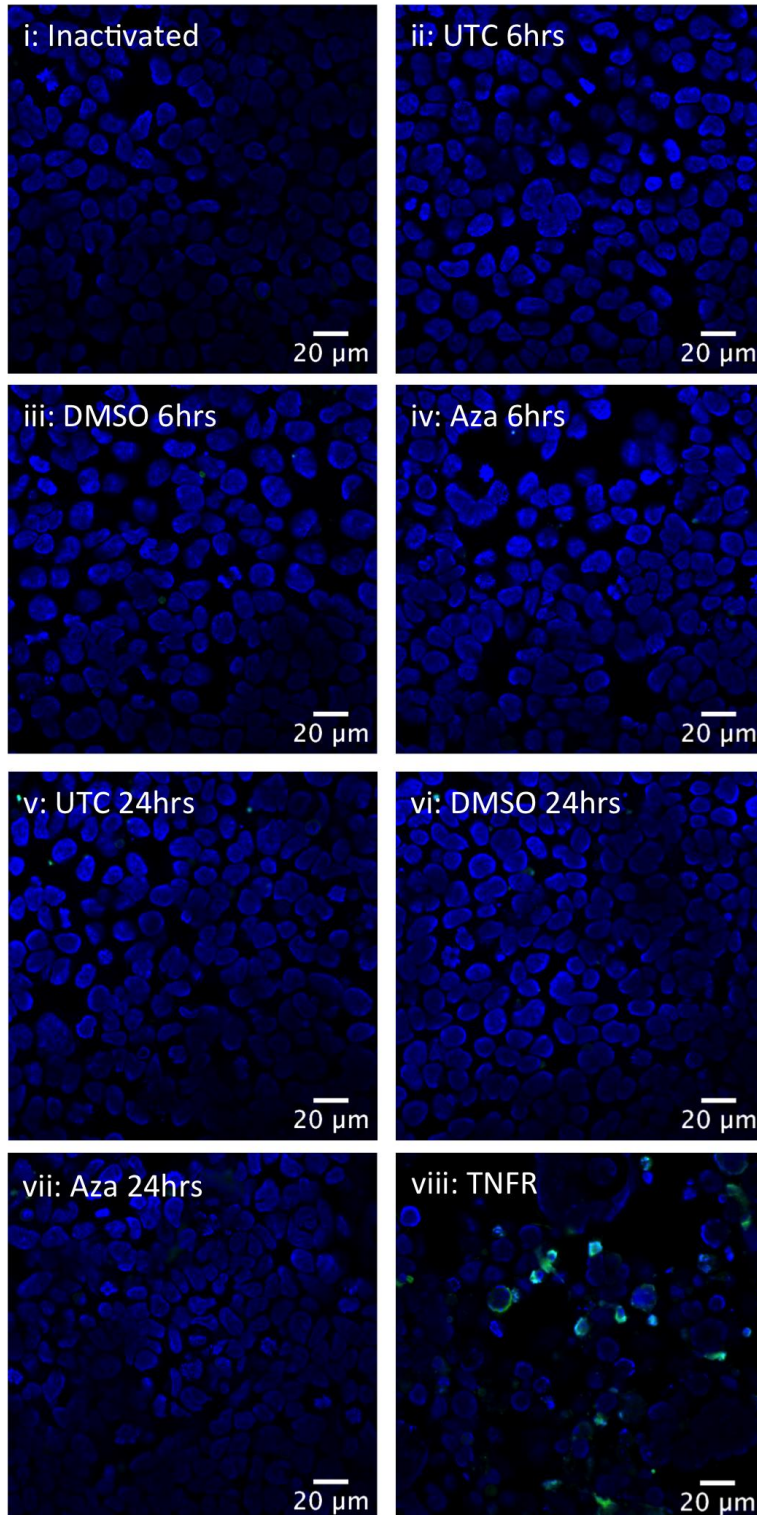
HEK293 cells were untreated; treated with DMSO (vehicle control) or 120 μ M azathioprine for 6 and 24 hours, or transfected with 0.5 μ g of TNF receptor plasmid and rested for 24 hours. Protein lysates separated on 10% SDS-page gel were immunoblotted for PARP and actin (i). ImageJ software was used for western densitometry. PARP and cleaved-PARP density normalized to actin was quantified (ii).

4.2.2 TUNEL Assay to Monitor Apoptosis in HEK293 cells treated with Azathioprine

Extensive DNA fragmentation is associated with the later stage of apoptosis and is induced during caspase-independent apoptosis by AIF and Endonuclease G release from the mitochondria following (MOMP). This can be detected using the TUNEL assay kit as the active enzyme Terminal deoxynucleotidyl transferase (TdT) binds to ends of double-stranded DNA breaks.

HEK293 cells were left untreated, treated with DMSO or with azathioprine for 6 and 24 hours, or transfected with 0.5 μ g of TNFR plasmid. After staining with the TUNEL kit, apoptotic cells positive for TdT (FITC) were enumerated and expressed as a percentage of total cells. A slight increase in TdT stained cells was observed with azathioprine at 24

hours from 2.3% of untreated cells at 24 hours to 5% (Figure 4.2). However a more considerable increase was observed with TNFR transfection to 14% (Figure 4.2). Importantly, at the optimum time-point for autophagy induction with azathioprine as shown in Chapter 3 (6 hours), apoptosis was not detected (1.7%) (Figure 4.2).



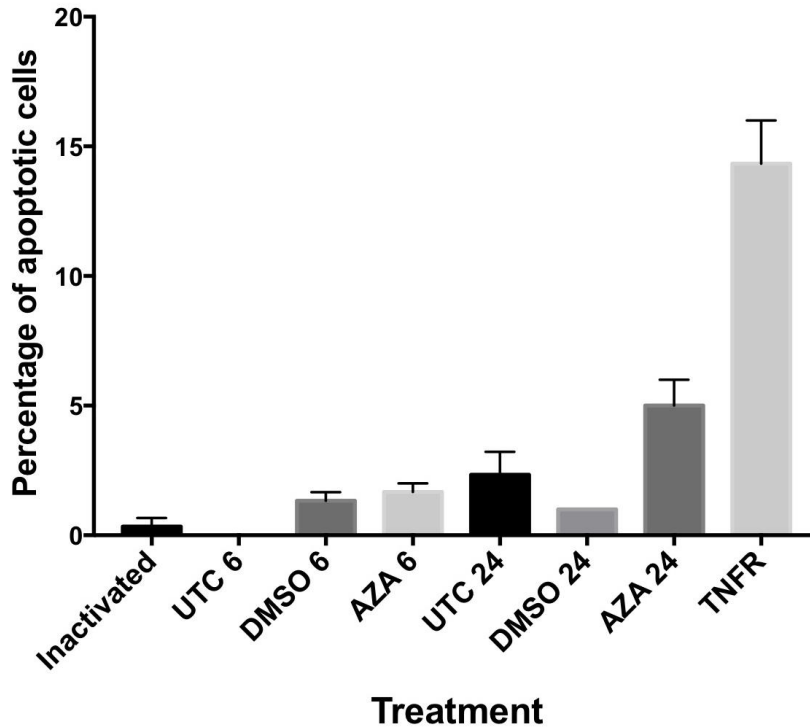


Figure 4.2: TUNEL Assay to Monitor Apoptosis in Cells Treated with Azathioprine

HEK293 cells were untreated (ii, v); treated with DMSO (vehicle control) (iii, vi) or 120 μ M azathioprine (iv, vii) for 6 and 24 hours, or transfected with 0.5 μ g of TNF receptor plasmid and rested for 24 hours (viii). Cells were then stained using the TUNEL assay kit and mounted with DAPI Vectashield (blue) for confocal microscopy imaging. A staining control of inactivated TdT is also shown (i). Total cells were counted in 3 fields of view and a percentage of TdT stained/apoptotic (FITC: green) was calculated (+/- SEM) (ix).

4.2.3 Annexin-V/PI Flow Cytometry to Monitor Apoptosis and Necrosis in HEK293 cells and THP-1-derived macrophages treated with Azathioprine

Annexin-V/Propidium Iodide (PI) flow cytometry can differentiate between early stage apoptosis, late stage apoptosis and necrosis. In viable cells, the cell membrane phospholipid, phosphatidylserine (PS), is located on the inner surface of the membrane. However, in early stage apoptosis the asymmetry of the phospholipid bilayer is altered and PS becomes exposed on the external surface of the cell membrane. Exposed PS is bound by Annexin-V to a high affinity; therefore, cells in early-stage apoptosis are stained solely with Annexin-V (AnnexinV⁺/PI⁻). PI is a DNA stain that can only enter cells

with disrupted cell membranes. Late-stage apoptotic cells have permeabilised cell membranes that enable PI staining of nuclear material but also are positive for Annexin-V staining due to exposed PS (AnnexinV⁺/PI⁺). PI staining alone occurs in necrotic cells that have compromised cell membranes exposing nuclear material but due to PS degradation Annexin-V staining is absent (AnnexinV⁻/PI⁺).

The effect of azathioprine treatment on early and late apoptosis, and necrosis in HEK293 and THP-1-derived macrophages was analysed. Apoptosis was triggered in HEK293 cells via the extrinsic pathway by overexpressing TNFR and as a positive control for PI staining HEK293 cells were mechanically detached by scraping, which compromised cell membrane integrity (Figure 4.3). HEK293 cells were also treated with DMSO and azathioprine for 6 and 24 hours (Figure 4.3). THP-1-derived macrophages were left untreated or treated with DMSO, azathioprine or 30µM camptothecin for 6 and 24 hours (Figure 4.4).

For both cell types the percentage of viable cells when untreated was between 84.9% and 86.4% at both 6 and 24 hours (Figure 4.3 and Figure 4.4). When cells were treated with DMSO or azathioprine for 6 and 24 hours, viability of cells was unaltered, ranging between 82.5% and 86.8% within the AnnexinV⁻/PI⁻ quadrant (Figure 4.3 and Figure 4.4). Therefore, we did not detect any effect of azathioprine treatment on viability in either THP-1-derived macrophages or HEK293 cells.

There was a significant decrease in percentage of viable HEK293 cells to 56.1% and 60.4% when cells were scraped or transfected with TNFR, respectively (Figure 4.3). In scraped cells the population primarily shifted to necrosis with an increase from 9.3% to 28.7% AnnexinV⁻/PI⁺ cells, but late apoptosis also increased slightly from 2.2% to 9.5% (AnnexinV⁺/PI⁺) (Figure 4.3 B and C: x). TNFR transfection was intended as a positive control for Annexin-V staining, but percentage of AnnexinV⁻/PI⁻ cells only increased slightly from 3.7% to 8.2% and AnnexinV⁺/PI⁺ increased from 2.2% to 5.4% (Figure 4.3 B and C: x). The decrease in viability of TNFR transfected cells was mainly due to an increase in percentage of AnnexinV⁻/PI⁺ cells to 25.6% (Figure 4.3 B and C: x).

When THP-1-derived macrophages were treated with camptothecin for 6 hours percentage of viable cells significantly decreased to 39.2% and percentage of positively stained cells significantly increased to 17.9%, 20.5% and 22.6% for AnnexinV⁺/PI⁻ (early

apoptosis), AnnexinV⁻/PI⁺ (necrosis) and AnnexinV⁺/PI⁺ (late apoptosis) staining, respectively (Figure 4.4A and C). When exposure to camptothecin was prolonged to 24 hours the significant decrease in viable cells was more pronounced with only 16.4% within the AnnexinV⁻/PI⁻ quadrant (Figure 4.4B and C). The percentage of early apoptotic cells did not increase, as the most prominent population shift was towards late stage apoptosis with 53% of cells AnnexinV⁺/PI⁺, and to a lesser extent, there was an increase in necrotic cells with 25.5% of cells AnnexinV⁻/PI⁺ (Figure 4.4B and C).

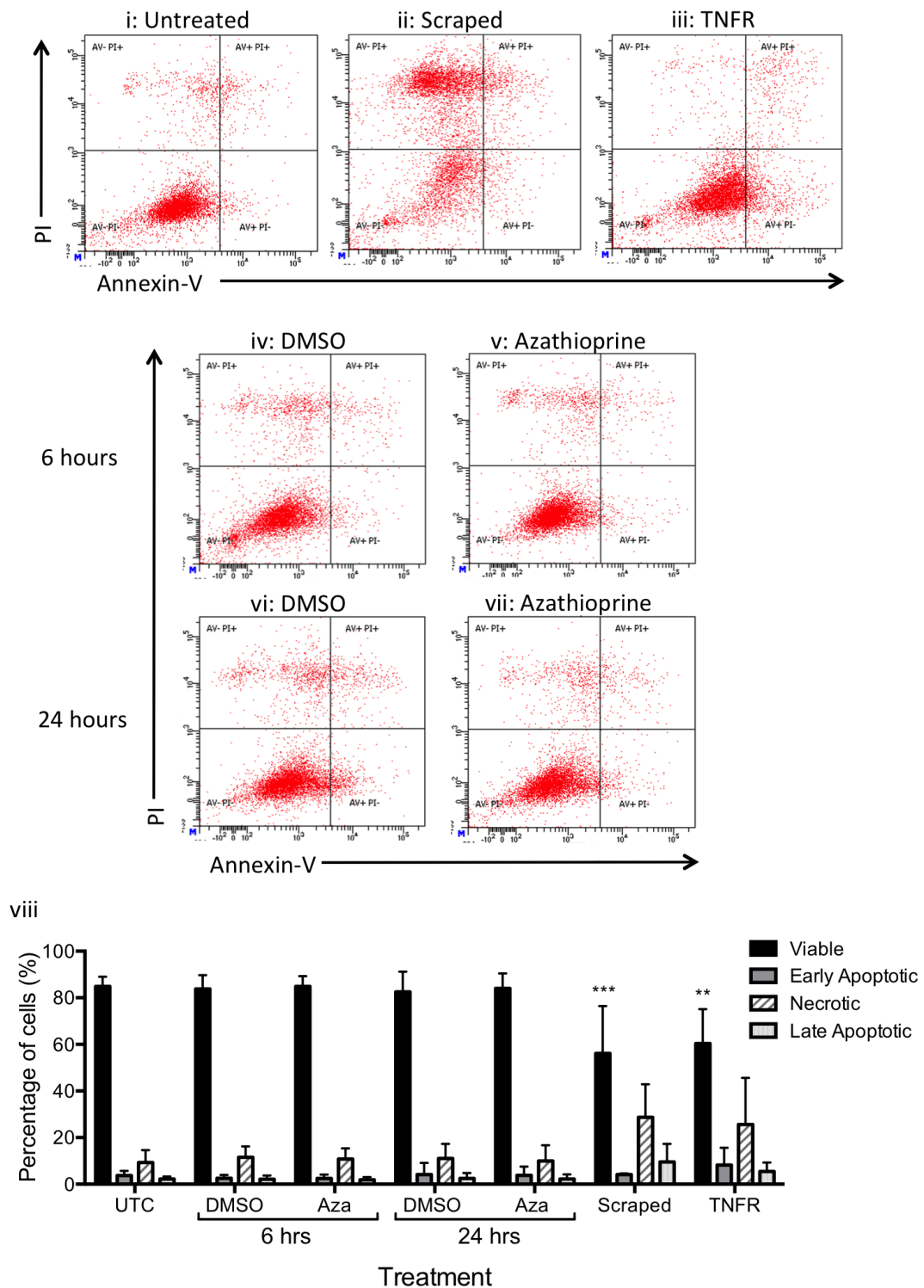
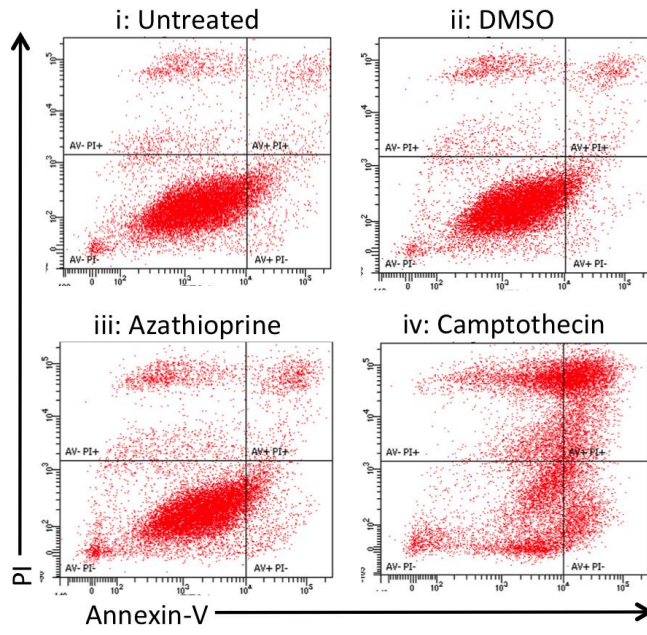


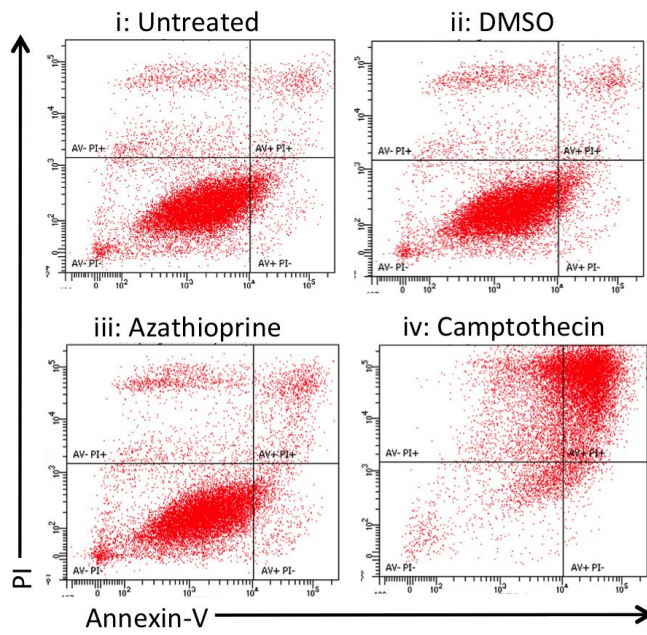
Figure 4.3: Annexin-V/PI Flow Cytometry to Monitor Apoptosis and Necrosis in HEK293 Cells Treated with Azathioprine

HEK293 cells were untreated (i), detached mechanically by scraping (ii) or transfected with p53 TNFR plasmid (iii). Cells were stained with Annexin-V/PI kit and analysed by flow cytometry. Representative blots from n=3. Mean percentage population in each quadrant from n=3 (+/- SEM) was quantified (viii). Two-way ANOVA was used with Tukey's multiple comparisons between treatments within each quadrant. **p < 0.01, ***p < 0.001 compared to untreated for corresponding time-point and quadrant.

A: 6 hours



B: 24 hours



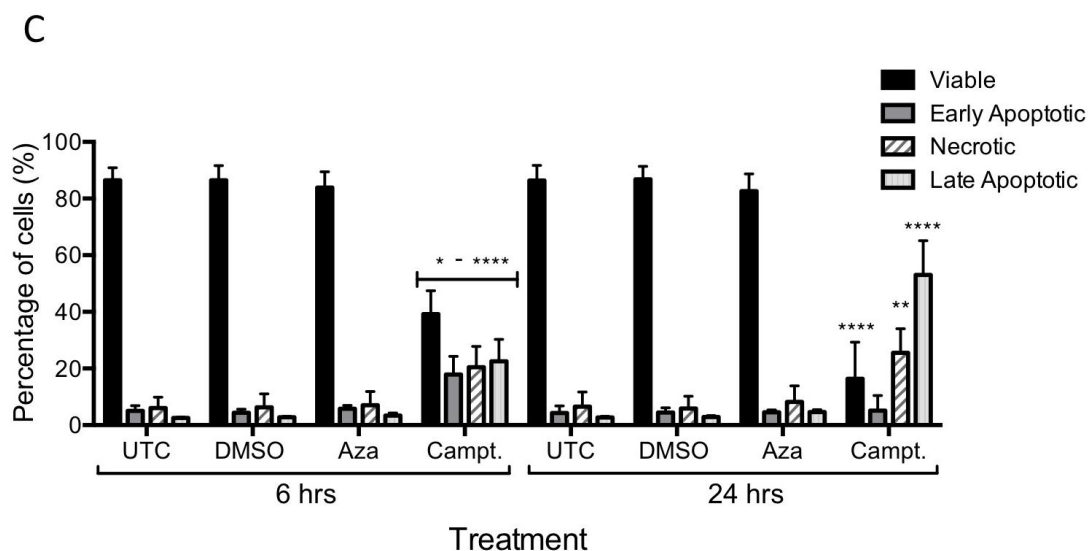


Figure 4.4: Annexin-V/PI Flow Cytometry to Monitor Apoptosis and Necrosis in THP-1-derived macrophages Treated with Azathioprine

THP-1-derived macrophages were either untreated (i) or treated with DMSO (ii), 120 μ M azathioprine (iii) or 30 μ M camptothecin (iv) for 6 (A) and 24 hours (B). Cells were stained with Annexin-V/PI kit and analysed by flow cytometry. Representative blots from n=3 shown. Mean percentage population in each quadrant from n=3 (+/- SEM) was quantified (C). Two-way ANOVA was used with Tukey's multiple comparisons between treatments within each quadrant. * p < 0.05, **p < 0.01, ***p < 0.001, ****p < 0.0001 compared to untreated for corresponding time-point and quadrant.

4.3 Summary

Azathioprine did not induce cell death in the HEK293 cell line or THP-1-derived macrophages at the concentration range and incubation times investigated. The complementary methods used investigated various types of cell death and were verified using positive controls for cell death induction. Caspase-dependent and caspase-independent apoptosis were monitored in HEK293 cells by western immunoblot for PARP and the TUNEL assay, respectively. Furthermore, in both HEK293 cells and THP-1-derived macrophages, flow cytometry for Annexin-V/PI assessed the effect of azathioprine on early/late apoptosis and necrosis.

If, in response to azathioprine, autophagy was accompanied by cell death or preceded cell death, it could be suggested that azathioprine is inducing cellular stress and autophagy is stimulated as a mechanism to cope with the stress and promote survival. However, as there is no cell death apparent at the optimum time-point for autophagy

or at subsequent time-points this suggests that azathioprine induces autophagy independently of apoptosis.

5 IBD Drug Modulation of Autophagy and UPR Signalling Pathways

5.1 Introduction

The mechanism of action of azathioprine in the context of autophagy was examined in THP-1-derived macrophages. Regulation of autophagy responses incorporates several coordinated signalling networks, which intertwine with signalling pathways from other cellular processes, such as the UPR and apoptosis. To explore the expanse of signalling pathways involved in autophagy regulation, the RT² Profiler™ PCR Array for Human Autophagy genes was used. This encompasses a wide range of autophagy-related genes and genes involved in autophagy signalling. Although autophagy induction is most commonly monitored on a protein level, in particular post-translational modifications, there are some autophagy proteins that are transcriptionally altered when autophagy is induced (Klionsky et al., 2016). Following identification of differentially expressed genes in the PCR array, these leads were investigated further by qPCR and western immunoblot. Furthermore, the effect of azathioprine on the activity of the mTORC1 regulatory hub was examined.

5.2 Results

5.2.1 Human Autophagy RT-PCR Array in THP-1-Derived Macrophages Treated with Azathioprine

For the RT² Profiler™ PCR Array for Human Autophagy genes, gene expression in THP-1-derived macrophages treated with azathioprine for 6 hours was compared with untreated cells. An LC3 immunostain was performed in conjunction to ensure autophagy induction was observed in the cells to be analysed by qPCR (Supplementary Figure 10.3). Percentage of cells with >5 LC3 foci increased from 24% in untreated cells to 48% in azathioprine-treated cells (Supplementary Figure 10.3).

The Autophagy PCR Array includes 84 genes related to autophagy or autophagy signalling. Figure 5.1 shows the fold-change expression of all genes in cells treated with

azathioprine, normalized to untreated. The red lines indicate 1.5-fold-change, which was considered as the threshold for differential regulation. Overall there are more genes downregulated, with a higher magnitude in downregulated fold-change compared to upregulation, in azathioprine-treated cells (Figure 5.1).

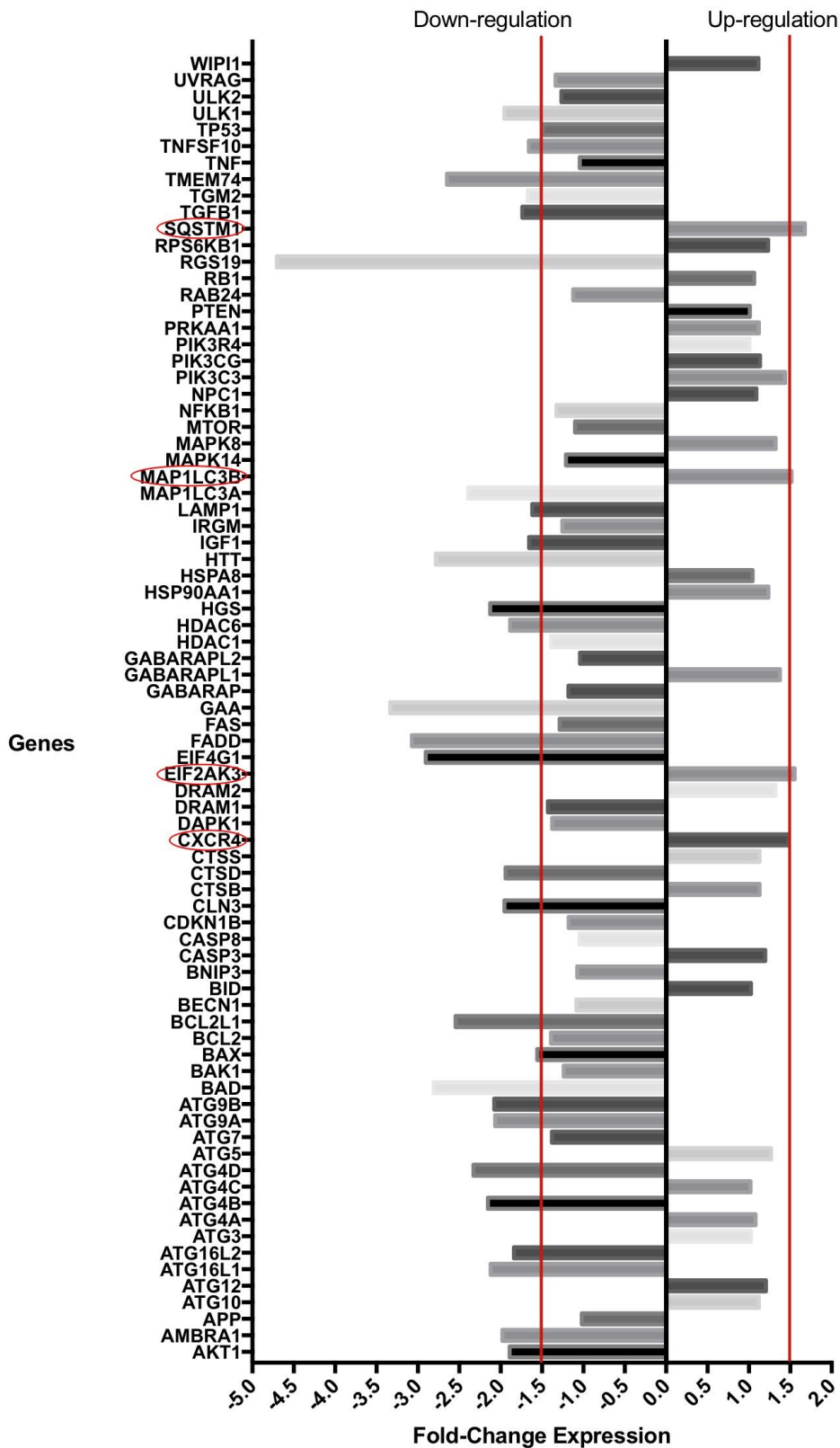


Figure 5.1: RT² Profiler™ PCR Array for Human Autophagy Genes for Analysis of Azathioprine-Induced Autophagy

THP-1-derived macrophages were untreated or treated with 120µM azathioprine for 6 hours. mRNA was extracted and converted to cDNA for RT-qPCR analysis using the RT² Profiler™ PCR Array for Human Autophagy genes according to manufacturer

instructions. The calibrating sample was untreated cells and relative expression for azathioprine treatment is displayed as fold-change, with upregulated genes calculated as $2^{-\text{ddCT}}$ and downregulated genes as 2^{ddCT} . The red lines indicate 1.5-fold change in expression, which was considered the threshold for differential expression. Upregulated genes are circled in red: *SQSTM1* (p62); *EIF2AK3* (PERK).

An overview of differentially expressed genes with fold-changes and a summary of their function are detailed in Table 5.1. Azathioprine upregulated the genes encoding the key autophagy proteins, MAP1LC3B and p62, the UPR kinase PERK, and chemokine receptor, CXCR4 (Table 5.1).

Certain genes for autophagy regulation were downregulated, such as *Akt1*, *AMBRA1* and *ULK1*, and several genes that translate to components of the autophagy machinery were also downregulated (Table 5.1). Furthermore, genes involved in lysosome biogenesis were downregulated by azathioprine treatment (Table 5.1).

Several apoptosis genes were downregulated with azathioprine treatment (Table 5.1). Most of these genes were pro-apoptotic, however, some of the downregulated genes had anti-apoptotic activity. In addition to the genes involved in apoptosis that are highlighted in Table 5.1, some genes within the table that have distinct primary functions can also modulate apoptosis. Huntingtin (HTT) protein, which was transcriptionally downregulated, has a primary function in the cytoskeleton and mitochondrial transportation, but has also been implicated in both pro- and anti-apoptotic regulation (S.-H. Li et al., 2000; Rigamonti et al., 2000; Saudou et al., 1998). *IGF-1* can act to induce cell proliferation and inhibit apoptosis via *Akt* pathway (Fernández et al., 2004), and both *IGF-1* and *Akt* are downregulated. Furthermore, *CLN3*, which is involved in lysosome function, can have anti-apoptotic functions and is downregulated by azathioprine (Mao et al., 2015).

Table 5.1: Differentially Expressed Genes from RT² Profiler™ PCR Array for Human Autophagy Genes

Differentially expressed genes are shown, with 1.5-fold change in expression considered as the threshold for differential expression. Fold-change, with upregulated genes calculated as $2^{-\text{ddCT}}$ and downregulated genes as 2^{ddCT} . Primary function of genes indicated. *Bcl-2-associated death promoter (BAD)*, *Fas-associated death domain (FADD)*, *Regulator Of G Protein Signaling 19 (RGS19)*, *transglutaminase 2 (TGM2)*, *Eukaryotic Translation Initiation Factor 4 Gamma 1 (EIF4G1)*, *Histone Deacetylase 6 (HDAC6)*, *Hepatocyte growth factor (HGS)*, *Insulin-like growth factor 1 (IGF1)*. (Fridman and Lowe, 2003¹; Gupta et al., 2004²; Howells et al., 2011³; Jänicke et al., 2008⁴; Sánchez-Capelo, 2005⁵; Tatsukawa et al., 2016⁶; Thorburn, 2007⁷; Zheng et al., 2016⁸).

	Gene	Fold-Change	Function
Up-regulation	<i>SQSTM1/p62</i>	1.7	Autophagy-adaptor molecule
	<i>EIF2AK3 (PERK)</i>	1.6	Unfolded Protein Response kinase
	<i>MAP1LC3B</i>	1.5	Autophagosome formation
	<i>CXCR4</i>	1.5	Chemokine/cytokine receptor
Down-regulation	<i>Akt1</i>	1.8	Apoptosis and mTORC1 regulation
	<i>AMBRA1</i>	2.0	Autophagy regulation
	<i>ULK1</i>	2.0	
	<i>ATG16L1</i>	2.1	Autophagy proteins
	<i>ATG16L2</i>	1.8	
	<i>ATG4B</i>	2.2	
	<i>ATG4D</i>	2.3	
	<i>ATG9A</i>	2.1	
	<i>ATG9B</i>	2.1	
	<i>LC3A</i>	2.4	
	<i>RGS19</i>	4.7	
	<i>TMEM74</i>	2.7	
	<i>BAD</i>	2.8	Co-Regulators of Autophagy and Apoptosis: Pro-apoptotic ^{1, 4, 5, 6}
	<i>Bax</i>	3.1	
	<i>FADD</i>	2.5	
	<i>TRAIL (TNFSF10)</i>	1.7	
	<i>BCL2L1 (BCLXL)</i>	1.6	
	<i>p53</i>	1.5	Co-Regulators of Autophagy and Apoptosis: Anti-apoptotic and Pro-apoptotic (context dependent) ^{2, 3, 7}
	<i>TGFB1</i>	1.7	
	<i>TGM2</i>	1.7	
	<i>CLN3 (Battenin)</i>	2.0	Lysosome function
	<i>CTSD (Cathepsin D)</i>	1.9	Lysosomal protease
	<i>GAA (Glucosidase α)</i>	3.3	Maintains lysosome integrity
	<i>LAMP1</i>	1.6	
	<i>EIF4G1</i>	2.9	Translation factor
	<i>HDAC6</i>	1.9	Ubiquitination
	<i>HGS</i>	2.1	Growth factors
	<i>IGF1</i>	1.7	
	<i>HTT (Huntingtin)</i>	2.9	Role in cytoskeleton and mitochondrial transport

5.2.2 *CXCR4* Expression Altered by Azathioprine Treatment in THP-1-Derived Macrophages

CXCR4 is a chemokine receptor for CXCL12 and macrophage migration inhibitory factor (MIF) (Bernhagen et al., 2007). Upregulation of *CXCR4* in response to treatment with azathioprine, which was identified in the PCR array, was confirmed by qPCR (Supplementary Figure 10.4). Prior to this a geNorm was performed to identify the most appropriate reference genes, which were *ribosomal protein L13a (RPL13A)* and *β-actin* (data not shown).

A time-course was undertaken in THP-derived macrophages treated with DMSO, azathioprine and EBSS (Supplementary Figure 10.4A). EBSS upregulated *CXCR4* expression by 1.9- to 8.4-fold, at 2, 6, 8 and 16 hours, but cells were not treated with EBSS for 24 hours. Azathioprine only upregulated *CXCR4* expression at 6 hours, with a 3.5-fold increase and the optimal time-point for EBSS upregulation of *CXCR4* was 6 hours.

Further investigation of *CXCR4* expression when treated with azathioprine at 6 hours revealed a clear, but non-significant, increase in *CXCR4* relative expression with a 3.5-fold increase (Supplementary Figure 10.4B). EBSS induced a significant increase in *CXCR4* expression with a 5.5-fold increase.

5.2.3 Expression of Unfolded Protein Response Markers Altered by Azathioprine Treatment

Up-regulation of *EIF2AK3 (Eukaryotic Translation Initiation Factor 2 Alpha Kinase 3)*, also known as the UPR kinase *PERK*, was identified in the PCR array and was investigated further by qPCR. Initially, brefeldin A treatment was optimised as a positive control for induction of ER stress and subsequent stimulation of UPR, by blocking protein transport from the ER to Golgi apparatus (Nebenführ et al., 2002). Cells were treated with varying concentrations of brefeldin A for 2, 4 and 6 hours and expression of *BiP* and *PERK* were then analysed by qPCR (Supplementary Figure 10.5).

Optimal upregulation of 13.4-fold and 10.3-fold in the expression of *PERK* and *BiP*, respectively, were observed at 6 hours. *BiP* was optimally upregulated with 1µg/ml, whereas *PERK* was optimally upregulated with 0.5µg/ml. Therefore, treatment of THP-

1-derived macrophages with 0.5µg/ml Brefeldin A for 6 hours was used as a positive control in subsequent experiments.

THP-1-derived macrophages were treated with DMSO, azathioprine, and EBSS for 2, 4, 6, 16 and 24 hours (Figure 5.2: i). *PERK* upregulation was only observed at 6 hours with azathioprine inducing 2.6- to 3.2-fold-increases in a concentration dependent manner. EBSS also upregulated *PERK*, by 2.1-fold, at 6 hours.

Further investigation by qPCR assessed relative expression of several genes involved in the UPR, including *PERK*, *ATF4*, *CHOP* and *PDI* at the optimal 6hr time-point. THP-1-derived macrophages were then treated with DMSO, azathioprine, EBSS and brefeldin A for 6 hours (Figure 5.2: ii-vi). Azathioprine induced a 1.8-fold increase and a significant 2.6-fold-increase in *PERK* with increasing concentration (Figure 5.2: ii). EBSS upregulated *PERK* by 2.3-fold and brefeldin A induced a 10.9-fold-increase.

Both *ATF4* and *CHOP* are transcriptionally upregulated by PERK activation (Harding et al., 2000). Azathioprine induced a slight upregulation of *ATF4* with a 1.6-fold-increase (Figure 5.2: iii). EBSS and brefeldin A upregulated *ATF4* expression significantly by 4.6- and 4.8-fold. Azathioprine increased *CHOP* expression by 1.6- and 2.1-fold with increasing concentration (Figure 5.2: iv). A 4.5-fold-increase in *CHOP* expression was induced by EBSS and a significant up-regulation in *CHOP* by 14.5-fold was induced by brefeldin A. *PDI* is involved in protein refolding in the ER lumen and is transcriptionally regulated by the IRE1α–XBP1 pathway (Lee et al., 2003; Osowski and Urano, 2011). *PDI* was upregulated by 120µM azathioprine with a 1.9-fold-increase and brefeldin A increased *PDI* expression by 2.2-fold (Figure 5.2: v). EBSS significantly upregulated *PDI* expression by 2.6-fold (Figure 5.2: v).

For analysis of expression of the gene for ER stress chaperon protein BiP/Grp78, cells were also treated for 24 hours. Azathioprine did not upregulate *BiP* expression above 1.5-fold. EBSS had a slight stimulatory effect on *BiP* expression with a 1.7-fold-increase and brefeldin A upregulated *BiP* expression by 3.8-fold, at 6 hours.

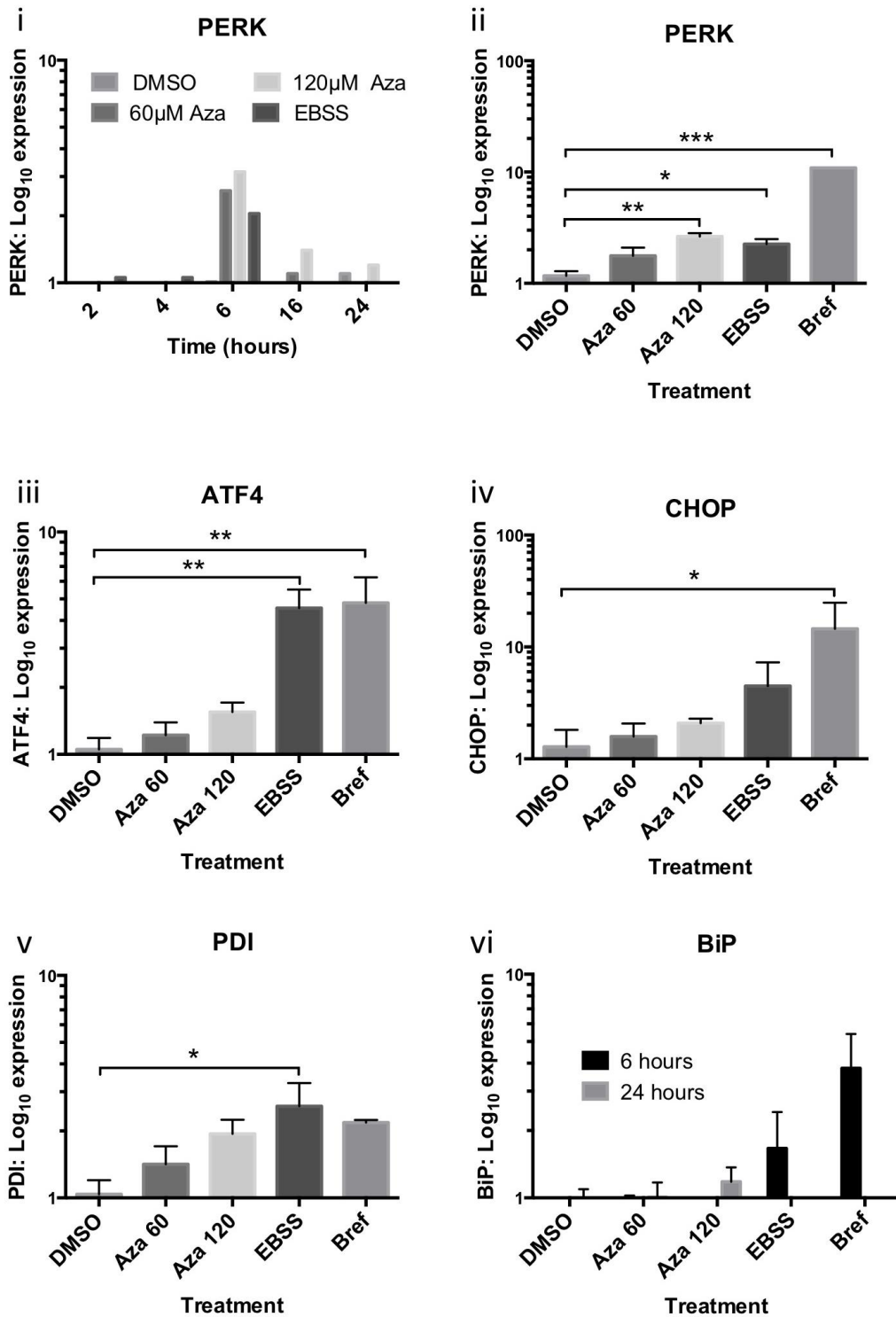


Figure 5.2: RT-qPCR for Unfolded Protein Response Markers

THP-1-derived macrophages were untreated or treated with DMSO (vehicle control), 60μM and 120μM azathioprine or EBSS for nutrient deprivation for 2, 4, 6, 16 and 24 hours (n=3) (i). Cells were additionally treated with 0.5μg/ml brefeldin A for 6 hours (ii-vi). For BiP RT-qPCR cells were also treated for 24 hours (vi). mRNA was extracted and converted to cDNA for qPCR analysis using primers for *PERK* (i-ii), *ATF4* (iii), *CHOP* (iv), *PDI* (v) and *BiP* (vi). Reference genes were *RPL13A* and *actin* and the calibrating sample was untreated cells for corresponding time-points. Relative expression was calculated

as $2^{-\text{ddCT}}$ and is displayed as Log_{10} or Log_{100} of fold-change (\pm SEM). One-way ANOVA and Dunnett's multiple comparisons was performed. * $p < 0.05$, ** $p < 0.01$, *** $p < 0.001$ using $2^{-\text{ddCT}}$ values.

5.2.4 Western Immunoblot for UPR markers in THP-1-Derived Macrophages Treated with Azathioprine

To further investigate the effects of azathioprine on ER stress and the UPR, protein expression was analysed by western immunoblot. THP-1-derived macrophages were treated with DMSO and azathioprine for 6 and 24 hours, and EBSS and brefeldin A for 6 hours. Protein lysates were prepared and run on a 10% gel followed by immunoblotting for BiP, PDI and β -actin (Figure 5.3).

Immunoblotting for BiP revealed two protein bands, which represent the two isoforms of BiP that occur due to alternative splicing of pre-mRNA (Ni et al., 2009). At 6 and 24 hours there was no increase in either of the BiP isoforms when treated with azathioprine (Figure 5.3: i-iii). At 6 hours there was a 1.4-fold-increase in both BiP isoforms when cells were treated with EBSS. Brefeldin A treatment increased BiP protein to a higher degree, with 2.4- and 1.8-fold-increase in BiP 1 and 2, respectively.

Fold-change in PDI was calculated from DMSO, due to an un-transferred protein band in an untreated sample in one of the immunoblots (immunoblot not shown). In some immunoblots a faint PDI band at 51kDa was visible, which was likely a degradation product (Mezghrani et al., 2000), but as this band was not resolved for all immunoblots, PDI was quantified from the protein band at 57kDa. There was no effect of azathioprine on PDI protein levels at 24 hours (Figure 5.3: i, iv, v). At 6 hours there was a very modest 1.3-fold-increase in PDI with azathioprine treatment. EBSS treatment increased PDI by 1.4-fold and a significant increase in PDI was induced by brefeldin A with a 1.6-fold-increase.

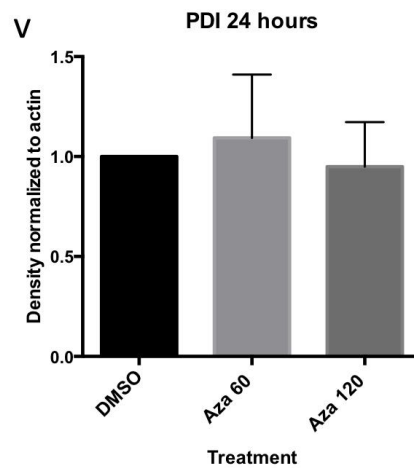
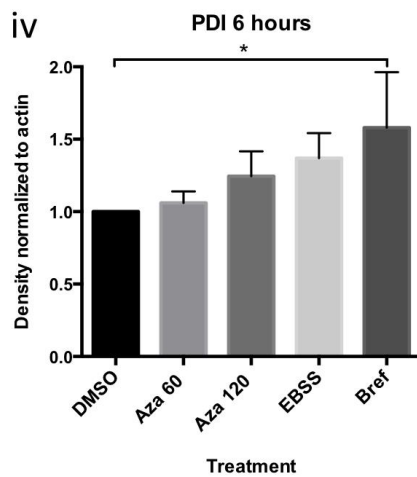
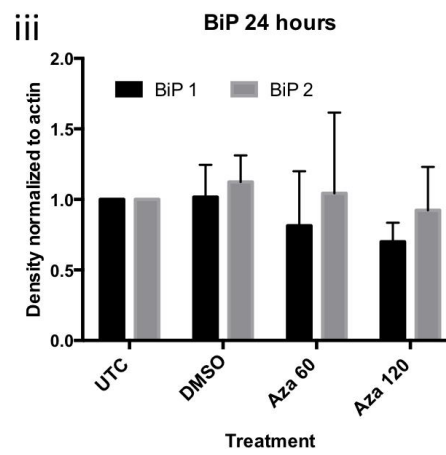
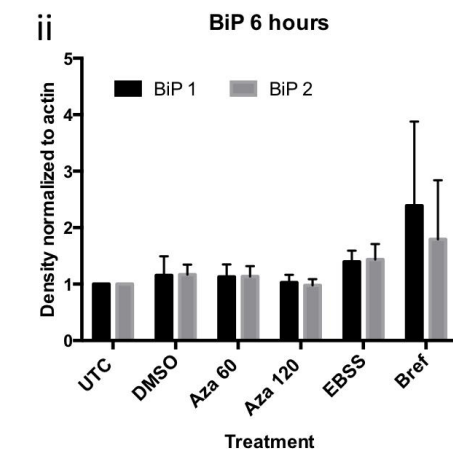
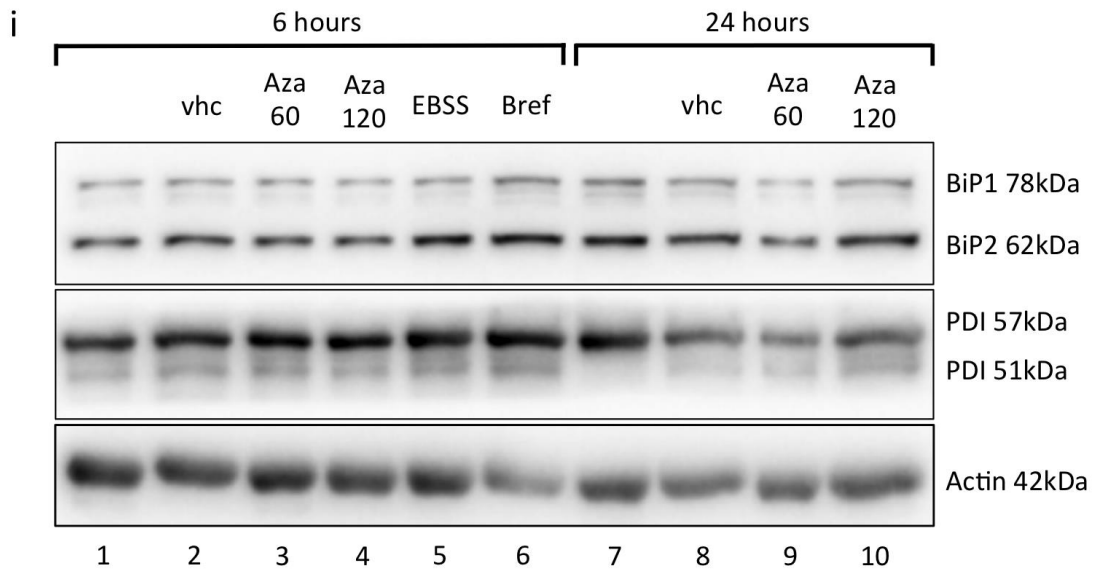


Figure 5.3: Unfolded Protein Response Markers Protein Expression Modulated by Azathioprine

THP-1-derived macrophages were untreated or treated with DMSO (vhc), 60 μ M or 120 μ M azathioprine for 6 hours and 24 hours; and also treated with EBSS for nutrient deprivation or 0.5 μ g/ml brefeldin A for 6 hours (n=3). Protein lysates separated on 10%

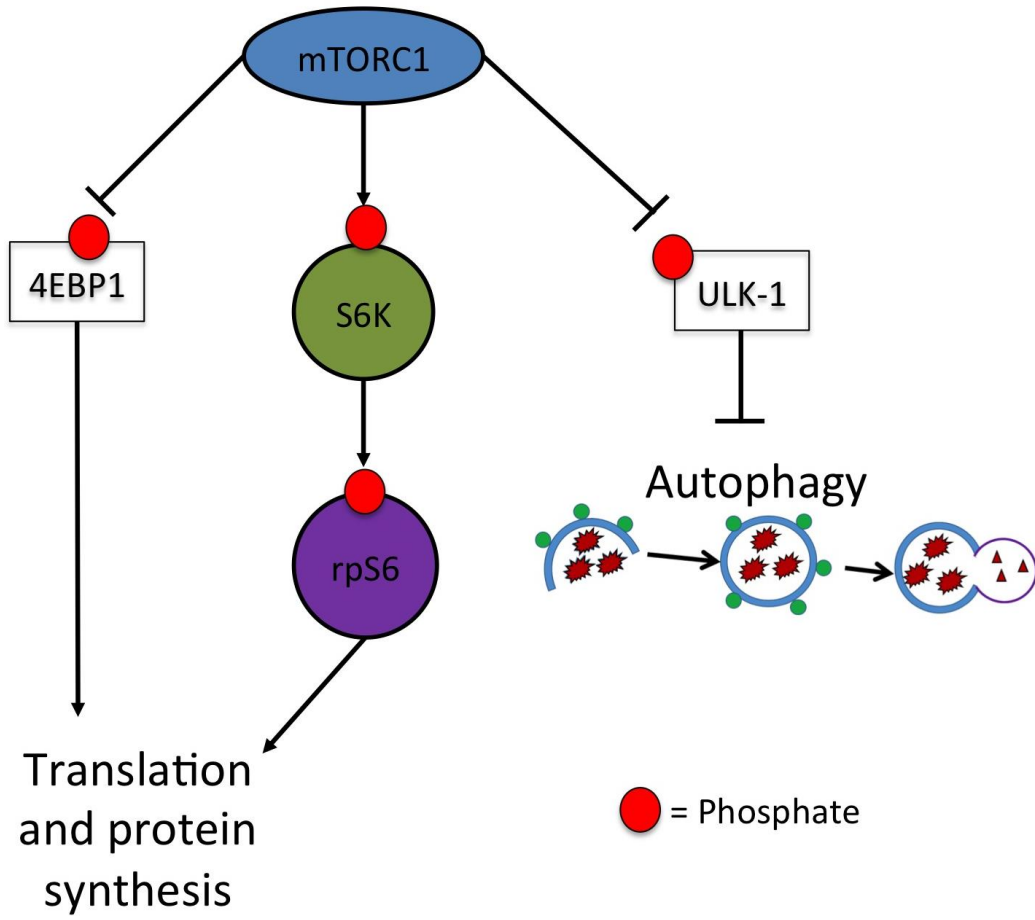
SDS-page gel were immunoblotted for BiP, PDI and β -actin, with a representative western immunoblot from n=3 shown (i). ImageJ software was used for western densitometry and fold-change from untreated in BiP bands (1 and 2) (ii-iii) and fold-change from DMSO in PDI bands (iv-v) normalized to β -actin was quantified for corresponding time-points (+/- SEM). One-way ANOVA with Tukey's multiple comparisons test was performed on data for each time-point. *p <0.05 compared to DMSO.

5.2.5 Western Immunoblot for rpS6 and Phosphorylated rpS6 to Monitor mTORC1 Activity in THP-1-Derived Macrophages

When active, mTORC1 upregulates protein translation via inhibition of eukaryotic initiation factor 4E (EIF4E) binding protein 1 [4EBP1] and phosphorylation of S6 ribosomal protein kinase (S6K) (Ma and Blenis, 2009). Phosphorylated S6K in turn phosphorylates and activates S6 ribosomal protein (rpS6) (Figure 5.4A). Therefore, depletion of phosphorylated rpS6 (p-rpS6) is an indirect indicator of mTORC1 inhibition. Western immunoblotting was used to monitor the levels of total rpS6 protein and phosphorylated rpS6 in THP-1-derived macrophages.

THP-1-derived macrophages were treated with DMSO, a concentration range of azathioprine, EBSS or rapamycin for 6 hours. Phosphorylated rpS6 density decreased slightly to 83% when treated with DMSO (Figure 5.4: i-ii). A more notable decrease was observed with 60 μ M azathioprine to 55% (Figure 5.4: i-ii). Significant decreases in phospho-rpS6 density were induced by higher concentrations of azathioprine to 29%, 30% and 23% (Figure 5.4: ii). As expected, EBSS and rapamycin treatment decreased phospho-S6 density significantly to 18% and 5% (Figure 5.4: i-ii). Total rpS6 also fluctuated, with increases when cells were treated with azathioprine and decreases with EBSS (Figure 5.4: i, iii).

A



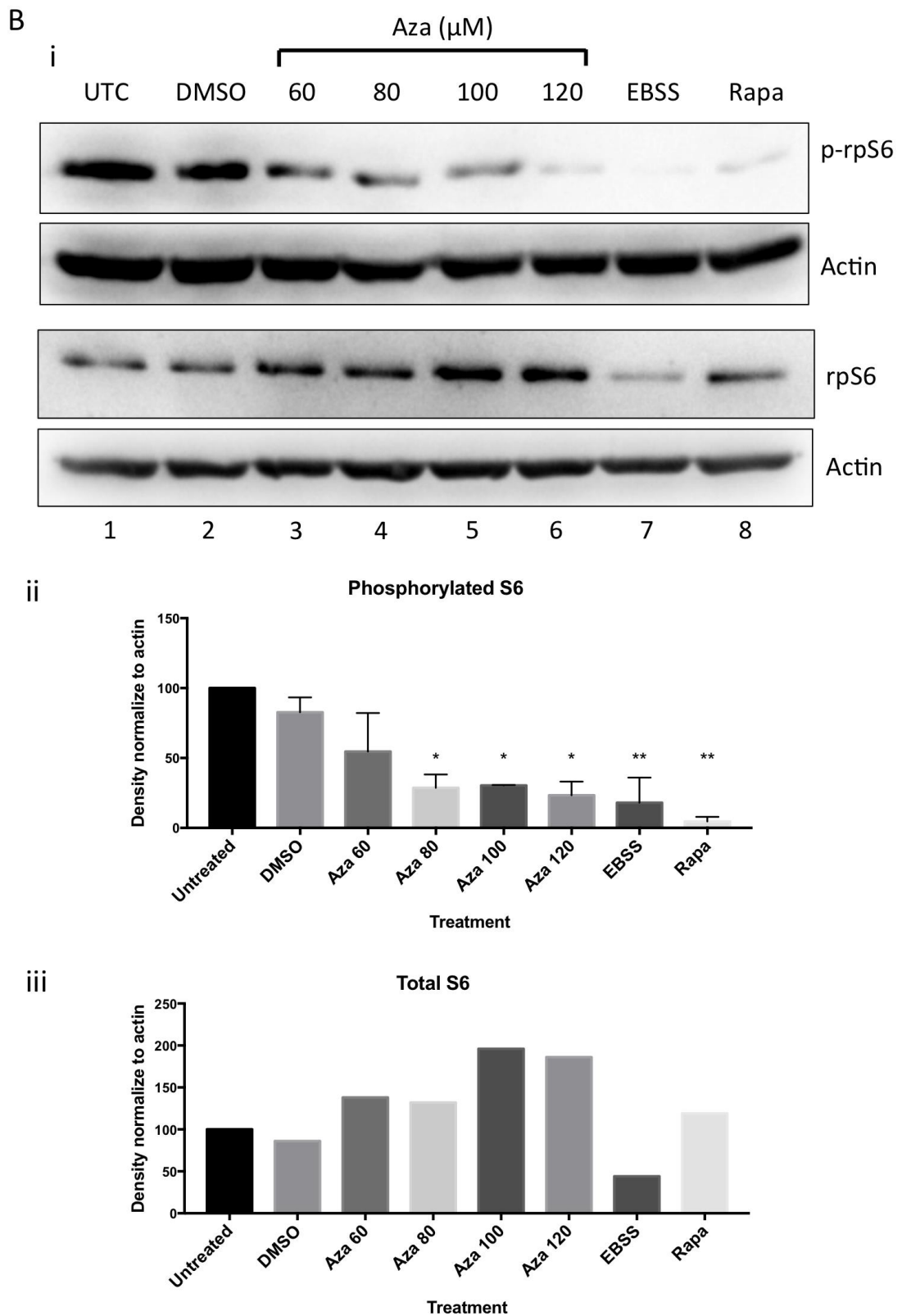


Figure 5.4: Western Immunoblot for rpS6 and Phospho-rpS6 to Monitor mTORC1 Activity Modulation by Azathioprine

A: Active mTORC1 increases translation and protein synthesis through phosphorylation of S6 kinase (S6K), which subsequently phosphorylates ribosomal protein S6 (rpS6), and inhibition of eukaryotic translation initiation factor 4E-binding protein 1 (4EBP1) via

phosphorylation. To inhibit autophagy mTORC1 phosphorylates ULK-1 to prevent formation of the ULK1-ATG13-FIP200 complex.

B: THP-1-derived macrophages were untreated or treated with DMSO (vehicle control), 60-120 μ M azathioprine, EBSS for nutrient deprivation or 100nM rapamycin for 6 hours. Protein lysates separated on a 10% SDS-page gel were immunoblotted for rpS6, phosphorylated rpS6 (p-rpS6 (S235/236)) and actin, with a representative western immunoblot from n=3 shown (i). ImageJ software was used for western densitometry and percentage change from untreated in phospho-rpS6 (ii) and total rpS6 (iii) bands normalized to β -actin was quantified from n=3 (+/- SEM). One-way ANOVA with Tukey's multiple comparisons test was performed on data. *p <0.05; **p <0.01 compared to DMSO.

5.2.6 Azathioprine inhibits mTORC1 activity independent of PERK

To test whether the inhibition of mTORC1 observed with azathioprine is dependent on PERK, cells were treated with azathioprine in the absence or presence of a pharmacologic inhibitor of PERK. THP-1-derived macrophages were untreated or treated with PERK inhibitor for 30 minutes prior to treatment with DMSO, azathioprine, EBSS or brefeldin A for 6 hours.

To confirm PERK inhibitor activity, phosphorylation of eIF2 α (p-eIF2 α), a well-characterised substrate of PERK, was assessed. The results show an increase in p-eIF2 α from 13% in untreated cells to 35% and 54% with EBSS and brefeldin A treatment, respectively (Figure 5.5: iii). A more modest increase in p-eIF2 α with azathioprine treatment to 20% was observed (Figure 5.5: iii). There is a clear reduction in eIF2 α phosphorylation in the presence of PERK inhibitor (Figure 5.5: i, iii).

Azathioprine again caused a decrease in p-rpS6 from 90% in untreated cells to 24% in azathioprine treated cells. However, the PERK inhibitor did not significantly alter this effect, as azathioprine decreased p-rpS6 from 77% to 31% in the presence of PERK inhibitor (Figure 5.5: i, compare lanes 3 and 8, and quantified in ii).

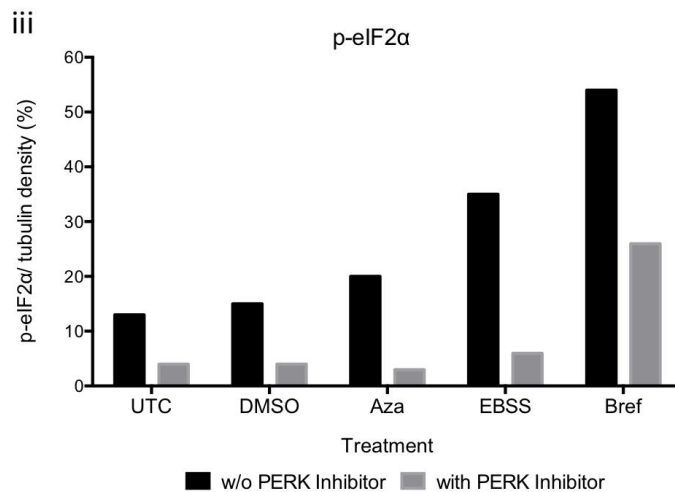
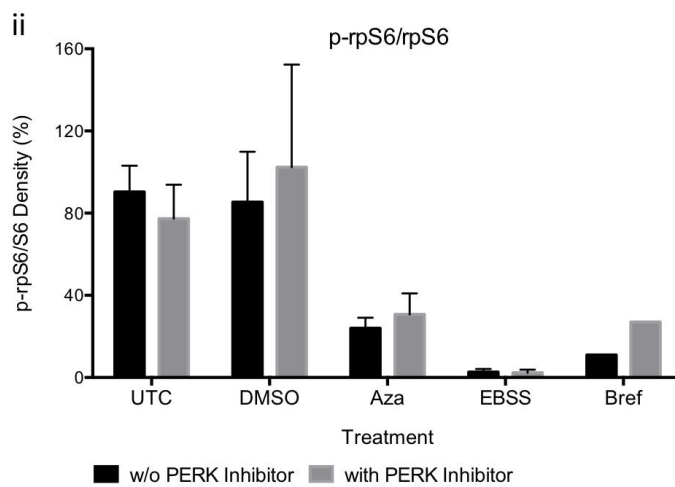
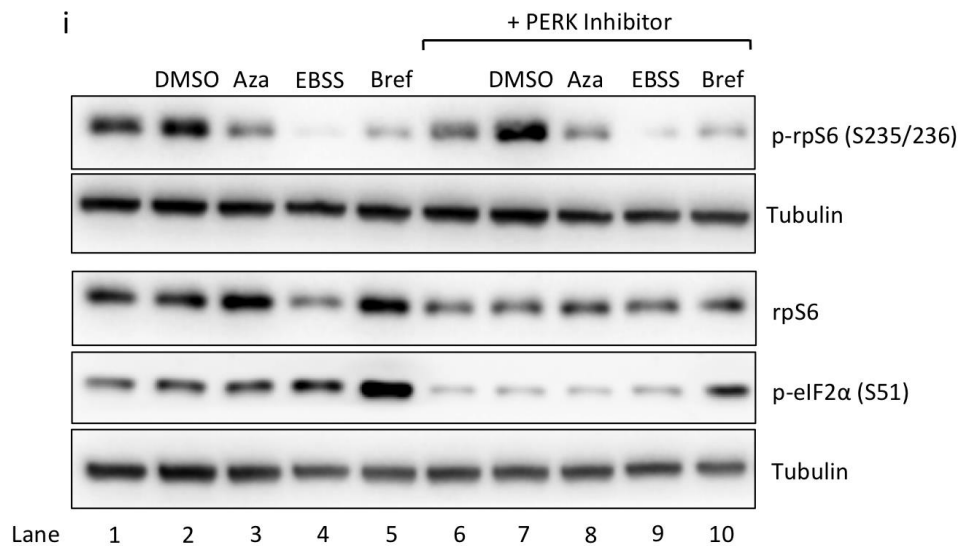


Figure 5.5: Azathioprine-induced inhibition of mTORC1 is not PERK dependent

THP-1-derived macrophages were untreated, or treated with DMSO, 120μM azathioprine, EBSS, or 0.5μg/ml Brefeldin A for 6 hours without (lanes 1-5) and with (lanes 6-10) 50nM PERK inhibitor I. Protein lysates separated on 10% SDS-page gel were immunoblotted for rpS6, phosphorylated rpS6 (p-rpS6 (S235/236)), phosphorylated

eIF2 α (p-eIF2 α (S51)) and tubulin (i). Representative blot from n=3. ImageJ software was used for western densitometry. rpS6/p-rpS6 density normalized to tubulin (+/- SEM) (ii) and p-eIF2 α normalized to tubulin was quantified (iii).

5.2.7 Azathioprine-induced autophagy is dependent on PERK

To determine whether the UPR is required for azathioprine-induced autophagy, THP-1-derived macrophages were treated with azathioprine or EBSS in the absence or presence of PERK inhibitor and then immunostained for LC3 (Figure 5.6). DMSO vehicle control (not shown) had 20.3% cells with >5 LC3 foci. Both azathioprine and EBSS significantly increased percentage of cells with >5 LC3 foci from 10% in untreated cells to between 59% and 60% (Figure 5.6: vii). In the presence of PERK inhibitor, azathioprine-induced autophagy was specifically attenuated as percentage of cells with >5 LC3 foci were between 13% and 15% in untreated and azathioprine-treated cells (Figure 5.6: compare panel ii and v, and quantified in vii). EBSS-induced autophagy was maintained with 48% of cells with >5 LC3 foci (Figure 5.6: compare panel iii and vi, and quantified in vii).

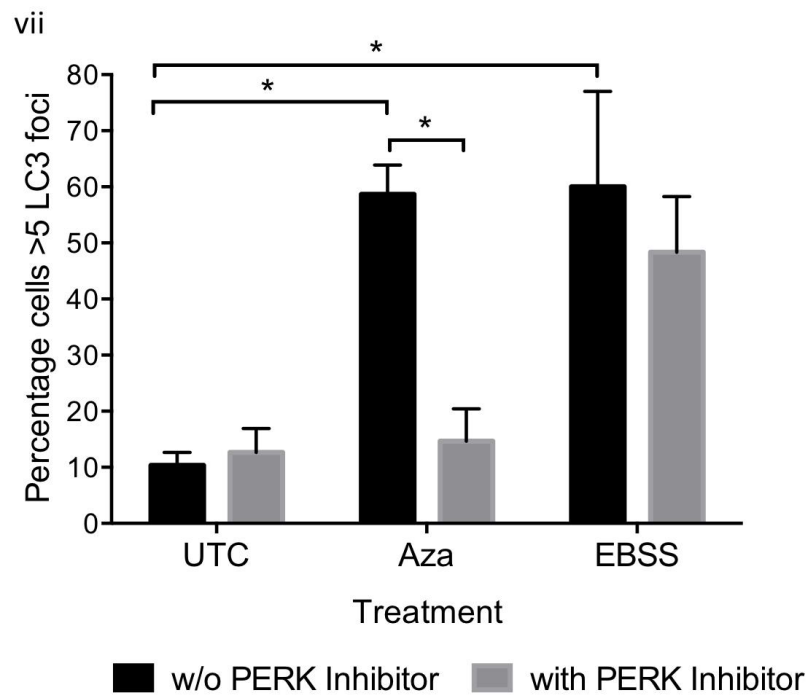
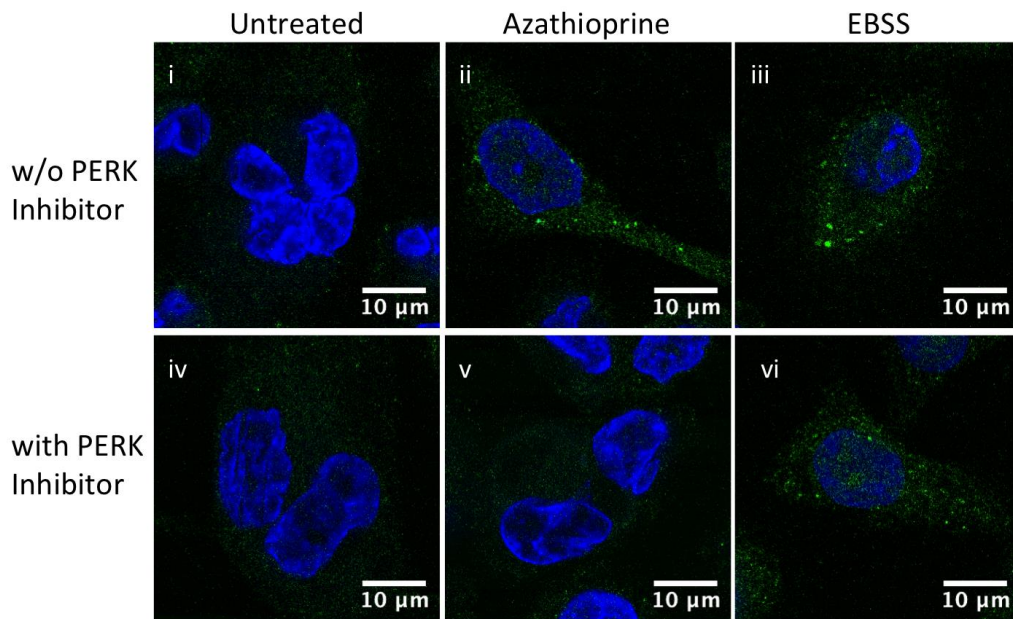


Figure 5.6: Azathioprine-induced autophagy is PERK dependent

THP-1-derived macrophages were untreated (i), or treated with 120 μ M azathioprine (ii) or EBSS (iii) for 6 hours without (i-iii) and with (iv-vi) 50nM PERK inhibitor I. Cells were then immunostained for LC3 (FITC: green) and mounted with DAPI Vectashield (blue). 100 cells were counted per treatment and percentage cells with >5 GFP-LC3 foci quantified (+/- SEM) from n=3 (vii). Two-way ANOVA with Tukey's multiple comparisons was performed *p < 0.05.

5.3 Summary

By using the RT² Profiler™ PCR Array for Human Autophagy genes it was possible to screen the effects of azathioprine on several autophagy and autophagy-related signalling pathways. The genes encoding the key autophagy proteins, MAP1LC3B and p62, were upregulated by azathioprine. In addition, upregulation of both *PERK* and *CXCR4* was confirmed with further investigation using qPCR.

Most genes encoding ATG proteins and major autophagy regulatory proteins were not transcriptionally upregulated by azathioprine in the PCR array, and some were shown to be downregulated. Genes involved in lysosome biogenesis and apoptosis, both pro- and anti-apoptotic, were also downregulated by azathioprine treatment.

In addition to UPR kinase, PERK, azathioprine increased the expression of UPR genes *ATF4*, *CHOP* and *PDI*, to a lesser extent. However, azathioprine did not increase expression of ER chaperone *BiP*. Western immunoblot also revealed a slight increase in PDI protein at 6 hours, but no increase in BiP when cells were treated with azathioprine.

A major regulator of autophagy activity, the mTORC1 pathway, was also investigated. Azathioprine decreased phosphorylation of rpS6, which indicates inhibition of mTORC1 activity, and an increase in total rpS6 emphasized the decrease in phosphorylation of the protein. Inhibiting PERK activity did not affect mTORC1 inhibition by azathioprine but had a pronounced affect on azathioprine-induced autophagy.

In conclusion, several interesting leads were identified using the PCR array; however, with further investigation of the UPR pathway, a link between UPR and autophagy signalling was identified in the context of azathioprine mechanism of action. It was also determined that inhibition of mTORC1 activity was involved in azathioprine-induced autophagy.

6. Effects of Azathioprine-induced Autophagy on Clearance of CD-associated Adherent Invasive *E. coli*

6.1 Introduction

Dysregulated immune responses to intestinal microflora are a crucial contributing factor to IBD pathogenesis (Boyapati et al., 2015). Although IBD cannot be attributed to one specific bacterial species, examination of the disease-associated microbiome has implicated several potentially causative agents (Frank et al., 2011). Most notably *E. coli* strains with an adherent and invasive phenotype (AIEC), are highly prevalent in CD (Boudeau et al., 1999; Darfeuille-Michaud et al., 2004; Frank et al., 2011; Martin et al., 2004; Thomazini et al., 2011). AIEC strains are persistent in intestinal macrophages from CD patients, leading to prolonged TNF- α production, continued recruitment of immune cells and granuloma formation (Bringer et al., 2012; Glasser et al., 2001; Meconi et al., 2007).

THP-1-derived macrophages were used to represent intestinal monocyte-derived macrophages and the AIEC CUICD541-10 strain isolated from a CD patient was used as it had previously been characterised for several key virulence genes (Baumgart et al., 2007). The effect of azathioprine on intracellular AIEC survival and pro-inflammatory responses was analysed and autophagy levels were monitored to determine if autophagic clearance of intracellular pathogens (xenophagy) was enhanced with azathioprine treatment.

6.2 Results

6.2.1 AIEC infection of THP-1-derived macrophages

THP-1-derived macrophages were infected with AIEC CUICD541-10 strain and gentamicin protection assay was used to optimise infection conditions. THP-1-derived macrophages were infected with MOI 10, 20 or 100 for 1, 2 or 3 hours prior to gentamicin treatment. An MOI of 100 appeared to infect cells to an excessive extent, as

did MOI 20 at 3 hours (Supplementary Figure 10.6). Optimal infection time for MOI 10 was 3 hours (Supplementary Figure 10.6).

THP-1-derived macrophages were then infected with AIEC CUICD541-10-mCherry strain and live-cell imaging was used to assess efficacy of bacterial internalisation in host cells. Cells were treated with IPTG to induce mCherry fluorescence in viable AIEC and Cell Tracker™ Green BODIPY® was used to demark the boundary of host cells. Enumeration of intracellular bacteria per host cell (indicated with white arrows) was carried out for up to 3 hours after infection, and revealed that detectable numbers of intracellular AIEC were apparent at 1 hour with 0.3 AIEC per host cell (Supplementary Figure 10.7: iii, vi). This increased to 0.6 and 0.9 AIEC per host cell at 2 and 3 hours, respectively (Supplementary Figure 10.7: iv-vi).

6.2.2 Azathioprine decreased intracellular AIEC survival as monitored by live-cell imaging

To ensure azathioprine does not have a direct anti-bacterial effect, a growth curve assay of AIEC bacterial cells was performed. There was no variation in growth of AIEC when treated with azathioprine or DMSO (Figure 6.1).

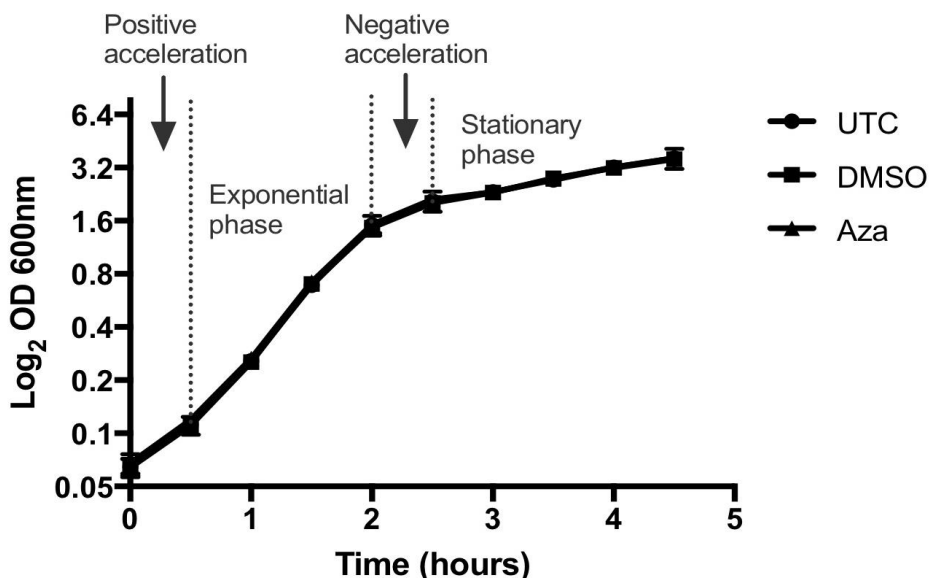


Figure 6.1: AIEC growth curve when treated with Azathioprine

LB broth was inoculated from an overnight culture of AIEC to an optical density of 0.05 at 600nm. The cultures were untreated, or treated with DMSO, or 120µM of azathioprine and incubated at 37°C, with shaking at 200RPM (n=3). Optical density at

600nm was measured every 0.5 hours and plotted in Log₂ scale to show growth phases (+/-SD). Experimental procedure performed by Ms Suzie McGinley under the supervision of Ms Kirsty Hooper.

THP-1-derived macrophages were infected with AIEC-mCherry for 3 hours and intracellular AIEC were maintained in low levels of gentamicin for 24 hours. For the final 6 hours of the gentamicin survival assay, cells were untreated or treated with azathioprine, as well as IPTG to induce mCherry fluorescence in AIEC. Live-cell imaging was used to monitor the percentage of THP-1-derived macrophages infected with AIEC (i) and the number of intracellular AIEC per host cell (ii) throughout the 6 hours (Figure 6.2).

At 0 hours, percentage of infection in both untreated and azathioprine-treated cells was between 30-40% (Figure 6.2: i). From 0.5 to 6 hours, between 38-48% of cells were infected when cells were untreated (Figure 6.2: i). In azathioprine-treated cells, 35% of cells were infected at 0.5 hours but this decreased to between 17-28% from 1 to 6 hours, which was significantly lower than untreated cells at the matched time-point (Figure 6.2: i). The optimal time-point for decreased percentage of infected cells with azathioprine treatment was 4 hours (Figure 6.2: i).

For quantification of intracellular AIEC per host cell, untreated cells had between 1.4 and 2.0 AIEC per cell from 0 to 6 hours (Figure 6.2: ii). When treated with azathioprine, intracellular AIEC per host cell remained between 0.9 and 1.3 from 0 to 1 hour (Figure 6.2: ii). However, from 2 to 6 hours of azathioprine treatment, intracellular bacteria per cell decreased to between 0.4 and 0.6 (Figure 6.2: ii). Intracellular AIEC per host cell numbers were significantly lower in azathioprine-treated cells at 0.53 compared to untreated cells at 1.9, at the 4-hour time-point (Figure 6.2: ii).

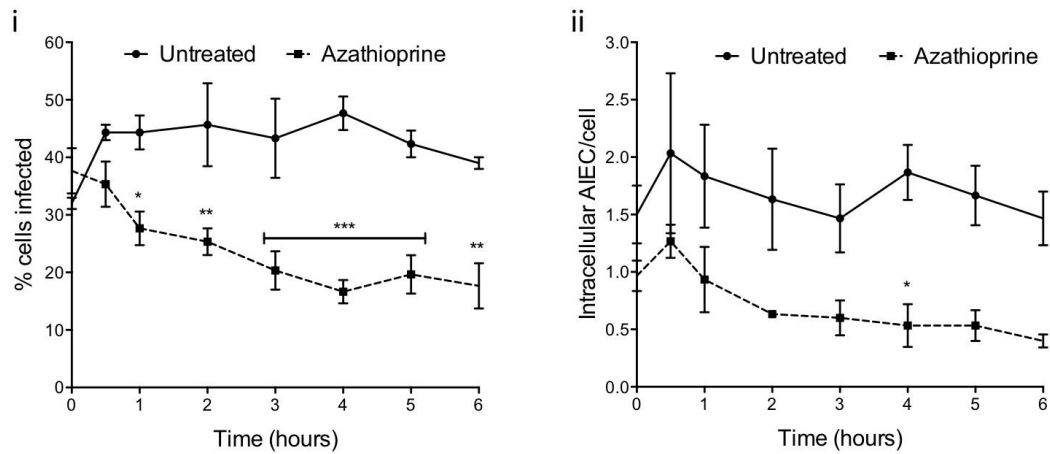


Figure 6.2: Azathioprine-induced clearance of mCherry AIEC monitored by live-cell imaging

THP-1-derived macrophages were infected with MOI 10 of mCherry-AIEC for 3 hours, treated with 100µg/ml gentamicin for 1 hour, and then maintained in 20µg/ml gentamicin for 24 hours. For the final 6 hours, cells were left untreated or treated with 120µM azathioprine and imaged by live-cell confocal microscopy (n=3). To induce mCherry fluorescence in AIEC, 0.1mM IPTG was added and 5µM Cell Tracker™ Green BODIPY® was added to visualise cells for the duration of the live-cell. 30 cells counted per image. Percentage cells with intracellular bacteria (+/- SEM) (i) and number of intracellular bacteria normalised to number of cells (+/- SEM) (ii) were quantified. A paired two-way ANOVA with Sidak's multiple comparisons was performed, with comparison of untreated and azathioprine treatment within each time-point *p < 0.05, **p < 0.01, ***p < 0.001.

6.2.3 Azathioprine decreased intracellular AIEC survival as monitored by gentamicin protection assay with enumeration of CFU

The effect of azathioprine on intracellular AIEC survival was then assessed using classical gentamicin protection assay with enumeration of CFU/ml. THP-1-derived macrophages, infected with AIEC, were untreated or treated with DMSO or azathioprine for the final 6 hours of the assay. A significant decrease in CFU/ml of intracellular AIEC was observed, with a roughly 2-fold decrease when cells were treated with azathioprine compared to DMSO-treated cells (Figure 6.3).

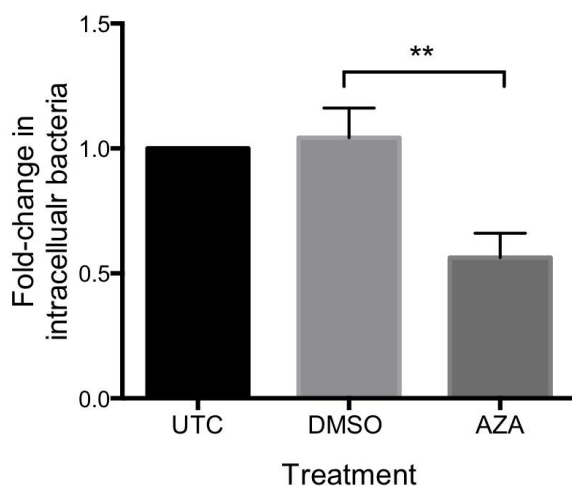


Figure 6.3: Azathioprine-induced clearance of AIEC monitored by gentamicin protection assay with CFU enumeration

THP-1-derived macrophages were infected with MOI 10 of AIEC for 3 hours, treated with 100µg/ml gentamicin for 1 hour, and then maintained in 20µg/ml gentamicin for 24 hours. For the final 6 hours, cells were left untreated or treated with DMSO or 120µM azathioprine (n=3). Cell lysates were prepared, spread on LB agar plates and incubated at 37°C overnight. CFU/ml of cell lysates was calculated and mean fold-change of CFU/ml normalised to untreated was calculated (+/- SEM). One-way ANOVA with Tukey's multiple comparison was performed **p < 0.01.

6.2.4 Azathioprine increased autophagy induction in correlation with enhanced bacterial clearance

THP-1-derived macrophages were infected with AIEC and left untreated (ii) treated with DMSO (iii) or treated with azathioprine (iv) for the final 6 hours of the gentamicin survival assay. Cells were immunostained for LC3 to evaluate autophagosome formation. Percentage of cells infected with AIEC and percentage of cells with >5 LC3 foci was quantified (Figure 6.4: v). Number of intracellular AIEC per host cell was also calculated (Figure 6.4: vi).

Confocal fluorescence imaging revealed a significant decrease in the percentage of cells infected, from 52% in untreated cells to 24% in azathioprine-treated cells (Figure 6.4: v). There was also a significant increase in percentage of cells exhibiting >5 LC3 foci, when comparing DMSO treatment to cells treated with azathioprine, from 20% to 52%, respectively (Figure 6.4: v). A notable decrease in the number of intracellular AIEC per host cell was observed from between 1.6 and 1.7 in untreated cells and DMSO-treated cells, to 0.6 in cells treated with azathioprine (Figure 6.4: vi).

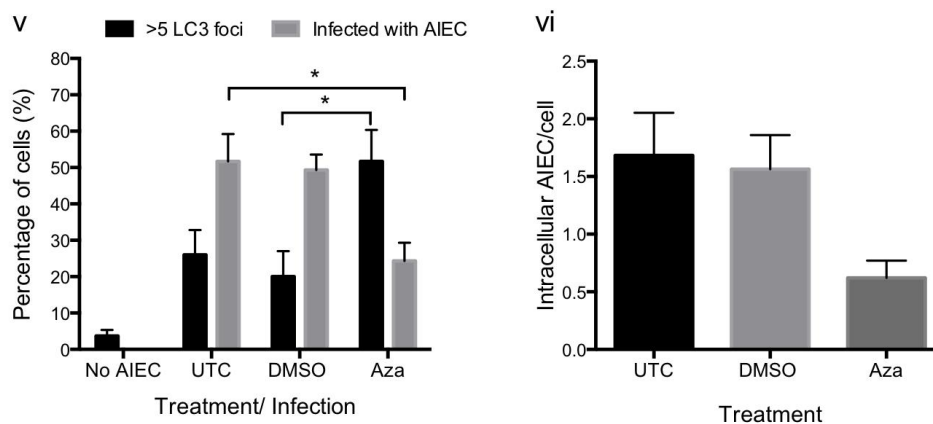
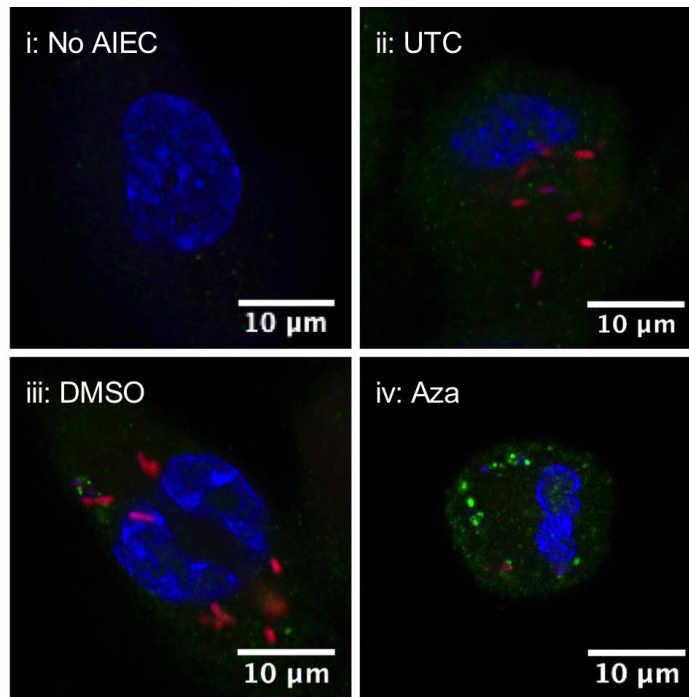


Figure 6.4: Azathioprine-induced clearance of mCherry AIEC and autophagy stimulation monitored by LC3 immunostaining

THP-1-derived macrophages were infected with MOI 10 of mCherry-AIEC for 3 hours, treated with 100 μ g/ml gentamicin for 1 hour, and then maintained in 20 μ g/ml gentamicin for 24 hours. For the final 6 hours cells were left untreated (ii), or treated with DMSO (iii) or 120 μ M azathioprine (iv). 30 minutes prior to fixation 0.1mM IPTG was added, then cells were immunostained for endogenous LC3 (FITC: green) and mounted with DAPI Vectashiled (blue). 100 cells were counted per condition. Percentage cells with >5 LC3 foci and with intracellular AIEC was quantified from n=3 (+/- SEM) (v) and number of intracellular bacteria normalised to number of cells (+/- SEM) (vi) were quantified. One-way ANOVA with Tukey's multiple comparison was performed *p < 0.05.

6.2.5 Azathioprine dampens pro-inflammatory cytokine responses to both AIEC infection and LPS

The effect of azathioprine treatment on AIEC- or LPS-induced pro-inflammatory cytokine expression was assessed in THP-1-derived macrophages using RT-qPCR. Cells were either not infected or infected with AIEC, then untreated or treated with DMSO or azathioprine for the final 6 hours of the gentamicin survival assay. Alternatively, cells were treated appropriately with/without combination with 200ng/ml lipopolysaccharide (LPS) for 6 hours (Figure 6.5: iv). Expression of IL-1 β (i), IL-6 (ii) and TNF α (iii-iv) was significantly upregulated by AIEC infection and LPS treatment and this was reduced when cells were treated with azathioprine (Figure 6.5). The dampening of TNF α expression was significant when infected cells were treated azathioprine (Figure 6.5: iii). Azathioprine had no effect on the expression of these cytokines in unstimulated cells (Figure 6.5).

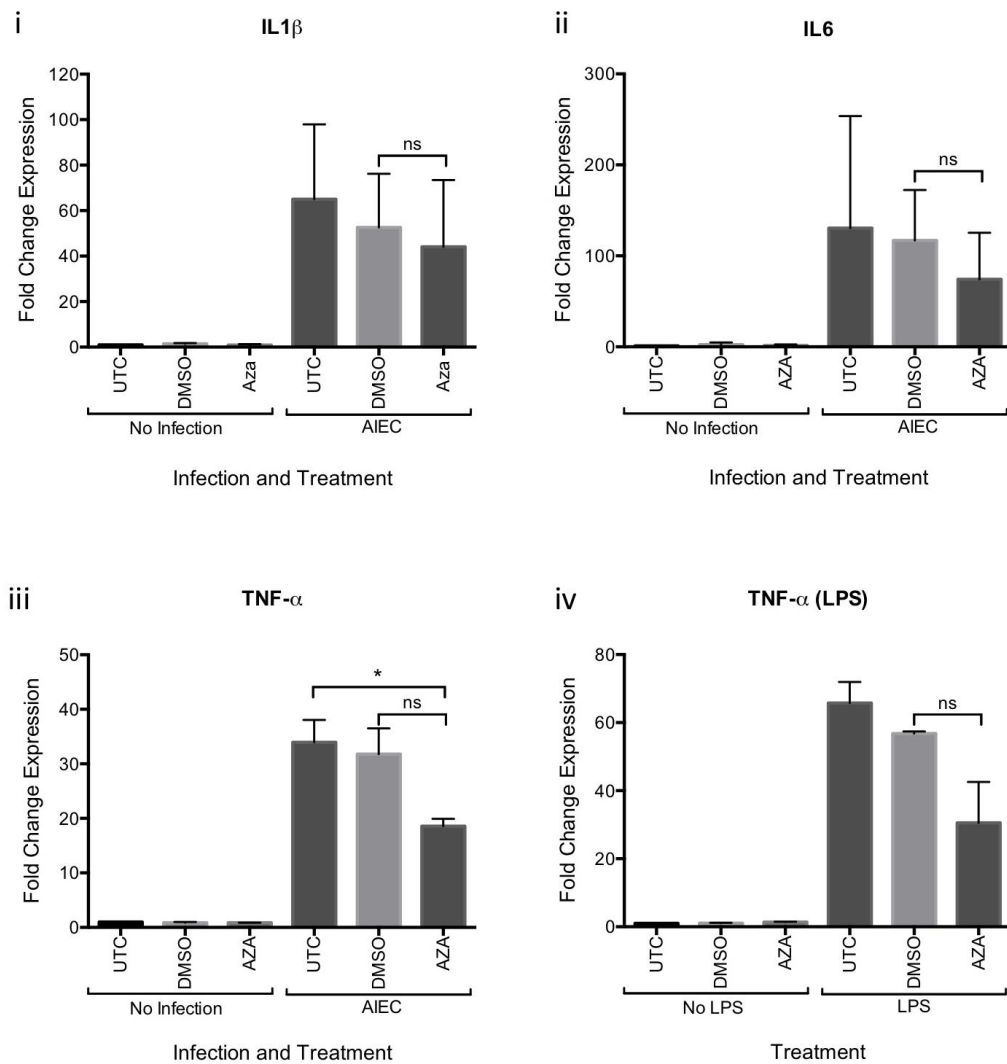


Figure 6.5: Azathioprine dampens AIEC- and LPS-induced pro-inflammatory cytokine expression

THP-1-derived macrophages were infected with MOI 10 of AIEC for 3 hours, treated with 100 μ g/ml gentamicin for 1 hour, and then maintained in 20 μ g/ml gentamicin for 24 hours (i-iii). For the final 6 hours cells were left untreated, or treated with DMSO or 120 μ M azathioprine. Cells were also untreated, or treated with DMSO or 120 μ M azathioprine either alone or in combination with 200ng/ml LPS for 6 hours (iv). mRNA was collected and converted to cDNA for RT-qPCR analysis of IL-1 β (i), IL-6 (ii) and TNF- α (iii-iv). Differential expression, normalized to untreated, was determined and mean fold-change expression is quantified from n=3 (+/- SEM) (i-ii). One-way ANOVA with Tukey's multiple comparison was performed using dCT *p < 0.05. Significant difference (p < 0.001 - p < 0.0001) for non-infected vs. infected, and untreated vs. LPS not shown.

6.3 Summary

Live-cell confocal imaging revealed that the CD-associated AIEC CUICD541-10-mCherry strain was able to infect THP-1-derived macrophages. Importantly, AIEC growth curves

demonstrated that azathioprine had no direct effect on growth of the bacteria. With this established, THP-1-derived macrophages were infected with AIEC, and live-cell imaging revealed that azathioprine decreased survival of intracellular bacteria between 1 and 6 hours of treatment, with an optimum time-point of 4 hours. This was verified using the classical gentamicin protection assay at the 6-hour time-point.

A key finding, demonstrated by LC3 immunostaining, was that azathioprine treatment increased clearance of intracellular AIEC in conjunction with enhanced autophagy activity. Additionally, azathioprine abrogated pro-inflammatory cytokine responses to AIEC infection, as assessed by RT-qPCR for IL-1 β , IL-6 and TNF α . Furthermore, azathioprine also reduced the expression of TNF α in cells treated with LPS. Overall, azathioprine increased clearance of intracellular AIEC, while dampening pro-inflammatory responses, potentially due to enhanced autophagy activity.

7. The IDEA Study - Azathioprine modulation of autophagy in paediatric IBD patient samples

7.1 Introduction

Alterations in IECs and immune cells have been linked to IBD, as detailed in section 1.1.4 and 1.1.5. Aberrant Paneth cell and goblet cell functions can drive IBD pathogenesis, and deficiencies in autophagy are key to these abnormalities (Section 1.3). Innate and adaptive immune cells both within the GI environment and systemically have also been associated with IBD. Due to autophagy's integral role in regulation, differentiation, development and survival of these cell types, this pathway can either directly or indirectly link these populations to IBD pathogenesis (Section 1.3). Furthermore, presentation of CD-associated variants in *NOD2* and *ATG16L1* can drive dysfunction in specific GI and systemic cells (Section 1.3). Importantly, enhancing autophagy levels in these cell types within the distinct physiological environments could have therapeutic benefits in IBD.

The aims of the IDEA (Inflammatory Bowel Disease Drug Effect on Autophagy) study were two-fold; measure autophagy in PBMCs and GI biopsies collected from paediatric IBD patients, and assess the effect of *ex vivo* azathioprine treatment on autophagy levels in PBMCs. Immunohistochemistry was used to measure endogenous LC3 in GI biopsies and flow cytometry was used to measure endogenous LC3 in PBMCs. Genotyping for CD-associated *NOD2* and *ATG16L1* variants determined the effect of genotype on basal autophagy activity and autophagy responses to azathioprine.

7.2 Results

7.2.1 Paediatric patient genotype: *ATG16L1* and *NOD2* CD-associated variants

The paediatric patients within the cohort were genotyped for CD-associated *ATG16L1* and *NOD2* variants. CD-associated *NOD2* variants were present in 1 out of 8 non-IBD patients, 2 out of 12 CD patients and 1 out of 7 UC patients (Table 7.1). No patients

carried the *NOD2 L1007fs* variant. One CD patient was homozygous for *NOD2 G908R* SNP and one CD patient was heterozygous for *NOD2 R702W* (Table 7.1). One non-IBD patient and one UC patient were homozygous for the *NOD2 R702W* SNP (Table 7.1).

ATG16L1 genotype of one non-IBD patient (AUT007) could not be determined. CD-associated *ATG16L1 T300A* SNP was present heterozygously, in 3 out of 7 non-IBD, 6 out of 12 CD and 3 out of 7 UC patients (Table 7.1). Homozygous presentation of the risk allele was apparent in 3 out of 7 non-IBD, 4 out of 12 CD and 3 out of 7 UC patients (Table 7.1). In the overall cohort, 4 patients presented the WT alleles for *ATG16L1*, 12 patients were heterozygous for *T300A* risk allele and 10 patients were homozygous.

Table 7.1: IDEA Study Paediatric Patient Genotypes

DNA was isolated from saliva samples collected from paediatric patients. Taqman Genotyping for each sample was undertaken for the following SNPs: *ATG16L1 T300A* (rs2241880), *NOD2 L1007f/s* (p.Leu1007fsX1008) (rs2066847), *NOD2 R702W* (rs2066844) and *NOD2 G908R* (rs2066845). This was performed by the Genetics Core at Edinburgh Clinical Research Facility, University of Edinburgh.

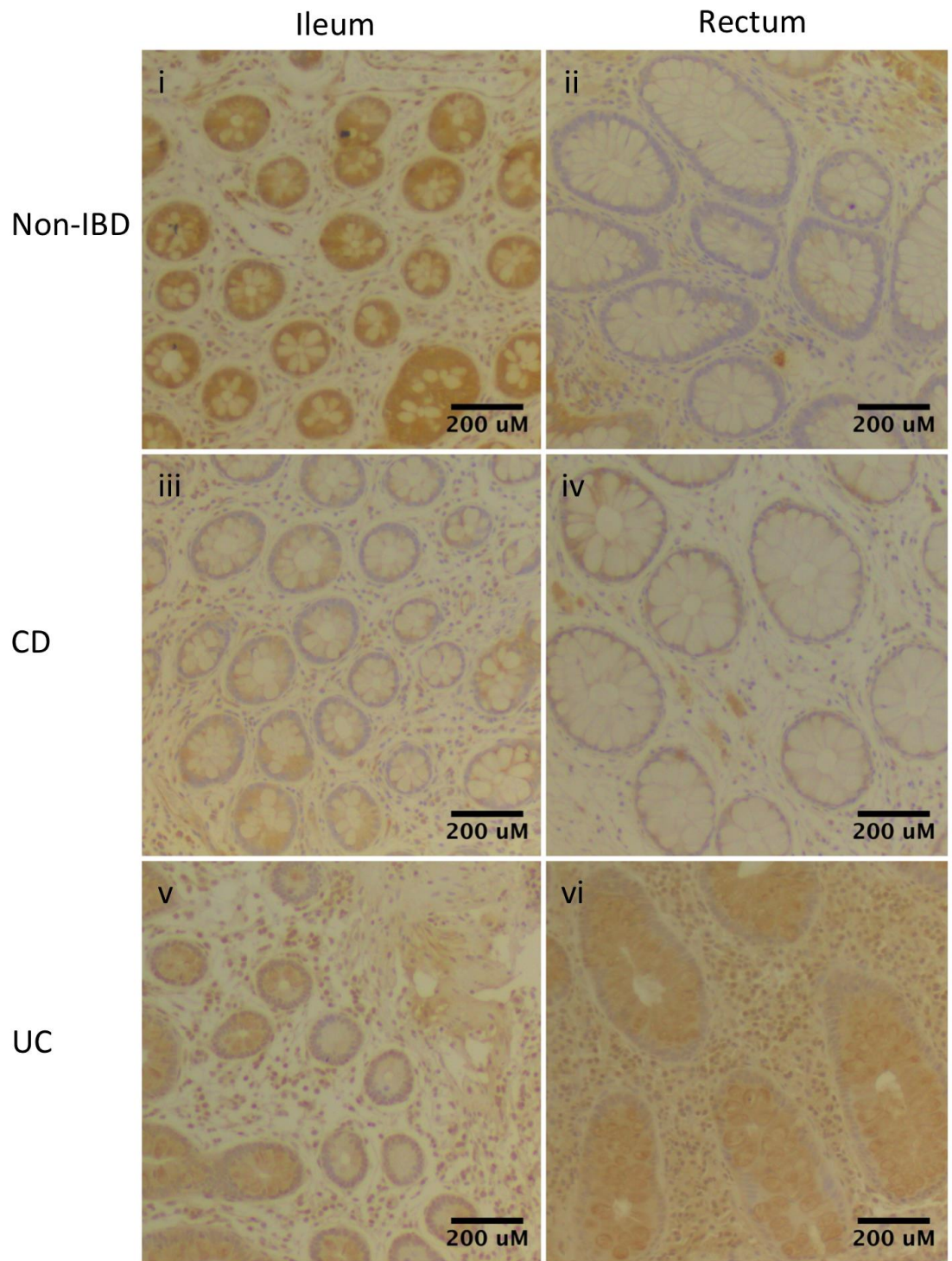
	Non-IBD	CD	UC	IBDU
Genotype <i>ATG16L1 T300A</i> (n=26)				
Wildtype	1	2	1	N/A
Heterozygous risk	3	6	3	N/A
Homozygous risk	3	4	3	N/A
Genotype <i>NOD2 L1007fs</i> (n=27)				
Wildtype	8	12	7	N/A
Heterozygous risk	0	0	0	N/A
Homozygous risk	0	0	0	N/A
Genotype <i>NOD2 G908R</i> (n=27)				
Wildtype	8	11	7	N/A
Heterozygous risk	0	0	0	N/A
Homozygous risk	0	1	0	N/A
Genotype <i>NOD2 R702W</i> (n=27)				
Wildtype	7	11	6	N/A
Heterozygous risk	0	1	0	N/A
Homozygous risk	1	0	1	N/A

7.2.2 Comparison of autophagy levels in GI biopsies from non-IBD and IBD paediatric patients

Immunohistochemical staining for LC3 in GI biopsies revealed differences in LC3 intensity between the patient groups (Figure 3.4). Figure 3.4 shows representative images of ileum and rectum biopsies from each patient group, with mean LC3 intensity in epithelial cells (vii) and mononuclear cells (viii) quantified in ileum/caecum and rectum biopsies from all patient groups. In non-IBD patients, high levels of LC3 staining were observed in epithelial cells in ileum/caecum biopsies (Figure 3.4: i, vii), which was

slightly decreased in UC patients (Figure 3.4: v, vii) and markedly decreased in CD (Figure 3.4: iii, vii). LC3 staining of mononuclear cells in ileum/caecum biopsies was constant for all patient groups (Figure 3.4: viii).

In rectal biopsies LC3 expression was slightly decreased in epithelial and mononuclear cells when compared to ileum/caecum, except for in UC patients where there was no difference between biopsy locations (Figure 3.4: i-viii). In rectal biopsies, UC patients had the highest levels of LC3 in both epithelial and mononuclear cells compared to other patients groups (Figure 3.4: vi-viii), which was slightly decreased in non-IBD patients (Figure 3.4: ii, vii-viii) and more substantially decreased in CD (Figure 3.4: iv, vii-viii).



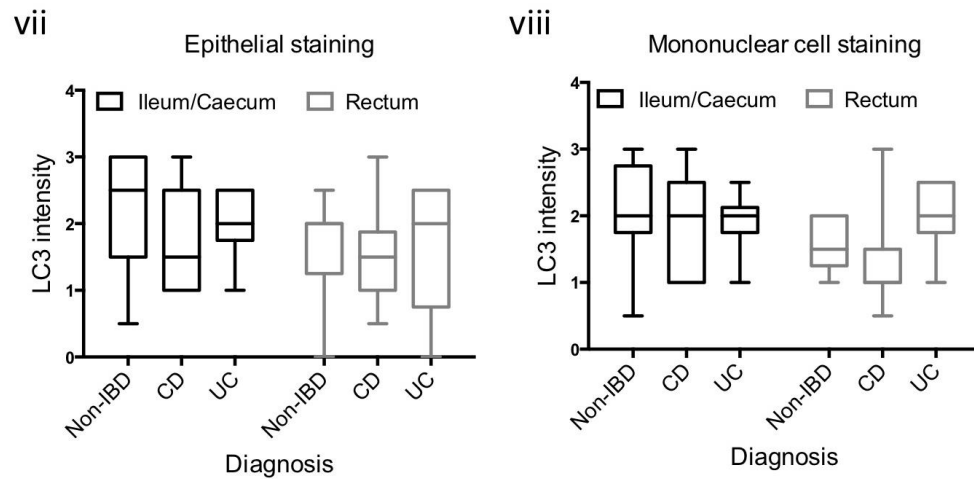


Figure 7.1: LC3 immunohistochemistry in paediatric patient GI biopsies

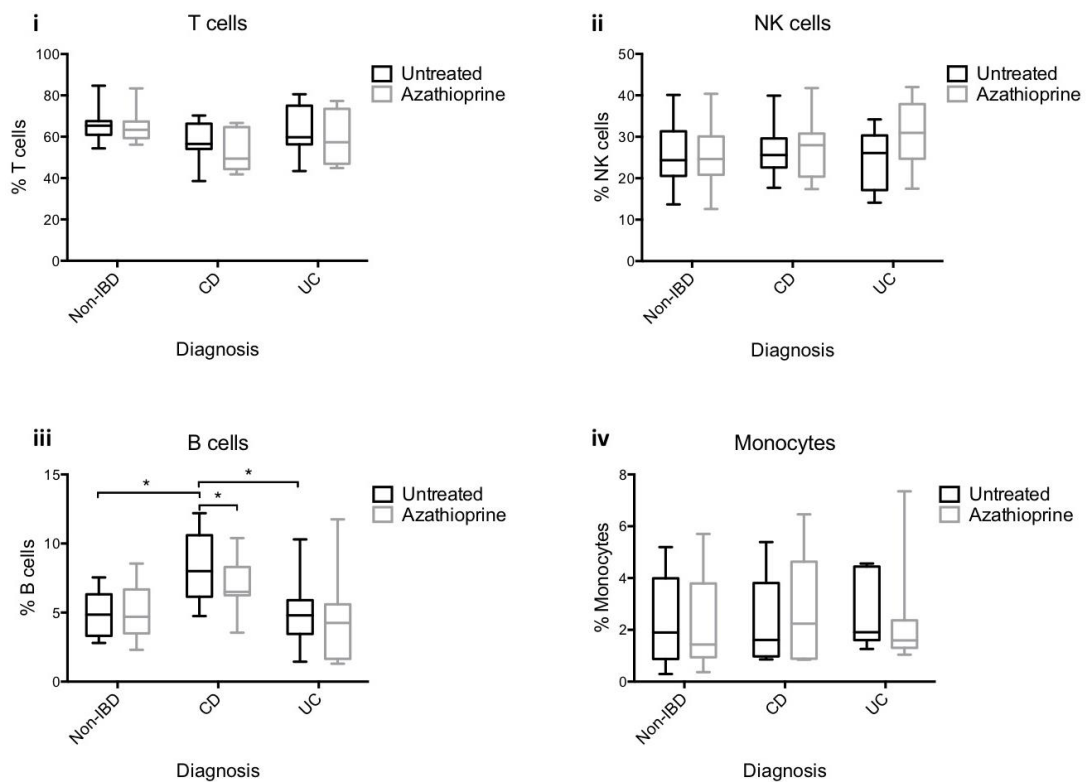
Biopsies taken from rectum (ii, iv, vi, viii) and either ileum or caecum (i, iii, v, vii) from non-IBD control (i-ii), CD (iii-iv) and UC (v-vi) patients were stained by immunohistochemistry for LC3 with DAB and haematoxylin counterstain. Two biopsies were taken per location. LC3 intensity of either epithelial cells (vii) or mononuclear cells (viii) was scored blind by two independent investigators and mean intensity score (+/- SEM) for each non-IBD and IBD patient group is shown for ileum/caecum and rectum (vii). Biopsies were sectioned at Centre for Comparative Pathology, University of Edinburgh, and remaining experimental procedures were performed by Ms. Sadie Kemp under the supervision of Ms. Kirsty Hooper.

7.2.3 Effect of azathioprine on PBMC sub-populations

A flow cytometry PBMC surface marker panel that stratified T cells, NK cells, B cells and monocytes was used to explore the effect of azathioprine on patient PBMC sub-populations. Cells were untreated or treated with azathioprine for 6 hours before immunostaining for flow cytometry analysis. Due to very low event count acquired for one CD patient (AUT020), this data was excluded from LC3 flow cytometry analysis. Percentages of the different PBMC subsets within the overall PBMC populations were analysed, and untreated cells were compared between the patient groups. Percentages of B cells were significantly increased in PBMCs from CD patients compared to non-IBD and UC patients (Figure 3.5A: iii). Comparisons were also made between untreated and azathioprine treated cells within each patient group. This revealed a significant reduction in B cell populations from CD patients when treated with azathioprine (Figure 3.5A: iii). All other cell populations were similar between patient groups and unaltered by azathioprine treatment (Figure 3.5A).

HLA-DR is a MHC II cell surface receptor that is constitutively expressed on B lymphocytes, monocytes and macrophages, and signifies late stages of T cell and NK cell activation (Bajnok et al., 2017). Initially, percentage of untreated cells that were HLA-DR+ was compared between the patient groups. HLA-DR expression was significantly increased in PBMCs from CD patients compared to non-IBD patient cells and in T cells from CD patients compared to cells from non-IBD and UC patients (Figure 3.5B: i-ii). There was also a significant increase in percentage of HLA-DR+ NK cells from UC patients compared to non-IBD patients (Figure 3.5B: iii). To determine the effects of azathioprine treatment on HLA-DR expression, percentage of untreated and azathioprine treated cells that were HLA-DR+ was compared within patient groups. There was a significant decrease in HLA-DR expression in B cells from non-IBD patients (Figure 3.5B: iv).

A



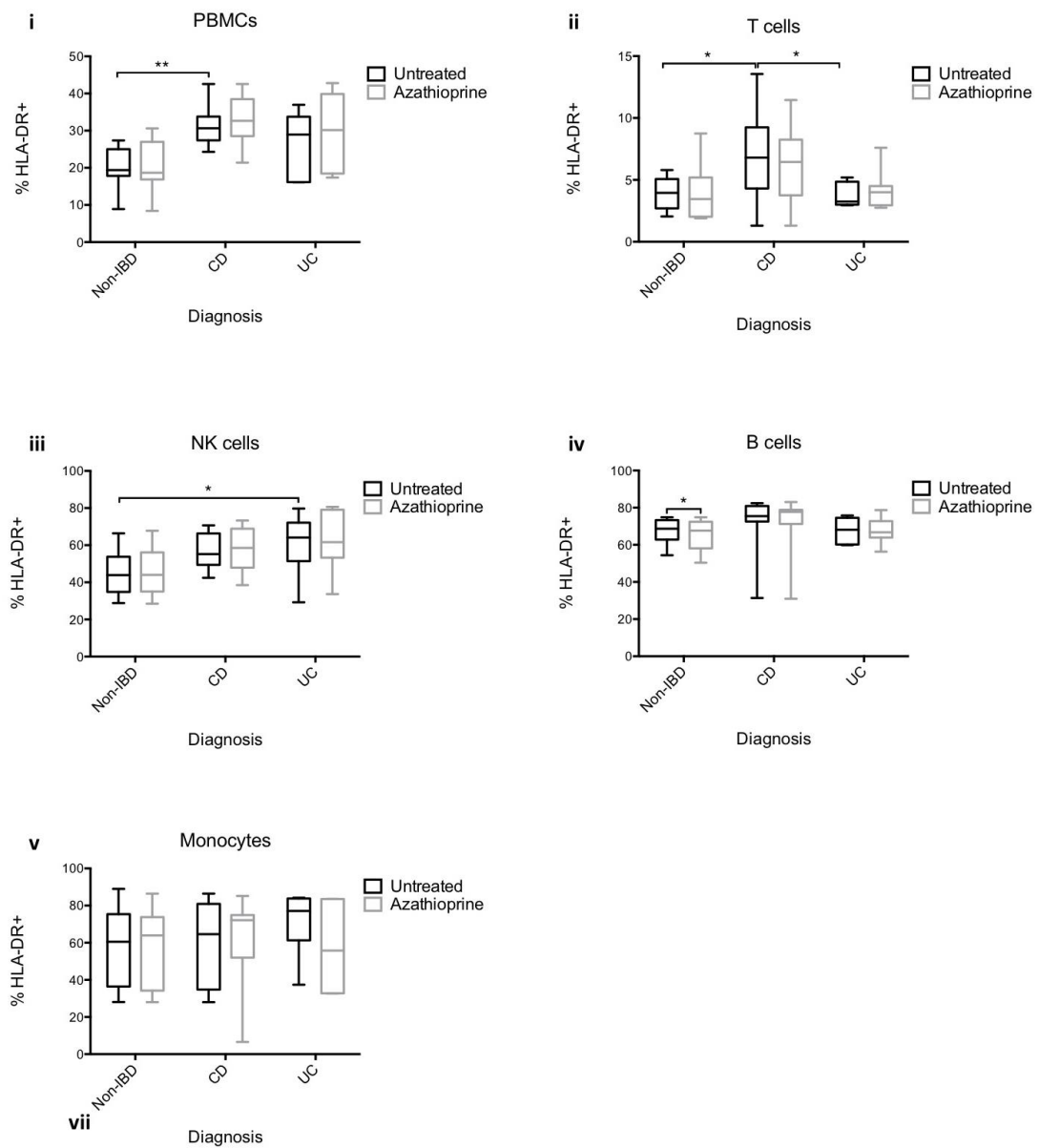
B

Figure 7.2: Paediatric patient PBMC populations

PBMCs isolated from non-IBD control and IBD patients were left untreated or treated with 120 μ M azathioprine for 6 hours. PBMCs were stained with surface markers for classification into populations and then washed with 0.05% saponin to remove cytosolic LC3. Cells were immunostained for endogenous LC3. Following flow cytometry acquisition, PBMC populations were analysed using FACSDiva software. PBMC populations are expressed as a mean percentage of PBMCs (+/- SEM) for non-IBD and IBD patient groups. One-way ANOVA with Tukey's multiple comparisons was used to compare untreated cells between the patient groups. Paired two-tailed t-test was used to compare untreated and azathioprine treated cells within each patient group. *p < 0.05, **p < 0.01, ***p < 0.001.

A: T cells (i), NK cells (ii), B cells (iii) and monocytes (iv) are expressed as a percentage of PBMCs.

B: Percentage of each PBMC populations positive for expression of HLA-DR is shown for PBMCs (i), T cells (ii), NK cells (iii), B cells (iv) and monocytes (v).

7.2.4 Effect of azathioprine on autophagy in PBMCs

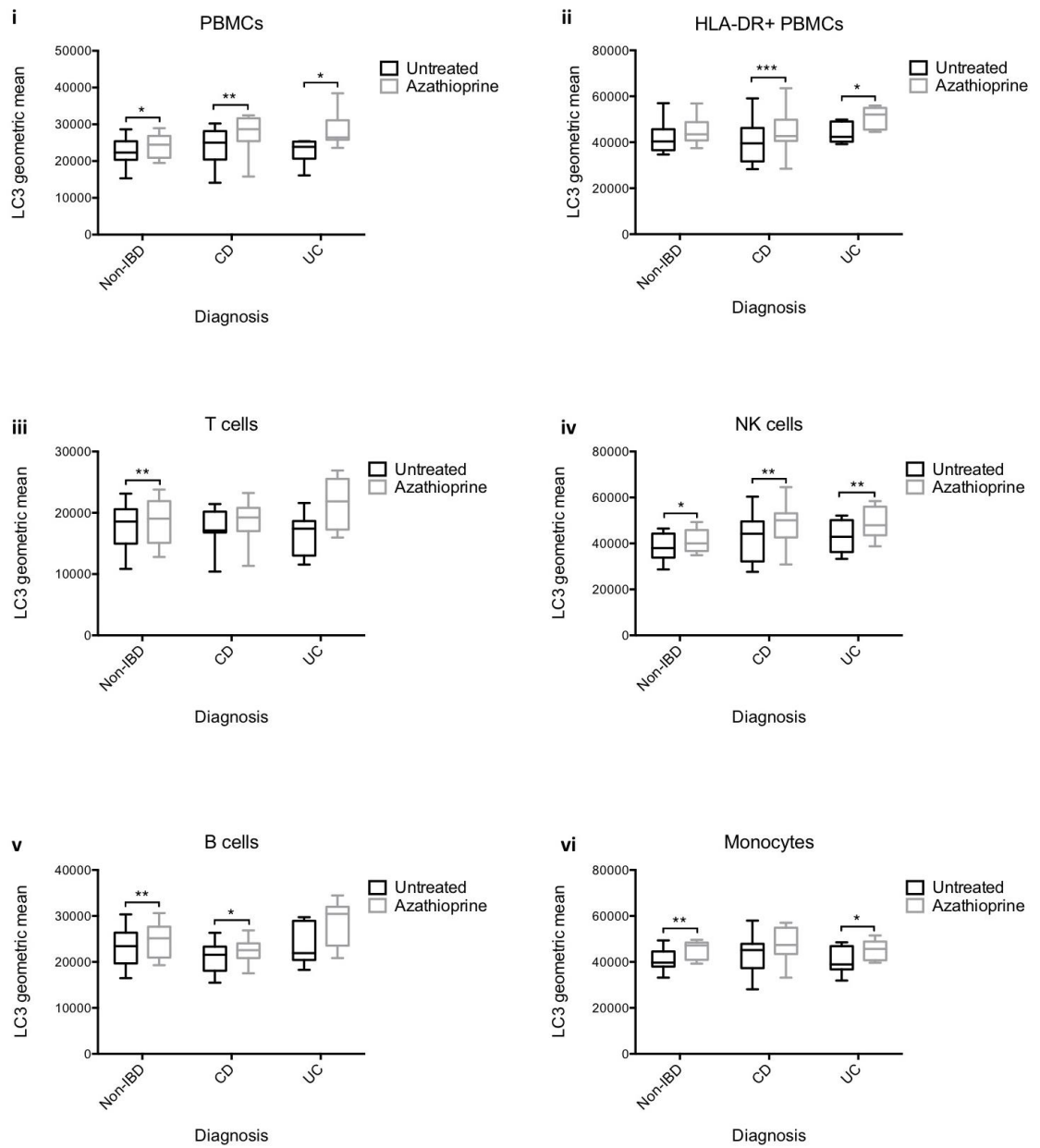
Flow cytometry for endogenous LC3 was coupled with a PBMC surface marker panel to analyse autophagy in different PBMC populations. There were no significant differences observed in basal levels of autophagy between patient groups when LC3 geometric mean of untreated cells was compared between the groups. However, azathioprine treatment induced a significant increase in LC3 in PBMC populations from non-IBD, CD and UC patients (Figure 7.3A). There was a significant increase in LC3 geometric mean in general PBMC populations from non-IBD, CD and UC patients, and in HLA-DR+ PBMCs from CD and UC patients, when treated with azathioprine (Figure 7.3A: i-ii). This was reflected in NK cells in all patient groups and in T cells from non-IBD patients only (Figure 7.3A: iii-iv). An azathioprine-induced increase in LC3 geometric mean was observed in B cells from non-IBD and CD patients and in monocytes from non-IBD patients and UC patients (Figure 7.3A: v-vi). As there was only one patient diagnosed with IBDU, no statistical analysis could be undertaken, although a similar azathioprine-induced increase in LC3 can be observed for all PBMC populations from the IBDU patient. These results confirm that azathioprine robustly induces autophagy in primary PBMCs *ex vivo*, supporting our *in vitro* findings.

7.2.5 *Ex vivo* azathioprine treatment preferentially increases autophagy in paediatric patient PBMC populations with *ATG16L1 T300A* SNP

To determine the effect of *ATG16L1* genotype (WT, *T300A* heterozygous and *T300A* homozygous) on azathioprine modulation of autophagosome-bound LC3, data was also analysed by sub-categorisation of *ATG16L1* genotype in the overall cohort. LC3 geometric mean of untreated and azathioprine-treated cells was compared within each patient genotype group. Azathioprine induced significant increases in LC3 in PBMCs, specifically from patients with the CD-associated *ATG16L1 T300A* SNP (Figure 7.3B). LC3 geometric mean of untreated cells was compared between *ATG16L1* genotype groups.

However, there were no significant differences in basal levels of autophagy between these groups (Figure 7.3B).

A



B

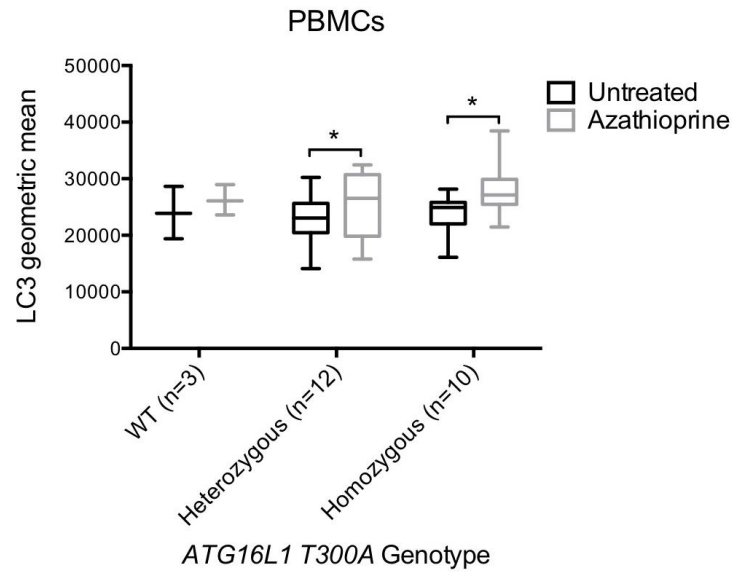


Figure 7.3: Paediatric patient PBMC LC3 flow cytometry

PBMCs isolated from non-IBD and IBD patients were left untreated or treated with 120 μ M azathioprine for 6 hours. PBMCs were stained with surface markers for classification into populations and then washed with 0.05% saponin to remove cytosolic LC3. Cells were immunostained for endogenous LC3 and geometric mean of LC3 intensity of cells was quantified by flow cytometry and analysed using FACSDiva software.

A: Mean of LC3 geometric mean (+/-SEM) is shown for PBMCs (i) and, then after gating for surface markers for PBMC populations, for HLA-DR+ PBMCs (ii), T cells (iii), NK cells (iv), B cells (v) and monocytes (vi) from each non-IBD and IBD patient group. One-way ANOVA with Tukey's multiple comparisons was used to compare untreated cells between the patient groups. Paired two-tailed t-test was used to compare untreated and azathioprine treated cells within each patient group. *p < 0.05, **p < 0.01, ***p < 0.001.

B: Mean of LC3 geometric mean (+/-SEM) is shown for PBMCs from each *ATG16L1 T300A* genotype patient group. Patients had either wild-type (WT) alleles or were heterozygous/homozygous for *ATG16L1 T300A* SNP. One-way ANOVA with Tukey's multiple comparisons was used to compare untreated cells between genotype groups. Paired two-tailed t-test was used to compare untreated and azathioprine treated cells within each genotype group *p < 0.05.

7.3 Summary

In the GI tract we observed decreased LC3 levels in CD patients compared to non-IBD patients, but basal levels of autophagy remained constant between patient groups in untreated PBMCs. *Ex vivo* treatment with azathioprine enhanced autophagy activity in both innate and adaptive systemic immune cells, and in activated, HLA-DR+, PBMC

populations. Interestingly, enhanced autophagy was more prominent in PBMCs derived from patients with the *ATG16L1 T300A* SNP.

Flow cytometry analysis also showed very similar percentages of PBMC populations in the distinct patient disease groups and the percentages of the populations was not altered with *ex vivo* azathioprine treatment. The exception to this was expansion of B cells in CD patients, which subsided upon azathioprine treatment. HLA-DR expression was altered in CD patient-derived PBMCs and T cells, and in UC patient-derived NK cells, compared to non-IBD patient-derived cells. Interestingly, azathioprine treatment decreased HLA-DR expression in B cells from non-IBD patients.

8 Discussion

8.1 Summary of results

By screening a panel of IBD drugs, it was identified that immunosuppressant drug azathioprine is a strong inducer of the autophagy pathway. Subsequent analysis determined that azathioprine induced autophagy independently of apoptosis, and via UPR kinase PERK signalling and inhibition of mTORC1 activity. Azathioprine also increased clearance of intracellular AIEC and dampened pro-inflammatory responses to infection. Finally, azathioprine increased autophagy activity in PBMCs derived from non-IBD and IBD paediatric patients, and this response was more pronounced in cells from patients harbouring the CD-associated *ATG16L1 T300A* SNP. By expanding the understanding of the mechanism of action of azathioprine its therapeutic use could be improved.

8.2 The effect of anti-TNF- α agents on autophagy

Initial testing of the IBD drug panel in HEK293 cells revealed that infliximab possessed modest autophagy modulating activity; however, this could not be confirmed with further investigation. Several studies have identified that the cytokine TNF- α harbours autophagy-inducing properties (Bell et al., 2013; Cha et al., 2014; Connor et al., 2012; Keller et al., 2011), and infliximab has been shown to reactivate *Mycobacterium tuberculosis* infection, at least partially through autophagy impairment (Harris and Keane, 2010). However, there is growing evidence that anti-TNF- α agents have the ability to enhance autophagy activity. In particular, infliximab has been shown to promote development of regulatory macrophage populations, in part through autophagy stimulation, and this response in patients was determined by *ATG16L1* genotype (Levin et al., 2016; Vos et al., 2012). Additionally, stimulation of the autophagy pathway has been proven to be key for the effectiveness of anti-TNF- α therapy (Wildenberg et al., 2013). As macrophages play a crucial role in innate immunity and inflammation within the GI tract, further investigation of the effects of anti-TNF- α on autophagy in this cell type will be particularly relevant to IBD. Although we could not confirm infliximab-induced autophagy in HEK293 cells, it is possible that autophagy responses to infliximab would have been more pronounced in macrophages. Also, as

infliximab acts via the neutralization of TNF- α , the effects of infliximab may be augmented when treating an inflamed area that has elevated TNF- α levels.

8.3 The effect of corticosteroids, aminosalisylates and immunomodulators on autophagy

Autophagy modulation was not observed in HEK293 GFP-LC3 cells treated with methylprednisolone, sulfasalazine or methotrexate, despite many studies previously exhibiting autophagy-modulating properties in these drug classes, as described in section 1.5 and shown in Table 1.3 (Hooper et al., 2017). There is a plethora of evidence showing that corticosteroids can modulate autophagy activity with many studies linking the mechanism to mTORC1 and apoptosis. miRNA and mRNA profiles in the rectal mucosa of UC patients showed differential expression of DDIT4, an inhibitor of mTORC1 activity, in responders to corticosteroid treatment (Naves et al., 2015). Several other *in vitro* and *in vivo* studies showed that mTORC1 is inhibited by corticosteroids (Fatkhullina et al., 2014; Ozmen et al., 2016; Wang et al., 2015), resulting in enhanced autophagy levels (J. Gao et al., 2016; He et al., 2016; Xue et al., 2016). Taken together these studies strongly suggest that inhibition of the mTORC1 pathway and subsequent enhancement of autophagy play an important role in the response to corticosteroid treatment. This opposes our results that showed minimal effect of methylprednisolone on autophagy activity. However, most of these aforementioned studies focused on dexamethasone and corticosterone that are more commonly used in cancer therapy.

Methylprednisolone and prednisolone, which are more commonly used for paediatric IBD treatment, suppressed autophagy activity in a neuroblastoma cell line (Neuro-2a) (W. Gao et al., 2016), in a rat model of osteoporosis (Tang et al., 2018) and in a rat model of spinal cord injury (Chen et al., 2012). This suggests that methylprednisolone and prednisolone may have mechanisms of action that differ slightly from the other drugs within the corticosteroid drug class, resulting in opposing effects on autophagy. Due to low basal levels of autophagy in our cell lines, it may not have been possible to detect autophagy suppression. To determine if methylprednisolone does inhibit autophagy activity, a future avenue of investigation would be to combine the drug with a known

autophagy modulator such as rapamycin or bafilomycin, to allow detection of decreases in autophagosome accumulation.

Sulfasalazine has opposing effects on autophagy, as the drug has been shown to decrease autophagy activity in a murine model of cancer cachexia (Chacon-Cabrera et al., 2014), but has also enhanced autophagic cell death in an oral squamous cell carcinoma (OSCC) cell line (Han et al., 2014). Dosage is difficult to compare between *in vitro* and *in vivo* studies, however it is possible that the induction of autophagic cell death observed by Han et al. (2014) may be representative of a concentration range that is cytotoxic. Therefore, the lack of autophagy modulation observed in HEK293 cells could be explained by the use of non-toxic concentrations in this cell line.

In various human cell lines, methotrexate has been shown both to enhance (Varshney and Saini, 2018; Xu et al., 2015) and suppress (Tsai et al., 2013) the autophagy pathway. The lack of autophagy modulation observed in our cell line may be due to differing effects of this immunosuppressant drug in HEK293 cells. It could also be possible that methotrexate was suppressing autophagy in our cell line, but this was not detected due to low basal levels of autophagy.

8.4 The effect of thiopurines on autophagy and apoptosis

Autophagy induction by thiopurines has previously been shown in a variety of cell types including HCT116 and HT29 cells (Chaabane et al., 2016; Oancea, 2016; Zeng et al., 2007; Zeng and Kinsella, 2010, 2008), human endometrial cancer cells (HEC59) (Zeng et al., 2007), HeLa cells, human hepatocytes cell line (HepG2), murine Ralph and William's cell line (RAW) macrophage-like cells and primary murine fibroblasts (Oancea, 2016). The majority of these studies focused solely on 6-TG, which is commonly used for cancer therapy. To date, only one study has shown autophagy induction mediated by azathioprine, which was in HCT116 and HT29 cells (Chaabane et al., 2016).

As previous studies focused on human epithelial cell lines, our observation that azathioprine induced autophagy in human THP-1-derived macrophages, a cell type distinctively relevant in IBD pathogenesis, is both novel and interesting. A recent study

investigated the effects of 6-TG on the mobility of DCs, which are another monocyte-derived cell type implicated in IBD pathogenesis. In DCs derived from individuals harbouring the *ATG16L1 T300A* SNP, defects in migration caused by autophagy deficiency could be restored by 6-TG treatment (Wildenberg et al., 2017). Although this study did not directly demonstrate autophagy induction by 6-TG, it does suggest that thiopurines are capable of inducing autophagy in primary innate immune cells. It would be valuable to confirm our THP-1-derived macrophage findings in primary monocyte-derived macrophages, and determine whether *ATG16L1 T300A* genotype affects responses to azathioprine in this cell type.

Despite demonstrating that azathioprine strongly induced autophagy, most genes encoding autophagy-related proteins were not transcriptionally upregulated in our RT² PCR array (Chapter 5). When transcription factor E2F1 binds to the *LC3B* promoter, expression of several autophagy genes have been shown to increase, resulting in increased autophagy (Haim et al., 2015; Kovsan et al., 2011). We found that the only autophagy genes upregulated by azathioprine were for LC3B and p62. However, it has been observed that increases in expression of *ATG* genes are usually very modest and dependent on cell type (Klionsky et al., 2016). Furthermore, autophagy proteins that are involved in autophagosome formation and maturation, such as ATG5 and ATG12, are not necessarily required for autophagy initiation. Therefore, transcriptional increases in these genes are more likely to be required for replenishment of protein when autophagy flux is extensive or prolonged (Kouroku et al., 2007; Rouschop et al., 2010; Sandri, 2010). This suggests that at the time-points we investigated, the upregulation of autophagy genes may not be apparent with azathioprine treatment, as autophagy flux is not excessive.

In some cases, azathioprine downregulated the expression of *ATG* genes: *ATG16L1*, *ATG16L2*, *ATG4B*, *ATG4D*, *ATG9A*, *ATG9B*, *LC3A*, *RGS19* and *TMEM74*. The downregulation of these genes may be part of a mechanism to limit autophagosome formation to prevent excessive autophagy in response to stimuli. For instance, the *NR1D1* and *ZKSCAN3* transcription factors are responsible for repressing autophagy genes in such a scenario (Chauhan et al., 2013; Klionsky et al., 2016).

From our array data, we identified that genes involved in lysosome biogenesis were downregulated with azathioprine treatment. This would suggest that azathioprine

decreases lysosome biogenesis, which may impair the fusion of autophagosomes and lysosomes that is necessary for autophagy flux. It was shown in Chapter 3, that autophagy flux is enhanced with azathioprine treatment. Therefore, despite impaired transcription of some key lysosome proteins, there appears to be sufficient lysosome formation to facilitate autophagy flux upon azathioprine treatment. Investigating the effect of azathioprine on lysosomal regulators, as well as regulators of autophagy would aid the understanding of the influence of this drug on autophagy flux.

Our array data also indicated that several genes involved in the modulation of apoptosis were downregulated with azathioprine treatment. Most of these genes were pro-apoptotic; however, some of the downregulated genes had anti-apoptotic activity. This highlights the complex signalling pathways involved in autophagy and apoptosis regulation, as genes with opposing functions can be altered simultaneously. Due to the contradictory effects on apoptosis signalling, it is therefore important to highlight the overall effect of azathioprine on apoptosis activity. As such, downregulation of mainly pro-apoptotic genes by azathioprine supports our observation that azathioprine-induced autophagy is independent of apoptosis induction (Chapter 4).

In previous studies thiopurine-induced autophagy was accompanied by apoptosis in HCT116 and HT29 cells (Chaabane et al., 2016; Zeng et al., 2007; Zeng and Kinsella, 2010, 2008) and HEC59 (Zeng et al., 2007). In one study, HCT116 and HT29 cells were treated with azathioprine at 50 μ M or 100 μ M for 24 hours followed by a 72 hour rest (Chaabane et al., 2016). Another study that focused solely on cytotoxicity, observed a decrease in the viability of human hepatocytes at 96 hours when treated with 5-25 μ M azathioprine (Petit et al., 2008). We found that the optimum time-point for monitoring autophagy induction in our model was 6 hours post-treatment, and prolonging incubation with 120 μ M of azathioprine to 24 hours did not induce cell death. Given that previous studies have used longer time-points, induction of apoptosis may have occurred if incubation with azathioprine were prolonged further. However, pre-mortem autophagy (autophagy preceding apoptosis) increases cell surface expression of phosphatidyl-serine to encourage phagocytic clearance of apoptotic cells (heterophagy) in an attempt reduce tissue inflammation (Qu et al., 2007). If azathioprine-induced autophagy were preceding apoptosis, then annexin-V staining of phosphatidyl-serine would likely be increased, which was not apparent at 6- or 24-hour time-points. This could suggest that

the azathioprine-induced autophagy observed in our cell model is mediated via a mechanism of action that is distinct from cytotoxicity.

The proposed mechanism of dual autophagy and apoptosis induction by thiopurines has been linked to MMR processing of damaged DNA, which caused mitochondrial PTP and subsequently increased ROS production (Chaabane et al., 2016; Zeng et al., 2007; Zeng and Kinsella, 2010, 2008). Mitochondrial PTP triggered mitophagy (Chaabane et al., 2016), and it has been shown that enhanced ROS can influence autophagy by enhancing ATG4 activity to promote autophagosome expansion (Scherz-Shouval et al., 2007). Enhanced mitophagy activity promoted cell survival in response to thiopurine treatment due to removal of damaged mitochondria; however, when ROS production and mitochondrial damage were extensive apoptosis was stimulated (Chaabane et al., 2016; Zeng and Kinsella, 2010). Both HEK293 cells and THP-1 cells are MMR proficient (Cannavo et al., 2005; Hangaishi et al., 1997), therefore would be capable of this response.

Metabolism of azathioprine inherently produces more ROS than 6-MP due to the reduction of the imidazole group when azathioprine is converted to 6-MP (Aarbakke et al., 1997; A. U. Lee and Farrell, 2001). It was observed in an immortalized human hepatic (IHH) cell line and a non-tumour intestinal human colon epithelial cell line (HCEC), that only azathioprine, and not 6-TG or 6-MP, increased ROS production (Pelin et al., 2015). In this study, the cytotoxic effects of these drugs were not linked to ROS production, but anti-proliferative effects of azathioprine were ROS-dependent. It was therefore suggested that ROS production in response to thiopurines is less pronounced in non-tumour cells, as in human colorectal cancer cells (HCT116 and HT29) enhanced ROS production was integral to autophagy and apoptosis induction by all three thiopurine drugs (Chaabane et al., 2016). A decreased propensity for ROS production or a higher tolerance of ROS may account for the lack of cell death accompanying azathioprine-induced autophagy in HEK293 cells and THP-1-derived macrophages. HEK293 cells are transformed healthy human embryonic kidney cells, and THP-1 cells, although leukaemia-derived, are a monocyte-like cell line, which produce high levels of antioxidants to combat the generation of ROS during respiratory bursts (Pietarinen-Runtti et al., 2000). Interestingly, 6-MP exposure did not induce autophagy in our own assays. Therefore, it can be speculated that azathioprine, but not 6-MP, induces levels

of ROS that cross a threshold for autophagy activation, but as HEK293 and THP-1 cells are more resistant to ROS, induction of cytotoxicity is not apparent. A key step in conclusively determining this would be to monitor ROS levels and antioxidant levels in our experimental model. Also, further experimental work is also required to delineate the role of the imidazole group and thiopurine metabolism in autophagy modulation.

When azathioprine is metabolised to 6-MP the imidazole moiety is released in a non-enzymatic reaction (De MIRANDA et al., 1973). Although the main active metabolites of azathioprine and 6-MP are the same, responses to these drugs can be drastically different with a higher incidence of intolerance to azathioprine than 6-MP (Fraser and Jewell, 2000). In patients intolerant to azathioprine but not 6-MP there were no differences in the activity of key enzymes required for thiopurine metabolism, such as TPMT (McGovern et al., 2002). Therefore, it was suggested that the non-enzymatic reaction cleaving the imidazole moiety might be integral to the differences in the drugs mechanism of action, as imidazole derivative can exert independent immunomodulatory activity (McGovern et al., 2002). Autophagy was clearly modulated by azathioprine and not 6-MP in our study, therefore, it would be interesting to determine if this was dependent on imidazole activity. Interestingly, one study found that imidazole blocked autophagy flux in HEC-1B cells while inducing apoptosis potentially due to its lysosomotropic properties (Liu et al., 2015). This contradictory effect of imidazole in this study to our hypothesis may be dependent on specific conditions and cell types; however, this facet of thiopurine metabolism would need to be investigated further for clarification.

It is likely that the increased autophagy activity observed in HEK293 and THP-1-derived macrophages could be a pro-survival mechanism, potentially to remove damaged mitochondria, in response to the low level ROS production and cellular stress caused by azathioprine. However, the autophagy response in HEK293 and THP-1-derived macrophages could also be mediated, at least in part, by mechanisms independent of cytotoxicity, ROS production and mitochondrial damage, as investigated in Chapter 5. It has been suggested that at lower therapeutic concentrations of thiopurines, which are typically used when treating IBD compared to their use in cancer therapy, there is less cytotoxicity and RAC1-dependent mechanisms that modulate autophagy are more prominent (Wildenberg et al., 2017).

8.5 Azathioprine mechanism of action in the context of autophagy

The major regulatory hub of autophagy is the mTORC1 pathway, which acts to inhibit autophagy activity. We demonstrated in THP-1-derived macrophages that azathioprine decreased phosphorylation of rpS6, which indicates inhibition of mTORC1 activity. This suggests that azathioprine-induced autophagy is mediated, in part, through mTORC1 inhibition. Furthermore, in our RT² PCR array, *Akt* was downregulated, which is a known activator of mTORC1 (Miyazaki et al., 2010; Sancak et al., 2007). Therefore, *Akt* downregulation may contribute to decreased mTORC1 activity. In HCT116 cells, it was shown that 6-TG induced both autophagy and apoptosis via positive regulation of mTORC1 and S6K1 (Zeng and Kinsella, 2008). As this is contrary to the established role of mTORC1 in autophagy regulation, it was suggested that positive regulation of mTORC1 increased translation of proteins required for autophagy induction, which superseded mTORC1's negative regulation of autophagy. The opposing mechanism observed in our cell model was reflected in human leukaemia T cells, where 6-MP decreased ATP production, which activated AMPK to subsequently inhibit mTORC1 (Fernández-Ramos et al., 2017). This recent study demonstrated that 6-MP can alter glycolytic and glutaminolytic fluxes in leukaemia T cells. Interestingly p53 can also modulate metabolic checkpoints and cell metabolism (Jones et al., 2005), and previous studies have exhibited p53-dependent autophagy induction with 6-TG treatment (Zeng et al., 2007). This could suggest that azathioprine-induced autophagy involves both p53 activation and mTORC1 inhibition that intersect at metabolic checkpoints.

The RT² PCR array was as a valuable tool to identify autophagy or autophagy-related genes that were modulated by azathioprine. One of the genes upregulated by azathioprine in THP-1-derived macrophages was *CXCR4*, a chemokine receptor for CXCL12 and MIF. MIF has a role in inflammatory diseases and tumorigenesis (Bernhagen et al., 2007; Chen et al., 2015; Lourenco et al., 2015), and can induce autophagy through TNF- α and IL-1 β induction, ROS generation during inflammation (Chuang et al., 2012) or through inhibition of mTORC1 (Hashimoto et al., 2008). Future investigation of the role of CXCR4-MIF signalling in azathioprine-induced autophagy is required. It would be valuable to determine if inhibition of mTORC1 by azathioprine is, in part, facilitated by CXCR4-MIF pathway. Furthermore, as this cytokine is known to mediate macrophage

migration, it would be intriguing to determine the effects of azathioprine on this process, which is a key requirement for an effective innate immune response.

The PCR array also identified azathioprine-induced upregulation of UPR kinase *PERK*, which was of particular interest due to the association between the UPR, autophagy and IBD (section 1.4.2). Further investigation revealed that azathioprine also increased expression of *ATF4* and *CHOP*, which are downstream of *PERK*; and *PDI*, which is transcriptionally regulated by the IRE1 α –XBP1 pathway (Lee et al., 2003; Osowski and Urano, 2011). Azathioprine also induced a slight increase in PDI protein and phosphorylation of eIF2 α , which is an indicator of PERK activity. It could be speculated that azathioprine activated autophagy and the UPR to restore ER homeostasis. However, a growing body of work suggests that the UPR is regulated by a diverse range of stimuli independent of ER-stress (Rutkowski and Hegde, 2010) and stressors such as nutrient deprivation and hypoxia have been shown to activate UPR signalling (Appenzeller-Herzog and Hall, 2012). In our own study, azathioprine did not appear to increase gene or protein expression of the ER chaperone BiP. The upregulation of UPR signalling, but does not ER stress chaperones, may therefore suggest that azathioprine can directly modulate UPR kinases and not exert its effects via direct induction of ER stress (Lee, 2005). However, azathioprine induction of ER stress cannot yet be dismissed and may have an additive effect on stimulation of the UPR. To conclusively determine the effect of azathioprine on ER stress, robust techniques for analysing ER lumen dilation by electron microscopy (Osowski and Urano, 2011) and ER redox reporter assays (Merksamer et al., 2008) could be used in future studies.

It is well known that the UPR can stimulate autophagy activity (Hart et al., 2012; Li et al., 2008; Ogata et al., 2006; Shimodaira et al., 2014; W. Wang et al., 2016). Furthermore, PERK signalling plays an established role in the enhancement of autophagy (Jia et al., 2015; Kouroku et al., 2007; Moon et al., 2016; Zhao et al., 2013). PERK has also been implicated in the maintenance of mitochondrial homeostasis (Rainbolt et al., 2014). One example of this is PERK-mediated upregulation of *Parkin*, which ubiquitinates damaged mitochondria to enhance mitophagy (Bouman et al., 2011). As our data showed azathioprine-induced upregulation of *PERK* and its downstream effectors, PERK signalling could be a contributing factor in azathioprine-induced autophagy. Furthermore, as defective mitophagy has been implicated in the mitochondrial damage

that is observed in IBD (Novak and Mollen, 2015), it would be intriguing to determine the effects of azathioprine-induced PERK signalling specifically on mitophagy.

UPR activation has been linked to mTORC1 inhibition and can occur both upstream and downstream of mTORC1 (Appenzeller-Herzog and Hall, 2012). Although PERK has been shown to inhibit mTORC1 (Avivar-Valderas et al., 2013; Ji et al., 2015; Laplante and Sabatini, 2012), there is also evidence that inhibiting mTORC1 can induce PERK activation (Freis et al., 2017), with both scenarios resulting in enhanced autophagy activity. In our cell model, PERK inhibitor did not affect mTORC1 inhibition by azathioprine, but dramatically decreased azathioprine-induced autophagy. This demonstrated that azathioprine-induced autophagy is dependent on PERK signalling but this is not mediated via downstream inhibition of mTORC1. Two conclusions could be drawn from these results: either mTORC1 and PERK signalling mediate azathioprine-induced autophagy as independent processes, or mTORC1 inhibition is acting upstream of PERK activation (Figure 8.1). As PERK inhibition caused such a dramatic decrease in azathioprine-induced autophagy, it could be speculated that mTORC1 inhibition is likely acting upstream of PERK activation, if it is assumed that both mTORC1 inhibition and PERK activation are indeed integral for azathioprine-induced autophagy (Figure 8.1). To conclusively determine this, the effects of preventing mTORC1 inhibition would have to be explored.

Interestingly, RAC1, a known target of thiopurines, can activate mTORC1 (Saci et al., 2011). RAC1 inhibition by thiopurines has been associated with the restoration of mobility in autophagy-deficient DCs (Wildenberg et al., 2017). We therefore speculate that inhibition of RAC1 may also contribute to mTORC1 inhibition and stimulation of autophagy (Figure 8.1).

Genetic studies have identified ER-stress and UPR genes associated with IBD, most notably the transcription factor *XBP1* and *AGR2*, which is a member of the PDI family (Kaser et al., 2008; Zheng et al., 2006). Furthermore, the major risk factors for CD, *NOD2* and *ATG16L1* functionally intersect with the UPR. One study demonstrated a direct link between *NOD1/2* and ER stress-induced inflammation (Keestra-Gounder et al., 2016). In addition, in Paneth cells of CD patients harbouring an *ATG16L1 T300A* risk allele, BiP and p-eIF2 α were highly expressed (Deuring et al., 2014). Elevated ER stress is a common outcome when either UPR or autophagy are not functional, especially in cells types such

as Paneth cells that naturally secrete large amounts of protein (Adolph et al., 2013; Todd et al., 2008). This suggests that the *ATG16L1 T300A* variant may define a subtype of CD characterized by abnormal Paneth cell functions due to deficiency in autophagy and UPR (Deuring et al., 2014). These studies highlight the coefficient and compensatory relationship between UPR and autophagy, which is contextualised by the CD-associated SNPs in *ATG16L1* and *XBP1*. Azathioprine signalling via an mTORC1-PERK pathway could have synergistic outcomes, as a well-established function of both mTORC1 inhibition and PERK-eIF2 α stimulation is to inhibit global protein translation, meaning ER stress is relieved by both autophagic degradation of proteins and inhibition of protein synthesis. Ultimately, this could have a significant impact in cell types, such as Paneth cells, where ER stress can become particularly elevated. The proposed mechanism of action we have highlighted (Figure 8.1) not only aids the understanding of how azathioprine can act, but also identifies another potential therapeutic effect of the drug.

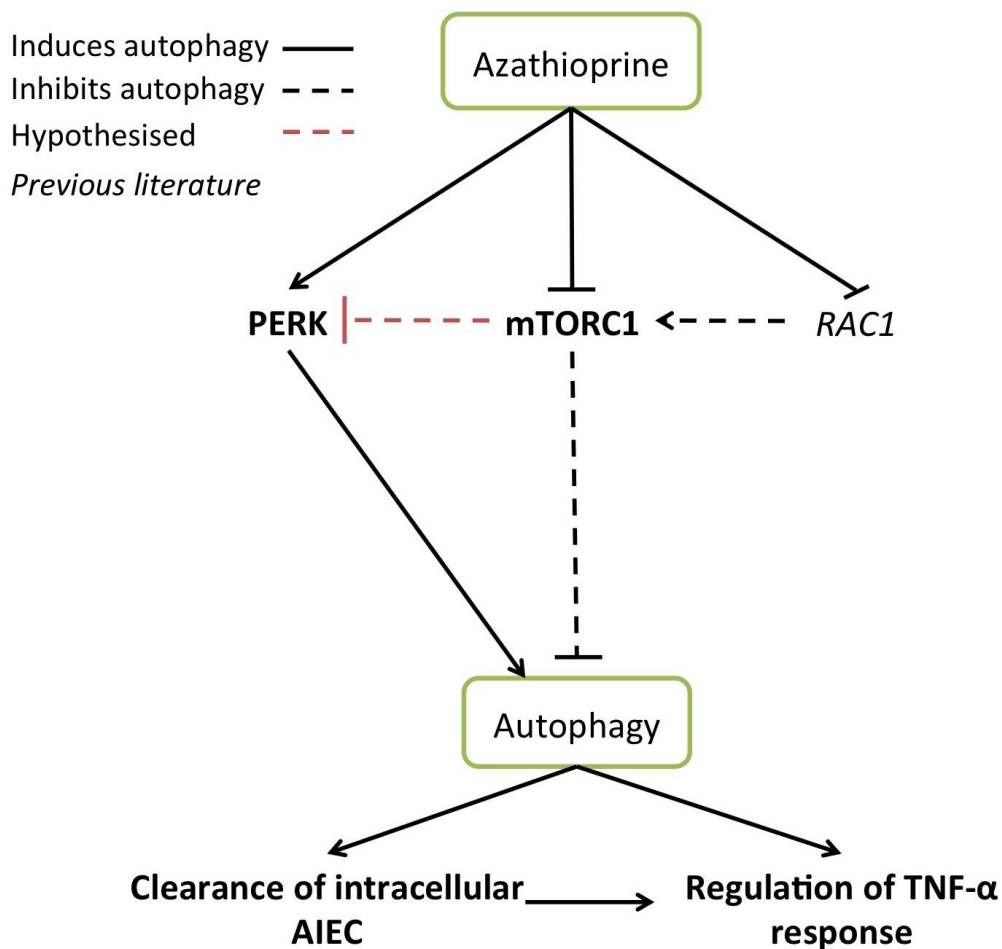


Figure 8.1: Proposed mechanism of action of azathioprine in the context of autophagy

In this study it was shown that azathioprine induces autophagy via mTORC1 inhibition and PERK activation. As PERK inhibition blocks azathioprine-induced autophagy but not inhibition of mTORC1, it can be speculated that mTORC1 is acting upstream of PERK. Azathioprine is also known as an inhibitor of RAC1 (Tiede et al., 2003), which is known to activate mTORC1 (Saci et al., 2011). Enhanced autophagy resulted in increased clearance of intracellular AIEC and dampened pro-inflammatory cytokine release.

8.6 The effect of azathioprine-induced autophagy on clearance of AIEC

A major factor in CD pathogenesis is microbial dysbiosis, as well as infection with specific pathogens, such as AIEC. Autophagy-mediated clearance of pathogens (xenophagy) is vital for efficient degradation of intracellular bacteria, and is also necessary for controlling pro-inflammatory responses to infection. Importantly, deficient autophagy has been implicated in the prolonged survival of intracellular pathogens and excessive pro-inflammatory signalling in CD (Cooney et al., 2010; Homer et al., 2010; Lapaquette et al., 2010, 2012; Negroni et al., 2016; Sadabad et al., 2015; Wolfkamp et al., 2014). Therefore, investigating the role of azathioprine-induced autophagy in bacterial handling and pro-inflammatory responses establishes a stronger link to its therapeutic benefit in CD.

We demonstrated that azathioprine enhanced clearance of AIEC in THP-1-derived macrophages and attenuated pro-inflammatory responses to infection and LPS treatment, and we speculate that this is mediated by autophagy induction (Figure 8.1). This hypothesis is reflected in our findings that azathioprine increased autophagy levels in conjunction with these effects. To corroborate this, a previous study found that 6-MP attenuated LPS-induced TNF α production in microglial cells via inhibition of PI3K-Akt/mTORC1 pathway (Huang et al., 2016). As we also identified mTORC1 inhibition by azathioprine in THP-1-derived macrophages, this advocates a link between autophagy induction via mTORC1 inhibition and TNF α downregulation.

The link between impaired autophagy and excessive pro-inflammatory signalling has been extensively investigated. Loss of functional ATG16L1 protein can result in increased pro-inflammatory IL-1 β and IL-18 production in response to NOD2 ligand in murine studies (Lassen et al., 2014; Saitoh et al., 2008) and in human PBMCs (Glubb et al., 2011; Plantinga et al., 2011; Salem et al., 2015). It has been suggested that when bound to

NOD2, ATG16L1 shifts NOD2 activity towards autophagy, but loss of functional ATG16L1 skews NOD2 activity towards pro-inflammatory signalling (Plantinga et al., 2011). In our findings, attenuation of LPS-induced expression of TNF α in the presence of azathioprine demonstrates that azathioprine impairment of pro-inflammatory cytokines is likely not simply due to decreases in bacterial load. We would suggest that further characterisation of azathioprine-mediated effects on pro-inflammatory signalling at the protein and genomic level should therefore be undertaken to fully characterise this finding in a therapeutic context.

To more conclusively determine the functional link between these effects, we elected to characterise inhibition of the autophagy pathway through pharmacological intervention and siRNA of essential ATG proteins. Knockdown of the essential autophagy protein ATG5 with siRNA was attempted, in parallel with the use of the PI3K inhibitor, 3-MA. Although siRNA knockdown was successful at a transcriptional level, we established that autophagy activity was still maintained in our model. Treatment regimens utilising 3-MA were also not successful, likely due to the temporal effects of 3-MA that result in both autophagy enhancing and inhibiting activity of this drug (Y.-T. Wu et al., 2010). Therefore, we established that neither technique could be used to confidently block autophagy activity in this context. However, in order to clarify the link between azathioprine-induced autophagy and bacterial clearance, alternative siRNA sequences or siRNA knockdown of other ATG proteins could be considered in a future study.

It has previously been shown that infliximab does not decrease infection of monocyte-derived macrophages from CD patients (Vazeille et al., 2015), despite evidence that blocking TNF α inhibits AIEC replication (Bringer et al., 2012). Therefore, azathioprine may be better suited at controlling bacterial replication in macrophages through autophagy induction, which in turn controls TNF α release, as opposed to simply neutralizing TNF α with infliximab. Furthermore, in a recent study the rapid local bacterial conversion of the 6-thioguanine pro-drug to an active metabolite was shown to augment autophagy in epithelial cells, resulting in increased intracellular bacterial killing, and decreased intestinal inflammation and immune activation in animal colitis models (Oancea, 2016). Therefore, the effects of azathioprine *in vivo* may be more pronounced, depending on the local microbial community.

Azathioprine-induced autophagy plays a potential role in clearance of intracellular AIEC and regulation of pro-inflammatory responses. The combined effects of azathioprine therefore represent a promising therapeutic option for treating subsets of patients with confirmed AIEC infection and deficiency in autophagy. Further studies are required to determine the effects of azathioprine-induced autophagy on clearance of other CD-associated pathogens within more complex microbial communities.

8.7 The IDEA study

8.7.1 Autophagy levels in GI biopsies from paediatric patients

PBMC populations and GI biopsies from non-IBD patients or patients with the diagnosis of IBD were analysed to determine basal autophagy levels and response to azathioprine treatment *ex vivo*. In GI biopsies from CD and IBDU patients there was a subtle decrease in levels of LC3 expression compared to non-IBD controls. This is an interesting observation due to the genetic association between autophagy genes particularly in CD pathogenesis.

These results are in contrast with other published studies showing that LC3-II levels were increased in protein lysates from colonic mucosal biopsies and unchanged in ileal biopsies from paediatric CD and UC patients compared to controls (Negroni et al., 2016). In another cohort, LC3 levels were specifically increased in Paneth cells in the duodenum and ileum in paediatric CD patients when compared to control, UC and celiac patients (Thachil et al., 2012). Finally, in adult patients with ileocecal CD, it has been reported that LC3-II levels were increased in protein lysates from terminal ileum biopsies compared to controls, whereas in adjacent mesenteric fat tissue autophagy levels were decreased compared to controls (Leal et al., 2012). There is clear disparity between the findings of these studies, possibly due to sample location, diversity between cohorts and varying techniques used such as LC3 western blot and LC3 IHC.

Analysing autophagy by IHC can be problematic as LC3 foci are difficult to distinguish. Some papers have described methods to detect LC3 foci in tissue (Rosenfeldt et al., 2012), but in our paediatric patient biopsies distinct autophagosomes could not be observed. However, previously published studies have quantified endogenous levels of

LC3 in tissue to monitor autophagy activity (Hiniker et al., 2013; Thachil et al., 2012). This method was used to indicate autophagy levels in our paediatric biopsies, but to support this technique, p62 IHC can also be used in future examinations. Additionally, in GI biopsies from CD patients, characteristics of pathogenic changes in the tissue are not consistent throughout the GI tract. Therefore, autophagy levels may differ dependent on whether biopsies are collected from highly localised inflamed or non-inflamed regions, and to determine this, pathological analysis of tissue would be required. These limitations may therefore explain why our results do not align with previous studies. However, they do complement several murine studies showing that deficient autophagy is a prominent factor in colitis development (Cadwell et al., 2010, 2008; Murthy et al., 2014; Saitoh et al., 2008; Tsuboi et al., 2015).

8.7.2 Effects of azathioprine on PBMC populations and autophagy in paediatric patient PBMCs

In PBMC populations isolated from paediatric patients, it was possible to compare the impact of patient diagnosis and genotype on basal levels of autophagy, but importantly we were also able to investigate the effect of *ex vivo* treatment with azathioprine on autophagy responses. Furthermore, flow cytometry with PBMCs allowed analysis of percentages of PBMC populations in the distinct patient disease groups and the effect of drug treatment on these populations. In CD patients, B cell populations were expanded and *ex vivo* azathioprine treatment decreased this enlarged population. It has been previously shown in patients with lupus nephritis and chronic glomerulonephritis that azathioprine treatment depletes T-cell and B-cell lymphocyte populations (Tareyeva et al., 1980). Slight alterations in B-cell sub-populations can impact lymphocyte homeostasis; therefore, it would need to be determined whether azathioprine decreases IBD-associated populations of B cells, subsequently dampening production of auto-reactive antibodies (Mizoguchi and Bhan, 2012), or whether regulatory B cell populations are also decreased (Oka et al., 2014; Zheng et al., 2017). As we determined that azathioprine treatment increased autophagy activity in B-cells from CD patients (Figure 8.2), it would be interesting to determine if the decrease in CD-associated B cell expansion due to enhanced autophagy or the suppression of DNA replication.

HLA-DR is a MHC class II cell surface receptor that is constitutively expressed on B lymphocytes, monocytes and macrophages, but signifies late stages of T cell and NK cell activation (Bajnok et al., 2017). HLA-class II gene SNPs have been associated with susceptibility to IBD (Stokkers et al., 1999). Furthermore, several studies have shown increased expression of the activation marker, HLA-DR, in intestinal epithelial cells (Horie et al., 1990, Selby et al., 1983, Hirata et al., 1986), lamina propria lymphocytes (Hirata et al., 1986) and intestinal macrophages (Selby et al., 1983) from CD patients. In the blood, T cells from CD patients are also enriched for HLA-DR (Ebert et al., 2005; Funderburg et al., 2013). HLA-DR⁺ NK cells have increased proliferation activity, enhanced cytokine-induced IFN- γ production and increased propensity to degranulate (Erokhina et al., 2018). Increases in this population of NK cells have also been associated with UC (Ng et al., 2009). In our results, HLA-DR expression profiles mirror these previous studies as PBMCs and T cells from CD patients have higher levels of HLA-DR, and NK cells from UC patients have increased HLA-DR expression.

Interestingly, azathioprine treatment decreased HLA-DR expression on B cells from non-IBD patients. Cross-linking of HLA-DR molecules on the surface of B cells has been shown to enhance presentation of antigens to T cells and increase production of IgM antibodies (Tabata et al., 2000). Reduced expression of HLA-DR could decrease T cell activation via B cell antigen presentation. However, diminution of HLA-DR could also decrease IgM⁺ B cells, which has been associated with IBD (Sabatino et al., 2005). Therefore, the implications of decreasing HLA-DR expression on B cells would need to be investigated further in the context of CD.

Although azathioprine-induced reduction in HLA-DR expression was not observed in any cell types derived from CD patients, increases in autophagy levels were apparent in these activated cells from CD patients. Azathioprine-induced autophagy in HLA-DR⁺ populations may play a role in dampening the hyper-inflammatory responses in these activated populations.

In PBMCs, our results indicate that there was no difference between patient groups in autophagy levels of untreated cells. This was in contrast to the GI biopsy results, which showed decreased LC3 expression in CD, highlighting the differences in autophagy activity between the GI tract and systemic immune cells. In this context, our findings

shed light on the role of autophagy in IBD pathogenesis by emphasizing its distinct activity in varying cell types and physiological systems.

Although deficient autophagy in cells from IBD patients may not be apparent in unstimulated PBMCs, treatment with MDP, LPS or infection with CD-associated bacteria can highlight the inability of these cells to mount an appropriate xenophagy response to resolve inflammation (Cooney et al., 2010; Homer et al., 2010). Therefore, it is of particular significance that azathioprine was able to induce increases in autophagosome-bound LC3 in PBMCs as this could resolve defects in autophagy responses of CD-derived PBMC populations (Figure 8.2).

In terms of autophagy detection, the technique used for flow cytometric analysis of autophagy in PBMCs was able to identify increases in autophagosomes but could not distinguish between increased autophagosome formation or decreased degradation resulting in autophagosome accumulation. Therefore, the effect of azathioprine on autophagy flux in PBMCs was not investigated. However, as autophagy flux was observed in HEK293 cells treated with azathioprine, we would propose that the mechanism of action is similar in PBMCs and therefore increases in autophagosome number are assumed as an indication of enhanced autophagy activity.

Azathioprine-induced autophagy was observed *ex vivo* in both innate and adaptive systemic immune cells, and in activated, HLA-DR+, PBMC populations (Figure 8.2). Deficient autophagy in monocytes, monocyte-derived cells and T cells has been linked to IBD pathogenesis, and autophagy is key to homeostasis and development of B and NK cells, which have both been linked to IBD when regulation of these populations is aberrant (described in section 1.1.5). In a recent study, *ex vivo* treatment of CD patient-derived DCs with thiopurines corrected a dysfunctional migration phenotype that was associated with deficient autophagy activity (Wildenberg et al., 2017). Autophagy is key for monocyte to macrophage differentiation, which prevents monocyte apoptosis (Zhang et al., 2012) and differentiation of monocytes to a regulatory phenotype is dependent on autophagy (Levin et al., 2016). Therefore, enhancing autophagy activity in systemic immune cells could have therapeutic benefit in IBD. To clarify this, it would be of interest to determine if enhancing autophagy with azathioprine in circulating monocytes could reduce IBD-related defects in intestinal macrophages and DCs post-differentiation.

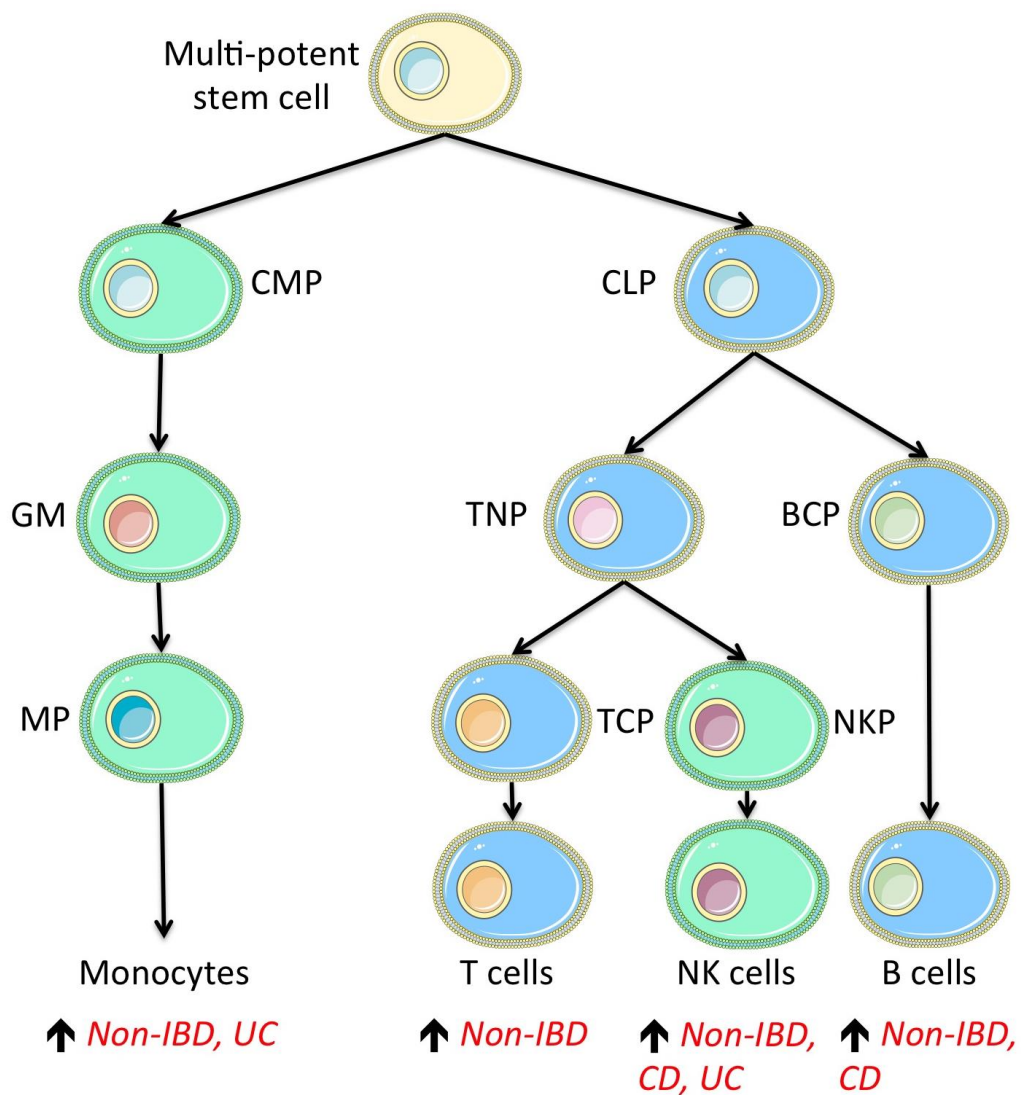
CD has been associated with imbalances in regulatory and effector T cell sub-populations, in part attributed to insufficient autophagy (Kabat et al., 2016; Shale et al., 2013). As azathioprine increased autophagy in T cells in our study (Figure 8.2), it would be interesting to determine these effects in T cell sub-populations and whether azathioprine-induced autophagy could enhance Treg expansion. However, it is worth noting that azathioprine treatment has previously been linked to lymphopenia due to enhanced T cell apoptosis (Tiede et al., 2003). As well as decreased numbers of CD4+ T cells, azathioprine can cause diminished Treg suppressive activity in systemic lupus erythematosus patients (Gómez-Martín et al., 2011). Furthermore, azathioprine treatment in CD patients was shown to reduce Treg populations (Saruta et al., 2007). This was replicated in a subsequent study with high doses of azathioprine, however, it was noted that lower concentrations of azathioprine actually expanded Treg populations (Daniel et al., 2016). This reiterates previous suggestions that high concentrations of azathioprine primarily cause cytotoxic effects, whereas lower concentrations function via distinct pathways that enhance autophagy (Wildenberg et al., 2017) and the enhanced autophagy could expand Treg populations. Furthermore, in our study, azathioprine treatment did not significantly decrease the T cell population, suggesting T cell apoptosis was not induced, but this would need to be confirmed with viability assays.

Autophagy in monocyte-derived DCs has an indirect effect on T cell activation, as it can destabilize immunological synapses between DCs and T cells (Wildenberg et al., 2012). Interestingly, azathioprine has also been shown to destabilize APC-T cell synapses via RAC1 inhibition (Poppe et al., 2006). As a previous study has linked azathioprine inhibition of RAC1 to autophagy induction (Wildenberg et al., 2017), it could be speculated that azathioprine-induced autophagy in DCs could destabilize immunological synapses via RAC1 inhibition, subsequently decreasing T cell activation.

In CD and UC there is an increase in CD16+ NK cells with an immature and pro-inflammatory phenotype (Steel et al., 2010). It has previously been shown that azathioprine treatment decreases NK cell activation and IFN-gamma responses, preferentially in this CD16+ subpopulation (Steel *et al.*, 2010). Although we did not observe decreases in NK cells with azathioprine treatment, there was a consistent increase in autophagy in NK cells. As autophagy in NK cells has been associated with

their proper development and maturation (S. Wang et al., 2016), it can be suggested that azathioprine-induced autophagy could help prevent expansion of immature and highly inflammatory NK cells that are associated with IBD.

Interestingly, the *ATG16L1 T300A* genotype was associated with significant increases in autophagy with azathioprine treatment, whereas increases in autophagy in cells from patients with the WT *ATG16L1* genotype were not significant. Therefore, *ATG16L1 T300A* genotype appears to be associated with a more pronounced autophagy response to azathioprine. The *T300A* SNP may be an indicator of the response of immune cells to azathioprine treatment.



↑: Aza significantly increased LC3

Figure 8.2 Summary of effect of azathioprine on autophagy activity in PBMC populations

Diagram of systemic immune cells indicating significant azathioprine-induced increases in autophagosome-bound LC3 in PBMC populations from different paediatric patient groups, as assessed by LC3 flow cytometry.

8.8 Clinical Implications of azathioprine-induced autophagy

A recent study identified an association between *ATG16L1 T300A* SNP and an enhanced therapeutic effect of thiopurines (Wildenberg et al., 2017). Furthermore, this genotype has been associated with a subset of patients that exhibit deficiencies in both UPR and

autophagy (Deuring et al., 2014). It is plausible that the enhanced therapeutic effect in patients with *ATG16L1 T300A* SNP is, in part, caused by heightened autophagy and UPR responses to this IBD drug.

Genetic polymorphisms of enzymes involved in azathioprine metabolism have been implicated in efficacy and toxicity of this drug. A variant in *TPMT* causes accumulation of toxic metabolites, whereas deletion in *GST-M1* for the GST enzyme and an *ITPA C94A* polymorphism for the ITPA enzyme causes increased levels of inactive metabolites (Stocco et al., 2014). One study identified a 32-gene transcriptomic signature that predicts lack of response to thiopurines, which implicated aberrant cell cycle, DNA mismatched repair and RAC1-dependent mechanisms in thiopurine resistance (Chouchana et al., 2015).

In the context of targeted therapeutic approaches, the FDA recommends *TPMT* genotyping prior to azathioprine administration, to identify patients that would be at risk of severe adverse effects and would benefit from alternative medication or reduced doses (Dean, 2012). By additionally genotyping patients for *ATG16L1 T300A*, this could help predict patients that are more likely to clinically respond to the drug. As roughly only 30% of CD patients achieve steroid-free remission after 6 months of azathioprine treatment (Colombel et al., 2010), predicting response to this drug prior to administration would have great clinical benefit. Through this genetic stratification, long relapse periods with interchanging therapeutic approaches could be avoided, thus accelerating the progression towards remission.

Monitoring efficacy and adverse effects of thiopurines at various administered doses could discriminate between cytotoxic effects and autophagy modulating capacity of the drug. Erythrocyte concentrations of thiopurine metabolites are routinely monitored to maintain therapeutic levels and avoid toxicity (Gardiner et al., 2008). Therefore, future clinical studies could fine tune appropriate doses of azathioprine by correlating erythrocyte concentrations of thiopurine metabolites with autophagy and cytotoxic effects. This could differ depending on genotype and therefore, a dose of azathioprine that enhances autophagy without eliciting cytotoxic effects may vary depending upon CD-associated genotype. It is possible that specific concentration ranges could be set based on predicted response to azathioprine treatment.

Another important consideration is that our findings were generated from paediatric patient samples. It is valuable to specifically investigate paediatric IBD, as there are distinct characteristics compared to adult IBD. Certain IBD drugs are more effective in paediatric cases (Akobeng and Zachos, 2004; Ruemmele et al., 2009), whereas some cause more adverse effects (Kirschner, 1998; Stocco et al., 2015). This could be due to discrepancies in aetiology between paediatric and adult IBD, which may suggest that the effect of azathioprine on autophagy could differ based on age of diagnosis. Genetic susceptibility is more prominent in paediatric IBD and *ATG16L1 T300A* confers greater risk for CD in paediatric patients as opposed to adult patients (Amre et al., 2009; Zhang et al., 2009). This could imply that the enhanced azathioprine-induced autophagy response in *T300A* patients could be more prominent in paediatric patients compared to adult patients. As the incidence of paediatric IBD is rising (Benchimol et al., 2014; Henderson et al., 2012), optimising therapies for these patients is pertinent. However, it would be valuable to determine if our results are reflected in an adult cohort.

Finally, the effect of azathioprine on autophagy could be harnessed in combination treatments for IBD. As certain IBD drugs have been shown to harbour autophagy-inhibiting properties, combination with a drug known to enhance autophagy, such as azathioprine may be beneficial. Treatment of refractory CD with mTORC1 inhibitor, sirolimus, has previously been demonstrated (Massey et al., 2008; Mutalib et al., 2014), however, as azathioprine is an established IBD drug it may be a preferential option to enhance autophagy activity. The autophagy-enhancing properties of azathioprine, combined with its effects on the UPR, could be enhanced through combination treatments and dosage control for its optimal therapeutic use in a more personalised approach.

8.9 On-going and Future research

Due to inherent limitations with *in vitro* research, alternative *ex vivo* systems, such as intestinal organoid models, can be used as a more physiological representation of the GI tract. Pluripotent stem cells from the crypts of the GI tract can be isolated from murine models of colitis or surgical resections from IBD patients. Supplying these stem cells with specific growth factors can influence differentiation into a 3-dimensional

tissue structure with multiple cell types. The effect of azathioprine, and other IBD drugs, on autophagy and associated pathways, could be investigated in intestinal organoids. This could determine the effects of these drugs in various cell types of the GI tract and would factor in altered pharmacokinetics and pharmacodynamics within tissue compared to cell lines. However, despite the limitations, *in vitro* findings remain valuable for delineating the signalling pathways and specific effects in a given cell type. In the cell line model, many variable factors are absent, allowing further characterisation of azathioprine mechanism of action in a controlled environment. These findings can act as the foundation for translation of the research into a more complex system.

A major challenge with *in vitro* research is translating pharmacological concentrations of drugs. A previous study determined that at therapeutic doses of 2-3mg/kg, concentrations in the tissue are unlikely to exceed 10 μ M (Lennard et al., 1997). In another study, mice were administered a 6-MP pro-drug, known as *cis*-AVTP, at 42.5 μ mol/kg (roughly 12mg/kg) and it was determined that thiopurine metabolites did not exceed 16 μ M in plasma, RBCs, intestine or liver (Gunnarsdottir and Elfarra, 2003). In our study a supra-pharmacological concentration range of azathioprine (60-120 μ M) was selected with reference to concentrations used in similar studies of autophagy and apoptosis responses to azathioprine treatment in cell lines (Chaabane et al., 2016; Pelin et al., 2015; Petit et al., 2008). Despite supra-pharmacological concentrations being used, there was absence of cytotoxicity in our cell lines, which suggests that thiopurine metabolites did not accumulate to concentrations that were toxic in our cell lines at the time-points used. It would therefore be useful to determine the levels of thiopurine metabolites in our cell lines treated with 120 μ M azathioprine as this may reflect the concentrations of metabolites in patient and murine tissue. As thiopurine metabolites can accumulate to toxic concentrations in patients the absence of toxicity in our cell lines suggests the concentrations used were not excessive and findings remain clinically relevant. Furthermore, a more recent study determined that patient weight and body composition do not correlate with blood levels of 6-TGN or 6-MMP metabolites (Holt et al., 2016), which have been shown to reflect the eventual tissue concentrations of thiopurine metabolites (Goel et al., 2015). This study suggested that enzyme levels of TPMT are more relevant predictors of appropriate therapeutic dose range (Holt et al., 2016), which could mean that tissue concentrations of thiopurine metabolites could

exceed predicted levels in patients with certain enzyme genotypes. This advocates for exploring higher concentrations of thiopurine drugs *in vitro*.

To expand the *in vitro* findings of this study, a pilot murine study has been undertaken. A DSS-induced colitis model was used to assess the effect of therapeutically appropriate concentrations of azathioprine on autophagy in the GI tract and in splenic mononuclear cells. This provides an opportunity to confidently translate our findings to an *in vivo* system.

Although a previous study has identified that both 6-MP and azathioprine induce autophagy (Chaabane et al., 2016); 6-MP did not modulate autophagy in our experimental model. This needs to be confirmed with further investigation using varying techniques to assess autophagy, and in different experimental models. If this is confirmed, it would then have to be determined if these drugs have distinct mechanisms of action and whether this is due to discrepancies in ROS levels or the release of the imidazole ring from azathioprine. Thiopurine administration is considered interchangeable, as 6-MP is often well tolerated with relatively high efficacy in azathioprine-intolerant patients (Domènech et al., 2005; Hindorf et al., 2006; Lees et al., 2008). However, if there are discrepancies in their mechanism of action, these drugs may vary in efficacy in distinct patients groups, based on phenotype or genotype. If this were the case, then more caution may be required when selecting a thiopurine drug or interchanging the drugs.

In our study, *ex vivo* treatment of patient samples allowed the use of a much more clinically appropriate cell model. However, due to the small cohort, sample size in each patient group was relatively small, which is emphasized when genotype analysis is considered. A larger cohort would allow analysis of autophagy levels in samples from patients that were administered drugs *in vivo*, which would be more relevant than *ex vivo* treatment of samples. Nevertheless, the IDEA study provided valuable data, which can aid the understanding of azathioprine mechanism of action and how its use can potentially be targeted to patients that would experience greater clinical benefit.

8.10 Final Conclusions

Azathioprine has been identified as a robust inducer of autophagy in cell lines and PBMCs from paediatric non-IBD and IBD patients. This activity was independent of apoptosis. However, azathioprine-induced autophagy was associated with upregulation of the UPR and inhibition of mTORC1. Through pharmacological inhibition of the UPR kinase, it was determined that PERK activation was vital for autophagy stimulation. Furthermore, by inhibiting PERK, a pathway was delineated, suggesting azathioprine inhibition of mTORC1 could be upstream of PERK activation. Azathioprine also enhanced clearance of CD-associated AIEC and dampened pro-inflammatory responses, in conjunction with autophagy stimulation, which demonstrates the functional effects of azathioprine-induced autophagy.

In patient PBMCs, azathioprine increased autophagy levels in both innate and adaptive immune cells. Enhancing autophagy in these cell types could be therapeutically beneficial for CD by promoting effective innate immune responses in the GI tract and controlling subsequent adaptive immune responses. Furthermore, azathioprine-induced autophagy was more pronounced in cells from patients with the *ATG16L1 T300A* SNP. Therefore, this genotype could predict patients that are more likely to therapeutically benefit from azathioprine treatment, thus, contributing to the progression towards a more personalised approach to IBD treatment.

9. Supplementary Results:

Optimisation of techniques to monitor autophagy

9.1 Introduction

The most established marker protein for monitoring autophagy is the mammalian homologue of Atg8, LC3. When autophagy is activated the LC3 precursor is converted into LC3-I and is then conjugated to phosphatidylethanolamine (PE) to form lipidated LC3-II (Klionsky et al., 2016). This allows LC3-II to bind to the isolation membrane to promote autophagosome formation.

Increased levels of LC3-II can be detected by western immunoblot and correlate with autophagy induction. LC3-II has a greater molecular weight than LC3-I, however due to its hydrophobicity, it migrates faster on a SDS-PAGE. When bound to autophagosome membranes, LC3-II forms distinct foci within the cell cytosol, which can be detected by anti-LC3 immunofluorescence staining or by utilising a reporter consisting of Green Fluorescent Protein (GFP) fused to LC3. LC3-II or GFP-LC3-II foci can be quantified and indicate autophagy levels within the cell.

The Human Embryonic Kidney (HEK293) cell line has been used extensively for investigating autophagy (Musiwaro et al., 2013), therefore it was selected as a model for the initial stage of the project. In this chapter the autophagy techniques described above were optimized in the HEK293 cell line using well-characterised modulators of autophagy induction and inhibition including bafilomycin, rapamycin and nutrient deprivation. Bafilomycin is a vacuolar proton pump inhibitor that blocks the fusion of autophagosomes with lysosomes by increasing the lysosomal pH and altering its membrane potential (Yamamoto et al., 1998). This causes accumulation of autophagosome-associated LC3. Rapamycin and nutrient deprivation cause an increase in autophagosome-associated LC3 due to the induction of autophagy and increased autophagosome formation. Rapamycin induces autophagy by inhibiting the regulatory mTORC1 pathway and nutrient deprivation induces autophagy through PI3K-dependent signalling pathways.

Resident macrophages play an important role in maintaining homeostasis in the (GI) tract, as they are responsible for effective clearance of pathogens and mounting appropriate innate immune responses. The THP-1 monocyte-like cell line can be differentiated with PMA into a macrophage like-cell, and was therefore a useful model, for GI macrophages. In this chapter the development of techniques to monitor endogenous LC3 in THP-1-derived macrophages are also described.

9.2 Results

9.2.1 Optimisation of the autophagy response: Confocal imaging of HEK293 GFP-LC3 cells

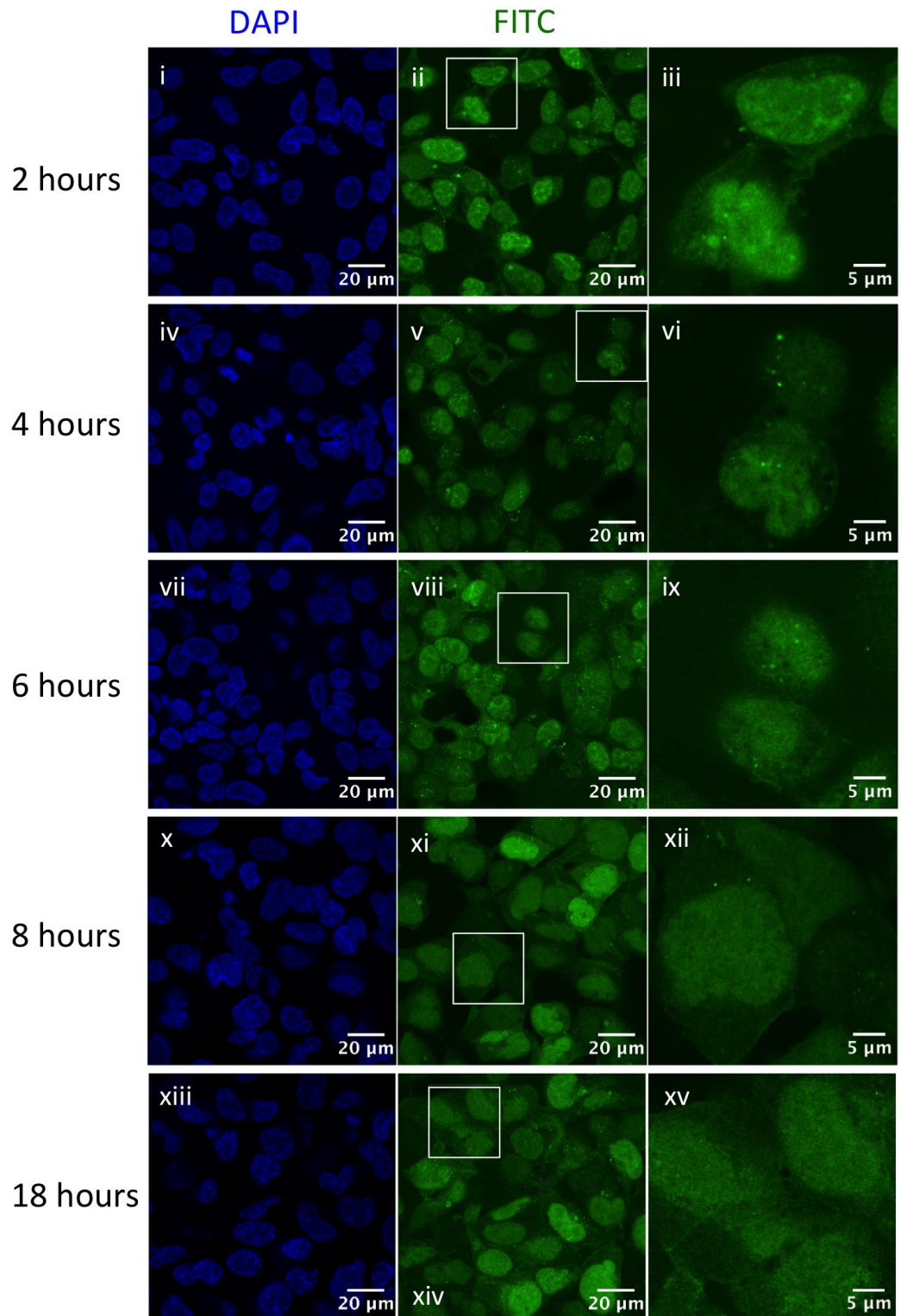
HEK293 cells stably expressing GFP-LC3 were treated with bafilomycin (Baf), rapamycin or complete medium without FBS (serum starvation) for 2, 4, 6, 8 and 18 hours before confocal microscopy imaging. Autophagy activation was determined as the percentage of cells exhibiting >5 GFP-LC3 foci for all time-points (i) and for the 6-hour time-point (ii) (Supplementary Figure 9.1E). It can be seen in Supplementary Figure 9.1E that a very low percentage of untreated cells, between 6 and 17%, were positive for autophagy throughout the time-course. Bafilomycin treatment at 2 hours, had a very modest effect on LC3 accumulation as only 22% of cells have >5 foci (Supplementary Figure 9.1E). However, after 4 hours of bafilomycin treatment GFP-LC3 accumulation increased considerably, varying between 97-99% of cells containing >5 foci for the remainder of the time-course (Supplementary Figure 9.1E).

Treatments of rapamycin and serum starvation showed increases in autophagy levels as early as 2 hours, with 59% and 62% autophagy positive cells, respectively (Supplementary Figure 9.1E). Serum starvation had a relatively modest effect on autophagy induction, throughout the time-course but reaches a maximum level after 6-hour treatments, with 69% of cells positive for autophagy induction (Supplementary Figure 9.1E). Rapamycin had a similar effect to bafilomycin treatment and after 4 hours of treatment induced high levels of autophagy, fluctuating between 80% and 100% (Supplementary Figure 9.1E).

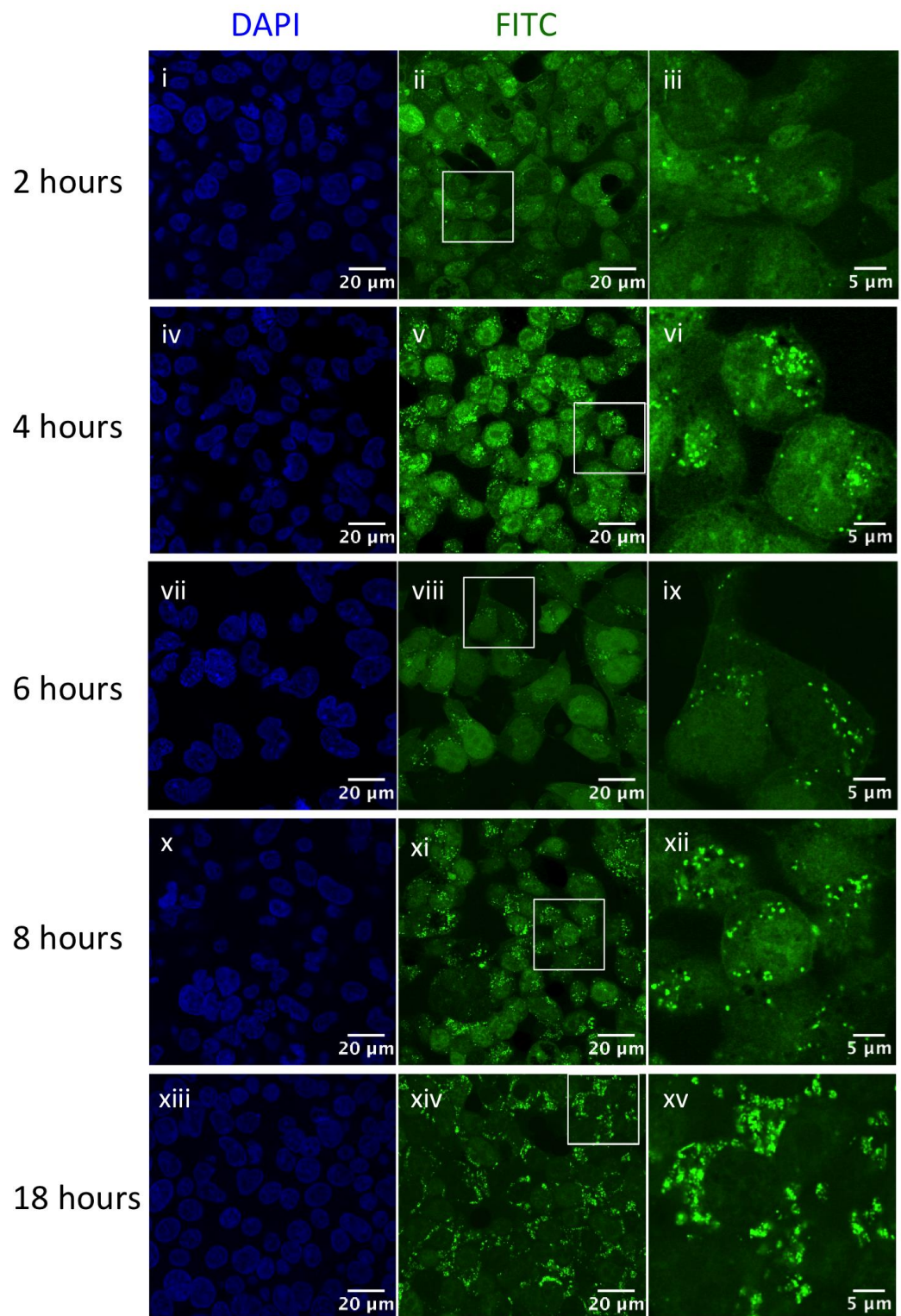
From the results in Supplementary Figure 9.1, 6-hour incubations were considered the most appropriate for all autophagy controls. From n=3 quantification for the 6-hour

time-point (ii), 6% of untreated cells were positive for autophagy, which significantly increased to 63%, 66% and 97% for serum starvation, rapamycin and bafilomycin treatment, respectively (Supplementary Figure 9.1E).

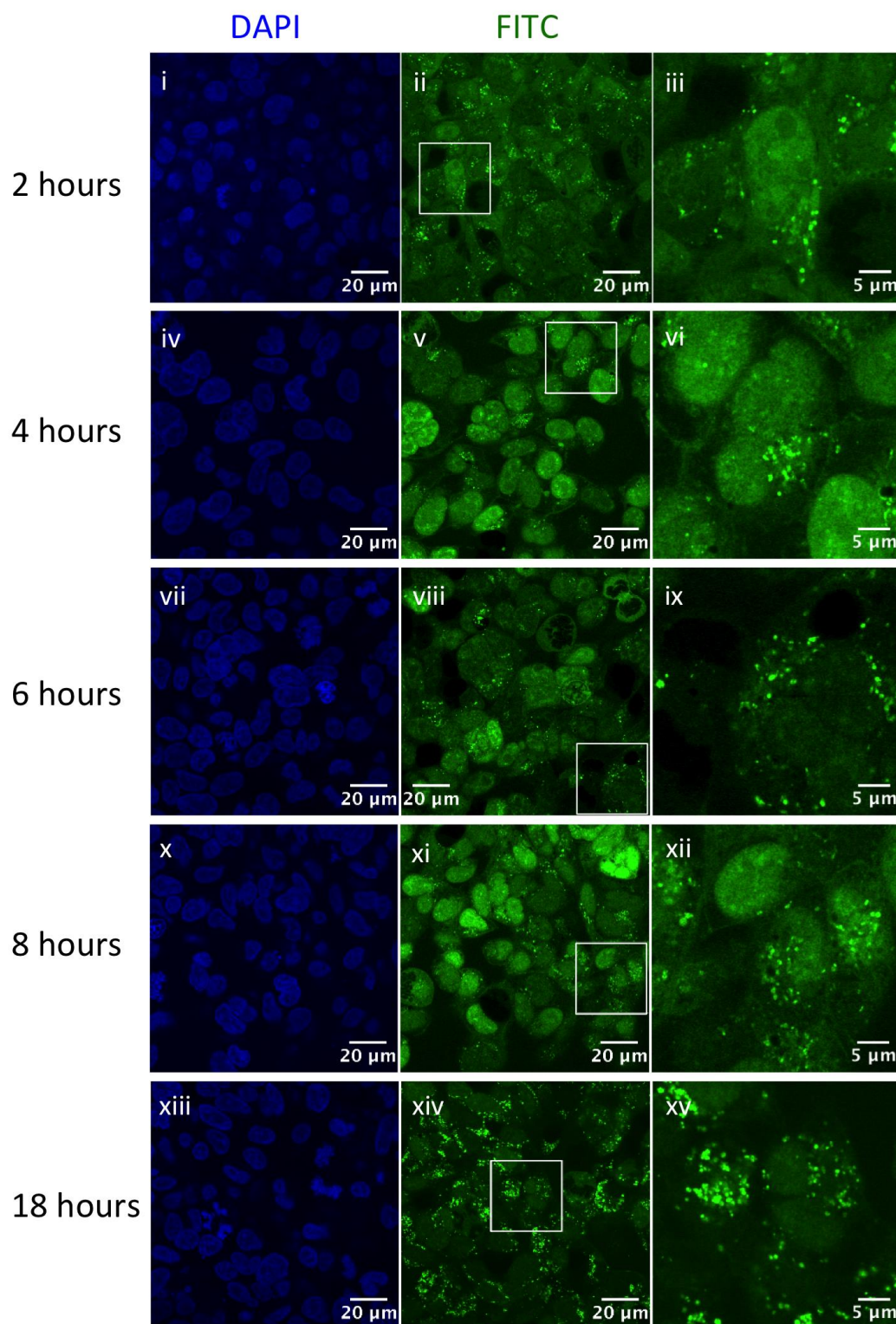
A: Untreated



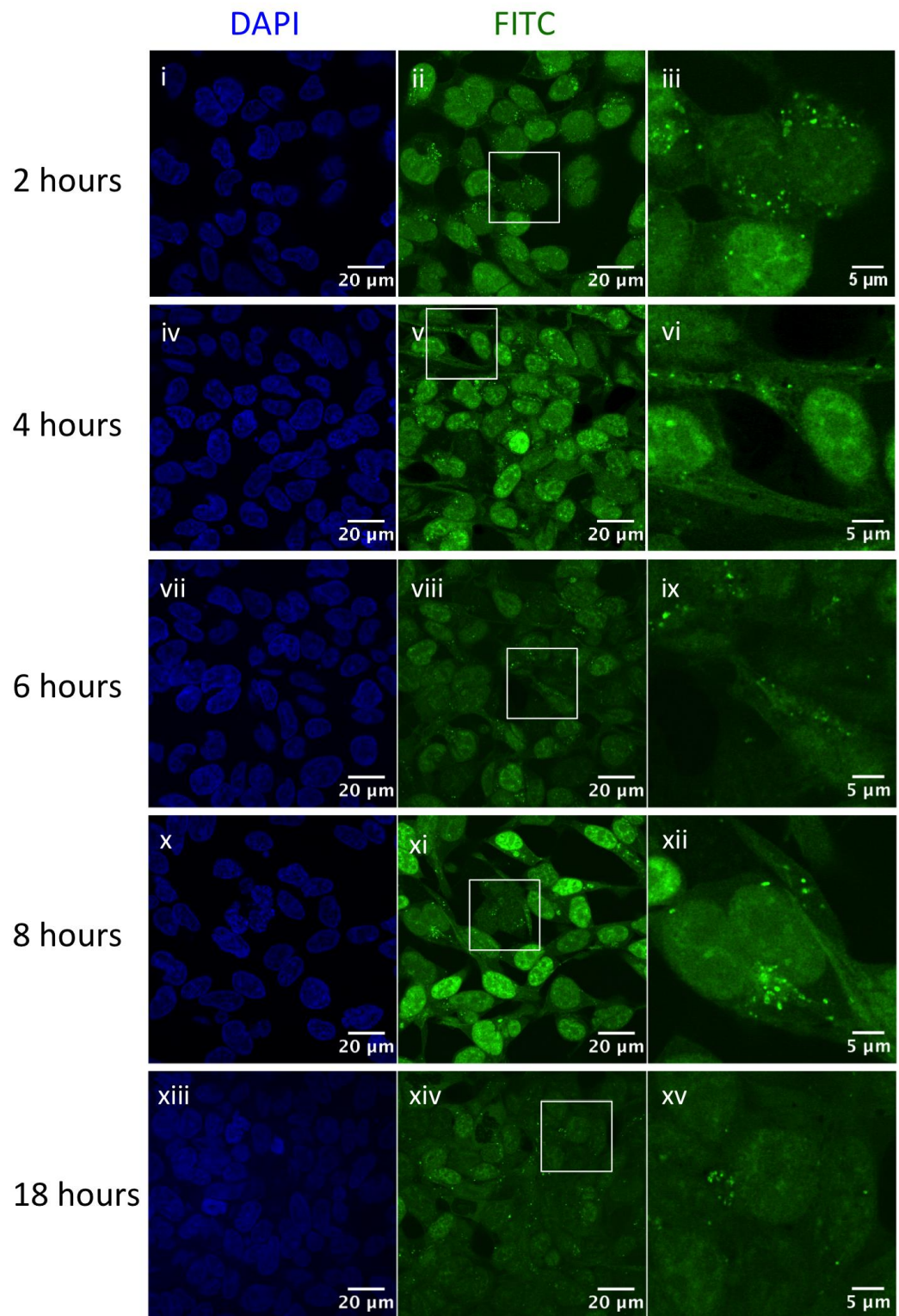
B: Bafilomycin



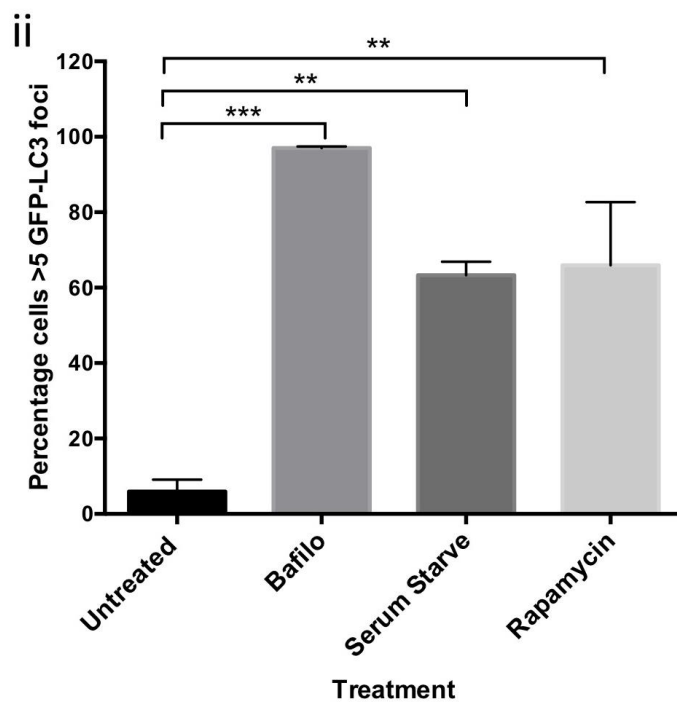
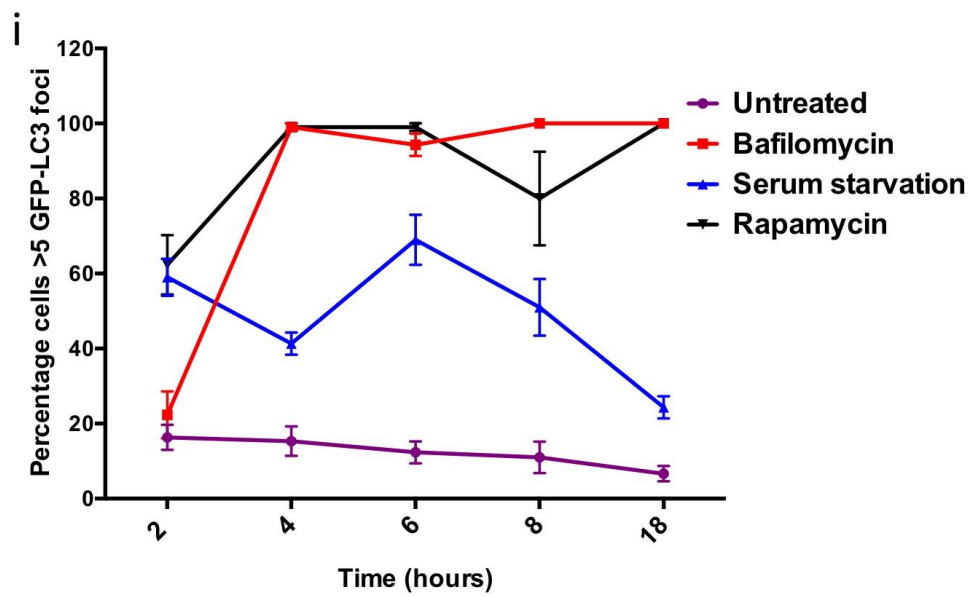
C: Rapamycin



D: Serum starvation



E



Supplementary Figure 9.1: Confocal Microscopy Imaging of HEK293 GFP-LC3 cells to Analyse Response to Autophagy Modulating Agents

HEK293 GFP-LC3 cells were treated with autophagy modulators for 2, 4, 6, 8 and 18 hours and fixed with 4% paraformaldehyde. GFP-LC3 (FITC: green) and nuclear material, stained with DAPI Vectashield (blue) mounting buffer were visualized by confocal microscopy.

A: Untreated HEK293 GFP-LC3 cells incubated in DMEM media with 10% FBS (normal growth media)

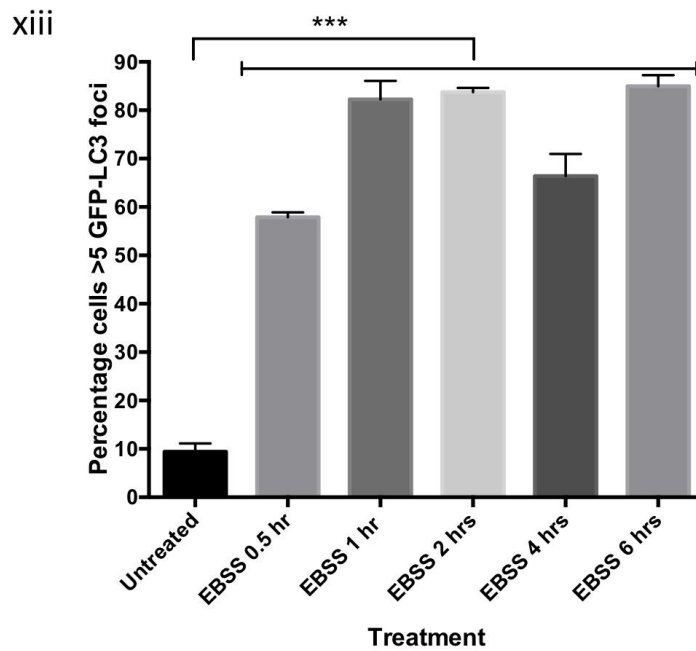
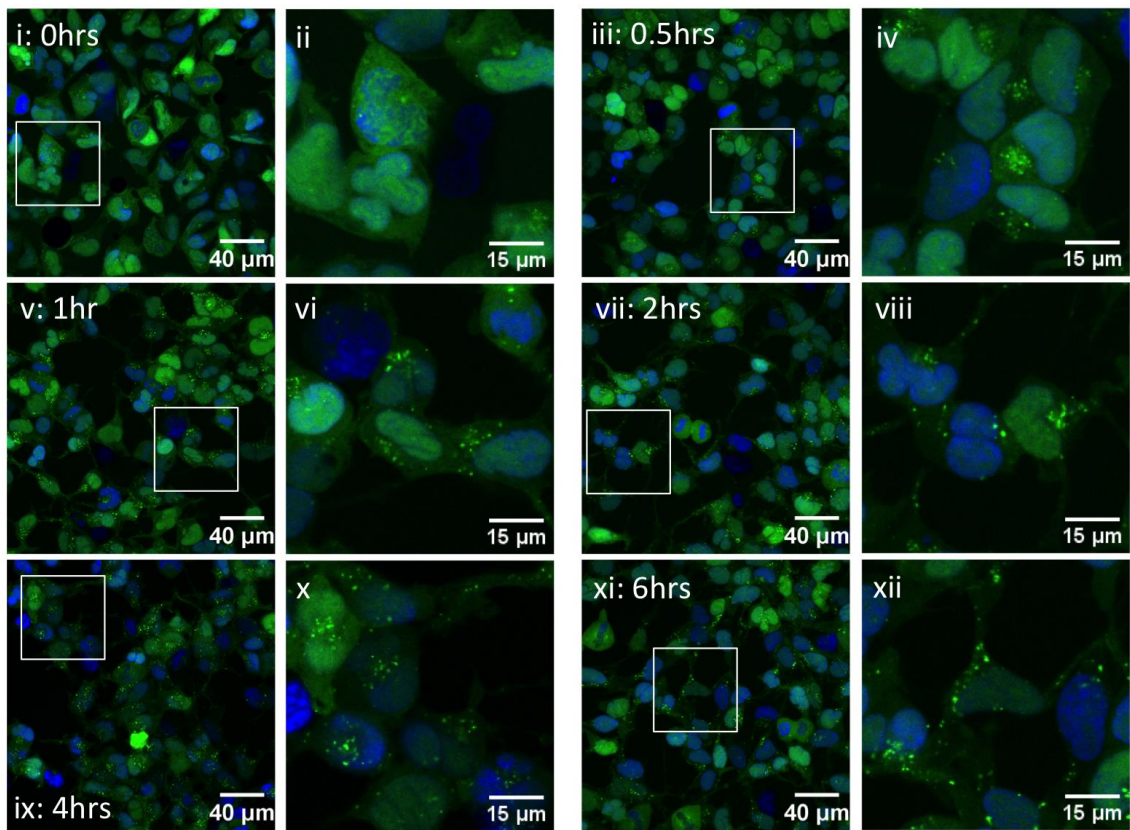
B: HEK293 GFP-LC3 cells treated with 160nM Bafilomycin

C: HEK293 GFP-LC3 cells treated with 100nM Rapamycin

D: HEK293 GFP-LC3 cells incubated in DMEM media without FBS (serum starvation)

E: Cells with >5 GFP-LC3 foci were considered positive for autophagy modulation. 30 cells were counted per field of view and mean percentage of cells with >5 GFP-LC3 foci in each field of view are displayed for each time-point (+/- SEM) (i). Mean percentage cells with >5 GFP-LC3 foci for 6-hour time-point was calculated from n=3 (+/- SEM) (ii). One-way ANOVA with Tukey's multiple comparison test was performed **p <0.01 (ii).

Methods for nutrient deprivation to induce autophagy can vary in efficacy depending on cell line. Therefore, Earle's Balanced Salts Solution (EBSS) was used instead of serum starvation to determine if this was more effective at inducing autophagy. Cells were left untreated or incubated with EBSS for 0.5, 1, 2, 4, and 6 hours and GFP-LC3 foci formation was imaged by fluorescent microscopy. Quantification revealed 9% of untreated cells with >5 GFP-LC3 foci (Supplementary Figure 9.2: xiii). At 0.5 hours percentage of autophagy positive cells increased significantly to 58% and this response was sustained for the 6 hours of incubation, fluctuating between 68% and 85% (Supplementary Figure 9.2).



Supplementary Figure 9.2: HEK293 GFP-LC3 Cells Treated with EBSS for Autophagy Induction via Nutrient Deprivation

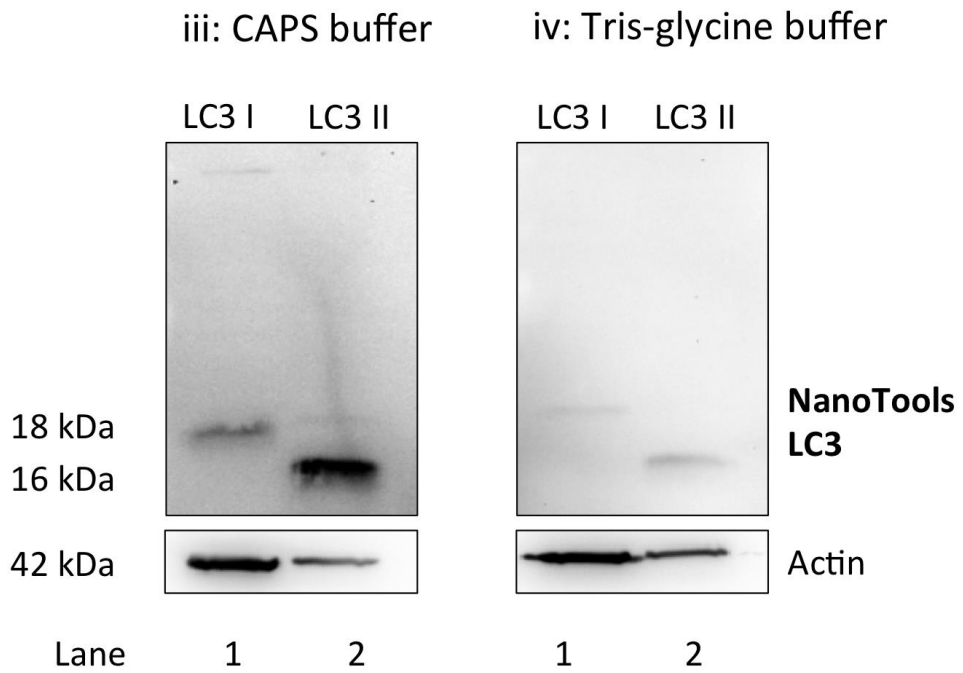
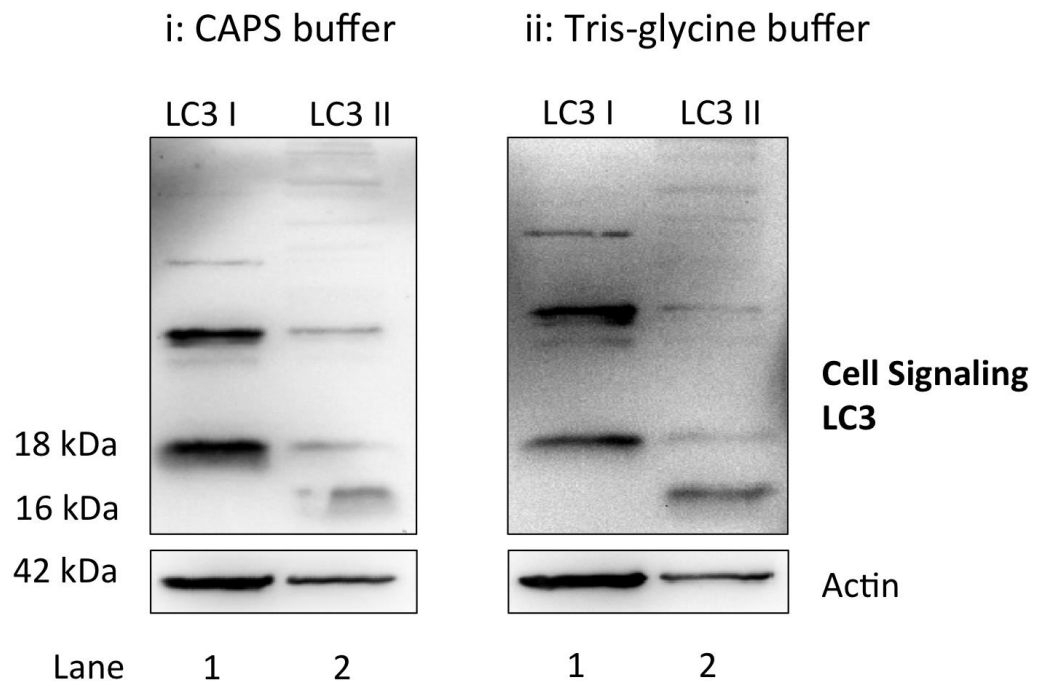
HEK293 GFP-LC3 cells were untreated (i-ii) or treated with EBSS media for nutrient deprivation for 0.5, 1, 2, 4 and 6 hours (iii-xii). Cells were fixed with 4% paraformaldehyde. GFP-LC3 (FITC: green) and nuclear material, stained with DAPI Vectashield (blue) mounting buffer were visualized by confocal microscopy. Cells with >5 GFP-LC3 foci were considered positive for autophagy modulation. A mean of percentage of total cells with >5 GFP-LC3 foci in each field of view is displayed for each

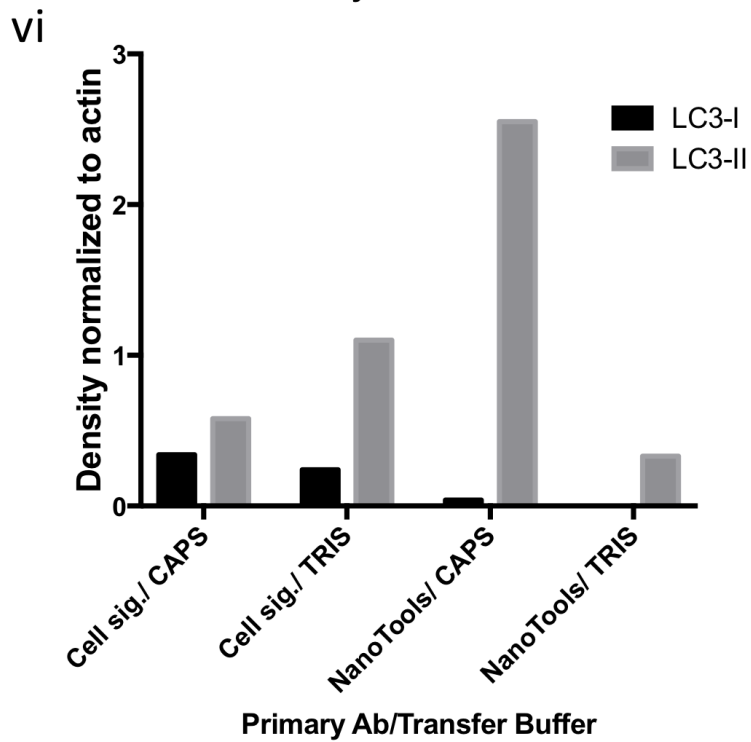
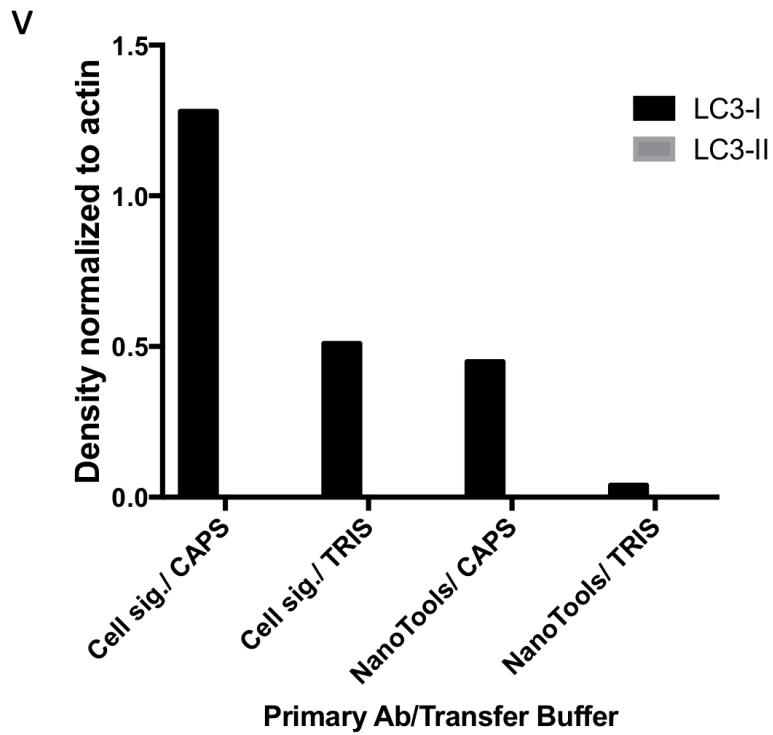
time-point (+/- SEM) (xii). One-way ANOVA with Tukey's multiple comparison test was performed ***p value <0.001 (xii).

9.2.2 Optimisation of the autophagy response: Western Immunoblot of LC3 in PC3 cells

Western immunoblot for endogenous LC3 was also optimized as a method to identify and quantify modulation of autophagy. LC3-I and LC3-II enriched cell fractions from the human prostate cancer PC3 cell line were supplied with the NanoTools anti-LC3 antibody. These cell fractions were used as positive controls to identify the most appropriate anti-LC3 antibody and western immunoblot transfer buffer (Supplementary Figure 9.3). The anti-LC3 antibodies compared were a mouse monoclonal antibody from Nanotools and a rabbit polyclonal antibody from Cell Signalling. A CAPS (3-(Cyclohexylamino)-1-propanesulfonic acid) transfer buffer was compared to a TRIS (2-Amino-2-(hydroxymethyl)-1,3-propanediol)-glycine transfer buffer. As LC3-II is the active form of LC3, conditions optimal for LC3-II detection rather than LC3-I were considered most appropriate.

Although 20µl of cell lysate was resolved in all the lanes, which is stated by NanoTools to be equivalent to approximately 1×10^5 cells per lane, it appears that there was more protein from the LC3-I samples due to the higher density of β -actin observed at 42kDa. This may be due higher levels of protein lysate concentrations in the LC3-I controls despite the number of cells being equal. Nonetheless, it is clear from the results that the NanoTools mouse monoclonal antibody to LC3 combined with the CAPS transfer buffer allowed for optimal LC3-II detection at 16 kDa (lane 2 of iii) (Supplementary Figure 9.3). This was confirmed by densitometry (vi), showing that LC3-II in lane 2 was 254.7% of β -actin density with these optimal conditions (iii) compared to 57.5% and 110.2% with Cell Signalling antibody (i-ii) and 33.0% with TRIS-glycine buffer with NanoTools anti-LC3 (iv) (Supplementary Figure 9.3). Furthermore, it is clear there is more non-specific antibody binding when using Cell Signalling antibody to LC3 (i-ii) compared with the NanoTools antibody (iii-iv) (Supplementary Figure 9.3). From these results it can be concluded that the NanoTools antibody is most appropriate for LC3 western immunoblot.





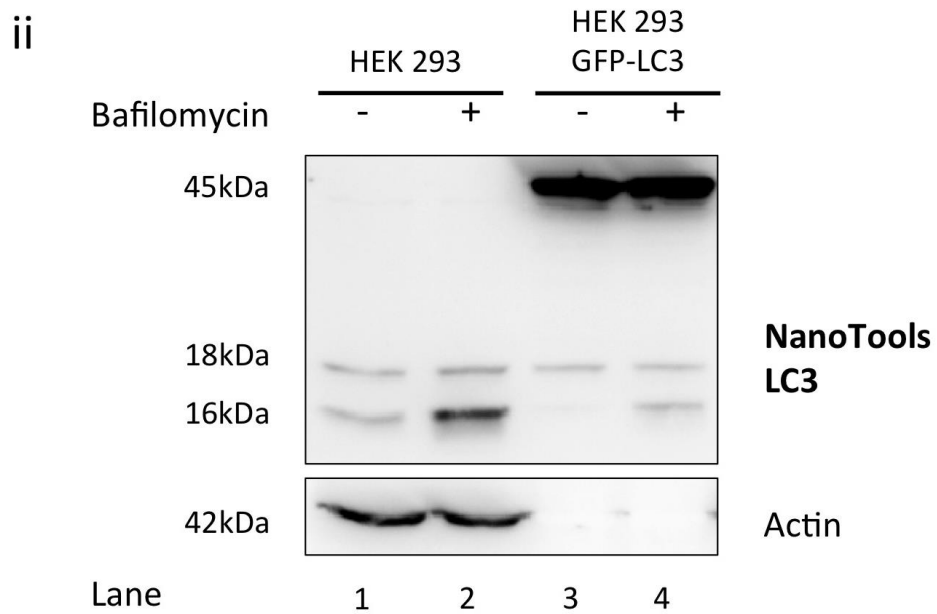
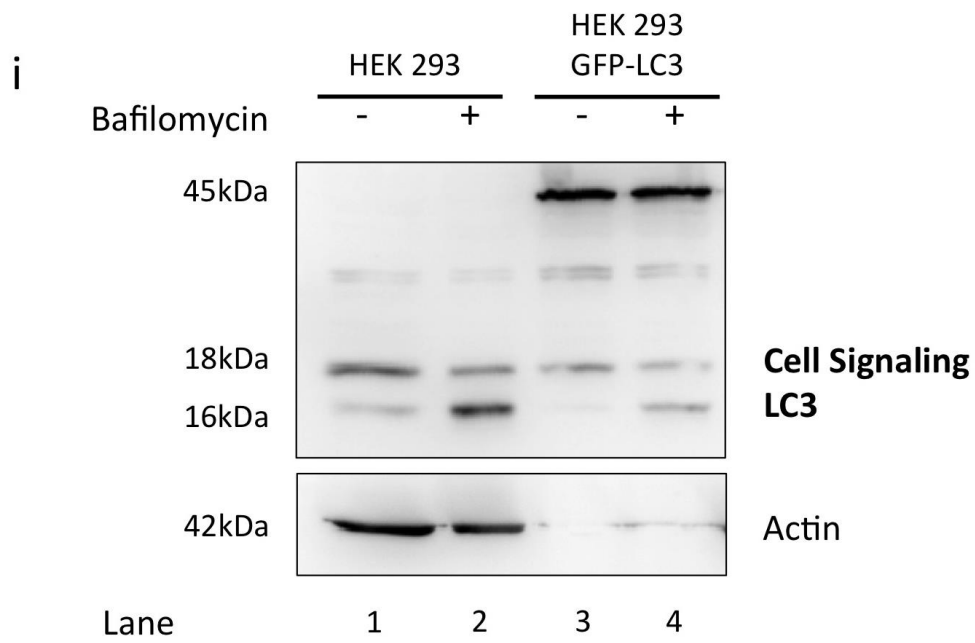
Supplementary Figure 9.3: Optimisation of LC3 Western Immunoblot of LC3-I and LC3-II Positive Protein Lysates

LC3 western immunoblot using either Cell Signalling (i-ii) or Nanotools (iii-iv) anti-LC3 antibodies (both 1 in 1000). 20 μ l (approximately 1×10^5 cells per lane) of LC3-I and LC3-II enriched cell fractions from the human prostate cancer PC3 cell line, supplied by

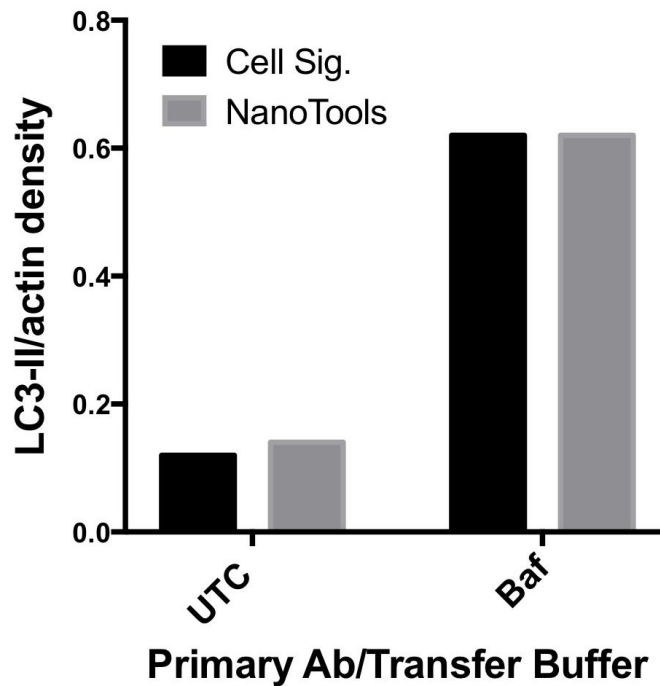
NanoTools, were separated on a 15% SDS-page gel. Protein was transferred to the nitrocellulose membrane using either CAPS transfer buffer (i and iii) or TRIS transfer buffer (ii and iv). ImageJ software was used for western densitometry and the LC3-I and LC3-II bands were expressed as a percentage of β -actin density for both LC3 I- (i) and LC3 II- (ii) positive protein lysates.

9.2.3 Optimisation of the autophagy response: western immunoblot of LC3 in HEK293 cells

LC3 western immunoblot was further optimised by comparing NanoTools and Cell Signalling anti-LC3 antibodies, using cell lysates from HEK293 and HEK293 GFP-LC3 cells that were treated with bafilomycin for 6 hours. In response to bafilomycin, a clear increase in endogenous LC3-II was detected in both HEK293 and HEK293 GFP-LC3 cell lines with both antibodies (Supplementary Figure 9.4). Higher levels of LC3-II were detected from HEK293 cells, possibly due to suppression in endogenous LC3 protein expression in HEK293 GFP-LC3 cells due to high levels of GFP-LC3 from the transfected plasmid (Supplementary Figure 9.4). As there is expression of full length, unprocessed, GFP-LC3 protein at 45kDa, the immunoblot could not be re-probed for β -actin and, therefore, western densitometry could only be performed for HEK293 in lanes 1 and 2 (Supplementary Figure 9.4). LC3-II levels, quantified as a percentage of β -actin density, were very similar with both antibodies. LC3-II levels for untreated control cells were 14.1% and 12.2% of β -actin density for Cell Signalling (i) and NanoTools (ii) antibodies, respectively (Supplementary Figure 9.4). LC3-II levels increased with bafilomycin treatment to 62.1% of β -actin density for both Cell Signalling and NanoTools antibodies (Supplementary Figure 9.4). However, there was non-specific binding seen with Cell Signalling antibody at around 25 kDa (i), meaning Nanotools antibody was more specific to LC3 in HEK293 cell lines.



iii



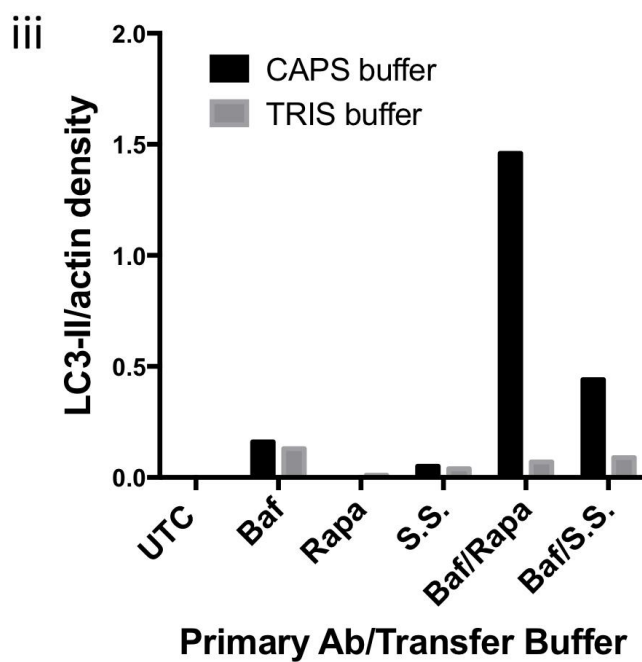
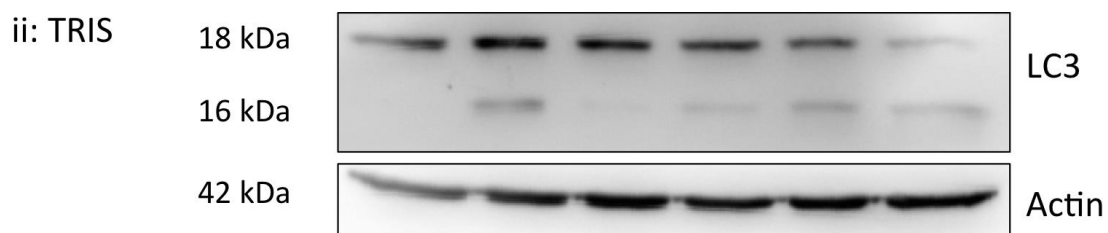
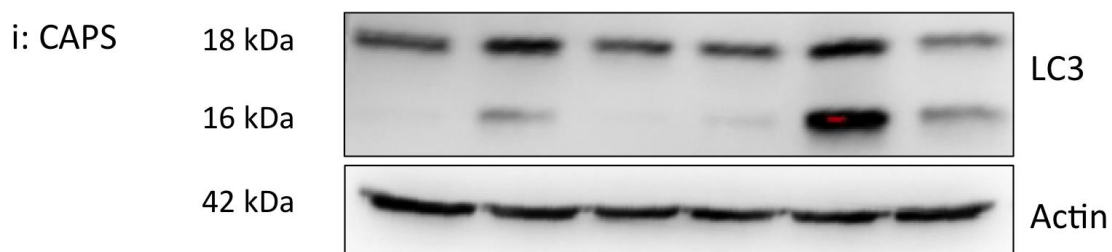
Supplementary Figure 9.4: Comparison of LC3 Antibodies for Western immunoblot of HEK293 and HEK293 GFP-LC3 Cells Treated with Bafilomycin

HEK293 and HEK293 GFP-LC3 cells were either untreated or treated with 160nM bafilomycin for 6 hours. Protein lysates were separated on a 15% SDS-page gel and proteins were transferred to nitrocellulose membrane using TRIS transfer buffer and were immunoblotted using either Cell Signalling (i) or Nanotools (ii) anti-LC3 antibodies (both 1 in 1000). ImageJ software was used for western densitometry and LC3-II bands were expressed as a percentage of β -actin density for the HEK293 cells only (iii).

HEK293 cells were then treated with bafilomycin, rapamycin and serum starvation for 6 hours, and CAPS and TRIS-glycine transfer buffer were compared. LC3-II was not detected in untreated lysates and bafilomycin treatment resulted in a modest increase in LC3-II to 13% and 16% for TRIS (i) and CAPS (ii) buffers, respectively (Supplementary Figure 9.5). There were minimal increases in LC3-II with serum starvation and rapamycin to between 1% and 5% for both buffers (Supplementary Figure 9.5). Rapamycin and serum starvation were combined with bafilomycin to prevent degradation of LC3-II (lanes 5 and 6) (Supplementary Figure 9.5). This resulted in considerable increases in LC3-II levels with CAPS buffer to 146% and 44% with rapamycin and serum starvation treatments combined with bafilomycin, respectively (Supplementary Figure 9.5: ii). This increase in LC3-II was not observed using the TRIS-glycine buffer (Supplementary Figure

9.5: i). These results confirm that CAPS buffer combined with NanoTools antibody are optimal for western immunoblot of LC3 with HEK293 cells.

S.S.	-	-	-	+	-	+
Rapamycin	-	-	+	-	+	-
Bafilomycin	-	+	-	-	+	+

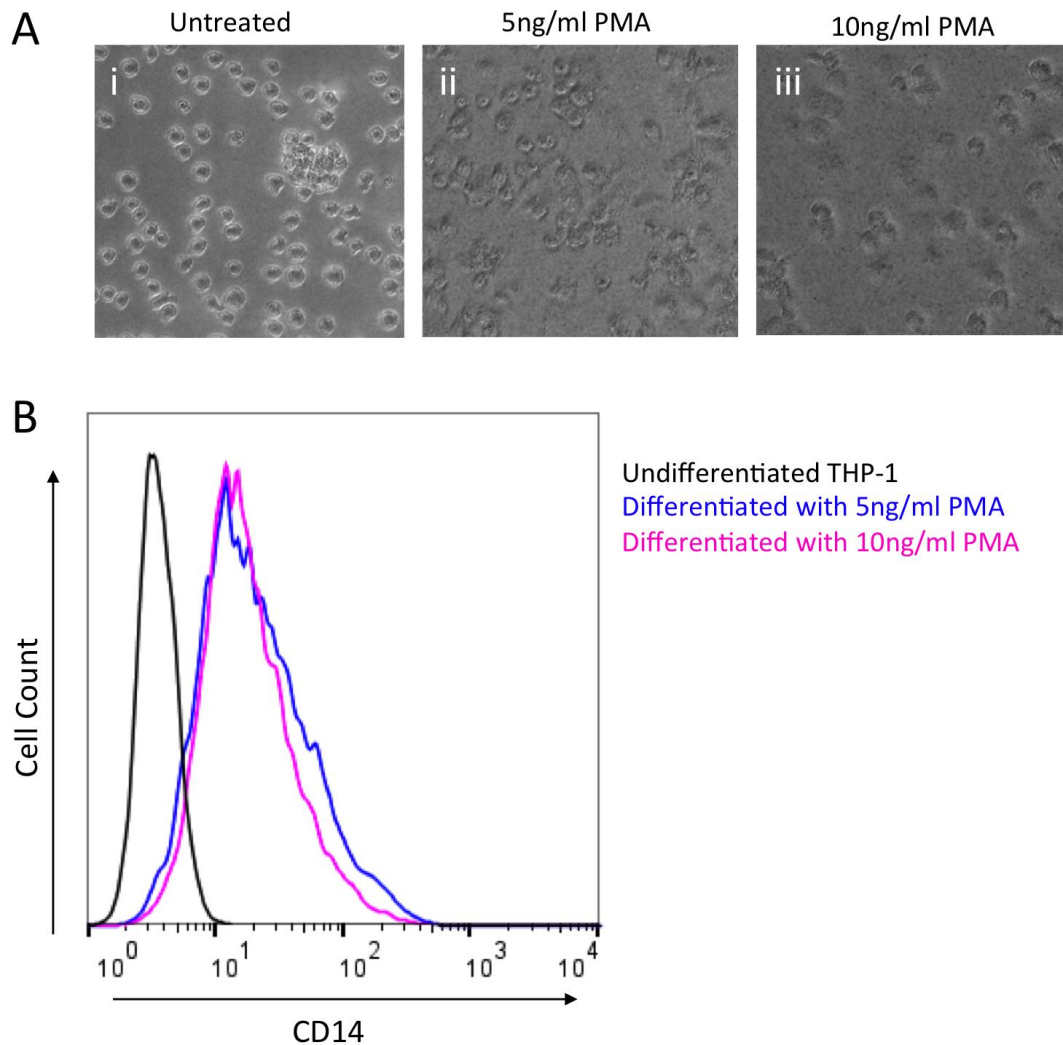


Supplementary Figure 9.5: Comparison of Transfer Buffers for LC3 western Immunoblot of HEK293 cells

HEK293 cells were untreated or treated with 160nM bafilomycin or/and 100nM rapamycin, DMEM without FBS (serum starvation) or DMEM without FBS (serum starvation) with 160nM bafilomycin for 6 hours. Protein lysates separated on 15% SDS-page gel and proteins were transferred to nitrocellulose membrane using either CAPS (i) or TRIS (ii) transfer buffer and were immunoblotted with Nanotools anti-LC3 antibody (1 in 1000). ImageJ software was used for western densitometry and LC3-II bands were expressed as a percentage of β -actin density (iii).

9.2.4 Differentiation of THP-1 monocytes into macrophage-like cells

When THP-1 cells differentiate into macrophages they undergo morphological changes from suspension to adherent cells (Supplementary Figure 9.6A). However, to confirm differentiation the CD14 surface protein, which is a well-established marker for monocyte to macrophage differentiation (Aldo et al., 2013), was analysed by flow cytometry. THP-1s were seeded with PMA and incubated for 72 hours, then incubated in normal growth media for 24 hours. There was a clear increase in CD14 expression when cells were exposed to PMA (Supplementary Figure 9.6B). Although, the level of CD14 expression is not dependent on the concentration of PMA used, there were pronounced morphological alterations with the higher PMA concentration (Supplementary Figure 9.6A). Therefore, it was determined that 10ng/ml of PMA was optimal to stimulate THP-1 differentiation into macrophage-like cells.



Supplementary Figure 9.6: THP-1 Cell Line Differentiated to Macrophage-Like Cells

THP-1 cells were incubated with 5ng/ml or 10ng/ml of PMA for 72 hours. PMA was removed by washing in PBS twice and cells were rested in normal growth media for a further 24 hours.

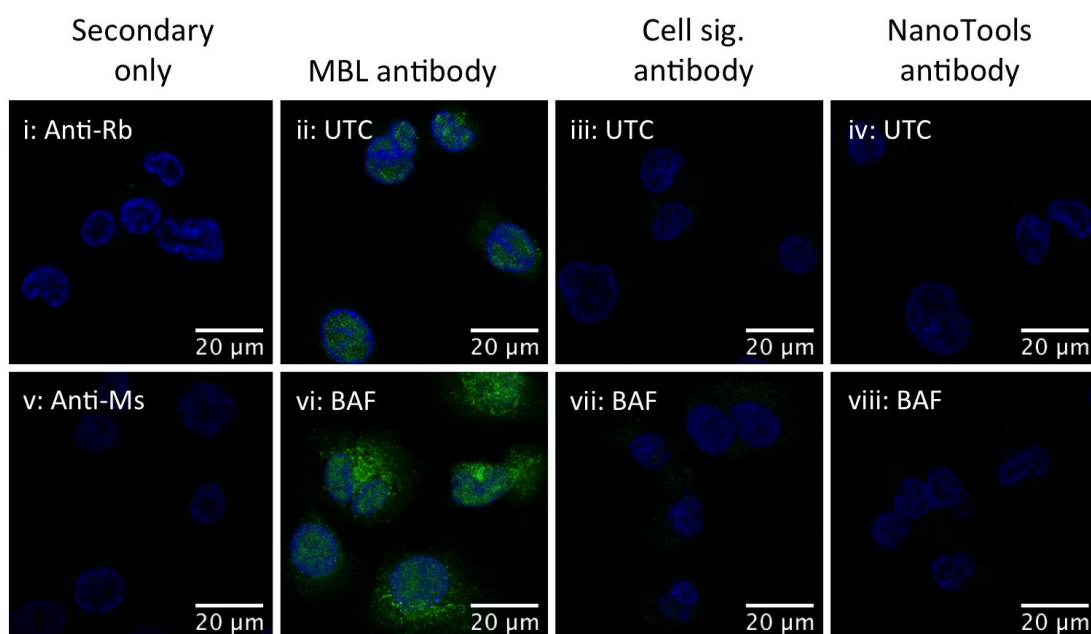
A: Brightfield images showing morphological differences between untreated (i), 5ng/ml (ii) or 10ng/ml (iii) PMA.

B: Cells were detached and stained for CD14 surface marker for flow cytometry acquisition. Geometric mean of CD14 intensity of cells was quantified by flow cytometry and analysed using FlowJo software.

9.2.5 Endogenous LC3 Immunostaining in THP-1-derived Macrophages

THP-1-derived macrophages were left untreated or treated with bafilomycin for 4 hours then anti-LC3 antibodies from NanoTools, Cell Signalling and MBL were compared for

immunostaining. There was no non-specific secondary antibody binding visible (Supplementary Figure 9.7: i, v). NanoTools and Cell Signalling anti-LC3 antibodies were unable to detect endogenous LC3 in untreated and bafilomycin-treated THP-1-derived macrophages (Supplementary Figure 9.7: iii, iv, vii, viii). However, MBL anti-LC3 detected basal levels of LC3 in untreated cells (Figure 3.8: ii). When THP-1-derived macrophages were treated with bafilomycin increased expression of LC3 was visible, with distinct LC3 foci also identified (Supplementary Figure 9.7: vi). Therefore, immunostaining with the MBL antibody allows detection of basal autophagy as well as increases in autophagosome accumulation due to autophagy modulation.

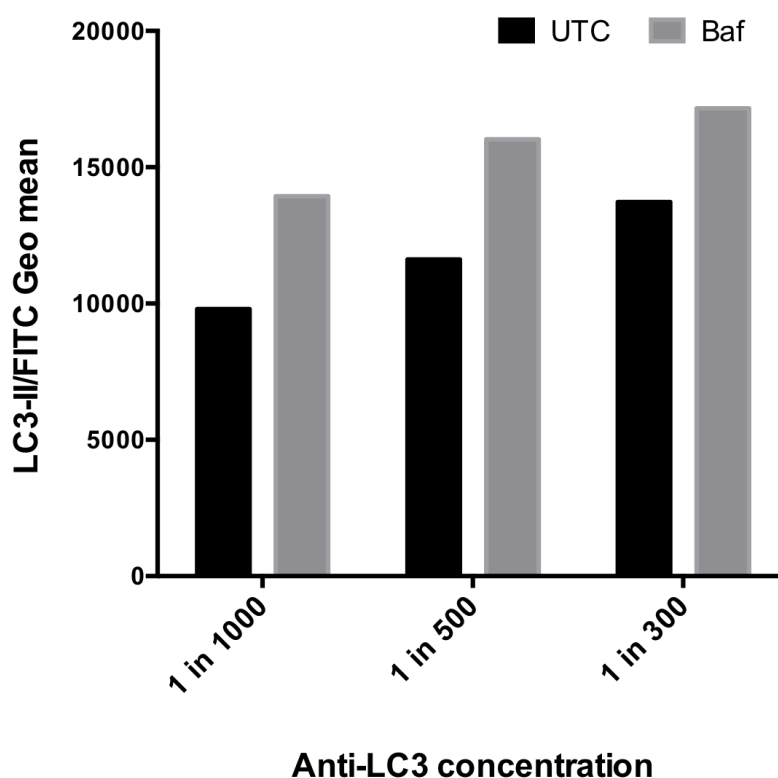


Supplementary Figure 9.7: Comparison of LC3 antibodies for immunostaining in THP-1-derived macrophages

LC3 immunostain using either MBL (ii, vi), Cell Signalling (iii-vii) or Nanotools (iv-viii) anti-LC3 antibodies (1 in 1000). Cells were untreated (i-v), or treated with 160nM bafilomycin for 4 hours (vi-viii). Cells were then immunostained for LC3 (FITC: green) and mounted with DAPI Vectashield (blue). Anti-Rb (for MBL and Cell Signalling) (i) and anti-Ms (for NanoTools) (v) secondary only staining controls were also included.

9.2.6 Endogenous LC3 flow cytometry in THP-1-derived Macrophages

To facilitate analysis of autophagosome-bound LC3-II by flow cytometry, unbound cytosolic LC3-I can be removed by permeabilisation of the cell membrane with 0.05% saponin prior to fixation (Eng et al., 2010). THP-1-derived macrophages were left untreated or treated with Baf for 4 hours. After removal of cytosolic LC3, immunostaining with a concentration range of MBL anti-LC3 antibody was undertaken. There was a notable increase in LC3 geometric mean when cells are treated with bafilomycin and with increasing concentrations of antibody (Supplementary Figure 9.8). However, the most substantial increase in LC3 staining between untreated and bafilomycin was observed with an antibody concentration of 1 in 500 (Supplementary Figure 9.8). These optimal conditions for endogenous LC3 flow cytometry allow the detection of bafilomycin-induced autophagosome accumulation.



Supplementary Figure 9.8: Optimisation of antibody concentration for endogenous LC3 Flow cytometry in THP-1-derived macrophages

Flow cytometry with MBL anti-LC3 antibody, comparing concentrations of 1 in 1000, 1 in 500 and 1 in 300. THP-1-derived macrophages were untreated or treated with 160nM

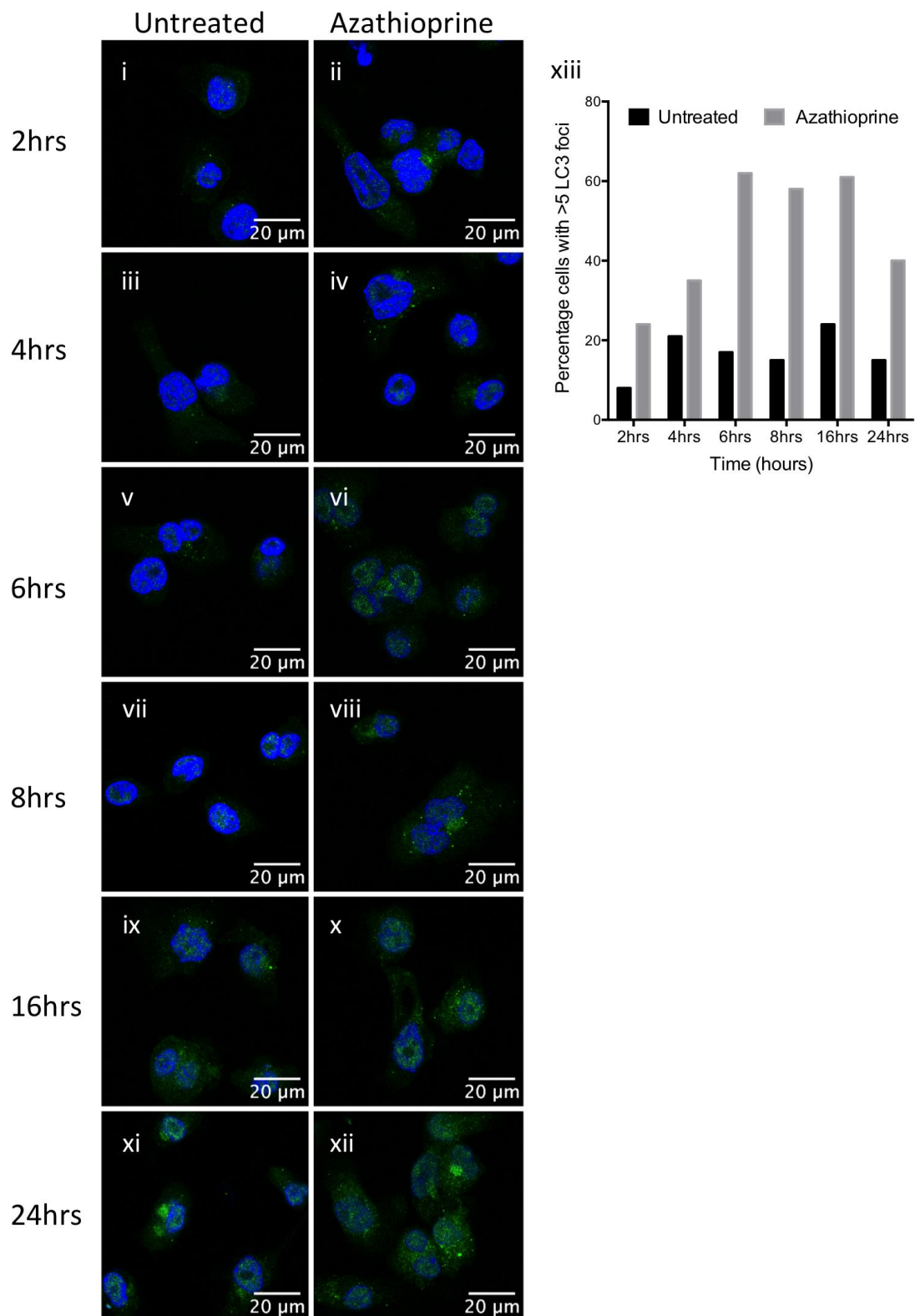
bafilomycin. After 4-hour incubation, cells were washed with 0.05% saponin and immunostained for LC3. Geometric mean of LC3 intensity of cells was quantified by flow cytometry and analysed using FlowJo software.

9.3 Summary

HEK293 cells have a fully functional autophagy pathway and respond as expected to autophagy modulating control treatments including bafilomycin, rapamycin and serum starvation. When cells were treated with autophagy controls, GFP-LC3 autophagosomes accumulated between 2- and 18- hour time points to varying degrees, however optimal accumulation was observed at 6 hours. Immunoblotting for LC3 was optimal when using a combination of NanoTools antibody and CAPS transfer buffer.

THP-1 differentiation to macrophage-like cells was successfully induced by PMA. In these THP-1-derived macrophages, detection of endogenous LC3 and autophagosome accumulation in response to bafilomycin was optimised. Therefore, LC3 immunostaining and flow cytometry, using the MBL antibody, can be used as complementary techniques to monitor responses to autophagy modulation in this cell line. The optimisation of techniques to monitor autophagy was an essential first step to allow subsequent investigations with IBD drugs to be carried out with confidence.

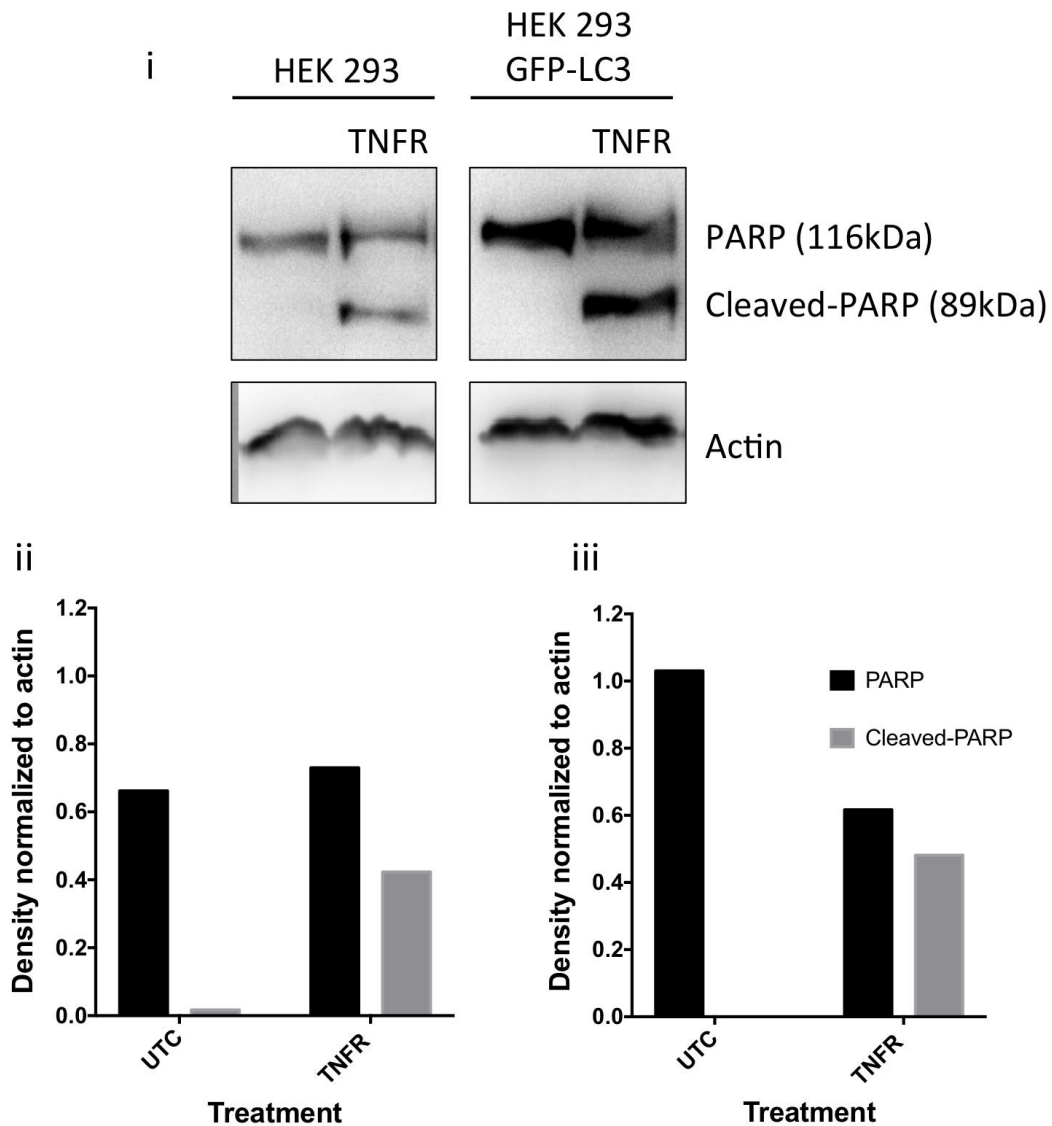
10. Supplementary Figures



Supplementary Figure 10.1: Azathioprine-Induced Autophagy in THP-1-derived Macrophages Monitored by LC3 Immunostaining

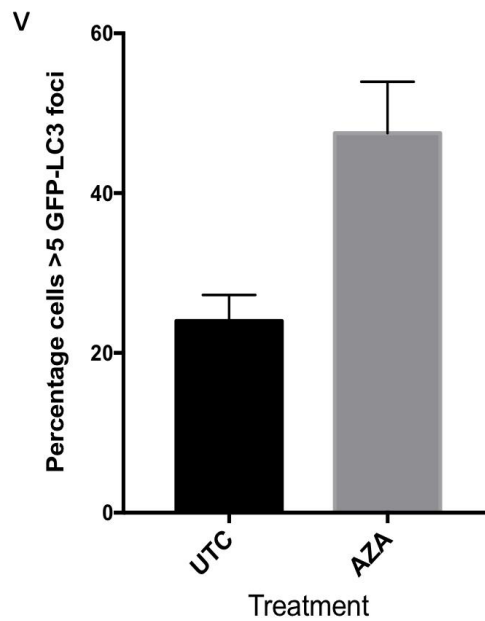
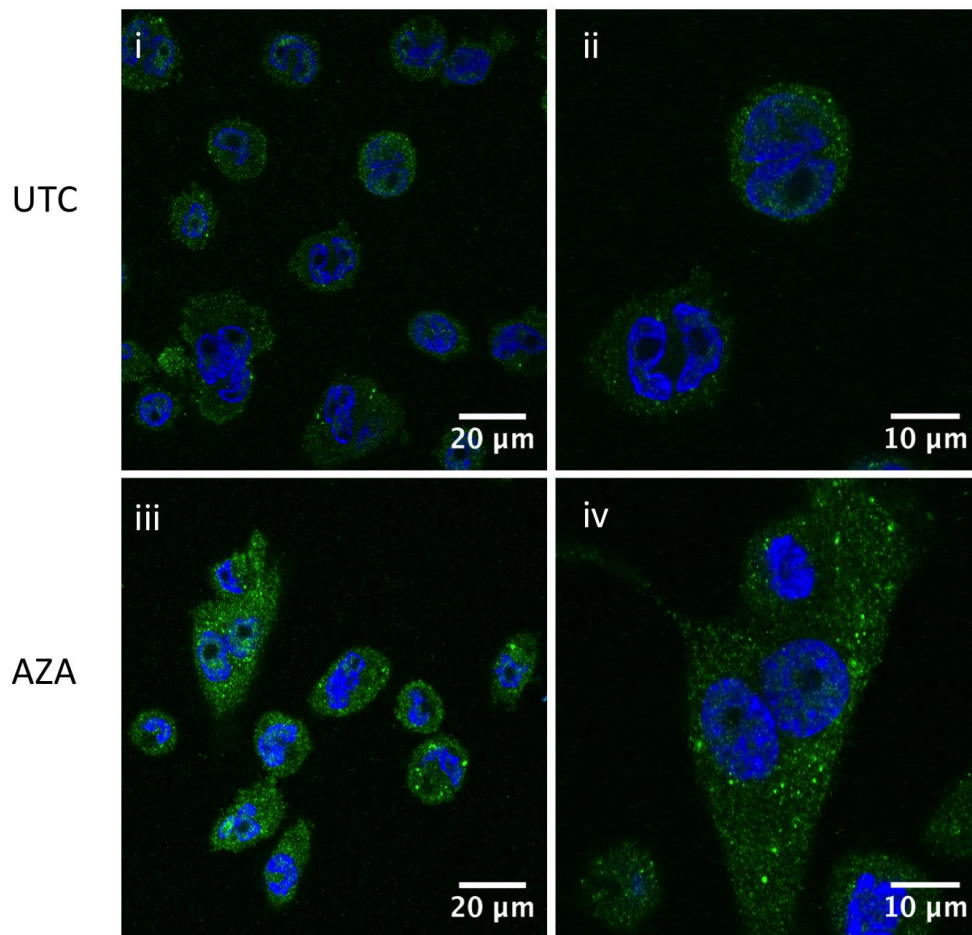
THP-1-derived macrophages were untreated (i, iii, v, vii, ix, xi) or treated with 120 μM azathioprine (ii, iv, vi, viii, x, xii) for 2 (i, ii), 4 (iii, iv), 6 (v, vi), 8(vii, viii), 16 (ix, x) and 24

hours (xi, xii) (n=1). Cells were then immunostained for LC3 (green) and mounted with DAPI Vectashield (blue). 30 cells were counted in 3 fields of view per treatment and percentage cells with >5 GFP-LC3 foci quantified (n=1).



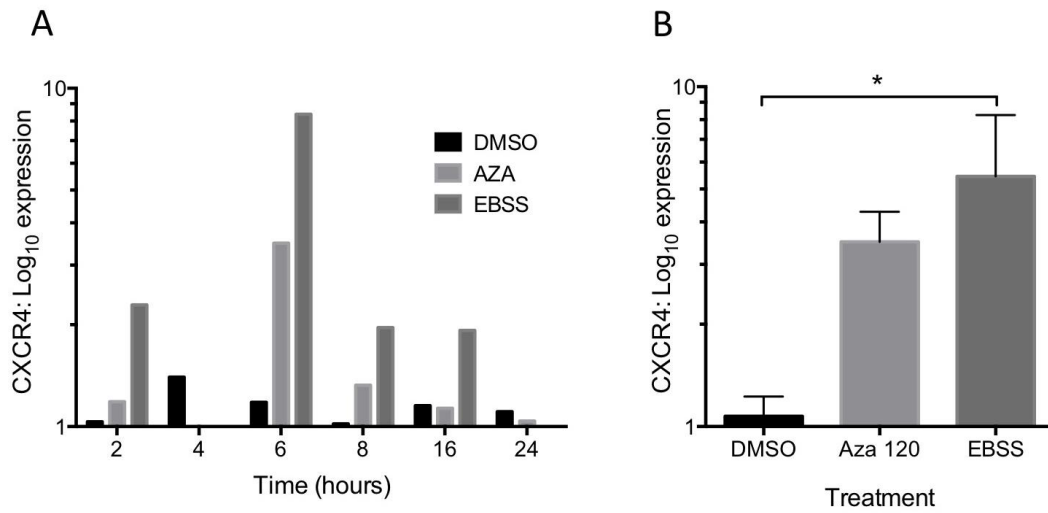
Supplementary Figure 10.2: Cleaved-PARP Western Immunoblot to Monitor Apoptosis

HEK293 and HEK293 GFP-LC3 cells were untreated or transfected by electroporation with 0.5 μ g of TNF receptor plasmid and rested for 24 hours. Protein lysates separated on 10% SDS-page gel were immunoblotted for PARP and actin (i). ImageJ software was used for western densitometry. PARP and cleaved-PARP density normalized to actin was quantified for HEK 293 (ii) and HEK 293 GFP-LC3 cells (iii).



Supplementary Figure 10.3: LC3 Immunostaining to Monitor Autophagy Activity for Human Autophagy Gene Array

Cells were untreated (i-ii) or treated with 120μM azathioprine (iii-iv) for 6 hours. Cells were then immunostained for LC3 (FITC: green) and mounted with DAPI Vectashield (blue). 30 cells were counted in 3 fields of view per treatment and percentage cells with >5 GFP-LC3 foci were quantified (+/- SEM) (v).

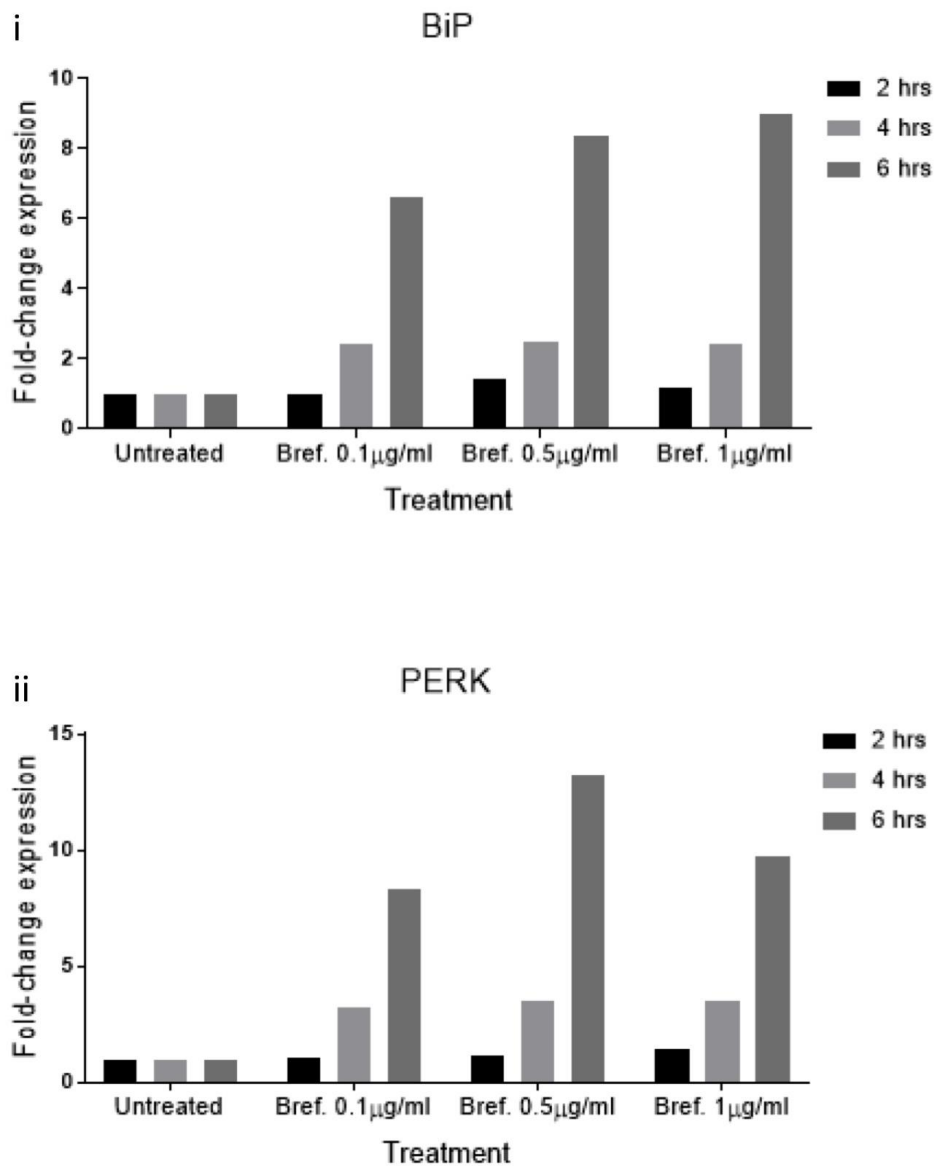


Supplementary Figure 10.4: *CXCR4* Gene Expression Up-Regulated by Azathioprine in THP-1-Derived Macrophages

mRNA was extracted and converted to cDNA for qPCR analysis using primers for *CXCR4*. Reference genes were *RPL13A* and *actin*, and the calibrating sample was untreated cells for corresponding time-points. Relative expression was calculated as 2^{-ddCT} and is displayed as Log_{10} of fold-change (2^{-ddCT}).

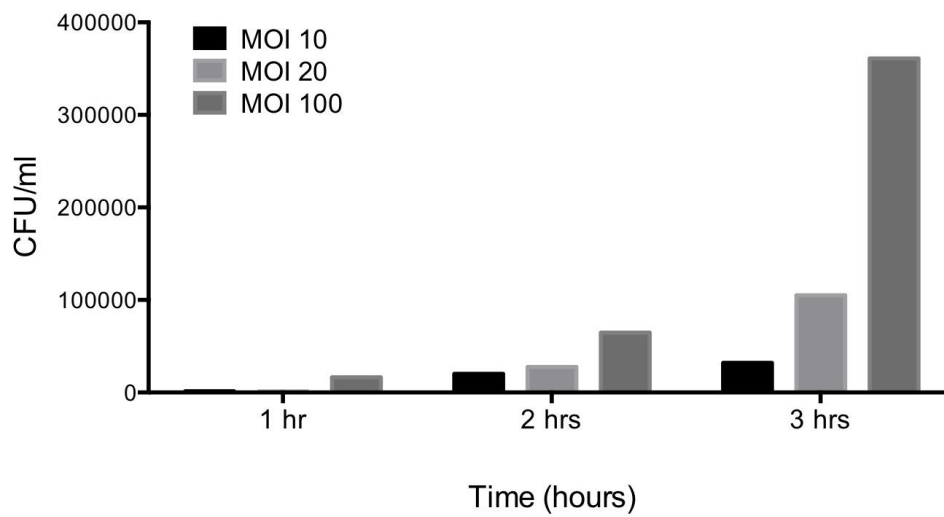
A: THP-1-derived macrophages were untreated or treated with DMSO (vehicle control), 120 μM azathioprine or EBSS for nutrient deprivation for 2, 4, 6, 8, 16 and 24 hours.

B: THP-1-derived macrophages were untreated or treated with DMSO (vehicle control), 120 μM azathioprine or EBSS for nutrient deprivation for 6 hours ($n=3$). Log_{10} of fold-change expression (\pm SEM) is shown. One-way ANOVA with Dunnett's multiple comparison test was performed on dCT values. * $p < 0.05$ compared to untreated.



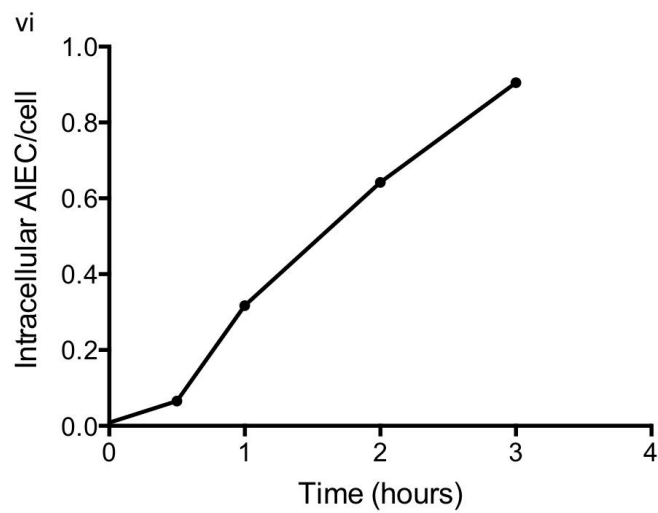
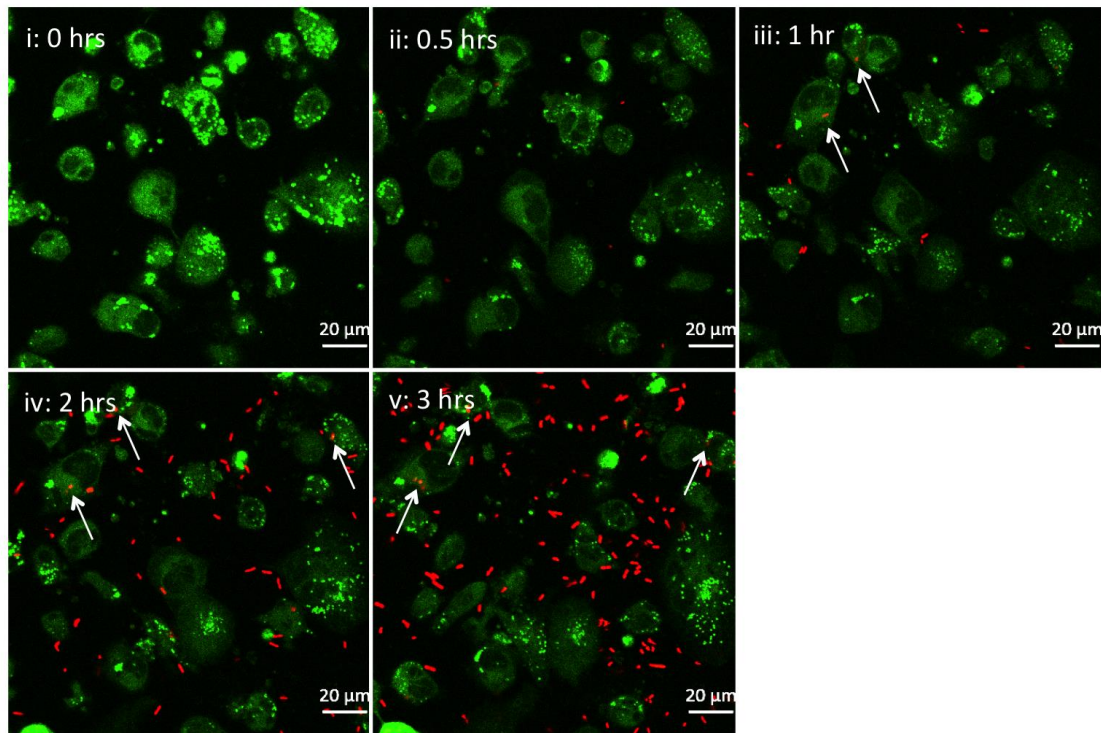
Supplementary Figure 10.5: Optimisation of Brefeldin A treatment as a positive control for BiP and PERK qPCR

THP-1-derived macrophages were untreated or treated with 0.1, 0.5 and 1 µg/ml brefeldin A for 2, 4 and 6 hours. mRNA was extracted and converted to cDNA for RT-qPCR analysis using primers for *BiP* (i) and *PERK* (ii) (n=1). Reference genes were *RPL13A* and *Actin*, and the calibrating sample was untreated cells for corresponding time-points. Relative expression was calculated and displayed as 2^{-ddCT} (fold-change).



Supplementary Figure 10.6: Optimisation of THP-1-derived macrophages infection with AIEC

THP-1-derived macrophages were infected with MOI 10, 20 and 100 of AIEC for 1, 2 and 3 hours, then treated with 100 μ g/ml gentamicin for 1 hour. Cell lysates were prepared, spread on LB agar plates and incubated at 37 $^{\circ}$ C overnight. CFU/ml of cell lysates was calculated.



Supplementary Figure 10.7: Live-cell confocal imaging of THP-1-derived macrophages infected with mCherry-AIEC

THP-1-derived macrophages were infected with MOI 10 of AIEC CUICD541-10-mCherry strain for 3 hours. To induce mCherry fluorescence in AIEC, 0.1mM IPTG was added and 5 μ M Cell Tracker™ Green BODIPY® was added to visualise cells for the duration of the live-cell. Number of intracellular bacteria normalised to number of host cells was quantified at 0, 0.5, 1, 2 and 3 hours (vi).

11. Review Paper

Journal of Crohn's and Colitis, 2017, 118–127
doi:10.1093/ecco-jcc/jjw127
Advance Access publication July 5, 2016
Review Article

OXFORD

Review Article

Inflammatory Bowel Disease Drugs: A Focus on Autophagy

Kirsty M. Hooper,^a Peter G. Barlow,^a Craig Stevens,^{a*} Paul Henderson,^{b,c*}

^aSchool of Life, Sport & Social Sciences, Edinburgh Napier University, Edinburgh, UK ^bChild Life and Health, University of Edinburgh, Edinburgh, UK ^cDepartment of Paediatric Gastroenterology and Nutrition, Royal Hospital for Sick Children, Edinburgh, UK

*Joint senior authors

Corresponding author: Dr Craig Stevens, BSc, PhD, FHEA, School of Life, Sport & Social Sciences, Edinburgh Napier University, Sighthill Campus, Sighthill Court, Edinburgh, EH11 4BN, UK. Tel.: 00 44 131 455 2930; email: C.Stevens@napier.ac.uk

Abstract

Inflammatory bowel disease [IBD] is characterized by chronic inflammation of the gastrointestinal tract. Medications such as corticosteroids, thiopurines, immunomodulators and biologic agents are used to induce and maintain remission; however, response to these drugs is variable and can diminish over time. Defective autophagy has been strongly linked to IBD pathogenesis, with evidence showing that enhancing autophagy may be therapeutically beneficial by regulating inflammation and clearing intestinal pathogens. It is plausible that the therapeutic effects of some IBD drugs are mediated in part through modulation of the autophagy pathway, with studies investigating a wide range of diseases and cell types demonstrating autophagy pathway regulation by these agents. This review will highlight the current evidence, both *in vitro* and *in vivo*, for the modulation of autophagy by drugs routinely used in IBD. A clearer understanding of their mechanisms of action will be invaluable to utilize these drugs in a more targeted and personalized manner in this diverse and often complex group of patients.

Key Words: Autophagy; drugs; IBD; Crohn's disease

1. Introduction

The major inflammatory bowel diseases [IBD], Crohn's disease [CD] and ulcerative colitis [UC], are characterized by chronic inflammation of the gastrointestinal [GI] tract and affect up to 1 in 250 people in the UK.¹ A recent National Health Service [NHS] review estimated IBD treatment costs of £720 million per year,¹ with roughly a quarter of these costs directly attributed to drug treatments.² At present there is no cure for IBD, and medications are aimed at inducing and maintaining remission of disease by modifying inflammatory processes.³ The efficacy of current drugs for the treatment of IBD continues to come under scrutiny, as response to treatment often diminishes over time, resulting in disease complications. A recent review of European cohorts estimates that 10–35% of CD patients required surgery within 1 year of diagnosis and up to 61% by 10 years.⁴ Development of new drugs is a long and expensive process

associated with high failure rates; therefore, making better use of drugs that have already been approved for clinical use is essential. The Crohn's and Colitis Foundation of America has recently highlighted this need for research into optimizing medical therapies,⁵ with patient stratification and personalized medicine of key importance in this context.⁶ In order to improve the efficacy of existing drugs, a more comprehensive characterization of their mechanism of action is required. Here we give an overview of IBD drugs that have been linked to the modulation of autophagy, a cellular process that has been implicated in CD pathogenesis, and summarize what is currently known regarding their mechanism of action.

2. Aetiology of IBD

The aetiopathogenesis of IBD remains poorly understood but is almost certainly multifactorial in nature, with genetic predisposition,

© European Crohn's and Colitis Organisation (ECCO) 2016.

This is an Open Access article distributed under the terms of the Creative Commons Attribution Non-Commercial License (<http://creativecommons.org/licenses/by-nc/4.0/>), which permits non-commercial re-use, distribution, and reproduction in any medium, provided the original work is properly cited. For commercial re-use, please contact journals.permissions@oup.com

118

environmental triggers [such as smoking, antibiotics and diet] and a dysregulated immune response to intestinal microflora all contributing.⁷ Genome-wide association studies [GWAS] have now identified multiple susceptibility loci for CD and confirmed the previously recognized association of nucleotide-binding oligomerization domain-containing protein 2 [NOD2], genes involved in T cell-dependent immunity and autophagy, including autophagy-related protein 16-1 [ATG16L1], immunity-related GTPase family M protein [IRGM] and leucine rich repeat kinase 2 [LRRK2].⁸ Genetic association with the transcription factor x-box-binding protein 1 [XBP1], a key component of the endoplasmic reticulum [ER]-stress response, with both forms of IBD have also been identified and replicated.⁹ These genetic studies have led to an increase in research linking autophagy dysregulation to CD pathogenesis.

2.1. Autophagy

Autophagy is an intracellular process that degrades excessive, damaged or aged proteins and organelles to maintain cellular homeostasis.¹⁰ These homeostatic functions impact on many essential cellular processes including development and differentiation, survival, senescence and innate and adaptive immunity, with dysregulated autophagy linked to a multitude of diseases.¹¹ When macroautophagy [hereafter referred to as autophagy] is initiated, the isolation membrane, an expanding lipid bilayer, forms a double membrane vesicle [the autophagosome] around the cargo to be degraded [Figure 1]. The mature autophagosome then fuses with a lysosome to form an autophagolysosome, in which lysosomal enzymes degrade the inner membrane and cargo. The process of autophagy is controlled by the coordinated activity of ATG [autophagy-related] proteins. The further detailed and complex molecular machinery involved in biogenesis of the isolation membrane and autophagosome is beyond the scope of this focused review and has been discussed comprehensively elsewhere¹²; however, it is appropriate to highlight the role of ATG16L1 in this process. Two ubiquitin-like molecules, LC3 [microtubule-associated proteins 1A/1B light chain 3A]/ATG8 and ATG12 are involved in autophagosome biogenesis. LC3/ATG8 is conjugated to phosphatidylethanolamine [PE] to form lipidated LC3-II and is associated with autophagosome formation. ATG12 is conjugated to ATG5 and forms a complex with ATG16L1 [ATG16L1 complex].

The ATG16L1 complex is proposed to specify the site of LC3 lipidation for autophagosome formation [Figure 1].¹³

2.2. Autophagy signalling pathways

Autophagy is active at a basal level in most cell types to maintain homeostasis, and this activity is modulated in response to a myriad of stresses and stimuli that include starvation, hypoxia, infection and ER stress.¹⁴ Autophagy is largely regulated, but not exclusively, by the mTORC1 [mechanistic target of rapamycin complex 1] and Beclin1/B cell lymphoma 2 [Bcl-2] signalling pathways [Figure 2]. The mTORC1 pathway plays a central role in the inhibition of autophagy, for example blocking mTORC1 activity with the small macrolide antibiotic rapamycin stimulates induction of autophagy. Class I phosphatidylinositol 3-kinases [PI3K], Akt and Ras/Mek/Erk signalling pathways are involved in the activation of mTORC1 and subsequent inhibition of autophagy.¹⁴ mTORC1 inhibits autophagy via phosphorylation of Unc-51 like autophagy activating kinase 1 [ULK1] and ATG13 to inhibit the ULK1-ATG13-FIP200 complex, which is important for initiation of autophagosome formation.¹⁵ Conversely, AMP-activated protein kinase [AMPK] is involved in the inhibition of mTORC1 and stimulates autophagy via phosphorylation of ULK1 at sites distinct from mTORC1.¹⁶ Activated ULK1 and AMPK subsequently phosphorylate Beclin1 for the induction of autophagy.^{16,17} Beclin1 induces autophagy through the formation of the class III PI3K complex consisting of Vps34-Vps15-Beclin1.¹⁸ Interaction of the class III PI3K complex with ATG14 is important for recruitment of autophagy proteins, including the ATG16L1 complex and LC3/ATG8, to the autophagosome membrane during early stages of the pathway [Figure 2].¹²

Beclin1 was originally identified as an interacting protein with Bcl-2¹⁹, an anti-apoptotic protein that inhibits autophagy when it is in complex with Beclin1.^{20,21} In response to nutrient deprivation, c-Jun N-terminal kinase [JNK]-1-mediated phosphorylation of Bcl-2 occurs, causing the dissociation of the Beclin1-Bcl-2 complex and induction of autophagy.²² However, during periods of prolonged nutrient deprivation, increased levels of Bcl-2 phosphorylation prevent Bcl-2 from binding to and inhibiting proapoptotic proteins including Bcl-2 associated X protein [BAX] and Bcl-2-antagonist/killer [Bak].^{23,24} Therefore, Bcl-2 phosphorylation

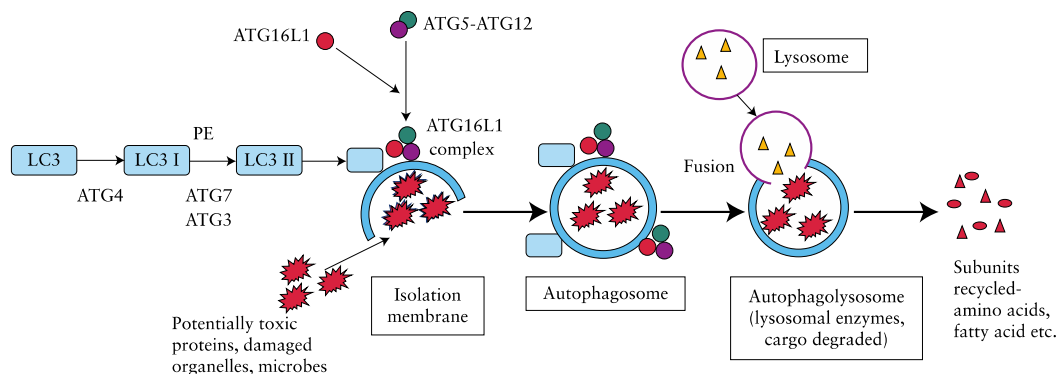


Figure 1. The autophagy pathway. During the initial stages of autophagy, the isolation membrane forms a double membrane vesicle [the autophagosome] around the cargo to be degraded. The mature autophagosome then fuses with a lysosome to form an autophagolysosome, in which cargo are degraded by lysosomal enzymes and subunits are recycled. Autophagy is controlled by the coordinated activity of ATG proteins. Two ubiquitin-like molecules, LC3 and ATG12, are involved in autophagosome biogenesis. LC3 is conjugated to PE to form lipidated LC3-II and is associated with the autophagosome outer membrane. ATG12 is conjugated to ATG5 and forms a complex with ATG16L1 [ATG16L1 complex]. The ATG16L1 complex is proposed to specify the site of LC3 lipidation for autophagosome formation.

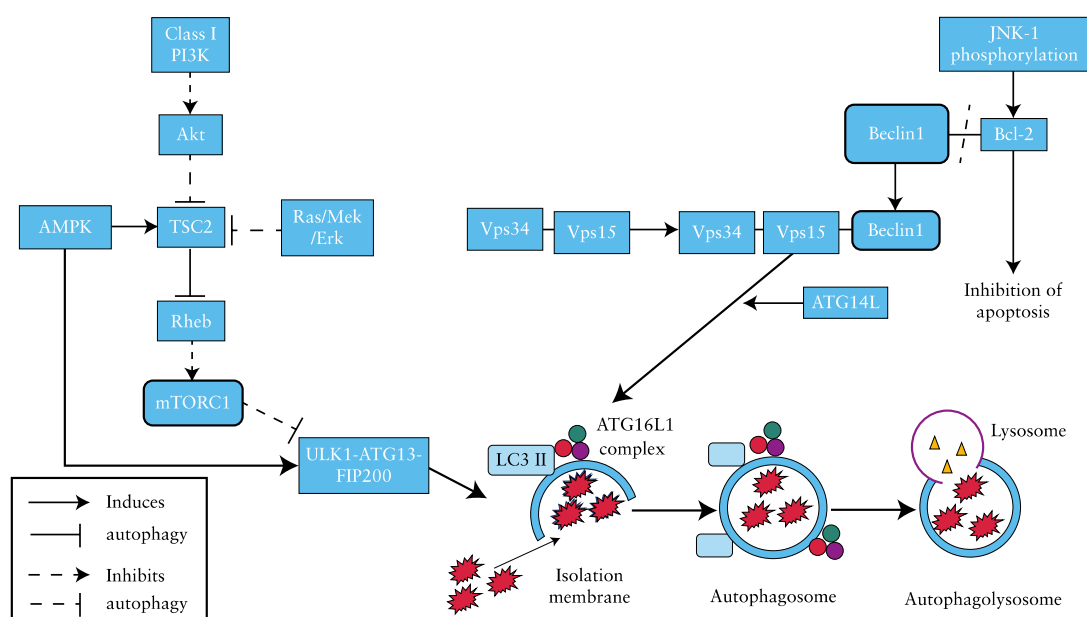


Figure 2. Autophagy regulation. The central pathways in autophagy regulation are mTORC1 and Beclin1/Bcl-2. class I PI3K, via Akt and Ras/Mek/Erk signalling pathways phosphorylate Tuberin [TSC2] to promote Rheb-dependent activation of mTORC1. When active, mTORC1 inhibits formation of the ULK1-ATG13-FIP200 complex, which is necessary for initiation of autophagy. Conversely, AMPK is involved in the inhibition of mTORC1 and stimulates autophagy via phosphorylation of ULK1 at sites distinct from mTORC1. Bcl-2 is dissociated from Beclin1 due to JNK-1-dependent phosphorylation of Bcl-2. Bcl-2 is then free to inhibit apoptosis through binding of BAX and Bak. Beclin1 is free to bind Vps34-Vps15 [the mammalian homologue of Vps15 is p150] to induce autophagy. The Vps34-Vps15-Beclin1 complex binds to ATG14L to induce further ATG protein recruitment and elongation of the isolation membrane in the initial stages of autophagy. Activated ULK1 and AMPK can also directly phosphorylate Beclin1 for the induction of autophagy [not shown].

can act as a switch between autophagy, a pro-survival response to cellular stress and apoptosis, a mechanism to limit damage to neighbouring cells under conditions of prolonged stress.²⁴ A rheostat model proposed by Pattingre *et al.*²⁰ suggests that when autophagy exceeds physiological levels, then autophagic-cell death can occur due to over-digestion of essential cellular components. The complex relationship between autophagy and apoptotic cell death has been reviewed elsewhere.²⁵

3. Autophagy and Crohn's Disease

Xenophagy [a specific type of autophagy that degrades microorganisms] is central to the innate immune response. It can target and degrade intracellular pathogens, stimulate the production of host defence peptides and present antigens to initiate the adaptive immune response.²⁶ During infection, microbe-associated molecular patterns [MAMPs] are detected by a family of proteins called pattern recognition receptors [PRRs] located within host cells. PRRs involved in xenophagy include the Nod-like receptors [NLRs], Toll-like receptors [TLRs] and sequestosome 1/p62-like receptors [SLRs]²⁷.

The PRR *NOD2* was the first gene to be linked to CD susceptibility in 2001,^{28–30} with the three most common CD-associated *NOD2* single nucleotide polymorphism [SNP] variants [R702W, G908R and L1007f/s] identified in roughly one-third of patients.³¹ Furthermore, homozygous mutation of the *NOD2* gene increases the risk of developing CD 20- to 40-fold.^{31,32} The *NOD2* L1007f/s variant is unable to detect muramyl dipeptide [MDP], a component of bacterial cell walls, which results in deficient nuclear factor

kappa-light-chain-enhancer of activated B cells [NFκB] signalling and host defence peptide secretion.³³ In 2007 the first autophagy gene, *ATG16L1*, was linked to CD susceptibility,³⁴ followed by the identification of variants in autophagy genes including *IRGM* and *LRKK2*.⁸ An SNP identified in *ATG16L1*, that encodes for a single amino acid substitution [T300A],³⁴ has been modelled in hypomorphic mice.³⁵ These mice do not spontaneously develop intestinal inflammation but do show evidence of Paneth cell dysfunction that is similar to Paneth cells from patients homozygous for the T300A allele.³⁶ A recent functional study using a T300A knock-in mouse model has demonstrated that the T300A variant creates a caspase cleavage site, making *ATG16L1* more susceptible to caspase-3-mediated degradation.³⁷

The majority of functional studies have focused on *NOD2* and *ATG16L1*, which are among the strongest risk factors in CD. These studies have reported decreased autophagy levels in a range of cell types derived from CD patients, and cells harbouring *NOD2* L1007f/s or *ATG16L1* T300A variants exhibit a number of disrupted functions linked to autophagy, including impaired autophagosome formation and degradation of cytoplasmic microorganisms, defective presentation of bacterial antigens to CD4⁺ T cells and alterations in Paneth cell granule formation.^{33,38–41} Importantly, in intestinal epithelial cells and dendritic cells [DCs] that harbour the *NOD2* L1007f/s or *ATG16L1* T300A variants, MDP-induced autophagy is diminished, leading to ineffective killing of pathogens such as *Salmonella typhimurium*, *Shigella flexneri* and Adherent Invasive *Escherichia coli* [AIEC].³³ It has been suggested this may be due to the inability of *NOD2* L1007f/s to recruit *ATG16L1* T300A protein and the autophagy machinery to

sites of bacterial entry at the cytoplasmic membrane.⁴² The increased levels of pro-inflammatory cytokines observed in CD patients have also been linked to autophagy dysregulation. Loss of functional *ATG16L1* protein results in increased pro-inflammatory IL-1 β and IL-18 production in murine studies³⁹ and in human peripheral blood mononuclear cells.⁴⁰ It has been suggested that when bound to NOD2, *ATG16L1* acts as a modulator of NOD2 activity, shifting the balance between autophagy and cytokine production; loss of functional *ATG16L1* shifts NOD2 activity towards pro-inflammatory signalling.⁴⁰ Autophagy is required for presentation of antigens derived from degraded bacterial components to the adaptive immune system.²⁶ This is of particular importance as dysregulation of T-cell responses are a key feature of CD pathogenesis. DCs from CD patients expressing the NOD2 L1007fs or *ATG16L1* T300A variants have disrupted antigen sampling and processing⁴¹ and are incapable of antigen presentation via major histocompatibility complex [MHC] II.³³

Little is known about the function of *IRGM* and *LRRK2* in CD. A deletion polymorphism immediately upstream of *IRGM* found in strong linkage disequilibrium with the most strongly CD-associated SNP, causes *IRGM* to segregate into CD risk variant [deletion] and protective variant [no deletion].⁴³ Subsequently it has been shown that a family of microRNAs [miRNAs], miR-196, that is overexpressed in the inflammatory intestinal epithelia of individuals with CD, down-regulates the *IRGM* protective variant but not the risk-associated variant. Functionally, the loss of *IRGM* protective variant expression compromises autophagy and control of the intracellular replication of CD-associated AIEC.⁴⁴ Interestingly, a recent study has placed *IRGM* in a central role for the orchestration of core autophagy machinery in response to microbial infection.⁴⁴ It was shown that *IRGM* regulates the formation of a complex containing NOD2 and *ATG16L1* that is necessary for the induction of xenophagy. The interaction of *IRGM* with NOD2 also stimulates phosphorylation cascades involving AMPK, ULK1 and Beclin1 that regulate autophagy initiation complexes.⁴⁴ *LRRK2* expression is enriched in human immune cells and is increased in colonic biopsy specimens from patients with CD.⁴⁵ Functionally, *LRRK2* can enhance NF κ B-dependent transcription, whereas small interfering RNA [siRNA] knockdown of *LRRK2* in RAW 264.7 macrophages interferes with reactive oxygen species production and bacterial killing.⁴⁵

Common upstream signalling pathways regulate autophagy; however, its activation can have different functional outcomes that operate in a cell-type specific manner. Consistent with this conditional knockout mouse models of autophagy genes *ATG16L1* and *ATG5* are selectively important for the biology of the Paneth cell, with notable abnormalities observed in the granule exocytosis pathway.³⁶ *IRGM1*-deficient mice also exhibit abnormalities in Paneth cell location and granule morphology, accompanied with increased susceptibility to inflammation in the colon and ileum.⁴⁶ *LRRK2* deficiency confers enhanced susceptibility to experimental colitis in mice; however, this was associated with enhanced nuclear localization of the transcription factor nuclear factor of activated T cells [NFAT1], important for regulating innate immune responses.⁴⁷ Specifically, it was found that there was aberrant activation of bone marrow-derived macrophages from the *LRRK2* deficient mice following exposure to various stimulators of innate immunity. Clearly, a comprehensive understanding of the cell-specific nature of autophagy and autophagy-related proteins is essential for understanding its role in IBD.

3.1. ER stress and autophagy

ER stress results from unfolded and misfolded protein accumulation in the ER, with cells that naturally secrete large amounts of protein,

such as Paneth cells, being more susceptible to ER stress.⁴⁸ The ability of highly secretory cells to respond to and resolve the ER stress depends on the unfolded protein response [UPR].⁴⁸ Genetic studies have identified several ER stress/UPR genes that are associated with IBD,⁴⁹ most notably *XBP1*, and there is evidence that ER stress levels are increased in the intestines of patients with IBD.⁹ Autophagy activity is high in Paneth cells⁵⁰ and can act to counterbalance ER stress⁵¹; therefore ER stress is a significant risk when the UPR or autophagy is not functional. Consistent with this, targeted deletion of either *XBP1* or *ATG16L1* in intestinal epithelial cells is associated with severe spontaneous CD-like transmural ileitis if both genes are compromised.⁵⁰ Importantly, in Paneth cells of patients harbouring an *ATG16L1* T300A risk allele, the ER-stress markers 78 kDa glucose-regulated protein [GRP78] and phospho-eukaryotic initiation factor 2 α subunit [pEIF2 α] were highly expressed.⁵² This has led to suggestion that the *ATG16L1* T300A variant may define a specific subtype of patients with CD, characterized by Paneth cell ER stress, which correlates with bacterial persistence and reduced antimicrobial functionality.⁵² Interestingly, a recent study has demonstrated a direct link between NOD1/2 and ER stress-induced inflammation.⁵³ In mouse and human cells, the ER stress inducers thapsigargin and dithiothreitol trigger the production of the pro-inflammatory cytokine IL-6 in a NOD1/2-dependent manner. Furthermore, IL-6 production induced by the intracellular pathogen *Brucella abortus*, which also induces ER stress, was dependent upon NOD1/2-signalling. Therefore, it is significant that major risk factors for CD, *ATG16L1* and NOD2, functionally intersect with ER stress and the UPR. The convergence between autophagy and ER stress provides new opportunity for the treatment of IBD. For example, modulation of the UPR in combination with autophagy inducers is a promising therapeutic strategy.

3.2. Current IBD drugs

The mechanism of action of current IBD drugs remains incompletely understood [Table 1]. However, progress has been made in recent years towards characterising their effects, with the modulation of immunoregulatory signalling pathways often linked directly or indirectly to the autophagy response [Table 2]. Importantly these heterogeneous studies have been conducted in a wide variety of disease settings and cell types; highlighting the need to explore the effect of these drugs on autophagy pathway activity in the context of IBD.

3.3. Corticosteroids

The first-line treatment for CD and UC is often corticosteroids. Corticosteroids downregulate pro-inflammatory cytokines including IL-1, IL-6 and tumor necrosis factor alpha (TNF α), by inhibiting the transcription of genes involved in their production and affecting the stability of messenger RNA [mRNA] to inhibit protein expression.⁵⁴ Furthermore, inflammatory signalling induced by NF κ B is decreased due to interaction with corticosteroid receptors.⁵⁴ Although there is limited knowledge of the effect of corticosteroids on autophagy in IBD, there has been some progress in understanding their effect on autophagy in other disease settings.

The clinical response to corticosteroids in UC patients has been linked to mTORC1 [Figure 3]. In a transcriptomics study, it was observed that miRNA and mRNA profiles in the rectal mucosa of UC patients differed between responders and non-responders to corticosteroid treatment.⁵⁵ The mRNA with the most significant differential expression between groups was DNA damage-induced transcript 4 [DDIT4], an inhibitor of mTORC1 activity, which was upregulated in responders after 3 days of corticosteroid treatment.

Table 1. IBD drugs mechanism of action.

Drug class	Examples	Mechanism of action
Corticosteroids	Prednisolone, budesonide	<ul style="list-style-type: none"> • Downregulation of pro-inflammatory cytokines⁵⁴ • Interference with NFκB inflammatory signalling⁵⁴
Aminosalicylates	Sulphasalazine, mesalazine	<ul style="list-style-type: none"> • Scavenging of damaging reactive oxygen species [ROS], upregulation of endogenous antioxidant systems, inhibition of leukocyte motility and leukotriene and platelet activation, interference with NFκB, TNFα, IL-1 and TGF-β, inhibition of nitric oxide formation, prevention of mitochondrial damage and colonic epithelial cell arrest in S-phase⁹
Thiopurines	Azathioprine, 6-mercaptopurine	<ul style="list-style-type: none"> • Inhibition of DNA, RNA and protein synthesis, causing results in immune suppression and cytotoxicity⁷⁵ • Induce T cell apoptosis through co-stimulation of CD28 due to the blockage of RAC1 activation of NFκB⁷⁶
Immunomodulators	Methotrexate, cyclosporin and tacrolimus	<ul style="list-style-type: none"> • Methotrexate inhibits DNA and RNA synthesis in rapidly dividing cells⁸³ • Cyclosporin and tacrolimus alter IL-2 transcription causing reduced T-cell activity⁸³
Biologics [Anti-TNF agents]	Infliximab, adalimumab	<ul style="list-style-type: none"> • Anti-TNFα antibodies neutralize TNFα to prevent pro-inflammatory functions

Table 2. Inflammatory bowel disease drugs linked to autophagy modulation.

Drug class	Evidence of autophagy modulation
Corticosteroids	<ul style="list-style-type: none"> • Corticosteroids upregulated mTORC1 inhibitors to induce autophagy in skeletal muscle <i>in vivo</i>, L6 myoblasts⁵⁷ and primary human lymphocytes⁵⁸ • Dexamethasone induced autophagy in T lymphocytes⁶²⁻⁶⁴
Aminosalicylates	<ul style="list-style-type: none"> • Inhibition of autophagy in human monocytes infected with <i>Aspergillus fumigatus</i>⁶⁵ • Sulphasalazine decreased autophagy via NFκB inhibition in an <i>in vivo</i> murine model of cachectic cancer⁷⁰ • Sulphasalazine induced autophagic cell death through inhibition of the Akt pathway and activation of the ERK pathway in an oral squamous cell carcinoma cell line⁷²
Thiopurines	<ul style="list-style-type: none"> • Autophagy is activated in hepatocytes treated with thiopurines⁷³ • Increased autophagy in epithelial cells of animal colitis model due to rapid local bacterial conversion of thioguanine pro-drug to active metabolite⁸⁰
Immunomodulators	<ul style="list-style-type: none"> • Cyclosporin cytotoxicity induced autophagy as a survival process in malignant glioma cells⁸³, primary cultured human renal tubular cells and <i>in vivo</i> with rat kidneys⁸⁴ and in kidney proximal tubule epithelial cells⁸⁵ • Cyclosporin induced autophagic-cell death in a rat pituitary cell line⁸⁶. • Tacrolimus induced autophagy in mouse neuroblastoma and microglial cell lines and in the brains of tacrolimus-treated mice⁸⁰
Biologics [Anti-TNF agents]	<ul style="list-style-type: none"> • Anti-TNF agents can induce reactivation of TB, at least partially due to decreased autophagy⁹⁷ • TNF stimulates autophagy in synovial fibroblasts from rheumatoid arthritis patients,⁹³ in skeletal muscle,⁹⁴ in atherosclerotic vascular smooth cells,⁹⁹ in trophoblastic cells⁹⁵ and in mouse macrophages⁹⁶

Furthermore, three miRNAs that were differentially expressed in responders could potentially target DDIT4.

In the hippocampus of rats, it has also been shown that corticosterone treatment affects mTORC1 signalling pathways.⁵⁶ In this study, corticosterone upregulated the expression of DDIT4, as well as FK506-binding protein 51 [FKBP51], but downregulated DDIT3. DDIT4 and FKBP51 inhibit mTORC1 activity, whereas the pro-apoptotic transcription factor DDIT3 is itself regulated by mTORC1.⁵⁶ In agreement, Wang *et al.*⁵⁷ found that dexamethasone treatment of *in vivo* skeletal muscle and cultured L6 myoblasts increased DDIT4 expression and confirmed that DDIT4 downregulates mTORC1 activity. Another study, investigating the effects of dexamethasone treatment on T lymphocytes from healthy donors, found that there was a reduction in mTORC1 expression.⁵⁸ Taken together, these studies strongly suggest that the mTORC1 pathway and autophagy play an important role in the response to treatment with corticosteroids.

Corticosteroid treatment is often associated with secondary osteoporosis and several studies have investigated the effects of corticosteroids on osteocyte cell fate. It has been shown *in vitro* and *in vivo* that low doses of prednisolone and dexamethasone induce autophagy in osteocytes and this is associated with osteocyte viability.^{59,60} However, higher doses of corticosteroids induce apoptosis, suggesting that autophagy may act as a protective mechanism against the cytotoxic effects of corticosteroids.⁵⁹ Autophagy is also activated in spinal cord injuries [SCL] along with apoptosis and necrosis; however, rats treated with methylprednisolone exhibited decreased autophagy post-SCL.⁶¹ The effects of methylprednisolone on autophagy in this study may therefore be attributed to direct inhibition of autophagy or to a decrease in inflammation associated with injury, which indirectly reduces autophagy.

Corticosteroids are also used to treat lymphoid malignancies by blocking cell proliferation and inducing apoptosis in immature T cells. It has been shown that glucocorticoids induce autophagy in

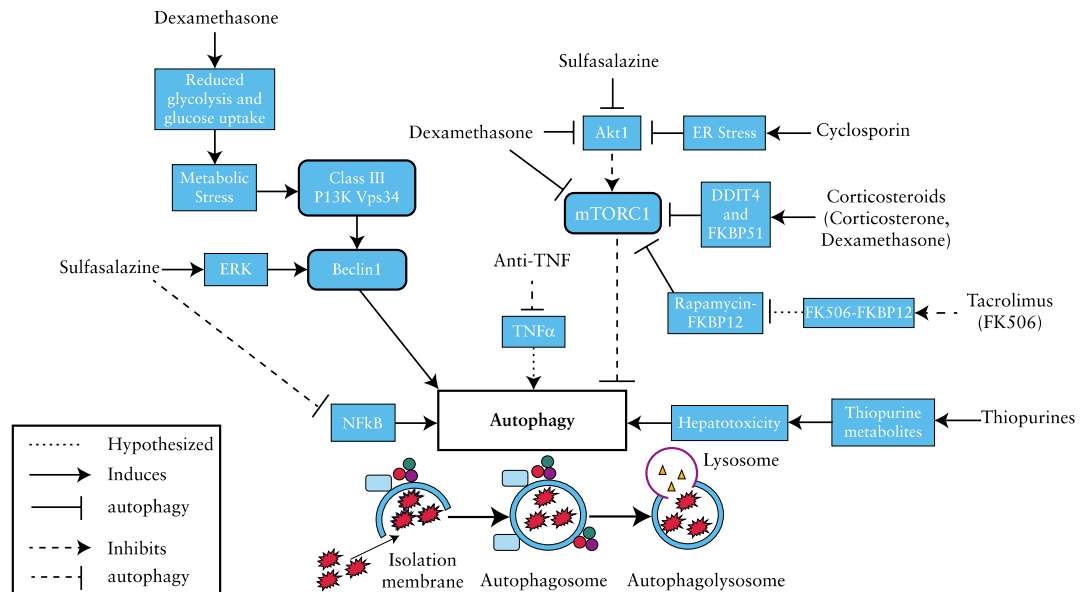


Figure 3. Current inflammatory bowel disease drugs modulation of autophagy pathways. Refer to the text and Table 2 for details.

immature T cell populations,⁶² lymphoid cell lines⁶³ and primary leukaemia cells.⁶⁴ The dexamethasone-induced increase in autophagy was also associated with inhibition of mTORC1, possibly through regulation of the Src kinase Fyn.⁶² Swerdlow *et al.*⁶³ suggested that a contributing factor to dexamethasone-induced autophagy could be metabolic stress caused by reduced glycolysis and glucose uptake in corticosteroid-treated lymphocytes [Figure 3]. Autophagy stimulation by glucocorticoids is relevant for treatment of lymphoid malignancies as it is intimately linked to the induction of apoptosis in T lymphocytes.^{63,64} Corticosteroids are able to induce apoptosis in immature T lymphocytes, as these cells lack the inhibitor of apoptosis protein Bcl-2. When Bcl-2 was overexpressed in immature T lymphocytes, dexamethasone-induced apoptosis was shown to be inhibited.⁶³ Although Bcl-2 usually inhibits autophagy by binding to Beclin1 [Figure 2], it has been shown that overexpression of Bcl-2 in immature T lymphocytes can increase autophagy levels, presumably due to inhibition of apoptosis.⁶³ Furthermore, autophagy induction prolonged the survival of dexamethasone-treated cells, and autophagy inhibition decreased survival time.⁶³ In contrast, Laane *et al.*⁶⁴ found that autophagy played a positive role in dexamethasone-induced apoptosis in lymphoid leukaemia cells. In this study, dexamethasone induced cell death through promyelocytic leukaemia [PML] protein-dependent dephosphorylation of the autophagy inhibitor Akt, stimulating the induction of autophagy [Figure 3].

Investigating fungal pathogen elimination in human monocytes demonstrated that corticosteroids could block autophagy protein recruitment to pathogen-containing phagosomes.⁶⁵ Detection of the fungal ligand β -glucan by Dectin-1 receptors triggered Syk kinase-dependent production of reactive oxygen species [ROS], which stimulate autophagy when cells are infected by *Aspergillus fumigatus*.⁶⁵ When autophagy was directly inhibited, or cells were treated with corticosteroids [*in vivo* and *ex vivo*], phagosome maturation [including fusion with the lysosome] and *A. fumigatus* killing were impaired.⁶⁵ This highlights the importance of autophagy as a

defence mechanism against fungal infections, but contradicts studies suggesting that autophagy is induced by corticosteroid treatment. Whereas this study focused on the effects of corticosteroids on xenophagy with *A. fumigatus*, other studies investigating T lymphocytes focused on non-selective macroautophagy induced by cellular stress. The contrasting results could be due to differences between the types of immune cells investigated, the disease pathogenesis, the types of corticosteroids used or the different types of autophagy that were investigated, and serves to highlight the cell-type specific nature of autophagy and the need to investigate the effect of corticosteroids on cell types that are relevant to IBD.

3.4. Aminosalicylates

Aminosalicylates are effective as first-line drugs to induce and maintain remission in mild to moderate cases of UC.⁶⁶ Despite a lack of evidence for their efficacy in CD treatment, they are often prescribed as adjuvant therapy due to minimal side effects, low cost and chemo-preventative properties.^{3,67} Sulphasalazine or salicylazosulphapyridine [SASP] was originally developed for rheumatoid arthritis and contains 5-aminosalicylate [5-ASA] bound to sulphapyridine.⁶⁸ Sulphapyridine exhibits direct antimicrobial activity and treatments with sulphapyridine have been linked to alterations in faecal bacterial profiles.⁶⁹ Sulphapyridine has been associated with additional adverse effects,³ leading to the development of other forms of aminosalicylates including mesalazine. These consist of only the active moiety of SASP and does not contain sulphapyridine; pro-drugs of mesalazine, for example balsalazide and olsalazine, are also in use.⁶⁸ The anti-inflammatory activities of 5-ASA include the scavenging of damaging ROS, upregulation of endogenous antioxidant systems, inhibition of leukocyte motility, leukotriene and platelet activation, interference with NF κ B, TNF α , IL-1 and TGF- β , inhibition of nitric oxide formation, prevention of mitochondrial damage and colonic epithelial cell-cycle arrest in S-phase.⁶⁹ In theory, many of these activities could directly or indirectly affect autophagy

due to a reduction of cellular stress. One study, investigating sulphasalazine as an NF κ B inhibitor in an *in vivo* murine model of cancer cachexia, reported a decrease in autophagy⁷⁰ [Figure 3]. This could be due to a direct effect of NF κ B inhibition, as NF κ B signalling regulates autophagy in a context-dependent manner,⁷¹ or through one or more of the other pathways regulated by sulphasalazine. In addition, this response may be specific to the disease or to the muscle tissues being examined in murine models. In contrast, Han *et al.*⁷² reported that sulphasalazine treatment in an oral squamous cell carcinoma [OSCC] cell line, HSC-4, induced autophagic cell death through inhibition of the Akt pathway and activation of the ERK pathway [Figure 3]. The seemingly opposing effects of sulphasalazine observed in these studies may be due to differences in dosage. Dosage is extremely difficult to compare between *in vitro* and *in vivo* studies; however, it is possible that the induction of autophagic cell death observed by Han *et al.*⁷² may be representative of a concentration range that is cytotoxic.

3.5. Thiopurines

Thiopurines, including azathioprine, 6-mercaptopurine and 6-thioguanine, are immunosuppressant drugs used to treat IBD.⁷³ They have a relatively slow onset but can maintain remission in moderate to severe cases of CD and have also shown some effectiveness for the induction of remission.^{3,74} The commonly used pro-drug azathioprine is converted to 6-mercaptopurine [6-MP] by glutathione in the intestinal wall. Through a multi-step enzymatic pathway, the drug is broken down to thiopurine metabolites, thioguanine nucleotides [TGN] and methylmercaptopurine nucleotides [MMPN]. These nucleotides act as purine antagonists causing the inhibition of DNA, RNA and protein synthesis, which results in immunosuppression and cytotoxicity.⁷⁵ Azathioprine can also generate 6-thioguanine GTP, which has been shown to induce T cell apoptosis through co-stimulation of the CD28 receptor due to blockage of Ras-related C3 botulinum toxin substrate [Rac1] activation of NF κ B.⁷⁶ Erythrocyte concentrations of thiopurine metabolites are now carefully monitored in many centres, to maintain therapeutic levels and to assess adherence, as increases in blood concentration have been associated with hepatotoxicity.⁷⁷ Other severe adverse effects associated with thiopurines are pancreatitis and myelosuppression,³ with 15–20% of patients treated with thiopurines having to discontinue treatment due to these side effects.⁷⁵

Due to the severe adverse effects of thiopurines, a potential protective role for autophagy in hepatocytes has been investigated. Autophagy is activated in hepatocytes treated with thiopurines, possibly as a secondary response to the hepatotoxic effects of the drug [Figure 3]; however, it could also indicate that autophagy is directly modulated to balance immune responses in patients.^{73,78} Despite the lack of understanding of the mechanism of action of thiopurines, it has been shown that autophagy has a protective role in hepatocytes during thiopurine therapy,⁷³ suggesting that a combination treatment of thiopurines with drugs that induce autophagy may reduce their adverse effects, enhancing their efficacy and safety.

A very recent study has correlated ATG16L1 genotype and response to thiopurines in two IBD cohorts and found that the ATG16L1 risk variant associates with response to thiopurine treatment specifically in patients with CD but not with UC.⁷⁹ Furthermore, a defect in the autophagosomal regulation of active Rac1, a member of the Rho family of GTPases linked to the regulation of diverse cellular functions including cytoskeletal rearrangement, underlies the association between ATG16L1 and CD through decreased myeloid cell migration.⁷⁹ As thiopurine can inhibit Rac1 activity, the authors suggest that ATG16L1 genotyping may be used to identify patients who would benefit from thiopurine treatment. In another new study,

the rapid local bacterial conversion of thioguanine pro-drug to active metabolite was shown to augment autophagy in epithelial cells, resulting in increased intracellular bacterial killing and decreased intestinal inflammation and immune activation in spontaneous and induced animal colitis models.⁸⁰

3.6. Methotrexate, cyclosporin and tacrolimus

Methotrexate, cyclosporin and tacrolimus are immunomodulatory drugs used mainly as second-line treatments to maintain remission in severe, steroid-refractory CD,⁸¹ with more recent evidence suggesting a role for tacrolimus in UC.⁸² Methotrexate inhibits DNA and RNA synthesis in rapidly dividing cells, and cyclosporin and tacrolimus alter IL-2 transcription causing reduced T cell activity.⁸³ Although some evidence suggests that cyclosporin and tacrolimus modulate autophagy as part of their mechanism of action, no link has been identified between methotrexate and autophagy modulation.

Cyclosporin, originally used to prevent organ transplant rejection, acts by blocking lymphocyte and other immune cell activation.⁸³ As this drug has very cytotoxic effects, several studies have shown that treatment with cyclosporin can induce autophagy in response to the toxicity either as a survival process or as part of a cell death mechanism.^{83–86} Toxic levels of cyclosporin induced autophagy *in vivo* and *in vitro* in malignant glioma cells.⁸³ This was accompanied by mTORC1 inhibition and an ER stress response, with blockage of ER signalling decreasing accumulation of the autophagy marker LC3-II⁸³ [Figure 3]. Furthermore, when autophagy is inhibited by blocking ULK1, ATG5 or ATG7, cyclosporin-induced cell death was shown to increase.⁸³ These results suggest that autophagy is induced as a protective response to the cytotoxic effects of cyclosporin.

In a study of cyclosporin-induced nephrotoxicity, ER stress-dependent autophagy induction [Figure 3] has been demonstrated in primary cultured human renal tubular cells and *in vivo* within rat kidneys.⁸⁴ In addition, cyclosporin can cause chronic metabolic stress, which leads to autophagy induction in kidney proximal tubule epithelial cells.⁸⁵ In this study, autophagy-competent cells allow for metabolic adaptation to cyclosporin treatment, whereas autophagy deficiency resulted in cyclosporin-induced deterioration of the tricarboxylic acid [TCA] cycle and the overall energy status of the cell. In a rat pituitary cell line model, cyclosporin induced apoptosis and autophagic-cell death in a dose-dependent manner.⁸⁶ From these studies, it appears that autophagy is stimulated by cyclosporin only as a secondary response to the drug's cytotoxic effects.

The mechanism of action of tacrolimus, also known as FK506, is similar to that of cyclosporin as both drugs inhibit the protein phosphatase calcineurin to block T cell function and IL-2 transcription. FK506 inhibits calcineurin by forming a complex with the immunophilin FKBP12 [FK506 binding protein], which is involved in immunoregulation.⁸⁷ FKBP12 is also the direct target of rapamycin, an inhibitor of mTORC1.

A recent study by Ge *et al.*⁸⁸ investigating a novel activator of mTORC1, 3-benzyl-5-[[2-nitrophenoxy] methyl]-dihydrofuran-2[3H]-one [3BDO], demonstrated that 3BDO could activate mTORC1 by occupying the rapamycin-binding site in FKBP12.⁸⁹ This study suggested that FK506, through a mechanism involving the formation of an FK506-FKBP12 complex, has the potential to act as an mTORC1 activator and autophagy inhibitor [Figure 3]. In another study investigating the use of FK506 as a novel therapeutic for prion infections, FK506 was shown to induce autophagy in mouse neuroblastoma [N2a58] and mouse microglial [MG20] cell lines and in the brains of mice.⁹⁰ FK506 treatment significantly increased LC3-II, ATG5, ATG7 and autolysosome formation,

concomitant with decreased prion protein levels in cell cultures and increased survival of mice due to delayed accumulation of prion proteins.⁹⁰

3.7. Biologic agents

Overproduction of pro-inflammatory cytokines and chemokines are a common feature associated with inflammatory diseases. Monoclonal antibodies that target and neutralise cytokines such as TNF α , IL-12, IL-23, IL-21, IL-22, IL-32 and IFN- γ , with a view to decreasing pro-inflammatory signaling, are used for the treatment of IBD.⁹¹ These biologic agents are usually reserved for the treatment of refractory CD or steroid-dependent patients to induce and maintain remission.

The most commonly used biologic agent for IBD is the anti-TNF α antibody, infliximab. Other anti-TNF α treatments approved for treatment of IBD patients include adalimumab, golimumab for UC only, and certolizumab pegol, which is approved in the USA, Switzerland and Russia. Anti-TNF α biosimilars, which are cheaper versions of licensed biologic agents whose patents have now expired, have also recently been developed.⁹²

TNF α plays a major role in modulating the inflammatory response, and while the effects of TNF α have been extensively studied in a variety of cell types, its mechanism of action in the gut remains unknown. One confirmed effect of TNF α is the modulation of autophagy, which has been observed in synovial fibroblasts from rheumatoid arthritis patients,⁹³ in skeletal muscle,⁹⁴ in atherosclerotic vascular smooth cells⁹⁵ and in trophoblastic cells.⁹⁵ The effect of TNF α on mitophagy, a specific type of autophagy that involves the degradation of mitochondrial proteins and the mitochondrial organelle, has also been demonstrated in mouse macrophages.⁹⁶ This study found that macrophages activated by TNF α have increased mitophagy, resulting in increased mitochondrial protein degradation and presentation to T cells via MHC I on the cell surface of the macrophages. As macrophages play a crucial role in innate immunity and inflammation within the gastrointestinal tract, further investigation of the effects of TNF α on autophagy in this cell type will be particularly relevant to IBD.

Taken together, these studies suggest that anti-TNF agents would inhibit autophagy [Figure 3]. Although there are no studies that have directly confirmed this, there is support for this hypothesis; anti-TNF agents can induce reactivation of *Mycobacterium tuberculosis*, at least partially due to decreased autophagy.⁹⁷ This effect is likely due to the protective antibacterial and anti-inflammatory roles of autophagy in epithelial cells infected with this non-motile bacillus.⁹⁸ It is worth noting however, that TNF α can also have inhibitory effects on autophagy in some contexts. A study investigating the effects of elevated TNF α on congestive heart failure in H9C2 rat cardiomyoblasts found that, although TNF α induces autophagy, autophagic protein degradation is disrupted, as evidenced by accumulation of p62 and increased ubiquitin-proteasome pathway activity.⁹⁹ Additionally, *Andrographis paniculata* plant extract [HMPL-400], which is currently being studied in IBD trials for reduction of TNF α , IL-1 β , IFN- γ and IL-22 expression, has been shown to inhibit autophagy in cancer.¹⁰⁰ This may be due to the reduction of cytokines or another mechanism affected by HMPL-400.

4. Conclusions

The modulation of autophagy represents an exciting therapeutic option for the treatment of IBD, and evidence is already emerging that drugs currently used for the treatment of IBD can affect

the autophagy pathway. The cross-talk between autophagy and ER stress offers new options for how IBD could be targeted, and combination treatments aimed at modulating both the UPR and autophagy warrant further investigation. However, to date there is little evidence that modulation of autophagy can be directly linked to amelioration of disease, with only one published case study of the mTORC1 inhibitor sirolimus [rapamycin] improving symptoms and healing in a patient with severe refractory CD.¹⁰¹ A major caveat is that autophagy is cell type specific, which makes it difficult to mechanistically link drug-induced autophagy to modulation of disease. Irrespective of this there is a pressing need to determine how these drugs modulate the autophagy pathway, specifically in patients with known mutations in the genes regulating the autophagy apparatus, and this must begin with consolidating studies in an *in vitro* setting in cell types directly relevant to IBD. A more comprehensive understanding of their mechanisms of action will undoubtedly allow for better-informed decisions regarding suitability of drug treatment for IBD on a patient-to-patient basis.

Funding

KMH is supported by a Crohn's in Childhood Research Association [CICRA] PhD studentship [PhD/S/2014/1]. PH is supported by an NHS Research Scotland Career Researcher Fellowship.

Conflict of Interest

None.

Author Contributions

KMH, PGB, CS and PH drafted the article and revised it critically for important intellectual content.

References

1. NHS England. *NHS Standard Contract For Colorectal: Complex Inflammatory Bowel Disease [Adult]*. London: NHS England, 2013/14.
2. Bassi A, Dodd S, Williamson P, Bodger K. Cost of illness of inflammatory bowel disease in the UK: A single centre retrospective study. *Gut* 2004;53:1471–8.
3. Diefenbach KA, Breuer CK. Pediatric inflammatory bowel disease. *World J Gastroenterol* 2006;12:3204–12.
4. Bernstein CN, Loftus EV Jr, Ng SC, Lakatos PL, Mow B. Hospitalisations and surgery in Crohn's disease. *Gut* 2012;61:622–9.
5. Denson LA, Long MD, McGovern DP, et al. Challenges in IBD research: Update on progress and prioritization of the CCFAs research agenda. *Inflamm Bowel Dis* 2013;19:677–82.
6. Fiocchi C. Tailoring treatment to the individual patient will inflammatory bowel disease medicine be personalized? *Dig Dis* 2015;33[Suppl 1]:82–9.
7. Boyapati R, Satsangi J, Ho GT. Pathogenesis of Crohn's disease. *F1000Prime Rep* 2015;7:44.
8. Jostins L, Ripke S, Weersma RK, et al. Host-microbe interactions have shaped the genetic architecture of inflammatory bowel disease. *Nature* 2012;491:119–24.
9. Kaser A, Lee AH, Franke A, et al. Xbp1 links ER stress to intestinal inflammation and confers genetic risk for human inflammatory bowel disease. *Cell* 2008;134:743–56.
10. Yang Z, Klionsky DJ. Eat or be eaten: A history of macroautophagy. *Nat Cell Biol* 2010;12:814–22.
11. Levine B, Kroemer G. Autophagy in the pathogenesis of disease. *Cell* 2008;132:27–42.
12. Lamb CA, Yoshimori T, Tooze SA. The autophagosome: Origins unknown, biogenesis complex. *Nat Rev Mol Cell Biol* 2013;14:759–74.

13. Fujita N, Itoh T, Omori H, et al. The atg16l complex specifies the site of lc3 lipidation for membrane biogenesis in autophagy. *Mol Biol Cell* 2008;19:2092–100.
14. Kroemer G, Marino G, Levine B. Autophagy and the integrated stress response. *Mol Cell* 2010;40:280–93.
15. Kim YC, Guan KL. Mtor: A pharmacologic target for autophagy regulation. *J Clin Invest* 2015;125:25–32.
16. Kim J, Kundu M, Viollet B, Guan KL. Ampk and mtor regulate autophagy through direct phosphorylation of ulk1. *Nat Cell Biol* 2011;13:132–41.
17. Russell RC, Tian Y, Yuan H, et al. Ulk1 induces autophagy by phosphorylating beclin-1 and activating vps34 lipid kinase. *Nat Cell Biol* 2013;15:741–50.
18. Levine B, Sinha S, Kroemer G. Bcl-2 family members: Dual regulators of apoptosis and autophagy. *Autophagy* 2008;4:600–6.
19. Liang XH, Kleeman LK, Jiang HH, et al. Protection against fatal sindbis virus encephalitis by beclin, a novel bcl-2-interacting protein. *J Virol* 1998;72:8586–96.
20. Pattingre S, Tassa A, Qu X, et al. Bcl-2 antiapoptotic proteins inhibit beclin-1-dependent autophagy. *Cell* 2005;122:927–39.
21. Maiuri MC, Le Toumelin G, Criollo A, et al. Functional and physical interaction between bcl-x[l] and a bh3-like domain in beclin-1. *Embo J* 2007;26:2527–39.
22. Wei Y, Pattingre S, Sinha S, Bassik M, Levine B. Jnk1-mediated phosphorylation of bcl-2 regulates starvation-induced autophagy. *Mol Cell* 2008;30:678–88.
23. Bassik MC, Scorrano L, Oakes SA, Pozzan T, Korsmeyer SJ. Phosphorylation of bcl-2 regulates er ca[2+] homeostasis and apoptosis. *EMBO J* 2004;23:1207–16.
24. Wei Y, Sinha S, Levine B. Dual role of jnk1-mediated phosphorylation of bcl-2 in autophagy and apoptosis regulation. *Autophagy* 2008;4:949–51.
25. Maiuri MC, Zalckvar E, Kimchi A, Kroemer G. Self-eating and self-killing: Crosstalk between autophagy and apoptosis. *Nat Rev Mol Cell Biol* 2007;8:741–52.
26. Deretic V, Saitoh T, Akira S. Autophagy in infection, inflammation and immunity. *Nat Rev Immunol* 2013;13:722–37.
27. Delgado M, Singh S, De Haro S, et al. Autophagy and pattern recognition receptors in innate immunity. *Immunol Rev* 2009;227:189–202.
28. Hugot JP, Chamaillard M, Zouali H, et al. Association of nod2 leucine-rich repeat variants with susceptibility to Crohn's disease. *Nature* 2001;411:599–603.
29. Hampe J, Cuthbert A, Croucher PJ, et al. Association between insertion mutation in nod2 gene and Crohn's disease in German and British populations. *Lancet* 2001;357:1925–8.
30. Ogura Y, Bonen DK, Inohara N, et al. A frameshift mutation in nod2 associated with susceptibility to Crohn's disease. *Nature* 2001;411:603–6.
31. Niess JH, Klaus J, Stephani J, et al. Nod2 polymorphism predicts response to treatment in Crohn's disease first steps to a personalized therapy. *Dig Dis Sci* 2012;57:879–86.
32. Lesage S, Zouali H, Cézard J-P, et al. Card15/nod2 mutational analysis and genotype-phenotype correlation in 612 patients with inflammatory bowel disease. *Am J Hum Genet* 2002;70:845–57.
33. Cooney R, Baker J, Brain O, et al. Nod2 stimulation induces autophagy in dendritic cells influencing bacterial handling and antigen presentation. *Nat Med* 2010;16:90–7.
34. Hampe J, Franke A, Rosenstiel P, et al. A genome-wide association scan of nonsynonymous snps identifies a susceptibility variant for Crohn disease in atg16l1. *Nat Genet* 2007;39:207–11.
35. Cadwell K, Patel KK, Maloney NS, et al. Virus-plus-susceptibility gene interaction determines Crohn's disease gene atg16l1 phenotypes in intestine. *Cell* 2010;141:1135–45.
36. Cadwell K, Liu JY, Brown SL, et al. A key role for autophagy and the autophagy gene atg16l1 in mouse and human intestinal paneth cells. *Nature* 2008;456:259–63.
37. Murthy A, Li Y, Peng I, et al. A Crohn's disease variant in atg16l1 enhances its degradation by caspase 3. *Nature* 2014;506:456–62.
38. Homer CR, Richmond AL, Rebert NA, Achkar JP, McDonald C. Atg16l1 and nod2 interact in an autophagy-dependent antibacterial pathway implicated in Crohn's disease pathogenesis. *Gastroenterology* 2010;139:1630–41.
39. Saitoh T, Fujita N, Jang MH, et al. Loss of the autophagy protein atg16l1 enhances endotoxin-induced il-1beta production. *Nature* 2008;456:264–8.
40. Plantinga TS, Crisan TO, Oosting M, et al. Crohn's disease-associated atg16l1 polymorphism modulates pro-inflammatory cytokine responses selectively upon activation of nod2. *Gut* 2011;60:1229–35.
41. Strisciuglio C, Miele E, Wildenberg ME, et al. T300a variant of autophagy atg16l1 gene is associated with decreased antigen sampling and processing by dendritic cells in pediatric Crohn's disease. *Inflamm Bowel Dis* 2013;19:2339–48.
42. Travassos LH, Carneiro LA, Ramjeet M, et al. Nod1 and nod2 direct autophagy by recruiting atg16l1 to the plasma membrane at the site of bacterial entry. *Nat Immunol* 2010;11:55–62.
43. McCarroll SA, Huett A, Kuballa P, et al. Deletion polymorphism upstream of irgm associated with altered irgm expression and Crohn's disease. *Nat Genet* 2008;40:1107–12.
44. Brest P, Lapaquette P, Souidi M, et al. A synonymous variant in irgm alters a binding site for mir-196 and causes deregulation of irgm-dependent xenophagy in Crohn's disease. *Nat Genet* 2011;43:242–5.
45. Gardet A, Benita Y, Li C, et al. Lrrk2 is involved in the ifn-gamma response and host response to pathogens. *J Immunol* 2010;185:5577–85.
46. Liu B, Gulati AS, Cantillana V, et al. Irgm1-deficient mice exhibit paneth cell abnormalities and increased susceptibility to acute intestinal inflammation. *Am J Physiol Gastrointest Liver Physiol* 2013;305:G573–84.
47. Liu Z, Lee J, Krummey S, et al. The kinase lrrk2 is a regulator of the transcription factor nfat that modulates the severity of inflammatory bowel disease. *Nat Immunol* 2011;12:1063–70.
48. Todd DJ, Lee AH, Glimcher LH. The endoplasmic reticulum stress response in immunity and autoimmunity. *Nat Rev Immunol* 2008;8:663–74.
49. McGuckin MA, Eri RD, Das I, Lourie R, Florin TH. ER stress and the unfolded protein response in intestinal inflammation. *Am J Physiol Gastrointest Liver Physiol* 2010;298:G820–32.
50. Adolph TE, Tomczak MF, Niederreiter L, et al. Paneth cells as a site of origin for intestinal inflammation. *Nature* 2013;503:272–6.
51. Ogata M, Hino S, Saito A, et al. Autophagy is activated for cell survival after endoplasmic reticulum stress. *Mol Cell Biol* 2006;26:9220–31.
52. Deuring JJ, Fuhler GM, Konstantinov SR, et al. Genomic atg16l1 risk allele-restricted paneth cell ER stress in quiescent Crohn's disease. *Gut* 2014;63:1081–91.
53. Keestra-Gounder AM, Byndloss MX, Seyffert N, et al. Nod1 and nod2 signalling links ER stress with inflammation. *Nature* 2016;532:394–7.
54. Kuenzig ME, Rezaie A, Seow CH, et al. Budesonide for maintenance of remission in Crohn's disease. *Cochrane Database Syst Rev* 2014;8:CD002913.
55. Naves JE, Manye J, Loren V, et al. P042 response to corticosteroids in ulcerative colitis may be related to modulation of mtor signaling pathway genes by micromas. *J Crohns Colitis* 2015;9[Suppl 1]:S98.
56. Polman JA, Hunter RG, Speksnijder N, et al. Glucocorticoids modulate the mtor pathway in the hippocampus: Differential effects depending on stress history. *Endocrinology* 2012;153:4317–27.
57. Wang H, Kubica N, Ellisen LW, Jefferson LS, Kimball SR. Dexamethasone represses signaling through the mammalian target of rapamycin in muscle cells by enhancing expression of redd1. *J Biol Chem* 2006;281:39128–34.
58. Fatkhullina AR, Abramov SN, Skibo Iu V, Abramova ZI. [Dexamethasone affect on the expression of bcl-2 and mtor genes in t-lymphocytes from healthy donors]. *Tsitologiya* 2014;56:459–61.
59. Jia G, Cheng G, Gangahar DM, Agrawal DK. Insulin-like growth factor-1 and tnf-alpha regulate autophagy through c-jun n-terminal kinase and akt pathways in human atherosclerotic vascular smooth cells. *Immunol Cell Biol* 2006;84:448–54.
60. Xia X, Kar R, Gluhak-Heinrich J, et al. Glucocorticoid-induced autophagy in osteocytes. *J Bone Miner Res* 2010;25:2479–88.
61. Chen HC, Fong TH, Lee AW, Chiu WT. Autophagy is activated in injured neurons and inhibited by methylprednisolone after experimental spinal cord injury. *Spine* 2012;37:470–5.
62. Harr MW, McColl KS, Zhong F, Molitoris JK, Distelhorst CW. Glucocorticoids downregulate fyn and inhibit ip[3]-mediated calcium signaling to promote autophagy in t lymphocytes. *Autophagy* 2010;6:912–21.

63. Swerdlow S, McColl K, Rong Y, *et al.* Apoptosis inhibition by bcl-2 gives way to autophagy in glucocorticoid-treated lymphocytes. *Autophagy* 2008;4:612–20.
64. Laane E, Tamm KP, Buentke E, *et al.* Cell death induced by dexamethasone in lymphoid leukemia is mediated through initiation of autophagy. *Cell Death Differ* 2009;16:1018–29.
65. Kyrmizi I, Gresnigt MS, Akoumianaki T, *et al.* Corticosteroids block autophagy protein recruitment in aspergillus fumigatus phagosomes via targeting dectin-1/syk kinase signaling. *J Immunol* 2013;191:1287–99.
66. Turner D, Levine A, Escher JC, *et al.* Management of pediatric ulcerative colitis: Joint ECCO and ESPGHAN evidence-based consensus guidelines. *J Pediatr Gastroenterol Nutr* 2012;55:340–61.
67. Schoepfer AM, Bortolotti M, Pittet V, *et al.* The gap between scientific evidence and clinical practice: 5-aminosalicylates are frequently used for the treatment of Crohn's disease. *Aliment Pharmacol Ther* 2014;40:930–7.
68. Crohn's and Colitis Foundation of America. *Aminosalicylates*. 2013. www.ccf.org/assets/pdfs/aminosalicylates.pdf
69. Campregher C, Gasche C. Aminosalicylates. *Best Pract Res Clin Gastroenterol* 2011;25:535–46.
70. Chacon-Cabrera A, Fermoselle C, Urtreger AJ, *et al.* Pharmacological strategies in lung cancer-induced cachexia: Effects on muscle proteolysis, autophagy, structure, and weakness. *J Cell Physiol* 2014;229:1660–72.
71. Salminen A, Hyttinen JMT, Kauppinen A, Kaarniranta K. Context-dependent regulation of autophagy by ikk-nf-kb signaling: Impact on the aging process. *Int J Cell Biol* 2012;2012:849541.
72. Han HY, Kim H, Jeong SH, Lim DS, Ryu MH. Sulfasalazine induces autophagic cell death in oral cancer cells via akt and erk pathways. *Asian Pac J Cancer Prev* 2014;15:6939–44.
73. Guizarro LG, Roman ID, Fernandez-Moreno MD, Gisbert JP, Hernandez-Breijo B. Is the autophagy induced by thiopurines beneficial or deleterious? *Curr Drug Metab* 2012;13:1267–76.
74. Gisbert JP, Chaparro M, Gomollon F. Common misconceptions about 5-aminosalicylates and thiopurines in inflammatory bowel disease. *World J Gastroenterol* 2011;17:3467–78.
75. Stocco G, Cuzzoni E, De Iudicibus S, *et al.* Thiopurine metabolites variations during co-treatment with aminosalicylates for inflammatory bowel disease: Effect of n-acetyl transferase polymorphisms. *World J Gastroenterol* 2015;21:3571–8.
76. Tiede I, Fritz G, Strand S, *et al.* Cd28-dependent rac1 activation is the molecular target of azathioprine in primary human cd4+ t lymphocytes. *J Clin Invest* 2003;111:1133–45.
77. Gardiner SJ, Geary RB, Burt MJ, Ding SL, Barclay ML. Severe hepatotoxicity with high 6-methylmercaptopurine nucleotide concentrations after thiopurine dose escalation due to low 6-thioguanine nucleotides. *Eur J Gastroenterol Hepatol* 2008;20:1238–42.
78. Petit E, Langouet S, Akhdar H, *et al.* Differential toxic effects of azathioprine, 6-mercaptopurine and 6-thioguanine on human hepatocytes. *Toxicol In Vitro* 2008;22:632–42.
79. Wildenberg M, Koelink P, Diederik K, *et al.* Autophagy regulates dendritic cell migration through rac1: Implications for thiopurine therapy. *J Crohns Colitis* 2016;10[Suppl 1]:S3–S4.
80. Oancea I, Das I, Aguirre de Carcer D, *et al.* Bacterial activation of thioguanine results in lymphocyte independent improvement in murine colitis. *J Crohns Colitis* 2016;10[Suppl 1]:S117.
81. Markowitz J, Grancher K, Kohn N, Daum F. Immunomodulatory therapy for pediatric inflammatory bowel disease: Changing patterns of use, 1990–2000. *Am J Gastroenterol* 2002;97:928–32.
82. Nuki Y, Esaki M, Asano K, *et al.* Comparison of the therapeutic efficacy and safety between tacrolimus and infliximab for moderate-to-severe ulcerative colitis: A single center experience. *Scand J Gastroenterol* 2016;51:700–5.
83. Ciecchomska IA, Gabrusiewicz K, Szczepankiewicz AA, Kaminska B. Endoplasmic reticulum stress triggers autophagy in malignant glioma cells undergoing cyclosporine a-induced cell death. *Oncogene* 2013;32:1518–29.
84. Pallet N, Bouvier N, Legendre C, *et al.* Autophagy protects renal tubular cells against cyclosporine toxicity. *Autophagy* 2008;4:783–91.
85. Kimura T, Takahashi A, Takabatake Y, *et al.* Autophagy protects kidney proximal tubule epithelial cells from mitochondrial metabolic stress. *Autophagy* 2013;9:1876–86.
86. Kim HS, Choi S-I, Jeung E-B, Yoo Y-M. Cyclosporine a induces apoptotic and autophagic cell death in rat pituitary gh3 cells. *PLoS One* 2014;9:e108981.
87. Liu J, Albers MW, Wandless TJ, *et al.* Inhibition of t cell signaling by immunophilin-ligand complexes correlates with loss of calcineurin phosphatase activity. *Biochemistry* 1992;31:3896–901.
88. Ge D, Han L, Huang S, *et al.* Identification of a novel mtor activator and discovery of a competing endogenous rna regulating autophagy in vascular endothelial cells. *Autophagy* 2014;10:957–71.
89. Amiot A, Peyrin-Biroulet L. Current, new and future biological agents on the horizon for the treatment of inflammatory bowel diseases. *Ther Adv Gastroenterol* 2015;8:66–82.
90. Nakagaki T, Satoh K, Ishibashi D, *et al.* Fk506 reduces abnormal prion protein through the activation of autolysosomal degradation and prolongs survival in prion-infected mice. *Autophagy* 2013;9:1386–94.
91. Nys K, Agostinis P, Vermeire S. Autophagy: A new target or an old strategy for the treatment of Crohn's disease? *Nat Rev Gastroenterol Hepatol* 2013;10:395–401.
92. de Ridder L, Waterman M, Turner D, *et al.* Use of biosimilars in paediatric inflammatory bowel disease: A position statement of the ESPGHAN Paediatric IBD Porto group. *J Pediatr Gastroenterol Nutr* 2015;61:5038.
93. Connor AM, Mahomed N, Gandhi R, Keystone EC, Berger SA. Tnfalpha modulates protein degradation pathways in rheumatoid arthritis synovial fibroblasts. *Arthritis Res Ther* 2012;14:R62.
94. Keller CW, Fokken C, Turville SG, *et al.* Tnf- α induces macroautophagy and regulates mhc class ii expression in human skeletal muscle cells. *J Biol Chem* 2011;286:3970–80.
95. Cha HH, Hwang JR, Kim HY, *et al.* Autophagy induced by tumor necrosis factor alpha mediates intrinsic apoptosis in trophoblastic cells. *Reprod Sci* 2014;21:612–22.
96. Bell C, English L, Boulais J, *et al.* Quantitative proteomics reveals the induction of mitophagy in tumor necrosis factor- α -activated [tnfa] macrophages. *Mol Cell Proteomics* 2013;12:2394–407.
97. Harris J, Keane J. How tumour necrosis factor blockers interfere with tuberculosis immunity. *Clin Exp Immunol* 2010;161:1–9.
98. Castillo EF, Dekonenko A, Arko-Mensah J, *et al.* Autophagy protects against active tuberculosis by suppressing bacterial burden and inflammation. *Proc Natl Acad Sci U S A* 2012;109:E3168–76.
99. Opperman CM, Sishi BJ. Tumor necrosis factor alpha stimulates p62 accumulation and enhances proteasome activity independently of ros. *Cell Biol Toxicol* 2015;31:83–94.
100. Zhou J, Hu SE, Tan SH, *et al.* Andrographolide sensitizes cisplatin-induced apoptosis via suppression of autophagosome-lysosome fusion in human cancer cells. *Autophagy* 2012;8:338–49.
101. Massey DC, Bredin F, Parkes M. Use of sirolimus [rapamycin] to treat refractory Crohn's disease. *Gut* 2008;57:1294–6.

12. References

- Aarbakke, J., Janka-Schaub, G., Elion, G.B., 1997. Thiopurine biology and pharmacology. *Trends Pharmacol. Sci.* 18, 3–7. [https://doi.org/10.1016/S0165-6147\(96\)01007-3](https://doi.org/10.1016/S0165-6147(96)01007-3)
- Adams, J.M., Cory, S., 2007. The Bcl-2 apoptotic switch in cancer development and therapy. *Oncogene* 26, 1324–1337. <https://doi.org/10.1038/sj.onc.1210220>
- Adolph, T.E., Tomczak, M.F., Niederreiter, L., Ko, H.-J., Böck, J., Martinez-Naves, E., Glickman, J.N., Tschurtschenthaler, M., Hartwig, J., Hosomi, S., Flak, M.B., Cusick, J.L., Kohno, K., Iwawaki, T., Billmann-Born, S., Raine, T., Bharti, R., Lucius, R., Kweon, M.-N., Marciniak, S.J., Choi, A., Hagen, S.J., Schreiber, S., Rosenstiel, P., Kaser, A., Blumberg, R.S., 2013. Paneth cells as a site of origin for intestinal inflammation. *Nature*. <https://doi.org/10.1038/nature12599>
- Agnholt, J., Kalltoft, K., 2001. In situ activated intestinal T cells expanded in vitro--without addition of antigen--produce IFN-gamma and IL-10 and preserve their function during growth. *Exp. Clin. Immunogenet.* 18, 213–225. <https://doi.org/10.1159/000049200>
- Ahmad, T., Armuzzi, A., Bunce, M., Mulcahy-Hawes, K., Marshall, S.E., Orchard, T.R., Crawshaw, J., Large, O., de Silva, A., Cook, J.T., Barnardo, M., Cullen, S., Welsh, K.I., Jewell, D.P., 2002. The molecular classification of the clinical manifestations of Crohn's disease. *Gastroenterology* 122, 854–866.
- Ahn, S.-H., Shah, Y.M., Inoue, J., Morimura, K., Kim, I., Yim, S., Lambert, G., Kurotani, R., Nagashima, K., Gonzalez, F.J., Inoue, Y., 2008. Hepatocyte nuclear factor 4 α in the intestinal epithelial cells protects against inflammatory bowel disease. *Inflamm. Bowel Dis.* 14, 908–920. <https://doi.org/10.1002/ibd.20413>
- Akobeng, A.K., Zachos, M., 2004. Tumor necrosis factor-alpha antibody for induction of remission in Crohn's disease. *Cochrane Database Syst. Rev.* CD003574. <https://doi.org/10.1002/14651858.CD003574.pub2>
- Aldo, P.B., Craveiro, V., Guller, S., Mor, G., 2013. Effect of Culture Conditions on the Phenotype of THP-1 Monocyte Cell Line. *Am. J. Reprod. Immunol.* 70, 80–86. <https://doi.org/10.1111/aji.12129>
- Alers, S., Löffler, A.S., Wesselborg, S., Stork, B., 2012. Role of AMPK-mTOR-Ulk1/2 in the regulation of autophagy: cross talk, shortcuts, and feedbacks. *Mol Cell Biol* 32, 2–11. <https://doi.org/10.1128/mcb.06159-11>
- Amiot, A., Peyrin-Biroulet, L., 2015. Current, new and future biological agents on the horizon for the treatment of inflammatory bowel diseases. *Ther. Adv Gastroenterol* 8, 66–82. <https://doi.org/10.1177/1756283x14558193>
- Amir, M., Zhao, E., Fontana, L., Rosenberg, H., Tanaka, K., Gao, G., Czaja, M.J., 2013. Inhibition of hepatocyte autophagy increases tumor necrosis factor-dependent liver injury by promoting caspase-8 activation. *Cell Death Differ.* 20, 878–887. <https://doi.org/10.1038/cdd.2013.21>
- Amre, D.K., Mack, D.R., Morgan, K., Krupoves, A., Costea, I., Lambrette, P., Grimard, G., Dong, J., Feguery, H., Bucionis, V., Deslandres, C., Levy, E., Seidman, E.G., 2009. Autophagy gene ATG16L1 but not IRGM is associated with Crohn's disease in Canadian children. *Inflamm. Bowel Dis.* 15, 501–507. <https://doi.org/10.1002/ibd.20785>
- Appenzeller-Herzog, C., Hall, M.N., 2012. Bidirectional crosstalk between endoplasmic reticulum stress and mTOR signaling. *Trends Cell Biol.* 22, 274–282. <https://doi.org/10.1016/j.tcb.2012.02.006>

- Arnold, J., Murera, D., Arbogast, F., Fauny, J.-D., Muller, S., Gros, F., 2016. Autophagy is dispensable for B-cell development but essential for humoral autoimmune responses. *Cell Death Differ.* 23, 853–864. <https://doi.org/10.1038/cdd.2015.149>
- Asada, R., Saito, A., Kawasaki, N., Kanemoto, S., Iwamoto, H., Oki, M., Miyagi, H., Izumi, S., Imaizumi, K., 2012. The Endoplasmic Reticulum Stress Transducer OASIS Is involved in the Terminal Differentiation of Goblet Cells in the Large Intestine. *J. Biol. Chem.* 287, 8144–8153. <https://doi.org/10.1074/jbc.M111.332593>
- Ashton, J.J., Ennis, S., Beattie, R.M., 2017. Early-onset paediatric inflammatory bowel disease. *Lancet Child Adolesc. Health* 1, 147–158. [https://doi.org/10.1016/S2352-4642\(17\)30017-2](https://doi.org/10.1016/S2352-4642(17)30017-2)
- Avivar-Valderas, A., Bobrovnikova-Marjon, E., Diehl, J.A., Bardeesy, N., Debnath, J., Aguirre-Ghiso, J., 2013. Regulation of autophagy during ECM detachment is linked to a selective inhibition of mTORC1 by PERK. *Oncogene* 32, 4932–4940. <https://doi.org/10.1038/onc.2012.512>
- Avivar-Valderas, A., Salas, E., Bobrovnikova-Marjon, E., Diehl, J.A., Nagi, C., Debnath, J., Aguirre-Ghiso, J.A., 2011. PERK Integrates Autophagy and Oxidative Stress Responses To Promote Survival during Extracellular Matrix Detachment. *Mol. Cell. Biol.* 31, 3616–3629. <https://doi.org/10.1128/MCB.05164-11>
- Baillie, J.K., Arner, E., Daub, C., Hoon, M.D., Itoh, M., Kawaji, H., Lassmann, T., Carninci, P., Forrest, A.R.R., Hayashizaki, Y., Consortium, F., Faulkner, G.J., Wells, C.A., Rehli, M., Pavli, P., Summers, K.M., Hume, D.A., 2017. Analysis of the human monocyte-derived macrophage transcriptome and response to lipopolysaccharide provides new insights into genetic aetiology of inflammatory bowel disease. *PLOS Genet.* 13, e1006641. <https://doi.org/10.1371/journal.pgen.1006641>
- Bajnok, A., Ivanova, M., Rigó, J., Toldi, G., 2017. The Distribution of Activation Markers and Selectins on Peripheral T Lymphocytes in Preeclampsia [WWW Document]. *Mediators Inflamm.* <https://doi.org/10.1155/2017/8045161>
- Barnich, N., Aguirre, J.E., Reinecker, H.-C., Xavier, R., Podolsky, D.K., 2005. Membrane recruitment of NOD2 in intestinal epithelial cells is essential for nuclear factor- κ B activation in muramyl dipeptide recognition. *J. Cell Biol.* 170, 21–26. <https://doi.org/10.1083/jcb.200502153>
- Barnich, N., Boudeau, J., Claret, L., Darfeuille-Michaud, A., 2003. Regulatory and functional co-operation of flagella and type 1 pili in adhesive and invasive abilities of AIEC strain LF82 isolated from a patient with Crohn's disease. *Mol. Microbiol.* 48, 781–794.
- Barnich, N., Bringer, M.-A., Claret, L., Darfeuille-Michaud, A., 2004. Involvement of lipoprotein Nlpl in the virulence of adherent invasive Escherichia coli strain LF82 isolated from a patient with Crohn's disease. *Infect. Immun.* 72, 2484–2493.
- Barrett, J.C., Hansoul, S., Nicolae, D.L., Cho, J.H., Duerr, R.H., Rioux, J.D., Brant, S.R., Silverberg, M.S., Taylor, K.D., Barmada, M.M., Bitton, A., Dassopoulos, T., Datta, L.W., Green, T., Griffiths, A.M., Kistner, E.O., Murtha, M.T., Ragueiro, M.D., Rotter, J.I., Schumm, L.P., Steinhart, A.H., Targan, S.R., Xavier, R.J., Libioulle, C., Sandor, C., Lathrop, M., Belaiche, J., Dewit, O., Gut, I., Heath, S., Laukens, D., Mni, M., Rutgeerts, P., Van Gossum, A., Zelenika, D., Franchimont, D., Hugot, J.P., de Vos, M., Vermeire, S., Louis, E., Cardon, L.R., Anderson, C.A., Drummond, H., Nimmo, E., Ahmad, T., Prescott, N.J., Onnie, C.M., Fisher, S.A., Marchini, J., Ghorji, J., Bumpstead, S., Gwilliam, R., Tremelling, M., Deloukas, P., Mansfield, J., Jewell,

- D., Satsangi, J., Mathew, C.G., Parkes, M., Georges, M., Daly, M.J., 2008. Genome-wide association defines more than 30 distinct susceptibility loci for Crohn's disease. *Nat Genet* 40, 955–62. <https://doi.org/10.1038/ng.175>
- Bassi, A., Dodd, S., Williamson, P., Bodger, K., 2004. Cost of illness of inflammatory bowel disease in the UK: a single centre retrospective study. *Gut* 53, 1471–8. <https://doi.org/10.1136/gut.2004.041616>
- Bassik, M.C., Scorrano, L., Oakes, S.A., Pozzan, T., Korsmeyer, S.J., 2004. Phosphorylation of BCL-2 regulates ER Ca²⁺ homeostasis and apoptosis. *EMBO J.* 23, 1207–1216. <https://doi.org/10.1038/sj.emboj.7600104>
- Baumgart, M., Dogan, B., Rishniw, M., Weitzman, G., Bosworth, B., Yantiss, R., Orsi, R.H., Wiedmann, M., McDonough, P., Kim, S.G., Berg, D., Schukken, Y., Scherl, E., Simpson, K.W., 2007. Culture independent analysis of ileal mucosa reveals a selective increase in invasive *Escherichia coli* of novel phylogeny relative to depletion of Clostridiales in Crohn's disease involving the ileum. *ISME J.* 1, 403–418. <https://doi.org/10.1038/ismej.2007.52>
- Baxt, L.A., Garza-Mayers, A.C., Goldberg, M.B., 2013. Bacterial subversion of host innate immune pathways. *Science* 340, 697–701. <https://doi.org/10.1126/science.1235771>
- B'chir, W., Maurin, A.-C., Carraro, V., Averous, J., Jousse, C., Muranishi, Y., Parry, L., Stepien, G., Fafournoux, P., Bruhat, A., 2013. The eIF2 α /ATF4 pathway is essential for stress-induced autophagy gene expression. *Nucleic Acids Res.* 41, 7683–7699. <https://doi.org/10.1093/nar/gkt563>
- Becker, C., Wirtz, S., Blessing, M., Pirhonen, J., Strand, D., Bechthold, O., Frick, J., Galle, P.R., Autenrieth, I., Neurath, M.F., 2003. Constitutive p40 promoter activation and IL-23 production in the terminal ileum mediated by dendritic cells. *J. Clin. Invest.* 112, 693–706. <https://doi.org/10.1172/JCI17464>
- Bell, C., English, L., Boulais, J., Chemali, M., Caron-Lizotte, O., Desjardins, M., Thibault, P., 2013. Quantitative proteomics reveals the induction of mitophagy in tumor necrosis factor- α -activated (TNF α) macrophages. *Mol. Cell. Proteomics* 12, 2394–2407.
- Benchimol, E.I., Mack, D.R., Nguyen, G.C., Snapper, S.B., Li, W., Mojaverian, N., Quach, P., Muise, A.M., 2014. Incidence, outcomes, and health services burden of very early onset inflammatory bowel disease. *Gastroenterology* 147, 803-813.e7; quiz e14-15. <https://doi.org/10.1053/j.gastro.2014.06.023>
- Benjamin, J., Makharia, G.K., Ahuja, V., Kalaivani, M., Joshi, Y.K., 2008. Intestinal permeability and its association with the patient and disease characteristics in Crohn's disease. *World J. Gastroenterol.* WJG 14, 1399–1405. <https://doi.org/10.3748/wjg.14.1399>
- Bernard, A., Jin, M., González-Rodríguez, P., Füllgrabe, J., Delorme-Axford, E., Backues, S.K., Joseph, B., Klionsky, D.J., 2015. Rph1/KDM4 mediates nutrient-limitation signaling that leads to the transcriptional induction of autophagy. *Curr. Biol.* CB 25, 546–555. <https://doi.org/10.1016/j.cub.2014.12.049>
- Bernard, A., Klionsky, D.J., 2015. Rph1 mediates the nutrient-limitation signaling pathway leading to transcriptional activation of autophagy. *Autophagy* 11, 718–719. <https://doi.org/10.1080/15548627.2015.1018503>
- Bernhagen, J., Krohn, R., Lue, H., Gregory, J.L., Zerneck, A., Koenen, R.R., Dewor, M., Georgiev, I., Schober, A., Leng, L., Kooistra, T., Fingerle-Rowson, G., Ghezzi, P., Kleemann, R., McColl, S.R., Bucala, R., Hickey, M.J., Weber, C., 2007. MIF is a

- noncognate ligand of CXC chemokine receptors in inflammatory and atherogenic cell recruitment. *Nat. Med.* 13, 587–596. <https://doi.org/10.1038/nm1567>
- Bernstein, C.N., Loftus, E.V., Jr., Ng, S.C., Lakatos, P.L., Moum, B., 2012. Hospitalisations and surgery in Crohn's disease. *Gut* 61, 622–9. <https://doi.org/10.1136/gutjnl-2011-301397>
- Bertolotti, A., Wang, X., Novoa, I., Jungreis, R., Schlessinger, K., Cho, J.H., West, A.B., Ron, D., 2001. Increased sensitivity to dextran sodium sulfate colitis in IRE1 β -deficient mice. *J. Clin. Invest.* 107, 585–593.
- Betin, V.M.S., Lane, J.D., 2009. Caspase cleavage of Atg4D stimulates GABARAP-L1 processing and triggers mitochondrial targeting and apoptosis. *J. Cell Sci.* 122, 2554–2566. <https://doi.org/10.1242/jcs.046250>
- Birgisdottir, Å.B., Lamark, T., Johansen, T., 2013. The LIR motif - crucial for selective autophagy. *J. Cell Sci.* 126, 3237–3247. <https://doi.org/10.1242/jcs.126128>
- Birmingham, C.L., Canadien, V., Gouin, E., Troy, E.B., Yoshimori, T., Cossart, P., Higgins, D.E., Brumell, J.H., 2007. *Listeria monocytogenes* evades killing by autophagy during colonization of host cells. *Autophagy* 3, 442–451.
- Boada-Romero, E., Serramito-Gómez, I., Sacristán, M.P., Boone, D.L., Xavier, R.J., Pimentel-Muiños, F.X., 2016. The T300A Crohn's disease risk polymorphism impairs function of the WD40 domain of ATG16L1. *Nat. Commun.* 7, 11821. <https://doi.org/10.1038/ncomms11821>
- Bonen, D.K., Ogura, Y., Nicolae, D.L., Inohara, N., Saab, L., Tanabe, T., Chen, F.F., Foster, S.J., Duerr, R.H., Brant, S.R., Cho, J.H., Nuñez, G., 2003. Crohn's disease-associated NOD2 variants share a signaling defect in response to lipopolysaccharide and peptidoglycan. *Gastroenterology* 124, 140–146. <https://doi.org/10.1053/gast.2003.50019>
- Boudeau, J., Barnich, N., Darfeuille-Michaud, A., 2001. Type 1 pili-mediated adherence of *Escherichia coli* strain LF82 isolated from Crohn's disease is involved in bacterial invasion of intestinal epithelial cells. *Mol. Microbiol.* 39, 1272–1284. <https://doi.org/10.1111/j.1365-2958.2001.02315.x>
- Boudeau, J., Glasser, A.-L., Masseret, E., Joly, B., Darfeuille-Michaud, A., 1999. Invasive Ability of an *Escherichia coli* Strain Isolated from the Ileal Mucosa of a Patient with Crohn's Disease. *Infect. Immun.* 67, 4499–4509.
- Bouman, L., Schlierf, A., Lutz, A.K., Shan, J., Deinlein, A., Kast, J., Galehdar, Z., Palmisano, V., Patenge, N., Berg, D., Gasser, T., Augustin, R., Trümbach, D., Irrcher, I., Park, D.S., Wurst, W., Kilberg, M.S., Tatzelt, J., Winklhofer, K.F., 2011. Parkin is transcriptionally regulated by ATF4: evidence for an interconnection between mitochondrial stress and ER stress. *Cell Death Differ.* 18, 769–782. <https://doi.org/10.1038/cdd.2010.142>
- Boya, P., Kroemer, G., 2008. Lysosomal membrane permeabilization in cell death. *Oncogene* 27, 6434–6451. <https://doi.org/10.1038/onc.2008.310>
- Boyapati, R., Satsangi, J., Ho, G.T., 2015. Pathogenesis of Crohn's disease. *F1000Prime Rep* 7, 44. <https://doi.org/10.12703/p7-44>
- Boyapati, R.K., Dorward, D.A., Tamborska, A., Kalla, R., Ventham, N.T., Doherty, M.K., Whitfield, P.D., Gray, M., Loane, J., Rossi, A.G., Satsangi, J., Ho, G.-T., 2018. Mitochondrial DNA Is a Pro-Inflammatory Damage-Associated Molecular Pattern Released During Active IBD. *Inflamm. Bowel Dis.* <https://doi.org/10.1093/ibd/izy095>
- Boyapati, R.K., Ho, G.-T., Satsangi, J., 2017. Can Thiopurines Prevent Formation of Antibodies Against Tumor Necrosis Factor Antagonists After Failure of These

- Therapies? Clin. Gastroenterol. Hepatol. 15, 76–78. <https://doi.org/10.1016/j.cgh.2016.09.152>
- Brandl, K., Rutschmann, S., Li, X., Du, X., Xiao, N., Schnabl, B., Brenner, D.A., Beutler, B., 2009. Enhanced sensitivity to DSS colitis caused by a hypomorphic Mbtps1 mutation disrupting the ATF6-driven unfolded protein response. Proc. Natl. Acad. Sci. U. S. A. 106, 3300–3305. <https://doi.org/10.1073/pnas.0813036106>
- Brandtzaeg, P., Carlsen, H.S., Halstensen, T.S., 2006. The B-cell system in inflammatory bowel disease. Adv. Exp. Med. Biol. 579, 149–167. https://doi.org/10.1007/0-387-33778-4_10
- Brant, S.R., Picco, M.F., Achkar, J.-P., Bayless, T.M., Kane, S.V., Brzezinski, A., Nouvet, F.J., Bonen, D., Karban, A., Dassopoulos, T., Karaliukas, R., Beaty, T.H., Hanauer, S.B., Duerr, R.H., Cho, J.H., 2003. Defining complex contributions of NOD2/CARD15 gene mutations, age at onset, and tobacco use on Crohn's disease phenotypes. Inflamm. Bowel Dis. 9, 281–289.
- Brest, P., Lapaquette, P., Souidi, M., Lebrigand, K., Cesaro, A., Vouret-Craviari, V., Mari, B., Barbry, P., Mosnier, J.F., Hebuterne, X., Harel-Bellan, A., Mograbi, B., Darfeuille-Michaud, A., Hofman, P., 2011. A synonymous variant in IRGM alters a binding site for miR-196 and causes deregulation of IRGM-dependent xenophagy in Crohn's disease. Nat Genet 43, 242–5. <https://doi.org/10.1038/ng.762>
- Bringer, M.-A., Barnich, N., Glasser, A.-L., Bardot, O., Darfeuille-Michaud, A., 2005. HtrA Stress Protein Is Involved in Intramacrophagic Replication of Adherent and Invasive Escherichia coli Strain LF82 Isolated from a Patient with Crohn's Disease. Infect. Immun. 73, 712–721. <https://doi.org/10.1128/IAI.73.2.712-721.2005>
- Bringer, M.-A., Billard, E., Glasser, A.-L., Colombel, J.-F., Darfeuille-Michaud, A., 2012. Replication of Crohn's disease-associated AIEC within macrophages is dependent on TNF- α secretion. Lab. Invest. 92, 411. <https://doi.org/10.1038/labinvest.2011.156>
- Bringer, M.-A., Glasser, A.-L., Tung, C.-H., Méresse, S., Darfeuille-Michaud, A., 2006. The Crohn's disease-associated adherent-invasive Escherichia coli strain LF82 replicates in mature phagolysosomes within J774 macrophages. Cell. Microbiol. 8, 471–484. <https://doi.org/10.1111/j.1462-5822.2005.00639.x>
- Buffie, C.G., Pamer, E.G., 2013. Microbiota-mediated colonization resistance against intestinal pathogens. Nat. Rev. Immunol. 13, 790–801. <https://doi.org/10.1038/nri3535>
- Burt, B.M., Plitas, G., Nguyen, H.M., Stableford, J.A., Bamboat, Z.M., DeMatteo, R.P., 2008. Circulating HLA-DR+ natural killer cells have potent lytic ability and weak antigen-presenting cell function. Hum. Immunol. 69, 469–474. <https://doi.org/10.1016/j.humimm.2008.06.009>
- Byun, J.-Y., Yoon, C.-H., An, S., Park, I.-C., Kang, C.-M., Kim, M.-J., Lee, S.-J., 2009. The Rac1/MKK7/JNK pathway signals upregulation of Atg5 and subsequent autophagic cell death in response to oncogenic Ras. Carcinogenesis 30, 1880–1888. <https://doi.org/10.1093/carcin/bgp235>
- Cader, M.Z., Kaser, A., 2013. Recent advances in inflammatory bowel disease: mucosal immune cells in intestinal inflammation. Gut 62, 1653–1664. <https://doi.org/10.1136/gutjnl-2012-303955>
- Cadwell, K., Liu, J., Brown, S.L., Miyoshi, H., Loh, J., Lennerz, J., Kishi, C., KC, W., Carrero, J.A., Hunt, S., Stone, C., Brunt, E.M., Xavier, R.J., Sleckman, B.P., Li, E., Mizushima, N., Stappenbeck, T.S., Virgin, H.W., 2008. A unique role for autophagy and

- Atg16L1 in Paneth cells in murine and human intestine. *Nature* 456, 259–263. <https://doi.org/10.1038/nature07416>
- Cadwell, K., Patel, K.K., Maloney, N.S., Liu, T.-C., Ng, A.C.Y., Storer, C.E., Head, R.D., Xavier, R., Stappenbeck, T.S., Virgin, H.W., 2010. Virus-Plus-Susceptibility Gene Interaction Determines Crohn's Disease Gene Atg16L1 Phenotypes in Intestine. *Cell* 141, 1135–1145. <https://doi.org/10.1016/j.cell.2010.05.009>
- Calfon, M., Zeng, H., Urano, F., Till, J.H., Hubbard, S.R., Harding, H.P., Clark, S.G., Ron, D., 2002. IRE1 couples endoplasmic reticulum load to secretory capacity by processing the XBP-1 mRNA. *Nature* 415, 92–96. <https://doi.org/10.1038/415092a>
- Campregher, C., Gasche, C., 2011. Aminosalicylates. *Best Pract. Res. Clin. Gastroenterol.* 25, 535–546. <https://doi.org/10.1016/j.bpg.2011.10.013>
- Cannavo, E., Marra, G., Sabates-Bellver, J., Menigatti, M., Lipkin, S.M., Fischer, F., Cejka, P., Jiricny, J., 2005. Expression of the MutL Homologue hMLH3 in Human Cells and its Role in DNA Mismatch Repair. *Cancer Res.* 65, 10759–10766. <https://doi.org/10.1158/0008-5472.CAN-05-2528>
- Cao, B., Zhou, X., Ma, J., Zhou, W., Yang, W., Fan, D., Hong, L., 2017. Role of MiRNAs in Inflammatory Bowel Disease. *Dig. Dis. Sci.* 62, 1426–1438. <https://doi.org/10.1007/s10620-017-4567-1>
- Cao, S.S., 2015. Endoplasmic Reticulum Stress and Unfolded Protein Response in Inflammatory Bowel Disease: *Inflamm. Bowel Dis.* 21, 636–644. <https://doi.org/10.1097/MIB.0000000000000238>
- Cao, S.S., Wang, M., Harrington, J.C., Chuang, B.-M., Eckmann, L., Kaufman, R.J., 2014. Phosphorylation of eIF2 α Is Dispensable for Differentiation but Required at a Posttranscriptional Level for Paneth Cell Function and Intestinal Homeostasis in Mice: *Inflamm. Bowel Dis.* 20, 712–722. <https://doi.org/10.1097/MIB.0000000000000010>
- Cao, S.S., Zimmermann, E.M., Chuang, B., Song, B., Nwokoyo, A., Wilkinson, J.E., Eaton, K.A., Kaufman, R.J., 2013. The Unfolded Protein Response and Chemical Chaperones Reduce Protein Misfolding and Colitis in Mice. *Gastroenterology* 144, 989-1000.e6. <https://doi.org/10.1053/j.gastro.2013.01.023>
- Cario, E., Podolsky, D.K., 2000. Differential alteration in intestinal epithelial cell expression of toll-like receptor 3 (TLR3) and TLR4 in inflammatory bowel disease. *Infect. Immun.* 68, 7010–7017.
- Carrière, J., Darfeuille-Michaud, A., Nguyen, H.T.T., 2014. Infectious etiopathogenesis of Crohn's disease. *World J. Gastroenterol. WJG* 20, 12102–12117. <https://doi.org/10.3748/wjg.v20.i34.12102>
- Castillo, E.F., Dekonenko, A., Arko-Mensah, J., Mandell, M.A., Dupont, N., Jiang, S., Delgado-Vargas, M., Timmins, G.S., Bhattacharya, D., Yang, H., Hutt, J., Lyons, C.R., Dobos, K.M., Deretic, V., 2012. Autophagy protects against active tuberculosis by suppressing bacterial burden and inflammation. *Proc Natl Acad Sci U S A* 109, E3168-76. <https://doi.org/10.1073/pnas.1210500109>
- Castillo, K., Rojas-Rivera, D., Lisbona, F., Caballero, B., Nassif, M., Court, F., Schuck, S., Ibar, C., Walter, P., Sierralta, J., Glavic, A., Hetz, C., 2011. BAX inhibitor-1 regulates autophagy by controlling the IRE1 α branch of the unfolded protein response. *EMBO J.* 30, 4465–78. <https://doi.org/10.1038/emboj.2011.318>
- CCFA, 2013. Aminosalicylates.

- Cha, H.H., Hwang, J.R., Kim, H.Y., Choi, S.J., Oh, S.Y., Roh, C.R., 2014. Autophagy induced by tumor necrosis factor alpha mediates intrinsic apoptosis in trophoblastic cells. *Reprod Sci* 21, 612–22. <https://doi.org/10.1177/1933719113508816>
- Chaabane, W., Appell, M.L., Chaabane, W., Appell, M.L., 2016. Interconnections between apoptotic and autophagic pathways during thiopurine-induced toxicity in cancer cells: the role of reactive oxygen species. *Oncotarget* 7, 75616–75634. <https://doi.org/10.18632/oncotarget.12313>
- Chacon-Cabrera, A., Fermoselle, C., Urtreger, A.J., Mateu-Jimenez, M., Diamant, M.J., de Kier Joffé, E.D.B., Sandri, M., Barreiro, E., 2014. Pharmacological Strategies in Lung Cancer-Induced Cachexia: Effects on Muscle Proteolysis, Autophagy, Structure, and Weakness: MUSCLE BIOLOGY, STRUCTURE, AND FUNCTION IN CACHEXIA. *J. Cell. Physiol.* 229, 1660–1672. <https://doi.org/10.1002/jcp.24611>
- Chan, E.Y.W., Longatti, A., McKnight, N.C., Tooze, S.A., 2009. Kinase-inactivated ULK proteins inhibit autophagy via their conserved C-terminal domains using an Atg13-independent mechanism. *Mol. Cell. Biol.* 29, 157–171. <https://doi.org/10.1128/MCB.01082-08>
- Chang, C.-P., Su, Y.-C., Hu, C.-W., Lei, H.-Y., 2013. TLR2-dependent selective autophagy regulates NF- κ B lysosomal degradation in hepatoma-derived M2 macrophage differentiation. *Cell Death Differ.* 20, 515–523. <https://doi.org/10.1038/cdd.2012.146>
- Chargui, A., Cesaro, A., Mimouna, S., Fareh, M., Brest, P., Naquet, P., Darfeuille-Michaud, A., Hébuterne, X., Mograbi, B., Vouret-Craviari, V., Hofman, P., 2012. Subversion of Autophagy in Adherent Invasive Escherichia coli-Infected Neutrophils Induces Inflammation and Cell Death. *PLOS ONE* 7, e51727. <https://doi.org/10.1371/journal.pone.0051727>
- Chauhan, S., Mandell, M.A., Deretic, V., 2015. IRGM governs the core autophagy machinery to conduct antimicrobial defense. *Mol Cell* 58, 507–21. <https://doi.org/10.1016/j.molcel.2015.03.020>
- Chauhan, Santosh, Goodwin, J.G., Chauhan, Swati, Manyam, G., Wang, J., Kamat, A.M., Boyd, D.D., 2013. ZKSCAN3 is a master transcriptional repressor of autophagy. *Mol. Cell* 50, 16–28. <https://doi.org/10.1016/j.molcel.2013.01.024>
- Chen, H.C., Fong, T.H., Lee, A.W., Chiu, W.T., 2012. Autophagy is activated in injured neurons and inhibited by methylprednisolone after experimental spinal cord injury. *Spine Phila Pa* 1976 37, 470–5. <https://doi.org/10.1097/BRS.0b013e318221e859>
- Chen, H.-R., Chuang, Y.-C., Chao, C.-H., Yeh, T.-M., 2015. Macrophage migration inhibitory factor induces vascular leakage via autophagy. *Biol. Open* 4, 244–252. <https://doi.org/10.1242/bio.201410322>
- Choi, M.S., Kim, Y., Jung, J.-Y., Yang, S.H., Lee, T.R., Shin, D.W., 2013. Resveratrol induces autophagy through death-associated protein kinase 1 (DAPK1) in human dermal fibroblasts under normal culture conditions. *Exp. Dermatol.* 22, 491–494. <https://doi.org/10.1111/exd.12175>
- Chouchana, L., Fernández-Ramos, A.A., Dumont, F., Marchetti, C., Ceballos-Picot, I., Beaune, P., Gurwitz, D., Lorient, M.-A., 2015. Molecular insight into thiopurine resistance: transcriptomic signature in lymphoblastoid cell lines. *Genome Med.* 7, 37. <https://doi.org/10.1186/s13073-015-0150-6>
- Chuang, Y.-C., Su, W.-H., Lei, H.-Y., Lin, Y.-S., Liu, H.-S., Chang, C.-P., Yeh, T.-M., 2012. Macrophage Migration Inhibitory Factor Induces Autophagy via Reactive Oxygen

- Species Generation. PLoS ONE 7, e37613.
<https://doi.org/10.1371/journal.pone.0037613>
- Ciechomska, I.A., Gabrusiewicz, K., Szczepankiewicz, A.A., Kaminska, B., 2013. Endoplasmic reticulum stress triggers autophagy in malignant glioma cells undergoing cyclosporine a-induced cell death. *Oncogene* 32, 1518–29. <https://doi.org/10.1038/onc.2012.174>
- Ciechomska, I.A., Kaminska, B., 2012. ER stress and autophagy contribute to CsA-induced death of malignant glioma cells. *Autophagy* 8, 1526–1528. <https://doi.org/10.4161/auto.21155>
- Cieza, R.J., Hu, J., Ross, B.N., Sbrana, E., Torres, A.G., 2015. The IbeA Invasin of Adherent-Invasive Escherichia coli Mediates Interaction with Intestinal Epithelia and Macrophages. *Infect. Immun.* 83, 1904–1918. <https://doi.org/10.1128/IAI.03003-14>
- Colombel, J.F., Sandborn, W.J., Reinisch, W., Mantzaris, G.J., Kornbluth, A., Rachmilewitz, D., Lichtiger, S., D’haens, G., Diamond, R.H., Broussard, D.L., 2010. Infliximab, azathioprine, or combination therapy for Crohn’s disease. *N. Engl. J. Med.* 362, 1383–1395.
- Cong, Y., Feng, T., Fujihashi, K., Schoeb, T.R., Elson, C.O., 2009. A dominant, coordinated T regulatory cell-IgA response to the intestinal microbiota. *Proc. Natl. Acad. Sci. U. S. A.* 106, 19256–19261. <https://doi.org/10.1073/pnas.0812681106>
- Connor, A.M., Mahomed, N., Gandhi, R., Keystone, E.C., Berger, S.A., 2012. TNF α modulates protein degradation pathways in rheumatoid arthritis synovial fibroblasts. *Arthritis Res Ther* 14, R62. <https://doi.org/10.1186/ar3778>
- Conte, M.P., Longhi, C., Marazzato, M., Conte, A.L., Aleandri, M., Lepanto, M.S., Zagaglia, C., Nicoletti, M., Aloï, M., Totino, V., Palamara, A.T., Schippa, S., 2014. Adherent-invasive Escherichia coli (AIEC) in pediatric Crohn’s disease patients: phenotypic and genetic pathogenic features. *BMC Res. Notes* 7, 748. <https://doi.org/10.1186/1756-0500-7-748>
- Cooney, R., Baker, J., Brain, O., Danis, B., Pichulik, T., Allan, P., Ferguson, D.J.P., Campbell, B.J., Jewell, D., Simmons, A., 2010. NOD2 stimulation induces autophagy in dendritic cells influencing bacterial handling and antigen presentation. *Nat. Med.* 16, 90–97. <https://doi.org/10.1038/nm.2069>
- Coskun, M., 2014. Intestinal Epithelium in Inflammatory Bowel Disease. *Front. Med.* 1. <https://doi.org/10.3389/fmed.2014.00024>
- Coskun, M., Olsen, A.K., Holm, T.L., Kvist, P.H., Nielsen, O.H., Riis, L.B., Olsen, J., Troelsen, J.T., 2012. TNF- α -induced down-regulation of CDX2 suppresses MEP1A expression in colitis. *Biochim. Biophys. Acta BBA - Mol. Basis Dis.* 1822, 843–851. <https://doi.org/10.1016/j.bbadis.2012.01.012>
- Cros, J., Cagnard, N., Woollard, K., Patey, N., Zhang, S.-Y., Senechal, B., Puel, A., Biswas, S.K., Moshous, D., Picard, C., Jais, J.-P., D’Cruz, D., Casanova, J.-L., Trouillet, C., Geissmann, F., 2010. Human CD14^{dim} monocytes patrol and sense nucleic acids and viruses via TLR7 and TLR8 receptors. *Immunity* 33, 375–386. <https://doi.org/10.1016/j.immuni.2010.08.012>
- Daniel, V., Trojan, K., Opelz, G., 2016. Immunosuppressive drugs affect induction of IFN γ + Treg in vitro. *Hum. Immunol.* 77, 146–152. <https://doi.org/10.1016/j.humimm.2015.11.006>
- Darfeuille-Michaud, A., Boudeau, J., Bulois, P., Neut, C., Glasser, A.-L., Barnich, N., Bringer, M.-A., Swidsinski, A., Beaugerie, L., Colombel, J.-F., 2004. High prevalence of adherent-invasive Escherichia coli associated with ileal mucosa in

- Crohn's disease. *Gastroenterology* 127, 412–421. <https://doi.org/10.1053/j.gastro.2004.04.061>
- Darfeuille-Michaud, A., Neut, C., Barnich, N., Lederman, E., Di Martino, P., Desreumaux, P., Gambiez, L., Joly, B., Md, A., Colombel, J.F., 1999. Presence of adherent *Escherichia coli* strains in ileal mucosa of patients with Crohn's disease. *Gastroenterology* 115, 1405–13. [https://doi.org/10.1016/S0016-5085\(98\)70019-8](https://doi.org/10.1016/S0016-5085(98)70019-8)
- De MIRANDA, P., Beacham, L.M., Creagh, T.H., Elion, G.B., 1973. The metabolic fate of the methylnitroimidazole moiety of azathioprine in the rat. *J. Pharmacol. Exp. Ther.* 187, 588–601.
- de Ridder, L., Waterman, M., Turner, D., Bronsky, J., Hauer, A.C., Dias, J.A., Strisciuglio, C., Ruemmele, F.M., Levine, A., Lionetti, P., 2015. Use of Biosimilars in Paediatric Inflammatory Bowel Disease: A Position Statement of the ESPGHAN Paediatric IBD Porto Group. *J Pediatr Gastroenterol Nutr.* <https://doi.org/10.1097/mpg.0000000000000903>
- Dean, L., 2012. Azathioprine Therapy and TPMT Genotype, in: Pratt, V., McLeod, H., Dean, L., Malheiro, A., Rubinstein, W. (Eds.), *Medical Genetics Summaries*. National Center for Biotechnology Information (US), Bethesda (MD).
- Delgado, M., Singh, S., De Haro, S., Master, S., Ponpuak, M., Dinkins, C., Ornatowski, W., Vergne, I., Deretic, V., 2009. Autophagy and pattern recognition receptors in innate immunity. *Immunol Rev* 227, 189–202. <https://doi.org/10.1111/j.1600-065X.2008.00725.x>
- Denson, L.A., Long, M.D., McGovern, D.P., Kugathasan, S., Wu, G.D., Young, V.B., Pizarro, T.T., de Zoeten, E.F., Stappenbeck, T.S., Plevy, S.E., Abraham, C., Nusrat, A., Jobin, C., McCole, D.F., Siegel, C.A., Higgins, P.D., Herfarth, H.H., Hyams, J., Sandborn, W.J., Loftus, E.V., Jr., Kappelman, M.D., Lewis, J.D., Parkos, C.A., Sartor, R.B., 2013. Challenges in IBD research: update on progress and prioritization of the CCFAs' research agenda. *Inflamm Bowel Dis* 19, 677–82. <https://doi.org/10.1097/MIB.0b013e31828134b3>
- Denton, D., Shrivage, B., Simin, R., Mills, K., Berry, D.L., Baehrecke, E.H., Kumar, S., 2009. Autophagy, not apoptosis, is essential for midgut cell death in *Drosophila*. *Curr. Biol. CB* 19, 1741–1746. <https://doi.org/10.1016/j.cub.2009.08.042>
- Deretic, V., Saitoh, T., Akira, S., 2013. Autophagy in infection, inflammation and immunity. *Nat Rev Immunol* 13, 722–37. <https://doi.org/10.1038/nri3532>
- Deuring, J.J., de Haar, C., Koelewijn, C.L., Kuipers, E.J., Peppelenbosch, M.P., van der Woude, C.J., 2012. Absence of ABCG2-mediated mucosal detoxification in patients with active inflammatory bowel disease is due to impeded protein folding. *Biochem. J.* 441, 87–93. <https://doi.org/10.1042/BJ20111281>
- Deuring, J.J., Fuhler, G.M., Konstantinov, S.R., Peppelenbosch, M.P., Kuipers, E.J., de Haar, C., van der Woude, C.J., 2014. Genomic ATG16L1 risk allele-restricted Paneth cell ER stress in quiescent Crohn's disease. *Gut* 63, 1081–1091. <https://doi.org/10.1136/gutjnl-2012-303527>
- Devereaux, K., Dall'Armi, C., Alcazar-Roman, A., Ogasawara, Y., Zhou, X., Wang, F., Yamamoto, A., De Camilli, P., Di Paolo, G., 2013. Regulation of mammalian autophagy by class II and III PI 3-kinases through PI3P synthesis. *PLoS One* 8, e76405. <https://doi.org/10.1371/journal.pone.0076405>
- Dibble, C.C., Elis, W., Menon, S., Qin, W., Klekota, J., Asara, J.M., Finan, P.M., Kwiatkowski, D.J., Murphy, L.O., Manning, B.D., 2012. TBC1D7 is a third subunit

- of the TSC1-TSC2 complex upstream of mTORC1. *Mol. Cell* 47, 535–546. <https://doi.org/10.1016/j.molcel.2012.06.009>
- Diefenbach, K.A., Breuer, C.K., 2006. Pediatric inflammatory bowel disease. *World J Gastroenterol* 12, 3204–12.
- Ding, W.-X., Ni, H.-M., Gao, W., Yoshimori, T., Stolz, D.B., Ron, D., Yin, X.-M., 2007. Linking of Autophagy to Ubiquitin-Proteasome System Is Important for the Regulation of Endoplasmic Reticulum Stress and Cell Viability. *Am. J. Pathol.* 171, 513–524. <https://doi.org/10.2353/ajpath.2007.070188>
- Ding, W.-X., Ni, H.-M., Li, M., Liao, Y., Chen, X., Stolz, D.B., Dorn, G.W., Yin, X.-M., 2010. Nix is critical to two distinct phases of mitophagy, reactive oxygen species-mediated autophagy induction and Parkin-ubiquitin-p62-mediated mitochondrial priming. *J. Biol. Chem.* 285, 27879–27890. <https://doi.org/10.1074/jbc.M110.119537>
- Domènech, E., Nos, P., Papo, M., López-San Román, A., Garcia-Planella, E., Gassull, M.A., 2005. 6-mercaptopurine in patients with inflammatory bowel disease and previous digestive intolerance of azathioprine. *Scand. J. Gastroenterol.* 40, 52–55.
- Dorn, S.D., Abad, J.F., Panagopoulos, G., Korelitz, B.I., 2004. Clinical characteristics of familial versus sporadic Crohn’s disease using the Vienna Classification. *Inflamm. Bowel Dis.* 10, 201–206.
- Dreux, N., Denizot, J., Martinez-Medina, M., Mellmann, A., Billig, M., Kisiela, D., Chattopadhyay, S., Sokurenko, E., Neut, C., Gower-Rousseau, C., Colombel, J.-F., Bonnet, R., Darfeuille-Michaud, A., Barnich, N., 2013. Point Mutations in FimH Adhesin of Crohn’s Disease-Associated Adherent-Invasive Escherichia coli Enhance Intestinal Inflammatory Response. *PLOS Pathog.* 9, e1003141. <https://doi.org/10.1371/journal.ppat.1003141>
- Dubinsky, M.C., 2004. Azathioprine, 6-mercaptopurine in inflammatory bowel disease: pharmacology, efficacy, and safety. *Clin. Gastroenterol. Hepatol. Off. Clin. Pract. J. Am. Gastroenterol. Assoc.* 2, 731–743.
- Dumortier, J., Lapalus, M.-G., Guillaud, O., Poncet, G., Gagnieu, M.-C., Partensky, C., Scoazec, J.-Y., 2008. Everolimus for refractory Crohn’s disease: A case report. *Inflamm. Bowel Dis.* 14, 874–877. <https://doi.org/10.1002/ibd.20395>
- Dupaul-Chicoine, J., Dagenais, M., Saleh, M., 2013. Crosstalk Between the Intestinal Microbiota and the Innate Immune System in Intestinal Homeostasis and Inflammatory Bowel Disease. *Inflamm. Bowel Dis.* 19, 2227–2237. <https://doi.org/10.1097/MIB.0b013e31828dcac7>
- Dupont, N., Lacas-Gervais, S., Bertout, J., Paz, I., Freche, B., Van Nhieu, G.T., van der Goot, F.G., Sansonetti, P.J., Lafont, F., 2009. Shigella phagocytic vacuolar membrane remnants participate in the cellular response to pathogen invasion and are regulated by autophagy. *Cell Host Microbe* 6, 137–149. <https://doi.org/10.1016/j.chom.2009.07.005>
- Eaves-Pyles, T., Allen, C.A., Taormina, J., Swidsinski, A., Tutt, C.B., Eric Jezek, G., Islas-Islas, M., Torres, A.G., 2008. Escherichia coli isolated from a Crohn’s disease patient adheres, invades, and induces inflammatory responses in polarized intestinal epithelial cells. *Int. J. Med. Microbiol.* 298, 397–409. <https://doi.org/10.1016/j.ijmm.2007.05.011>
- Ebert, E.C., Mehta, V., Das, K.M., 2005. Activation antigens on colonic T cells in inflammatory bowel disease: effects of IL-10. *Clin. Exp. Immunol.* 140, 157–165. <https://doi.org/10.1111/j.1365-2249.2005.02722.x>

- Egan, D.F., Shackelford, D.B., Mihaylova, M.M., Gelino, S.R., Kohnz, R.A., Mair, W., Vasquez, D.S., Joshi, A., Gwinn, D.M., Taylor, R., Asara, J.M., Fitzpatrick, J., Dillin, A., Viollet, B., Kundu, M., Hansen, M., Shaw, R.J., 2011. Phosphorylation of ULK1 (hATG1) by AMP-activated protein kinase connects energy sensing to mitophagy. *Science* 331, 456–461. <https://doi.org/10.1126/science.1196371>
- Eisenberg-Lerner, A., Kimchi, A., 2012. PKD is a kinase of Vps34 that mediates ROS-induced autophagy downstream of DAPk. *Cell Death Differ.* 19, 788–797. <https://doi.org/10.1038/cdd.2011.149>
- Eklund, B.I., Moberg, M., Bergquist, J., Mannervik, B., 2006. Divergent activities of human glutathione transferases in the bioactivation of azathioprine. *Mol. Pharmacol.* 70, 747–754. <https://doi.org/10.1124/mol.106.025288>
- Elgendy, M., Sheridan, C., Brumatti, G., Martin, S.J., 2011. Oncogenic Ras-induced expression of Noxa and Beclin-1 promotes autophagic cell death and limits clonogenic survival. *Mol. Cell* 42, 23–35. <https://doi.org/10.1016/j.molcel.2011.02.009>
- Elion, G.B., 1989. The purine path to chemotherapy. *Science* 244, 41–47. <https://doi.org/10.1126/science.2649979>
- Elson, C.O., Alexander, K.L., 2015. Host-Microbiota Interactions in the Intestine. *Dig. Dis.* 33, 131–136. <https://doi.org/10.1159/000369534>
- Elson, C.O., Cong, Y., 2012. Host-microbiota interactions in inflammatory bowel disease. *Gut Microbes* 3, 332–44. <https://doi.org/10.4161/gmic.20228>
- Eng, K.E., Panas, M.D., Karlsson Hedestam, G.B., McInerney, G.M., 2010. A novel quantitative flow cytometry-based assay for autophagy. *Autophagy* 6, 634–641. <https://doi.org/10.4161/auto.6.5.12112>
- Erdélyi, P., Borsos, E., Takács-Vellai, K., Kovács, T., Kovács, A.L., Sigmond, T., Hargitai, B., Pásztor, L., Sengupta, T., Dengg, M., Pécsi, I., Tóth, J., Nilsen, H., Vértessy, B.G., Vellai, T., 2011. Shared developmental roles and transcriptional control of autophagy and apoptosis in *Caenorhabditis elegans*. *J. Cell Sci.* 124, 1510–1518. <https://doi.org/10.1242/jcs.080192>
- Eri, R.D., Adams, R.J., Tran, T.V., Tong, H., Das, I., Roche, D.K., Oancea, I., Png, C.W., Jeffery, P.L., Radford-Smith, G.L., Cook, M.C., Florin, T.H., McGuckin, M.A., 2011. An intestinal epithelial defect conferring ER stress results in inflammation involving both innate and adaptive immunity. *Mucosal Immunol.* 4, 354–364. <https://doi.org/10.1038/mi.2010.74>
- Erokhina, Streltsova, Kanevskiy, Telford, Sapozhnikov, Kovalenko, 2018. HLA-DR+ NK cells are mostly characterized by less mature phenotype and high functional activity. *Immunol. Cell Biol.* 96, 212–228. <https://doi.org/10.1111/imcb.1032>
- Fakhoury, M., Negrulj, R., Mooranian, A., Al-Salami, H., 2014. Inflammatory bowel disease: clinical aspects and treatments. *J. Inflamm. Res.* 7, 113–120. <https://doi.org/10.2147/JIR.S65979>
- Fatkhullina, A.R., Abramov, S.N., Skibo lu, V., Abramova, Z.I., 2014. [Dexamethasone affect on the expression of bcl-2 and mTOR genes in T-lymphocytes from healthy donors]. *Tsitologiya* 56, 459–61.
- Fernandes, M.A., Verstraete, S.G., Garnett, E.A., Heyman, M.B., 2016. Addition of Histology to the Paris Classification of Pediatric Crohn’s Disease Alters Classification of Disease Location. *J. Pediatr. Gastroenterol. Nutr.* 62, 242–245. <https://doi.org/10.1097/MPG.0000000000000967>

- Fernández, M., Sánchez-Franco, F., Palacios, N., Sánchez, I., Fernández, C., Cacicedo, L., 2004. IGF-I inhibits apoptosis through the activation of the phosphatidylinositol 3-kinase/Akt pathway in pituitary cells. *J. Mol. Endocrinol.* 33, 155–163.
- Fernández-Ramos, A.A., Marchetti-Laurent, C., Poindessous, V., Antonio, S., Laurent-Puig, P., Bortoli, S., Lorient, M.-A., Pallet, N., 2017. 6-mercaptopurine promotes energetic failure in proliferating T cells. *Oncotarget* 8, 43048–43060. <https://doi.org/10.18632/oncotarget.17889>
- Filimonenko, M., Isakson, P., Finley, K.D., Anderson, M., Jeong, H., Melia, T.J., Bartlett, B.J., Myers, K.M., Birkeland, H.C.G., Lamark, T., Krainc, D., Brech, A., Stenmark, H., Simonsen, A., Yamamoto, A., 2010. The selective macroautophagic degradation of aggregated proteins requires the PI3P-binding protein Alfy. *Mol. Cell* 38, 265–279. <https://doi.org/10.1016/j.molcel.2010.04.007>
- Fiocchi, C., 2015. Tailoring Treatment to the Individual Patient - Will Inflammatory Bowel Disease Medicine Be Personalized? *Dig Dis* 33 Suppl 1, 82–89. <https://doi.org/10.1159/000437086>
- Frank, D.N., Robertson, C.E., Hamm, C.M., Kpadeh, Z., Zhang, T., Chen, H., Zhu, W., Sartor, R.B., Boedeker, E.C., Harpaz, N., Pace, N.R., Li, E., 2011. Disease phenotype and genotype are associated with shifts in intestinal-associated microbiota in inflammatory bowel diseases. *Inflamm. Bowel Dis.* 17, 179–184. <https://doi.org/10.1002/ibd.21339>
- Frank, D.N., St. Amand, A.L., Feldman, R.A., Boedeker, E.C., Harpaz, N., Pace, N.R., 2007. Molecular-phylogenetic characterization of microbial community imbalances in human inflammatory bowel diseases. *Proc. Natl. Acad. Sci. U. S. A.* 104, 13780–13785. <https://doi.org/10.1073/pnas.0706625104>
- Franke, A., McGovern, D.P., Barrett, J.C., Wang, K., Radford-Smith, G.L., Ahmad, T., Lees, C.W., Balschun, T., Lee, J., Roberts, R., Anderson, C.A., Bis, J.C., Bumpstead, S., Ellinghaus, D., Festen, E.M., Georges, M., Green, T., Haritunians, T., Jostins, L., Latiano, A., Mathew, C.G., Montgomery, G.W., Prescott, N.J., Raychaudhuri, S., Rotter, J.I., Schumm, P., Sharma, Y., Simms, L.A., Taylor, K.D., Whiteman, D., Wijmenga, C., Baldassano, R.N., Barclay, M., Bayless, T.M., Brand, S., Buning, C., Cohen, A., Colombel, J.F., Cottone, M., Stronati, L., Denson, T., De Vos, M., D’Inca, R., Dubinsky, M., Edwards, C., Florin, T., Franchimont, D., Gearry, R., Glas, J., Van Gossom, A., Guthery, S.L., Halfvarson, J., Verspaget, H.W., Hugot, J.P., Karban, A., Laukens, D., Lawrance, I., Lemann, M., Levine, A., Libioulle, C., Louis, E., Mowat, C., Newman, W., Panes, J., Phillips, A., Proctor, D.D., Regueiro, M., Russell, R., Rutgeerts, P., Sanderson, J., Sans, M., Seibold, F., Steinhardt, A.H., Stokkers, P.C., Torkvist, L., Kullak-Ublick, G., Wilson, D., Walters, T., Targan, S.R., Brant, S.R., Rioux, J.D., D’Amato, M., Weersma, R.K., Kugathasan, S., Griffiths, A.M., Mansfield, J.C., Vermeire, S., Duerr, R.H., Silverberg, M.S., Satsangi, J., Schreiber, S., Cho, J.H., Annesse, V., Hakonarson, H., Daly, M.J., Parkes, M., 2010. Genome-wide meta-analysis increases to 71 the number of confirmed Crohn’s disease susceptibility loci. *Nat Genet* 42, 1118–25. <https://doi.org/10.1038/ng.717>
- Fraser, A.G., Jewell, D.P., 2000. Side effects of azathioprine treatment given for inflammatory bowel disease—a 30 year audit. *Gastroenterology* 118, A787. [https://doi.org/10.1016/S0016-5085\(00\)85289-0](https://doi.org/10.1016/S0016-5085(00)85289-0)
- Freis, P., Bollard, J., Lebeau, J., Massoma, P., Favre, J., Vercherat, C., Walter, T., Manié, S., Roche, C., Scoazec, J.-Y., Ferraro-Peyret, C., 2017. mTOR inhibitors activate PERK signaling and favor viability of gastrointestinal neuroendocrine cell lines. *Oncotarget* 8, 20974–20987. <https://doi.org/10.18632/oncotarget.15469>

- Fridman, J.S., Lowe, S.W., 2003. Control of apoptosis by p53. *Oncogene* 22, 9030–9040. <https://doi.org/10.1038/sj.onc.1207116>
- Fujimoto, T., Imaeda, H., Takahashi, K., Kasumi, E., Bamba, S., Fujiyama, Y., Andoh, A., 2013. Decreased abundance of *Faecalibacterium prausnitzii* in the gut microbiota of Crohn's disease. *J. Gastroenterol. Hepatol.* 28, 613–619. <https://doi.org/10.1111/jgh.12073>
- Fujita, N., Itoh, T., Omori, H., Fukuda, M., Noda, T., Yoshimori, T., 2008. The Atg16L complex specifies the site of LC3 lipidation for membrane biogenesis in autophagy. *Mol Biol Cell* 19, 2092–100. <https://doi.org/10.1091/mbc.E07-12-1257>
- Funderburg, Stubblefield Park, Sung, Hardy, Clagett Brian, Ignatz-Hoover, Harding, Fu, Katz, Lederman, Levine, 2013. Circulating CD4+ and CD8+ T cells are activated in inflammatory bowel disease and are associated with plasma markers of inflammation. *Immunology* 140, 87–97. <https://doi.org/10.1111/imm.12114>
- Furth, R. van, Cohn, Z.A., 1968. The Origin and Kinetics of Mononuclear Phagocytes. *J. Exp. Med.* 128, 415–435. <https://doi.org/10.1084/jem.128.3.415>
- Gade, P., Manjegowda, S.B., Nallar, S.C., Maachani, U.B., Cross, A.S., Kalvakolanu, D.V., 2014. Regulation of the Death-Associated Protein Kinase 1 Expression and Autophagy via ATF6 Requires Apoptosis Signal-Regulating Kinase 1. *Mol. Cell. Biol.* 34, 4033–4048. <https://doi.org/10.1128/MCB.00397-14>
- Gade, P., Ramachandran, G., Maachani, U.B., Rizzo, M.A., Okada, T., Prywes, R., Cross, A.S., Mori, K., Kalvakolanu, D.V., 2012. An IFN- γ -stimulated ATF6-C/EBP- β -signaling pathway critical for the expression of Death Associated Protein Kinase 1 and induction of autophagy. *Proc. Natl. Acad. Sci. U. S. A.* 109, 10316–10321. <https://doi.org/10.1073/pnas.1119273109>
- Galluzzi, L., Kepp, O., Kroemer, G., 2012. Mitochondria: master regulators of danger signalling. *Nat. Rev. Mol. Cell Biol.* 13, 780–788. <https://doi.org/10.1038/nrm3479>
- Galonek, H.L., Hardwick, J.M., 2006. Upgrading the BCL-2 network. *Nat. Cell Biol.* 8, 1317–1319. <https://doi.org/10.1038/ncb1206-1317>
- Gao, J., Cheng, T.S., Qin, A., Pavlos, N.J., Wang, T., Song, K., Wang, Y., Chen, L., Zhou, L., Jiang, Q., Takayanagi, H., Yan, S., Zheng, M., 2016. Glucocorticoid impairs cell-cell communication by autophagy-mediated degradation of connexin 43 in osteocytes. *Oncotarget* 7, 26966–26978. <https://doi.org/10.18632/oncotarget.9034>
- Gao, P., Liu, H., Huang, H., Zhang, Q., Strober, W., Zhang, F., 2017. The Inflammatory Bowel Disease-Associated Autophagy Gene Atg16L1T300A Acts as a Dominant Negative Variant in Mice. *J. Immunol. Baltim. Md 1950* 198, 2457–2467. <https://doi.org/10.4049/jimmunol.1502652>
- Gao, W., Chen, S., Wu, M., Gao, K., Li, Y., Wang, H., Li, C., Li, H., 2016. Methylprednisolone exerts neuroprotective effects by regulating autophagy and apoptosis. *Neural Regen. Res.* 11, 823–828. <https://doi.org/10.4103/1673-5374.182711>
- Gardet, A., Benita, Y., Li, C., Sands, B.E., Ballester, I., Stevens, C., Korzenik, J.R., Rioux, J.D., Daly, M.J., Xavier, R.J., Podolsky, D.K., 2010. LRRK2 is involved in the IFN- γ response and host response to pathogens. *J Immunol* 185, 5577–85. <https://doi.org/10.4049/jimmunol.1000548>
- Gardiner, S.J., Gearry, R.B., Burt, M.J., Ding, S.L., Barclay, M.L., 2008. Severe hepatotoxicity with high 6-methylmercaptopurine nucleotide concentrations

- after thiopurine dose escalation due to low 6-thioguanine nucleotides. *Eur J Gastroenterol Hepatol* 20, 1238–42. <https://doi.org/10.1097/MEG.0b013e3282ffda37>
- Gasparetto, M., Guariso, G., 2013. Highlights in IBD Epidemiology and Its Natural History in the Paediatric Age. *Gastroenterol Res Pr.* 2013, 829040. <https://doi.org/10.1155/2013/829040>
- Ge, D., Han, L., Huang, S., Peng, N., Wang, P., Jiang, Z., Zhao, J., Su, L., Zhang, S., Zhang, Y., Kung, H., Zhao, B., Miao, J., 2014. Identification of a novel MTOR activator and discovery of a competing endogenous RNA regulating autophagy in vascular endothelial cells. *Autophagy* 10, 957–971. <https://doi.org/10.4161/auto.28363>
- Geerling, B.J., Badart-Smook, A., van Deursen, C., van Houwelingen, A.C., Russel, M.G., Stockbrügger, R.W., Brummer, R.J., 2000. Nutritional supplementation with N-3 fatty acids and antioxidants in patients with Crohn's disease in remission: effects on antioxidant status and fatty acid profile. *Inflamm. Bowel Dis.* 6, 77–84.
- Geisler, S., Holmström, K.M., Skujat, D., Fiesel, F.C., Rothfuss, O.C., Kahle, P.J., Springer, W., 2010. PINK1/Parkin-mediated mitophagy is dependent on VDAC1 and p62/SQSTM1. *Nat. Cell Biol.* 12, 119–131. <https://doi.org/10.1038/ncb2012>
- Gewirtz, A.T., Navas, T.A., Lyons, S., Godowski, P.J., Madara, J.L., 2001. Cutting edge: bacterial flagellin activates basolaterally expressed TLR5 to induce epithelial proinflammatory gene expression. *J. Immunol. Baltim. Md 1950* 167, 1882–1885.
- Girón, M.D., Vílchez, J.D., Shreeram, S., Salto, R., Manzano, M., Cabrera, E., Campos, N., Edens, N.K., Rueda, R., López-Pedrosa, J.M., 2015. β -Hydroxy- β -Methylbutyrate (HMB) Normalizes Dexamethasone-Induced Autophagy-Lysosomal Pathway in Skeletal Muscle. *PLoS ONE* 10. <https://doi.org/10.1371/journal.pone.0117520>
- Gisbert, J.P., Chaparro, M., Gomollon, F., 2011. Common misconceptions about 5-aminosalicylates and thiopurines in inflammatory bowel disease. *World J Gastroenterol* 17, 3467–78. <https://doi.org/10.3748/wjg.v17.i30.3467>
- Giverhaug, T., Klemetsdal, B., Lysaa, R., Aarbakke, J., 1996. Intraindividual variability in red blood cell thiopurine methyltransferase activity. *Eur. J. Clin. Pharmacol.* 50, 217–220.
- Glas, J., Seiderer, J., Fries, C., Tillack, C., Pfennig, S., Weidinger, M., Beigel, F., Olszak, T., Lass, U., Göke, B., Ochsenkühn, T., Wolf, C., Lohse, P., Müller-Myhsok, B., Diegelmann, J., Czamara, D., Brand, S., 2011. CEACAM6 Gene Variants in Inflammatory Bowel Disease. *PLOS ONE* 6, e19319. <https://doi.org/10.1371/journal.pone.0019319>
- Glasser, A.-L., Boudeau, J., Barnich, N., Perruchot, M.-H., Colombel, J.-F., Darfeuille-Michaud, A., 2001. Adherent Invasive Escherichia coli Strains from Patients with Crohn's Disease Survive and Replicate within Macrophages without Inducing Host Cell Death. *Infect. Immun.* 69, 5529–5537. <https://doi.org/10.1128/IAI.69.9.5529-5537.2001>
- Glick, D., Barth, S., Macleod, K.F., 2010. Autophagy: cellular and molecular mechanisms. *J Pathol* 221, 3–12. <https://doi.org/10.1002/path.2697>
- Glubb, D.M., Gearry, R.B., Barclay, M.L., Roberts, R.L., Pearson, J., Keenan, J.I., McKenzie, J., Bentley, R.W., 2011. NOD2 and ATG16L1 polymorphisms affect monocyte responses in Crohn's disease. *World J. Gastroenterol.* 17, 2829–2837. <https://doi.org/10.3748/wjg.v17.i23.2829>
- Goel, R.M., Blaker, P., Mentzer, A., Fong, S.C.M., Marinaki, A.M., Sanderson, J.D., 2015. Optimizing the use of thiopurines in inflammatory bowel disease. *Ther. Adv. Chronic Dis.* 6, 138–146. <https://doi.org/10.1177/2040622315579063>

- Gómez-Martín, D., Díaz-Zamudio, M., Vanoye, G., Crispín, J.C., Alcocer-Varela, J., 2011. Quantitative and functional profiles of CD4+ lymphocyte subsets in systemic lupus erythematosus patients with lymphopenia. *Clin. Exp. Immunol.* 164, 17–25. <https://doi.org/10.1111/j.1365-2249.2010.04309.x>
- Grip, O., Bredberg, A., Lindgren, S., Henriksson, G., 2007. Increased subpopulations of CD16(+) and CD56(+) blood monocytes in patients with active Crohn's disease. *Inflamm. Bowel Dis.* 13, 566–572. <https://doi.org/10.1002/ibd.20025>
- Guan, B.-J., Krokowski, D., Majumder, M., Schmotzer, C.L., Kimball, S.R., Merrick, W.C., Koromilas, A.E., Hatzoglou, M., 2014. Translational control during endoplasmic reticulum stress beyond phosphorylation of the translation initiation factor eIF2 α . *J. Biol. Chem.* 289, 12593–12611. <https://doi.org/10.1074/jbc.M113.543215>
- Guijarro, L.G., Roman, I.D., Fernandez-Moreno, M.D., Gisbert, J.P., Hernandez-Breijo, B., 2012. Is the autophagy induced by thiopurines beneficial or deleterious? *Curr Drug Metab* 13, 1267–76.
- Gunnarsdottir, S., Elfarra, A.A., 2003. Distinct Tissue Distribution of Metabolites of the Novel Glutathione-Activated Thiopurine Prodrugs Cis-6-(2-Acetylvinythio)purine and Trans-6-(2-Acetylvinythio)guanine and 6-Thioguanine in the Mouse. *Drug Metab. Dispos.* 31, 718–726. <https://doi.org/10.1124/dmd.31.6.718>
- Gupta, S., Kim, C., Yel, L., Gollapudi, S., 2004. A role of fas-associated death domain (FADD) in increased apoptosis in aged humans. *J. Clin. Immunol.* 24, 24–29. <https://doi.org/10.1023/B:JOCI.0000018059.56924.99>
- Gwinn, D.M., Shackelford, D.B., Egan, D.F., Mihaylova, M.M., Mery, A., Vasquez, D.S., Turk, B.E., Shaw, R.J., 2008. AMPK phosphorylation of raptor mediates a metabolic checkpoint. *Mol Cell* 30, 214–26. <https://doi.org/10.1016/j.molcel.2008.03.003>
- Haim, Y., Blüher, M., Slutsky, N., Goldstein, N., Klötting, N., Harman-Boehm, I., Kirshtein, B., Ginsberg, D., Gericke, M., Guiu Jurado, E., Kovsan, J., Tarnovskii, T., Kachko, L., Bashan, N., Gepner, Y., Shai, I., Rudich, A., 2015. Elevated autophagy gene expression in adipose tissue of obese humans: A potential non-cell-cycle-dependent function of E2F1. *Autophagy* 11, 2074–2088. <https://doi.org/10.1080/15548627.2015.1094597>
- Hampe, J., Cuthbert, A., Croucher, P.J., Mirza, M.M., Mascheretti, S., Fisher, S., Frenzel, H., King, K., Hasselmeyer, A., MacPherson, A.J., Bridger, S., van Deventer, S., Forbes, A., Nikolaus, S., Lennard-Jones, J.E., Foelsch, U.R., Krawczak, M., Lewis, C., Schreiber, S., Mathew, C.G., 2001. Association between insertion mutation in NOD2 gene and Crohn's disease in German and British populations. *Lancet* 357, 1925–8. [https://doi.org/10.1016/s0140-6736\(00\)05063-7](https://doi.org/10.1016/s0140-6736(00)05063-7)
- Hampe, J., Franke, A., Rosenstiel, P., Till, A., Teuber, M., Huse, K., Albrecht, M., Mayr, G., De La Vega, F.M., Briggs, J., Gunther, S., Prescott, N.J., Onnie, C.M., Hasler, R., Sipos, B., Folsch, U.R., Lengauer, T., Platzer, M., Mathew, C.G., Krawczak, M., Schreiber, S., 2007. A genome-wide association scan of nonsynonymous SNPs identifies a susceptibility variant for Crohn disease in ATG16L1. *Nat Genet* 39, 207–11. <https://doi.org/10.1038/ng1954>
- Han, H.-Y., Kim, H., Jeong, S.-H., Lim, D.-S., Ryu, M.H., 2014. Sulfasalazine Induces Autophagic Cell Death in Oral Cancer Cells via Akt and ERK Pathways. *Asian Pac. J. Cancer Prev.* 15, 6939–6944. <https://doi.org/10.7314/APJCP.2014.15.16.6939>

- Hangaishi, A., Ogawa, S., Mitani, K., Hosoya, N., Chiba, S., Yazaki, Y., Hirai, H., 1997. Mutations and loss of expression of a mismatch repair gene, hMLH1, in leukemia and lymphoma cell lines. *Blood* 89, 1740–1747.
- Harding, H.P., Zhang, Y., Bertolotti, A., Zeng, H., Ron, D., 2000. Perk Is Essential for Translational Regulation and Cell Survival during the Unfolded Protein Response. *Mol. Cell* 5, 897–904. [https://doi.org/10.1016/S1097-2765\(00\)80330-5](https://doi.org/10.1016/S1097-2765(00)80330-5)
- Harr, M.W., McColl, K.S., Zhong, F., Molitoris, J.K., Distelhorst, C.W., 2010. Glucocorticoids downregulate Fyn and inhibit IP(3)-mediated calcium signaling to promote autophagy in T lymphocytes. *Autophagy* 6, 912–21. <https://doi.org/10.4161/auto.6.7.13290>
- Harris, J., Keane, J., 2010. How tumour necrosis factor blockers interfere with tuberculosis immunity: TNF blockers and TB immunity. *Clin. Exp. Immunol.* no-no. <https://doi.org/10.1111/j.1365-2249.2010.04146.x>
- Hart, L.S., Cunningham, J.T., Datta, T., Dey, S., Tameire, F., Lehman, S.L., Qiu, B., Zhang, H., Cerniglia, G., Bi, M., Li, Y., Gao, Y., Liu, H., Li, C., Maity, A., Thomas-Tikhonenko, A., Perl, A.E., Koong, A., Fuchs, S.Y., Diehl, J.A., Mills, I.G., Ruggero, D., Koumenis, C., 2012. ER stress-mediated autophagy promotes Myc-dependent transformation and tumor growth. *J. Clin. Invest.* 122, 4621–4634. <https://doi.org/10.1172/JCI62973>
- Hashimoto, I., Koizumi, K., Tatematsu, M., Minami, T., Cho, S., Takeno, N., Nakashima, A., Sakurai, H., Saito, S., Tsukada, K., Saiki, I., 2008. Blocking on the CXCR4/mTOR signalling pathway induces the anti-metastatic properties and autophagic cell death in peritoneal disseminated gastric cancer cells. *Eur. J. Cancer* 44, 1022–1029. <https://doi.org/10.1016/j.ejca.2008.02.043>
- Haze, K., Yoshida, H., Yanagi, H., Yura, T., Mori, K., 1999. Mammalian transcription factor ATF6 is synthesized as a transmembrane protein and activated by proteolysis in response to endoplasmic reticulum stress. *Mol. Biol. Cell* 10, 3787–3799.
- He, B., Zhang, N., Zhao, R., 2016. Dexamethasone Downregulates SLC7A5 Expression and Promotes Cell Cycle Arrest, Autophagy and Apoptosis in BeWo Cells. *J Cell Physiol* 231, 233–42. <https://doi.org/10.1002/jcp.25076>
- He, C., Bassik, M.C., Moresi, V., Sun, K., Wei, Y., Zou, Z., An, Z., Loh, J., Fisher, J., Sun, Q., Korsmeyer, S., Packer, M., May, H.I., Hill, J.A., Virgin, H.W., Gilpin, C., Xiao, G., Bassel-Duby, R., Scherer, P.E., Levine, B., 2012. Exercise-induced BCL2-regulated autophagy is required for muscle glucose homeostasis. *Nature* 481, 511–515. <https://doi.org/10.1038/nature10758>
- Heazlewood, C.K., Cook, M.C., Eri, R., Price, G.R., Tauro, S.B., Taupin, D., Thornton, D.J., Png, C.W., Crockford, T.L., Cornall, R.J., Adams, R., Kato, M., Nelms, K.A., Hong, N.A., Florin, T.H.J., Goodnow, C.C., McGuckin, M.A., 2008. Aberrant Mucin Assembly in Mice Causes Endoplasmic Reticulum Stress and Spontaneous Inflammation Resembling Ulcerative Colitis. *PLoS Med.* 5. <https://doi.org/10.1371/journal.pmed.0050054>
- Henderson, P., 2013. Paediatric inflammatory bowel disease—bench to bedside and nationwide: a detailed analysis of Scottish children with IBD.
- Henderson, P., Hansen, R., Cameron, F.L., Gerasimidis, K., Rogers, P., Bisset, W.M., Reynish, E.L., Drummond, H.E., Anderson, N.H., Van Limbergen, J., Russell, R.K., Satsangi, J., Wilson, D.C., 2012. Rising incidence of pediatric inflammatory bowel disease in Scotland. *Inflamm Bowel Dis* 18, 999–1005. <https://doi.org/10.1002/ibd.21797>

- Henderson, P., van Limbergen, J.E., Schwarze, J., Wilson, D.C., 2011. Function of the intestinal epithelium and its dysregulation in inflammatory bowel disease. *Inflamm. Bowel Dis.* 17, 382–395. <https://doi.org/10.1002/ibd.21379>
- Hetz, C., Thielen, P., Matus, S., Nassif, M., Court, F., Kiffin, R., Martinez, G., Cuervo, A.M., Brown, R.H., Glimcher, L.H., 2009. XBP-1 deficiency in the nervous system protects against amyotrophic lateral sclerosis by increasing autophagy. *Genes Dev.* 23, 2294–2306. <https://doi.org/10.1101/gad.1830709>
- Heuschkel, R., 2009. Enteral nutrition should be used to induce remission in childhood Crohn's disease. *Dig. Dis. Basel Switz.* 27, 297–305. <https://doi.org/10.1159/000228564>
- Hindorf, U., Lindqvist, M., Hildebrand, H., Fagerberg, U., Almer, S., 2006. Adverse events leading to modification of therapy in a large cohort of patients with inflammatory bowel disease. *Aliment. Pharmacol. Ther.* 24, 331–342. <https://doi.org/10.1111/j.1365-2036.2006.02977.x>
- Hiniker, A., Daniels, B.H., Lee, H.S., Margeta, M., 2013. Comparative utility of LC3, p62 and TDP-43 immunohistochemistry in differentiation of inclusion body myositis from polymyositis and related inflammatory myopathies. *Acta Neuropathol. Commun.* 1, 29. <https://doi.org/10.1186/2051-5960-1-29>
- Hino, K., Saito, A., Asada, R., Kanemoto, S., Imaizumi, K., 2014. Increased Susceptibility to Dextran Sulfate Sodium-Induced Colitis in the Endoplasmic Reticulum Stress Transducer OASIS Deficient Mice. *PLoS ONE* 9. <https://doi.org/10.1371/journal.pone.0088048>
- Hirsch, I., Weiwad, M., Prell, E., Ferrari, D.M., 2014. ERp29 deficiency affects sensitivity to apoptosis via impairment of the ATF6-CHOP pathway of stress response. *Apoptosis Int. J. Program. Cell Death* 19, 801–815. <https://doi.org/10.1007/s10495-013-0961-0>
- Ho, G.-T., Aird, R.E., Liu, B., Boyapati, R.K., Kennedy, N.A., Dorward, D.A., Noble, C.L., Shimizu, T., Carter, R.N., Chew, E.T.S., Morton, N.M., Rossi, A.G., Sartor, R.B., Iredale, J.P., Satsangi, J., 2018. MDR1 deficiency impairs mitochondrial homeostasis and promotes intestinal inflammation. *Mucosal Immunol.* 11, 120–130. <https://doi.org/10.1038/mi.2017.31>
- Hollien, J., 2006. Decay of Endoplasmic Reticulum-Localized mRNAs During the Unfolded Protein Response. *Science* 313, 104–107. <https://doi.org/10.1126/science.1129631>
- Holt, D.Q., Strauss, B.J., Moore, G.T., 2016. Weight and Body Composition Compartments do Not Predict Therapeutic Thiopurine Metabolite Levels in Inflammatory Bowel Disease. *Clin. Transl. Gastroenterol.* 7, e199. <https://doi.org/10.1038/ctg.2016.56>
- Homer, C.R., Richmond, A.L., Rebert, N.A., Achkar, J.-P., McDonald, C., 2010. ATG16L1 and NOD2 interact in an autophagy-dependent, anti-bacterial pathway implicated in Crohn's disease pathogenesis. *Gastroenterology* 139, 1630–1641.e2. <https://doi.org/10.1053/j.gastro.2010.07.006>
- Hooper, K.M., Barlow, P.G., Stevens, C., Henderson, P., 2017. Inflammatory Bowel Disease Drugs: A Focus on Autophagy. *J. Crohns Colitis* 11, 118–127. <https://doi.org/10.1093/ecco-jcc/jjw127>
- Hou, W., Han, J., Lu, C., Goldstein, L.A., Rabinowich, H., 2010. Autophagic degradation of active caspase-8: a crosstalk mechanism between autophagy and apoptosis. *Autophagy* 6, 891–900. <https://doi.org/10.4161/auto.6.7.13038>

- Howells, C.C., Baumann, W.T., Samuels, D.C., Finkielstein, C.V., 2011. The Bcl-2-associated death promoter (BAD) lowers the threshold at which the Bcl-2-interacting domain death agonist (BID) triggers mitochondria disintegration. *J. Theor. Biol.* 271, 114–123. <https://doi.org/10.1016/j.jtbi.2010.11.040>
- Hsieh, S.-Y., Shih, T.-C., Yeh, C.-Y., Lin, C.-J., Chou, Y.-Y., Lee, Y.-S., 2006. Comparative proteomic studies on the pathogenesis of human ulcerative colitis. *Proteomics* 6, 5322–5331. <https://doi.org/10.1002/pmic.200500541>
- Huang, H.-Y., Chang, H.-F., Tsai, M.-J., Chen, J.-S., Wang, M.-J., 2016. 6-Mercaptopurine attenuates tumor necrosis factor- α production in microglia through Nur77-mediated transrepression and PI3K/Akt/mTOR signaling-mediated translational regulation. *J. Neuroinflammation* 13. <https://doi.org/10.1186/s12974-016-0543-5>
- Huang, J., Manning, B.D., 2009. A complex interplay between Akt, TSC2, and the two mTOR complexes. *Biochem. Soc. Trans.* 37, 217–222. <https://doi.org/10.1042/BST0370217>
- Hugot, J.P., Chamaillard, M., Zouali, H., Lesage, S., Cezard, J.P., Belaiche, J., Almer, S., Tysk, C., O’Morain, C.A., Gassull, M., Binder, V., Finkel, Y., Cortot, A., Modigliani, R., Laurent-Puig, P., Gower-Rousseau, C., Macry, J., Colombel, J.F., Sahbatou, M., Thomas, G., 2001. Association of NOD2 leucine-rich repeat variants with susceptibility to Crohn’s disease. *Nature* 411, 599–603. <https://doi.org/10.1038/35079107>
- Hui, K.Y., Fernandez-Hernandez, H., Hu, J., Schaffner, A., Pankratz, N., Hsu, N.-Y., Chuang, L.-S., Carmi, S., Villaverde, N., Li, X., Rivas, M., Levine, A.P., Bao, X., Labrias, P.R., Haritunians, T., Ruane, D., Gettler, K., Chen, E., Li, D., Schiff, E.R., Pontikos, N., Barzilai, N., Brant, S.R., Bressman, S., Cheifetz, A.S., Clark, L.N., Daly, M.J., Desnick, R.J., Duerr, R.H., Katz, S., Lencz, T., Myers, R.H., Ostrer, H., Ozelius, L., Payami, H., Peter, Y., Rioux, J.D., Segal, A.W., Scott, W.K., Silverberg, M.S., Vance, J.M., Ubarretxena-Belandia, I., Foroud, T., Atzmon, G., Pe’er, I., Ioannou, Y., McGovern, D.P.B., Yue, Z., Schadt, E.E., Cho, J.H., Peter, I., 2018. Functional variants in the LRRK2 gene confer shared effects on risk for Crohn’s disease and Parkinson’s disease. *Sci. Transl. Med.* 10. <https://doi.org/10.1126/scitranslmed.aai7795>
- Hunter, M.M., Wang, A., Parhar, K.S., Johnston, M.J.G., Rooijen, N.V., Beck, P.L., McKay, D.M., 2010. In Vitro-Derived Alternatively Activated Macrophages Reduce Colonic Inflammation in Mice. *Gastroenterology* 138, 1395–1405. <https://doi.org/10.1053/j.gastro.2009.12.041>
- Inoki, K., Li, Y., Zhu, T., Wu, J., Guan, K.-L., 2002. TSC2 is phosphorylated and inhibited by Akt and suppresses mTOR signalling. *Nat. Cell Biol.* 4, 648–657. <https://doi.org/10.1038/ncb839>
- Jänicke, R.U., Sohn, D., Schulze-Osthoff, K., 2008. The dark side of a tumor suppressor: anti-apoptotic p53. *Cell Death Differ.* 15, 959–976. <https://doi.org/10.1038/cdd.2008.33>
- Janssen, C.E.I., Rose, C.D., De Hertogh, G., Martin, T.M., Bader Meunier, B., Cimaz, R., Harjacek, M., Quartier, P., Ten Cate, R., Thomee, C., Desmet, V.J., Fischer, A., Roskams, T., Wouters, C.H., 2012. Morphologic and immunohistochemical characterization of granulomas in the nucleotide oligomerization domain 2-related disorders Blau syndrome and Crohn disease. *J. Allergy Clin. Immunol.* 129, 1076–1084. <https://doi.org/10.1016/j.jaci.2012.02.004>

- Ji, G., Yu, N., Xue, X., Li, Z., 2015. PERK-mediated Autophagy in Osteosarcoma Cells Resists ER Stress-induced Cell Apoptosis. *Int. J. Biol. Sci.* 11, 803–812. <https://doi.org/10.7150/ijbs.11100>
- Jia, G., Cheng, G., Gangahar, D.M., Agrawal, D.K., 2006. Insulin-like growth factor-1 and TNF-alpha regulate autophagy through c-jun N-terminal kinase and Akt pathways in human atherosclerotic vascular smooth cells. *Immunol Cell Biol* 84, 448–54. <https://doi.org/10.1111/j.1440-1711.2006.01454.x>
- Jia, X.-E., Ma, K., Xu, T., Gao, L., Wu, S., Fu, C., Zhang, W., Wang, Z., Liu, K., Dong, M., others, 2015. Mutation of *kri1l* causes definitive hematopoiesis failure via PERK-dependent excessive autophagy induction. *Cell Res.* 25, 946.
- Jin, M., He, D., Backues, S.K., Freeberg, M.A., Liu, X., Kim, J.K., Klionsky, D.J., 2014. Transcriptional regulation by Pho23 modulates the frequency of autophagosome formation. *Curr. Biol. CB* 24, 1314–1322. <https://doi.org/10.1016/j.cub.2014.04.048>
- Johansen, T., Lamark, T., 2011. Selective autophagy mediated by autophagic adapter proteins. *Autophagy* 7, 279–296.
- Jones, R.G., Plas, D.R., Kubek, S., Buzzai, M., Mu, J., Xu, Y., Birnbaum, M.J., Thompson, C.B., 2005. AMP-activated protein kinase induces a p53-dependent metabolic checkpoint. *Mol. Cell* 18, 283–293. <https://doi.org/10.1016/j.molcel.2005.03.027>
- Jostins, L., Ripke, S., Weersma, R.K., Duerr, R.H., McGovern, D.P., Hui, K.Y., Lee, J.C., Philip Schumm, L., Sharma, Y., Anderson, C.A., Essers, J., Mitrovic, M., Ning, K., Cleyne, I., Theatre, E., Spain, S.L., Raychaudhuri, S., Goyette, P., Wei, Z., Abraham, C., Achkar, J.-P., Ahmad, T., Amininejad, L., Ananthakrishnan, A.N., Andersen, V., Andrews, J.M., Baidoo, L., Balschun, T., Bampton, P.A., Bitton, A., Boucher, G., Brand, S., Büning, C., Cohain, A., Cichon, S., D’Amato, M., De Jong, D., Devaney, K.L., Dubinsky, M., Edwards, C., Ellinghaus, D., Ferguson, L.R., Franchimont, D., Fransen, K., Gearry, R., Georges, M., Gieger, C., Glas, J., Haritunians, T., Hart, A., Hawkey, C., Hedl, M., Hu, X., Karlson, T.H., Kupcinskis, L., Kugathasan, S., Latiano, A., Laukens, D., Lawrance, I.C., Lees, C.W., Louis, E., Mahy, G., Mansfield, J., Morgan, A.R., Mowat, C., Newman, W., Palmieri, O., Ponsioen, C.Y., Potocnik, U., Prescott, N.J., Regueiro, M., Rotter, J.I., Russell, R.K., Sanderson, J.D., Sans, M., Satsangi, J., Schreiber, S., Simms, L.A., Sventoraityte, J., Targan, S.R., Taylor, K.D., Tremelling, M., Verspaget, H.W., De Vos, M., Wijmenga, C., Wilson, D.C., Winkelmann, J., Xavier, R.J., Zeissig, S., Zhang, B., Zhang, C.K., Zhao, H., Silverberg, M.S., Annese, V., Hakonarson, H., Brant, S.R., Radford-Smith, G., Mathew, C.G., Rioux, J.D., Schadt, E.E., Daly, M.J., Franke, A., Parkes, M., Vermeire, S., Barrett, J.C., Cho, J.H., 2012. Host–microbe interactions have shaped the genetic architecture of inflammatory bowel disease. *Nature* 491, 119–124. <https://doi.org/10.1038/nature11582>
- Jounai, N., Kobiyama, K., Shiina, M., Ogata, K., Ishii, K.J., Takeshita, F., 2011. NLRP4 negatively regulates autophagic processes through an association with beclin1. *J. Immunol. Baltim. Md* 1950 186, 1646–1655. <https://doi.org/10.4049/jimmunol.1001654>
- Kaakoush, N.O., Day, A.S., Leach, S.T., Lemberg, D.A., Nielsen, S., Mitchell, H.M., 2015. Effect of exclusive enteral nutrition on the microbiota of children with newly diagnosed Crohn’s disease. *Clin. Transl. Gastroenterol.* 6, e71. <https://doi.org/10.1038/ctg.2014.21>

- Kabat, A.M., Harrison, O.J., Riffelmacher, T., Moghaddam, A.E., Pearson, C.F., Laing, A., Abeler-Dörner, L., Forman, S.P., Grecnis, R.K., Sattentau, Q., Simon, A.K., Pott, J., Maloy, K.J., 2016. The autophagy gene Atg16l1 differentially regulates Treg and TH2 cells to control intestinal inflammation. *eLife* 5. <https://doi.org/10.7554/eLife.12444>
- Kabeya, Y., Mizushima, N., Ueno, T., Yamamoto, A., Kirisako, T., Noda, T., Kominami, E., Ohsumi, Y., Yoshimori, T., 2000. LC3, a mammalian homologue of yeast Apg8p, is localized in autophagosome membranes after processing. *EMBO J.* 19, 5720–5728. <https://doi.org/10.1093/emboj/19.21.5720>
- Kamada, N., Hisamatsu, T., Okamoto, S., Chinen, H., Kobayashi, T., Sato, T., Sakuraba, A., Kitazume, M.T., Sugita, A., Koganei, K., Akagawa, K.S., Hibi, T., 2008. Unique CD14 intestinal macrophages contribute to the pathogenesis of Crohn disease via IL-23/IFN-gamma axis. *J. Clin. Invest.* 118, 2269–2280. <https://doi.org/10.1172/JCI34610>
- Kamada, N., Kim, Y.-G., Sham, H.P., Vallance, B.A., Puente, J.L., Martens, E.C., Núñez, G., 2012. Regulated virulence controls the ability of a pathogen to compete with the gut microbiota. *Science* 336, 1325–1329. <https://doi.org/10.1126/science.1222195>
- Kaneko, M., Niinuma, Y., Nomura, Y., 2003. Activation Signal of Nuclear Factor- κ B in Response to Endoplasmic Reticulum Stress is Transduced via IRE1 and Tumor Necrosis Factor Receptor-Associated Factor 2. *Biol. Pharm. Bull.* 26, 931–5. <https://doi.org/10.1248/bpb.26.931>
- Kang, Y.-A., Sanalkumar, R., O'Geen, H., Linnemann, A.K., Chang, C.-J., Bouhassira, E.E., Farnham, P.J., Keles, S., Bresnick, E.H., 2012. Autophagy driven by a master regulator of hematopoiesis. *Mol. Cell. Biol.* 32, 226–239. <https://doi.org/10.1128/MCB.06166-11>
- Kaser, A., Lee, A.-H., Franke, A., Glickman, J.N., Zeissig, S., Tilg, H., Nieuwenhuis, E.E.S., Higgins, D.E., Schreiber, S., Glimcher, L.H., Blumberg, R.S., 2008. XBP1 Links ER Stress to Intestinal Inflammation and Confers Genetic Risk for Human Inflammatory Bowel Disease. *Cell* 134, 743–756. <https://doi.org/10.1016/j.cell.2008.07.021>
- Kassam, Z., Belga, S., Roifman, I., Hirota, S., Jijon, H., Kaplan, G.G., Ghosh, S., Beck, P.L., 2014. Inflammatory Bowel Disease Cause-specific Mortality: A Primer for Clinicians. *Inflamm. Bowel Dis.* 20, 2483–2492. <https://doi.org/10.1097/MIB.0000000000000173>
- Kathiria, A.S., Butcher, L.D., Feagins, L.A., Souza, R.F., Boland, C.R., Theiss, A.L., 2012. Prohibitin 1 Modulates Mitochondrial Stress-Related Autophagy in Human Colonic Epithelial Cells. *PLOS ONE* 7, e31231. <https://doi.org/10.1371/journal.pone.0031231>
- Keestra-Gounder, A.M., Byndloss, M.X., Seyffert, N., Young, B.M., Chávez-Arroyo, A., Tsai, A.Y., Cevallos, S.A., Winter, M.G., Pham, O.H., Tiffany, C.R., de Jong, M.F., Kerrinnes, T., Ravindran, R., Luciw, P.A., McSorley, S.J., Bäumlner, A.J., Tsolis, R.M., 2016. NOD1 and NOD2 signalling links ER stress with inflammation. *Nature* 532, 394–397. <https://doi.org/10.1038/nature17631>
- Keller, C.W., Fokken, C., Turville, S.G., Lünemann, A., Schmidt, J., Münz, C., Lünemann, J.D., 2011. TNF- α induces macroautophagy and regulates MHC class II expression in human skeletal muscle cells. *J. Biol. Chem.* 286, 3970–3980.

- Kim, H.J., Lee, S., Jung, J.U., 2010. When autophagy meets viruses: a double-edged sword with functions in defense and offense. *Semin. Immunopathol.* 32, 323–341. <https://doi.org/10.1007/s00281-010-0226-8>
- Kim, H.S., Choi, S.-I., Jeung, E.-B., Yoo, Y.-M., 2014. Cyclosporine A Induces Apoptotic and Autophagic Cell Death in Rat Pituitary GH3 Cells. *PLoS ONE* 9, e108981. <https://doi.org/10.1371/journal.pone.0108981>
- Kim, J., Kim, Y.C., Fang, C., Russell, R.C., Kim, J.H., Fan, W., Liu, R., Zhong, Q., Guan, K.-L., 2013. Differential regulation of distinct Vps34 complexes by AMPK in nutrient stress and autophagy. *Cell* 152, 290–303. <https://doi.org/10.1016/j.cell.2012.12.016>
- Kim, J., Kundu, M., Viollet, B., Guan, K.-L., 2011. AMPK and mTOR regulate autophagy through direct phosphorylation of Ulk1. *Nat. Cell Biol.* 13, 132–141. <https://doi.org/10.1038/ncb2152>
- Kimura, S., Noda, T., Yoshimori, T., 2007. Dissection of the autophagosome maturation process by a novel reporter protein, tandem fluorescent-tagged LC3. *Autophagy* 3, 452–460.
- Kimura, T., Takahashi, A., Takabatake, Y., Namba, T., Yamamoto, T., Kaimori, J., Matsui, I., Kitamura, H., Niimura, F., Matsusaka, T., Soga, T., Rakugi, H., Isaka, Y., 2013. Autophagy protects kidney proximal tubule epithelial cells from mitochondrial metabolic stress. *Autophagy* 9, 1876–1886. <https://doi.org/10.4161/auto.25418>
- Kirisako, T., Baba, M., Ishihara, N., Miyazawa, K., Ohsumi, M., Yoshimori, T., Noda, T., Ohsumi, Y., 1999. Formation process of autophagosome is traced with Apg8/Aut7p in yeast. *J. Cell Biol.* 147, 435–446.
- Kirkin, V., Lamark, T., Sou, Y.-S., Bjørkøy, G., Nunn, J.L., Bruun, J.-A., Shvets, E., McEwan, D.G., Clausen, T.H., Wild, P., Bilusic, I., Theurillat, J.-P., Øvervatn, A., Ishii, T., Elazar, Z., Komatsu, M., Dikic, I., Johansen, T., 2009. A role for NBR1 in autophagosomal degradation of ubiquitinated substrates. *Mol. Cell* 33, 505–516. <https://doi.org/10.1016/j.molcel.2009.01.020>
- Kirschner, B.S., 1998. Safety of azathioprine and 6-mercaptopurine in pediatric patients with inflammatory bowel disease. *Gastroenterology* 115, 813–821.
- Klionsky, D.J., Abdelmohsen, K., Abe, A., Abedin, M.J., Abeliovich, H., Acevedo Arozena, A., Adachi, H., Adams, C.M., Adams, P.D., Adeli, K., Adhihetty, P.J., Adler, S.G., Agam, G., Agarwal, R., Aghi, M.K., Agnello, M., Agostinis, P., Aguilar, P.V., Aguirre-Ghiso, J., Airoidi, E.M., Ait-Si-Ali, S., Akematsu, T., Akporiaye, E.T., Al-Rubeai, M., Albaiceta, G.M., Albanese, C., Albani, D., Albert, M.L., Aldudo, J., Algül, H., Alirezaei, M., Alloza, I., Almasan, A., Almonte-Beceril, M., Alnemri, E.S., Alonso, C., Altan-Bonnet, N., Altieri, D.C., Alvarez, S., Alvarez-Erviti, L., Alves, S., Amadoro, G., Amano, A., Amantini, C., Ambrosio, S., Amelio, I., Amer, A.O., Amessou, M., Amon, A., An, Z., Anania, F.A., Andersen, S.U., Andley, U.P., Andreadi, C.K., Andrieu-Abadie, N., Anel, A., Ann, D.K., Anoopkumar-Dukie, S., Antonielli, M., Aoki, H., Apostolova, N., Aquila, S., Aquilano, K., Araki, K., Arama, E., Aranda, A., Araya, J., Arcaro, A., Arias, E., Arimoto, H., Ariosa, A.R., Armstrong, J.L., Arnould, T., Arsov, I., Asanuma, K., Askanas, V., Asselin, E., Atarashi, R., Atherton, S.S., Atkin, J.D., Attardi, L.D., Auberger, P., Auburger, G., Aurelian, L., Autelli, R., Avagliano, L., Avantaggiati, M.L., Avrahami, L., Awale, S., Azad, N., Bachetti, T., Backer, J.M., Bae, D.-H., Bae, J.-S., Bae, O.-N., Bae, S.H., Baehrecke, E.H., Baek, S.-H., Baghdiguian, S., Bagniewska-Zadworna, A., Bai, H., Bai, J., Bai, X.-Y., Bailly, Y., Balaji, K.N., Balduini, W., Ballabio, A., Balzan, R., Banerjee, R., Bánhegyi, G., Bao, H., Barbeau, B., Barrachina, M.D., Barreiro, E., Bartel, B., Bartolomé, A.,

Bassham, D.C., Bassi, M.T., Bast, R.C., Basu, A., Batista, M.T., Batoko, H., Battino, M., Bauckman, K., Baumgarner, B.L., Bayer, K.U., Beale, R., Beaulieu, J.-F., Beck, G.R., Becker, C., Beckham, J.D., Bédard, P.-A., Bednarski, P.J., Begley, T.J., Behl, C., Behrends, C., Behrens, G.M., Behrns, K.E., Bejarano, E., Belaid, A., Belleudi, F., Bénard, G., Berchem, G., Bergamaschi, D., Bergami, M., Berkhout, B., Berliocchi, L., Bernard, A., Bernard, M., Bernassola, F., Bertolotti, A., Bess, A.S., Besteiro, S., Bettuzzi, S., Bhalla, S., Bhattacharyya, S., Bhutia, S.K., Biagosch, C., Bianchi, M.W., Biard-Piechaczyk, M., Billes, V., Bincoletto, C., Bingol, B., Bird, S.W., Bitoun, M., Bjedov, I., Blackstone, C., Blanc, L., Blanco, G.A., Blomhoff, H.K., Boada-Romero, E., Böckler, S., Boes, M., Boesze-Battaglia, K., Boise, L.H., Bolino, A., Boman, A., Bonaldo, P., Bordi, M., Bosch, J., Botana, L.M., Botti, J., Bou, G., Bouché, M., Bouchecareilh, M., Boucher, M.-J., Boulton, M.E., Bouret, S.G., Boya, P., Boyer-Guittaut, M., Bozhkov, P.V., Brady, N., Braga, V.M., Brancolini, C., Braus, G.H., Bravo-San Pedro, J.M., Brennan, L.A., Bresnick, E.H., Brest, P., Bridges, D., Bringer, M.-A., Brini, M., Brito, G.C., Brodin, B., Brookes, P.S., Brown, E.J., Brown, K., Broxmeyer, H.E., Bruhat, A., Brum, P.C., Brumell, J.H., Brunetti-Pierri, N., Bryson-Richardson, R.J., Buch, S., Buchan, A.M., Budak, H., Bulavin, D.V., Bultman, S.J., Bultynck, G., Bumbasirevic, V., Burelle, Y., Burke, R.E., Burmeister, M., Bütikofer, P., Caberlotto, L., Cadwell, K., Cahova, M., Cai, D., Cai, J., Cai, Q., Calatayud, S., Camougrand, N., Campanella, M., Campbell, G.R., Campbell, M., Campello, S., Candau, R., Caniggia, I., Cantoni, L., Cao, L., Caplan, A.B., Caraglia, M., Cardinali, C., Cardoso, S.M., Carew, J.S., Carleton, L.A., Carlin, C.R., Carloni, S., Carlsson, S.R., Carmona-Gutierrez, D., Carneiro, L.A., Carnevali, O., Carra, S., Carrier, A., Carroll, B., Casas, C., Casas, J., Cassinelli, G., Castets, P., Castro-Obregon, S., Cavallini, G., Ceccherini, I., Cecconi, F., Cederbaum, A.I., Ceña, V., Cenci, S., Cerella, C., Cervia, D., Cetrullo, S., Chaachouay, H., Chae, H.-J., Chagin, A.S., Chai, C.-Y., Chakrabarti, G., Chamilos, G., Chan, E.Y., Chan, M.T., Chandra, D., Chandra, P., Chang, C.-P., Chang, R.C.-C., Chang, T.Y., Chatham, J.C., Chatterjee, S., Chauhan, S., Che, Y., Cheetham, M.E., Cheluvappa, R., Chen, C.-J., Chen, Gang, Chen, G.-C., Chen, Guoqiang, Chen, H., Chen, J.W., Chen, J.-K., Chen, Min, Chen, Mingzhou, Chen, P., Chen, Qi, Chen, Quan, Chen, S.-D., Chen, S., Chen, S.S.-L., Chen, Wei, Chen, W.-J., Chen, W.Q., Chen, Wenli, Chen, X., Chen, Y.-H., Chen, Y.-G., Chen, Yin, Chen, Yingyu, Chen, Yongshun, Chen, Y.-J., Chen, Y.-Q., Chen, Yujie, Chen, Zhen, Chen, Zhong, Cheng, A., Cheng, C.H., Cheng, H., Cheong, H., Cherry, S., Chesney, J., Cheung, C.H.A., Chevet, E., Chi, H.C., Chi, S.-G., Chiacchiera, F., Chiang, H.-L., Chiarelli, R., Chiariello, M., Chieppa, M., Chin, L.-S., Chiong, M., Chiu, G.N., Cho, D.-H., Cho, S.-G., Cho, W.C., Cho, Y.-Y., Cho, Y.-S., Choi, A.M., Choi, E.-J., Choi, E.-K., Choi, J., Choi, M.E., Choi, S.-I., Chou, T.-F., Chouaib, S., Choubey, D., Choubey, V., Chow, K.-C., Chowdhury, K., Chu, C.T., Chuang, T.-H., Chun, T., Chung, H., Chung, T., Chung, Y.-L., Chwae, Y.-J., Cianfanelli, V., Ciarcia, R., Ciechomska, I.A., Ciriolo, M.R., Cirone, M., Claerhout, S., Clague, M.J., Clària, J., Clarke, P.G., Clarke, R., Clementi, E., Cleyrat, C., Cnop, M., Coccia, E.M., Cocco, T., Codogno, P., Coers, J., Cohen, E.E., Colecchia, D., Coletto, L., Coll, N.S., Colucci-Guyon, E., Comincini, S., Condello, M., Cook, K.L., Coombs, G.H., Cooper, C.D., Cooper, J.M., Coppens, I., Corasaniti, M.T., Corazzari, M., Corbalan, R., Corcelle-Termeau, E., Cordero, M.D., Corral-Ramos, C., Corti, O., Cossarizza, A., Costelli, P., Costes, S., Cotman, S.L., Coto-Montes, A., Cottet, S., Couve, E., Covey, L.R., Cowart, L.A., Cox, J.S., Coxon, F.P., Coyne, C.B., Cragg, M.S., Craven, R.J., Crepaldi, T., Crespo, J.L., Criollo, A., Crippa, V., Cruz,

M.T., Cuervo, A.M., Cuezva, J.M., Cui, T., Cutillas, P.R., Czaja, M.J., Czyzyk-Krzeska, M.F., Dagda, R.K., Dahmen, U., Dai, C., Dai, W., Dai, Y., Dalby, K.N., Dalla Valle, L., Dalmasso, G., D'Amelio, M., Damme, M., Darfeuille-Michaud, A., Dargemont, C., Darley-Usmar, V.M., Dasarathy, S., Dasgupta, B., Dash, S., Dass, C.R., Davey, H.M., Davids, L.M., Dávila, D., Davis, R.J., Dawson, T.M., Dawson, V.L., Daza, P., de Belleruche, J., de Figueiredo, P., de Figueiredo, R.C.B.Q., de la Fuente, J., De Martino, L., De Matteis, A., De Meyer, G.R., De Milito, A., De Santi, M., de Souza, W., De Tata, V., De Zio, D., Debnath, J., Dechant, R., Decuypere, J.-P., Deegan, S., Dehay, B., Del Bello, B., Del Re, D.P., Delage-Mourroux, R., Delbridge, L.M., Deldicque, L., Delorme-Axford, E., Deng, Y., Dengjel, J., Denizot, M., Dent, P., Der, C.J., Deretic, V., Derrien, B., Deutsch, E., Devarenne, T.P., Devenish, R.J., Di Bartolomeo, S., Di Daniele, N., Di Domenico, F., Di Nardo, A., Di Paola, S., Di Pietro, A., Di Renzo, L., DiAntonio, A., Díaz-Araya, G., Díaz-Laviada, I., Diaz-Meco, M.T., Diaz-Nido, J., Dickey, C.A., Dickson, R.C., Diederich, M., Digard, P., Dikic, I., Dinesh-Kumar, S.P., Ding, C., Ding, W.-X., Ding, Z., Dini, L., Distler, J.H., Diwan, A., Djavaheri-Mergny, M., Dmytruk, K., Dobson, R.C., Doetsch, V., Dokladny, K., Dokudovskaya, S., Donadelli, M., Dong, X.C., Dong, X., Dong, Z., Donohue, T.M., Doran, K.S., D'Orazi, G., Dorn, G.W., Dosenko, V., Dridi, S., Drucker, L., Du, J., Du, L.-L., Du, L., du Toit, A., Dua, P., Duan, L., Duann, P., Dubey, V.K., Duchen, M.R., Duchosal, M.A., Duez, H., Dugail, I., Dumit, V.I., Duncan, M.C., Dunlop, E.A., Dunn, W.A., Dupont, N., Dupuis, L., Durán, R.V., Durcan, T.M., Duvezin-Caubet, S., Duvvuri, U., Eapen, V., Ebrahimi-Fakhari, D., Echard, A., Eckhart, L., Edelstein, C.L., Edinger, A.L., Eichinger, L., Eisenberg, T., Eisenberg-Lerner, A., Eissa, N.T., El-Deiry, W.S., El-Khoury, V., Elazar, Z., Eldar-Finkelman, H., Elliott, C.J., Emanuele, E., Emmenegger, U., Engedal, N., Engelbrecht, A.-M., Engelder, S., Enserink, J.M., Erdmann, R., Erenpreisa, J., Eri, R., Eriksen, J.L., Erman, A., Escalante, R., Eskelinen, E.-L., Espert, L., Esteban-Martínez, L., Evans, T.J., Fabri, M., Fabrias, G., Fabrizi, C., Facchiano, A., Færgeman, N.J., Faggioni, A., Fairlie, W.D., Fan, C., Fan, D., Fan, J., Fang, S., Fanto, M., Fanzani, A., Farkas, T., Faure, M., Favier, F.B., Fearnhead, H., Federici, M., Fei, E., Felizardo, T.C., Feng, H., Feng, Yibin, Feng, Yuchen, Ferguson, T.A., Fernández, Á.F., Fernandez-Barrena, M.G., Fernandez-Checa, J.C., Fernández-López, A., Fernandez-Zapico, M.E., Feron, O., Ferraro, E., Ferreira-Halder, C.V., Fesus, L., Feuer, R., Fiesel, F.C., Filippi-Chiela, E.C., Filomeni, G., Fimia, G.M., Fingert, J.H., Finkbeiner, S., Finkel, T., Fiorito, F., Fisher, P.B., Flajolet, M., Flamigni, F., Florey, O., Florio, S., Floto, R.A., Folini, M., Follo, C., Fon, E.A., Fornai, F., Fortunato, F., Fraldi, A., Franco, R., Francois, A., François, A., Frankel, L.B., Fraser, I.D., Frey, N., Freyssenet, D.G., Frezza, C., Friedman, S.L., Frigo, D.E., Fu, D., Fuentes, J.M., Fueyo, J., Fujitani, Y., Fujiwara, Y., Fujiya, M., Fukuda, M., Fulda, S., Fusco, C., Gabryel, B., Gaestel, M., Gailly, P., Gajewska, M., Galadari, S., Galili, G., Galindo, I., Galindo, M.F., Galliciotti, G., Galluzzi, Lorenzo, Galluzzi, Luca, Galy, V., Gammoh, N., Gandy, S., Ganesan, A.K., Ganesan, S., Ganley, I.G., Gannagé, M., Gao, F.-B., Gao, F., Gao, J.-X., García Nannig, L., García Vescovi, E., Garcia-Macia, M., Garcia-Ruiz, C., Garg, A.D., Garg, P.K., Gargini, R., Gassen, N.C., Gatica, D., Gatti, E., Gavard, J., Gavathiotis, E., Ge, L., Ge, P., Ge, S., Gean, P.-W., Gelmetti, V., Genazzani, A.A., Geng, J., Genschik, P., Gerner, L., Gestwicki, J.E., Gewirtz, D.A., Ghavami, S., Ghigo, E., Ghosh, D., Giammarioli, A.M., Giampieri, F., Giampietri, C., Giatromanolaki, A., Gibbings, D.J., Gibellini, L., Gibson, S.B., Ginet, V., Giordano, A., Giorgini, F., Giovannetti, E., Girardin, S.E., Gispert, S., Giuliano, S., Gladson,

C.L., Glavic, A., Gleave, M., Godefroy, N., Gogal, R.M., Gokulan, K., Goldman, G.H., Goletti, D., Goligorsky, M.S., Gomes, A.V., Gomes, L.C., Gomez, H., Gomez-Manzano, C., Gómez-Sánchez, R., Gonçalves, D.A., Goncu, E., Gong, Q., Gongora, C., Gonzalez, C.B., Gonzalez-Alegre, P., Gonzalez-Cabo, P., González-Polo, R.A., Goping, I.S., Gorbea, C., Gorbunov, N.V., Goring, D.R., Gorman, A.M., Gorski, S.M., Goruppi, S., Goto-Yamada, S., Gotor, C., Gottlieb, R.A., Gozes, I., Gozuacik, D., Graba, Y., Graef, M., Granato, G.E., Grant, G.D., Grant, S., Gravina, G.L., Green, D.R., Greenhough, A., Greenwood, M.T., Grimaldi, B., Gros, F., Grose, C., Groulx, J.-F., Gruber, F., Grumati, P., Grune, T., Guan, J.-L., Guan, K.-L., Guerra, B., Guillen, C., Gulshan, K., Gunst, J., Guo, C., Guo, L., Guo, M., Guo, W., Guo, X.-G., Gust, A.A., Gustafsson, Å.B., Gutierrez, E., Gutierrez, M.G., Gwak, H.-S., Haas, A., Haber, J.E., Hadano, S., Hagedorn, M., Hahn, D.R., Halayko, A.J., Hamacher-Brady, A., Hamada, K., Hamai, A., Hamann, A., Hamasaki, M., Hamer, I., Hamid, Q., Hammond, E.M., Han, F., Han, W., Handa, J.T., Hanover, J.A., Hansen, M., Harada, M., Harhaji-Trajkovic, L., Harper, J.W., Harrath, A.H., Harris, A.L., Harris, J., Hasler, U., Hasselblatt, P., Hasui, K., Hawley, R.G., Hawley, T.S., He, C., He, C.Y., He, F., He, G., He, R.-R., He, X.-H., He, Y.-W., He, Y.-Y., Heath, J.K., Hébert, M.-J., Heinzen, R.A., Helgason, G.V., Hensel, M., Henske, E.P., Her, C., Herman, P.K., Hernández, A., Hernandez, C., Hernández-Tiedra, S., Hetz, C., Hiesinger, P.R., Higaki, K., Hilfiker, S., Hill, B.G., Hill, J.A., Hill, W.D., Hino, K., Hofius, D., Hofman, P., Höglinger, G.U., Höhfeld, J., Holz, M.K., Hong, Y., Hood, D.A., Hoozemans, J.J., Hoppe, T., Hsu, C., Hsu, C.-Y., Hsu, L.-C., Hu, D., Hu, G., Hu, H.-M., Hu, H., Hu, M.C., Hu, Y.-C., Hu, Z.-W., Hua, F., Hua, Y., Huang, C., Huang, H.-L., Huang, K.-H., Huang, K.-Y., Huang, Shile, Huang, Shiqian, Huang, W.-P., Huang, Y.-R., Huang, Yong, Huang, Yunfei, Huber, T.B., Huebbe, P., Huh, W.-K., Hulmi, J.J., Hur, G.M., Hurley, J.H., Husak, Z., Hussain, S.N., Hussain, S., Hwang, J.J., Hwang, S., Hwang, T.I., Ichihara, A., Imai, Y., Imbriano, C., Inomata, M., Into, T., Iovane, V., Iovanna, J.L., Iozzo, R.V., Ip, N.Y., Irazoqui, J.E., Iribarren, P., Isaka, Y., Isakovic, A.J., Ischiropoulos, H., Isenberg, J.S., Ishaq, M., Ishida, H., Ishii, I., Ishmael, J.E., Isidoro, C., Isobe, K.-I., Isono, E., Issazadeh-Navikas, S., Itahana, K., Itakura, E., Ivanov, A.I., Iyer, A.K.V., Izquierdo, J.M., Izumi, Y., Izzo, V., Jäättelä, M., Jaber, N., Jackson, D.J., Jackson, W.T., Jacob, T.G., Jacques, T.S., Jagannath, C., Jain, A., Jana, N.R., Jang, B.K., Jani, A., Janji, B., Jannig, P.R., Jansson, P.J., Jean, S., Jendrach, M., Jeon, J.-H., Jessen, N., Jeung, E.-B., Jia, K., Jia, L., Jiang, Hong, Jiang, Hongchi, Jiang, L., Jiang, T., Jiang, Xiaoyan, Jiang, Xuejun, Jiang, Xuejun, Jiang, Ying, Jiang, Yongjun, Jiménez, A., Jin, C., Jin, H., Jin, L., Jin, M., Jin, S., Jinwal, U.K., Jo, E.-K., Johansen, T., Johnson, D.E., Johnson, G.V., Johnson, J.D., Jonasch, E., Jones, C., Joosten, L.A., Jordan, J., Joseph, A.-M., Joseph, B., Joubert, A.M., Ju, D., Ju, J., Juan, H.-F., Juenemann, K., Juhász, G., Jung, H.S., Jung, J.U., Jung, Y.-K., Jungbluth, H., Justice, M.J., Jutten, B., Kaakoush, N.O., Kaarniranta, K., Kaasik, A., Kabuta, T., Kaeffer, B., Kågedal, K., Kahana, A., Kajimura, S., Kakhlon, O., Kalia, M., Kalvakolanu, D.V., Kamada, Y., Kambas, K., Kaminsky, V.O., Kampinga, H.H., Kandouz, M., Kang, C., Kang, R., Kang, T.-C., Kanki, T., Kanneganti, T.-D., Kanno, H., Kanthasamy, A.G., Kantorow, M., Kaparakis-Liaskos, M., Kapuy, O., Karantza, V., Karim, M.R., Karmakar, P., Kaser, A., Kaushik, S., Kawula, T., Kaynar, A.M., Ke, P.-Y., Ke, Z.-J., Kehrl, J.H., Keller, K.E., Kemper, J.K., Kenworthy, A.K., Kepp, O., Kern, A., Kesari, S., Kessel, D., Ketteler, R., Kettelhut, I. do C., Khambu, B., Khan, M.M., Khandelwal, V.K., Khare, S., Kiang, J.G., Kiger, A.A., Kihara, A., Kim, A.L., Kim, C.H., Kim, D.R., Kim, D.-H., Kim, E.K., Kim, H.Y., Kim, H.-R., Kim, J.-S., Kim, Jeong Hun,

Kim, J.C., Kim, Jin Hyoung, Kim, K.W., Kim, M.D., Kim, M.-M., Kim, P.K., Kim, S.W., Kim, S.-Y., Kim, Y.-S., Kim, Y., Kimchi, A., Kimmelman, A.C., Kimura, T., King, J.S., Kirkegaard, K., Kirkin, V., Kirshenbaum, L.A., Kishi, S., Kitajima, Y., Kitamoto, K., Kitaoka, Y., Kitazato, K., Kley, R.A., Klimecki, W.T., Klinkenberg, M., Klucken, J., Knævelsrud, H., Knecht, E., Knuppertz, L., Ko, J.-L., Kobayashi, S., Koch, J.C., Koechlin-Ramonatxo, C., Koenig, U., Koh, Y.H., Köhler, K., Kohlwein, S.D., Koike, M., Komatsu, M., Kominami, E., Kong, D., Kong, H.J., Konstantakou, E.G., Kopp, B.T., Korcsmaros, T., Korhonen, L., Korolchuk, V.I., Koshkina, N.V., Kou, Y., Koukourakis, M.I., Koumenis, C., Kovács, A.L., Kovács, T., Kovacs, W.J., Koya, D., Kraft, C., Krainc, D., Kramer, H., Kravic-Stevovic, T., Krek, W., Kretz-Remy, C., Krick, R., Krishnamurthy, M., Kriston-Vizi, J., Kroemer, G., Kruer, M.C., Kruger, R., Ktistakis, N.T., Kuchitsu, K., Kuhn, C., Kumar, A.P., Kumar, Anuj, Kumar, Ashok, Kumar, Deepak, Kumar, Dhiraj, Kumar, R., Kumar, S., Kundu, M., Kung, H.-J., Kuno, A., Kuo, S.-H., Kuret, J., Kurz, T., Kwok, T., Kwon, T.K., Kwon, Y.T., Kyrmizi, I., La Spada, A.R., Lafont, F., Lahm, T., Lakkaraju, A., Lam, T., Lamark, T., Lancel, S., Landowski, T.H., Lane, D.J.R., Lane, J.D., Lanzi, C., Lapaquette, P., Lapierre, L.R., Laporte, J., Laukkarinen, J., Laurie, G.W., Lavandero, S., Lavie, L., LaVoie, M.J., Law, B.Y.K., Law, H.K.-W., Law, K.B., Layfield, R., Lazo, P.A., Le Cam, L., Le Roch, K.G., Le Stunff, H., Leardkamolkarn, V., Lecuit, M., Lee, B.-H., Lee, C.-H., Lee, E.F., Lee, G.M., Lee, H.-J., Lee, H., Lee, J.K., Lee, J., Lee, J.-H., Lee, J.H., Lee, M., Lee, M.-S., Lee, P.J., Lee, S.W., Lee, Seung-Jae, Lee, Shiow-Ju, Lee, S.Y., Lee, S.H., Lee, S.S., Lee, Sung-Joon, Lee, S., Lee, Y.-R., Lee, Y.J., Lee, Y.H., Leeuwenburgh, C., Lefort, S., Legouis, R., Lei, J., Lei, Q.-Y., Leib, D.A., Leibowitz, G., Lekli, I., Lemaire, S.D., Lemasters, J.J., Lemberg, M.K., Lemoine, A., Leng, S., Lenz, G., Lenzi, P., Lerman, L.O., Lettieri Barbato, D., Leu, J.I.-J., Leung, H.Y., Levine, B., Lewis, P.A., Lezoualc'h, F., Li, C., Li, F., Li, F.-J., Li, J., Li, K., Li, L., Li, M., Li, M., Li, Q., Li, R., Li, S., Li, W., Li, W., Li, X., Li, Y., Lian, J., Liang, C., Liang, Q., Liao, Y., Liberal, J., Liberski, P.P., Lie, P., Lieberman, A.P., Lim, H.J., Lim, K.-L., Lim, K., Lima, R.T., Lin, C.-S., Lin, C.-F., Lin, Fang, Lin, Fangming, Lin, F.-C., Lin, K., Lin, K.-H., Lin, P.-H., Lin, T., Lin, W.-W., Lin, Y.-S., Lin, Y., Linden, R., Lindholm, D., Lindqvist, L.M., Lingor, P., Linkermann, A., Liotta, L.A., Lipinski, M.M., Lira, V.A., Lisanti, M.P., Liton, P.B., Liu, B., Liu, C., Liu, C.-F., Liu, F., Liu, H.-J., Liu, J., Liu, J.-J., Liu, J.-L., Liu, K., Liu, Leyuan, Liu, Liang, Liu, Q., Liu, R.-Y., Liu, Shiming, Liu, Shuwen, Liu, W., Liu, X.-D., Liu, Xiangguo, Liu, X.-H., Liu, Xinfeng, Liu, Xu, Liu, Xueqin, Liu, Yang, Liu, Yule, Liu, Zexian, Liu, Zhe, Liuzzi, J.P., Lizard, G., Ljujic, M., Lodhi, I.J., Logue, S.E., Lokeshwar, B.L., Long, Y.C., Lonial, S., Loos, B., López-Otín, C., López-Vicario, C., Lorente, M., Lorenzi, P.L., Lőrincz, P., Los, M., Lotze, M.T., Lovat, P.E., Lu, Binfeng, Lu, Bo, Lu, J., Lu, Q., Lu, S.-M., Lu, S., Lu, Y., Luciano, F., Luckhart, S., Lucocq, J.M., Ludovico, P., Lugea, A., Lukacs, N.W., Lum, J.J., Lund, A.H., Luo, H., Luo, J., Luo, S., Luparello, C., Lyons, T., Ma, J., Ma, Yi, Ma, Yong, Ma, Z., Machado, J., Machado-Santelli, G.M., Macian, F., MacIntosh, G.C., MacKeigan, J.P., Macleod, K.F., MacMicking, J.D., MacMillan-Crow, L.A., Madeo, F., Madesh, M., Madrigal-Matute, J., Maeda, A., Maeda, T., Maegawa, G., Maellaro, E., Maes, H., Magariños, M., Maiese, K., Maiti, T.K., Maiuri, L., Maiuri, M.C., Maki, C.G., Malli, R., Malorni, W., Maloyan, A., Mami-Chouaib, F., Man, N., Mancias, J.D., Mandelkow, E.-M., Mandell, M.A., Manfredi, A.A., Manié, S.N., Manzoni, C., Mao, K., Mao, Z., Mao, Z.-W., Marambaud, P., Marconi, A.M., Marelja, Z., Marfe, G., Margeta, M., Margittai, E., Mari, M., Mariani, F.V., Marin, C., Marinelli, S., Mariño, G., Markovic, I., Marquez, R., Martelli, A.M., Martens, S., Martin, K.R.,

Martin, S.J., Martin, S., Martin-Acebes, M.A., Martín-Sanz, P., Martinand-Mari, C., Martinet, W., Martinez, J., Martinez-Lopez, N., Martinez-Outschoorn, U., Martínez-Velázquez, M., Martinez-Vicente, M., Martins, W.K., Mashima, H., Mastrianni, J.A., Matarese, G., Matarrese, P., Mateo, R., Matoba, S., Matsumoto, N., Matsushita, T., Matsuura, A., Matsuzawa, T., Mattson, M.P., Matus, S., Maugeri, N., Mauvezin, C., Mayer, A., Maysinger, D., Mazzolini, G.D., McBrayer, M.K., McCall, K., McCormick, C., McInerney, G.M., McIver, S.C., McKenna, S., McMahon, J.J., McNeish, I.A., Mehta-Grigoriou, F., Medema, J.P., Medina, D.L., Megyeri, K., Mehrpour, M., Mehta, J.L., Mei, Y., Meier, U.-C., Meijer, A.J., Meléndez, A., Melino, G., Melino, S., de Melo, E.J.T., Mena, M.A., Meneghini, M.D., Menendez, J.A., Menezes, R., Meng, L., Meng, L.-H., Meng, S., Menghini, R., Menko, A.S., Menna-Barreto, R.F., Menon, M.B., Meraz-Ríos, M.A., Merla, G., Merlini, L., Merlot, A.M., Meryk, A., Meschini, S., Meyer, J.N., Mi, M.-T., Miao, C.-Y., Micale, L., Michaeli, S., Michiels, C., Migliaccio, A.R., Mihailidou, A.S., Mijaljica, D., Mikoshiba, K., Milan, E., Miller-Fleming, L., Mills, G.B., Mills, I.G., Minakaki, G., Minassian, B.A., Ming, X.-F., Minibayeva, F., Minina, E.A., Mintern, J.D., Minucci, S., Miranda-Vizueté, A., Mitchell, C.H., Miyamoto, S., Miyazawa, K., Mizushima, N., Mnich, K., Mograbi, B., Mohseni, S., Moita, L.F., Molinari, Marco, Molinari, Maurizio, Møller, A.B., Mollereau, B., Mollinedo, F., Mongillo, M., Monick, M.M., Montagnaro, S., Montell, C., Moore, D.J., Moore, M.N., Mora-Rodriguez, R., Moreira, P.I., Morel, E., Morelli, M.B., Moreno, S., Morgan, M.J., Moris, A., Moriyasu, Y., Morrison, J.L., Morrison, L.A., Morselli, E., Moscat, J., Moseley, P.L., Mostowy, S., Motori, E., Mottet, D., Mottram, J.C., Moussa, C.E.-H., Mpakou, V.E., Mukhtar, H., Mulcahy Levy, J.M., Muller, S., Muñoz-Moreno, R., Muñoz-Pinedo, C., Münz, C., Murphy, M.E., Murray, J.T., Murthy, A., Mysorekar, I.U., Nabi, I.R., Nabissi, M., Nader, G.A., Nagahara, Y., Nagai, Y., Nagata, K., Nagelkerke, A., Nagy, P., Naidu, S.R., Nair, S., Nakano, H., Nakatogawa, H., Nanjundan, M., Napolitano, G., Naqvi, N.I., Nardacci, R., Narendra, D.P., Narita, M., Nascimbeni, A.C., Natarajan, R., Navegantes, L.C., Nawrocki, S.T., Nazarko, T.Y., Nazarko, V.Y., Neill, T., Neri, L.M., Netea, M.G., Netea-Maier, R.T., Neves, B.M., Ney, P.A., Nezis, I.P., Nguyen, H.T., Nguyen, H.P., Nicot, A.-S., Nilsen, H., Nilsson, P., Nishimura, M., Nishino, I., Niso-Santano, M., Niu, H., Nixon, R.A., Njar, V.C., Noda, T., Noegel, A.A., Nolte, E.M., Norberg, E., Norga, K.K., Noureini, S.K., Notomi, S., Notterpek, L., Nowikovsky, K., Nukina, N., Nürnberger, T., O'Donnell, V.B., O'Donovan, T., O'Dwyer, P.J., Oehme, I., Oeste, C.L., Ogawa, M., Ogretmen, B., Ogura, Y., Oh, Y.J., Ohmuraya, M., Ohshima, T., Ojha, R., Okamoto, K., Okazaki, T., Oliver, F.J., Ollinger, K., Olsson, S., Orban, D.P., Ordonez, P., Orhon, I., Orosz, L., O'Rourke, E.J., Orozco, H., Ortega, A.L., Ortona, E., Osellame, L.D., Oshima, J., Oshima, S., Osiewacz, H.D., Otomo, T., Otsu, K., Ou, J.-H.J., Outeiro, T.F., Ouyang, D.-Y., Ouyang, H., Overholtzer, M., Ozbun, M.A., Ozdinler, P.H., Ozpolat, B., Pacelli, C., Paganetti, P., Page, G., Pages, G., Pagnini, U., Pajak, B., Pak, S.C., Pakos-Zebrucka, K., Pakpour, N., Palková, Z., Palladino, F., Pallauf, K., Pallet, N., Palmieri, M., Paludan, S.R., Palumbo, C., Palumbo, S., Pampliega, O., Pan, H., Pan, W., Panaretakis, T., Pandey, A., Pantazopoulou, A., Papackova, Z., Papademetrio, D.L., Papassideri, I., Papini, A., Parajuli, N., Pardo, J., Parekh, V.V., Parenti, G., Park, J.-I., Park, J., Park, O.K., Parker, R., Parlato, R., Parys, J.B., Parzych, K.R., Pasquet, J.-M., Pasquier, B., Pasumarthi, K.B., Patschan, D., Patterson, C., Pattingre, S., Pattison, S., Pause, A., Pavenstädt, H., Pavone, F., Pedrozo, Z., Peña, F.J., Peñalva, M.A., Pende, M., Peng, J., Penna, F., Penninger,

J.M., Pensalfini, A., Pepe, S., Pereira, G.J., Pereira, P.C., Pérez-de la Cruz, V., Pérez-Pérez, M.E., Pérez-Rodríguez, D., Pérez-Sala, D., Perier, C., Perl, A., Perlmutter, D.H., Perrotta, I., Pervaiz, S., Pesonen, M., Pessin, J.E., Peters, G.J., Petersen, M., Petrache, I., Petrof, B.J., Petrovski, G., Phang, J.M., Piacentini, M., Pierdominici, M., Pierre, P., Pierrefite-Carle, V., Pietrocola, F., Pimentel-Muñíos, F.X., Pinar, M., Pineda, B., Pinkas-Kramarski, R., Pinti, M., Pinton, P., Piperdi, B., Piret, J.M., Platánias, L.C., Platta, H.W., Plowey, E.D., Pöggeler, S., Poirot, M., Polčič, P., Poletti, A., Poon, A.H., Popelka, H., Popova, B., Poprawa, I., Poulouse, S.M., Poulton, J., Powers, S.K., Powers, T., Pozuelo-Rubio, M., Prak, K., Prange, R., Prescott, M., Priault, M., Prince, S., Proia, R.L., Proikas-Cezanne, T., Prokisch, H., Promponas, V.J., Przyklenk, K., Puertollano, R., Pugazhenthii, S., Puglielli, L., Pujol, A., Puyal, J., Pyeon, D., Qi, X., Qian, W.-B., Qin, Z.-H., Qiu, Y., Qu, Z., Cuadrilátero, J., Quinn, F., Raben, N., Rabinowich, H., Radogna, F., Ragusa, M.J., Rahmani, M., Raina, K., Ramanadham, S., Ramesh, R., Rami, A., Randall-Demllo, S., Randow, F., Rao, H., Rao, V.A., Rasmussen, B.B., Rasse, T.M., Ratovitski, E.A., Rautou, P.-E., Ray, S.K., Razani, B., Reed, B.H., Reggiori, F., Rehm, M., Reichert, A.S., Rein, T., Reiner, D.J., Reits, E., Ren, J., Ren, X., Renna, M., Reusch, J.E., Revuelta, J.L., Reyes, L., Rezaie, A.R., Richards, R.I., Richardson, D.R., Richetta, C., Riehle, M.A., Rihn, B.H., Rikihisa, Y., Riley, B.E., Rimbach, G., Rippo, M.R., Ritis, K., Rizzi, F., Rizzo, E., Roach, P.J., Robbins, J., Roberge, M., Roca, G., Roccheri, M.C., Rocha, S., Rodrigues, C.M., Rodríguez, C.I., de Córdoba, S.R., Rodríguez-Muela, N., Roelofs, J., Rogov, V.V., Rohn, T.T., Rohrer, B., Romanelli, D., Romani, L., Romano, P.S., Roncero, M.I.G., Rosa, J.L., Rosello, A., Rosen, K.V., Rosenstiel, P., Rost-Roszkowska, M., Roth, K.A., Roué, G., Rouis, M., Rouschop, K.M., Ruan, D.T., Ruano, D., Rubinsztein, D.C., Rucker, E.B., Rudich, A., Rudolf, E., Rudolf, R., Ruegg, M.A., Ruiz-Roldan, C., Ruparelia, A.A., Rusmini, P., Russ, D.W., Russo, G.L., Russo, G., Russo, R., Rusten, T.E., Ryabovol, V., Ryan, K.M., Ryter, S.W., Sabatini, D.M., Sacher, M., Sachse, C., Sack, M.N., Sadoshima, J., Saftig, P., Sagi-Eisenberg, R., Sahni, S., Saikumar, P., Saito, T., Saitoh, T., Sakakura, K., Sakoh-Nakatogawa, M., Sakuraba, Y., Salazar-Roa, M., Salomoni, P., Saluja, A.K., Salvaterra, P.M., Salvioli, R., Samali, A., Sanchez, A.M., Sánchez-Alcázar, J.A., Sanchez-Prieto, R., Sandri, M., Sanjuan, M.A., Santaguida, S., Santambrogio, L., Santoni, G., Dos Santos, C.N., Saran, S., Sardiello, M., Sargent, G., Sarkar, P., Sarkar, S., Sarrias, M.R., Sarwal, M.M., Sasakawa, C., Sasaki, M., Sass, M., Sato, K., Sato, M., Satriano, J., Savaraj, N., Saveljeva, S., Schaefer, L., Schaible, U.E., Scharl, M., Schatzl, H.M., Schekman, R., Scheper, W., Schiavi, A., Schipper, H.M., Schmeisser, H., Schmidt, J., Schmitz, I., Schneider, B.E., Schneider, E.M., Schneider, J.L., Schon, E.A., Schönenberger, M.J., Schönthal, A.H., Schorderet, D.F., Schröder, B., Schuck, S., Schulze, R.J., Schwarten, M., Schwarz, T.L., Sciarretta, S., Scotto, K., Scovassi, A.I., Screatón, R.A., Screen, M., Seca, H., Sedej, S., Segatori, L., Segev, N., Seglen, P.O., Seguí-Simarro, J.M., Segura-Aguilar, J., Seki, E., Sell, C., Seiliez, I., Semenkovich, C.F., Semenza, G.L., Sen, U., Serra, A.L., Serrano-Puebla, A., Sesaki, H., Setoguchi, T., Settembre, C., Shacka, J.J., Shajahan-Haq, A.N., Shapiro, I.M., Sharma, S., She, H., Shen, C.-K.J., Shen, C.-C., Shen, H.-M., Shen, S., Shen, W., Sheng, R., Sheng, X., Sheng, Z.-H., Shepherd, T.G., Shi, J., Shi, Qiang, Shi, Qinghua, Shi, Y., Shibusani, S., Shibuya, K., Shidoji, Y., Shieh, J.-J., Shih, C.-M., Shimada, Y., Shimizu, S., Shin, D.W., Shinohara, M.L., Shintani, M., Shintani, T., Shioi, T., Shirabe, K., Shirisverdlov, R., Shirihi, O., Shore, G.C., Shu, C.-W., Shukla, D., Sibirny, A.A., Sica, V., Sigurdson, C.J., Sigurdsson, E.M., Sijwali, P.S., Sikorska, B., Silveira, W.A., Silvente-

Poirot, S., Silverman, G.A., Simak, J., Simmet, T., Simon, A.K., Simon, H.-U., Simone, C., Simons, M., Simonsen, A., Singh, R., Singh, S.V., Singh, S.K., Sinha, D., Sinha, S., Sinicrope, F.A., Sirko, A., Sirohi, K., Sishi, B.J., Sittler, A., Siu, P.M., Sivridis, E., Skwarska, A., Slack, R., Slaninová, I., Slavov, N., Smaili, S.S., Smalley, K.S., Smith, D.R., Soenen, S.J., Soleimanpour, S.A., Solhaug, A., Somasundaram, K., Son, J.H., Sonawane, A., Song, C., Song, F., Song, H.K., Song, J.-X., Song, W., Soo, K.Y., Sood, A.K., Soong, T.W., Soontornniyomkij, V., Sorice, M., Sotgia, F., Soto-Pantoja, D.R., Sotthibundhu, A., Sousa, M.J., Spaink, H.P., Span, P.N., Spang, A., Sparks, J.D., Speck, P.G., Spector, S.A., Spies, C.D., Springer, W., Clair, D.S., Stacchiotti, A., Staels, B., Stang, M.T., Starczynowski, D.T., Starokadomskyy, P., Steegborn, C., Steele, J.W., Stefanis, L., Steffan, J., Stellrecht, C.M., Stenmark, H., Stepkowski, T.M., Stern, S.T., Stevens, C., Stockwell, B.R., Stoka, V., Storchova, Z., Stork, B., Stratoulis, V., Stravopodis, D.J., Strnad, P., Strohecker, A.M., Ström, A.-L., Stromhaug, P., Stulik, J., Su, Y.-X., Su, Z., Subauste, C.S., Subramaniam, S., Sue, C.M., Suh, S.W., Sui, X., Sukseeree, S., Sulzer, D., Sun, F.-L., Sun, Jiaren, Sun, Jun, Sun, S.-Y., Sun, Yang, Sun, Yi, Sun, Yingjie, Sundaramoorthy, V., Sung, J., Suzuki, H., Suzuki, K., Suzuki, N., Suzuki, T., Suzuki, Y.J., Swanson, M.S., Swanton, C., Swärd, K., Swarup, G., Sweeney, S.T., Sylvester, P.W., Szatmari, Z., Szegezdi, E., Szlosarek, P.W., Taegtmeier, H., Tafani, M., Taillebourg, E., Tait, S.W., Takacs-Vellai, K., Takahashi, Y., Takáts, S., Takemura, G., Takigawa, N., Talbot, N.J., Tamagno, E., Tamburini, J., Tan, C.-P., Tan, L., Tan, M.L., Tan, M., Tan, Y.-J., Tanaka, K., Tanaka, M., Tang, Daolin, Tang, Dingzhong, Tang, G., Tanida, I., Tanji, K., Tannous, B.A., Tapia, J.A., Tasset-Cuevas, I., Tatar, M., Tavassoly, I., Tavernarakis, N., Taylor, A., Taylor, G.S., Taylor, G.A., Taylor, J.P., Taylor, M.J., Tchetina, E.V., Tee, A.R., Teixeira-Clerc, F., Telang, S., Tencomnao, T., Teng, B.-B., Teng, R.-J., Terro, F., Tettamanti, G., Theiss, A.L., Theron, A.E., Thomas, K.J., Thomé, M.P., Thomes, P.G., Thorburn, A., Thorner, J., Thum, T., Thumm, M., Thurston, T.L., Tian, L., Till, A., Ting, J.P.-Y., Titorenko, V.I., Toker, L., Toldo, S., Tooze, S.A., Topisirovic, I., Torgersen, M.L., Torosantucci, L., Torriglia, A., Torrisi, M.R., Tournier, C., Towns, R., Trajkovic, V., Travassos, L.H., Triola, G., Tripathi, D.N., Trisciuglio, D., Troncoso, R., Trougakos, I.P., Truttmann, A.C., Tsai, K.-J., Tschan, M.P., Tseng, Y.-H., Tsukuba, T., Tsung, A., Tsvetkov, A.S., Tu, S., Tuan, H.-Y., Tucci, M., Tumbarello, D.A., Turk, B., Turk, V., Turner, R.F., Tveita, A.A., Tyagi, S.C., Ubukata, M., Uchiyama, Y., Udelnow, A., Ueno, T., Umekawa, M., Umemiya-Shirafuji, R., Underwood, B.R., Ungermann, C., Ureshino, R.P., Ushioda, R., Uversky, V.N., Uzcátegui, N.L., Vaccari, T., Vaccaro, M.I., Váchová, L., Vakifahmetoglu-Norberg, H., Valdor, R., Valente, E.M., Vallette, F., Valverde, A.M., Van den Berghe, G., Van Den Bosch, L., van den Brink, G.R., van der Goot, F.G., van der Klei, I.J., van der Laan, L.J., van Doorn, W.G., van Egmond, M., van Golen, K.L., Van Kaer, L., van Lookeren Campagne, M., Vandenabeele, P., Vandenbergh, W., Vanhorebeek, I., Varela-Nieto, I., Vasconcelos, M.H., Vasko, R., Vavvas, D.G., Vega-Naredo, I., Velasco, G., Velentzas, A.D., Velentzas, P.D., Vellai, T., Vellenga, E., Vendelbo, M.H., Venkatachalam, K., Ventura, N., Ventura, S., Veras, P.S., Verdier, M., Vertessy, B.G., Viale, A., Vidal, M., Vieira, H.L.A., Vierstra, R.D., Vigneswaran, N., Vij, N., Vila, M., Villar, M., Villar, V.H., Villarroja, J., Vindis, C., Viola, G., Viscomi, M.T., Vitale, G., Vogl, D.T., Voitsekhovskaja, O.V., von Haefen, C., von Schwarzenberg, K., Voth, D.E., Vouret-Craviari, V., Vuori, K., Vyas, J.M., Waeber, C., Walker, C.L., Walker, M.J., Walter, J., Wan, L., Wan, X., Wang, B., Wang, Caihong, Wang, C.-Y., Wang, Chengshu, Wang, Chenran, Wang,

Chuangui, Wang, D., Wang, Fen, Wang, Fuxin, Wang, G., Wang, H.-J., Wang, Haichao, Wang, H.-G., Wang, Hongmin, Wang, H.-D., Wang, Jing, Wang, Junjun, Wang, M., Wang, M.-Q., Wang, P.-Y., Wang, P., Wang, R.C., Wang, S., Wang, T.-F., Wang, Xian, Wang, X.-J., Wang, X.-W., Wang, Xin, Wang, Xuejun, Wang, Yan, Wang, Yanming, Wang, Ying, Wang, Y.-J., Wang, Yipeng, Wang, Yu, Wang, Y.T., Wang, Yuqing, Wang, Z.-N., Wappner, P., Ward, C., Ward, D.M., Warnes, G., Watada, H., Watanabe, Y., Watase, K., Weaver, T.E., Weekes, C.D., Wei, J., Weide, T., Weihl, C.C., Weindl, G., Weis, S.N., Wen, L., Wen, X., Wen, Y., Westermann, B., Weyand, C.M., White, A.R., White, E., Whitton, J.L., Whitworth, A.J., Wiels, J., Wild, F., Wildenberg, M.E., Wileman, T., Wilkinson, D.S., Wilkinson, S., Willbold, D., Williams, C., Williams, K., Williamson, P.R., Winklhofer, K.F., Witkin, S.S., Wohlgemuth, S.E., Wollert, T., Wolvetang, E.J., Wong, E., Wong, G.W., Wong, R.W., Wong, V.K.W., Woodcock, E.A., Wright, K.L., Wu, C., Wu, D., Wu, G.S., Wu, Jian, Wu, Junfang, Wu, Mian, Wu, Min, Wu, S., Wu, W.K., Wu, Y., Wu, Z., Xavier, C.P., Xavier, R.J., Xia, G.-X., Xia, T., Xia, W., Xia, Y., Xiao, H., Xiao, J., Xiao, S., Xiao, W., Xie, C.-M., Xie, Zhiping, Xie, Zhonglin, Xilouri, M., Xiong, Y., Xu, Chuanshan, Xu, Congfeng, Xu, F., Xu, Haoxing, Xu, Hongwei, Xu, Jian, Xu, Jianzhen, Xu, Jinxian, Xu, L., Xu, X., Xu, Yangqing, Xu, Ye, Xu, Z.-X., Xu, Z., Xue, Y., Yamada, T., Yamamoto, A., Yamanaka, K., Yamashina, S., Yamashiro, S., Yan, Bing, Yan, Bo, Yan, X., Yan, Z., Yanagi, Y., Yang, D.-S., Yang, J.-M., Yang, L., Yang, M., Yang, P.-M., Yang, P., Yang, Q., Yang, W., Yang, W.Y., Yang, X., Yang, Yi, Yang, Ying, Yang, Zhifen, Yang, Zhihong, Yao, M.-C., Yao, P.J., Yao, X., Yao, Zhenyu, Yao, Zhiyuan, Yasui, L.S., Ye, M., Yedvobnick, B., Yeganeh, B., Yeh, E.S., Yeyati, P.L., Yi, F., Yi, L., Yin, X.-M., Yip, C.K., Yoo, Y.-M., Yoo, Y.H., Yoon, S.-Y., Yoshida, K.-I., Yoshimori, T., Young, K.H., Yu, H., Yu, J.J., Yu, J.-T., Yu, J., Yu, L., Yu, W.H., Yu, X.-F., Yu, Z., Yuan, J., Yuan, Z.-M., Yue, B.Y., Yue, J., Yue, Z., Zacks, D.N., Zacksenhaus, E., Zaffaroni, N., Zaglia, T., Zakeri, Z., Zecchini, V., Zeng, J., Zeng, M., Zeng, Q., Zervos, A.S., Zhang, D.D., Zhang, F., Zhang, G., Zhang, G.-C., Zhang, Hao, Zhang, Hong, Zhang, Hong, Zhang, Hongbing, Zhang, Jian, Zhang, Jian, Zhang, Jiangwei, Zhang, Jianhua, Zhang, J.-P., Zhang, Li, Zhang, Lin, Zhang, Lin, Zhang, Long, Zhang, M.-Y., Zhang, X., Zhang, X.D., Zhang, Yan, Zhang, Yang, Zhang, Yanjin, Zhang, Yingmei, Zhang, Yunjiao, Zhao, M., Zhao, W.-L., Zhao, X., Zhao, Y.G., Zhao, Ying, Zhao, Yongchao, Zhao, Y.-X., Zhao, Z., Zhao, Z.J., Zheng, D., Zheng, X.-L., Zheng, X., Zhivotovsky, B., Zhong, Q., Zhou, G.-Z., Zhou, G., Zhou, H., Zhou, S.-F., Zhou, X.-J., Zhu, Hongxin, Zhu, Hua, Zhu, W.-G., Zhu, W., Zhu, X.-F., Zhu, Y., Zhuang, S.-M., Zhuang, X., Ziparo, E., Zois, C.E., Zoladek, T., Zong, W.-X., Zorzano, A., Zughaiier, S.M., 2016. Guidelines for the use and interpretation of assays for monitoring autophagy (3rd edition). *Autophagy* 12, 1–222. <https://doi.org/10.1080/15548627.2015.1100356>

Kobayashi, K.S., 2005. Nod2-Dependent Regulation of Innate and Adaptive Immunity in the Intestinal Tract. *Science* 307, 731–734. <https://doi.org/10.1126/science.1104911>

Koch S., Kucharzik T., Heidemann J., Nusrat A., Luegering A., 2010. Investigating the role of proinflammatory CD16+ monocytes in the pathogenesis of inflammatory bowel disease. *Clin. Exp. Immunol.* 161, 332–341. <https://doi.org/10.1111/j.1365-2249.2010.04177.x>

Koike, M., Shibata, M., Tadakoshi, M., Gotoh, K., Komatsu, M., Waguri, S., Kawahara, N., Kuida, K., Nagata, S., Kominami, E., Tanaka, K., Uchiyama, Y., 2008. Inhibition of autophagy prevents hippocampal pyramidal neuron death after hypoxic-

- ischemic injury. *Am. J. Pathol.* 172, 454–469. <https://doi.org/10.2353/ajpath.2008.070876>
- Konrad, A., Cong, Y., Duck, W., Borlaza, R., Elson, C.O., 2006. Tight mucosal compartmentation of the murine immune response to antigens of the enteric microbiota. *Gastroenterology* 130, 2050–2059. <https://doi.org/10.1053/j.gastro.2006.02.055>
- Kouroku, Y., Fujita, E., Tanida, I., Ueno, T., Isoai, A., Kumagai, H., Ogawa, S., Kaufman, R.J., Kominami, E., Momoi, T., 2007. ER stress (PERK/eIF2 [alpha] phosphorylation) mediates the polyglutamine-induced LC3 conversion, an essential step for autophagy formation. *Cell Death Differ.* 14, 230.
- Kovsan, J., Blüher, M., Tarnovscki, T., Klötting, N., Kirshtein, B., Madar, L., Shai, I., Golan, R., Harman-Boehm, I., Schön, M.R., Greenberg, A.S., Elazar, Z., Bashan, N., Rudich, A., 2011. Altered autophagy in human adipose tissues in obesity. *J. Clin. Endocrinol. Metab.* 96, E268-277. <https://doi.org/10.1210/jc.2010-1681>
- Kroemer, G., Galluzzi, L., Brenner, C., 2007. Mitochondrial membrane permeabilization in cell death. *Physiol. Rev.* 87, 99–163. <https://doi.org/10.1152/physrev.00013.2006>
- Kroemer, G., Martin, S.J., 2005. Caspase-independent cell death. *Nat. Med.* 11, 725–730. <https://doi.org/10.1038/nm1263>
- Kuballa, P., Huett, A., Rioux, J.D., Daly, M.J., Xavier, R.J., 2008. Impaired autophagy of an intracellular pathogen induced by a Crohn's disease associated ATG16L1 variant. *PLoS One* 3, e3391. <https://doi.org/10.1371/journal.pone.0003391>
- Kuenzig, M.E., Rezaie, A., Seow, C.H., Otley, A.R., Steinhart, A.H., Griffiths, A.M., Kaplan, G.G., Benchimol, E.I., 2014. Budesonide for maintenance of remission in Crohn's disease. *Cochrane Database Syst Rev* 8, Cd002913. <https://doi.org/10.1002/14651858.CD002913.pub3>
- Kyrmizi, I., Gresnigt, M.S., Akoumianaki, T., Samonis, G., Sidiropoulos, P., Boumpas, D., Netea, M.G., van de Veerdonk, F.L., Kontoyiannis, D.P., Chamilos, G., 2013. Corticosteroids Block Autophagy Protein Recruitment in *Aspergillus fumigatus* Phagosomes via Targeting Dectin-1/Syk Kinase Signaling. *J. Immunol.* 191, 1287–1299. <https://doi.org/10.4049/jimmunol.1300132>
- Laane, E., Tamm, K.P., Buentke, E., Ito, K., Khahariza, P., Oscarsson, J., Corcoran, M., Björklund, A.C., Hultenby, K., Lundin, J., others, 2009. Cell death induced by dexamethasone in lymphoid leukemia is mediated through initiation of autophagy. *Cell Death Differ.* 16, 1018.
- Lamark, T., Johansen, T., 2012. Aggrephagy: Selective Disposal of Protein Aggregates by Macroautophagy [WWW Document]. *Int. J. Cell Biol.* <https://doi.org/10.1155/2012/736905>
- Lamb, C.A., Yoshimori, T., Tooze, S.A., 2013. The autophagosome: origins unknown, biogenesis complex. *Nat. Rev. Mol. Cell Biol.* 14, 759–774. <https://doi.org/10.1038/nrm3696>
- Lange, K.M. de, Moutsianas, L., Lee, J.C., Lamb, C.A., Luo, Y., Kennedy, N.A., Jostins, L., Rice, D.L., Gutierrez-Achury, J., Ji, S.-G., Heap, G., Nimmo, E.R., Edwards, C., Henderson, P., Mowat, C., Sanderson, J., Satsangi, J., Simmons, A., Wilson, D.C., Tremelling, M., Hart, A., Mathew, C.G., Newman, W.G., Parkes, M., Lees, C.W., Uhlig, H., Hawkey, C., Prescott, N.J., Ahmad, T., Mansfield, J.C., Anderson, C.A., Barrett, J.C., 2017. Genome-wide association study implicates immune activation of multiple integrin genes in inflammatory bowel disease. *Nat. Genet.* 49, 256–261. <https://doi.org/10.1038/ng.3760>

- Lapaquette, Glasser, A.-L., Huett, A., Xavier, R.J., Darfeuille-Michaud, A., 2010. Crohn's disease-associated adherent-invasive E. coli are selectively favoured by impaired autophagy to replicate intracellularly. *Cell. Microbiol.* 12, 99–113. <https://doi.org/10.1111/j.1462-5822.2009.01381.x>
- Lapaquette, P., Bringer, M.-A., Darfeuille-Michaud, A., 2012. Defects in autophagy favour adherent-invasive Escherichia coli persistence within macrophages leading to increased pro-inflammatory response. *Cell. Microbiol.* 14, 791–807. <https://doi.org/10.1111/j.1462-5822.2012.01768.x>
- Lapaquette, P., Glasser, A.L., Huett, A., Xavier, R.J., Darfeuille-Michaud, A., 2010. Crohn's disease-associated adherent-invasive E. coli are selectively favoured by impaired autophagy to replicate intracellularly. *Cell Microbiol* 12, 99–113. <https://doi.org/10.1111/j.1462-5822.2009.01381.x>
- Laplante, M., Sabatini, D.M., 2012. mTOR Signaling in Growth Control and Disease. *Cell* 149, 274–293. <https://doi.org/10.1016/j.cell.2012.03.017>
- Lassen, K.G., Kuballa, P., Conway, K.L., Patel, K.K., Becker, C.E., Peloquin, J.M., Villablanca, E.J., Norman, J.M., Liu, T.C., Heath, R.J., Becker, M.L., Fagbami, L., Horn, H., Mercer, J., Yilmaz, O.H., Jaffe, J.D., Shamji, A.F., Bhan, A.K., Carr, S.A., Daly, M.J., Virgin, H.W., Schreiber, S.L., Stappenbeck, T.S., Xavier, R.J., 2014. Atg16L1 T300A variant decreases selective autophagy resulting in altered cytokine signaling and decreased antibacterial defense. *Proc Natl Acad Sci U S A* 111, 7741–6. <https://doi.org/10.1073/pnas.1407001111>
- Leal, R.F., Coy, C.S.R., Velloso, L.A., Dalal, S., Portovedo, M., Rodrigues, V.S., Coope, A., Ayrizono, M.L.S., Fagundes, J.J., Milanski, M., 2012. Autophagy is decreased in mesenteric fat tissue but not in intestinal mucosae of patients with Crohn's disease. *Cell Tissue Res.* 350, 549–552. <https://doi.org/10.1007/s00441-012-1491-8>
- Lee, A.-H., Iwakoshi, N.N., Glimcher, L.H., 2003. XBP-1 Regulates a Subset of Endoplasmic Reticulum Resident Chaperone Genes in the Unfolded Protein Response. *Mol. Cell. Biol.* 23, 7448–7459. <https://doi.org/10.1128/MCB.23.21.7448-7459.2003>
- Lee, A.S., 2005. The ER chaperone and signaling regulator GRP78/BiP as a monitor of endoplasmic reticulum stress. *Methods* 35, 373–381. <https://doi.org/10.1016/j.ymeth.2004.10.010>
- Lee, Alice U., Farrell, G.C., 2001. Mechanism of azathioprine-induced injury to hepatocytes: roles of glutathione depletion and mitochondrial injury. *J. Hepatol.* 35, 756–764. [https://doi.org/10.1016/S0168-8278\(01\)00196-9](https://doi.org/10.1016/S0168-8278(01)00196-9)
- Lee, A. U., Farrell, G.C., 2001. Mechanism of azathioprine-induced injury to hepatocytes: roles of glutathione depletion and mitochondrial injury. *J. Hepatol.* 35, 756–764.
- Lee, J.C., Biasci, D., Roberts, R., Gearry, R.B., Mansfield, J.C., Ahmad, T., Prescott, N.J., Satsangi, J., Wilson, D.C., Jostins, L., Anderson, C.A., Consortium, U.I.G., Traherne, J.A., Lyons, P.A., Parkes, M., Smith, K.G.C., 2017. Genome-wide association study identifies distinct genetic contributions to prognosis and susceptibility in Crohn's disease. *Nat. Genet.* 49, 262–268. <https://doi.org/10.1038/ng.3755>
- Lee, J.-Y., Nagano, Y., Taylor, J.P., Lim, K.L., Yao, T.-P., 2010. Disease-causing mutations in parkin impair mitochondrial ubiquitination, aggregation, and HDAC6-dependent mitophagy. *J. Cell Biol.* 189, 671–679. <https://doi.org/10.1083/jcb.201001039>
- Lee, K., Tirasophon, W., Shen, X., Michalak, M., Prywes, R., Okada, T., Yoshida, H., Mori, K., Kaufman, R.J., 2002. IRE1-mediated unconventional mRNA splicing and S2P-

- mediated ATF6 cleavage merge to regulate XBP1 in signaling the unfolded protein response. *Genes Dev.* 16, 452–466. <https://doi.org/10.1101/gad.964702>
- Lees, C.W., Maan, A.K., Hansoti, B., Satsangi, J., Arnott, I.D.R., 2008. Tolerability and safety of mercaptopurine in azathioprine-intolerant patients with inflammatory bowel disease. *Aliment. Pharmacol. Ther.* 27, 220–227. <https://doi.org/10.1111/j.1365-2036.2007.03570.x>
- Lennard, L., Welch, J.C., Lilleyman, J.S., 1997. Thiopurine drugs in the treatment of childhood leukaemia: the influence of inherited thiopurine methyltransferase activity on drug metabolism and cytotoxicity. *Br. J. Clin. Pharmacol.* 44, 455–461. <https://doi.org/10.1046/j.1365-2125.1997.t01-1-00607.x>
- Lesage, S., Zouali, H., Cézard, J.-P., the, E.-I.B.D. group, Colombel, J.-F., the, E. group, Belaiche, J., the, G. group, Almer, S., Tysk, C., O’Morain, C., Gassull, M., Binder, V., Finkel, Y., Modigliani, R., Gower-Rousseau, C., Macry, J., Merlin, F., Chamailard, M., Jannot, A.-S., Thomas, G., Hugot, J.-P., 2002. CARD15/NOD2 Mutational Analysis and Genotype-Phenotype Correlation in 612 Patients with Inflammatory Bowel Disease. *Am. J. Hum. Genet.* 70, 845–857.
- Leung, G., Wang, A., Fernando, M., Phan, V.C., McKay, D.M., 2013. Bone marrow-derived alternatively activated macrophages reduce colitis without promoting fibrosis: participation of IL-10. *Am. J. Physiol. Gastrointest. Liver Physiol.* 304, G781-792. <https://doi.org/10.1152/ajpgi.00055.2013>
- Levin, A.D., Koelink, P.J., Bloemendaal, F.M., Vos, A.C.W., D’Haens, G.R., van den Brink, G.R., Wildenberg, M.E., 2016. Autophagy Contributes to the Induction of Anti-TNF Induced Macrophages. *J. Crohns Colitis* 10, 323–329. <https://doi.org/10.1093/ecco-jcc/jjv174>
- Levine, A., Griffiths, A., Markowitz, J., Wilson, D.C., Turner, D., Russell, R.K., Fell, J., Ruemmele, F.M., Walters, T., Sherlock, M., Dubinsky, M., Hyams, J.S., 2011. Pediatric modification of the Montreal classification for inflammatory bowel disease: the Paris classification. *Inflamm. Bowel Dis.* 17, 1314–1321. <https://doi.org/10.1002/ibd.21493>
- Levine, A., Koletzko, S., Turner, D., Escher, J.C., Cucchiara, S., de Ridder, L., Kolho, K.-L., Veres, G., Russell, R.K., Paerregaard, A., Buderus, S., Greer, M.-L.C., Dias, J.A., Veereman-Wauters, G., Lionetti, P., Sladek, M., Martin de Carpi, J., Staiano, A., Ruemmele, F.M., Wilson, D.C., European Society of Pediatric Gastroenterology, Hepatology, and Nutrition, 2014. ESPGHAN revised porto criteria for the diagnosis of inflammatory bowel disease in children and adolescents. *J. Pediatr. Gastroenterol. Nutr.* 58, 795–806. <https://doi.org/10.1097/MPG.0000000000000239>
- Levine, B., Kroemer, G., 2008. Autophagy in the pathogenesis of disease. *Cell* 132, 27–42. <https://doi.org/10.1016/j.cell.2007.12.018>
- Li, J., Ni, M., Lee, B., Barron, E., Hinton, D., Lee, A., 2008. The unfolded protein response regulator GRP78/BiP is required for endoplasmic reticulum integrity and stress-induced autophagy in mammalian cells. *Cell Death Differ.* 15, 1460–1471. <https://doi.org/10.1038/cdd.2008.81>
- Li, M., Baumeister, P., Roy, B., Phan, T., Foti, D., Luo, S., Lee, A.S., 2000. ATF6 as a transcription activator of the endoplasmic reticulum stress element: thapsigargin stress-induced changes and synergistic interactions with NF- κ B and YY1. *Mol. Cell. Biol.* 20, 5096–5106.

- Li, M.O., Flavell, R.A., 2008. Contextual regulation of inflammation: a duet by transforming growth factor-beta and interleukin-10. *Immunity* 28, 468–476. <https://doi.org/10.1016/j.immuni.2008.03.003>
- Li, S., Wandel, M.P., Li, F., Liu, Z., He, C., Wu, J., Shi, Y., Randow, F., 2013. Sterical hindrance promotes selectivity of the autophagy cargo receptor NDP52 for the danger receptor galectin-8 in antibacterial autophagy. *Sci. Signal.* 6, ra9. <https://doi.org/10.1126/scisignal.2003730>
- Li, S.-H., Lam, S., Cheng, A.L., Li, X.-J., 2000. Intranuclear huntingtin increases the expression of caspase-1 and induces apoptosis. *Hum. Mol. Genet.* 9, 2859–2867. <https://doi.org/10.1093/hmg/9.19.2859>
- Liang, X.H., Kleeman, L.K., Jiang, H.H., Gordon, G., Goldman, J.E., Berry, G., Herman, B., Levine, B., 1998. Protection against Fatal Sindbis Virus Encephalitis by Beclin, a Novel Bcl-2-Interacting Protein. *J. Virol.* 72, 8586–8596.
- Littman, D.R., Rudensky, A.Y., 2010. Th17 and regulatory T cells in mediating and restraining inflammation. *Cell* 140, 845–858. <https://doi.org/10.1016/j.cell.2010.02.021>
- Liu, B., Gulati, A.S., Cantillana, V., Henry, S.C., Schmidt, E.A., Daniell, X., Grossniklaus, E., Schoenborn, A.A., Sartor, R.B., Taylor, G.A., 2013. Irgm1-deficient mice exhibit Paneth cell abnormalities and increased susceptibility to acute intestinal inflammation. *Am. J. Physiol. - Gastrointest. Liver Physiol.* 305, G573–G584. <https://doi.org/10.1152/ajpgi.00071.2013>
- Liu, J., Albers, M.W., Wandless, T.J., Luan, S., Alberg, D.G., Belshaw, P.J., Cohen, P., MacKintosh, C., Klee, C.B., Schreiber, S.L., 1992. Inhibition of T cell signaling by immunophilin-ligand complexes correlates with loss of calcineurin phosphatase activity. *Biochemistry* 31, 3896–901.
- Liu, Z., Lee, J., Krummey, S., Lu, W., Cai, H., Lenardo, M.J., 2011. The kinase LRRK2 is a regulator of the transcription factor NFAT that modulates the severity of inflammatory bowel disease. *Nat Immunol* 12, 1063–70. <https://doi.org/10.1038/ni.2113>
- Liu, Z., Wang, Y., Zhao, S., Zhang, J., Wu, Y., Zeng, S., 2015. Imidazole inhibits autophagy flux by blocking autophagic degradation and triggers apoptosis via increasing FoxO3a-Bim expression. *Int. J. Oncol.* 46, 721–731. <https://doi.org/10.3892/ijo.2014.2771>
- Livak, K.J., Schmittgen, T.D., 2001. Analysis of relative gene expression data using real-time quantitative PCR and the 2(-Delta Delta C(T)) Method. *Methods San Diego Calif* 25, 402–408. <https://doi.org/10.1006/meth.2001.1262>
- Lodes, M.J., Cong, Y., Elson, C.O., Mohamath, R., Landers, C.J., Targan, S.R., Fort, M., Hershberg, R.M., 2004. Bacterial flagellin is a dominant antigen in Crohn disease. *J. Clin. Invest.* 113, 1296–1306. <https://doi.org/10.1172/JCI20295>
- Lourenco, S., Teixeira, V.H., Kalber, T., Jose, R.J., Floto, R.A., Janes, S.M., 2015. Macrophage Migration Inhibitory Factor–CXCR4 Is the Dominant Chemotactic Axis in Human Mesenchymal Stem Cell Recruitment to Tumors. *J. Immunol.* 194, 3463–3474. <https://doi.org/10.4049/jimmunol.1402097>
- Lu, Y., Gao, J., Zhang, S., Gu, J., Lu, H., Xia, Y., Zhu, Q., Qian, X., Zhang, F., Zhang, C., Shen, H., Hippen, K.L., Blazar, B.R., Lu, L., Wang, X., 2018. miR-142-3p regulates autophagy by targeting ATG16L1 in thymic-derived regulatory T cell (tTreg). *Cell Death Dis.* 9, 290. <https://doi.org/10.1038/s41419-018-0298-2>

- Luo, S., Rubinsztein, D.C., 2010. Apoptosis blocks Beclin 1-dependent autophagosome synthesis: an effect rescued by Bcl-xL. *Cell Death Differ.* 17, 268–277. <https://doi.org/10.1038/cdd.2009.121>
- Ma, X.M., Blenis, J., 2009. Molecular mechanisms of mTOR-mediated translational control. *Nat. Rev. Mol. Cell Biol.* 10, 307. <https://doi.org/10.1038/nrm2672>
- Maiuri, M.C., Le Toumelin, G., Criollo, A., Rain, J.C., Gautier, F., Juin, P., Tasdemir, E., Pierron, G., Troulinaki, K., Tavernarakis, N., Hickman, J.A., Geneste, O., Kroemer, G., 2007. Functional and physical interaction between Bcl-X(L) and a BH3-like domain in Beclin-1. *Embo J* 26, 2527–39. <https://doi.org/10.1038/sj.emboj.7601689>
- Mammucari, C., Milan, G., Romanello, V., Masiero, E., Rudolf, R., Del Piccolo, P., Burden, S.J., Di Lisi, R., Sandri, C., Zhao, J., Goldberg, A.L., Schiaffino, S., Sandri, M., 2007. FoxO3 controls autophagy in skeletal muscle in vivo. *Cell Metab.* 6, 458–471. <https://doi.org/10.1016/j.cmet.2007.11.001>
- Manzoni, C., Mamais, A., Roosen, D.A., Dihanich, S., Soutar, M.P.M., Plun-Favreau, H., Bandopadhyay, R., Hardy, J., Tooze, S.A., Cookson, M.R., Lewis, P.A., 2016. mTOR independent regulation of macroautophagy by Leucine Rich Repeat Kinase 2 via Beclin-1. *Sci. Rep.* 6. <https://doi.org/10.1038/srep35106>
- Mao, D., Che, J., Han, S., Zhao, H., Zhu, Y., Zhu, H., 2015. RNAi-mediated knockdown of the CLN3 gene inhibits proliferation and promotes apoptosis in drug-resistant ovarian cancer cells. *Mol. Med. Rep.* 12, 6635–6641. <https://doi.org/10.3892/mmr.2015.4238>
- Marcuzzi, A., Bianco, A.M., Girardelli, M., Tommasini, A., Martellosi, S., Monasta, L., Crovella, S., 2013. Genetic and functional profiling of Crohn's disease: autophagy mechanism and susceptibility to infectious diseases. *Biomed Res Int* 2013, 297501. <https://doi.org/10.1155/2013/297501>
- Margariti, A., Li, H., Chen, T., Martin, D., Vizcay-Barrena, G., Alam, S., Karamariti, E., Xiao, Q., Zampetaki, A., Zhang, Z., Wang, W., Jiang, Z., Gao, C., Ma, B., Chen, Y.-G., Cockerill, G., Hu, Y., Xu, Q., Zeng, L., 2013. XBP1 mRNA Splicing Triggers an Autophagic Response in Endothelial Cells through BECLIN-1 Transcriptional Activation. *J. Biol. Chem.* 288, 859–872. <https://doi.org/10.1074/jbc.M112.412783>
- Marini, M., Bamias, G., Rivera-Nieves, J., Moskaluk, C.A., Hoang, S.B., Ross, W.G., Pizarro, T.T., Cominelli, F., 2003. TNF- α neutralization ameliorates the severity of murine Crohn's-like ileitis by abrogation of intestinal epithelial cell apoptosis. *Proc. Natl. Acad. Sci.* 100, 8366–8371. <https://doi.org/10.1073/pnas.1432897100>
- Mariño, G., Niso-Santano, M., Baehrecke, E.H., Kroemer, G., 2014. Self-consumption: the interplay of autophagy and apoptosis. *Nat. Rev. Mol. Cell Biol.* 15, 81–94. <https://doi.org/10.1038/nrm3735>
- Markowitz, J., 2008. Current treatment of inflammatory bowel disease in children. *Dig Liver Dis* 40, 16–21. <https://doi.org/10.1016/j.dld.2007.07.167>
- Markowitz, J., Grancher, K., Kohn, N., Daum, F., 2002. Immunomodulatory therapy for pediatric inflammatory bowel disease: changing patterns of use, 1990-2000. *Am J Gastroenterol* 97, 928–32. <https://doi.org/10.1111/j.1572-0241.2002.05611.x>
- Martin, H.M., Campbell, B.J., Hart, C.A., Mpofu, C., Nayar, M., Singh, R., Englyst, H., Williams, H.F., Rhodes, J.M., 2004. Enhanced *Escherichia coli* adherence and invasion in Crohn's disease and colon cancer. *Gastroenterology* 127, 80–93. <https://doi.org/10.1053/j.gastro.2004.03.054>

- Martina, J.A., Chen, Y., Gucek, M., Puertollano, R., 2012. MTORC1 functions as a transcriptional regulator of autophagy by preventing nuclear transport of TFEB. *Autophagy* 8, 903–914. <https://doi.org/10.4161/auto.19653>
- Martinon, F., Chen, X., Lee, A.-H., Glimcher, L.H., 2010. TLR activation of the transcription factor XBP1 regulates innate immune responses in macrophages. *Nat. Immunol.* 11, 411–418. <https://doi.org/10.1038/ni.1857>
- Massey, D.C., Bredin, F., Parkes, M., 2008. Use of sirolimus (rapamycin) to treat refractory Crohn's disease. *Gut* 57, 1294–6. <https://doi.org/10.1136/gut.2008.157297>
- Matsuda, C., Ito, T., Song, J., Mizushima, T., Tamagawa, H., Kai, Y., Hamanaka, Y., Inoue, M., Nishida, T., Matsuda, H., Sawa, Y., 2007. Therapeutic effect of a new immunosuppressive agent, everolimus, on interleukin-10 gene-deficient mice with colitis. *Clin. Exp. Immunol.* 148, 348–359. <https://doi.org/10.1111/j.1365-2249.2007.03345.x>
- McCarroll, S.A., Huett, A., Kuballa, P., Chilewski, S.D., Landry, A., Goyette, P., Zody, M.C., Hall, J.L., Brant, S.R., Cho, J.H., Duerr, R.H., Silverberg, M.S., Taylor, K.D., Rioux, J.D., Altshuler, D., Daly, M.J., Xavier, R.J., 2008. Deletion polymorphism upstream of IRGM associated with altered IRGM expression and Crohn's disease. *Nat Genet* 40, 1107–12. <https://doi.org/10.1038/ng.215>
- McFarlane, S.M., Pashmi, G., Connell, M.C., Littlejohn, A.F., Tucker, S.J., Vandenabeele, P., MacEwan, D.J., 2002. Differential activation of nuclear factor- κ B by tumour necrosis factor receptor subtypes. TNFR1 predominates whereas TNFR2 activates transcription poorly. *FEBS Lett.* 515, 119–126. [https://doi.org/10.1016/S0014-5793\(02\)02450-X](https://doi.org/10.1016/S0014-5793(02)02450-X)
- McGovern, D.P.B., Travis, S.P.L., Duley, J., Shobowale-Bakre, E.M., Dalton, H.R., 2002. Azathioprine intolerance in patients with IBD may be imidazole-related and is independent of TPMT activity. *Gastroenterology* 122, 838–839.
- McGuckin, M.A., Eri, R.D., Das, I., Lourie, R., Florin, T.H., 2010. ER stress and the unfolded protein response in intestinal inflammation. *Am. J. Physiol. - Gastrointest. Liver Physiol.* 298, G820–G832. <https://doi.org/10.1152/ajpgi.00063.2010>
- Meconi, S., Vercellone, A., Levillain, F., Payré, B., Al Saati, T., Capilla, F., Desreumaux, P., Darfeuille-Michaud, A., Altare, F., 2007. Adherent-invasive *Escherichia coli* isolated from Crohn's disease patients induce granulomas in vitro. *Cell. Microbiol.* 9, 1252–1261. <https://doi.org/10.1111/j.1462-5822.2006.00868.x>
- Merksamer, P.I., Trusina, A., Papa, F.R., 2008. Real-time redox measurements during endoplasmic reticulum stress reveal interlinked protein folding functions. *Cell* 135, 933–947. <https://doi.org/10.1016/j.cell.2008.10.011>
- Mesquita, F.S., Thomas, M., Sachse, M., Santos, A.J.M., Figueira, R., Holden, D.W., 2012. The *Salmonella* deubiquitinase SseL inhibits selective autophagy of cytosolic aggregates. *PLoS Pathog.* 8, e1002743. <https://doi.org/10.1371/journal.ppat.1002743>
- Mezghrani, A., Courageot, J., Mani, J.C., Pugniere, M., Bastiani, P., Miquelis, R., 2000. Protein-disulfide Isomerase (PDI) in FRTL5 Cells pH-DEPENDENT THYROGLOBULIN/PDI INTERACTIONS DETERMINE A NOVEL PDI FUNCTION IN THE POST-ENDOPLASMIC RETICULUM OF THYROCYTES. *J. Biol. Chem.* 275, 1920–1929. <https://doi.org/10.1074/jbc.275.3.1920>
- Mijaljica, D., Prescott, M., Devenish, R.J., 2011. Microautophagy in mammalian cells: revisiting a 40-year-old conundrum. *Autophagy* 7, 673–682.

- Miller, B.C., Zhao, Z., Stephenson, L.M., Cadwell, K., Pua, H.H., Lee, H.K., Mizushima, N.N., Iwasaki, A., He, Y.-W., Swat, W., Virgin, H.W., 2008. The autophagy gene ATG5 plays an essential role in B lymphocyte development. *Autophagy* 4, 309–314.
- Miller, E.M., Nickoloff, J.A., 1995. *Escherichia coli* Electrotransformation, in: *Electroporation Protocols for Microorganisms, Methods in Molecular Biology™*. Humana Press, pp. 105–113. <https://doi.org/10.1385/0-89603-310-4:105>
- Mitroulis, I., Kourtzelis, I., Kambas, K., Rafail, S., Chrysanthopoulou, A., Speletas, M., Ritis, K., 2010. Regulation of the autophagic machinery in human neutrophils. *Eur. J. Immunol.* 40, 1461–1472. <https://doi.org/10.1002/eji.200940025>
- Miyazaki, M., McCarthy, J.J., Esser, K.A., 2010. Insulin like growth factor-1-induced phosphorylation and altered distribution of tuberous sclerosis complex (TSC)1/TSC2 in C2C12 myotubes. *FEBS J.* 277, 2180–2191. <https://doi.org/10.1111/j.1742-4658.2010.07635.x>
- Mizoguchi, A., Bhan, A.K., 2012. Immunobiology of B Cells in Inflammatory Bowel Disease, in: *Crohn's Disease and Ulcerative Colitis*. Springer, Boston, MA, pp. 161–168. https://doi.org/10.1007/978-1-4614-0998-4_12
- Mizushima, N., Yoshimori, T., Levine, B., 2010. Methods in Mammalian Autophagy Research. *Cell* 140, 313–326. <https://doi.org/10.1016/j.cell.2010.01.028>
- Moon, H., Kim, B., Gwak, H., Suh, D.H., Song, Y.S., 2016. Autophagy and protein kinase RNA-like endoplasmic reticulum kinase (PERK)/eukaryotic initiation factor 2 alpha kinase (eIF2 α) pathway protect ovarian cancer cells from metformin-induced apoptosis: THE EFFECT OF METFORMIN ON AUTOPHAGY AND PERK. *Mol. Carcinog.* 55, 346–356. <https://doi.org/10.1002/mc.22284>
- Moretti, J., Roy, S., Bozec, D., Martinez, J., Chapman, J.R., Ueberheide, B., Lamming, D.W., Chen, Z.J., Horng, T., Yeretssian, G., Green, D.R., Blander, J.M., 2017. STING Senses Microbial Viability to Orchestrate Stress-Mediated Autophagy of the Endoplasmic Reticulum. *Cell*. <https://doi.org/10.1016/j.cell.2017.09.034>
- Mortensen, M., Ferguson, D.J.P., Edelmann, M., Kessler, B., Morten, K.J., Komatsu, M., Simon, A.K., 2010. Loss of autophagy in erythroid cells leads to defective removal of mitochondria and severe anemia in vivo. *Proc. Natl. Acad. Sci. U. S. A.* 107, 832–837. <https://doi.org/10.1073/pnas.0913170107>
- Murthy, A., Li, Y., Peng, I., Reichelt, M., Katakam, A.K., Noubade, R., Roose-Girma, M., DeVoss, J., Diehl, L., Graham, R.R., van Lookeren Campagne, M., 2014. A Crohn's disease variant in Atg16l1 enhances its degradation by caspase 3. *Nature* 506, 456–462. <https://doi.org/10.1038/nature13044>
- Musiwaro, P., Smith, M., Manifava, M., Walker, S.A., Ktistakis, N.T., 2013. Characteristics and requirements of basal autophagy in HEK 293 cells. *Autophagy* 9, 1407–1417. <https://doi.org/10.4161/auto.25455>
- Mutalib, M., Borrelli, O., Blackstock, S., Kiparissi, F., Elawad, M., Shah, N., Lindley, K., 2014. The use of sirolimus (rapamycin) in the management of refractory inflammatory bowel disease in children. *J. Crohns Colitis* 8, 1730–1734. <https://doi.org/10.1016/j.crohns.2014.08.014>
- Muzes, G., Tulassay, Z., Sipos, F., 2013. Interplay of autophagy and innate immunity in Crohn's disease: a key immunobiologic feature. *World J Gastroenterol* 19, 4447–54. <https://doi.org/10.3748/wjg.v19.i28.4447>
- Nakagaki, T., Satoh, K., Ishibashi, D., Fuse, T., Sano, K., Kamatari, Y.O., Kuwata, K., Shigematsu, K., Iwamaru, Y., Takenouchi, T., Kitani, H., Nishida, N., Atarashi, R.,

2013. FK506 reduces abnormal prion protein through the activation of autolysosomal degradation and prolongs survival in prion-infected mice. *Autophagy* 9, 1386–1394. <https://doi.org/10.4161/auto.25381>
- Nara, A., Mizushima, N., Yamamoto, A., Kabeya, Y., Ohsumi, Y., Yoshimori, T., 2002. SKD1 AAA ATPase-dependent endosomal transport is involved in autolysosome formation. *Cell Struct. Funct.* 27, 29–37.
- Narendra, D., Tanaka, A., Suen, D.-F., Youle, R.J., 2008. Parkin is recruited selectively to impaired mitochondria and promotes their autophagy. *J. Cell Biol.* 183, 795–803. <https://doi.org/10.1083/jcb.200809125>
- Narendra, D.P., Jin, S.M., Tanaka, A., Suen, D.-F., Gautier, C.A., Shen, J., Cookson, M.R., Youle, R.J., 2010. PINK1 Is Selectively Stabilized on Impaired Mitochondria to Activate Parkin. *PLOS Biol.* 8, e1000298. <https://doi.org/10.1371/journal.pbio.1000298>
- Naves, J., Manye, J., Loren, V., Mañosa, M., Moret, I., García-Jaraquemada, A., Bastida, G., Beltrán, B., Cabré, E., Domènech, E., 2015. P042 Response to corticosteroids in Ulcerative Colitis may be related to modulation of mTOR signaling pathway genes by microRNAs. *J. Crohns Colitis* 9 (suppl 1). <https://doi.org/10.1093/ecco-jcc/jju027.160>
- Nebenführ, A., Ritzenthaler, C., Robinson, D.G., 2002. Brefeldin A: Deciphering an Enigmatic Inhibitor of Secretion. *Plant Physiol.* 130, 1102–1108. <https://doi.org/10.1104/pp.011569>
- Nedjic, J., Aichinger, M., Emmerich, J., Mizushima, N., Klein, L., 2008. Autophagy in thymic epithelium shapes the T-cell repertoire and is essential for tolerance. *Nature* 455, 396–400. <https://doi.org/10.1038/nature07208>
- Negróni, A., Colantoni, E., Vitali, R., Palone, F., Pierdomenico, M., Costanzo, M., Cesi, V., Cucchiara, S., Stronati, L., 2016. NOD2 induces autophagy to control AIEC bacteria infectiveness in intestinal epithelial cells. *Inflamm. Res.* 65, 803–813. <https://doi.org/10.1007/s00011-016-0964-8>
- Negróni, A., Costanzo, M., Vitali, R., Superti, F., Bertuccini, L., Tinari, A., Minelli, F., Di Nardo, G., Nuti, F., Pierdomenico, M., Cucchiara, S., Stronati, L., 2012. Characterization of adherent-invasive *Escherichia coli* isolated from pediatric patients with inflammatory bowel disease. *Inflamm Bowel Dis* 18, 913–24. <https://doi.org/10.1002/ibd.21899>
- Neurath, M.F., 2017. Current and emerging therapeutic targets for IBD. *Nat. Rev. Gastroenterol. Hepatol.* 14, nrgastro.2016.208. <https://doi.org/10.1038/nrgastro.2016.208>
- Newman, A.C., Scholefield, C.L., Kemp, A.J., Newman, M., McIver, E.G., Kamal, A., Wilkinson, S., 2012. TBK1 kinase addiction in lung cancer cells is mediated via autophagy of Tax1bp1/Ndp52 and non-canonical NF- κ B signalling. *PloS One* 7, e50672. <https://doi.org/10.1371/journal.pone.0050672>
- Ng, S.C., Plamondon, S., Al-Hassi, H.O., English, N., Gellatly, N., Kamm, M.A., Knight, S.C., Stagg, A.J., 2009. A novel population of human CD56+ human leucocyte antigen D-related (HLA-DR+) colonic lamina propria cells is associated with inflammation in ulcerative colitis. *Clin. Exp. Immunol.* 158, 205–218. <https://doi.org/10.1111/j.1365-2249.2009.04012.x>
- Ng, S.C., Shi, H.Y., Hamidi, N., Underwood, F.E., Tang, W., Benchimol, E.I., Panaccione, R., Ghosh, S., Wu, J.C.Y., Chan, F.K.L., Sung, J.J.Y., Kaplan, G.G., 2017. Worldwide incidence and prevalence of inflammatory bowel disease in the 21st century: a

- systematic review of population-based studies. *The Lancet* 390, 2769–2778. [https://doi.org/10.1016/S0140-6736\(17\)32448-0](https://doi.org/10.1016/S0140-6736(17)32448-0)
- Nguyen, H.T.T., Dalmasso, G., Müller, S., Carrière, J., Seibold, F., Darfeuille–Michaud, A., 2014. Crohn’s Disease–Associated Adherent Invasive *Escherichia coli* Modulate Levels of microRNAs in Intestinal Epithelial Cells to Reduce Autophagy. *Gastroenterology* 146, 508–519. <https://doi.org/10.1053/j.gastro.2013.10.021>
- NHS, C.B., 2013. 2013/14 NHS Standard Contract for Colorectal: Complex Inflammatory Bowel Disease (Adult).
- Ni, M., Zhou, H., Wey, S., Baumeister, P., Lee, A.S., 2009. Regulation of PERK Signaling and Leukemic Cell Survival by a Novel Cytosolic Isoform of the UPR Regulator GRP78/BiP. *PLoS ONE* 4, e6868. <https://doi.org/10.1371/journal.pone.0006868>
- Niederreiter, L., Fritz, T.M.J., Adolph, T.E., Krismer, A.-M., Offner, F.A., Tschurtschenthaler, M., Flak, M.B., Hosomi, S., Tomczak, M.F., Kaneider, N.C., Sarcevic, E., Kempster, S.L., Raine, T., Esser, D., Rosenstiel, P., Kohno, K., Iwawaki, T., Tilg, H., Blumberg, R.S., Kaser, A., 2013. ER stress transcription factor Xbp1 suppresses intestinal tumorigenesis and directs intestinal stem cells. *J. Exp. Med.* 210, 2041–2056. <https://doi.org/10.1084/jem.20122341>
- Niess, J.H., Klaus, J., Stephani, J., Pfluger, C., Degenkolb, N., Spaniol, U., Mayer, B., Lahr, G., von Boyen, G.B., 2012. NOD2 polymorphism predicts response to treatment in Crohn’s disease—first steps to a personalized therapy. *Dig Sci* 57, 879–86. <https://doi.org/10.1007/s10620-011-1977-3>
- Nishino, K., Nishida, A., Inoue, R., Kawada, Y., Ohno, M., Sakai, S., Inatomi, O., Bamba, S., Sugimoto, M., Kawahara, M., Naito, Y., Andoh, A., 2018. Analysis of endoscopic brush samples identified mucosa-associated dysbiosis in inflammatory bowel disease. *J. Gastroenterol.* 53, 95–106. <https://doi.org/10.1007/s00535-017-1384-4>
- Nishitoh, H., 2012. CHOP is a multifunctional transcription factor in the ER stress response. *J. Biochem. (Tokyo)* 151, 217–219. <https://doi.org/10.1093/jb/mvr143>
- Noronha, A.M., Liang, Y., Hetzel, J.T., Hasturk, H., Kantarci, A., Stucchi, A., Zhang, Y., Nikolajczyk, B.S., Farraye, F.A., Ganley-Leal, L.M., 2009. Hyperactivated B cells in human inflammatory bowel disease. *J. Leukoc. Biol.* 86, 1007–1016. <https://doi.org/10.1189/jlb.0309203>
- Novak, E.A., Mollen, K.P., 2015. Mitochondrial dysfunction in inflammatory bowel disease. *Front. Cell Dev. Biol.* 3. <https://doi.org/10.3389/fcell.2015.00062>
- Nuki, Y., Esaki, M., Asano, K., Maehata, Y., Umeno, J., Moriyama, T., Nakamura, S., Matsumoto, T., Kitazono, T., 2016. Comparison of the therapeutic efficacy and safety between tacrolimus and infliximab for moderate-to-severe ulcerative colitis: a single center experience. *Scand J Gastroenterol* 51, 700–5. <https://doi.org/10.3109/00365521.2016.1138239>
- Nys, K., Agostinis, P., Vermeire, S., 2013. Autophagy: a new target or an old strategy for the treatment of Crohn’s disease? *Nat. Rev. Gastroenterol. Hepatol.* 10, 395–401. <https://doi.org/10.1038/nrgastro.2013.66>
- Oancea, I., D., I...Aguirre de Carce, D...Movva, R...Schreiber, V...Yang, Y...Proctor, M...Wang, R...Sheng, Y...Lobb, M...Cuiv, P.O...Duley, J.A...Begun, J...Florin, T.H.J., 2016. Bacterial activation of thioguanine results in lymphocyte independent improvement in murine colitis. *J Crohns Colitis* 10(Supp 1), S117.
- Oancea, I., Movva, R., Das, I., Aguirre de Cárcer, D., Schreiber, V., Yang, Y., Purdon, A., Harrington, B., Proctor, M., Wang, R., Sheng, Y., Lobb, M., Lourie, R., Ó Cuív, P., Duley, J.A., Begun, J., Florin, T.H.J., 2017. Colonic microbiota can promote rapid

- local improvement of murine colitis by thioguanine independently of T lymphocytes and host metabolism. *Gut* 66, 59–69. <https://doi.org/10.1136/gutjnl-2015-310874>
- O'Brien, V., Brown, R., 2006. O'Brien V, Brown R Signalling cell cycle arrest and cell death through the MMR system. *Carcinogenesis* 27: 682–692. <https://doi.org/10.1093/carcin/bgi298>
- Ogata, M., Hino, S., Saito, A., Morikawa, K., Kondo, S., Kanemoto, S., Murakami, T., Taniguchi, M., Tanii, I., Yoshinaga, K., Shiosaka, S., Hammarback, J.A., Urano, F., Imaizumi, K., 2006. Autophagy is activated for cell survival after endoplasmic reticulum stress. *Mol Cell Biol* 26, 9220–31. <https://doi.org/10.1128/mcb.01453-06>
- Ogawa, M., Yoshimori, T., Suzuki, T., Sagara, H., Mizushima, N., Sasakawa, C., 2005. Escape of intracellular Shigella from autophagy. *Science* 307, 727–731. <https://doi.org/10.1126/science.1106036>
- Ogura, Y., Bonen, D.K., Inohara, N., Nicolae, D.L., Chen, F.F., Ramos, R., Britton, H., Moran, T., Karaliuskas, R., Duerr, R.H., Achkar, J.P., Brant, S.R., Bayless, T.M., Kirschner, B.S., Hanauer, S.B., Nunez, G., Cho, J.H., 2001a. A frameshift mutation in NOD2 associated with susceptibility to Crohn's disease. *Nature* 411, 603–6. <https://doi.org/10.1038/35079114>
- Ogura, Y., Inohara, N., Benito, A., Chen, F.F., Yamaoka, S., Nunez, G., 2001b. Nod2, a Nod1/Apaf-1 family member that is restricted to monocytes and activates NF-kappaB. *J. Biol. Chem.* 276, 4812–4818. <https://doi.org/10.1074/jbc.M008072200>
- Ogura, Y., Lala, S., Xin, W., Smith, E., Dowds, T.A., Chen, F.F., Zimmermann, E., Tretiakova, M., Cho, J.H., Hart, J., Greenson, J.K., Keshav, S., Nuñez, G., 2003. Expression of NOD2 in Paneth cells: a possible link to Crohn's ileitis. *Gut* 52, 1591–1597.
- Oka, A., Ishihara, S., Mishima, Y., Tada, Y., Kusunoki, R., Fukuba, N., Yuki, T., Kawashima, K., Matsumoto, S., Kinoshita, Y., 2014. Role of regulatory B cells in chronic intestinal inflammation: association with pathogenesis of Crohn's disease. *Inflamm. Bowel Dis.* 20, 315–328. <https://doi.org/10.1097/01.MIB.0000437983.14544.d5>
- Okatsu, K., Saisho, K., Shimanuki, M., Nakada, K., Shitara, H., Sou, Y.-S., Kimura, M., Sato, S., Hattori, N., Komatsu, M., Tanaka, K., Matsuda, N., 2010. p62/SQSTM1 cooperates with Parkin for perinuclear clustering of depolarized mitochondria. *Genes Cells Devoted Mol. Cell. Mech.* 15, 887–900. <https://doi.org/10.1111/j.1365-2443.2010.01426.x>
- Olson, T.S., Bamias, G., Naganuma, M., Rivera-Nieves, J., Burcin, T.L., Ross, W., Morris, M.A., Pizarro, T.T., Ernst, P.B., Cominelli, F., Ley, K., 2004. Expanded B cell population blocks regulatory T cells and exacerbates ileitis in a murine model of Crohn disease. *J. Clin. Invest.* 114, 389–398. <https://doi.org/10.1172/JCI20855>
- Opperman, C.M., Sishi, B.J., 2015. Tumor necrosis factor alpha stimulates p62 accumulation and enhances proteasome activity independently of ROS. *Cell Biol Toxicol* 31, 83–94. <https://doi.org/10.1007/s10565-015-9295-8>
- Oral, O., Oz-Arslan, D., Itah, Z., Naghavi, A., Deveci, R., Karacali, S., Gozuacik, D., 2012. Cleavage of Atg3 protein by caspase-8 regulates autophagy during receptor-activated cell death. *Apoptosis Int. J. Program. Cell Death* 17, 810–820. <https://doi.org/10.1007/s10495-012-0735-0>

- Orenstein, S.J., Cuervo, A.M., 2010. Chaperone-mediated autophagy: molecular mechanisms and physiological relevance. *Semin. Cell Dev. Biol.* 21, 719–726. <https://doi.org/10.1016/j.semcdb.2010.02.005>
- Oslowski, C.M., Urano, F., 2011. Measuring ER Stress and the Unfolded Protein Response Using Mammalian Tissue Culture System, in: *Methods in Enzymology*. Elsevier, pp. 71–92. <https://doi.org/10.1016/B978-0-12-385114-7.00004-0>
- Ozmen, A., Unek, G., Kipmen-Korgun, D., Cetinkaya, B., Avcil, Z., Korgun, E.T., 2015. Glucocorticoid exposure altered angiogenic factor expression via Akt/mTOR pathway in rat placenta. *Ann. Anat. Anat. Anz. Off. Organ Anat. Ges.* 198, 34–40. <https://doi.org/10.1016/j.aanat.2014.10.007>
- Ozmen, A., Unek, G., Kipmen-Korgun, D., Mendilcioglu, I., Sanhal, C., Sakıncı, M., Korgun, E.T., 2016. Glucocorticoid effects on angiogenesis are associated with mTOR pathway activity. *Biotech. Histochem. Off. Publ. Biol. Stain Comm.* 91, 296–306. <https://doi.org/10.3109/10520295.2016.1161234>
- Pagliarini, V., Wirawan, E., Romagnoli, A., Ciccocanti, F., Lisi, G., Lippens, S., Cecconi, F., Fimia, G.M., Vandenabeele, P., Corazzari, M., Piacentini, M., 2012. Proteolysis of Ambra1 during apoptosis has a role in the inhibition of the autophagic pro-survival response. *Cell Death Differ.* 19, 1495–1504. <https://doi.org/10.1038/cdd.2012.27>
- Pallet, N., Bouvier, N., Legendre, C., Gilleron, J., Codogno, P., Beaune, P., Thervet, E., Anglicheau, D., 2008. Autophagy protects renal tubular cells against cyclosporine toxicity. *Autophagy* 4, 783–91.
- Palmieri, M., Impey, S., Kang, H., di Ronza, A., Pelz, C., Sardiello, M., Ballabio, A., 2011. Characterization of the CLEAR network reveals an integrated control of cellular clearance pathways. *Hum. Mol. Genet.* 20, 3852–3866. <https://doi.org/10.1093/hmg/ddr306>
- Parkes, M., Barrett, J.C., Prescott, N., Tremelling, M., Anderson, C.A., Fisher, S.A., Roberts, R.G., Nimmo, E.R., Cummings, F.R., Soars, D., Drummond, H., Lees, C.W., Khawaja, S.A., Bagnall, R., Burke, D.A., Todhunter, C.E., Ahmad, T., Onnie, C.M., McArdle, W., Strachan, D., Bethel, G., Bryan, C., Deloukas, P., Forbes, A., Sanderson, J., Jewell, D.P., Satsangi, J., Mansfield, J.C., the Wellcome Trust Case Control, C., Cardon, L., Mathew, C.G., 2007. Sequence variants in the autophagy gene IRGM and multiple other replicating loci contribute to Crohn disease susceptibility. *Nat. Genet.* 39, 830–832. <https://doi.org/10.1038/ng2061>
- Pascal, V., Pozuelo, M., Borrueal, N., Casellas, F., Campos, D., Santiago, A., Martinez, X., Varela, E., Sarrabayrouse, G., Machiels, K., Vermeire, S., Sokol, H., Guarner, F., Manichanh, C., 2017. A microbial signature for Crohn's disease. *Gut* *gutjnl-2016-313235*. <https://doi.org/10.1136/gutjnl-2016-313235>
- Pattingre, S., Tassa, A., Qu, X., Garuti, R., Liang, X.H., Mizushima, N., Packer, M., Schneider, M.D., Levine, B., 2005. Bcl-2 antiapoptotic proteins inhibit Beclin 1-dependent autophagy. *Cell* 122, 927–39. <https://doi.org/10.1016/j.cell.2005.07.002>
- Pelin, M., Iudicibus, S.D., Fusco, L., Taboga, E., Pellizzari, G., Lagatolla, C., Martelossi, S., Ventura, A., Decorti, G., Stocco, G., 2015. Role of Oxidative Stress Mediated by Glutathione-S-transferase in Thiopurines' Toxic Effects. *Chem. Res. Toxicol.* 28, 1186–1195. <https://doi.org/10.1021/acs.chemrestox.5b00019>
- Petit, E., Langouet, S., Akhdar, H., Nicolas-Nicolaz, C., Guillouzo, A., Morel, F., 2008. Differential toxic effects of azathioprine, 6-mercaptopurine and 6-thioguanine

- on human hepatocytes. *Toxicol Vitro* 22, 632–42. <https://doi.org/10.1016/j.tiv.2007.12.004>
- Pietarinen-Runtti, P., Lakari, E., Raivio, K.O., Kinnula, V.L., 2000. Expression of antioxidant enzymes in human inflammatory cells. *Am. J. Physiol.-Cell Physiol.* 278, C118–C125.
- Plantinga, T.S., Crisan, T.O., Oosting, M., van de Veerdonk, F.L., de Jong, D.J., Philpott, D.J., van der Meer, J.W.M., Girardin, S.E., Joosten, L.A.B., Netea, M.G., 2011. Crohn's disease-associated ATG16L1 polymorphism modulates pro-inflammatory cytokine responses selectively upon activation of NOD2. *Gut* 60, 1229–1235. <https://doi.org/10.1136/gut.2010.228908>
- Png, C.W., Lindén, S.K., Gilshenan, K.S., Zoetendal, E.G., McSweeney, C.S., Sly, L.I., McGuckin, M.A., Florin, T.H.J., 2010. Mucolytic bacteria with increased prevalence in IBD mucosa augment in vitro utilization of mucin by other bacteria. *Am. J. Gastroenterol.* 105, 2420–2428. <https://doi.org/10.1038/ajg.2010.281>
- Polman, J.A., Hunter, R.G., Speksnijder, N., van den Oever, J.M., Korobko, O.B., McEwen, B.S., de Kloet, E.R., Datson, N.A., 2012. Glucocorticoids modulate the mTOR pathway in the hippocampus: differential effects depending on stress history. *Endocrinology* 153, 4317–27. <https://doi.org/10.1210/en.2012-1255>
- Poppe, D., Tiede, I., Fritz, G., Becker, C., Bartsch, B., Wirtz, S., Strand, D., Tanaka, S., Galle, P.R., Bustelo, X.R., Neurath, M.F., 2006. Azathioprine Suppresses Ezrin-Radixin-Moesin-Dependent T Cell-APC Conjugation through Inhibition of Vav Guanosine Exchange Activity on Rac Proteins. *J. Immunol.* 176, 640–651. <https://doi.org/10.4049/jimmunol.176.1.640>
- Pranculienė, G., Steponaitienė, R., Skiecevičienė, J., Kučinskienė, R., Kiudelis, G., Adamonis, K., Labanauskas, L., Kupčinskas, L., 2016. Associations between NOD2, IRGM and ORMDL3 polymorphisms and pediatric-onset inflammatory bowel disease in the Lithuanian population. *Med. Kaunas Lith.* 52, 325–330. <https://doi.org/10.1016/j.medic.2016.11.006>
- Qu, X., Zou, Z., Sun, Q., Luby-Phelps, K., Cheng, P., Hogan, R.N., Gilpin, C., Levine, B., 2007. Autophagy gene-dependent clearance of apoptotic cells during embryonic development. *Cell* 128, 931–946. <https://doi.org/10.1016/j.cell.2006.12.044>
- Ragusa, M.J., Stanley, R.E., Hurley, J.H., 2012. Architecture of the Atg17 complex as a scaffold for autophagosome biogenesis. *Cell* 151, 1501–1512. <https://doi.org/10.1016/j.cell.2012.11.028>
- Rainbolt, T.K., Saunders, J.M., Wiseman, R.L., 2014. Stress-responsive regulation of mitochondria through the ER unfolded protein response. *Trends Endocrinol. Metab.* 25, 528–537. <https://doi.org/10.1016/j.tem.2014.06.007>
- Reinisch, W., Panés, J., Lémann, M., Schreiber, S., Feagan, B., Schmidt, S., Sturniolo, G.C., Mikhailova, T., Alexeeva, O., Sanna, L., Haas, T., Korom, S., Mayer, H., 2008. A multicenter, randomized, double-blind trial of everolimus versus azathioprine and placebo to maintain steroid-induced remission in patients with moderate-to-severe active Crohn's disease. *Am. J. Gastroenterol.* 103, 2284–2292. <https://doi.org/10.1111/j.1572-0241.2008.02024.x>
- Rieger, M.A., Schroeder, T., 2012. Hematopoiesis. *Cold Spring Harb. Perspect. Biol.* 4. <https://doi.org/10.1101/cshperspect.a008250>
- Rigamonti, D., Bauer, J.H., De-Fraja, C., Conti, L., Sipione, S., Sciorati, C., Clementi, E., Hackam, A., Hayden, M.R., Li, Y., Cooper, J.K., Ross, C.A., Govoni, S., Vincenz, C., Cattaneo, E., 2000. Wild-type huntingtin protects from apoptosis upstream of caspase-3. *J. Neurosci. Off. J. Soc. Neurosci.* 20, 3705–3713.

- Riley, T., Sontag, E., Chen, P., Levine, A., 2008. Transcriptional control of human p53-regulated genes. *Nat. Rev. Mol. Cell Biol.* 9, 402–412. <https://doi.org/10.1038/nrm2395>
- Rioux, J.D., Xavier, R.J., Taylor, K.D., Silverberg, M.S., Goyette, P., Huett, A., Green, T., Kuballa, P., Barmada, M.M., Datta, L.W., Shugart, Y.Y., Griffiths, A.M., Targan, S.R., Ippoliti, A.F., Bernard, E.-J., Mei, L., Nicolae, D.L., Regueiro, M., Schumm, L.P., Steinhardt, A.H., Rotter, J.I., Duerr, R.H., Cho, J.H., Daly, M.J., Brant, S.R., 2007. Genome-wide association study identifies new susceptibility loci for Crohn disease and implicates autophagy in disease pathogenesis. *Nat. Genet.* 39, 596–604. <https://doi.org/10.1038/ng2032>
- Rivollier, A., He, J., Kole, A., Valatas, V., Kelsall, B.L., 2012. Inflammation switches the differentiation program of Ly6Chi monocytes from antiinflammatory macrophages to inflammatory dendritic cells in the colon. *J. Exp. Med.* 209, 139–155. <https://doi.org/10.1084/jem.20101387>
- Roca, H., Varsos, Z.S., Sud, S., Craig, M.J., Ying, C., Pienta, K.J., 2009. CCL2 and Interleukin-6 Promote Survival of Human CD11b+ Peripheral Blood Mononuclear Cells and Induce M2-type Macrophage Polarization. *J. Biol. Chem.* 284, 34342–34354. <https://doi.org/10.1074/jbc.M109.042671>
- Rodríguez-Muela, N., Germain, F., Mariño, G., Fitze, P.S., Boya, P., 2012. Autophagy promotes survival of retinal ganglion cells after optic nerve axotomy in mice. *Cell Death Differ.* 19, 162–169. <https://doi.org/10.1038/cdd.2011.88>
- Rolhion, N., Barnich, N., Bringer, M.-A., Glasser, A.-L., Ranc, J., Hebuterne, X., Hofman, P., Darfeuille-Michaud, A., 2010. Abnormally expressed ER stress response chaperone Gp96 in CD favours adherent-invasive Escherichia coli invasion. *Gut* 59, 1355–1362. <https://doi.org/10.1136/gut.2010.207456>
- Rolhion, N., Barnich, N., Claret, L., Darfeuille-Michaud, A., 2005. Strong decrease in invasive ability and outer membrane vesicle release in Crohn's disease-associated adherent-invasive Escherichia coli strain LF82 with the yfgL gene deleted. *J. Bacteriol.* 187, 2286–2296. <https://doi.org/10.1128/JB.187.7.2286-2296.2005>
- Rolhion, N., Carvalho, F.A., Darfeuille-Michaud, A., 2007. OmpC and the sigma(E) regulatory pathway are involved in adhesion and invasion of the Crohn's disease-associated Escherichia coli strain LF82. *Mol. Microbiol.* 63, 1684–1700. <https://doi.org/10.1111/j.1365-2958.2007.05638.x>
- Romani, N., Gruner, S., Brang, D., Kämpgen, E., Lenz, A., Trockenbacher, B., Konwalinka, G., Fritsch, P.O., Steinman, R.M., Schuler, G., 1994. Proliferating dendritic cell progenitors in human blood. *J. Exp. Med.* 180, 83–93. <https://doi.org/10.1084/jem.180.1.83>
- Roosen, D.A., Cookson, M.R., 2016. LRRK2 at the interface of autophagosomes, endosomes and lysosomes. *Mol. Neurodegener.* 11, 73. <https://doi.org/10.1186/s13024-016-0140-1>
- Ropolo, A., Grasso, D., Pardo, R., Sacchetti, M.L., Archange, C., Lo Re, A., Seux, M., Nowak, J., Gonzalez, C.D., Iovanna, J.L., Vaccaro, M.I., 2007. The pancreatitis-induced vacuole membrane protein 1 triggers autophagy in mammalian cells. *J. Biol. Chem.* 282, 37124–37133. <https://doi.org/10.1074/jbc.M706956200>
- Rosenfeldt, M.T., Nixon, C., Liu, E., Mah, L.Y., Ryan, K.M., 2012. Analysis of macroautophagy by immunohistochemistry. *Autophagy* 8, 963–969. <https://doi.org/10.4161/auto.20186>

- Rouschop, K.M.A., van den Beucken, T., Dubois, L., Niessen, H., Bussink, J., Savelkoul, K., Keulers, T., Mujcic, H., Landuyt, W., Voncken, J.W., Lambin, P., van der Kogel, A.J., Koritzinsky, M., Wouters, B.G., 2010. The unfolded protein response protects human tumor cells during hypoxia through regulation of the autophagy genes MAP1LC3B and ATG5. *J. Clin. Invest.* 120, 127–141. <https://doi.org/10.1172/JCI40027>
- Ruemmele, F.M., Lachaux, A., Cézard, J.-P., Morali, A., Maurage, C., Giniès, J.-L., Viola, S., Goulet, O., Lamireau, T., Scaillon, M., Breton, A., Sarles, J., Groupe Francophone d'Hépatologie, Gastroentérologie et Nutrition Pédiatrique, 2009. Efficacy of infliximab in pediatric Crohn's disease: a randomized multicenter open-label trial comparing scheduled to on demand maintenance therapy. *Inflamm. Bowel Dis.* 15, 388–394. <https://doi.org/10.1002/ibd.20788>
- Russell, R.C., Tian, Y., Yuan, H., Park, H.W., Chang, Y.-Y., Kim, J., Kim, H., Neufeld, T.P., Dillin, A., Guan, K.-L., 2013. ULK1 induces autophagy by phosphorylating Beclin-1 and activating Vps34 lipid kinase. *Nat. Cell Biol.* 15, 741–750. <https://doi.org/10.1038/ncb2757>
- Rutkowski, D.T., Hegde, R.S., 2010. Regulation of basal cellular physiology by the homeostatic unfolded protein response. *J. Cell Biol.* 189, 783–794. <https://doi.org/10.1083/jcb.201003138>
- Ryan, P., Kelly, R.G., Lee, G., Collins, J.K., O'Sullivan, G.C., O'Connell, J., Shanahan, F., 2004. Bacterial DNA within granulomas of patients with Crohn's disease--detection by laser capture microdissection and PCR. *Am. J. Gastroenterol.* 99, 1539–1543. <https://doi.org/10.1111/j.1572-0241.2004.40103.x>
- Rzymiski, T., Milani, M., Pike, L., Buffa, F., Mellor, H.R., Winchester, L., Pires, I., Hammond, E., Ragoussis, I., Harris, A.L., 2010. Regulation of autophagy by ATF4 in response to severe hypoxia. *Oncogene* 29, 4424–4435. <https://doi.org/10.1038/onc.2010.191>
- Sabatino, A.D., Rosado, M.M., Ciccocioppo, R., Cazzola, P., Morera, R., Corazza, G.R., Carsetti, R., 2005. Depletion of Immunoglobulin M Memory B Cells is Associated with Splenic Hypofunction in Inflammatory Bowel Disease. *Am. J. Gastroenterol.* 100, 1788–1795. <https://doi.org/10.1111/j.1572-0241.2005.41939.x>
- Saci, A., Cantley, L.C., Carpenter, C.L., 2011. Rac1 Regulates the Activity of mTORC1 and mTORC2 and Controls Cellular Size. *Mol. Cell* 42, 50–61. <https://doi.org/10.1016/j.molcel.2011.03.017>
- Sadabad, M.S., Regeling, A., Goffau, M.C. de, Blokzijl, T., Weersma, R.K., Penders, J., Faber, K.N., Harmsen, H.J.M., Dijkstra, G., 2015. The ATG16L1-T300A allele impairs clearance of pathosymbionts in the inflamed ileal mucosa of Crohn's disease patients. *Gut* 64, 1546–1552. <https://doi.org/10.1136/gutjnl-2014-307289>
- Saitoh, T., Fujita, N., Jang, M.H., Uematsu, S., Yang, B.-G., Satoh, T., Omori, H., Noda, T., Yamamoto, N., Komatsu, M., Tanaka, K., Kawai, T., Tsujimura, T., Takeuchi, O., Yoshimori, T., Akira, S., 2008. Loss of the autophagy protein Atg16L1 enhances endotoxin-induced IL-1 β production. *Nature* 456, 264–268. <https://doi.org/10.1038/nature07383>
- Salem, M., Nielsen, O.H., Nys, K., Yazdanyar, S., Seidelin, J.B., 2015. Impact of T300A Variant of *ATG16L1* on Antibacterial Response, Risk of Culture Positive Infections, and Clinical Course of Crohn's Disease. *Clin. Transl. Gastroenterol.* 6, e122. <https://doi.org/10.1038/ctg.2015.47>

- Salminen, A., Hyttinen, J.M.T., Kauppinen, A., Kaarniranta, K., 2012. Context-Dependent Regulation of Autophagy by IKK-NF- κ B Signaling: Impact on the Aging Process. *Int. J. Cell Biol.* 2012, 849541. <https://doi.org/10.1155/2012/849541>
- Sancak, Y., Thoreen, C.C., Peterson, T.R., Lindquist, R.A., Kang, S.A., Spooner, E., Carr, S.A., Sabatini, D.M., 2007. PRAS40 is an insulin-regulated inhibitor of the mTORC1 protein kinase. *Mol Cell* 25, 903–15. <https://doi.org/10.1016/j.molcel.2007.03.003>
- Sánchez-Capelo, A., 2005. Dual role for TGF-beta1 in apoptosis. *Cytokine Growth Factor Rev.* 16, 15–34. <https://doi.org/10.1016/j.cytogfr.2004.11.002>
- Sandri, M., 2010. Autophagy in health and disease. 3. Involvement of autophagy in muscle atrophy. *Am. J. Physiol. Cell Physiol.* 298, C1291-1297. <https://doi.org/10.1152/ajpcell.00531.2009>
- Sano, R., Reed, J.C., 2013. ER stress-induced cell death mechanisms. *Biochim. Biophys. Acta* 1833. <https://doi.org/10.1016/j.bbamcr.2013.06.028>
- Sardiello, M., Palmieri, M., di Ronza, A., Medina, D.L., Valenza, M., Gennarino, V.A., Di Malta, C., Donaudy, F., Embrione, V., Polishchuk, R.S., Banfi, S., Parenti, G., Cattaneo, E., Ballabio, A., 2009. A gene network regulating lysosomal biogenesis and function. *Science* 325, 473–477. <https://doi.org/10.1126/science.1174447>
- Saruta, M., Yu, Q.T., Fleshner, P.R., Mantel, P.-Y., Schmidt-Weber, C.B., Banham, A.H., Papadakis, K.A., 2007. Characterization of FOXP3+CD4+ regulatory T cells in Crohn's disease. *Clin. Immunol. Orlando Fla* 125, 281–290. <https://doi.org/10.1016/j.clim.2007.08.003>
- Saudou, F., Finkbeiner, S., Devys, D., Greenberg, M.E., 1998. Huntingtin acts in the nucleus to induce apoptosis but death does not correlate with the formation of intranuclear inclusions. *Cell* 95, 55–66.
- Scherz-Shouval, R., Shvets, E., Fass, E., Shorer, H., Gil, L., Elazar, Z., 2007. Reactive oxygen species are essential for autophagy and specifically regulate the activity of Atg4. *EMBO J.* 26, 1749–1760. <https://doi.org/10.1038/sj.emboj.7601623>
- Schindelin, J., Arganda-Carreras, I., Frise, E., Kaynig, V., Longair, M., Pietzsch, T., Preibisch, S., Rueden, C., Saalfeld, S., Schmid, B., Tinevez, J.-Y., White, D.J., Hartenstein, V., Eliceiri, K., Tomancak, P., Cardona, A., 2012. Fiji: an open-source platform for biological-image analysis. *Nat. Methods* 9, 676–682. <https://doi.org/10.1038/nmeth.2019>
- Schoepfer, A.M., Bortolotti, M., Pittet, V., Mottet, C., Gonvers, J.-J., Reich, O., Fournier, N., Vader, J.-P., Burnand, B., Michetti, P., Froehlich, F., 2014. The gap between scientific evidence and clinical practice: 5-aminosalicylates are frequently used for the treatment of Crohn's disease. *Aliment. Pharmacol. Ther.* 40, 930–937. <https://doi.org/10.1111/apt.12929>
- Schultz, C., Berg, F.M. van den, Kate, F.W. ten, Tytgat, G.N.J., Dankert, J., 1999. The intestinal mucus layer from patients with inflammatory bowel disease harbors high numbers of bacteria compared with controls. *Gastroenterology* 117, 1089–1097. [https://doi.org/10.1016/S0016-5085\(99\)70393-8](https://doi.org/10.1016/S0016-5085(99)70393-8)
- Settembre, C., Di Malta, C., Polito, V.A., Arencibia, M.G., Vetrini, F., Erdin, S., Erdin, S.U., Huynh, T., Medina, D., Colella, P., Sardiello, M., Rubinsztein, D.C., Ballabio, A., 2011. TFEB Links Autophagy to Lysosomal Biogenesis. *Science* 332, 1429–1433. <https://doi.org/10.1126/science.1204592>
- Settembre, C., Zoncu, R., Medina, D.L., Vetrini, F., Erdin, Serkan, Erdin, Serpil Uckac, Huynh, T., Ferron, M., Karsenty, G., Vellard, M.C., Facchinetti, V., Sabatini, D.M., Ballabio, A., 2012. A lysosome-to-nucleus signalling mechanism senses and

- regulates the lysosome via mTOR and TFEB. *EMBO J.* 31, 1095–1108. <https://doi.org/10.1038/emboj.2012.32>
- Sha, D., Chin, L.-S., Li, L., 2010. Phosphorylation of parkin by Parkinson disease-linked kinase PINK1 activates parkin E3 ligase function and NF-kappaB signaling. *Hum. Mol. Genet.* 19, 352–363. <https://doi.org/10.1093/hmg/ddp501>
- Shale, M., Schiering, C., Powrie, F., 2013. CD4+ T-cell subsets in intestinal inflammation. *Immunol. Rev.* 252, 164–182. <https://doi.org/10.1111/imr.12039>
- Shamu, C.E., Walter, P., 1996. Oligomerization and phosphorylation of the Ire1p kinase during intracellular signaling from the endoplasmic reticulum to the nucleus. *EMBO J.* 15, 3028–3039.
- Shaye, O.A., Yadegari, M., Abreu, M.T., Poordad, F., Simon, K., Martin, P., Papadakis, K.A., Ippoliti, A., Vasiliauskas, E., Tran, T.T., 2007. Hepatotoxicity of 6-mercaptopurine (6-MP) and Azathioprine (AZA) in adult IBD patients. *Am. J. Gastroenterol.* 102, 2488–2494. <https://doi.org/10.1111/j.1572-0241.2007.01515.x>
- Shen, J., Chen, X., Hendershot, L., Prywes, R., 2002. ER stress regulation of ATF6 localization by dissociation of BiP/GRP78 binding and unmasking of Golgi localization signals. *Dev. Cell* 3, 99–111.
- Shi, C.S., Shenderov, K., Huang, N.N., Kabat, J., Abu-Asab, M., Fitzgerald, K.A., Sher, A., Kehrl, J.H., 2012. Activation of autophagy by inflammatory signals limits IL-1beta production by targeting ubiquitinated inflammasomes for destruction. *Nat Immunol* 13, 255–63. <https://doi.org/10.1038/ni.2215>
- Shi, J., Wang, L., Zhang, H., Jie, Q., Li, X., Shi, Q., Huang, Q., Gao, B., Han, Y., Guo, K., Liu, J., Yang, L., Luo, Z., 2015. Glucocorticoids: Dose-related effects on osteoclast formation and function via reactive oxygen species and autophagy. *Bone* 79, 222–232. <https://doi.org/10.1016/j.bone.2015.06.014>
- Shimodaira, Y., Takahashi, S., Kinouchi, Y., Endo, K., Shiga, H., Kakuta, Y., Kuroha, M., Shimosegawa, T., 2014. Modulation of endoplasmic reticulum (ER) stress-induced autophagy by C/EBP homologous protein (CHOP) and inositol-requiring enzyme 1 α (IRE1 α) in human colon cancer cells. *Biochem. Biophys. Res. Commun.* 445, 524–533. <https://doi.org/10.1016/j.bbrc.2014.02.054>
- Shkoda, A., Ruiz, P.A., Daniel, H., Kim, S.C., Rogler, G., Sartor, R.B., Haller, D., 2007. Interleukin-10 Blocked Endoplasmic Reticulum Stress in Intestinal Epithelial Cells: Impact on Chronic Inflammation. *Gastroenterology* 132, 190–207. <https://doi.org/10.1053/j.gastro.2006.10.030>
- Siddiqui, K.R.R., Laffont, S., Powrie, F., 2010. E-cadherin marks a subset of inflammatory dendritic cells that promote T cell-mediated colitis. *Immunity* 32, 557–567. <https://doi.org/10.1016/j.immuni.2010.03.017>
- Simpson, K.W., Dogan, B., Rishniw, M., Goldstein, R.E., Klaessig, S., McDonough, P.L., German, A.J., Yates, R.M., Russell, D.G., Johnson, S.E., Berg, D.E., Harel, J., Bruant, G., McDonough, S.P., Schukken, Y.H., 2006. Adherent and invasive *Escherichia coli* is associated with granulomatous colitis in boxer dogs. *Infect. Immun.* 74, 4778–4792. <https://doi.org/10.1128/IAI.00067-06>
- Singh, S.B., Ornatowski, W., Vergne, I., Naylor, J., Delgado, M., Roberts, E., Ponpuak, M., Master, S., Pilli, M., White, E., Komatsu, M., Deretic, V., 2010. Human IRGM regulates autophagy and cell-autonomous immunity functions through mitochondria. *Nat Cell Biol* 12, 1154–65. <https://doi.org/10.1038/ncb2119>

- Singh, S.B., Wilson, M., Ritz, N., Lin, H.C., 2017. Autophagy Genes of Host Responds to Disruption of Gut Microbial Community by Antibiotics. *Dig. Dis. Sci.* 62, 1486–1497. <https://doi.org/10.1007/s10620-017-4589-8>
- Sluis, M.V. der, Koning, B.A.E.D., Bruijn, A.C.J.M.D., Velcich, A., Meijerink, J.P.P., Goudoever, J.B.V., Büller, H.A., Dekker, J., Seunigen, I.V., Renes, I.B., Einerhand, A.W.C., 2006. Muc2-Deficient Mice Spontaneously Develop Colitis, Indicating That MUC2 Is Critical for Colonic Protection. *Gastroenterology* 131, 117–129. <https://doi.org/10.1053/j.gastro.2006.04.020>
- Smythies, L.E., Sellers, M., Clements, R.H., Mosteller-Barnum, M., Meng, G., Benjamin, W.H., Orenstein, J.M., Smith, P.D., 2005. Human intestinal macrophages display profound inflammatory anergy despite avid phagocytic and bacteriocidal activity. *J. Clin. Invest.* 115, 66–75. <https://doi.org/10.1172/JCI19229>
- Sokol, H., Pigneur, B., Watterlot, L., Lakhdari, O., Bermúdez-Humarán, L.G., Gratadoux, J.-J., Blugeon, S., Bridonneau, C., Furet, J.-P., Corthier, G., Grangette, C., Vasquez, N., Pochart, P., Trugnan, G., Thomas, G., Blottière, H.M., Doré, J., Marteau, P., Seksik, P., Langella, P., 2008. Faecalibacterium prausnitzii is an anti-inflammatory commensal bacterium identified by gut microbiota analysis of Crohn disease patients. *Proc. Natl. Acad. Sci. U. S. A.* 105, 16731–16736. <https://doi.org/10.1073/pnas.0804812105>
- Song, S., Tan, J., Miao, Y., Zhang, Q., 2017. Crosstalk of ER stress-mediated autophagy and ER-phagy: involvement of UPR and the core autophagy machinery. *J. Cell. Physiol.*
- Steel, Mela C. M., Lindsay J. O., Gazzard B. G., Goodier M. R., 2010. Increased proportion of CD16+ NK cells in the colonic lamina propria of inflammatory bowel disease patients, but not after azathioprine treatment. *Aliment. Pharmacol. Ther.* 33, 115–126. <https://doi.org/10.1111/j.1365-2036.2010.04499.x>
- Stephan, J.S., Yeh, Y.-Y., Ramachandran, V., Deminoff, S.J., Herman, P.K., 2009. The Tor and PKA signaling pathways independently target the Atg1/Atg13 protein kinase complex to control autophagy. *Proc. Natl. Acad. Sci. U. S. A.* 106, 17049–17054. <https://doi.org/10.1073/pnas.0903316106>
- Stephenson, L.M., Miller, B.C., Ng, A., Eisenberg, J., Zhao, Z., Cadwell, K., Graham, D.B., Mizushima, N.N., Xavier, R., Virgin, H.W., Swat, W., 2009. Identification of Atg5-dependent transcriptional changes and increases in mitochondrial mass in Atg5-deficient T lymphocytes. *Autophagy* 5, 625–635.
- Stocco, G., Cuzzoni, E., De Iudicibus, S., Favretto, D., Malusa, N., Martelossi, S., Pozzi, E., Lionetti, P., Ventura, A., Decorti, G., 2015. Thiopurine metabolites variations during co-treatment with aminosaliclates for inflammatory bowel disease: Effect of N-acetyl transferase polymorphisms. *World J Gastroenterol* 21, 3571–8. <https://doi.org/10.3748/wjg.v21.i12.3571>
- Stocco, G., Cuzzoni, E., De Iudicibus, S., Franca, R., Favretto, D., Malusà, N., Londero, M., Cont, G., Bartoli, F., Martelossi, S., Ventura, A., Decorti, G., 2014. Deletion of Glutathione-S-Transferase M1 Reduces Azathioprine Metabolite Concentrations in Young Patients With Inflammatory Bowel Disease. *J. Clin. Gastroenterol.* 48, 43. <https://doi.org/10.1097/MCG.0b013e31828b2866>
- Stokkers, P.C.F., Reitsma, P.H., Tytgat, G.N.J., Deventer, S.J.H. van, 1999. HLA-DR and -DQ phenotypes in inflammatory bowel disease: a meta-analysis. *Gut* 45, 395–401. <https://doi.org/10.1136/gut.45.3.395>
- Strisciuglio, C., Miele, E., Wildenberg, M.E., Giugliano, F.P., Androozzi, M., Vitale, A., Capasso, F., Camarca, A., Barone, M.V., Staiano, A., Troncone, R., Gianfrani, C.,

2013. T300A Variant of Autophagy ATG16L1 Gene is Associated with Decreased Antigen Sampling and Processing by Dendritic Cells in Pediatric Crohn's Disease: *Inflamm. Bowel Dis.* 19, 2339–2348. <https://doi.org/10.1097/MIB.0b013e3182a6a11c>
- Sun, Y., Li, C., Shu, Y., Ju, X., Zou, Z., Wang, H., Rao, S., Guo, F., Liu, H., Nan, W., Zhao, Y., Yan, Y., Tang, J., Zhao, C., Yang, P., Liu, K., Wang, S., Lu, H., Li, X., Tan, L., Gao, R., Song, J., Gao, X., Tian, X., Qin, Y., Xu, K.-F., Li, D., Jin, N., Jiang, C., 2012. Inhibition of autophagy ameliorates acute lung injury caused by avian influenza A H5N1 infection. *Sci. Signal.* 5, ra16. <https://doi.org/10.1126/scisignal.2001931>
- Suzuki, K., Kubota, Y., Sekito, T., Ohsumi, Y., 2007. Hierarchy of Atg proteins in pre-autophagosomal structure organization. *Genes Cells* 12, 209–18. <https://doi.org/10.1111/j.1365-2443.2007.01050.x>
- Swann, P.F., Waters, T.R., Moulton, D.C., Xu, Y.-Z., Zheng, Q., Edwards, M., Mace, R., 1996. Role of Postreplicative DNA Mismatch Repair in the Cytotoxic Action of Thioguanine. *Science* 273, 1109–1111. <https://doi.org/10.1126/science.273.5278.1109>
- Swerdlow, S., McColl, K., Rong, Y., Lam, M., Gupta, A., Distelhorst, C.W., 2008. Apoptosis inhibition by Bcl-2 gives way to autophagy in glucocorticoid-treated lymphocytes. *Autophagy* 4, 612–20.
- Tabata, H., Matsuoka, T., Endo, F., Nishimura, Y., Matsushita, S., 2000. Ligation of HLA-DR Molecules on B Cells Induces Enhanced Expression of IgM Heavy Chain Genes in Association with Syk Activation. *J. Biol. Chem.* 275, 34998–35005. <https://doi.org/10.1074/jbc.M002089200>
- Takahashi, K., Nishida, A., Fujimoto, T., Fujii, M., Shioya, M., Imaeda, H., Inatomi, O., Bamba, S., Sugimoto, M., Andoh, A., 2016. Reduced Abundance of Butyrate-Producing Bacteria Species in the Fecal Microbial Community in Crohn's Disease. *Digestion* 93, 59–65. <https://doi.org/10.1159/000441768>
- Tang, Y.-H., Yue, Z.-S., Xin, D.-W., Zeng, L.-R., Xiong, Z.-F., Hu, Z.-Q., Xu, C.-D., 2018. β -Ecdysterone promotes autophagy and inhibits apoptosis in osteoporotic rats. *Mol. Med. Rep.* 17, 1591–1598.
- Tareyeva, I.E., Shilov, E.M., Gordovskaya, N.B., 1980. The effects of azathioprine and prednisolone on T- and B-lymphocytes in patients with lupus nephritis and chronic glomerulonephritis. *Clin. Nephrol.* 14, 233–237.
- Tasdemir, E., Maiuri, M.C., Galluzzi, L., Vitale, I., Djavaheri-Mergny, M., D'Amelio, M., Criollo, A., Morselli, E., Zhu, C., Harper, F., Nannmark, U., Samara, C., Pinton, P., Vicencio, J.M., Carnuccio, R., Moll, U.M., Madeo, F., Paterlini-Brechot, P., Rizzuto, R., Szabadkai, G., Pierron, G., Blomgren, K., Tavernarakis, N., Codogno, P., Cecconi, F., Kroemer, G., 2008. Regulation of autophagy by cytoplasmic p53. *Nat. Cell Biol.* 10, 676–687. <https://doi.org/10.1038/ncb1730>
- Tatsukawa, H., Furutani, Y., Hitomi, K., Kojima, S., 2016. Transglutaminase 2 has opposing roles in the regulation of cellular functions as well as cell growth and death. *Cell Death Dis.* 7, e2244. <https://doi.org/10.1038/cddis.2016.150>
- Thachil, E., Hugot, J.P., Arbeille, B., Paris, R., Grodet, A., Peuchmaur, M., Codogno, P., Barreau, F., Ogier-Denis, E., Berrebi, D., Viala, J., 2012. Abnormal activation of autophagy-induced crinophagy in Paneth cells from patients with Crohn's disease. *Gastroenterology* 142, 1097-1099.e4. <https://doi.org/10.1053/j.gastro.2012.01.031>
- Theiss, A.L., Idell, R.D., Srinivasan, S., Klapproth, J.-M., Jones, D.P., Merlin, D., Sitaraman, S.V., 2007. Prohibitin protects against oxidative stress in intestinal epithelial

- cells. *FASEB J. Off. Publ. Fed. Am. Soc. Exp. Biol.* 21, 197–206. <https://doi.org/10.1096/fj.06-6801com>
- Thomazini, C.M., Samegima, D.A.G., Rodrigues, M.A.M., Victoria, C.R., Rodrigues, J., 2011. High prevalence of aggregative adherent *Escherichia coli* strains in the mucosa-associated microbiota of patients with inflammatory bowel diseases. *Int. J. Med. Microbiol.* 301, 475–479. <https://doi.org/10.1016/j.ijmm.2011.04.015>
- Thorburn, A., 2007. Tumor necrosis factor-related apoptosis-inducing ligand (TRAIL) pathway signaling. *J. Thorac. Oncol. Off. Publ. Int. Assoc. Study Lung Cancer* 2, 461–465. <https://doi.org/10.1097/JTO.0b013e31805fea64>
- Thurston, T.L.M., Ryzhakov, G., Bloor, S., von Muhlinen, N., Randow, F., 2009. The TBK1 adaptor and autophagy receptor NDP52 restricts the proliferation of ubiquitin-coated bacteria. *Nat. Immunol.* 10, 1215–1221. <https://doi.org/10.1038/ni.1800>
- Thurston, T.L.M., Wandel, M.P., von Muhlinen, N., Foeglein, A., Randow, F., 2012. Galectin 8 targets damaged vesicles for autophagy to defend cells against bacterial invasion. *Nature* 482, 414–418. <https://doi.org/10.1038/nature10744>
- Tiede, I., Fritz, G., Strand, S., Poppe, D., Dvorsky, R., Strand, D., Lehr, H.A., Wirtz, S., Becker, C., Atreya, R., Mudter, J., Hildner, K., Bartsch, B., Holtmann, M., Blumberg, R., Walczak, H., Iven, H., Galle, P.R., Ahmadian, M.R., Neurath, M.F., 2003. CD28-dependent Rac1 activation is the molecular target of azathioprine in primary human CD4+ T lymphocytes. *J. Clin. Invest.* 111, 1133–1145. <https://doi.org/10.1172/JCI200316432>
- Timmermans, W.M.C., Laar, J.A.M. van, Houwen, T.B. van der, Kamphuis, L.S.J., Bartol, S.J.W., Lam, K.H., Ouwendijk, R.J., Sparrow, M.P., Gibson, P.R., Hagen, P.M. van, Zelm, M.C. van, 2016. B-Cell Dysregulation in Crohn's Disease Is Partially Restored with Infliximab Therapy. *PLOS ONE* 11, e0160103. <https://doi.org/10.1371/journal.pone.0160103>
- Tirasophon, W., Lee, K., Callaghan, B., Welihinda, A., Kaufman, R.J., 2000. The endoribonuclease activity of mammalian IRE1 autoregulates its mRNA and is required for the unfolded protein response. *Genes Dev.* 14, 2725–2736.
- Todd, D.J., Lee, A.H., Glimcher, L.H., 2008. The endoplasmic reticulum stress response in immunity and autoimmunity. *Nat Rev Immunol* 8, 663–74. <https://doi.org/10.1038/nri2359>
- Travassos, L.H., Carneiro, L.A.M., Ramjeet, M., Hussey, S., Kim, Y.-G., Magalhães, J.G., Yuan, L., Soares, F., Chea, E., Le Bourhis, L., Boneca, I.G., Allaoui, A., Jones, N.L., Nuñez, G., Girardin, S.E., Philpott, D.J., 2010. Nod1 and Nod2 direct autophagy by recruiting ATG16L1 to the plasma membrane at the site of bacterial entry. *Nat. Immunol.* 11, 55–62. <https://doi.org/10.1038/ni.1823>
- Tréton, X., Pédruzzi, E., Cazals-Hatem, D., Grodet, A., Panis, Y., Groyer, A., Moreau, R., Bouhnik, Y., Daniel, F., Ogier-Denis, E., 2011. Altered Endoplasmic Reticulum Stress Affects Translation in Inactive Colon Tissue From Patients With Ulcerative Colitis. *Gastroenterology* 141, 1024–1035. <https://doi.org/10.1053/j.gastro.2011.05.033>
- Troncoso, R., Paredes, F., Parra, V., Gatica, D., Vásquez-Trincado, C., Quiroga, C., Bravo-Sagua, R., López-Crisosto, C., Rodríguez, A.E., Oyarzún, A.P., Kroemer, G., Lavandero, S., 2014. Dexamethasone-induced autophagy mediates muscle atrophy through mitochondrial clearance. *Cell Cycle* 13, 2281–2295. <https://doi.org/10.4161/cc.29272>

- Tsai, C.-W., Lai, F.-J., Sheu, H.-M., Lin, Y.-S., Chang, T.-H., Jan, M.-S., Chen, S.-M., Hsu, P.-C., Huang, T.-T., Huang, T.-C., Sheen, M.-C., Chen, S.-T., Chang, W.-C., Chang, N.-S., Hsu, L.-J., 2013. WWOX suppresses autophagy for inducing apoptosis in methotrexate-treated human squamous cell carcinoma. *Cell Death Dis.* 4, e792. <https://doi.org/10.1038/cddis.2013.308>
- Tschurtschenthaler, M., Adolph, T.E., Ashcroft, J.W., Niederreiter, L., Bharti, R., Saveljeva, S., Bhattacharyya, J., Flak, M.B., Shih, D.Q., Fuhler, G.M., Parkes, M., Kohno, K., Iwawaki, T., Janneke van der Woude, C., Harding, H.P., Smith, A.M., Peppelenbosch, M.P., Targan, S.R., Ron, D., Rosenstiel, P., Blumberg, R.S., Kaser, A., 2017. Defective ATG16L1-mediated removal of IRE1 α drives Crohn's disease-like ileitis. *J. Exp. Med.* 214, 401–422. <https://doi.org/10.1084/jem.20160791>
- Tsuboi, K., Nishitani, M., Takakura, A., Imai, Y., Komatsu, M., Kawashima, H., 2015. Autophagy Protects against Colitis by the Maintenance of Normal Gut Microflora and Secretion of Mucus. *J. Biol. Chem.* 290, 20511–20526. <https://doi.org/10.1074/jbc.M114.632257>
- Tsuru, A., Fujimoto, N., Takahashi, S., Saito, M., Nakamura, D., Iwano, M., Iwawaki, T., Kadokura, H., Ron, D., Kohno, K., 2013. Negative feedback by IRE1 β optimizes mucin production in goblet cells. *Proc. Natl. Acad. Sci. U. S. A.* 110, 2864–2869. <https://doi.org/10.1073/pnas.1212484110>
- Turner, D., Levine, A., Escher, J.C., Griffiths, A.M., Russell, R.K., Dignass, A., Dias, J.A., Bronsky, J., Braegger, C.P., Cucchiara, S., de Ridder, L., Fagerberg, U.L., Hussey, S., Hugot, J.P., Kolacek, S., Kolho, K.L., Lionetti, P., Paerregaard, A., Potapov, A., Rintala, R., Serban, D.E., Staiano, A., Sweeny, B., Veerman, G., Veres, G., Wilson, D.C., Ruemmele, F.M., 2012. Management of pediatric ulcerative colitis: joint ECCO and ESPGHAN evidence-based consensus guidelines. *J. Pediatr. Gastroenterol Nutr* 55, 340–61. <https://doi.org/10.1097/MPG.0b013e3182662233>
- Uhlig, H.H., McKenzie, B.S., Hue, S., Thompson, C., Joyce-Shaikh, B., Stepankova, R., Robinson, N., Buonocore, S., Tlaskalova-Hogenova, H., Cua, D.J., Powrie, F., 2006. Differential activity of IL-12 and IL-23 in mucosal and systemic innate immune pathology. *Immunity* 25, 309–318. <https://doi.org/10.1016/j.immuni.2006.05.017>
- Uhlig, H.H., Schwerd, T., Koletzko, S., Shah, N., Kammermeier, J., Elkadri, A., Ouahed, J., Wilson, D.C., Travis, S.P., Turner, D., Klein, C., Snapper, S.B., Muise, A.M., 2014. The Diagnostic Approach to Monogenic Very Early Onset Inflammatory Bowel Disease. *Gastroenterology* 147, 990-1007.e3. <https://doi.org/10.1053/j.gastro.2014.07.023>
- Urano, F., Wang, X., Bertolotti, A., Zhang, Y., Chung, P., Harding, H.P., Ron, D., 2000. Coupling of Stress in the ER to Activation of JNK Protein Kinases by Transmembrane Protein Kinase IRE1. *Science* 287, 664–666. <https://doi.org/10.1126/science.287.5453.664>
- Van den Brande, J.M.H., Braat, H., van den Brink, G.R., Versteeg, H.H., Bauer, C.A., Hoedemaeker, I., van Montfrans, C., Hommes, D.W., Peppelenbosch, M.P., van Deventer, S.J.H., 2003. Infliximab but not etanercept induces apoptosis in lamina propria T-lymphocytes from patients with Crohn's disease. *Gastroenterology* 124, 1774–1785.
- Van Limbergen, J., Stevens, C., Nimmo, E.R., Wilson, D.C., Satsangi, J., 2009. Autophagy: from basic science to clinical application. *Mucosal Immunol* 2, 315–30. <https://doi.org/10.1038/mi.2009.20>

- Vandesompele, J., De Preter, K., Pattyn, F., Poppe, B., Van Roy, N., De Paepe, A., Speleman, F., 2002. Accurate normalization of real-time quantitative RT-PCR data by geometric averaging of multiple internal control genes. *Genome Biol.* 3, research0034. <https://doi.org/10.1186/gb-2002-3-7-research0034>
- Varshney, P., Saini, N., 2018. PI3K/AKT/mTOR activation and autophagy inhibition plays a key role in increased cholesterol during IL-17A mediated inflammatory response in psoriasis. *Biochim. Biophys. Acta BBA - Mol. Basis Dis.* 1864, 1795–1803. <https://doi.org/10.1016/j.bbadis.2018.02.003>
- Vaseva, A.V., Marchenko, N.D., Ji, K., Tsirka, S.E., Holzmann, S., Moll, U.M., 2012. p53 opens the mitochondrial permeability transition pore to trigger necrosis. *Cell* 149, 1536–1548. <https://doi.org/10.1016/j.cell.2012.05.014>
- Vattem, K.M., Wek, R.C., 2004. Reinitiation involving upstream ORFs regulates ATF4 mRNA translation in mammalian cells. *Proc. Natl. Acad. Sci. U. S. A.* 101, 11269–11274. <https://doi.org/10.1073/pnas.0400541101>
- Vazeille, E., Buisson, A., Bringer, M.-A., Goutte, M., Ouchchane, L., Hugot, J.-P., de Vallee, A., Barnich, N., Bommelaer, G., Darfeuille-Michaud, A., 2015. Monocyte-derived Macrophages from Crohn's Disease Patients Are Impaired in the Ability to Control Intracellular Adherent-Invasive Escherichia coli and Exhibit Disordered Cytokine Secretion Profile. *J. Crohns Colitis* 9, 410–420. <https://doi.org/10.1093/ecco-jcc/jjv053>
- Vázquez, P., Arroba, A.I., Cecconi, F., de la Rosa, E.J., Boya, P., de Pablo, F., 2012. Atg5 and Ambra1 differentially modulate neurogenesis in neural stem cells. *Autophagy* 8, 187–199. <https://doi.org/10.4161/auto.8.2.18535>
- Ventham, N.T., Kennedy, N.A., Adams, A.T., Kalla, R., Heath, S., O'Leary, K.R., Drummond, H., Lauc, G., Campbell, H., McGovern, D.P.B., Annesse, V., Zoldoš, V., Permberton, I.K., Wuhrer, M., Kolarich, D., Fernandes, D.L., Theodorou, E., Merrick, V., Spencer, D.I., Gardner, R.A., Doran, R., Shubhakar, A., Boyapati, R., Rudan, I., Lionetti, P., Akmačić, I.T., Krištić, J., Vučković, F., Štambuk, J., Novokmet, M., Pučić-Baković, M., Gornik, O., Andriulli, A., Cantoro, L., Sturniolo, G., Fiorino, G., Manetti, N., Latiano, A., Kohn, A., D'Incà, R., Danese, S., Arnott, I.D., Noble, C.L., Lees, C.W., Shand, A.G., Ho, G.-T., Dunlop, M.G., Murphy, L., Gibson, J., Evenden, L., Wrobel, N., Gilchrist, T., Fawkes, A., Kammeijer, G.S.M., Clerc, F., de Haan, N., Vojta, A., Samaržija, I., Markulin, D., Klasić, M., Dobrinić, P., Aulchenko, Y., van den Heuve, T., Jonkers, D., Pierik, M., Vatn, S., Ricanek, P., Jahnsen, J., You, P., Sjølvernes, J., Frengen, A.B., Tannæs, T.M., Moen, A.E.F., Dahl, F.A., Lindstrøm, J.C., Ekeland, G.S., Detlie, T.E., Keita, Å.V., Söderholm, J.D., Hjortswang, H., Halfvarson, J., Bergemalm, D., Gomollón, F., D'Amato, M., Törkvist, L., Hjelm, F., Gullberg, M., Nordberg, N., Ocklind, A., Pettersson, E., Ekman, D., Sundell, M., Modig, E., Veillard, A.-C., Schoemans, R., Poncelet, D., Sabatel, C., Gut, M., Bayes, M., Casén, C., Lindahl, T., Cierniejewska, E., Vatn, M.H., Wilson, D.C., Gut, I.G., Nimmo, E.R., Satsangi, J., 2016. Integrative epigenome-wide analysis demonstrates that DNA methylation may mediate genetic risk in inflammatory bowel disease. *Nat. Commun.* 7, 13507. <https://doi.org/10.1038/ncomms13507>
- Verstockt, B., Smith, K.G., Lee, J.C., 2018. Genome-wide association studies in Crohn's disease: Past, present and future. *Clin. Transl. Immunol.* 7, e1001. <https://doi.org/10.1002/cti2.1001>
- Vos, A.C.W., Wildenberg, M.E., Arijs, I., Duijvestein, M., Verhaar, A.P., de Hertogh, G., Vermeire, S., Rutgeerts, P., van den Brink, G.R., Hommes, D.W., 2012. Regulatory

- macrophages induced by infliximab are involved in healing in vivo and in vitro. *Inflamm. Bowel Dis.* 18, 401–408. <https://doi.org/10.1002/ibd.21818>
- Vos, A.C.W., Wildenberg, M.E., Duijvestein, M., Verhaar, A.P., Brink, G.R. van den, Hommes, D.W., 2011. Anti-Tumor Necrosis Factor- α Antibodies Induce Regulatory Macrophages in an Fc Region-Dependent Manner. *Gastroenterology* 140, 221-230.e3. <https://doi.org/10.1053/j.gastro.2010.10.008>
- Vousden, K.H., Lane, D.P., 2007. p53 in health and disease. *Nat. Rev. Mol. Cell Biol.* 8, 275–283. <https://doi.org/10.1038/nrm2147>
- Walker, A.W., Sanderson, J.D., Churcher, C., Parkes, G.C., Hudspith, B.N., Rayment, N., Brostoff, J., Parkhill, J., Dougan, G., Petrovska, L., 2011. High-throughput clone library analysis of the mucosa-associated microbiota reveals dysbiosis and differences between inflamed and non-inflamed regions of the intestine in inflammatory bowel disease. *BMC Microbiol.* 11, 7. <https://doi.org/10.1186/1471-2180-11-7>
- Wang, H., Kubica, N., Ellisen, L.W., Jefferson, L.S., Kimball, S.R., 2006. Dexamethasone represses signaling through the mammalian target of rapamycin in muscle cells by enhancing expression of REDD1. *J Biol Chem* 281, 39128–34. <https://doi.org/10.1074/jbc.M610023200>
- Wang, S., Xia, P., Huang, G., Zhu, P., Liu, J., Ye, B., Du, Y., Fan, Z., 2016. FoxO1-mediated autophagy is required for NK cell development and innate immunity. *Nat. Commun.* 7, 11023. <https://doi.org/10.1038/ncomms11023>
- Wang, W., Kang, H., Zhao, Y., Min, I., Wyrwas, B., Moore, M., Teng, L., Zarnegar, R., Jiang, X., Fahey, T.J., 2016. Targeting autophagy sensitizes BRAF-mutant thyroid cancer to vemurafenib. *J. Clin. Endocrinol. Metab.* jc.2016-1999. <https://doi.org/10.1210/jc.2016-1999>
- Wang, X.Z., Harding, H.P., Zhang, Y., Jolicoeur, E.M., Kuroda, M., Ron, D., 1998. Cloning of mammalian Ire1 reveals diversity in the ER stress responses. *EMBO J.* 17, 5708–5717. <https://doi.org/10.1093/emboj/17.19.5708>
- Weersma, R.K., Stokkers, P.C.F., van Bodegraven, A.A., van Hogezaand, R.A., Verspaget, H.W., de Jong, D.J., van der Woude, C.J., Oldenburg, B., Linskens, R.K., Festen, E. a. M., van der Steege, G., Hommes, D.W., Crusius, J.B.A., Wijmenga, C., Nolte, I.M., Dijkstra, G., Dutch Initiative on Crohn and Colitis (ICC), 2009. Molecular prediction of disease risk and severity in a large Dutch Crohn’s disease cohort. *Gut* 58, 388–395. <https://doi.org/10.1136/gut.2007.144865>
- Wehkamp, J., Harder, J., Weichenthal, M., Schwab, M., Schäffeler, E., Schlee, M., Herrlinger, K.R., Stallmach, A., Noack, F., Fritz, P., Schröder, J.M., Bevins, C.L., Fellermann, K., Stange, E.F., 2004. NOD2 (CARD15) mutations in Crohn’s disease are associated with diminished mucosal alpha-defensin expression. *Gut* 53, 1658–1664. <https://doi.org/10.1136/gut.2003.032805>
- Wei, Y., Sinha, S.C., Levine, B., 2008. Dual role of JNK1-mediated phosphorylation of Bcl-2 in autophagy and apoptosis regulation. *Autophagy* 4, 949–951.
- Weinstein, R.S., Jilka, R.L., Parfitt, A.M., Manolagas, S.C., 1998. Inhibition of osteoblastogenesis and promotion of apoptosis of osteoblasts and osteocytes by glucocorticoids. Potential mechanisms of their deleterious effects on bone. *J. Clin. Invest.* 102, 274–282.
- Wild, P., Farhan, H., McEwan, D.G., Wagner, S., Rogov, V.V., Brady, N.R., Richter, B., Korac, J., Waidmann, O., Choudhary, C., Dötsch, V., Bumann, D., Dikic, I., 2011. Phosphorylation of the autophagy receptor optineurin restricts Salmonella growth. *Science* 333, 228–233. <https://doi.org/10.1126/science.1205405>

- Wildenberg, M.E., Koelink, P.J., Diederens, K., te Velde, A.A., Wolfkamp, S.C.S., Nuij, V.J., Peppelenbosch, M.P., Nobis, M., Sansom, O.J., Anderson, K.I., van der Woude, C.J., D'Haens, G.R.A.M., van den Brink, G.R., 2017. The ATG16L1 risk allele associated with Crohn's disease results in a Rac1-dependent defect in dendritic cell migration that is corrected by thiopurines. *Mucosal Immunol.* 10, 352–360. <https://doi.org/10.1038/mi.2016.65>
- Wildenberg, M.E., Vos, A.C.W., Wolfkamp, S.C.S., Duijvestein, M., Verhaar, A.P., Te Velde, A.A., van den Brink, G.R., Hommes, D.W., 2012. Autophagy attenuates the adaptive immune response by destabilizing the immunologic synapse. *Gastroenterology* 142, 1493-1503.e6. <https://doi.org/10.1053/j.gastro.2012.02.034>
- Wilson, D.C., Thomas, A.G., Croft, N.M., Newby, E., Akobeng, A.K., Sawczenko, A., Fell, J.M.E., Murphy, M.S., Beattie, R.M., Sandhu, B.K., Mitton, S.G., IBD Working Group of the British Society of Paediatric Gastroenterology, Hepatology, and Nutrition, Casson, D., Elawad, M., Heuschkel, R., Jenkins, H., Johnson, T., Macdonald, S., Murch, S.H., 2010. Systematic review of the evidence base for the medical treatment of paediatric inflammatory bowel disease. *J. Pediatr. Gastroenterol. Nutr.* 50 Suppl 1, S14-34. <https://doi.org/10.1097/MPG.0b013e3181c92caa>
- Wirawan, E., Vande Walle, L., Kersse, K., Cornelis, S., Claerhout, S., Vanoverberghe, I., Roelandt, R., De Rycke, R., Verspurten, J., Declercq, W., Agostinis, P., Vanden Berghe, T., Lippens, S., Vandenabeele, P., 2010. Caspase-mediated cleavage of Beclin-1 inactivates Beclin-1-induced autophagy and enhances apoptosis by promoting the release of proapoptotic factors from mitochondria. *Cell Death Dis.* 1, e18. <https://doi.org/10.1038/cddis.2009.16>
- Wirth, M., Joachim, J., Tooze, S.A., 2013. Autophagosome formation--the role of ULK1 and Beclin1-PI3KC3 complexes in setting the stage. *Semin. Cancer Biol.* 23, 301–309. <https://doi.org/10.1016/j.semcancer.2013.05.007>
- Wittstock, M., Rommer, P.S., Schiffmann, F., Jügelt, K., Stüwe, S., Benecke, R., Schiffmann, D., Zettl, U.K., 2015. Effect of methylprednisolone on mammalian neuronal networks in vitro. *Cell. Mol. Neurobiol.* 35, 111–114. <https://doi.org/10.1007/s10571-014-0117-y>
- Woldt, E., Sebt, Y., Solt, L.A., Duhem, C., Lancel, S., Eeckhoutte, J., Hesselink, M.K.C., Paquet, C., Delhay, S., Shin, Y., Kamenecka, T.M., Schaart, G., Lefebvre, P., Nevière, R., Burris, T.P., Schrauwen, P., Staels, B., Duez, H., 2013. Rev-erb- α modulates skeletal muscle oxidative capacity by regulating mitochondrial biogenesis and autophagy. *Nat. Med.* 19, 1039–1046. <https://doi.org/10.1038/nm.3213>
- Wolfkamp, S.C., Verseyden, C., Vogels, E.W., Meisner, S., Boonstra, K., Peters, C.P., Stokkers, P.C., Te, A.V., 2014. ATG16L1 and NOD2 polymorphisms enhance phagocytosis in monocytes of Crohn's disease patients., ATG16L1 and NOD2 polymorphisms enhance phagocytosis in monocytes of Crohn's disease patients. *World J. Gastroenterol.* World J. Gastroenterol. WJG 20, 20, 2664, 2664–2672. <https://doi.org/10.3748/wjg.v20.i10.2664>, <https://doi.org/10.3748/wjg.v20.i10.2664>
- Wu, F., Guo, N.J., Tian, H., Marohn, M., Gearhart, S., Bayless, T.M., Brant, S.R., Kwon, J.H., 2011. Peripheral blood microRNAs distinguish active ulcerative colitis and Crohn's disease. *Inflamm. Bowel Dis.* 17, 241–250. <https://doi.org/10.1002/ibd.21450>

- Wu, F., Zhang, S., Dassopoulos, T., Harris, M.L., Bayless, T.M., Meltzer, S.J., Brant, S.R., Kwon, J.H., 2010. Identification of microRNAs associated with ileal and colonic Crohn's disease. *Inflamm. Bowel Dis.* 16, 1729–1738. <https://doi.org/10.1002/ibd.21267>
- Wu, Y.-T., Tan, H.-L., Shui, G., Bauvy, C., Huang, Q., Wenk, M.R., Ong, C.-N., Codogno, P., Shen, H.-M., 2010. Dual role of 3-methyladenine in modulation of autophagy via different temporal patterns of inhibition on class I and III phosphoinositide 3-kinase. *J. Biol. Chem.* 285, 10850–10861. <https://doi.org/10.1074/jbc.M109.080796>
- Xia, X., Kar, R., Gluhak-Heinrich, J., Yao, W., Lane, N.E., Bonewald, L.F., Biswas, S.K., Lo, W.K., Jiang, J.X., 2010. Glucocorticoid-induced autophagy in osteocytes. *J Bone Min. Res* 25, 2479–88. <https://doi.org/10.1002/jbmr.160>
- Xie, J., Zhu, R., Peng, Y., Gao, W., Du, J., Zhao, L., Chi, Y., Yang, L., 2017. Tumor necrosis factor-alpha regulates photoreceptor cell autophagy after retinal detachment. *Sci. Rep.* 7. <https://doi.org/10.1038/s41598-017-17400-3>
- Xiong, X., Tao, R., DePinho, R.A., Dong, X.C., 2012. The autophagy-related gene 14 (Atg14) is regulated by forkhead box O transcription factors and circadian rhythms and plays a critical role in hepatic autophagy and lipid metabolism. *J. Biol. Chem.* 287, 39107–39114. <https://doi.org/10.1074/jbc.M112.412569>
- Xu, K., Cai, Y., Lu, S.-M., Li, X., Liu, L., Li, Z., Liu, H., Xu, P., 2015. Autophagy induction contributes to the resistance to methotrexate treatment in rheumatoid arthritis fibroblast-like synovial cells through high mobility group box chromosomal protein 1. *Arthritis Res. Ther.* 17. <https://doi.org/10.1186/s13075-015-0892-y>
- Xue, E., Zhang, Y., Song, B., Xiao, J., Shi, Z., 2016. Effect of autophagy induced by dexamethasone on senescence in chondrocytes. *Mol. Med. Rep.* 14, 3037–3044. <https://doi.org/10.3892/mmr.2016.5662>
- Xue, Y., Du, M., Sheng, H., Hovde, C.J., Zhu, M.-J., 2017. *Escherichia coli* O157:H7 suppresses host autophagy and promotes epithelial adhesion via Tir-mediated and cAMP-independent activation of protein kinase A. *Cell Death Discov.* 3, 17055. <https://doi.org/10.1038/cddiscovery.2017.55>
- Yadav, P.K., Chen, C., Liu, Z., 2011. Potential Role of NK Cells in the Pathogenesis of Inflammatory Bowel Disease [WWW Document]. *BioMed Res. Int.* <https://doi.org/10.1155/2011/348530>
- Yamamoto, A., Tagawa, Y., Yoshimori, T., Moriyama, Y., Masaki, R., Tashiro, Y., 1998. Bafilomycin A1 prevents maturation of autophagic vacuoles by inhibiting fusion between autophagosomes and lysosomes in rat hepatoma cell line, H-4-II-E cells. *Cell Struct. Funct.* 23, 33–42.
- Yamazaki, H., Hiramatsu, N., Hayakawa, K., Tagawa, Y., Okamura, M., Ogata, R., Huang, T., Nakajima, S., Yao, J., Paton, A.W., Paton, J.C., Kitamura, M., 2009. Activation of the Akt-NF-kappaB pathway by subtilase cytotoxin through the ATF6 branch of the unfolded protein response. *J. Immunol. Baltim. Md* 1950 183, 1480–1487. <https://doi.org/10.4049/jimmunol.0900017>
- Yan, T., Berry-Miller, S., Desai, A., Kinsella, T., 2003. DNA mismatch repair (MMR) mediates 6-thioguanine Genotoxicity by introducing single-strand breaks to signal a G(2)-M arrest in MMR-proficient RKO cells. *Clin. Cancer Res.* 9, 2327–2334.
- Yang, M., Liu, J., Shao, J., Qin, Y., Ji, Q., Zhang, X., Du, J., 2014. Cathepsin S-mediated autophagic flux in tumor-associated macrophages accelerate tumor

- development by promoting M2 polarization. *Mol. Cancer* 13, 43. <https://doi.org/10.1186/1476-4598-13-43>
- Yang, Z., Klionsky, D.J., 2010. Eaten alive: a history of macroautophagy. *Nat. Cell Biol.* 12, 814–822. <https://doi.org/10.1038/ncb0910-814>
- Yang, Z., Ye, X., Wu, Q., Wu, K., Fan, D., 2014. A network meta-analysis on the efficacy of 5-aminosalicylates, immunomodulators and biologics for the prevention of postoperative recurrence in Crohn's disease. *Int J Surg* 12, 516–22. <https://doi.org/10.1016/j.ijso.2014.02.010>
- Ye, J., Rawson, R.B., Komuro, R., Chen, X., Davé, U.P., Prywes, R., Brown, M.S., Goldstein, J.L., 2000. ER stress induces cleavage of membrane-bound ATF6 by the same proteases that process SREBPs. *Mol. Cell* 6, 1355–1364.
- Yoshida, H., Matsui, T., Yamamoto, A., Okada, T., Mori, K., 2001. XBP1 mRNA is induced by ATF6 and spliced by IRE1 in response to ER stress to produce a highly active transcription factor. *Cell* 107, 881–891.
- Youle, R.J., Narendra, D.P., 2011a. Mechanisms of mitophagy. *Nat. Rev. Mol. Cell Biol.* 12, 9–14. <https://doi.org/10.1038/nrm3028>
- Youle, R.J., Narendra, D.P., 2011b. Mechanisms of mitophagy. *Nat. Rev. Mol. Cell Biol.* 12, 9–14. <https://doi.org/10.1038/nrm3028>
- Yousefi, S., Perozzo, R., Schmid, I., Ziemiecki, A., Schaffner, T., Scapozza, L., Brunner, T., Simon, H.-U., 2006. Calpain-mediated cleavage of Atg5 switches autophagy to apoptosis. *Nat. Cell Biol.* 8, 1124–1132. <https://doi.org/10.1038/ncb1482>
- Zalckvar, E., Berissi, H., Mizrachy, L., Idelchuk, Y., Koren, I., Eisenstein, M., Sabanay, H., Pinkas-Kramarski, R., Kimchi, A., 2009. DAP-kinase-mediated phosphorylation on the BH3 domain of beclin 1 promotes dissociation of beclin 1 from Bcl-XL and induction of autophagy. *EMBO Rep.* 10, 285–292. <https://doi.org/10.1038/embor.2008.246>
- Zeng, X., Kinsella, T.J., 2010. BNIP3 is essential for mediating 6-thioguanine- and 5-fluorouracil-induced autophagy following DNA mismatch repair processing. *Cell Res.* 20, 665–675. <https://doi.org/10.1038/cr.2010.40>
- Zeng, X., Kinsella, T.J., 2008. Mammalian Target of Rapamycin and S6 Kinase 1 Positively Regulate 6-thioguanine-Induced Autophagy. *Cancer Res.* 68, 2384–2390. <https://doi.org/10.1158/0008-5472.CAN-07-6163>
- Zeng, X., Yan, T., Schupp, J.E., Seo, Y., Kinsella, T.J., 2007. DNA Mismatch Repair Initiates 6-Thioguanine-Induced Autophagy through p53 Activation in Human Tumor Cells. *Clin. Cancer Res.* 13, 1315–1321. <https://doi.org/10.1158/1078-0432.CCR-06-1517>
- Zhai, Z., Wu, F., Dong, F., Chuang, A.Y., Messer, J.S., Boone, D.L., Kwon, J.H., 2014. Human autophagy gene ATG16L1 is post-transcriptionally regulated by MIR142-3p. *Autophagy* 10, 468–479. <https://doi.org/10.4161/auto.27553>
- Zhang, H., Zheng, L., McGovern, D.P.B., Hamill, A.M., Ichikawa, R., Kanazawa, Y., Luu, J., Kumagai, K., Cilluffo, M., Fukata, M., Targan, S.R., Underhill, D.M., Zhang, X., Shih, D.Q., 2017. Myeloid ATG16L1 Facilitates Host-Bacteria Interactions in Maintaining Intestinal Homeostasis. *J. Immunol. Baltim. Md 1950* 198, 2133–2146. <https://doi.org/10.4049/jimmunol.1601293>
- Zhang, H.-F., Qiu, L.-X., Chen, Y., Zhu, W.-L., Mao, C., Zhu, L.-G., Zheng, M.-H., Wang, Y., Lei, L., Shi, J., 2009. ATG16L1 T300A polymorphism and Crohn's disease susceptibility: evidence from 13,022 cases and 17,532 controls. *Hum. Genet.* 125, 627–631. <https://doi.org/10.1007/s00439-009-0660-7>

- Zhang, Y., Morgan, M.J., Chen, K., Choksi, S., Liu, Z., 2012. Induction of autophagy is essential for monocyte-macrophage differentiation. *Blood* 119, 2895–2905. <https://doi.org/10.1182/blood-2011-08-372383>
- Zhao, C., Yin, S., Dong, Y., Guo, X., Fan, L., Ye, M., Hu, H., 2013. Autophagy-dependent EIF2AK3 activation compromises ursolic acid-induced apoptosis through upregulation of MCL1 in MCF-7 human breast cancer cells. *Autophagy* 9, 196–207. <https://doi.org/10.4161/auto.22805>
- Zhao, J., Brault, J.J., Schild, A., Cao, P., Sandri, M., Schiaffino, S., Lecker, S.H., Goldberg, A.L., 2007. FoxO3 coordinately activates protein degradation by the autophagic/lysosomal and proteasomal pathways in atrophying muscle cells. *Cell Metab.* 6, 472–483. <https://doi.org/10.1016/j.cmet.2007.11.004>
- Zheng, J.H., Viacava Follis, A., Kriwacki, R.W., Moldoveanu, T., 2016. Discoveries and controversies in BCL-2 protein-mediated apoptosis. *FEBS J.* 283, 2690–2700. <https://doi.org/10.1111/febs.13527>
- Zheng, W., Rosenstiel, P., Huse, K., Sina, C., Valentonyte, R., Mah, N., Zeitlmann, L., Grosse, J., Ruf, N., Nürnberg, P., Costello, C.M., Onnie, C., Mathew, C., Platzer, M., Schreiber, S., Hampe, J., 2006. Evaluation of AGR2 and AGR3 as candidate genes for inflammatory bowel disease. *Genes Immun.* 7, 11–18. <https://doi.org/10.1038/sj.gene.6364263>
- Zheng, X., Tsuchiya, K., Okamoto, R., Iwasaki, M., Kano, Y., Sakamoto, N., Nakamura, T., Watanabe, M., 2011. Suppression of *hath1* gene expression directly regulated by *hes1* via notch signaling is associated with goblet cell depletion in ulcerative colitis. *Inflamm. Bowel Dis.* 17, 2251–2260. <https://doi.org/10.1002/ibd.21611>
- Zheng, Y., Ge, W., Ma, Y., Xie, G., Wang, W., Han, L., Bian, B., Li, L., Shen, L., 2017. miR-155 Regulates IL-10-Producing CD24^{hi}CD27⁺B Cells and Impairs Their Function in Patients with Crohn's Disease. *Front. Immunol.* 8, 914. <https://doi.org/10.3389/fimmu.2017.00914>
- Zhou, J., Hu, S.E., Tan, S.H., Cao, R., Chen, Y., Xia, D., Zhu, X., Yang, X.F., Ong, C.N., Shen, H.M., 2012. Andrographolide sensitizes cisplatin-induced apoptosis via suppression of autophagosome-lysosome fusion in human cancer cells. *Autophagy* 8, 338–49. <https://doi.org/10.4161/auto.18721>
- Ziegler-Heitbrock, L., Ancuta, P., Crowe, S., Dalod, M., Grau, V., Hart, D.N., Leenen, P.J.M., Liu, Y.-J., MacPherson, G., Randolph, G.J., Scherberich, J., Schmitz, J., Shortman, K., Sozzani, S., Strobl, H., Zembala, M., Austyn, J.M., Lutz, M.B., 2010. Nomenclature of monocytes and dendritic cells in blood. *Blood* 116, e74-80. <https://doi.org/10.1182/blood-2010-02-258558>
- Zigmond, E., Varol, C., Farache, J., Elmaliyah, E., Satpathy, A.T., Friedlander, G., Mack, M., Shpigel, N., Boneca, I.G., Murphy, K.M., Shakhar, G., Halpern, Z., Jung, S., 2012. Ly6C^{hi} monocytes in the inflamed colon give rise to proinflammatory effector cells and migratory antigen-presenting cells. *Immunity* 37, 1076–1090. <https://doi.org/10.1016/j.immuni.2012.08.026>